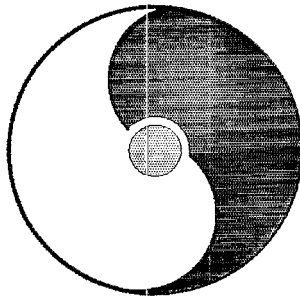


2002 Summer Program: Current and Future Directions at RHIC

August 5-23, 2002



Organizers:

A. Deshpande, A. Dumitru, J. Jalilian-Marian, N. Saito,
D. Teaney, R. Venugopalan, W. Vogelsang

RIKEN BNL Research Center

Building 510A, Brookhaven National Laboratory, Upton, NY 11973-5000, USA

DISCLAIMER

This report was prepared as an account of work sponsored by an agency of the United States Government. Neither the United States Government nor any agency thereof, nor any employees, nor any of their contractors, subcontractors or their employees, makes any warranty, express or implied, or assumes any legal liability or responsibility for the accuracy, completeness, or any third party's use or the results of such use of any information, apparatus, product, or process disclosed, or represents that its use would not infringe privately owned rights. Reference herein to any specific commercial product, process, or service by trade name, trademark, manufacturer, or otherwise, does not necessarily constitute or imply its endorsement, recommendation, or favoring by the United States Government or any agency thereof or its contractors or subcontractors. The views and opinions of authors expressed herein do not necessarily state or reflect those of the United States Government or any agency thereof.

Available electronically at-

<http://www.doe.gov/bridge>

Available to U.S. Department of Energy and its contractors in paper from-

U.S. Department of Energy
Office of Scientific and Technical Information
P.O. Box 62
Oak Ridge, TN 37831
(423) 576-8401

Available to the public from-

U.S. Department of Commerce
National Technical Information Service
5285 Port Royal Road
Springfield, VA 22131
(703) 487-4650



Printed on recycled paper

Preface to the Series

The RIKEN BNL Research Center (RBRC) was established in April 1997 at Brookhaven National Laboratory. It is funded by the "Rikagaku Kenkyusho" (RIKEN, The Institute of Physical and Chemical Research) of Japan. The Center is dedicated to the study of strong interactions, including spin physics, lattice QCD, and RHIC physics through the nurturing of a new generation of young physicists.

During the first year, the Center had only a Theory Group. In the second year, an Experimental Group was also established at the Center. At present, there are seven Fellows and seven Research Associates in these two groups. During the third year, we started a new Tenure Track Strong Interaction Theory RHIC Physics Fellow Program, with six positions in the first academic year, 1999-2000. This program had increased to include ten theorists and one experimentalist in academic year, 2001-2002. With recent graduations, the program presently has eight theorists and two experimentalists. Beginning last year a new RIKEN Spin Program (RSP) category was implemented at RBRC, presently comprising four RSP Researchers and five RSP Research Associates. In addition, RBRC has four RBRC Young Researchers.

The Center also has an active workshop program on strong interaction physics with each workshop focused on a specific physics problem. Each workshop speaker is encouraged to select a few of the most important transparencies from his or her presentation, accompanied by a page of explanation. This material is collected at the end of the workshop by the organizer to form proceedings, which can therefore be available within a short time. To date there are forty-eight proceeding volumes available.

The construction of a 0.6 teraflops parallel processor, dedicated to lattice QCD, begun at the Center on February 19, 1998, was completed on August 28, 1998. A 10 teraflops QCDOC computer is under development and expected to be completed in JFY 2003.

**T. D. Lee
November 22, 2002**

***Work performed under the auspices of U.S.D.O.E. Contract No. DE-AC02-98CH10886.**

CONTENTS

Preface to the Series

Introduction	i
Nuclear Effects Observed at High P_T in Single Hadron Spectra and Hadron Pair Spectra at Fermilab	
<i>R. McCarthy</i>	1
Energy Dependence of the High- p_T Tomography of $d + Au$ and $Au + Au$ as SPS, RHIC, and LHC	
<i>I. Vitev</i>	13
p_A in the Color Glass Condensate Model	
<i>F. Gelis</i>	21
What's Happening at High p_T ? New Results from Phenix	
<i>B. Jacak</i>	29
v_2 from Classical Yang-Mills	
<i>Y. Nara</i>	35
Elliptic Flow from Minijet Production in Heavy Ion Collisions	
<i>K. Tuchin</i>	41
Elliptic Flow at High p_T	
<i>K. Filimonov</i>	47
Scaling of Particle Production in High Energy Collisions	
<i>G. Roland</i>	55
Saturation and RHIC Data	
<i>E. Levin</i>	63
Recent Results from BRAHMS at RHIC	
<i>J. H. Lee</i>	71
Particle Production in AA Collisions from Saturation Physics	
<i>Y. Kovchegov</i>	79
E_T Distributions and Other Event-by-Event Fluctuations	
<i>M. Tannenbaum</i>	85

Two-Particle Interferometry at RHIC <i>S. Panitkin</i>	91
Strangeness Production at RHIC <i>H. Caines</i>	99
Jets and Dijets in p+p and Au+Au Collisions at RHIC <i>D. Hardtke</i>	105
Charm and J/PSI Measurement at RHIC <i>Y. Akiba</i>	113
PHENIX AA Related Upgrades <i>C. Woody</i>	119
Current and Future Physics at RHIC <i>D. Kharzeev</i>	127
Heavy Quark Production at RHIC <i>J. Raufeisen</i>	135
Violations of Parton-Hadron Duality in DIS Scattering <i>S. Liuti</i>	141
Leading and Higher Twist in e + A and p + A Collisions <i>R. Fries</i>	149
Diffractive DIS <i>F. Hautmann</i>	157
Small x Phenomena with Nuclei <i>M. Strikman</i>	163
Global Analysis of Nuclear DIS and Drell-Yan Data <i>S. Kumano</i>	169
Towards a New Global QCD Analysis: P.d.f. for Low-x <i>E. Levin</i>	175
Gluon Saturation and Wilson Line Distribution <i>H. Lam</i>	183
Hard Coherent Phenomena in eA and pA Collisions <i>L. Frankfurt</i>	191

Search for Color Transparency <i>A. Sandacz</i>	197
eRHIC. Accelerator Issues <i>V. Ptitsyn</i>	205
HERA III & THERA Plans <i>H. Kowalski</i>	211
QCD Results from CDF <i>F. Ukegawa</i>	217
Evidence for Hadronic Deconfinement and for a Significant Change in the Hadronization Conditions in $p\bar{p}$ Collisions @ 1.8 TeV <i>R. Scharenberg</i>	225
pp Neutral Pion Results from PHENIX Run-2 <i>H. Torii</i>	231
pp J/Psi Results from PHENIX Run-2 <i>H. Sato</i>	239
Fragmentation Functions in Hadron Production <i>X.-F. Zhang</i>	247
Resumed Cross-Section for Higgs Production at Hadron Colliders <i>D. de Florian</i>	253
Transverse Momentum Resummation in DIS Production of Light and Heavy Flavors <i>P. Nadolsky</i>	259
Physics Beyond RHIC Spin <i>K. Hagiwara</i>	265
NLO QCD Corrections to A^{π}_{LL} <i>M. Stratmann</i>	273
Hadron Production in Polarized pp Collisions at NLO <i>D. de Florian</i>	281
Polarization Effects in Drell-Yan <i>H. Yokoya</i>	287
W-Boson Physics at the Polarized RHIC <i>C.-P. Yuan</i>	293
QCD Analysis of Spin Structure Function Data from Present & Prospective Future Measurements <i>J. Lichtenstadt</i>	299

Polarized Light-Antiquark Flavor Asymmetry <i>S. Kumano</i>	309
Nucleon Matrix Elements with domain Wall Fermions <i>K. Orginos</i>	315
Single Spin Asymmetries in pp and ep Collisions <i>Y. Koike</i>	323
Extraction of Polarized Parton Distributions from Semi-Inclusive HERMES Data <i>P. Liebing</i>	329
Thoughts on Measuring Δ_S in Semi-Inclusive DIS <i>E. Kinney</i>	335
Fragmentation Functions from e^+e^- Annihilations and Semi-Inclusive DIS <i>S. Kretzer</i>	343
vp Elastic Scattering: A Direct Measure of Δ_S <i>S. Bass</i>	351
Studies of Exclusive Processes in ep Scattering at EIC <i>A. Sandacz</i>	357
Impact Parameter Space Interpretation for the Generalized Parton Distributions $H(X,0,T)$ and $E(X,0T)$ <i>M. Burkardt</i>	365
Azimuthal Asymmetries in Semi-Inclusive DIS <i>P. Nadolsky</i>	371
Measurements of the Structure of Proton and Virtual Photon at HERA <i>S. Schlenstedt</i>	377
Helicity Selection and Semi-Exclusive Meson Production <i>J. Lenaghan</i>	383
The Drell-Hearn-Gerasimov Sum Rule at EIC <i>S. Bass</i>	389
ΔG at RHIC-SPIN via Double J/ψ Production <i>J. Kodaira</i>	397
Perturbative Aspects of Azimuthal Asymmetries in Polarized ep <i>K. Oganessyan</i>	403

Nucleon Spin Physics at Jefferson Lab using the 12 GeV upgrade	
<i>Z. Meizani</i>	409
List of Registered Participants	415
Agenda	425
Additional RIKEN BNL Research Center Proceeding Volumes	429
Contact Information	

Introduction

The Relativistic Heavy Ion Collider (RHIC) was commissioned for heavy ion collisions and for polarized pp collisions in 2001. All principal components of the accelerator chain were commissioned (barring a few which will be operational in the 2003 RHIC run). This has indeed been a tremendous accelerator and machine physics achievement. The experimental collaborations are not too far behind either. Not only have they commissioned various components of their detectors, but they have already published more than 20 papers related to the heavy ion physics. Furthermore, exciting new spin results have recently been released for the first time and analysis efforts towards their publication are on the way. While discovery and study of the Quark Gluon Plasma (QGP) is the primary goal of the heavy ion physics, understanding the spin structure of the nucleon is the primary objective of the RHIC Spin program. The successful start of both these programs motivated the initial thought process for this Workshop on "Current & Future Directions at RHIC".

The aim of this Workshop was to bring together experts at the forefront of theoretical and experimental communities (in both heavy ion and spin physics) to present and understand the already available data, and to orient the experimental effort appropriately to uncover the surprises that RHIC may offer us in near future. From the variety and depth of presentations we had in this Workshop we believe we have achieved that, and hope the reader will agree with us. Many interesting discussions ensued which challenged dearly held ideas of the past, while new data clearly presented opportunities for predictions and new proposals.

With all the excitement around, it was also emphasized that thinking about not just the short term but also the long term future program at RHIC/BNL was necessary. Upgrades of the RHIC accelerator complex to enhance the luminosity of the AA and pp collisions was discussed, ideas about the physics program at the high luminosities and the necessities of detector upgrades were also presented. A major new effort to add a 10 GeV electron ring to the RHIC complex to enable polarized and unpolarized DIS at never before achieved high energies has been proposed as a upgrade of the facility. (eRHIC or the Electron Ion Collider, EIC) Not only the physics motivation for such a facility were discussed but also the relevance of such studies to the already existing heavy ion physics program at RHIC was debated.

The Workshop was three weeks long: the first one dedicated to the present and future plans for heavy ion physics after the RHIC luminosity upgrade, the second week focused on the unpolarized pp and e-A physics motivation and expectations at RHIC; and the third week was dedicated to the polarized pp and ep studies at RHIC and eRHIC/EIC.

We are grateful for the enthusiastic participation by the RHIC community. This Workshop was initially envisioned as part of the series of "summer workshops" conducted by the Nuclear Theory Division at BNL. This year it was combined with other efforts. The Workshop would not have been possible without the generous support from the RIKEN BNL Research Center. We also acknowledge support in part by the BSA/BNL Program Development Fund. We thank Brookhaven National Laboratory and the U.S. Department of Energy for providing the facilities for holding this Workshop.

Finally, our sincere thanks go to the RIKEN & BNL administrative staff, foremost to Pamela Esposito. Without her professional and efficient work it would not have been possible to run this Workshop. We also acknowledge gratefully help from Marcy Chaloupka and Tammy Heinz.

A. Deshpande (RBRC)
A. Dumitru(BNL)
J. Jalilian-Marian(BNL)
N. Saito(RBRC/Kyoto)
D. Teaney(BNL)
R. Venugopalan(RBRC/BNL)
W. Vogelsang(RBRC/BNL)

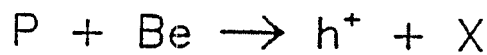
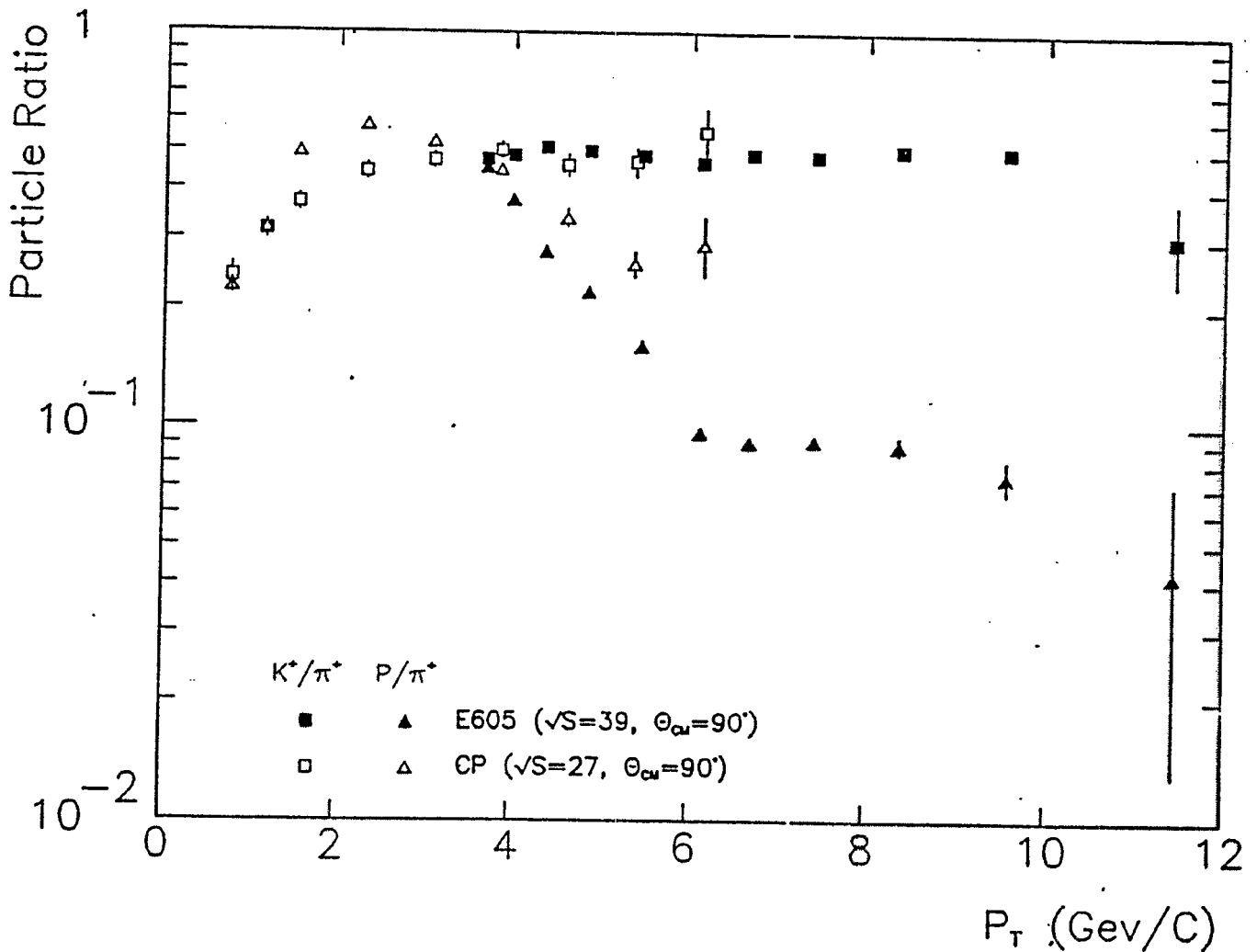
Nuclear Effects Observed
at High P_T
in Single Hadron Spectra
and Hadron Pair Spectra
at Fermilab

Bob McCarthy
SUNY at Stony Brook

Future Directions at RHIC
BNL 8/5/2002

Summary

1. Single hadrons appear to be produced by the fragmentation of single constituents for $p_T \gtrsim 3 \text{ GeV}$.
 \Rightarrow Study propagation of quarks in nuclear matter by varying A .
2. Single hadron production may be consistent with multiple scattering but a better theory is needed.
3. For single hadrons the anomalous nuclear enhancement fades away for $p_T \gtrsim 8 \text{ GeV}$.
4. For h^+h^- pairs $R_{w/Be}$ rises steeply versus p_{out} . This is expected in a constituent multiple scattering model.
5. For h^+h^- pairs $R_{w/Be} < 1$ for $m > 8 \text{ GeV}$. Multiple scattering models can not accommodate [K. Kastella, private communication]



ratios independent of p_T for $p_T > 6$
 as σ 's change by orders of
 magnitude
 \Rightarrow probably a simple explanation
 in u -quark fragmentation

$$\bar{s}/\bar{d} \approx K^+/\pi^+ = 0.48 \pm .02$$

$$(ud)/\bar{d} \approx P/\pi^+ = 0.09 \pm .02$$

Conclusion

Single hadron production at $p_T \gtrsim 3$ GeV appears to be dominated by the fragmentation of a single constituent.

For positives with $p_T > 6$ GeV this constituent is a u quark.

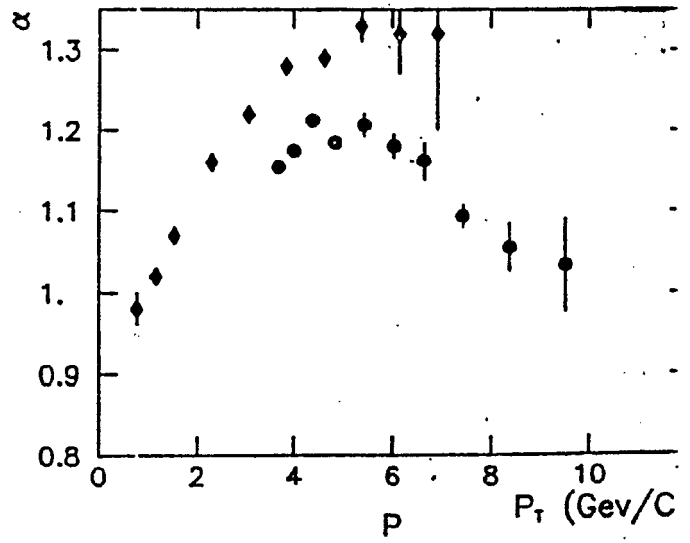
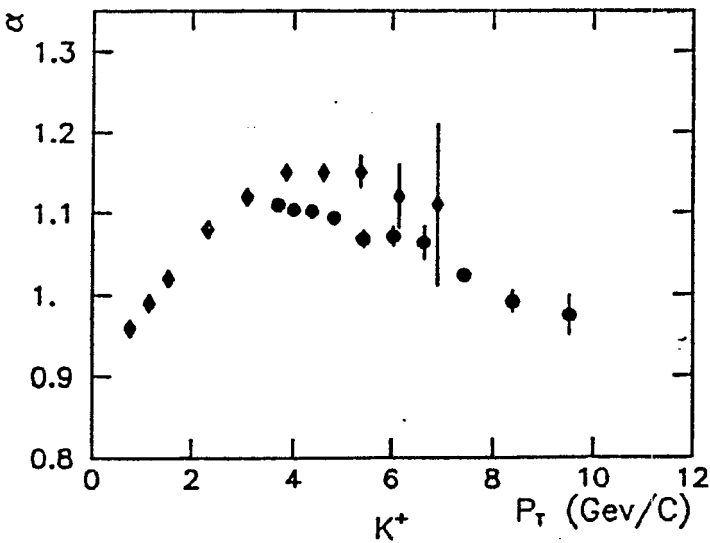
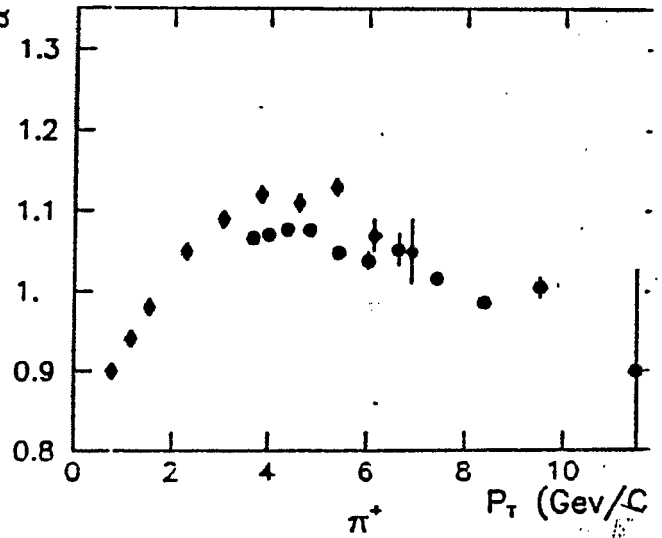
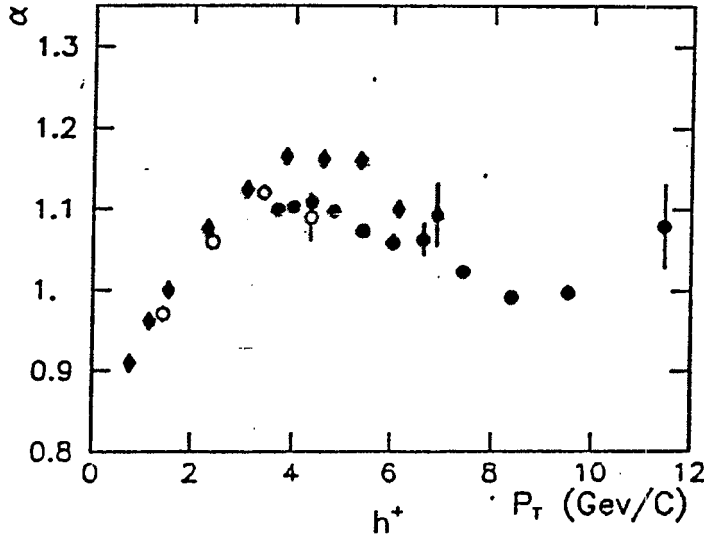
($P_{LAB} \sim 100$ GeV \Rightarrow fragments to hadron outside nucleus.)

A-Dependence

Now change the A of the target nucleus - increase the length of nuclear matter through which the above constituent must pass.

- E605 - This experiment $\sqrt{s} = 38.8 \text{ GeV}$
- ◆ CP - Antreasyan et al., Phys. Rev. D19, 764 (1979) $\sqrt{s} = 27.4$
- CFS - McCarthy et al., Phys. Rev. Lett. 40, 213 (1978) $\sqrt{s} = 27.4$

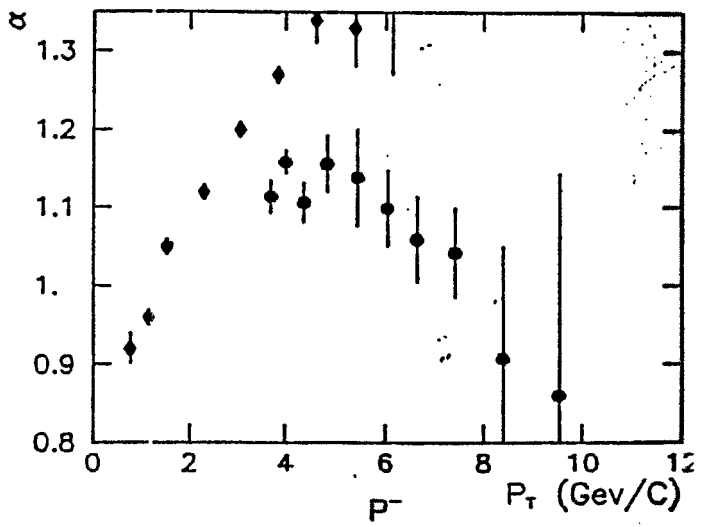
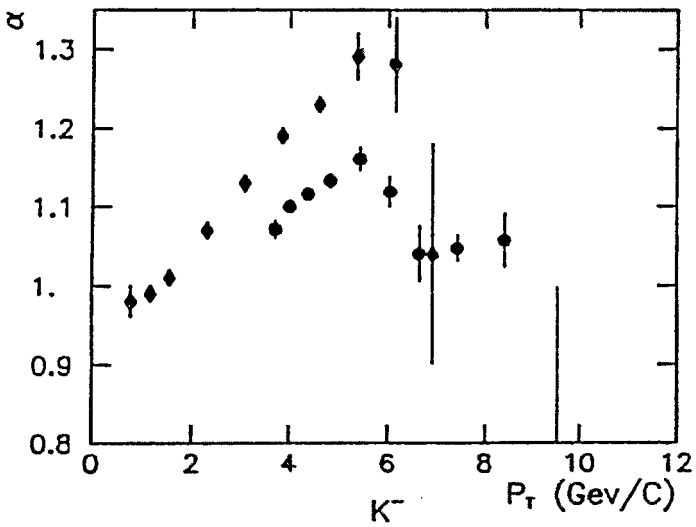
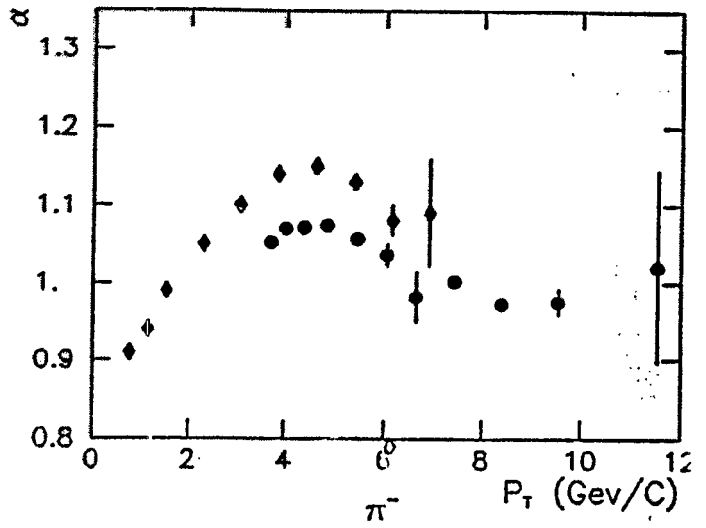
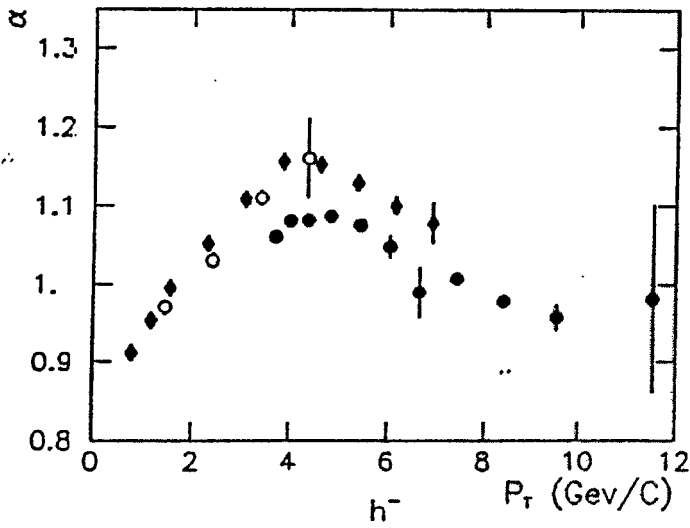
A Dependence for Singles $-0.13 < X_T < 0.14$



⇒ anomalous nuclear enhancement fades away for $P_T \gtrsim 8 \text{ GeV}$
decreases with increasing s

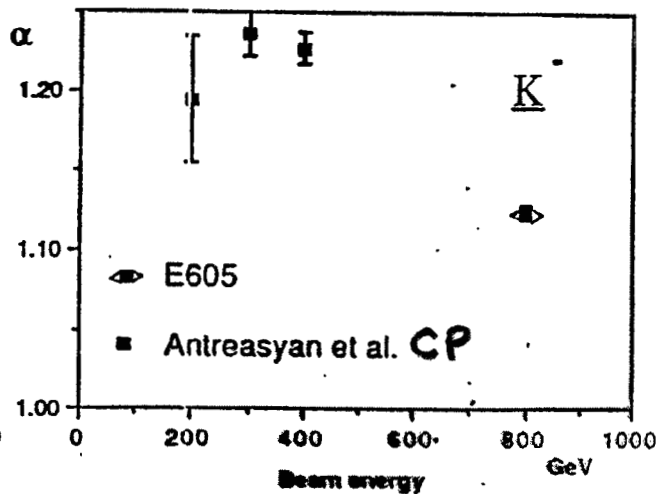
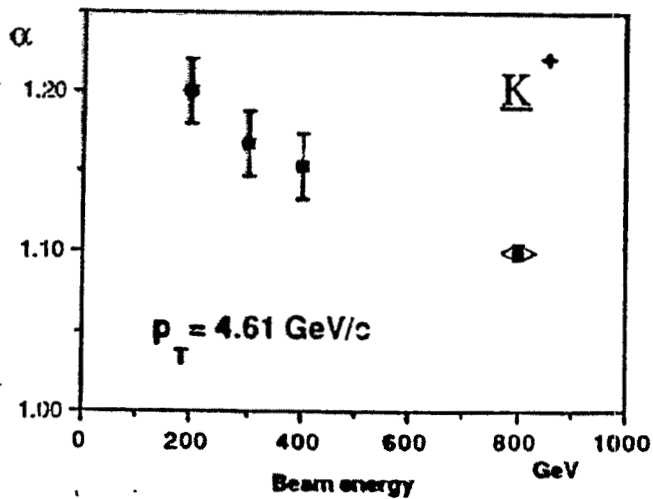
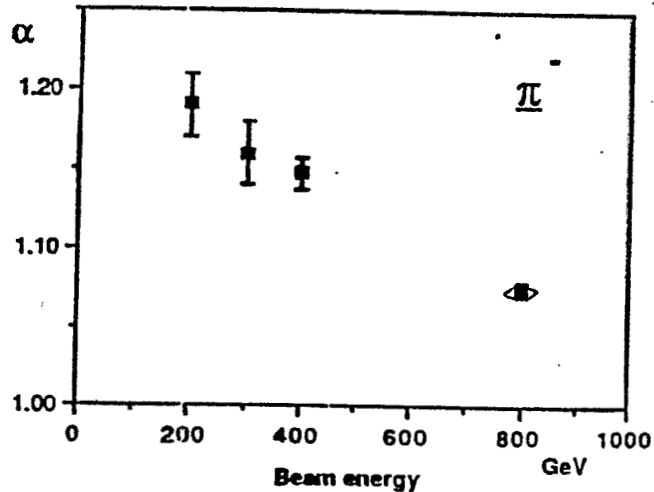
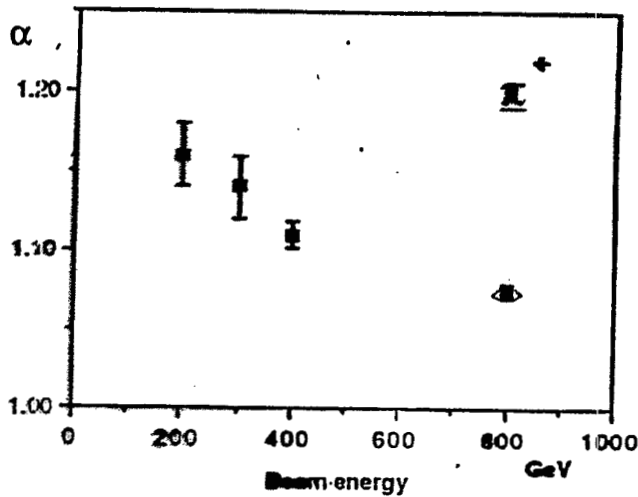
- E605 - This experiment
- ◆ CP -
- GFS -

" A Dependence for Singles $-0.13 < X_F < 0.14$

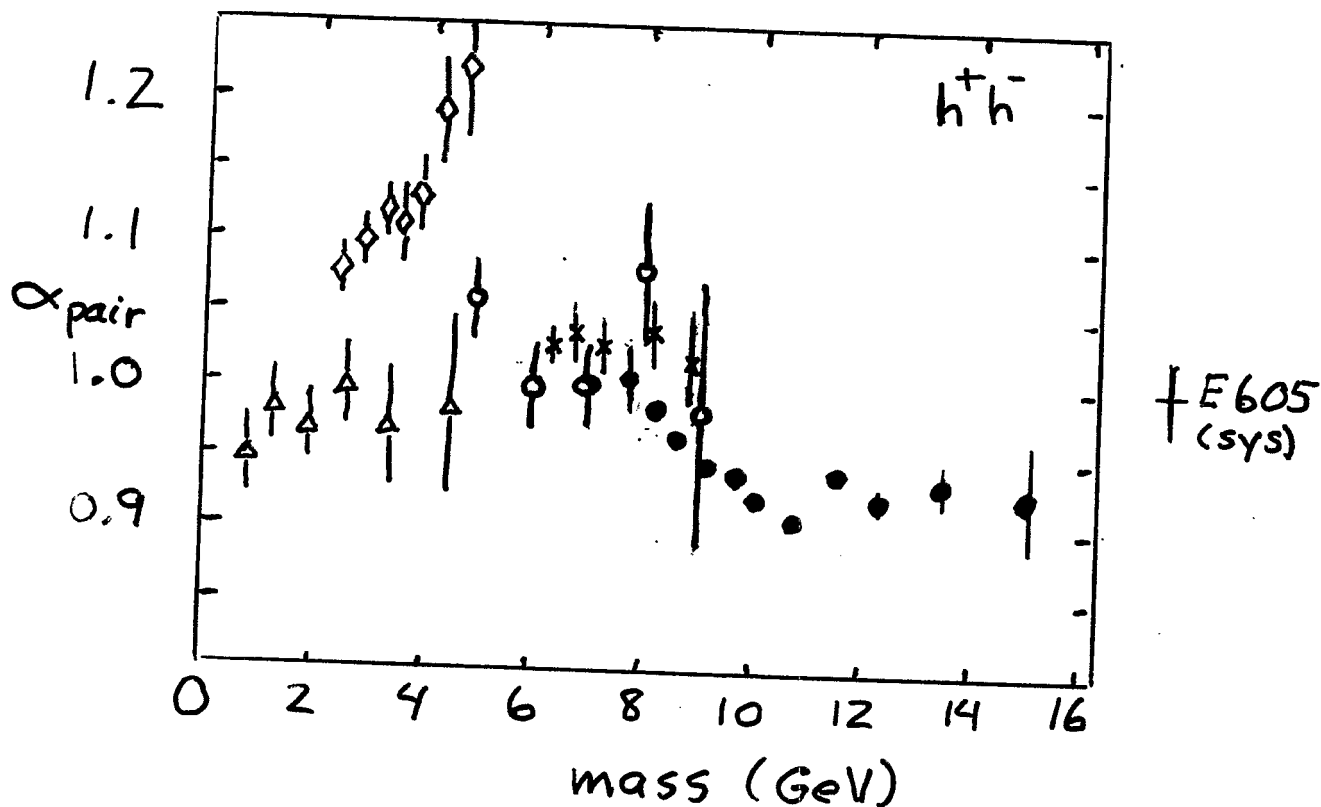


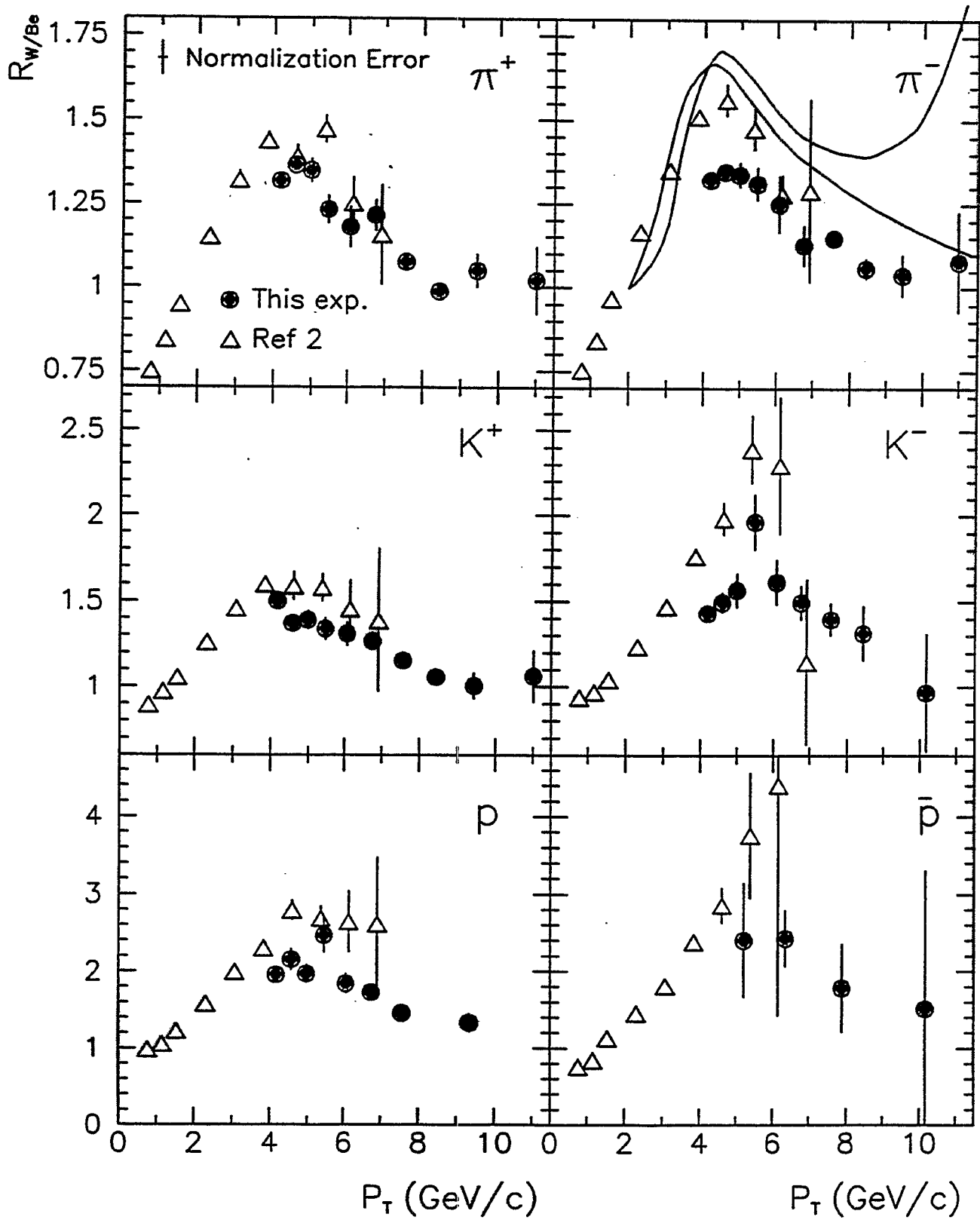
Energy Dependence

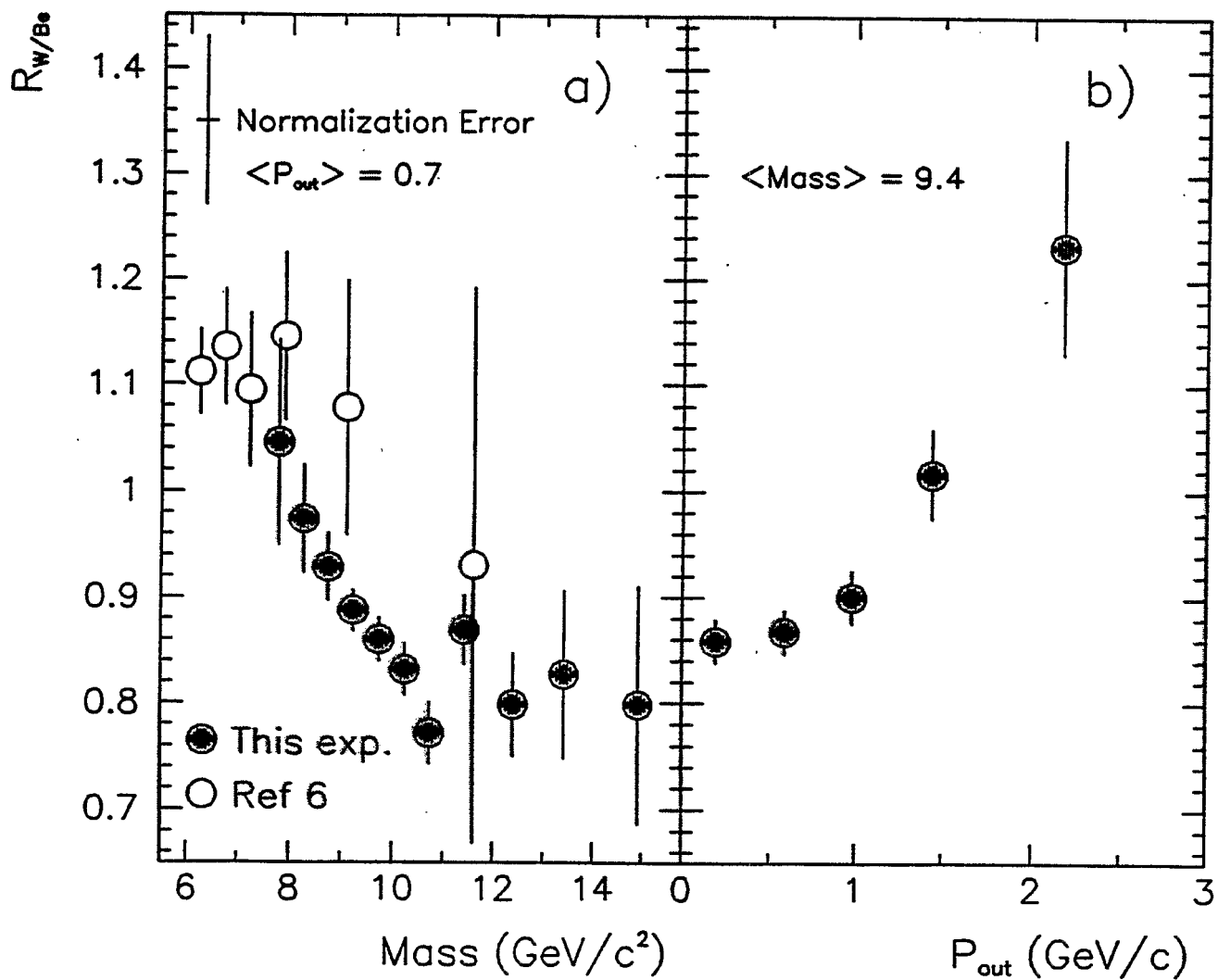
at $P_T = 4.61 \text{ GeV}$



- 400 GeV ○ McCarthy et al., P.R.L. 40, 213(1978) E494
 400 ◇ Finley et al., P.R.L. 42, 1031(1979)
 70 △ Abramov et al., JETP Lett. 38, 352(1983)
 800 ● Straub et al., submitted to PRL E605
 800 × K. Streets et al., Phys. Rev. Lett. 66, 864(1991)







Summary

1. Single hadrons appear to be produced by the fragmentation of single constituents for $p_T \gtrsim 3 \text{ GeV}$.
 \Rightarrow Study propagation of quarks in nuclear matter by varying A .
2. Single hadron production may be consistent with multiple scattering but a better theory is needed.
3. For single hadrons the anomalous nuclear enhancement fades away for $p_T \gtrsim 8 \text{ GeV}$.
4. For h^+h^- pairs R_{w/B_e} rises steeply versus p_{out} . This is expected in a constituent multiple scattering model.
5. For h^+h^- pairs $R_{w/B_e} < 1$ for $m > 8 \text{ GeV}$. Multiple scattering models can not accommodate!
[K. Kastella, private communication]

Energy Dependence of the High- p_T Tomography of $d + Au$ and $Au + Au$ at SPS, RHIC, and LHC

Ivan Vitev^a

^aDepartment of Physics, Columbia University,
538 West 120-th Street, New York, NY 10027, USA

The first systematic study of the manifestation of nuclear effects in inclusive hadron spectra in $d+Au$ and $Au+Au$ at $\sqrt{s_{NN}} = 17, 200, 5500$ GeV is presented versus the leading order PQCD-computed baseline for elementary $p + p(\bar{p} + p)$ collisions. We include the Eskola-Kolhinen-Slagado parameterization of nuclear shadowing, as well as initial parton broadening and final state medium-induced radiation evaluated in the Gyulassy-Levai-Vitev formalism. We find suppression/enhancement factors that are strikingly different in shape and magnitude at different center of mass energies.

1. SUMMARY OF RESULTS

The magnitude and the p_T dependence of the nuclear modification factor R_{AA} that compares inclusive hadron spectra to the geometrically scaled $p+p(\bar{p}+p)$ result are shown to be strongly correlated to the center of mass energy per nucleon. This dependence includes the shape of the underlying jet (quark and gluon) spectra, the initial gluon rapidity density which drives the non-Abelian energy loss, the x and Q^2 dependence of the nuclear shadowing, and the magnitude of the Cronin effect.

At SPS energies we find significant Cronin enhancement that does leave space for a factor ~ 2 suppression of high- p_T hadrons due to the non-Abelian jet energy loss. At RHIC we demonstrate that a consistent incorporation of initial and final state nuclear effects in the high- p_T hadron production phenomenology in $Au + Au$ leads to a constant p_T -independent quenching factor in the $5 \leq p_T \leq 20$ GeV range. At LHC shadowing and Cronin effect in the $5 \leq p_T \leq 100$ GeV range were found to give $\leq 20\%$ correction, while the effect of energy loss is large and its strong p_T dependence reflects the hardening of the particle spectra.

Energy Dependence of High p_T Tomography of B+A from SPS to LHC

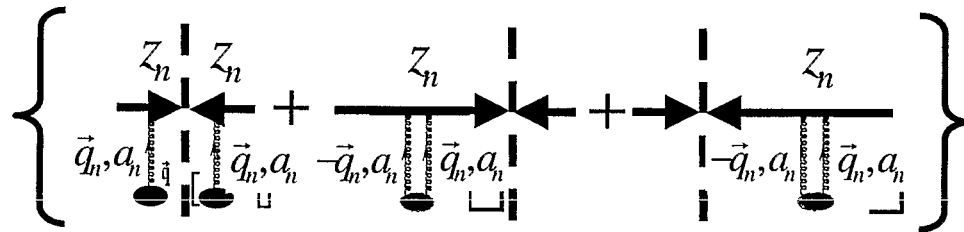
Ivan Vitev and Miklos Gyulassy
Columbia University, New York, NY 10027

Current and future directions at RHIC, August 5-23
BNL, Upton, NY

Initial Parton Broadening via the GLV Elastic Reaction Operator

- A systematic expansion technique that describes the multiple elastic and inelastic scatterings of fast partons in orders of $\chi = L/\lambda$

Elastic scattering case:



M.Gyulassy, P.Levai, I.V.,
nucl-th/0201078, Phys.Rev.D 66

M.Gyulassy, P.Levai, I.V.,
Nucl.Phys.B594, 371 (2001)

$$\hat{R}_n = \hat{D}_n^\dagger \hat{D}_n + \hat{V}_n + \hat{V}_n^\dagger$$

R.O. = all possible $t = \infty$
on-shell cuts through a new
Double Born interaction

$$dN(b) = \sum_{n=0}^{\infty} dN^n(b) = e^{T(b_0) \left(4\pi^2 \frac{d\sigma_{el}(b)}{d^2q} - \sigma_{el}^{tot} \right)} dN^0(b)$$

$$dN(p) = \sum_{n=0}^{\infty} e^{-\chi} \frac{\chi^n}{n!} \int \prod_{i=1}^n d^2q_i \frac{1}{\sigma_{el}} \frac{d\sigma_{el}}{d^2q_i} dN^0(p - q_1 - \dots - q_n)$$

The GLV approach
gives solutions for
any initial parton
distribution

Cronin Effect in p+W and p+Be

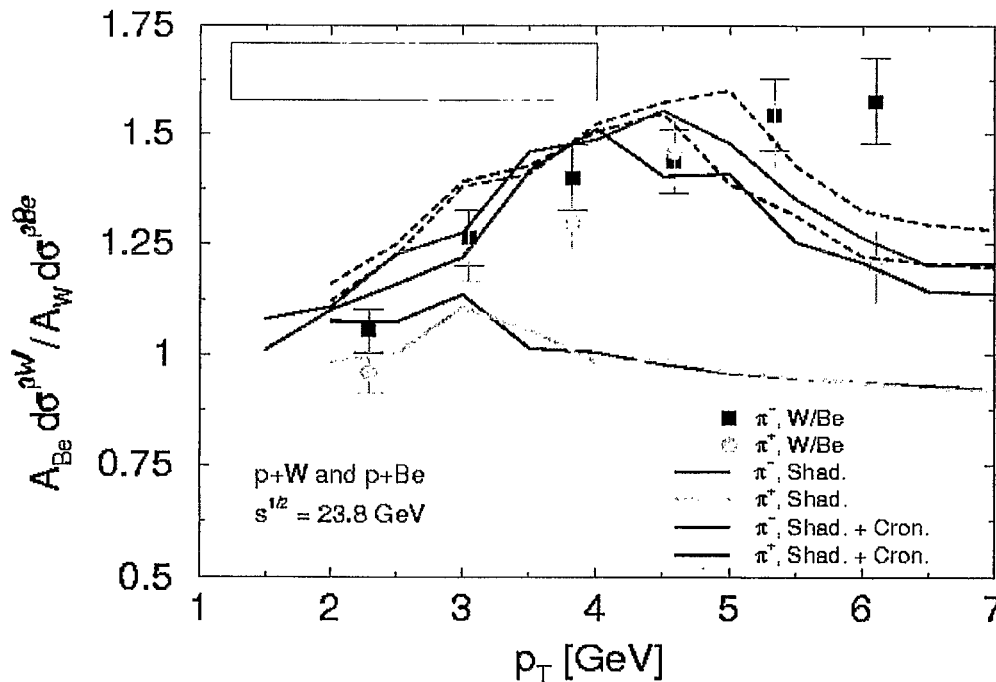
Take $\lambda \simeq d_N \simeq 2.5 \text{ fm}$, $\mu^2 \simeq 0.2 \text{ GeV}^2$

$$\frac{\mu^2}{\lambda} = 0.08 \text{ GeV}^2 / \text{fm}$$

For comparison from Drell-Yan data $\sim 0.056 \pm 0.036 \text{ GeV}^2 / \text{fm}$

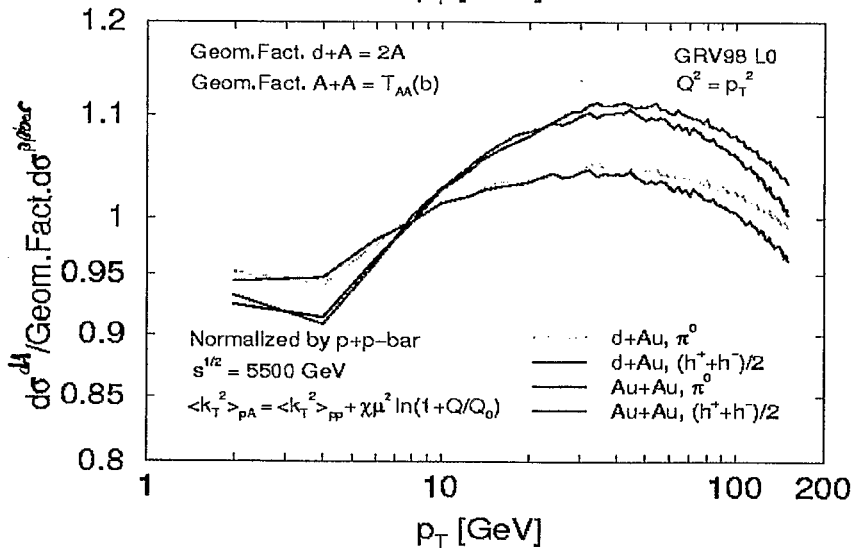
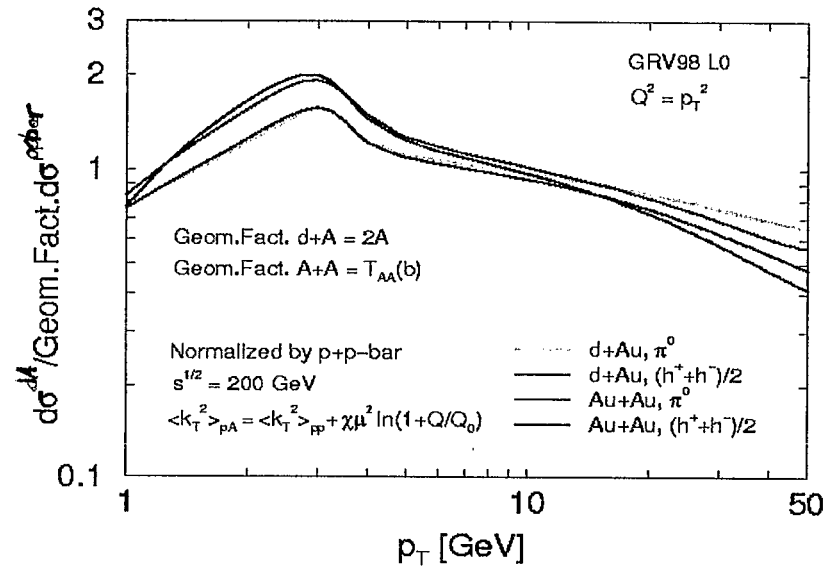
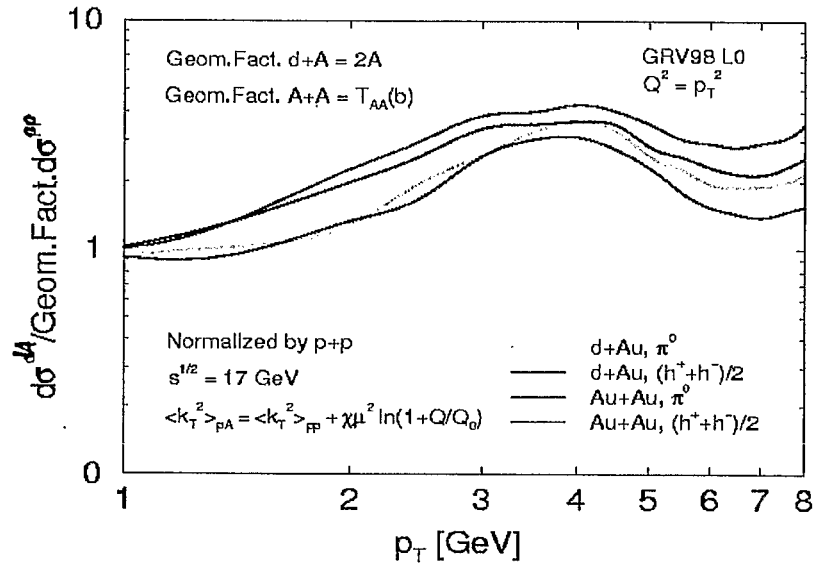
Compares to results for cold nuclear matter

F.Arleo, Phys.Lett. B532, 231 (2002)



- Shadowing alone gives a decreasing ratio with p_T
- Most, but not all, of the Cronin enhancement can be accounted for
- Careful parameterizations of the Q dependence may achieve better results

Predicted d+Au and Au+Au with Shadowing and Cronin



- SPS: factor 3-4 enhancement from Cronin. Leaves space for ~ 2 suppression!
- RHIC: factor 1.5-2 enhancement from Cronin. Some of it persists in peripheral reactions. At $p_T = 50$ GeV factor of 2 suppression from shadowing (EMC region)
- LHC: No detectable effect $\sim 10\%$

Gluon Probability Density

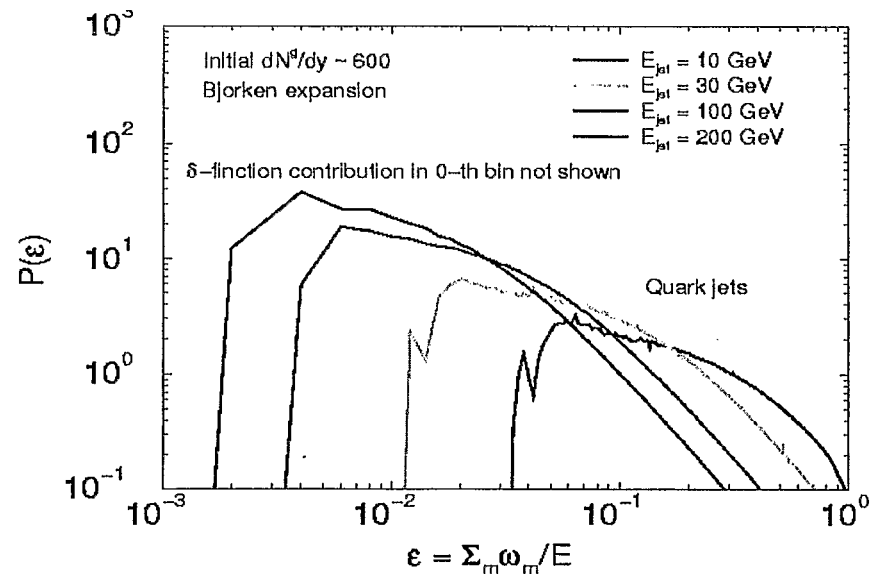
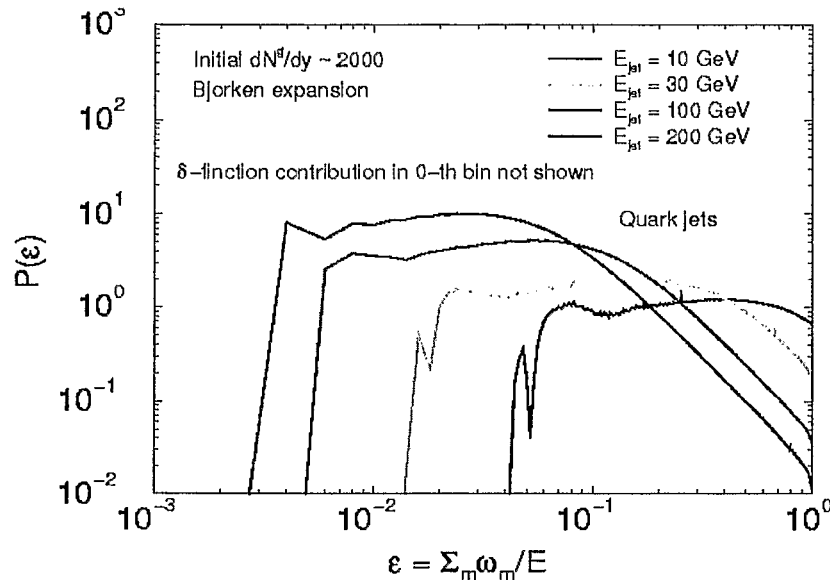
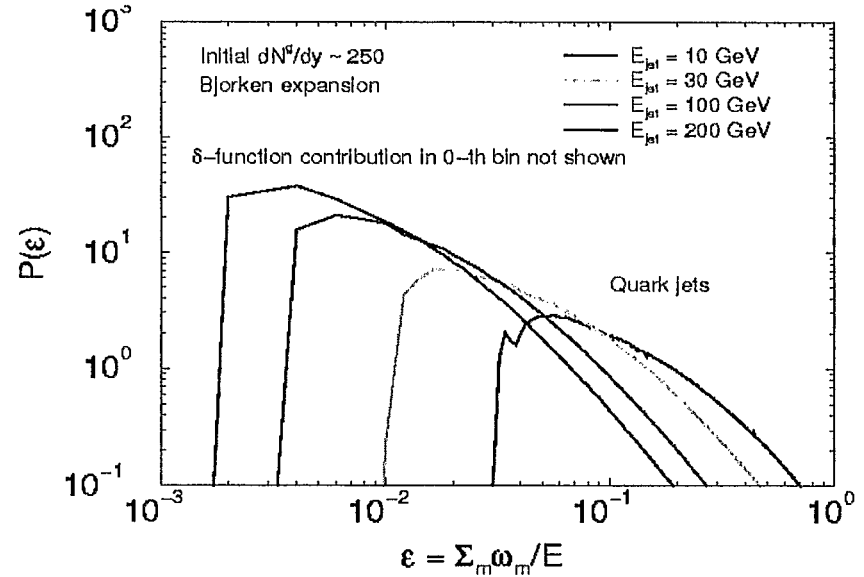
- Poisson approximation
- Non-negligible $\delta(\varepsilon)$ contribution

$$P(\varepsilon, E) = \sum_{n=0}^{\infty} P_n(\varepsilon, E) \quad \frac{\Delta E}{E} = \int_0^{\infty} d\varepsilon \varepsilon P(\varepsilon, E)$$

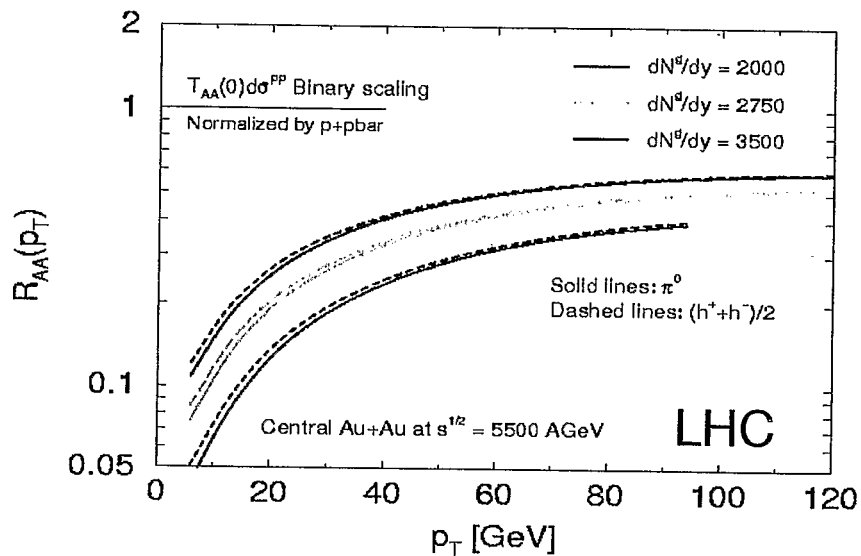
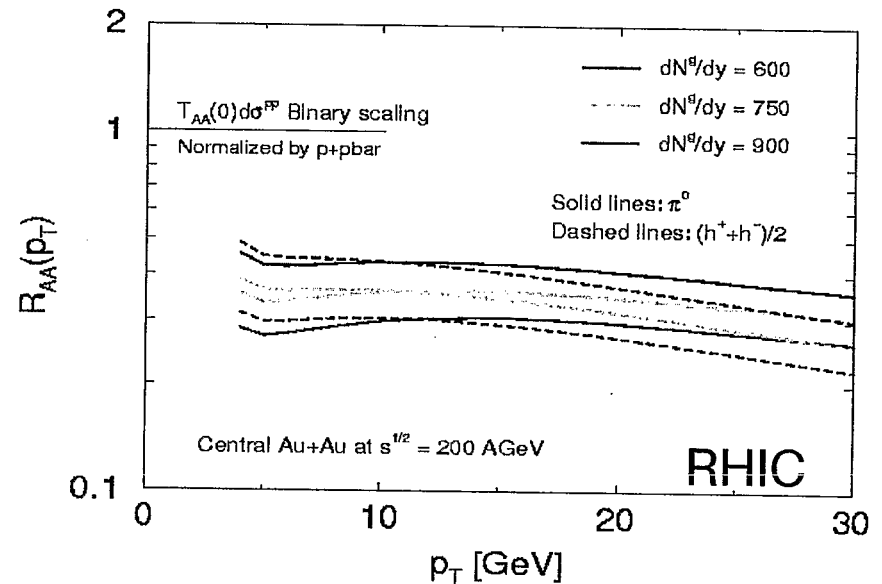
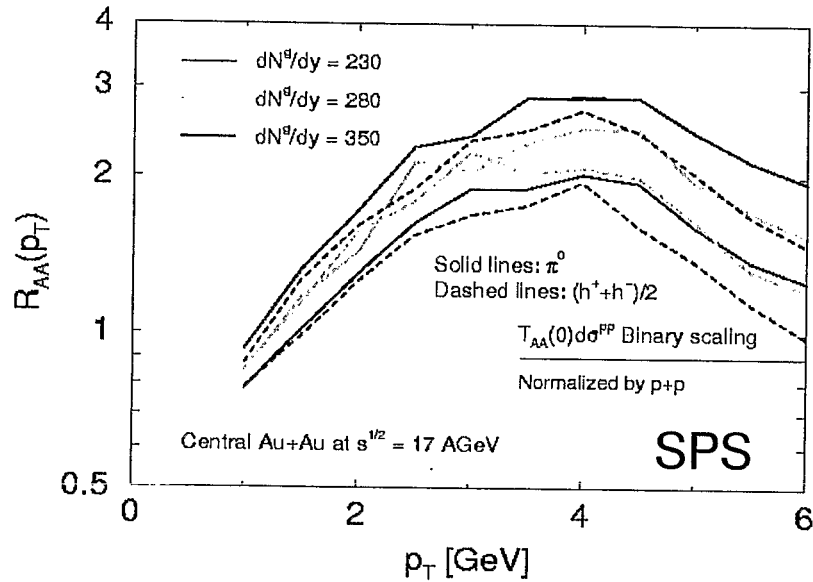
$$P_{n+1}(\varepsilon, E) = \frac{1}{n+1} \int_{x_0}^{1-x_0} dx_n \rho(x_n, E) P_n(\varepsilon - x_n, E)$$

$$P_1(\varepsilon, E) = e^{-\langle N_g \rangle} \rho(\varepsilon, E)$$

**M.Gyulassy, P.Levai, I.V.,
Phys.Lett.B538, 282 (2002)**



Suppression of Particle Spectra in Central Au+Au from $s^{1/2}=17$ AGeV to $s^{1/2}=5500$ AGeV



- The shape of the R_{AA} is different at SPS, RHIC, and LHC due to the different interplay of Cronin, shadowing, and energy loss.

- At SPS even with energy loss there is a factor $\sim 1.5-2$ enhancement, consistent with data.

- At RHIC in the $p_T=20-30$ GeV region 30% of the effect comes from shadowing. The rest is energy loss.

Conclusions: Results at SPS, RHIC, and LHC

SPS:

- ❑ Cronin effect + shadowing result in 2-2.5 fold enhancement in d+Au and 3-4 fold enhancement in Au+Au at $s^{1/2}=17$ AGeV relative to p+p.
- ❑ Energy loss driven by $dN^g/dy=280-350$ reduces this enhancement to 1.5-2 and brings it in line with the WA98 data in the $p_T=2-4$ GeV range.

RHIC:

- ❑ Cronin effect gives ~ 1.5 enhancement in d+Au and ~ 2 enhancement in Au+Au at $s^{1/2}=200$ AGeV in the $p_T=2-4$ GeV region relative to p+pbar. At $p_T=50$ GeV shadowing leads to 30%(50%) suppression in d+Au(Au+Au).
- ❑ Energy loss driven by $dN^g/dy=600-900$ results in an essentially constant suppression factor $R_{AA}=0.3-0.4$. The slight decrease is due to shadowing.

LHC:

- ❑ Cronin + shadowing at $s^{1/2}=5500$ AGeV in d+Au and Au+Au give results comparable with p+pbar within 10% for $p_T=5-150$ GeV.
- ❑ Energy loss driven by $dN^g/dy=2000-3500$ gives an evolving suppression factor: $R_{AA}=0.07-0.13$ at $p_T=10$ GeV to $R_{AA}=0.4-0.6$ at $p_T=120$ GeV.

pA in the Color Glass Condensate Model

François Gelis

Laboratoire de Physique Théorique
Bât. 210, Université ParisXO
91405 Orsay Cedex, France

Abstract:

The recently proposed Color Glass Condensate model is a framework designed to describe the universal properties of high-energy hadron or nucleus reactions. It is based on the fact that soft modes in the wave function of a high-energy hadron or nucleus have a very large occupation number, and can therefore be described in terms of classical color fields as first suggested by McLerran and Venugopalan. These soft modes are driven by the hard modes which act as “frozen” color sources.

A central part of my talk is devoted to explain how to compute the probability of some processes in this model. Indeed, the fact that the two colliding objects are described in terms of (strong) classical fields has several implications regarding what can be calculated and how. In particular, a key issue is that of the so-called “vacuum diagrams”. Vacuum diagrams are disconnected quasi-elastic sub-diagrams that appear as a prefactor of any amplitude calculated in a time-dependent external field. One can readily see that they are not negligible in strong fields, and that they play a central role in ensuring that the results are compatible with unitarity.

Then, I explain how one can compute probabilities with various degrees of inclusiveness in this model. The simplest case is the probability of a completely exclusive process (where the final state is completely prescribed), which simply requires to keep all the vacuum diagrams. However, it is sometimes more relevant to compute semi-inclusive probabilities (like the probability to produce exactly one particle of some sort, plus any number of particles of other species). At leading order in the strong coupling constant, there is a very simple rule in order to do that: one must calculate the amplitude with the requested particle in the final state and the vacuum diagrams corresponding to that particle, while all the other vacuum diagrams must be omitted. Note that this result can also be applied at leading order in order to compute the probability of events with rapidity gaps. Finally, an even more inclusive quantity is the average number of particles of some type produced in the collision: this is given at leading order by the retarded forward self-energy for this particle, and no vacuum diagrams are needed.

After that, I focus on pA collisions, for which extra simplifications can be performed based on the fact that the classical field of the proton is weaker than the classical field of the nucleus. As an example, I will show how photon/dilepton production, or photon-jet correlations can be used to test saturation effects in the nucleus.

The colored Glass Condensate

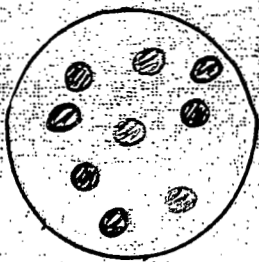
- At small momentum fraction x , BFKL predicts a rise of structure functions like:

$$\frac{1}{x^\delta} \quad (\delta > 0)$$

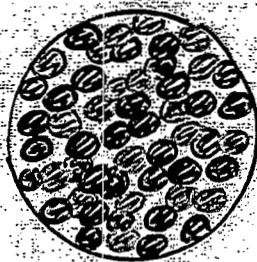
⇒ cross-sections grow like a power of the center-of-mass energy \sqrt{s}

⚠ This violates unitarity!

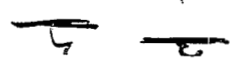
- Source of the problem: BFKL neglects gluon fusion, which should be important at large gluon densities.



A hadron at large x



A hadron at small x

⇒ When gluons overlap, the recombination process  becomes essential.

Field theory in an external field

- Generic problem:

- A classical field $A_{\text{ext}}^\mu(t, \vec{x})$ occupies all space-time
- we want the cross-section (or probability) for some processes to occur in this background.

For instance:

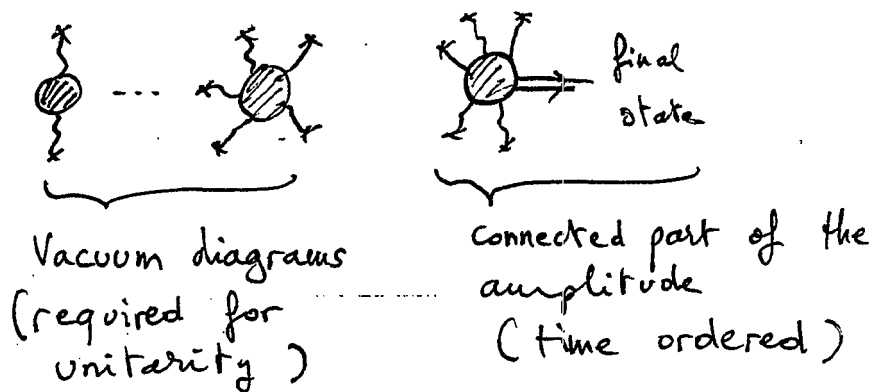
- gluon production
- $q\bar{q}$ production
- γ production

- Preliminary remarks:

- the "vacuum state" $|0\rangle$ is not really empty: it contains the external field.
- the external field is time dependent
 \Rightarrow so does $|0\rangle$
 $|0_{\text{in}}\rangle \neq |0_{\text{out}}\rangle$
- the external field carries some quantum numbers (color, ...)
 \Rightarrow so does $|0\rangle$
F : ...

- More and more inclusive quantities:

- Exclusive: the final state is completely specified.



- Semi-inclusive: we do not specify some particles in the final state.

Rule: the vacuum diagrams corresponding to the unspecified particles must be omitted

- Average multiplicity of some particle.

Rule: given by the imaginary part of the retarded self-energy of that particle.

Note: No vacuum diagrams here

Simplifications specific to pA

(20)

- At the same energy/nucleon, a proton has a smaller saturation momentum:
No $A^{1/3}$ enhancement in Q_s^2
 \Rightarrow One can assume:

$$\Lambda_{QCD}^2 \ll Q_s^2(\text{proton}) \ll Q_s^2(\text{nucleus})$$

- In terms of the classical fields:

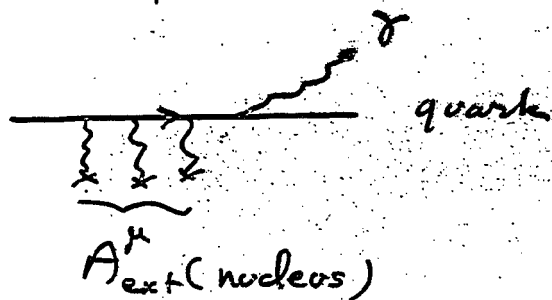
$$1 \ll A_{\text{ext}}(\text{proton}) \ll A_{\text{ext}}(\text{nucleus}) \sim \frac{1}{g}$$

\Rightarrow the fact that $g A_{\text{ext}}(\text{proton}) \ll 1$ enables to neglect multiple rescattering-rings of a particle in the external field created by the proton.

- Note: In case the condition $A_{\text{ext}}(\text{proton}) \gg 1$ is only marginally satisfied, one can describe the proton with standard p.d.f.s

Example: photon/dilepton emission in pA at high energy

- * In the wave function of a high-energy nucleus, there are many more gluons than quarks.
 \Rightarrow the partons in the proton see mostly gluons when they go through the nucleus
- * The soft gluons are in highly occupied states \Rightarrow they can be described by a classical color field.
- * At leading order in α_s , only a quark entering in the classical field can produce a photon:



Note: One only needs the quark propagator in the background field of the nucleus

Note: a dilepton is produced from a virtual photon:



What's happening at high p_T ? New Results from PHENIX

Barbara V. Jacak, Stony Brook University, SUNY

In my talk I showed that the suppression of high p_T particles in Au+Au collisions at RHIC previously reported by PHENIX continues to p_T of approximately 10 GeV/c. The suppression is seen both in identified neutral pions and in the production of charged hadrons. Uncertainties on the magnitude of the suppression are now much smaller, as PHENIX has measured the reference spectrum in 200 GeV c.m. energy p+p collisions. The neutral pion spectrum from p+p is now known to 13 GeV/c p_T , and is well described by a NLO pQCD calculation from Vogelsang. The x range reached at RHIC is approximately 1.6×10^{-2} , but not lower.

In central collisions, the number of neutral pions observed above $p_T = 5$ GeV/c is a factor of about 4 less than expected when scaling up the measured pions from the p-p data by the number of binary nucleon-nucleon collisions. Theoretical descriptions of the data need to include some energy loss of the partons in the medium in order to reproduce the observed yields.

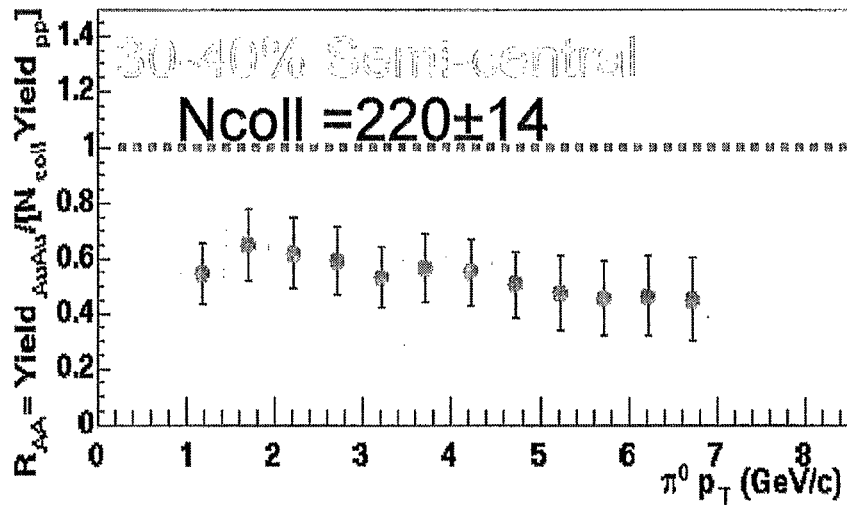
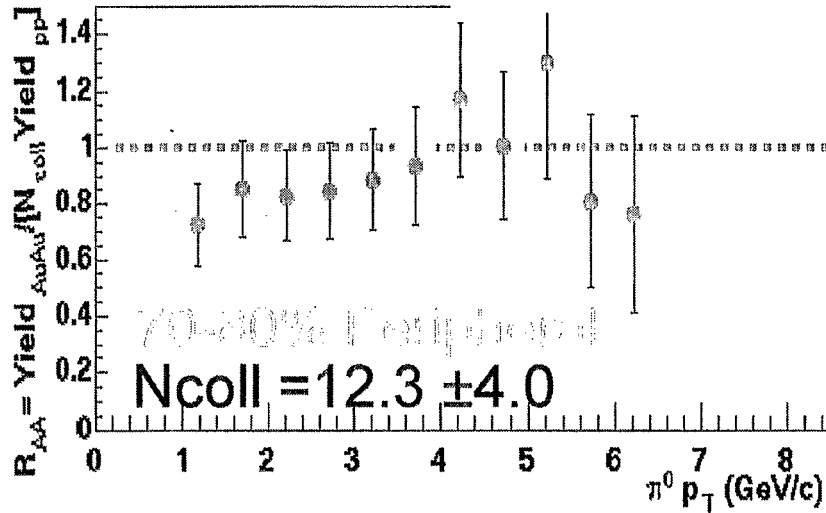
Measurement of the charged particle spectra as a function of AuAu collision centrality shows a gradual increase in the suppression, rather than a sudden onset at some threshold impact parameter. The apparent suppression of charged particles is smaller, as they include baryons and anti-baryons, which do not appear to be suppressed. The charged particle yields at high p_T scale neither with the number of participant nucleons, nor with the number of binary nucleon-nucleon collisions. For mid-central and central collisions, the yields come closer to participant scaling, but the deviations are at the 3σ level. Possible explanations of this include surface emission of the hadrons, in-medium re-interactions, or perhaps a purely accidental near-scaling.

PHENIX measures particle correlations to look for a jet signature. We select events with a leading photon with $p_T > 2.5$ GeV/c, and look at correlations of associated charged particles, and we also look at charged-charged correlations. These studies provide an unambiguous signal of jets in Au + Au collisions. We expect that v_2 at high p_T also sensitive to jets, and have devised several methods to disentangle collective flow effects from correlations due to jets. There is, however, a possible bias in the requirement of a leading particle. Systematic studies are underway to understand this.

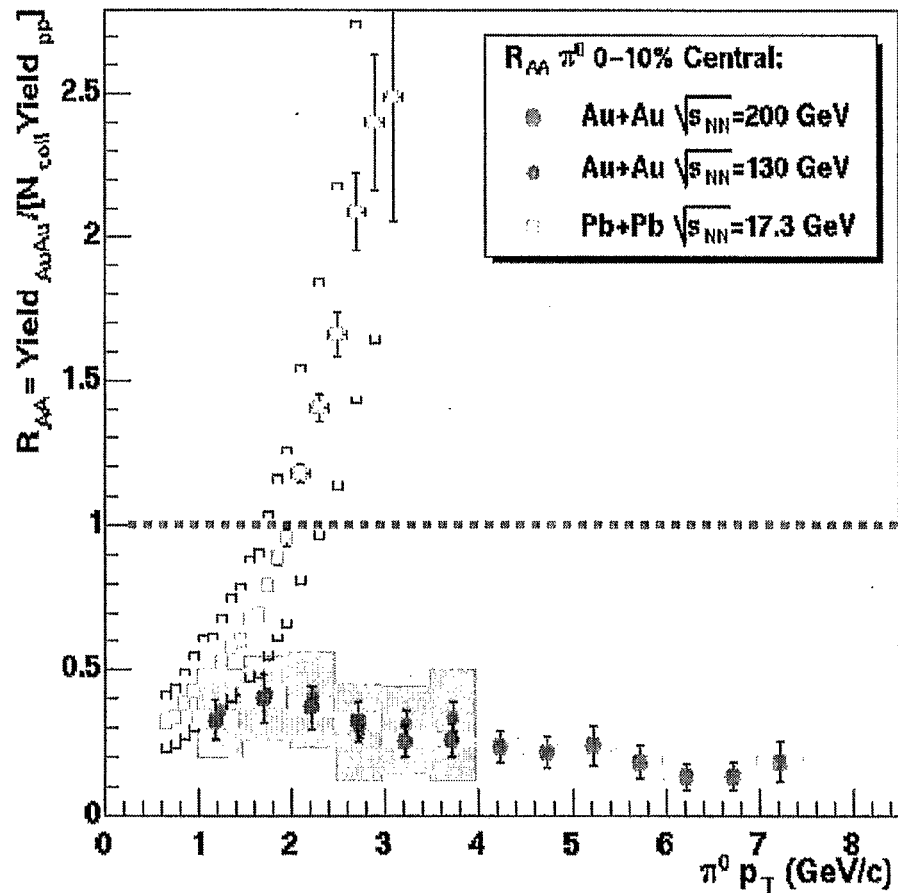
The hadronic composition at high p_T is somewhat mysterious, compared to the known jet fragmentation functions, and the composition changes with centrality. The proton and antiproton yields equal the pion yields above 2 GeV/c p_T . The p/π^+ and $pbar/\pi^-$ ratios in peripheral collisions are lower; the peripheral collision baryon/meson ratios agree with those observed in p+p collisions at the ISR, and more closely approach the hadronic composition of gluon jets at LEP. We study the ratio of neutral pions to charged hadrons as a function of p_T in central collisions, and find that the large baryon contribution continues out to 9 GeV/c p_T .

π^0 yield in AuAu vs. p-p collisions

PHENIX Preliminary



$$\frac{\text{Yield}_{\text{central}} / \langle N_{\text{binary}} \rangle_{\text{central}}}{\text{Yield}_{\text{pp}}}$$

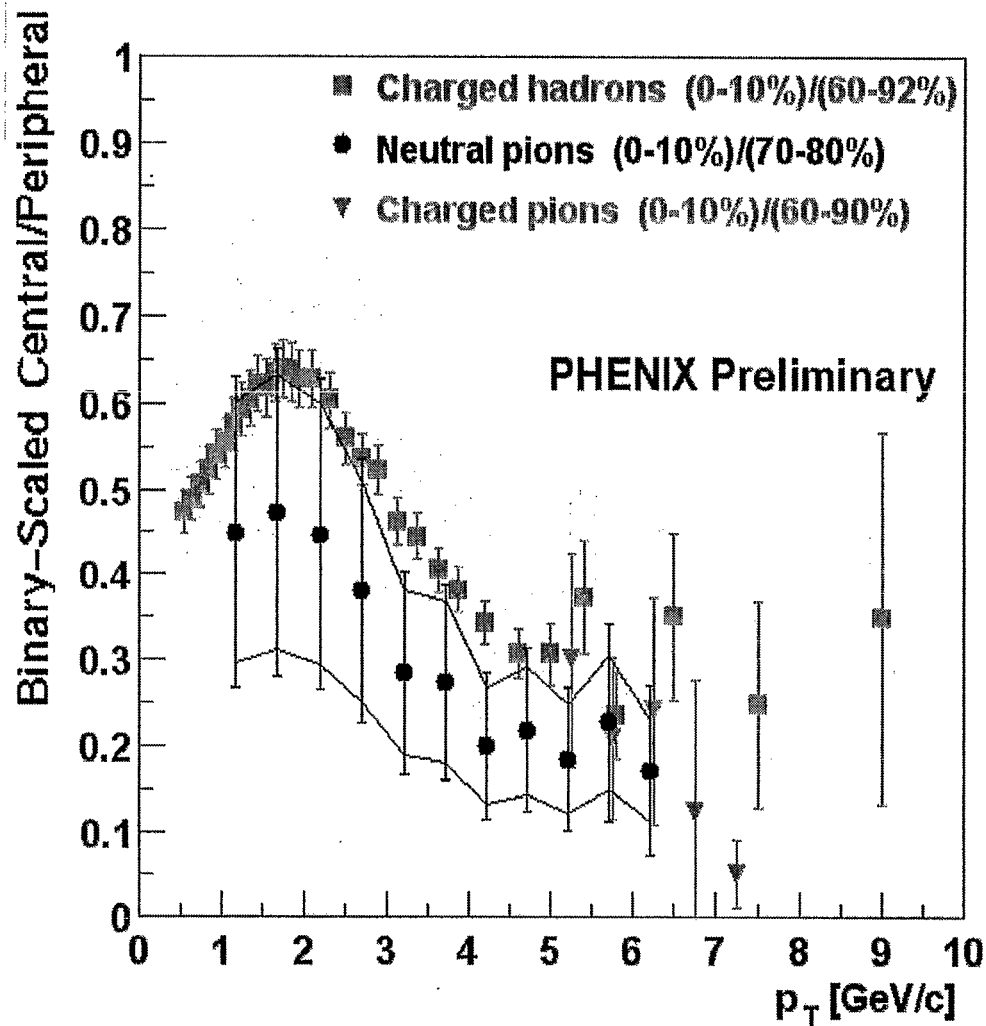


Comparing different channels

$$\text{Yield}_{\text{central}} / \langle N_{\text{binary}} \rangle_{\text{central}}$$

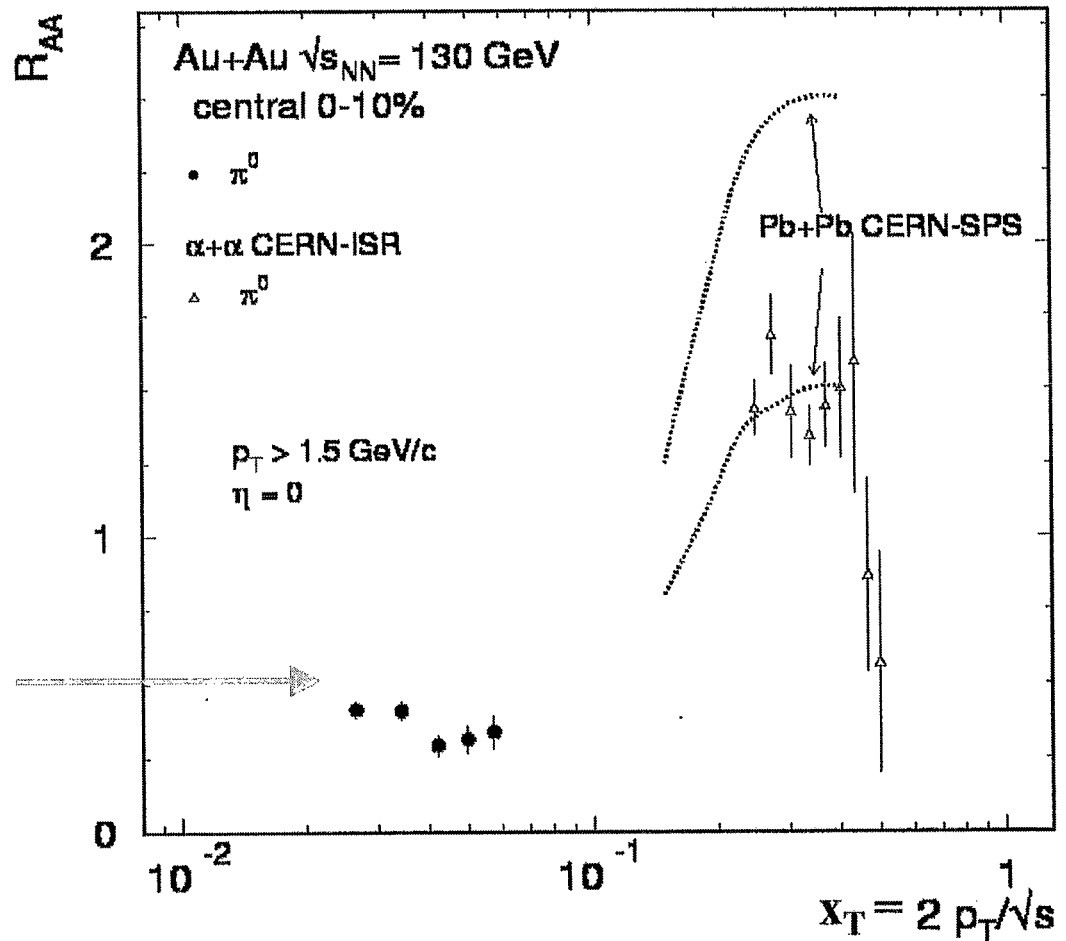
$$\text{Yield}_{\text{peripheral}} / \langle N_{\text{binary}} \rangle_{\text{peripheral}}$$

- **Suppression to 9 GeV/c!**
- **Factor consistent for 3 independent measurements**
- **Difference in charged hadron ratio and neutral pion ratio accounted for by particle composition**



x of struck parton

- if $p_{T(\text{had})} / p_{T(\text{jet})} \sim 1$ then $x_T \sim x(\text{parton})$ at $y=0$
- SPS and RHIC at different x!

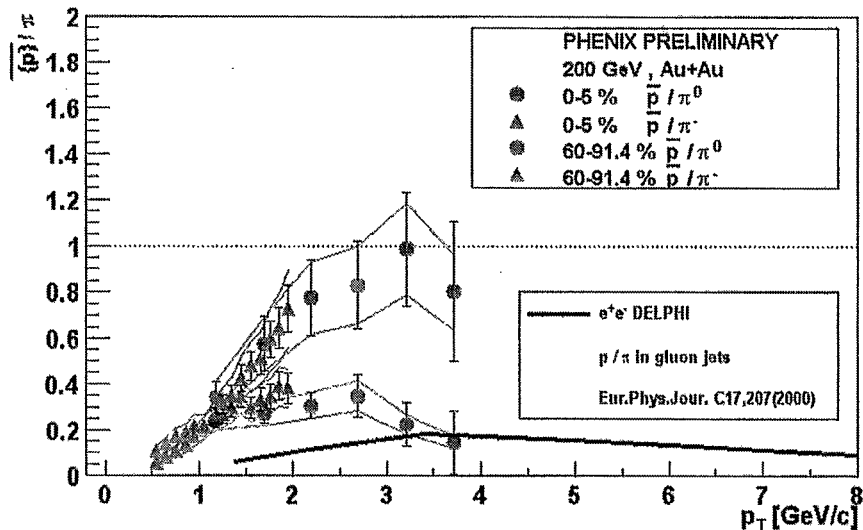
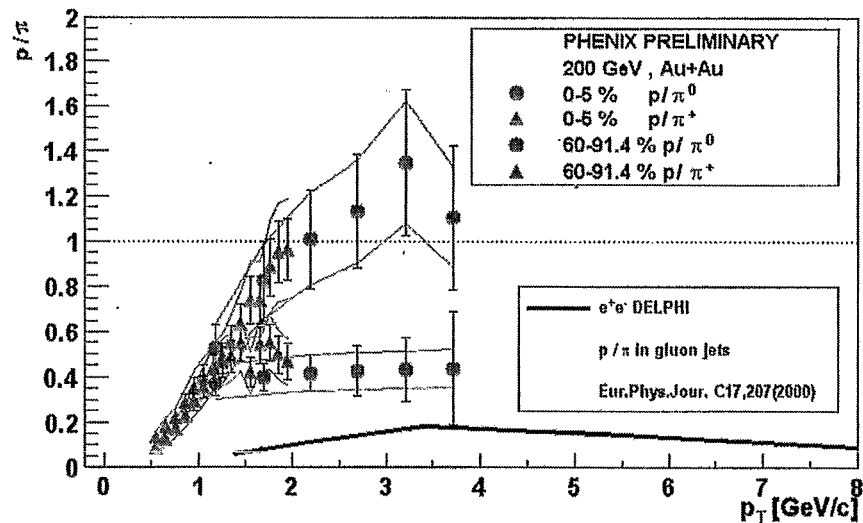


RHIC:
 $\sim 1.6 \times 10^{-2}$ at 200 GeV
 still not very small...

Centrality dependence of p/pi

• Ratios reach ~ 1 for central collisions

• Peripheral collisions lower, but still above gluon jet ratios at high p_T

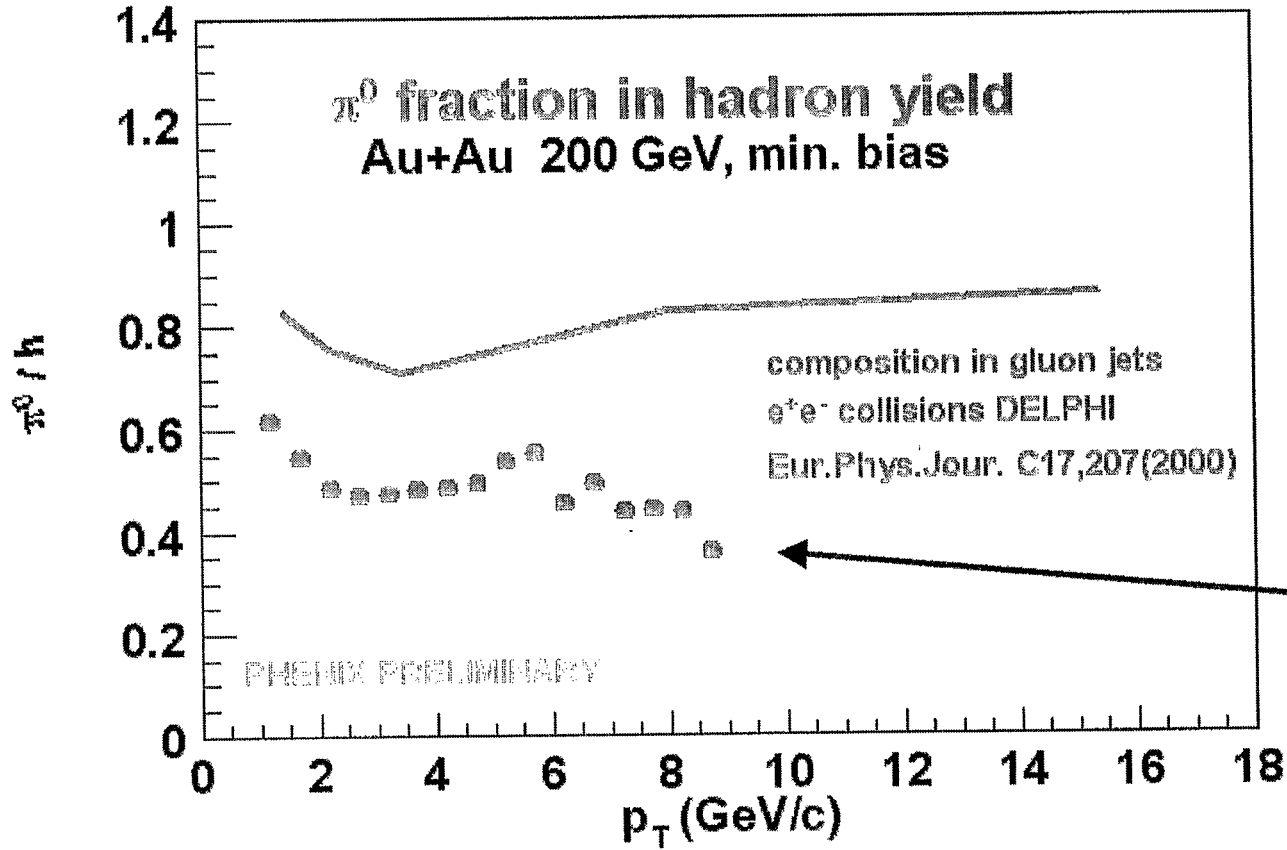


• Maybe not so surprising

- 1) "peripheral" means 60-91.4% of σ_{total}
- 2) $p/\pi = 0.3$ at ISR

Do junctions agree?

Use pi/h to look at higher p_T



What's this?
protons??

v_2 from Classical Yang-Mills

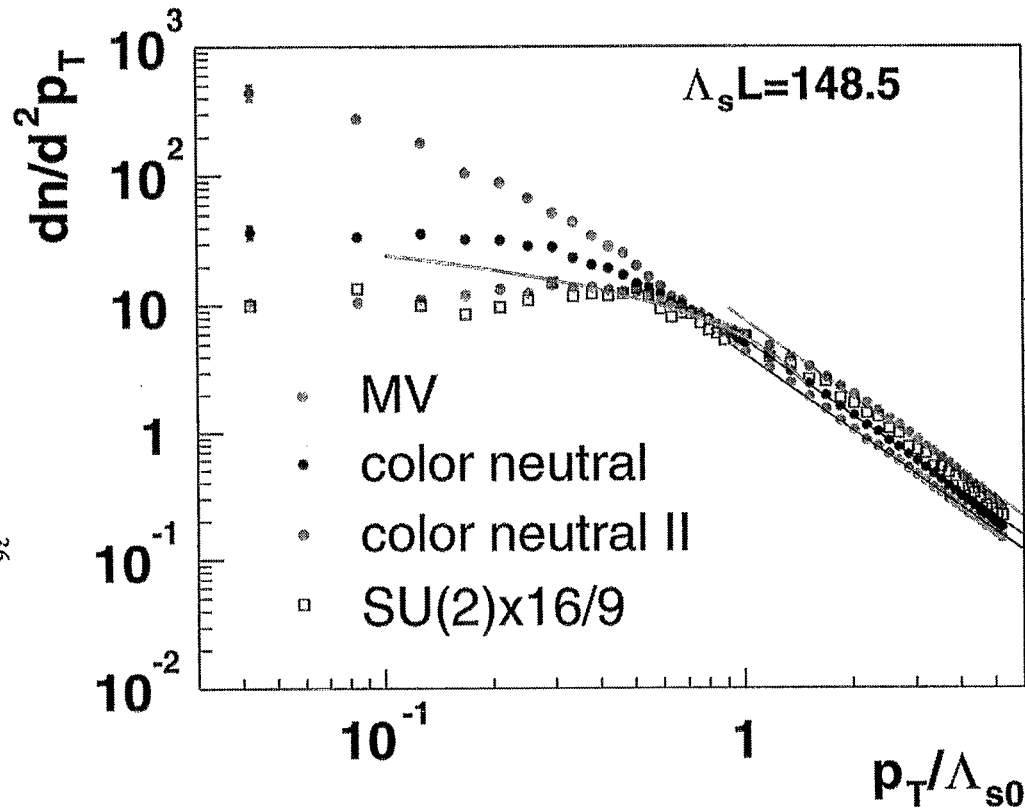
Alex Krasnitz¹, Yasushi Nara², Raju Venugopalan^{2,3}

1. CENTRA, Universidade do Algarve, Campus de Gambelas, P-8000 Faro, Portugal
2. RIKEN BNL Research Center, Brookhaven National Laboratory, Upton, N.Y. 11973, U.S.A.
3. Physics Department, Brookhaven National Laboratory, Upton, N.Y. 11973, U.S.A.

We extend previous work on high energy nuclear collisions in the Color Glass Condensate model to study collisions of finite ultrarelativistic nuclei. The changes implemented include a) open boundary conditions to treat the expansion of gluon fields into the vacuum, b) imposition of color neutrality at the nucleon level and c) realistic nuclear matter distributions. The saturation scale characterizing the fields of color charge is explicitly position dependent, $\Lambda_s = \Lambda_s(x_t)$. We compute gluon distributions both before and after the collisions. The gluon distribution in the nuclear wavefunction before the collision is significantly suppressed below the saturation scale when compared to the simple McLerran-Venugopalan model prediction, while the behavior at large momentum $k_t \gg \Lambda_s$ remains unchanged. We study the centrality dependence of produced gluons and compare it to the centrality dependence of charged hadrons exhibited by the RHIC data. We find that the classical Yang-Mills results for $k_t < \Lambda_s$ can be simply matched to a perturbative QCD computation for $k_t > \Lambda_s$. The resulting energy per particle is significantly lower than our previous estimates. Our results can be used as initial conditions for quantitative studies of the further evolution and possible equilibration the hot and dense gluonic matter produced in heavy ion collisions.

We compute the elliptic flow generated by classical gluon fields in a high energy nuclear collision with the extended model. A significant elliptic flow is generated only over time scales on the order of the system size R . The flow is dominated by soft modes $p_T \sim \Lambda_s/4$ which linearize at very late times $\tau \sim R \gg 1/\Lambda_s$. Field description should be invalid due to the strong expansion of the system. Therefore, at late times, our simulations do not include the interactions between soft modes and hard modes. This is the main reason why the flow is dominated by only soft modes. However, we have shown that Boltzmann solution in which only collision term among particle is included, is not able to reproduce elliptic flow. In order to treat correctly the interaction involving the hard modes, we need to solve *Boltzmann-Vlasov* type equation for the hard modes and YM equation for the soft modes.

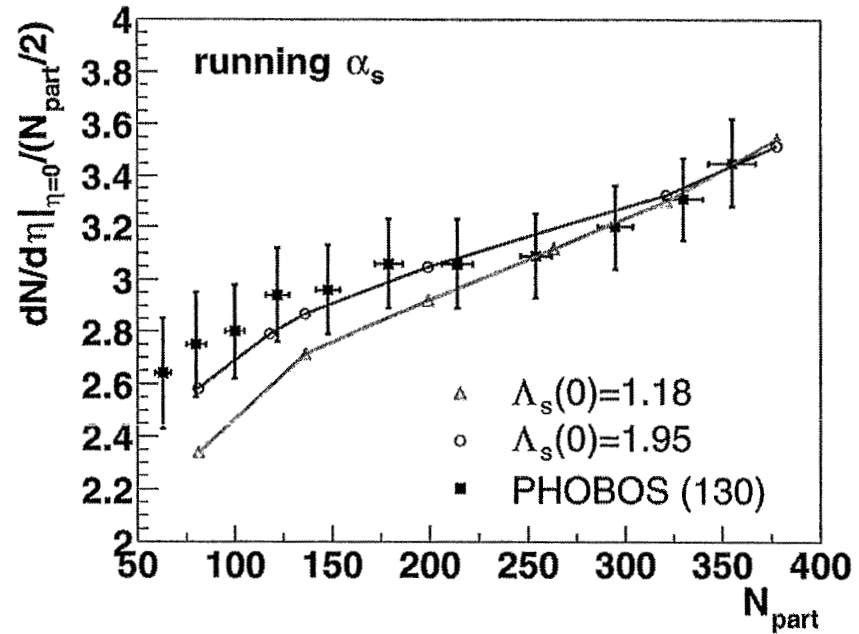
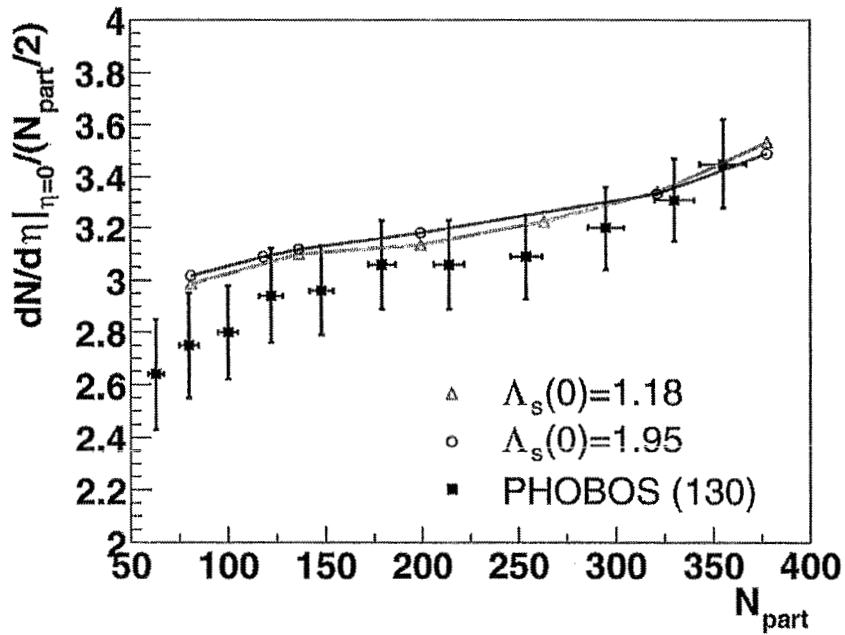
Gluon distribution before collision



- Suppression of gluon fields at $\Lambda_{s0} < p_T$ for color neutral.



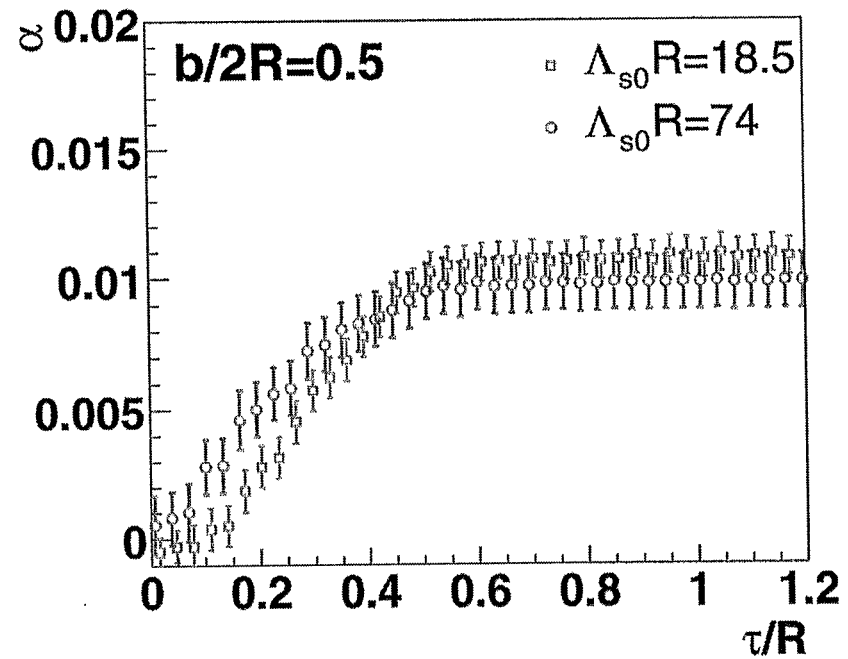
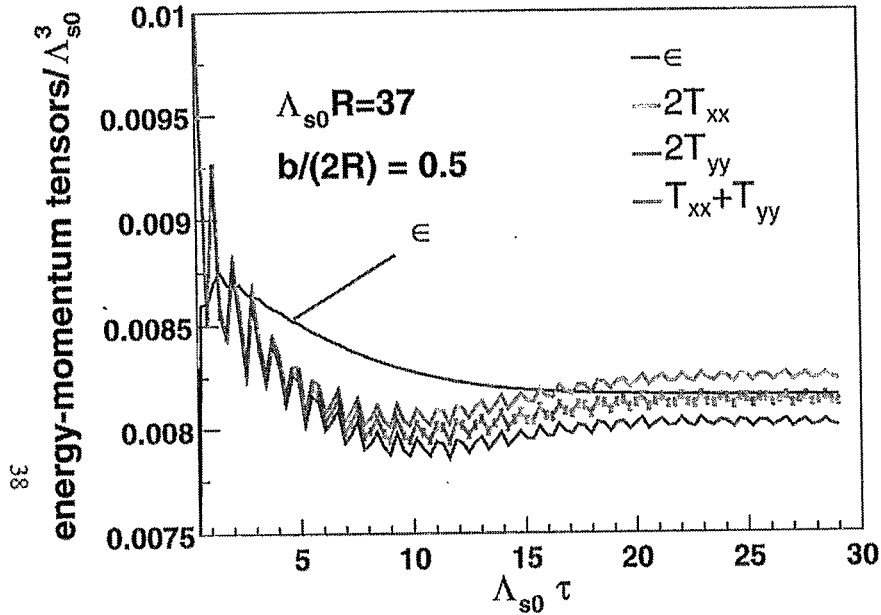
Centrality dependence of the gluon multiplicities



- Universal curve when coupling constant is not running; no color charge dependence.



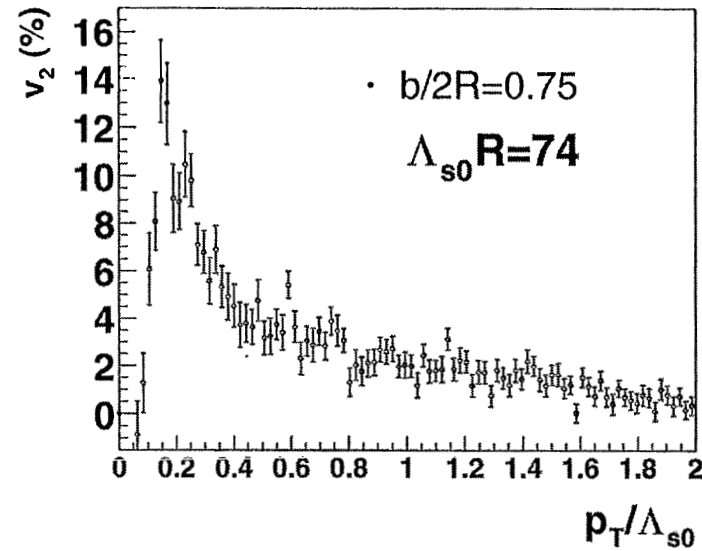
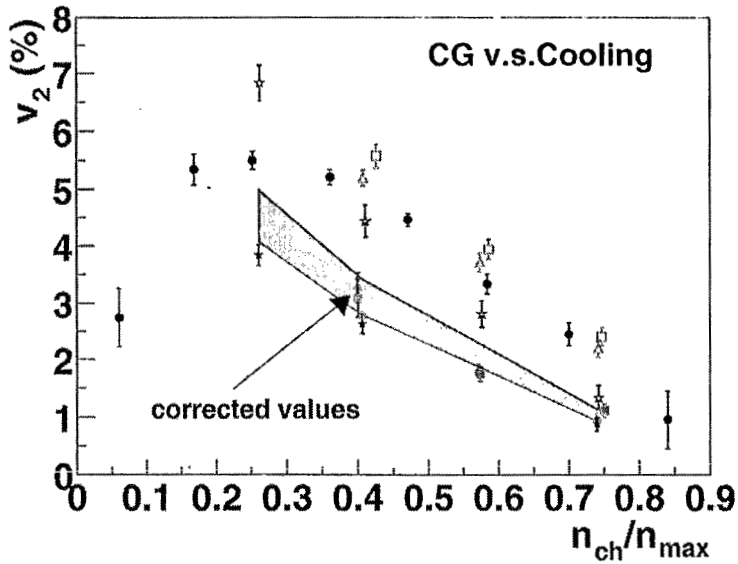
Time evolution of energy momentum tensor



- $\alpha = \langle T^{xx} - T^{yy} \rangle / \langle T^{xx} + T^{yy} \rangle$.
- Strongly interacting system at early times
- Free streaming in the transverse plane at later times $e = T^{xx} + T^{yy}$.



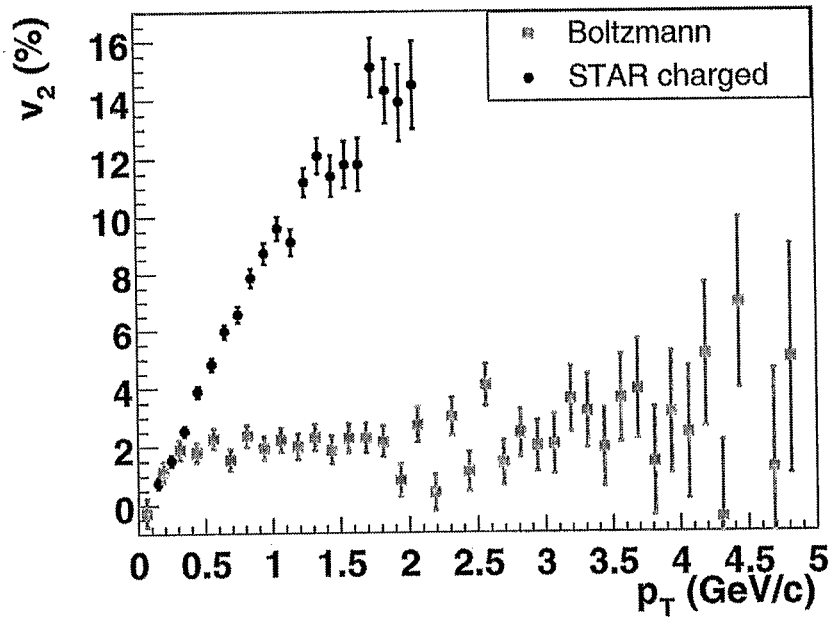
Centrality and Transverse momentum dependence of v_2



- Weak dependence on $\Lambda_s R$.
- Dominant component of the v_2 is soft modes of the gluon field.
- Totally different shape compared to experimental data.
- Need time evolution of gluons according to the Boltzmann type calculations using YM as a initial condition?



Switch to Boltzmann



- Solve classical YM up to $\tau_{sw} \sim 1/Q_s$.
- Convert field to particle at τ_{sw} .
- Solve Boltzmann equation:

$$p^\mu \partial_\mu f(x, p) = C$$

using test particle method.

- $m_D = 0.4$ GeV, $\sigma_{gg} = 11$ mb
- only elastic scattering included.
- initial transverse spatial distribution
→ number of participants



Elliptic Flow from Minijet Production in Heavy Ion Collisions

Kirill Tuchin

Institute for Nuclear Theory, University of Washington

in collaboration with Yuri Kovchegov

We propose a model of non-flow particle correlations in the initial stages of heavy ion collisions. The model is based on particle production mechanism in the high energy regime when gluon and quark distribution functions of the colliding nuclei reach saturation. As was suggested by McLerran and Venugopalan the dominant gluon production mechanism in the early stages of the collision is given by the classical field of the nuclei. At the high energies achieved by RHIC experiments the classical field alone can not account for particle production; thus quantum corrections become important. The essence of our model is the following: to estimate the non-flow contribution to $v_2(p_T)$ one has to calculate the single and double inclusive gluon production cross sections first in the framework of the simple McLerran-Venugopalan model and then include the nonlinear evolution effects in them. Two produced gluons in the double inclusive cross section are of course azimuthally correlated with each other. This correlation can contribute to v_2 after being averaged over all particle pairs, which is proportional to the total particle multiplicity squared. The latter was related to the single inclusive gluon production cross section. Two comments are in order here. First of all double gluon production cross section of course can not be given by the classical field and is therefore not a classical quantity. Calculating it thus corresponds to the first (order α_s) correction to McLerran-Venugopalan model. Secondly when the momenta of the produced two gluons are not extremely large the correlations are not only back-to-back since in the saturation regime it is not required anymore by transverse momentum conservation as some of the momentum can be carried away by other soft particles. So, in addition to back-to-back ($\Delta\phi = \pi$) there are also collinear ($\Delta\phi = 0$) correlations.

Since the exact double inclusive gluon production cross section is not known we constructed a simple model of single- and double- gluon production in the spirit of k_T -factorization approach. The model successfully describes the saturation of $v_2(p_T)$ at high p_T as well as centrality dependence of $v_2(B)$ at $\sqrt{s} = 130$ GeV. We also show that two-particle correlation functions in our model are consistent with the data reported by PHENIX if NLO corrections are taken into account.

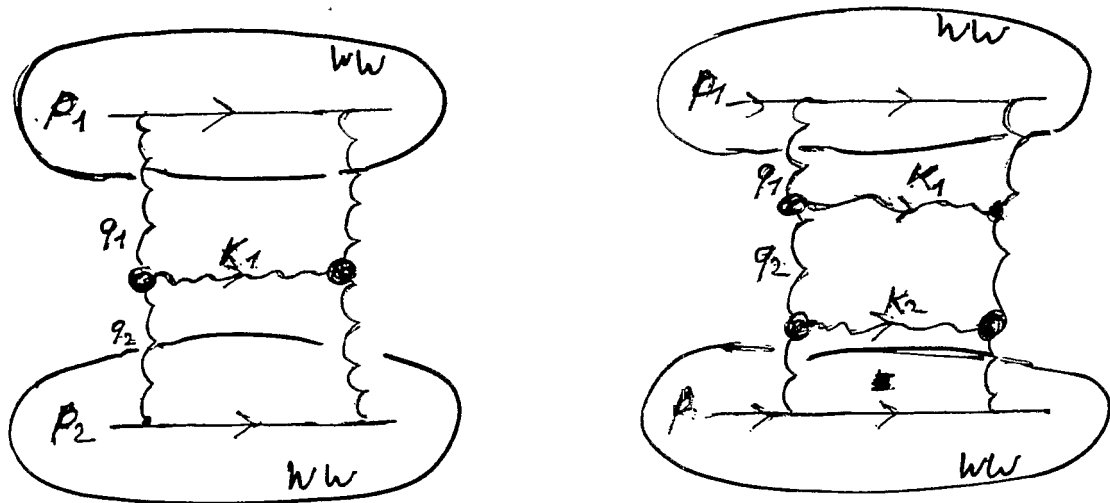
We demonstrate that even in the case of only non-flow correlations the distribution of particles with respect to experimentally determined reaction plane averaged over many events is proportional to $\cos 2(\phi - \Psi_R)$ in agreement with STAR data. (ϕ and Ψ_R are azimuthal angles of the particle and reaction plane correspondingly.) This distribution is due to the fact that the reaction plane is also determined from the second harmonic of the multiplicity distribution. Therefore the $\cos 2\phi$ shape of the distribution with respect to reaction plane does not reflect any physics. At the same time the amplitude of the distribution is given by physical correlations, that is by $2v_2$.

Our model

We assume that:

- 1) factorization holds
- 2) the nuclear gluonic fields are classical
- 3) quantum evolution is included by substitution

$$Q_{\text{classical}}^2 \rightarrow Q_s^2(y)$$



4) $y_1 \ll y_2$ or $y_2 \ll y_1$

5) nuclei are cylindrical

Mini-jet production part of the amplitude

Single particle distribution:

$$\frac{dN}{d^2k_1 dy_1} = \frac{2ds}{C_F S_\perp} \frac{1}{k_1^2} \int d^2q_1 \frac{dx_{GA}}{dq_1^2} \frac{dx_{GA}}{d(k_1 - q_1)^2}$$

$$\frac{dN_{corr}}{d^2k_1 dy_1 d^2k_2 dy_2} = \frac{N_c ds^2}{\pi^2 C_F S_\perp} \frac{1}{k_1^2 k_2^2} \int d^2q_1 \frac{dx_{GA}}{dq_1^2} \frac{dx_{GA}}{d(k_1 + k_2 - q_1)^2}$$

where $x_{GA} = A \frac{s C_F}{\pi} \ln \frac{q^2}{\mu^2}$

Inclusion of WW fields of nuclei

$$\begin{aligned} \frac{dx_{GA}(x, q^2)}{dq^2} &= \frac{2}{(2\bar{u})^2} \int d^2z e^{-i\bar{z} \cdot \underline{q}} \int d^2b \text{Tr} [A^{WW}(\underline{0}) A^{WW}(\underline{z})] \\ &= \frac{2}{\pi \cdot (2\bar{u})^2} \int d^2z e^{-i\bar{z} \cdot \underline{q}} \cdot \frac{S_\perp C_F}{2s \bar{z}^2} (1 - e^{-\frac{1}{2}\bar{z}^2 Q_s^2}) \end{aligned}$$

$$Q_s^2 = \frac{4\bar{u}^2 ds N_c}{N_c^2 - 1} f(x, 1/\bar{z}^2) T(\underline{b}) \rightarrow \text{the saturation scale at given (not too high) energy}$$

One and two-particle distributions

$$\frac{dN}{d^2K, dy_1} = \frac{C_F S_1}{ds K_1^2} \frac{4 K_1}{\pi^3} \int_0^\infty \frac{dz}{z^3} J_0(K, z) \left(1 - e^{-\frac{z^2 Q_s^2}{4}}\right)^2$$

$$\frac{dN_{\text{corr}}}{d^2K, dy_1, d^2K_2, dy_2} = \frac{N_c C_F S_1}{K_1^2 K_2^2} \frac{K_2}{\pi^6} \int d^2z \frac{1}{z^4} e^{-iz \cdot (\underline{K}_1 + \underline{K}_2)} \left(1 - e^{-\frac{z^2 Q_s^2}{4}}\right)^2$$

K_1, K_2 give correct normalization

* K_1 is found by comparing $\frac{dN}{dy}$ of our model to the total multiplicity at RHIC

* Fixing K_2 : at $\underline{K}_1 \sim \underline{K}_2 \sim \underline{p_T} \gg Q_s$

$$\frac{dN_{\text{corr}}}{d^2p_T^2 dy_1 dy_2} = K_2 \frac{9\pi ds^2}{4 p_T^4} [2G(x, p_T)]^2$$

$$\Rightarrow K_2 = 2$$

The final result:

$$v_2(p_T, \underline{B}) = \alpha_s \left(\frac{\pi N_c K_2}{2 \ln 2 C_F S_\perp Q_s^2 K_1^2} \right)^{1/2} \times$$
$$\times \frac{\int_0^\infty \frac{dz}{z^3} J_2(p_T z) (1 - e^{-z^2 Q_s^2/4})^2}{\int_0^\infty \frac{dz}{z^3} J_0(p_T z) (1 - e^{-z^2 Q_s^2/4})^2}$$

Note: $S_\perp Q_s^2 \sim N_{\text{part}} \Rightarrow v_2 \sim \frac{1}{\sqrt{N_p}}$

in the most central events $N_p \sim 350 \Rightarrow$

$v_2 \sim 5\%$ - this is order of magnitude estimate!

Conclusions

1. We calculated the contribution of pairwise correlations in minijet production to elliptic flow variable v_2 .

We observed a good agreement with RHIC data for:

- p_T dependence
- centrality dependence

2. We took into account NLO corrections and calculated the correlation function as defined at PHENIX.

3. We argued that the particle distribution with respect to reaction plane is independent of the nature of correlations. It always gives $\cos 2\phi$ shape.

4. Uncertainties of our model come from the following assumptions:
 - factorization
 - cylindrical shape of nucleus

Elliptic flow at high p_T

Kirill Filimonov

Lawrence Berkeley National Laboratory

for the STAR Collaboration

Elliptic Flow at High p_T

Kirill Filimonov, LBNL, for the STAR Collaboration

The monotonic rise of elliptic flow measured in Au+Au collisions at RHIC at transverse momenta $p_T < 2$ GeV/c is consistent with hydrodynamic behaviour of bulk matter developed early in the collision. The measurements of azimuthal anisotropy v_2 of charged particles with $p_T=3-6$ GeV/c reveal a saturation pattern of v_2 with values that decrease systematically with increasing centrality. $v_2(p_T)$ -dependence measured in collisions at 130 GeV and 200 GeV is compared. Larger values of v_2 are found at low ($p_T < 1-2$ GeV/c) transverse momenta at higher energy. In the saturation region, however, the azimuthal anisotropies are very similar at both energies, indicating, perhaps, the geometric origin of the observed saturation. The large asymmetries measured in the transverse momentum range where hard processes are expected to contribute significantly, combined with the observation of the suppression of charged particle yields at high transverse momenta relative to the binary collision scaling, maybe consistent with dissipative dynamics with finite parton energy loss.

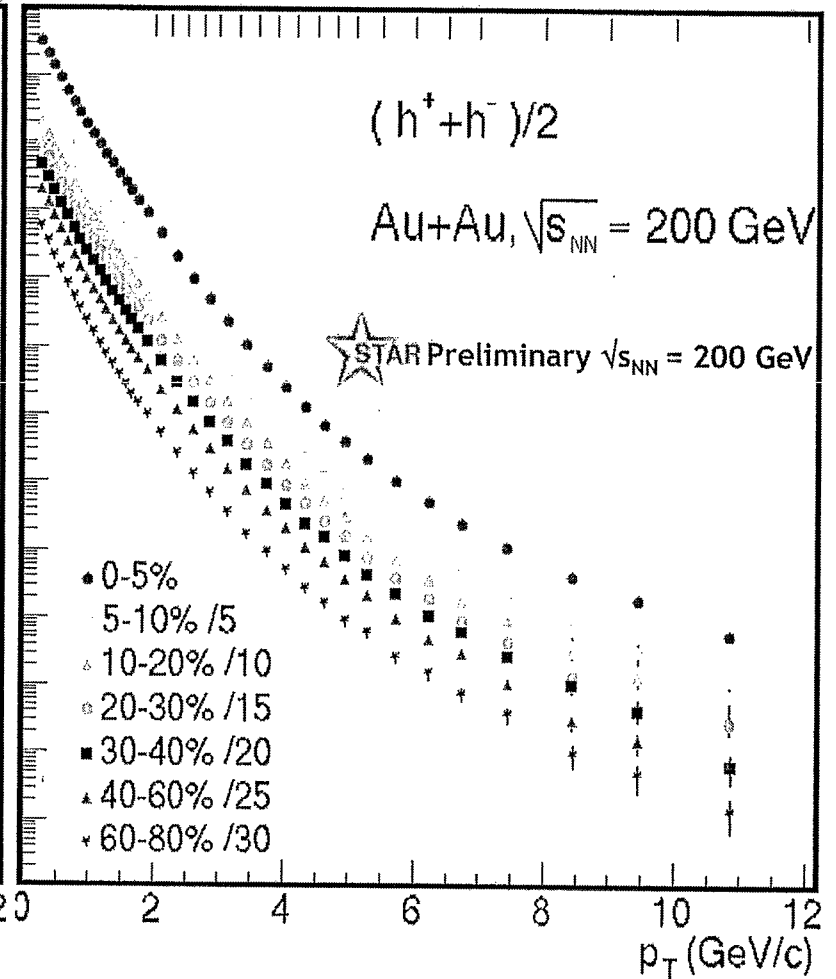
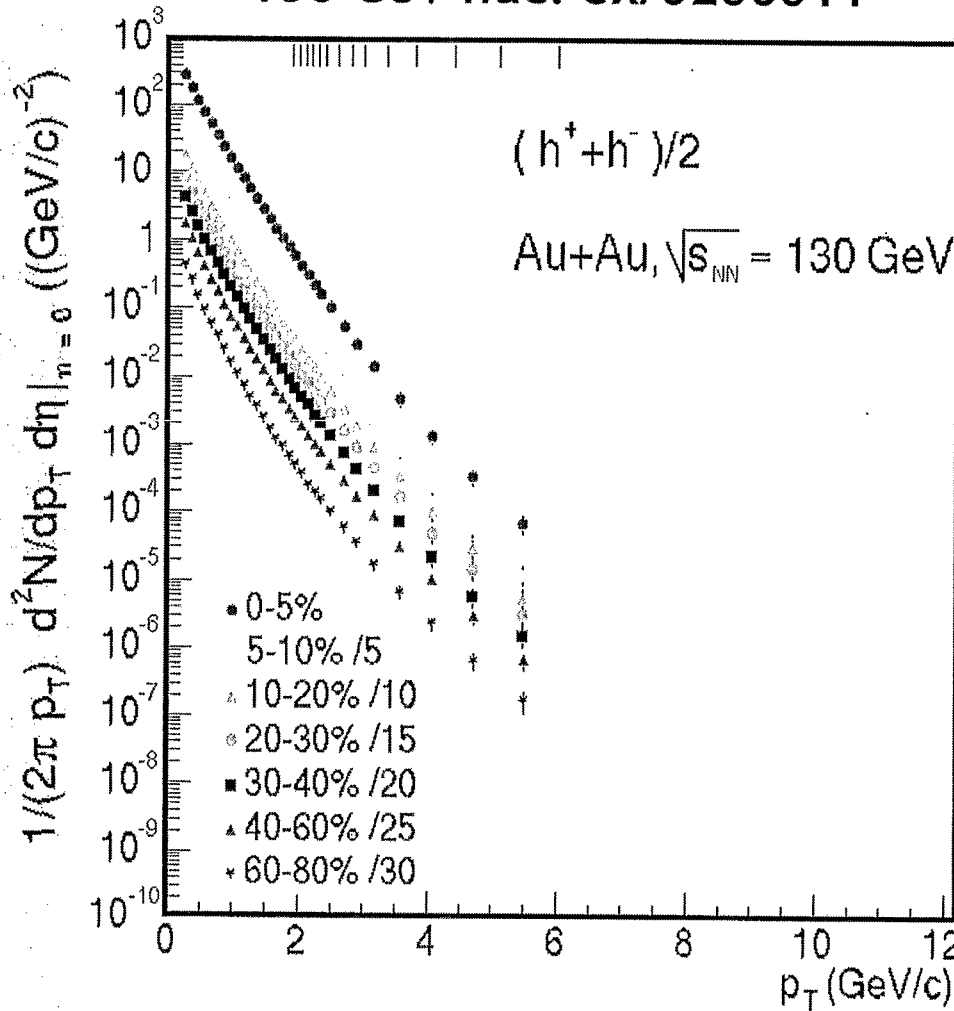
The p_T -dependence of elliptic flow for identified particles (pions, kaons, protons) is consistent with hydrodynamical calculations for transverse momenta $p_T < 1$ GeV/c. The elliptic flow of mesons (charged pions, kaons, and K_s^0) and baryons (protons, antiprotons, and Λ) is compared for p_T up to 3.5 GeV/c. At $p_T < 2$ GeV/c baryon flow is smaller than that of mesons, but for $p_T > 2$ GeV/c baryons exhibit larger values of v_2 than mesons.

Charged Hadron p_T Spectra

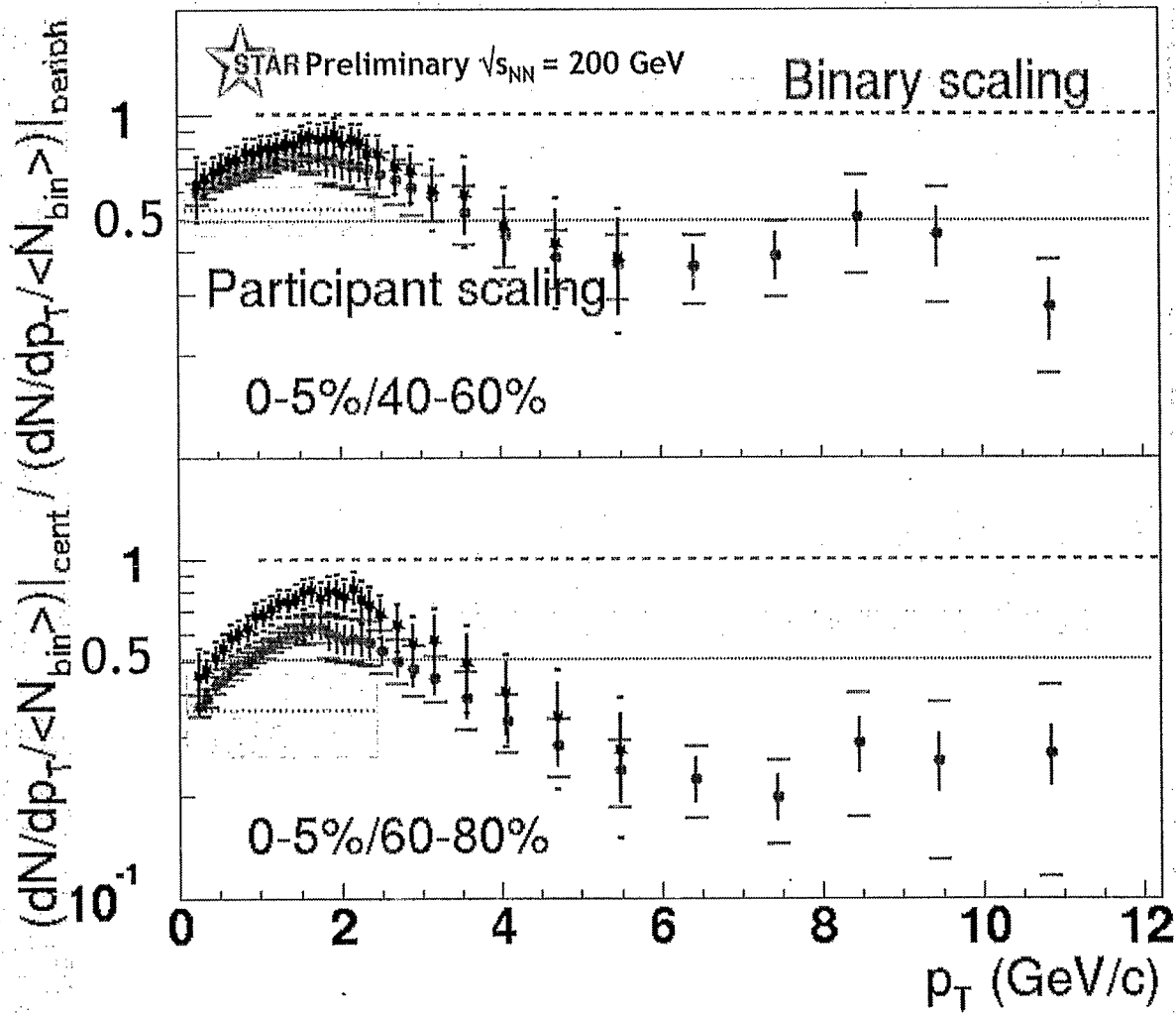
130 GeV nucl-ex/0206011



Preliminary $\sqrt{s_{NN}} = 200$ GeV



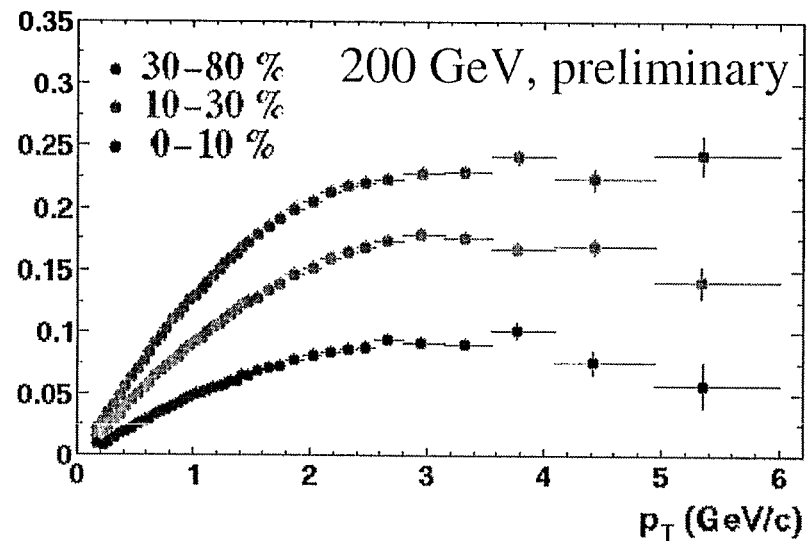
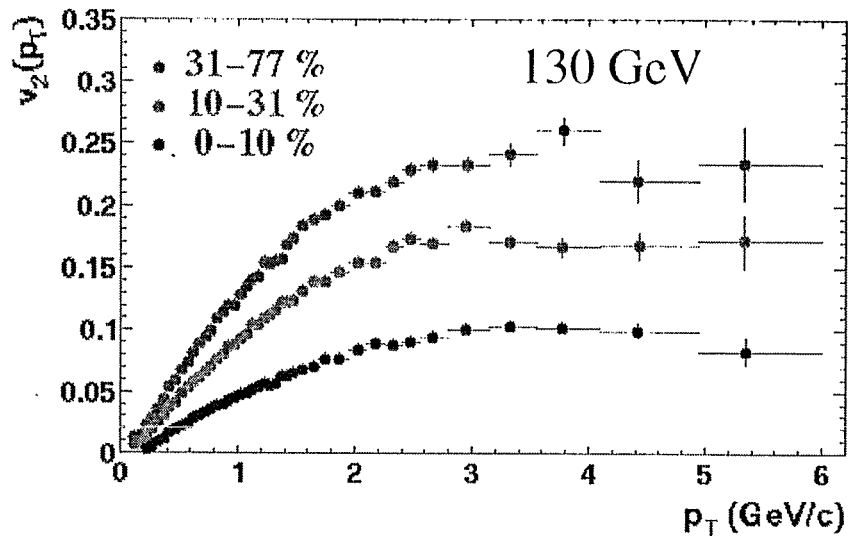
Central/Peripheral Comparison



At 130 GeV, the suppression increases up to $p_T = 6$ GeV/c. With higher p_T data from 200 GeV, we see that the suppression has saturated at $p_T \sim 6$ GeV/c

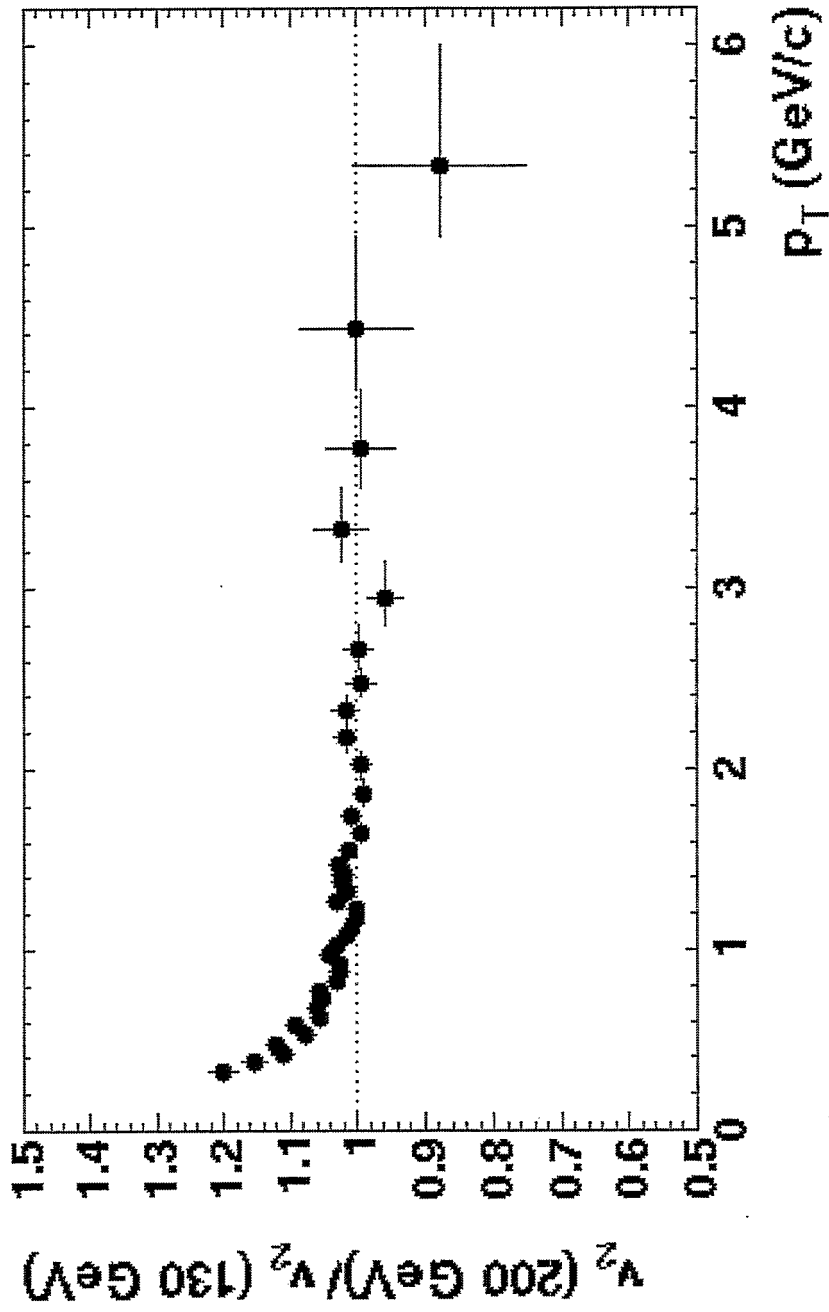
- ★ 130 GeV
- 200 GeV

Centrality dependence of $v_2(p_T)$



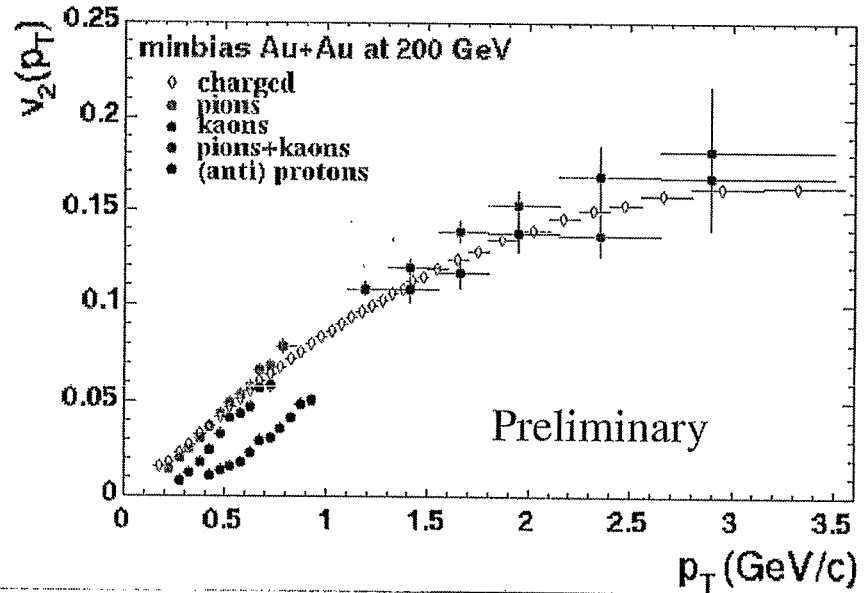
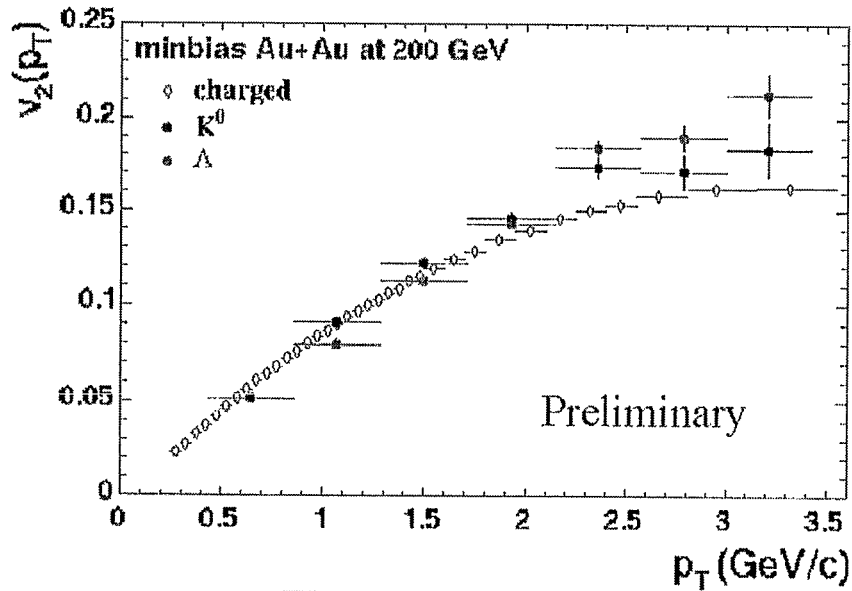
- v_2 saturates for $p_T > 3$ GeV/c for all centralities at both energies
- Indication of geometric origin?

Comparison of 130 GeV and 200 GeV



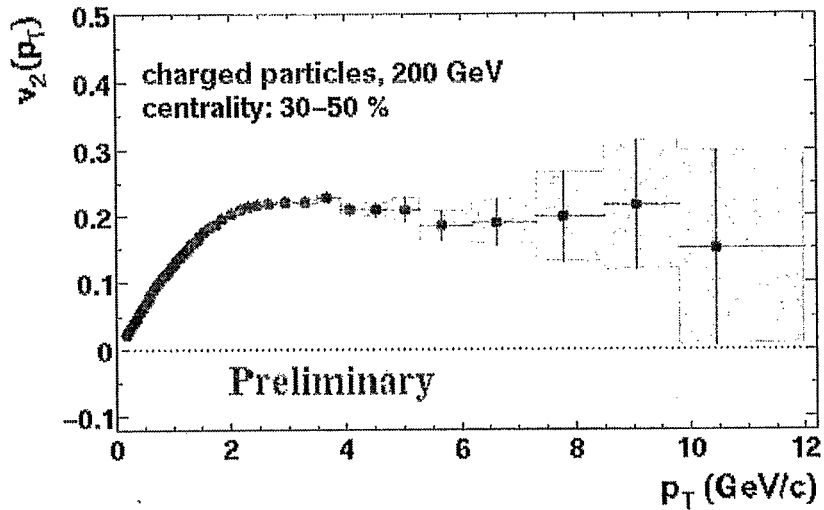
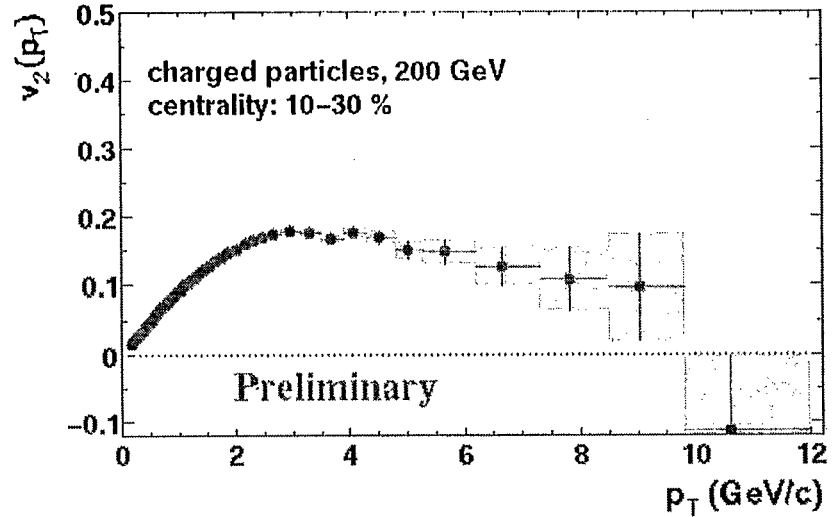
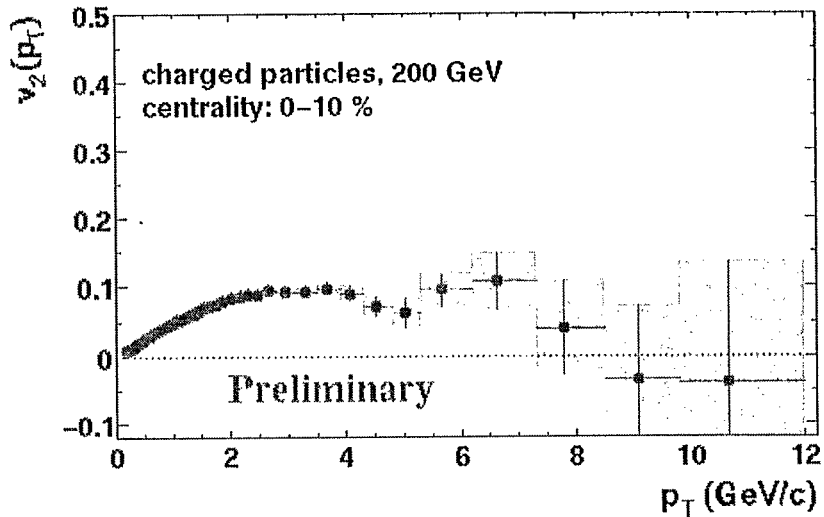
- Very similar, slight increase at 200 GeV at low p_T

v_2 of K^0 and Λ



- Similar to charged pions+kaons vs (anti)-protons

$v_2(p_T)$ up to 12 GeV/c



- Statistical errors only
- Finite v_2 up to 12 GeV/c in mid-peripheral bin

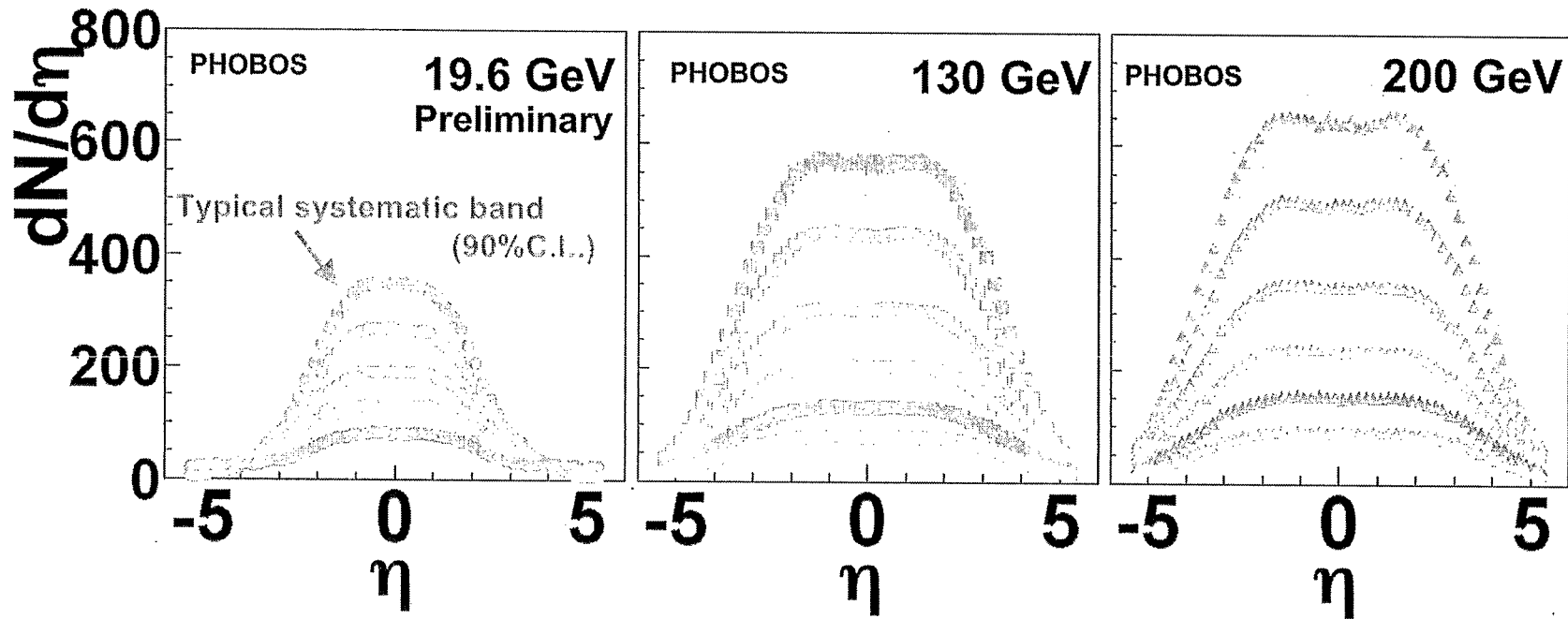
Scaling of Particle Production in High Energy Collisions

Gunther Roland
MIT

Scaling of Particle Production in High Energy Collisions

- Extensive data set
- Yields in Au+Au vs
 - Collision Energy
 - Collision Centrality
 - Pseudo-rapidity
 - Reaction plane
 - Transverse Momentum
- ‘Simple’ scaling behavior observed
 - $dN/d\eta$ vs N_{part}, \sqrt{s}
 - Limiting fragmentation
 - N_{ch} ‘Universality’
 - dN/dp_T vs N_{part}

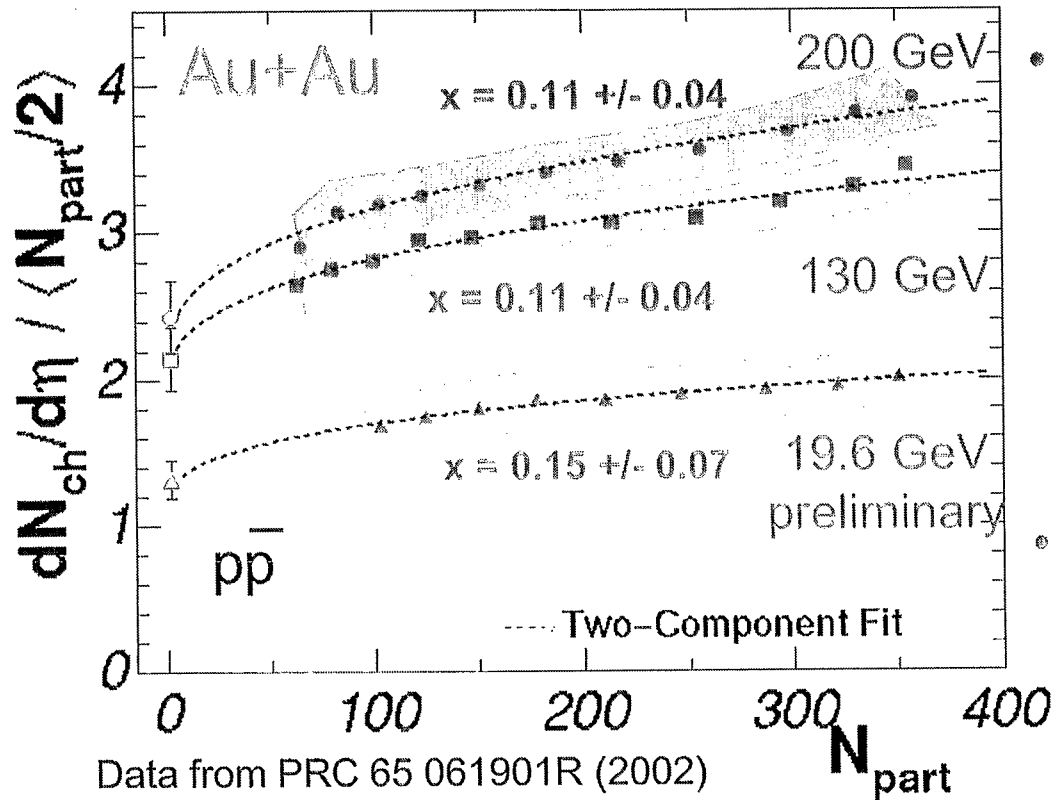
PHOBOS Au+Au Multiplicity Data



Au+Au collisions at $\sqrt{s}=19.6, 130, 200$ GeV

- $dN/d\eta$ for $|\eta| < 5.4$ over full azimuth
- Centrality from paddles (130/200) & N_{hits} (19.6)
- Top 50% of total cross section ($N_{\text{part}} \sim 65-360$)

Centrality Dependence at $|\eta| < 1$



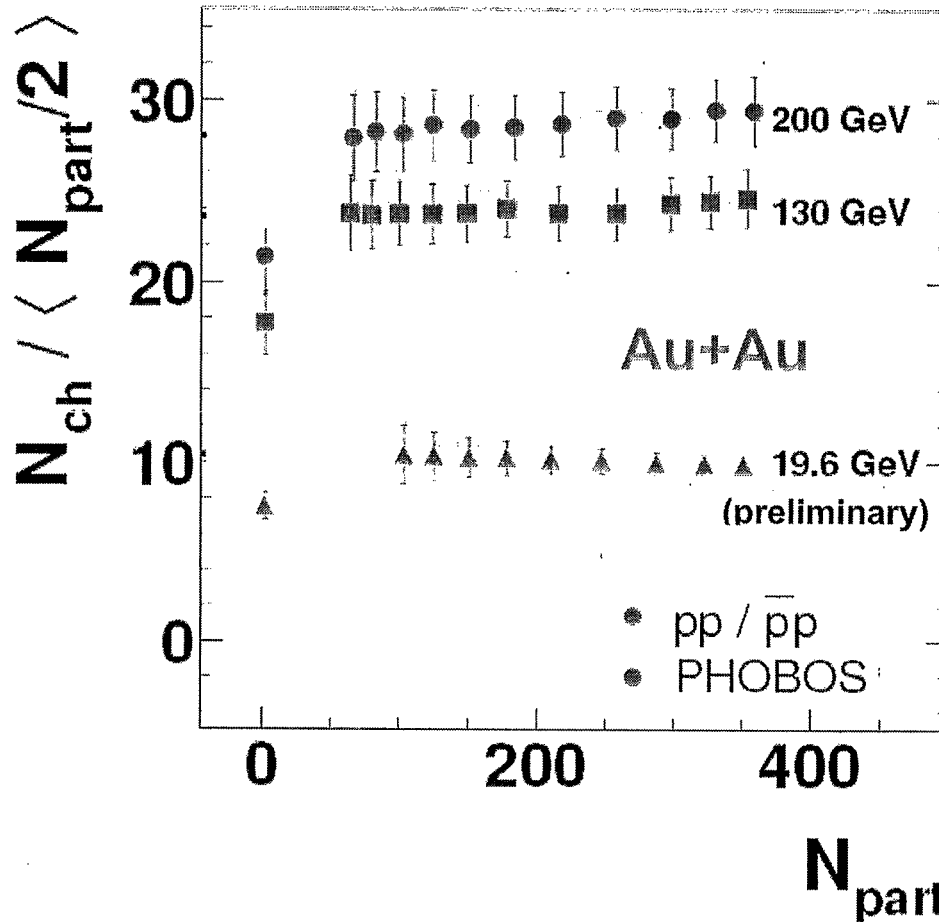
- 19.6, 130 and 200 GeV
 - Two-Component fit works at all energies
 - similar x (0.11-0.15) at 19.6, 130 and 200
 - it's not mini-jets
- Saturation?
 - hep/ph 0111315:
 - works at 22 GeV

Gunther Roland

$$\frac{dN}{d\eta} = (1-x)n_{pp}\frac{N_{part}}{2} + xn_{pp}N_{coll}$$

RHOBS

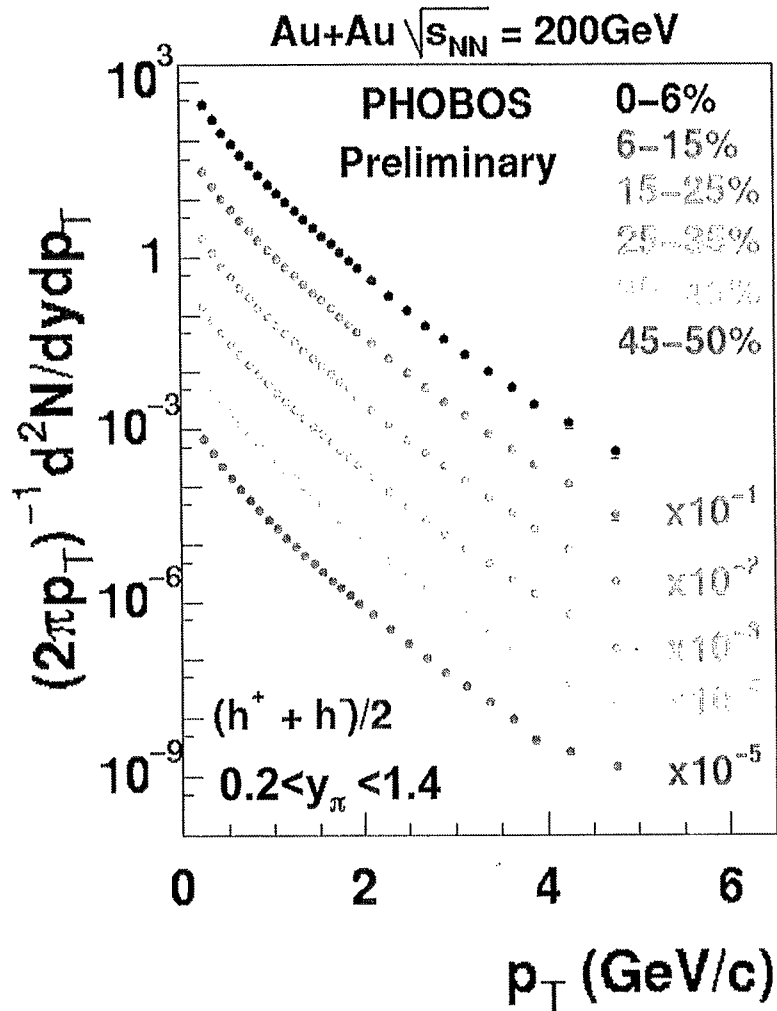
$\langle N_{ch} \rangle$ scaling vs N_{part}



Error bands due to high- η extrapolation

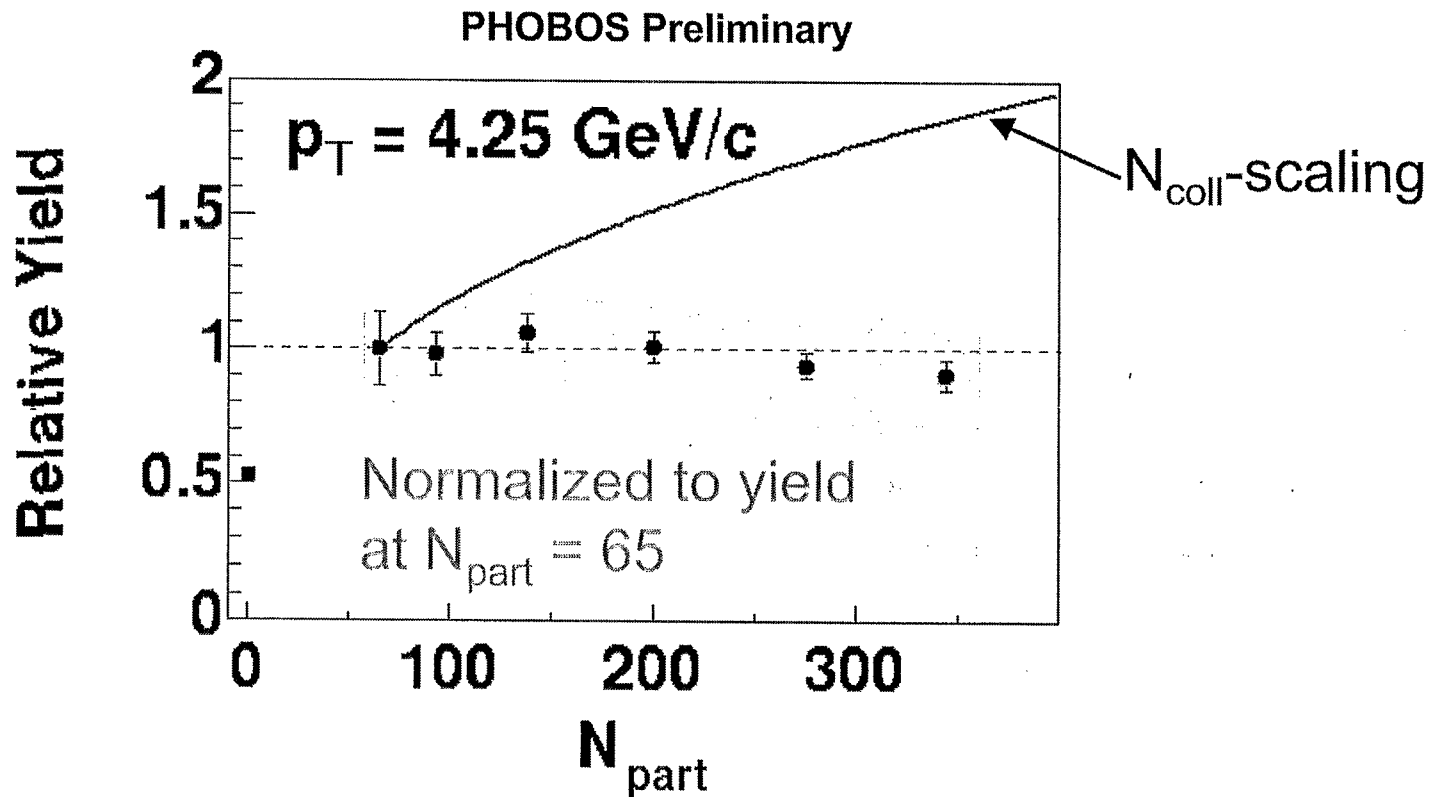
Total charged particle production $\sim N_{part}$

PHOBOS-Spectra @ 200GeV



- Spectra corrected for
 - Acceptance/Efficiency
 - Ghost Tracks
 - Momentum resolution
 - Variable bin width
 - Secondaries
- Acceptance $\sim y=1$
- Compare to 200GeV UA1 min. bias. $p\bar{p}$

N_{part} Scaling at high p_T



$\Rightarrow N_{\text{part}}$ scaling describes data at $p_T \sim 4.25 \text{ GeV/c}$

SATURATION and RHIC DATA

(KLN point of view)

E. Levin

Tel Aviv University / DESY

e-mail: leving@post.tau.ac.il

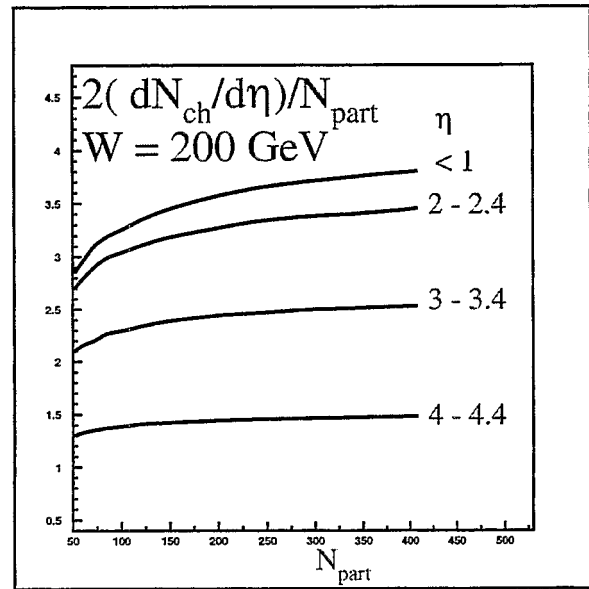
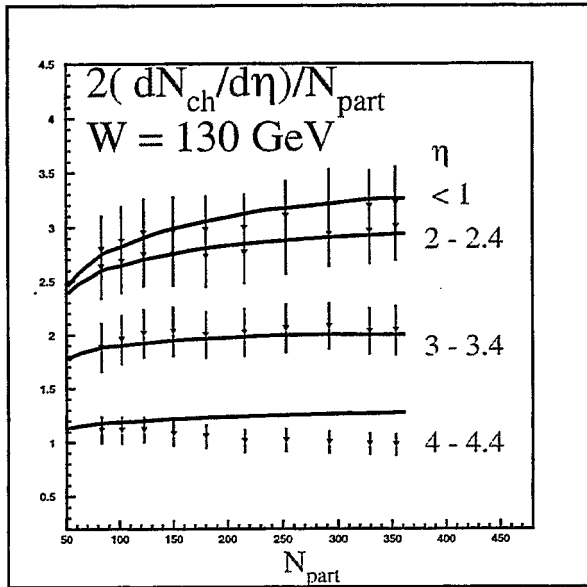
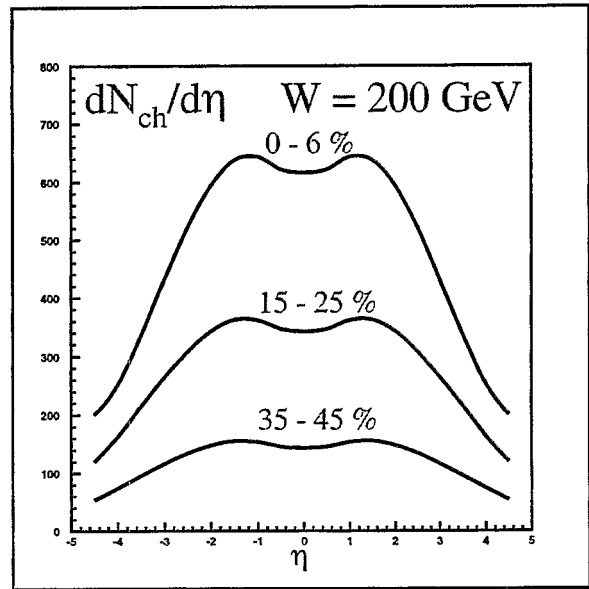
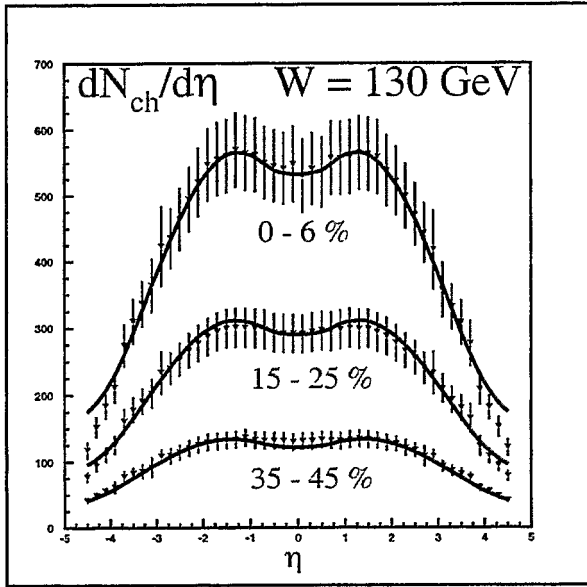
In this talk the KLN point of view is discussed that RHIC data give a clear evidence for a saturation in the quark - gluon system produced at the initial stage of heavy ion collisions. If it is true it would be a first experimental support for our (theorists) belief that saturation and thermalization will lead to quark-gluon plasma production.

We cannot expect that only our approach is able to describe RHIC data, due to a duality between parton and hadron degrees of freedom. Therefore, we believe that a plenty of different approaches will be work out. However, we firmly believe that (i) our approach follows directly from QCD; (ii) it gives the most economic description since we have to take from non-perturbative QCD (phenomenology) only a small number of parameters; and (iii) it has a predictive power which manifest itself in suggesting new experimental observables at RHIC (especially correlations of different types).

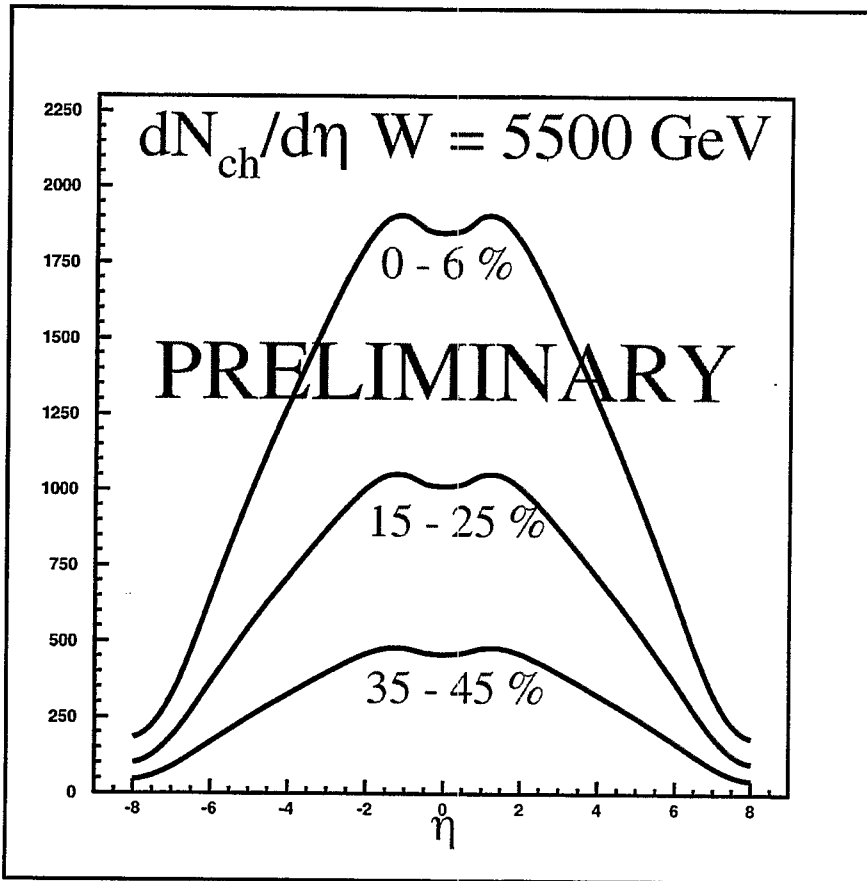
This talk demonstrates that

- The saturation scale at RHIC ($W = 130\text{GeV}$) $Q_s^2(\text{Gold}) = 2\text{ GeV}^2$;
- We can describe the RHIC data on multiplicity (transparency 1) and on the p_t distribution of the produced hadrons (transparency 3);
- Everything, that we used, agrees with the hadronic data on DIS (at HERA) or on "hard" processes at Tevatron;
- Our approach leads to predictions at higher energies (see transparency 2 which shows the multiplicity distributions for LHC energies);
- Our approach gives a rich spectrum of different prediction for correlations: transparencies 4 and 5 show the predictions for azimuthal correlation which demonstrate the simple intuitive expectation that the jet with sufficiently high p_t could be compensated by several particles with average parton transverse momentum (Q_s); transparency 6 shows that the ratio of two p_t distributions for different centrality cuts has a maximum at the saturation scale for less central events.

More detailed and selfconsistent presentation of the KLN approach you can find in the original papers: D. Kharzeev and M. Nardi, Phys. Lett. B507 (2001) 121; D. Kharzeev and E. Levin, Phys. Lett. B523 (2001) 79; D. Kharzeev, E. Levin and M. Nardi, hep-ph/0111315; D. Kharzeev and E. Levin, (in preparation).



Predictions for rapidity distribution for the LHC energy using Golec-Biernat and Wüsthoff model for Q_s .



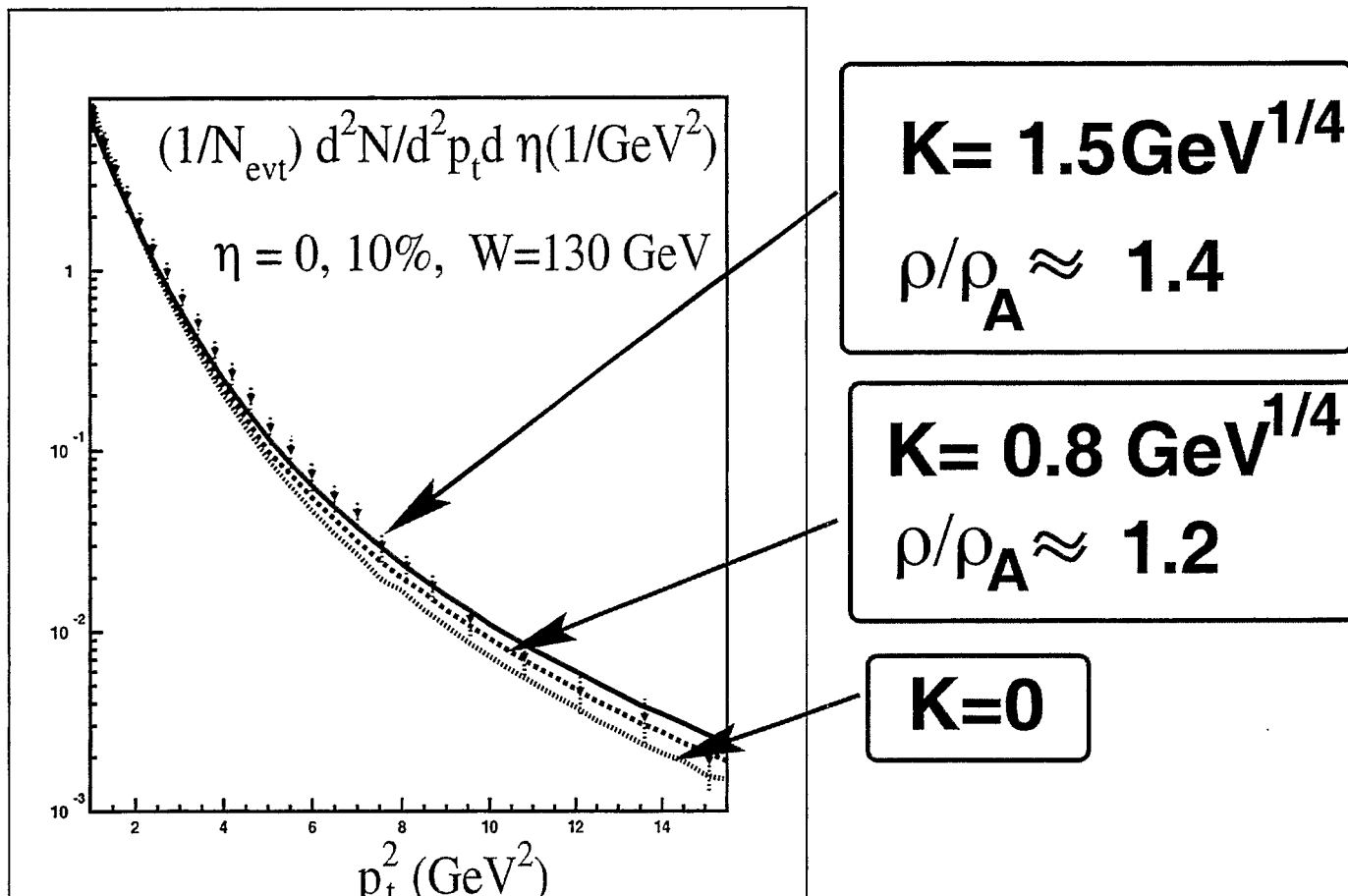
$$\frac{\frac{dN(y=0;W)}{dy}}{\frac{dN(y=0;W_0)}{dy}} = \left(\frac{W}{W_0}\right)^\lambda \left(1 + \lambda \frac{\ln \frac{W}{W_0}}{\ln \left(\frac{Q_s^2(s_0)}{\Lambda_{QCD}^2} \right)} \right)$$

where:

$$B = \frac{d \ln \frac{d\sigma}{d p_t^2}}{d \ln p_t}$$

L is the size of the nucleus;

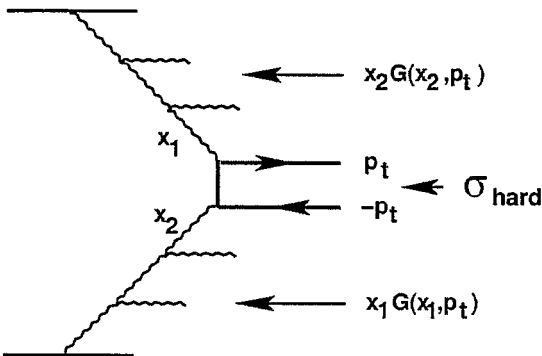
ρ - nucleon density in ion-ion collision while $\rho_A \approx 0.16 \text{ fm}^{-3}$;



Correlations

Asimuthal correlations

Factorization:



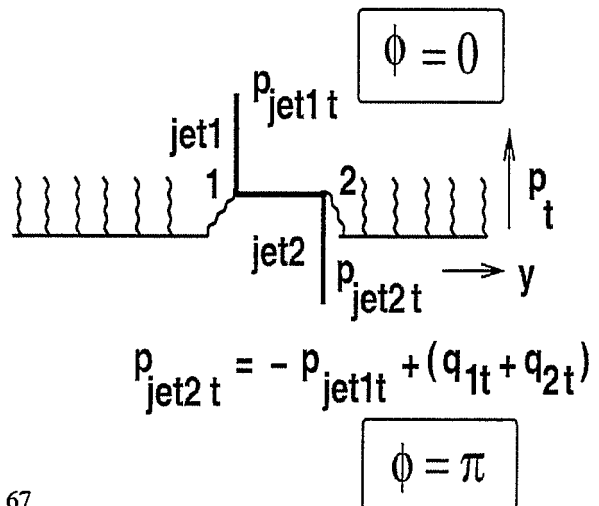
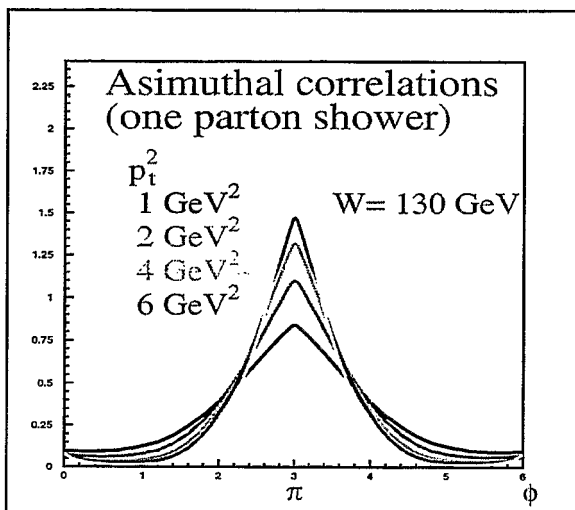
$$p_{jet1,t} \gg Q_s \quad \vec{p}_{jet1,t} \longrightarrow -\vec{p}_{jet2,t}$$

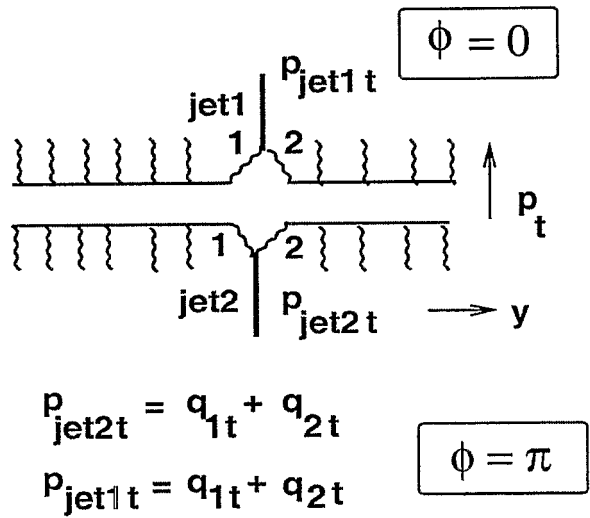
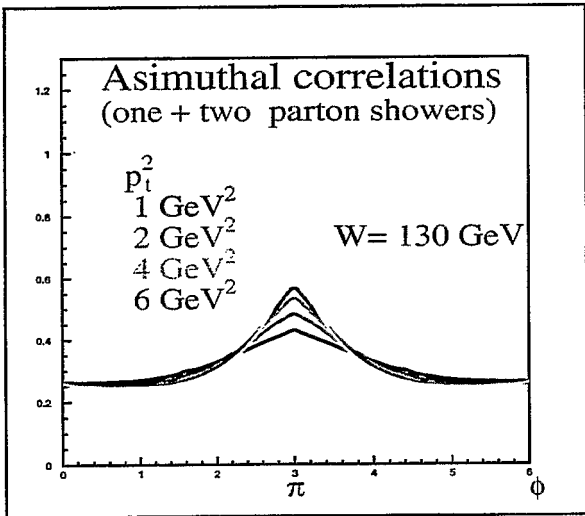
Strong correlation !!!

$$p_{jet1,t} \leq Q_s$$

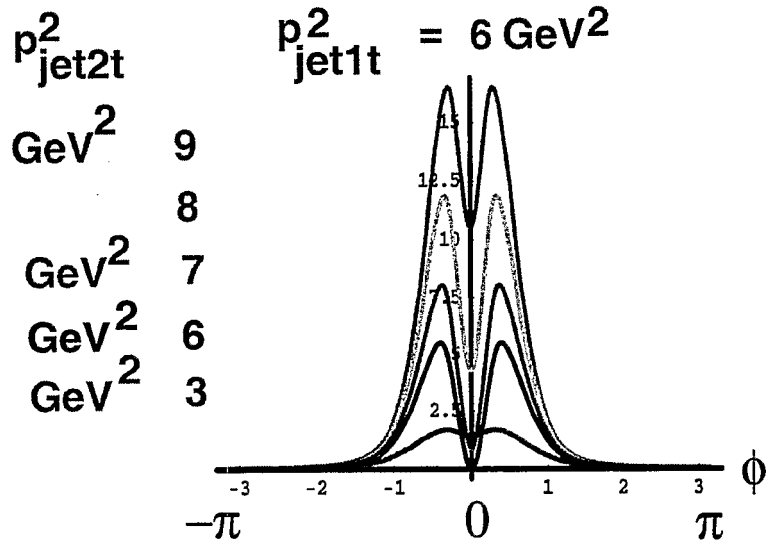
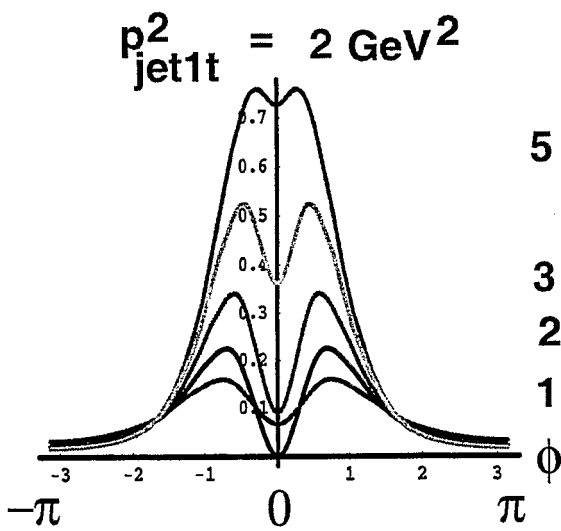
the production of two jet comes from two parton shower event.

No correlations !!!

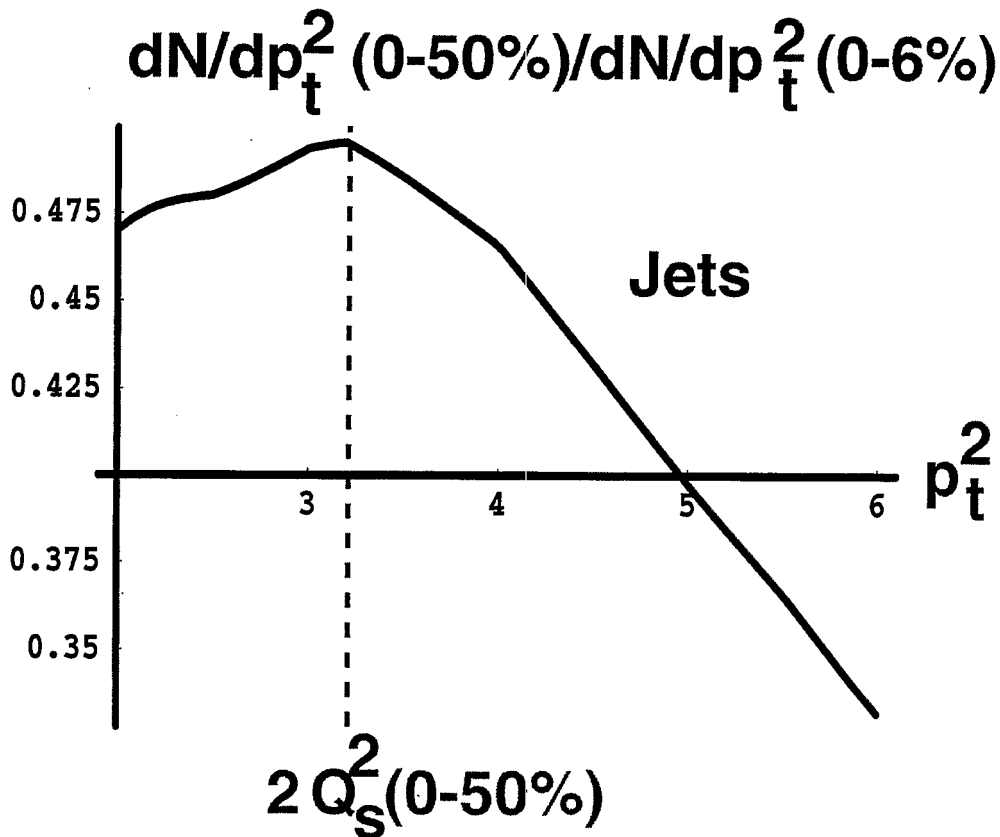




Ratio = $\frac{\text{one parton shower}}{\text{two parton showers}}$

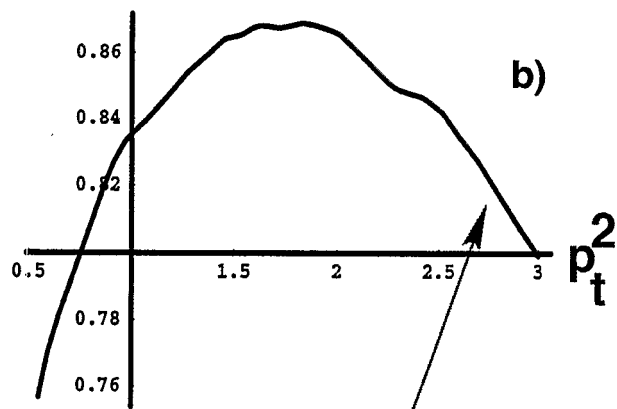
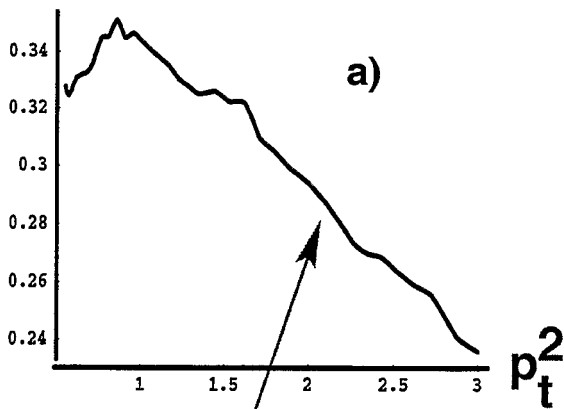


Ratio for different centralities



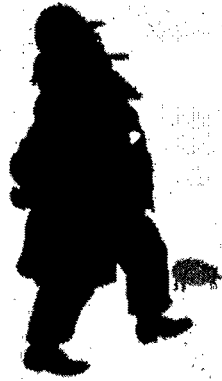
$\frac{dNdp_t^2 (0-50\%)}{dN/dp_t^2 (0-6\%)}$

HADRONS



D from KKP-paper

D from LPHD



Recent Results from BRAHMS at RHIC

J.H. Lee

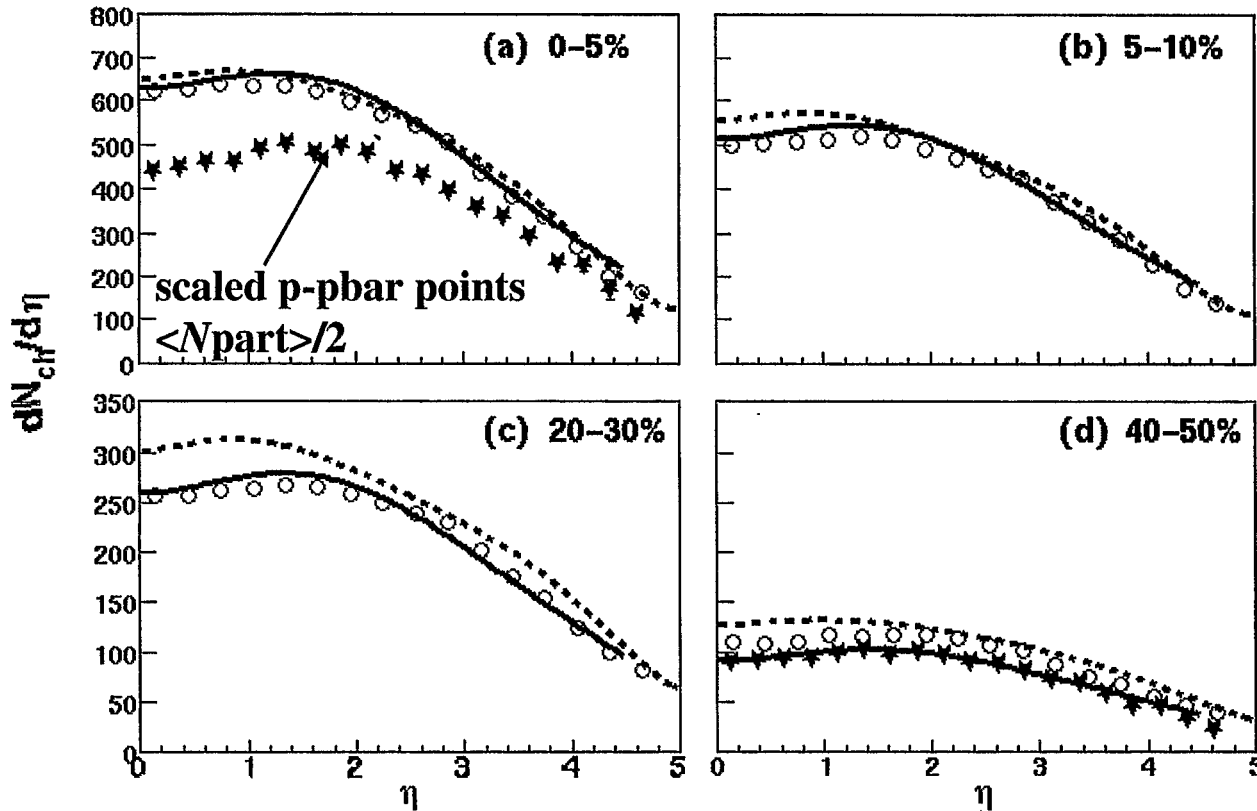
Physics Department
Brookhaven National Laboratory

For the BRAHMS Collaboration

Current and Future Directions at RHIC
Aug. 7 2002

$dN_{ch}/d\eta$ - Comparison to Model Predictions

$\sqrt{s_{NN}}=200\text{GeV}$

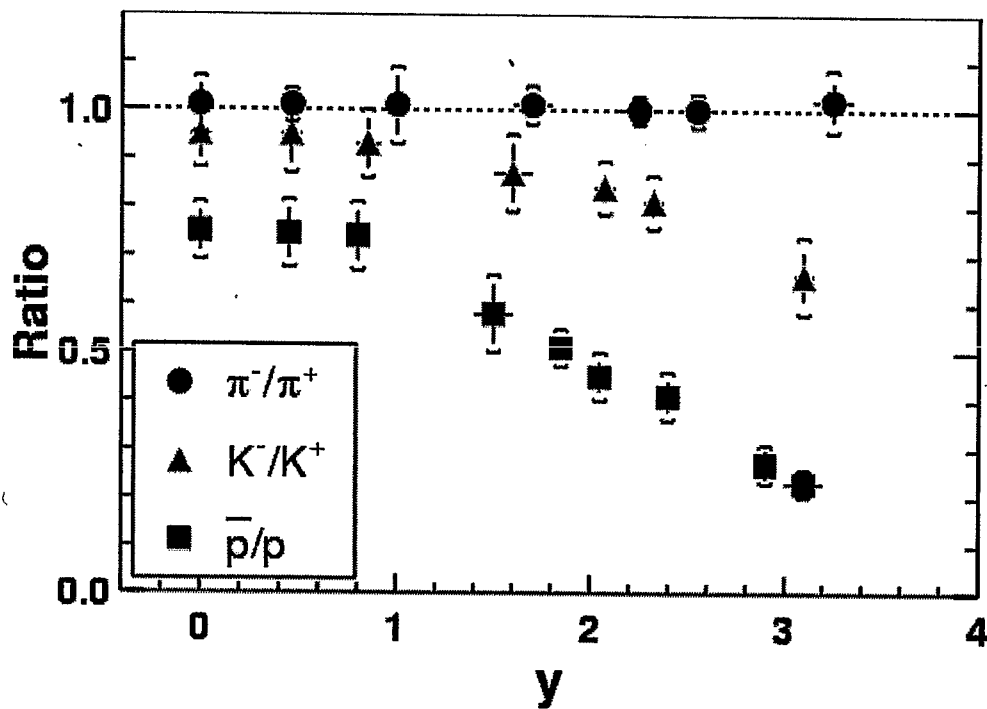


--- AMPT
 (HIJING + final-state re-scattering)

— High density QCD
 Gluon Saturation:
 Kharzeev and Levin,
 PLB523 (2001) 79

Strong enhancement
 relative to p-pbar for
 central collisions

Anti-particle/particle ratios vs rapidity at $\sqrt{s_{NN}}=200$ GeV

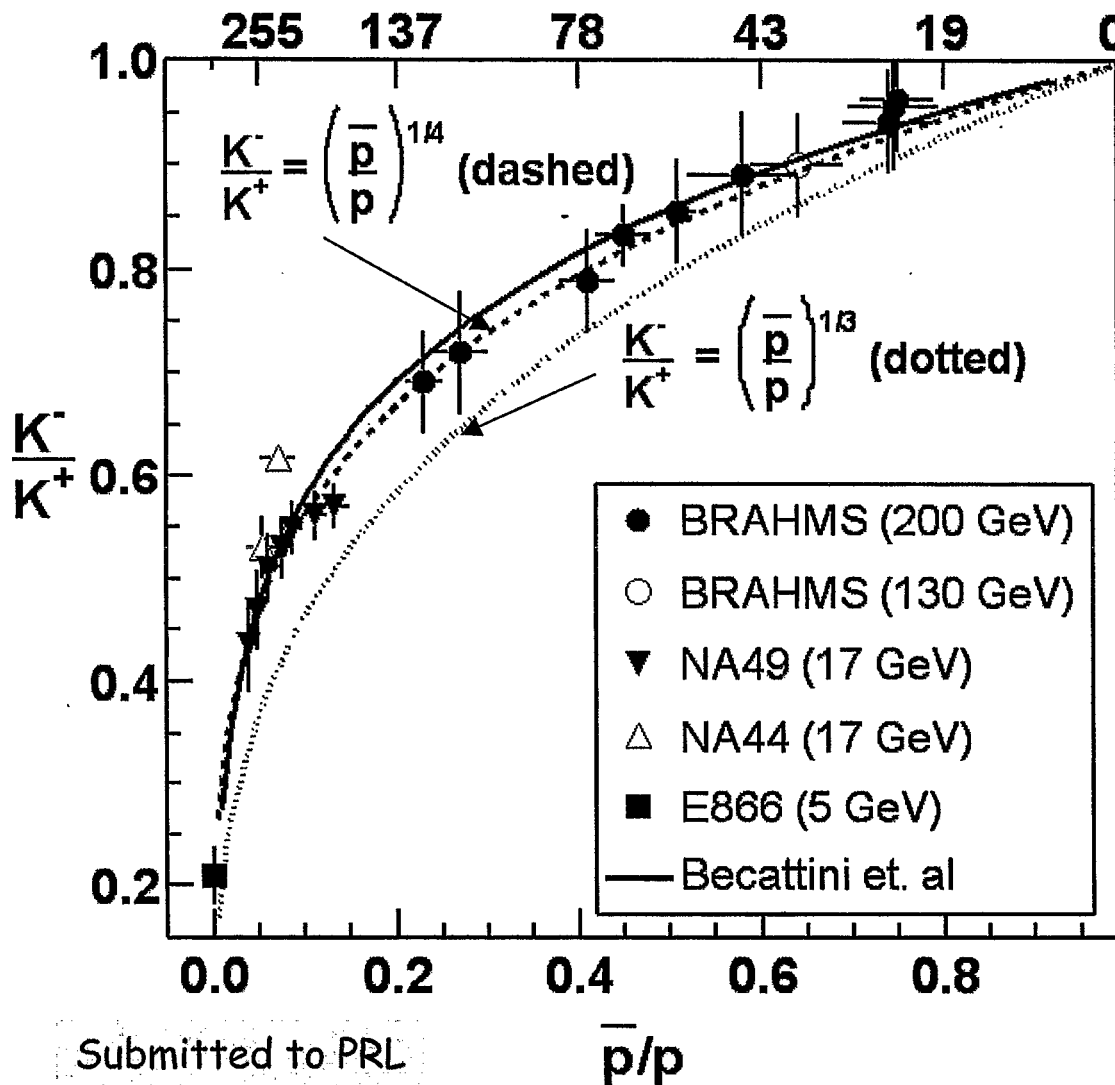


- At $y=0$ (20% central)
 $\bar{p}/p = 0.75 \pm 0.04$
 $K^-/K^+ = 0.95 \pm 0.05$
 $\pi^-/\pi^+ = 1.01 \pm 0.04$
- Highest \bar{p}/p ratio but still incomplete transparency (~17% increase from 130 GeV)
- Ratios ~identical over ± 1 unit around mid-rapidity.
- Weak centrality and p_T dependence
- No Hyperon feed down applied: less than 5% correction assuming $\Lambda/p \sim 0.5$ and $\bar{p}/p \sim \Lambda\text{-Bar}/\Lambda$

Submitted to PRL : nucl-ex/0207006

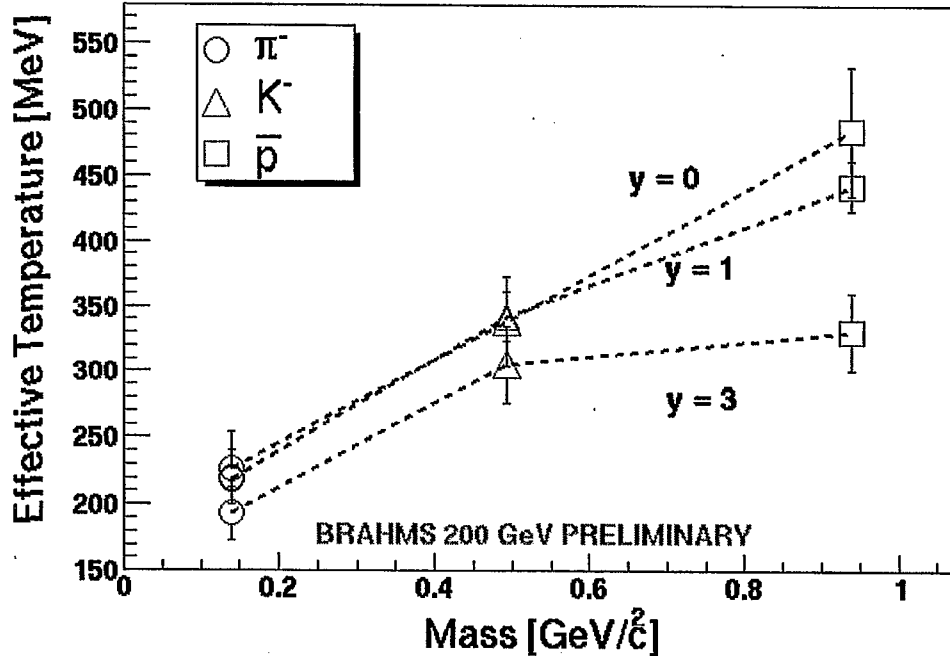
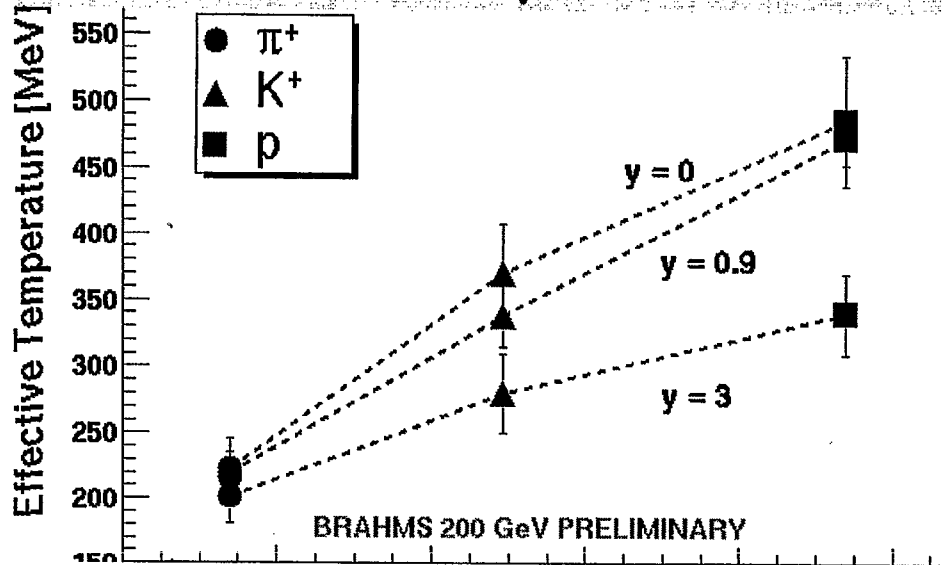
Universal Correlation in K^-/K^+ vs \bar{p}/p ?

μ_B (T=170MeV)



- K^-/K^+
 $= \exp(2\mu_s/T)\exp(-2\mu_q/T)$
 $= \exp(2\mu_s/T)(\bar{p}/p)^{1/3}$
- $K^-/K^+ = (\bar{p}/p)^{1/4}$ is a fit to the data points
- Good agreement with the statistical-thermal model prediction by Beccatini et al. (PRC64 2001): Based on SPS results and assuming $T=170$ MeV

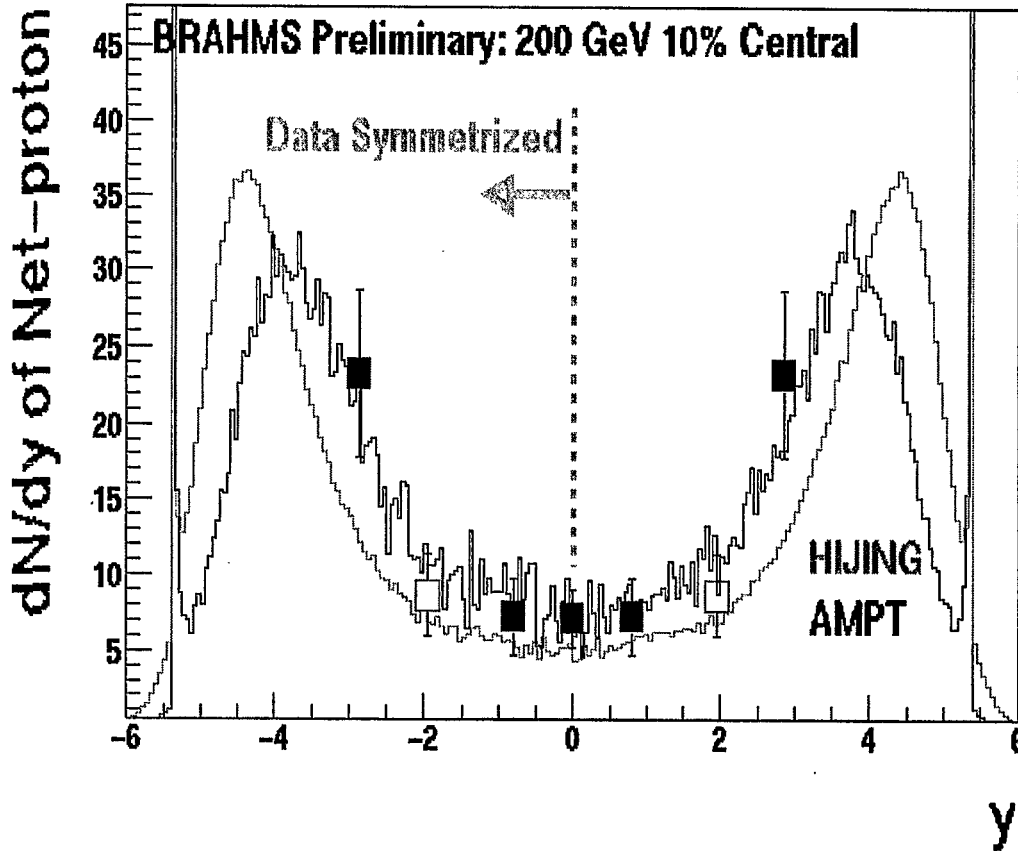
BRAHMS Preliminary: 200 GeV 10% Central



Inverse p_T Slope vs. mass

- All fits are in p_T :
over same range for all particles, at all rapidities
- Negative \approx Positive
- Inverse slope decreases as y increases
- Flow at all covered rapidities

dN/dy of Net-proton and Models



- "Plateau" at $|y| < \pm 2$
- Hyperon feed down will reduce the yields by 10-20%
- Net-baryon at $y = 0$: ~ 14.2
(if $N(\text{proton})/N(\text{neutron}) \approx 1$)
- More data to be analyzed (at $y \sim 2$, and $y \sim 3$)
- AMPT in reasonable agreement (HIJING + re-scattering!)

Summary:

BRAHMS Measurements of Au+Au at 200 GeV

- Highest particle multiplicity in nuclear collisions (21% increase from 130 GeV)
- At forward η : consistent with "limiting fragmentation" picture
- Partonic models: good general agreement with data
- K^-/K^+ , $pbar/p$: approximately constant over ± 1 unit of rapidity and fall off with y
- Universal correlation: $K^-/K^+ = (pbar/p)^{1/4}$
- Inverse slope decreases with rapidity
- Measured dN/dy over 3 units of rapidity
- near flat net-proton yield in $y < \pm 2$
- Significant increase in net protons at $y=3$
- Good agreement with AMPT: re-scattering still significant at RHIC

- Low to high chemical potential from $y=0$ to $y=3$
- Net baryon central plateau ($y < \pm 2$)
- Incomplete yet significant transparency
- More Complete measurements including pp, dA expected in Run3 and beyond

Particle Production in AA Collisions from Saturation Physics

Yuri V. Kovchegov*

*Department of Physics, University of Washington, Box 351560
Seattle, WA 98195*

We discuss the problem of particle production in nuclear collisions in the framework of parton saturation approach. We propose an ansatz for the analytical solution of the problem in the quasi-classical (multiple rescattering) approximation and conjecture a generalization of the resulting expression to include quantum evolution in energy.

Calculating the cross section of inclusive particle production at mid-rapidity in the regime when the wave functions of both colliding hadrons or nuclei have reached saturation is very important for understanding initial conditions for quark-gluon plasma (QGP) formation in AA collisions at RHIC and LHC, as well as for creating a unified framework for describing DIS (HERA) and pp (Tevatron) data. Therefore it is probably the most important still open problem of saturation physics today. Traditionally particle production in nuclear collisions is described employing collinear factorization framework for pairwise nucleon-nucleon interactions. This approach is valid only for production of particles with sufficiently high momentum so that one could neglect the higher-twist multiple rescatterings corrections. At the same time the resulting particle p_T spectrum is infrared divergent scaling as $1/p_T^4$, making the total number of produced gluons depend on the unknown infrared cutoff as $1/\Lambda^2$. Saturation physics resums all twists and therefore is applicable over a much wider p_T interval than collinear factorization approach. The total number of gluons in the saturation framework should become cutoff-independent, thus resolving many problems of collinear factorization.

The goal of the saturation physics approach could be illustrated using the example of total cross section of deep inelastic scattering (DIS). The first step is to include multiple rescatterings without any evolution in energy, restricting each gluon-nucleon interaction to a two-gluon exchange (see Transparency #1). The relevant resummation parameter is $\alpha_s^2 A^{1/3}$ [1]. This resummation has been accomplished by Mueller in 1990 resulting in the Glauber-Mueller formula for the $q\bar{q}$ dipole-nucleus cross section shown in Transparency #1. The second step of the saturation program for $\sigma_{tot}^{q\bar{q}A}$ is to include quantum evolution in energy (in the BFKL sense) into it. This corresponds to resummation of powers of $\alpha_s \ln s$, with s the center of mass energy of the system. The resummation has been performed in the large- N_c limit in [2] resulting in nonlinear evolution equation shown in Transparency #2. Our goal is to apply these techniques to inclusive cross sections in AA .

To resum multiple rescatterings in the single gluon production cross section for AA one has to employ the solution of the same problem for pA [1]. There in the light cone gauge of the nucleus all gluon mergers in the final state cancel and the gluon production is given by initial state interactions only [3,1] (see Transparency #3). While the physical cancellation mechanism is not clear the fact of cancellation has been rigorously established [3]. Assuming that cancellation of final state mergers persists in AA we derive the formula for the gluon's multiplicity distribution in AA shown in Transparency #4 [3]. This distribution is infrared safe and gives the value of the liberation coefficient $c^{AA} = 2 \ln 2$.

Note that distribution in Transparency #4 expresses inclusive gluon production cross section in terms of forward amplitudes of a scattering of a gluon dipole on a nucleus. The same was true in pA case [1] and in DIS [4]. In [5] it was shown for single gluon inclusive cross section in DIS (and pA) that in order to include quantum evolution in it one has to substitute the Glauber-Mueller expression for gluon dipole cross section on a nucleus by the cross section which is fully evolved using nonlinear evolution equation of [2]. This is discussed in Transparency #5. This observation allows one to conjecture the formula for produced gluon distribution in AA presented in Transparency #5 which includes the effects of nonlinear evolution in it.

[1] Yu. V. Kovchegov, A.H. Mueller, Nucl. Phys. B **529**, 451 (1998).

[2] I.I. Balitsky, Nucl. Phys. B **463**, 99 (1996); Phys. Rev. D **60**, 014020 (1999); Yu. V. Kovchegov, Phys. Rev. D **60**, 034008 (1999); D **61**, 074018 (2000).

[3] Yu. V. Kovchegov, Nucl. Phys. A **692**, 557 (2001).

[4] Yu. V. Kovchegov, Phys. Rev. D **64**, 114016 (2001).

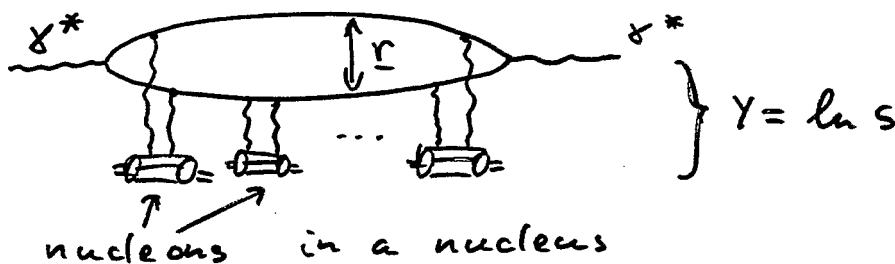
[5] Yu. V. Kovchegov, K. Tuchin, Phys. Rev. D **65**, 074026 (2002).

*This work is supported in part by the U. S. Department of Energy under Grant No. DE-FG-97ER41014.

What is the goal / program ?

→ DIS is a good example:

Stage 1 Inclusion of multiple rescatterings



Dipole-nucleus cross section is

$$\sigma_{\text{tot}}^{\gamma^* A} = 2 \int d^2 b N(\underline{r}, \underline{b}, \gamma)$$

with

$$N \Big|_{\gamma=0} = 1 - e^{-r^2 Q_s^2(b) / 4}$$

Glauber-Mueller
formula

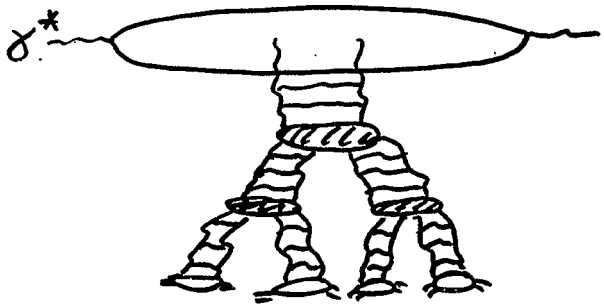
$$r^2 Q_s^2 \sim \sigma^{\gamma^* N} \sim \frac{r^2 \alpha_s \times G_N \cdot A}{\pi R^2} \sim A^{1/3}$$

Stage 2 Inclusion of quantum corrections

(evolution, brings in terms like

$\alpha_s \ln s$, with $\alpha_s \ll 1$ enhanced by

$\ln s \gg 1$ so that $\alpha_s \ln s \sim \alpha_s \gamma \sim 1$)



δ^* on top of multiple rescatterings may have mergers of ladders

(GLR '82)

Resulting evolution for dipoles is

$$\frac{\partial N}{\partial \gamma} = \alpha_s K_{\text{BFKL}} \otimes N - \alpha_s N^2$$

Balitsky '96

Kovchegov '99

(but: large N_c only)

↳ beyond large $N_c \sim \text{JIMWLK eq.}$

⇒ The Stage 1/2 process is (almost) complete

for DIS (for $\sigma_{\text{tot}} \sim F_2$)!

⇒ Can we do the same for inclusive observables such as gluon production cross section in AA / pA / pp / DIS ?

Same pA process in $A_+ = 0$ light cone gauge

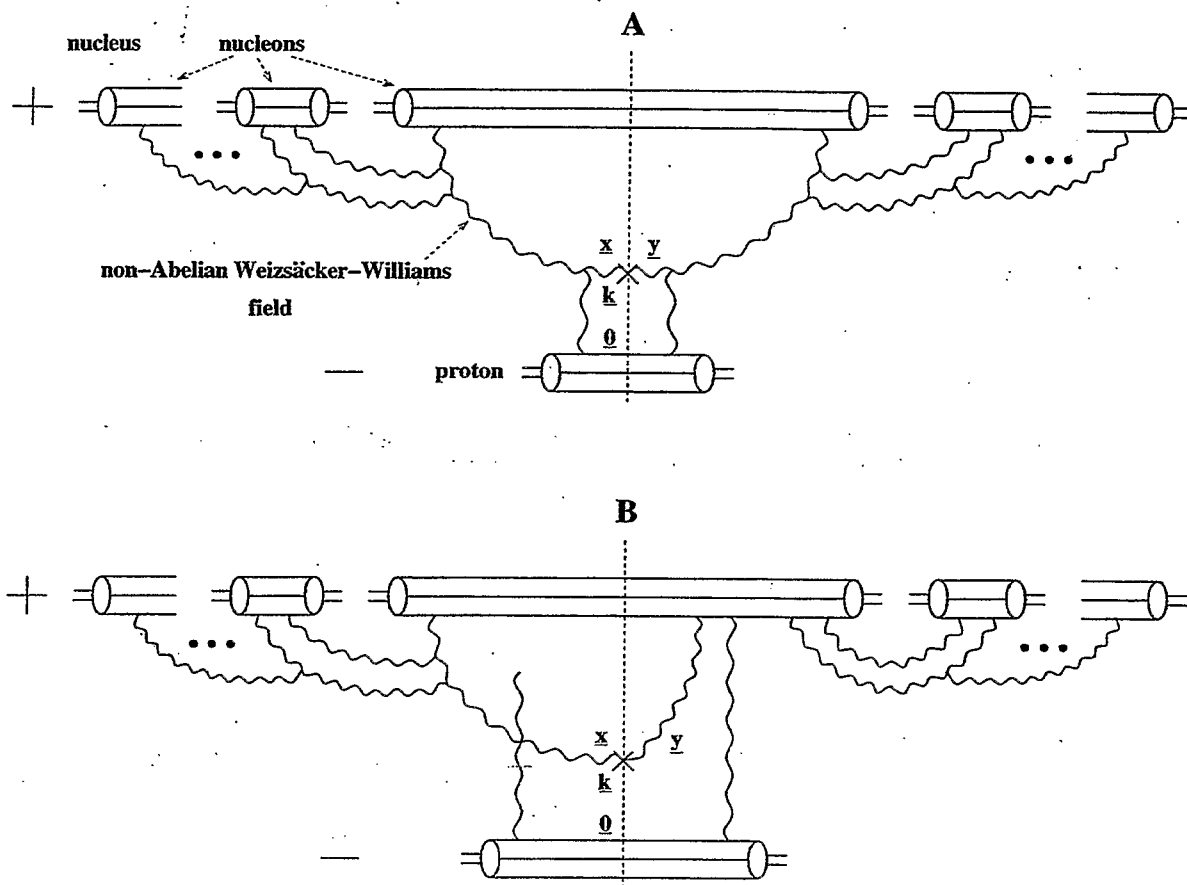
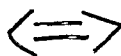


Figure 11: Gluon production in proton–nucleus collisions in $A_+ = 0$ light cone gauge.

Yu. K., hep-ph/0011252

Let us adopt a different strategy: we know the answer. Let us guess which diagrams give the same answer in $A_+ = 0$ light cone gauge. The diagrams are shown above.

Final state interactions
in $\partial \cdot A = 0$ gauge



Initial state interactions
in $A_+ = 0$ gauge

Nucleus-Nucleus Collisions (AA)

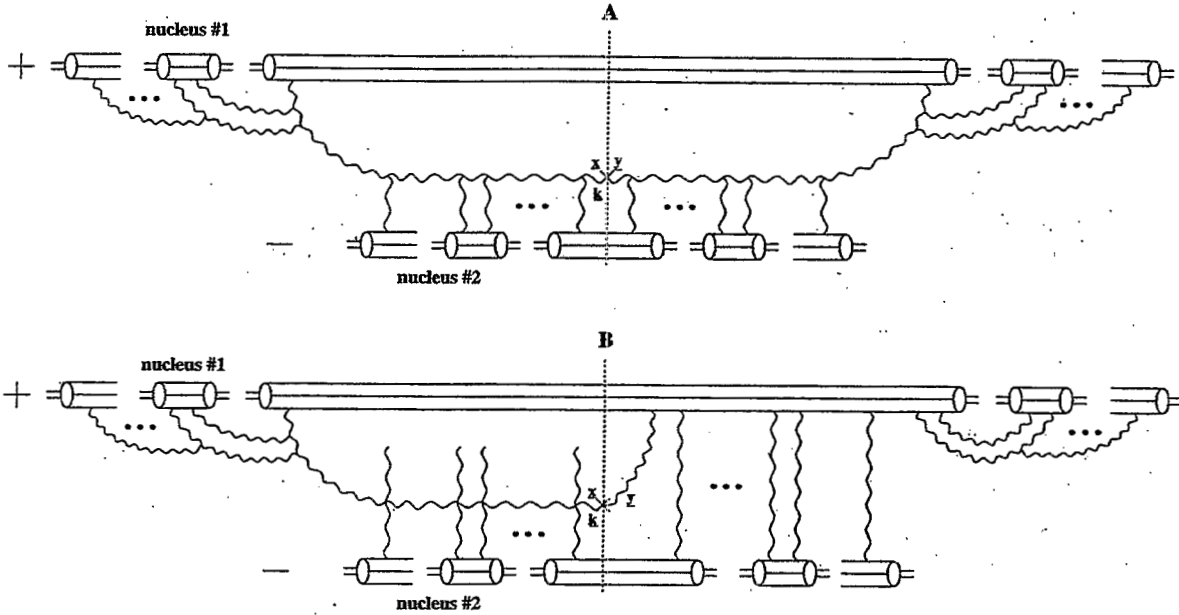


Figure 15: Diagrams contributing to the gluon production in nucleus-nucleus collisions in the $A_+ = 0$ light cone gauge.

main result:

$$\left. \begin{aligned}
 \frac{dN^{AA}}{d^2k d^2b dy} &= \frac{2C_F}{\alpha_S \pi^2} \left\{ - \int \frac{d^2z}{(2\pi)^2} e^{i\mathbf{k}\cdot\mathbf{z}} \frac{1}{z^2} \left(1 - e^{-z^2 Q_{s1}^2/4} \right) \right. \\
 &\times \left(1 - e^{-z^2 Q_{s2}^2/4} \right) + \int \frac{d^2x d^2y}{(2\pi)^3} e^{i\mathbf{k}\cdot(\mathbf{x}-\mathbf{y})} \frac{\mathbf{x}}{x^2} \cdot \frac{\mathbf{y}}{y^2} \left[\frac{1}{x^2 \ln \frac{1}{|x|\mu}} \right. \\
 &\times \left(1 - e^{-x^2 Q_{s1}^2/4} \right) \left(1 - e^{-x^2 Q_{s2}^2/4} \right) + \frac{1}{y^2 \ln \frac{1}{|y|\mu}} \left(1 - e^{-y^2 Q_{s1}^2/4} \right) \\
 &\left. \left. \left. \times \left(1 - e^{-y^2 Q_{s2}^2/4} \right) \right] \right\}.
 \end{aligned} \right.$$

Yu.K., hep-ph/0011252

Including Evolution in Energy

In the large- N_c limit the rule is very simple: substitute

$$1 - e^{-\underline{x}^2 Q_{0s}^2(\underline{b})/4} \longrightarrow N_G(\underline{x}, \underline{b}, y).$$

where $N_G(\underline{x}, \underline{b}, y)$ is the forward amplitude of a gluon dipole on a nucleus obtained from solving non-linear evolution equation.

Yu. K., K. Tuchin, '01 (proven for DIS)
inclusive x -section

One obtains the following simple formula for particle production in pp and AA

$$\frac{dN^{AA}}{d^2k d^2b dy} = \frac{C_F}{\alpha_S \pi^3} \int_0^\infty \frac{dx}{x} J_2(kx) N_G(\underline{x}, \underline{b}, y) \\ \times N_G(\underline{x}, \underline{b}, Y - y) \quad (\text{conjecture})$$

which can be used to describe both Fermilab and RHIC data.

For pA:

$$\frac{d\sigma^{pA}}{d^2k dy} = \frac{1}{2\bar{\alpha}} S_\perp^A \int_0^\infty dx \cdot x \cdot J_2(kx) \cdot N_G(\underline{x}, \underline{b}, y) \cdot x G_p(e^{-(Y-y)}, \frac{1}{x^2})$$

E_T Distributions and other Event-by-Event Fluctuations

M. J. Tannenbaum

for the PHENIX Collaboration

BNL, Upton, NY 11973-5000 USA

- The event by event average p_T for charged particles, denoted M_{p_T} , was discussed and results were presented for the PHENIX 200 GeV data.

$$M_{p_T} = \overline{p_T(n)} = \frac{1}{n} \sum_{i=1}^n p_{T_i} = \frac{1}{n} E_{Tc}$$

- “ M_{p_T} is not a Gaussian, it’s a Gamma distribution” because the semi-inclusive p_T distribution is a Gamma distribution and particle emission in Au+Au collision is very close to being a statistical independent sample from the semi-inclusive distribution.

- To see deviations from random emission, the measured M_{p_T} distributions as a function of centrality are compared to the ‘random baseline’ of mixed events which match the multiplicity and $\langle p_T \rangle$ of the data to high precision, much better than 1 %.

- A non-random fluctuation F_t on the order of a few percent of the standard deviation is observed which increases as the p_T range of the measurement is increased. (And may increase with solid angle according to STAR).

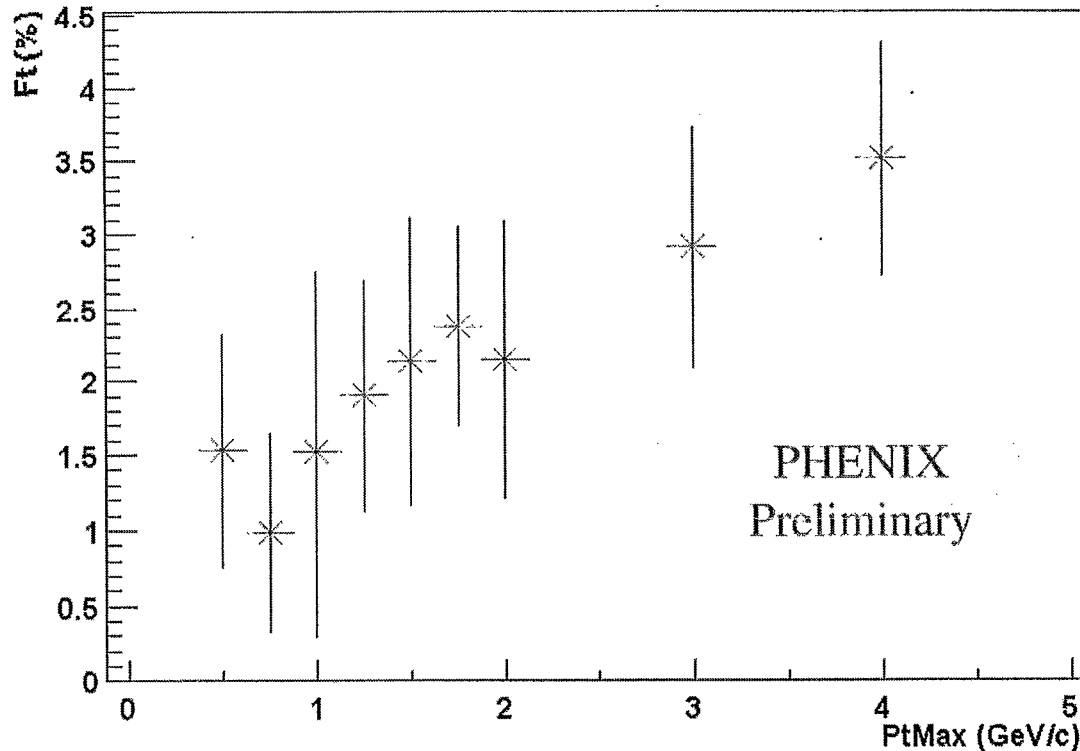
- E_T and multiplicity distributions measured by PHENIX at 200 GeV for Au+Au have a similar centrality dependence to the 130 GeV measurements, with an overall increase by a constant factor of ~ 1.15 .

- E_T and multiplicity distributions from p+p collisions when they become available will provide the basis for Wounded Nucleon style analyses of the entire Au+Au E_T distribution, including fluctuations of the upper edge, and may add additional enlightenment on any p_T correlations as possibly indicated by M_{p_T} .

- Event-by-event net charge fluctuations at 130 and 200 GeV are consistent with random emission of hadrons with conserved total charge, with some evidence for slight ($\sim\%$) short-range charge correlation due to resonance production.

CURRENT AND FUTURE DIRECTIONS AT RHIC, AUGUST 8, 2002

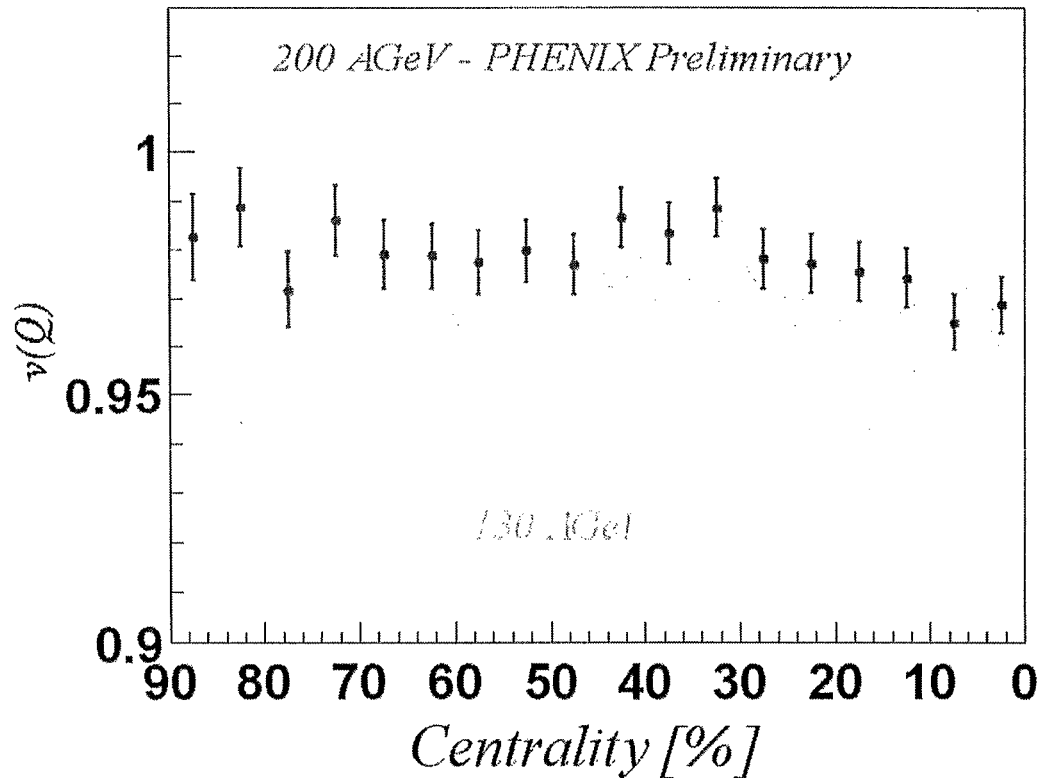
The fluctuation magnitude tends to increase as the p_T range used to calculate $\langle p_T \rangle$ is extended to higher values.



F_T vs. P_T range
 $(0.2 < p_T < p_{T, max})$

Centrality and p_T dependence similar to elliptic flow.
 Simulations using PHENIX preliminary p_T -dependent v_2 measurements wrt to the reaction plane can, however, not reproduce the signal.

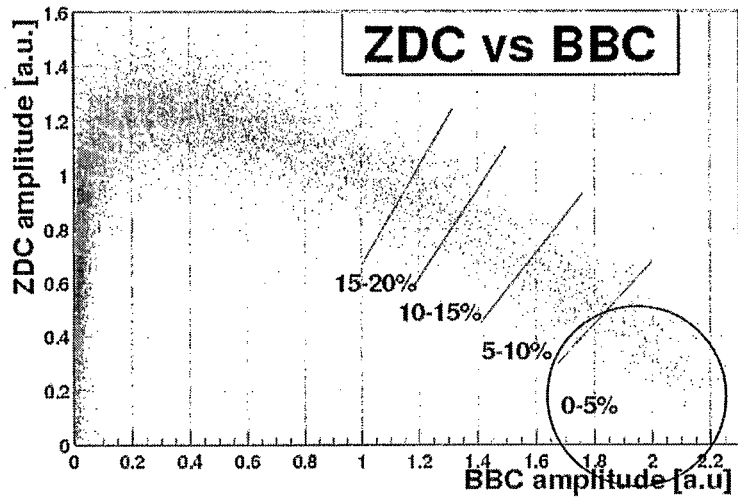
$v(Q)$ as a function of collision centrality



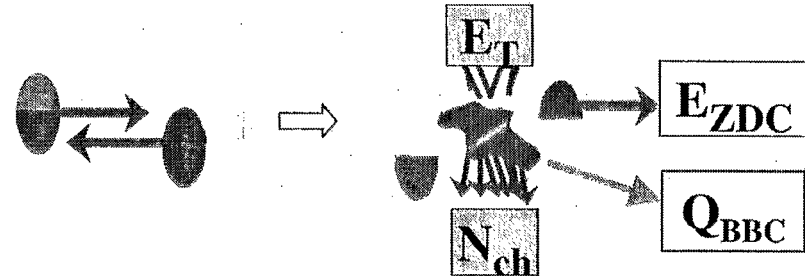
A small deviation from stochastic emission observed at 130 GeV
 K. Adcox et al. (PHENIX) nucl-ex/0203014 to appear in PRL

No dramatic change at 200 GeV - the upward shift of ~ 0.01 units can be explained by harder track quality cuts leading to a reduced acceptance.

Centrality Selection

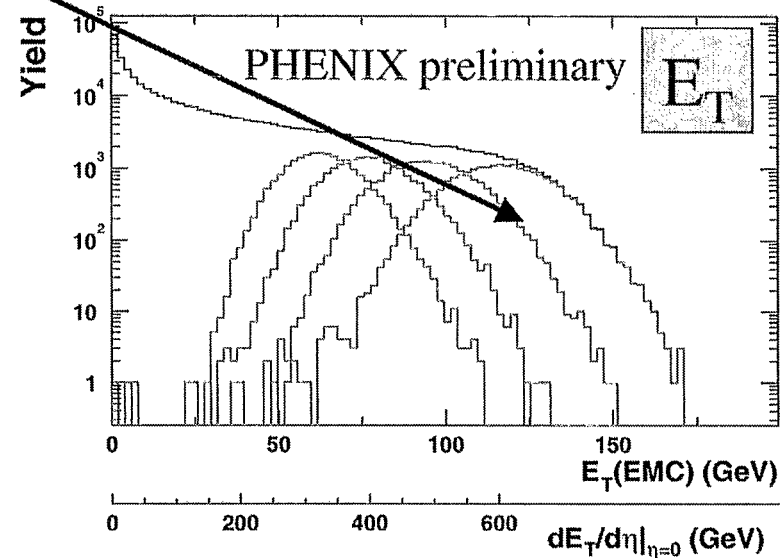
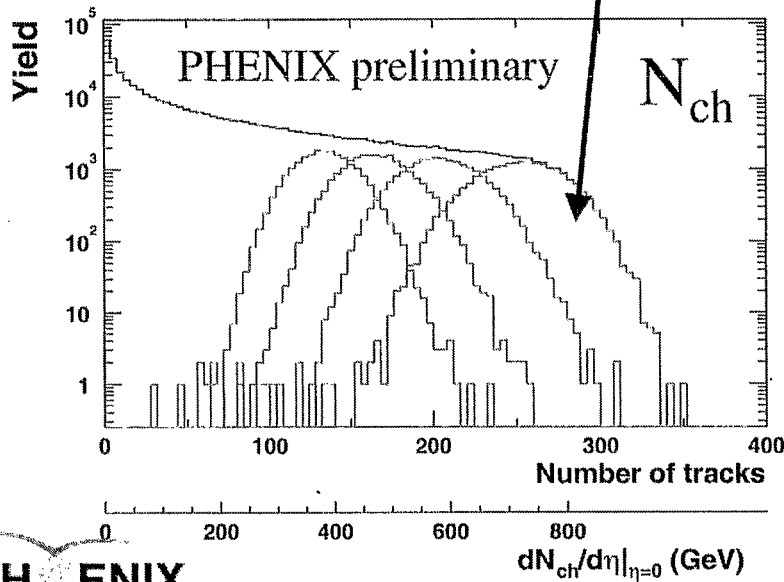


Define centrality classes: ZDC vs BBC

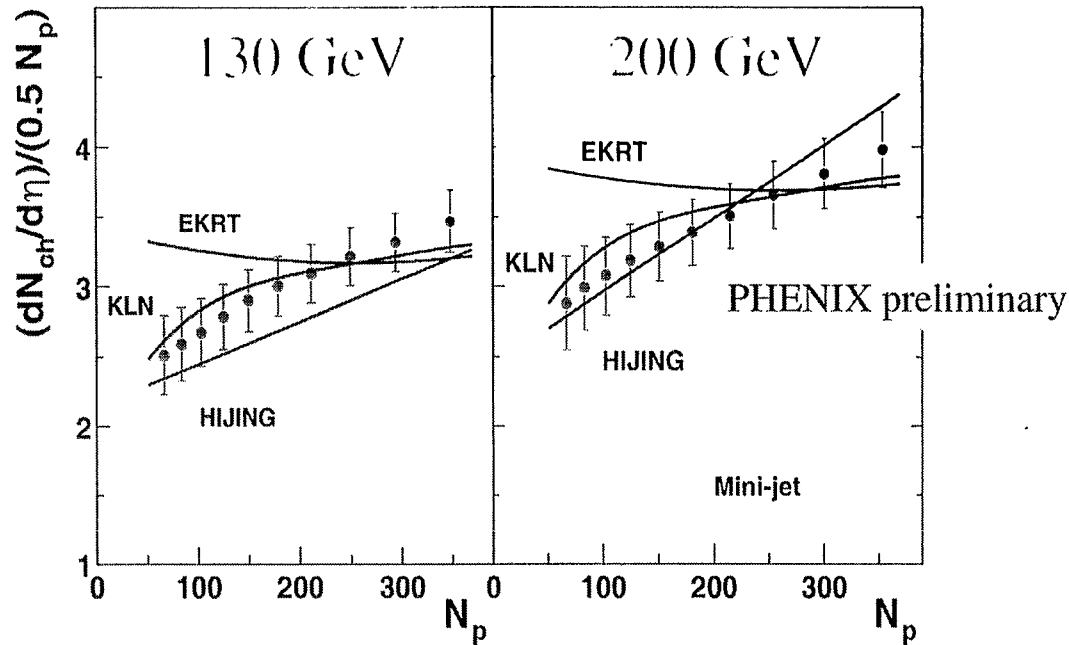


Extract N participants: Glauber model

88



Comparison to theory



HIJING X

X.N.Wang and M.Gyulassy,
PRL 86, 3498 (2001)

Mini-jet

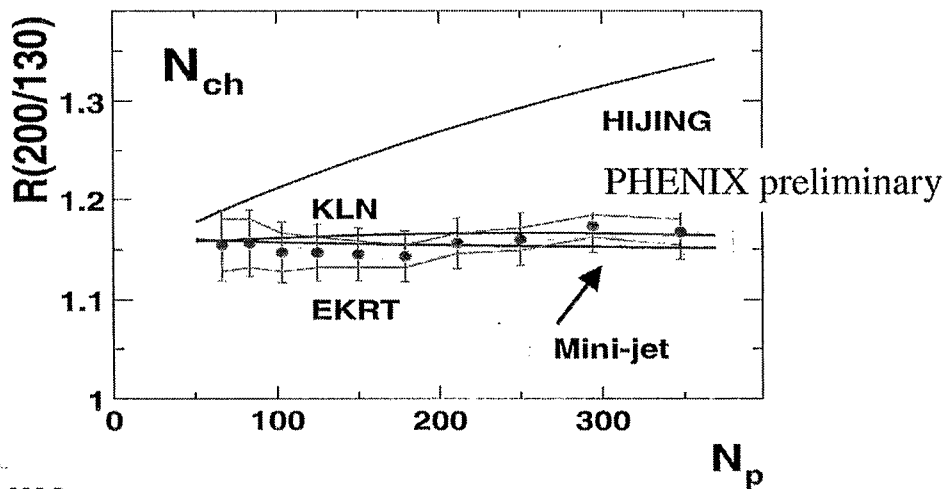
S.Li and X.N.Wang
Phys.Lett.B527:85-91 (2002)

EKRT X

K.J.Eskola et al,
Nucl Phys. B570, 379 and
Phys.Lett. B 497, 39 (2001)

KLN

D.Kharzeev and M. Nardi,
Phys.Lett. B503, 121 (2001)
D.Kharzeev and E.Levin,
Phys.Lett. B523, 79 (2001)



Two Particle Interferometry at RHIC

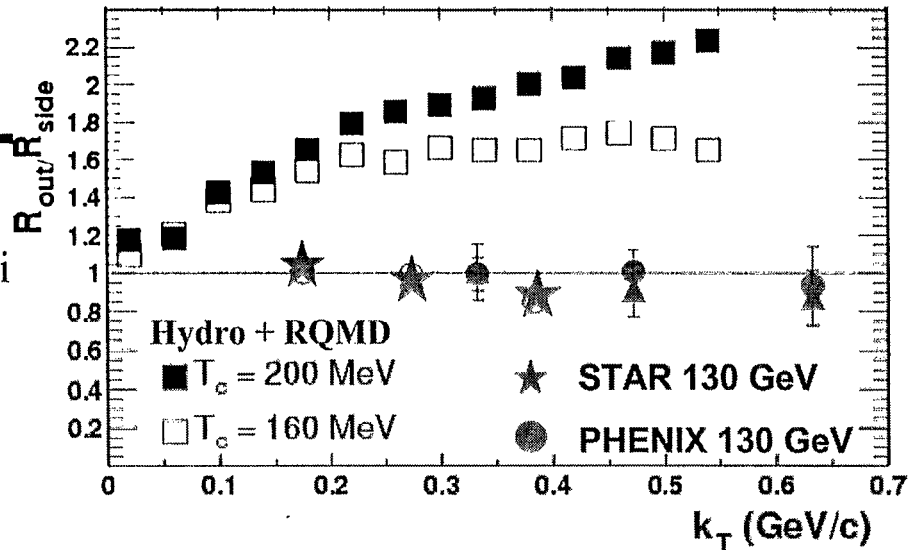
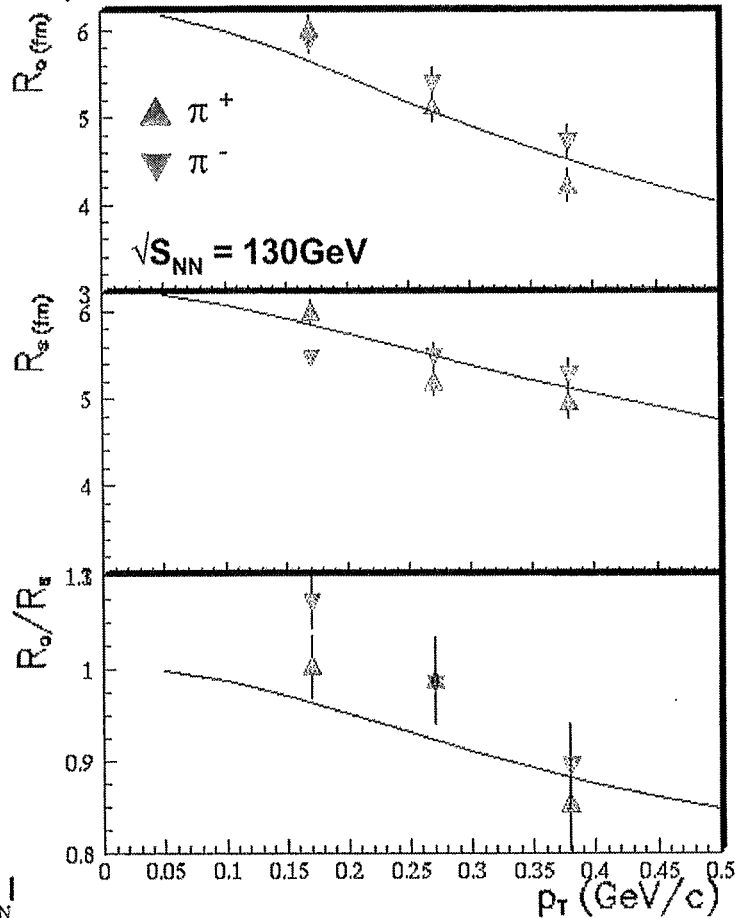
Sergey Panitkin

(Brookhaven National Laboratory)

RHIC HBT Puzzle

Most “reasonable” models still do not reproduce RHIC $\sqrt{s_{NN}} = 130\text{ GeV}$ HBT radii

$R_{y2}=13.500, s2=0.000, T=0.110, rho0=0.950, rhoa=0.000, tau=1.500$



PHENIX PRL 88 192302 (2002)

“Blast wave” parameterization (Sollfrank model)

can approximately describe data at 130 GeV

...but emission duration must be small

- $\langle \rho_0 \rangle = 0.6$ (radial flow)
 - $T = 110$ MeV
 - $R = 13.5 \pm 1$ fm (hard-sphere)
 - $\tau_{\text{emission}} = 1.5 \pm 1$ fm/c (Gaussian)
- } from spectra, v_2

PHOBOS Pion Correlations

$$C = 1 + \lambda e^{-Q_O^2 R_O^2 - Q_L^2 R_L^2 - Q_S^2 R_S^2 - 2Q_O Q_L R_{OL}^2}$$

$$0.2 < y < 1.5$$

$$0.15 < k_T < 0.35$$

Phobos preliminary

200 GeV Au-Au

15% most central events

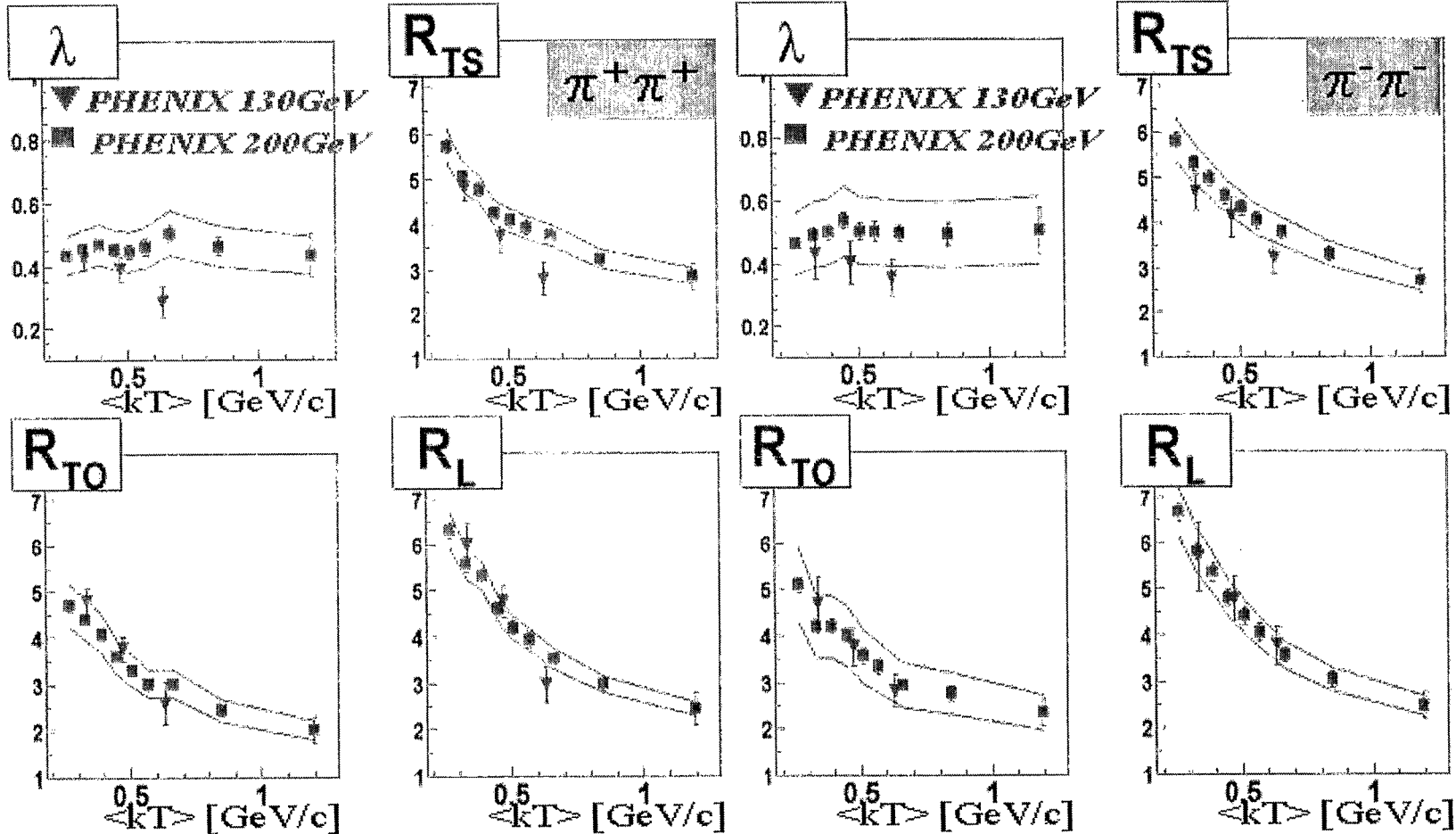
	λ	R_{out}	R_{side}	R_{long}	$R_{out-long}^2$
$\pi^- \pi^-$	0.54 ± 0.02	5.8 ± 0.2	5.1 ± 0.4	6.8 ± 0.3	4.9 ± 1.7
$\pi^+ \pi^+$	0.57 ± 0.03	5.8 ± 0.2	4.9 ± 0.4	7.3 ± 0.3	4.5 ± 1.9

Systematic error on radii of 1 fm, on λ of 0.06

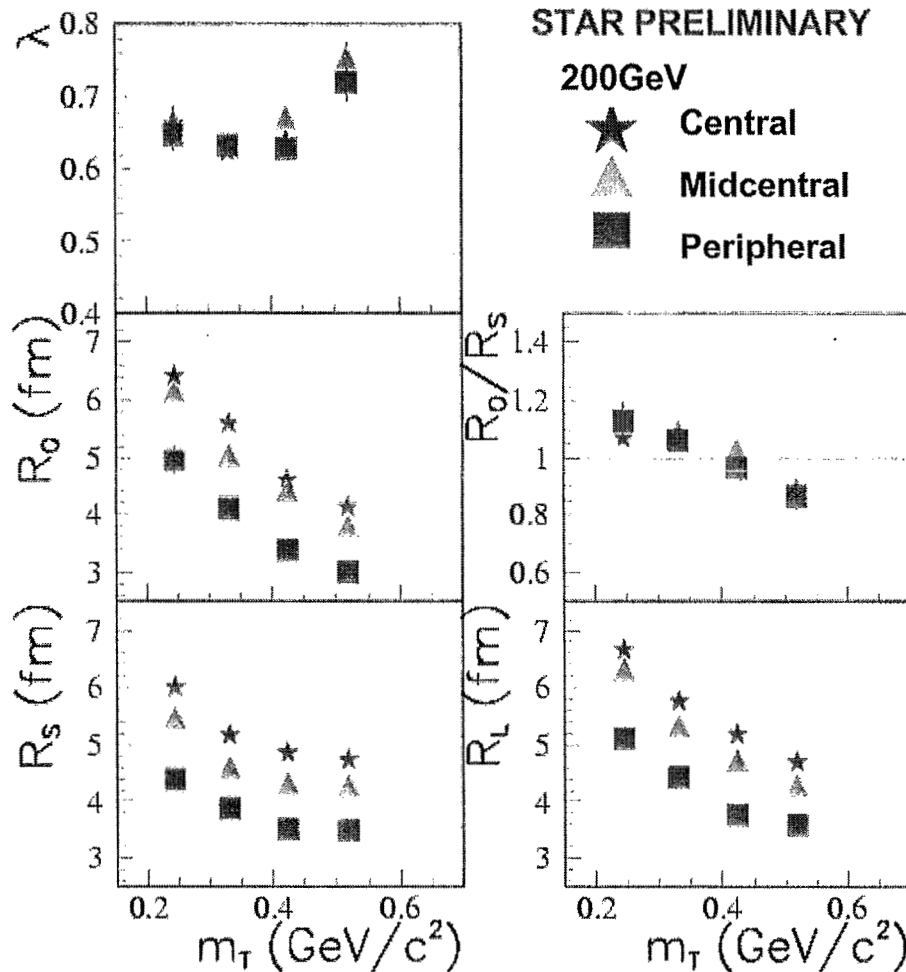
PHENIX kT dependence of source radii

Centrality is in top 30%

PHENIX PRELIMINARY



Centrality and m_T dependence at 200 GeV



R_L varies similar to R_O , R_S with centrality

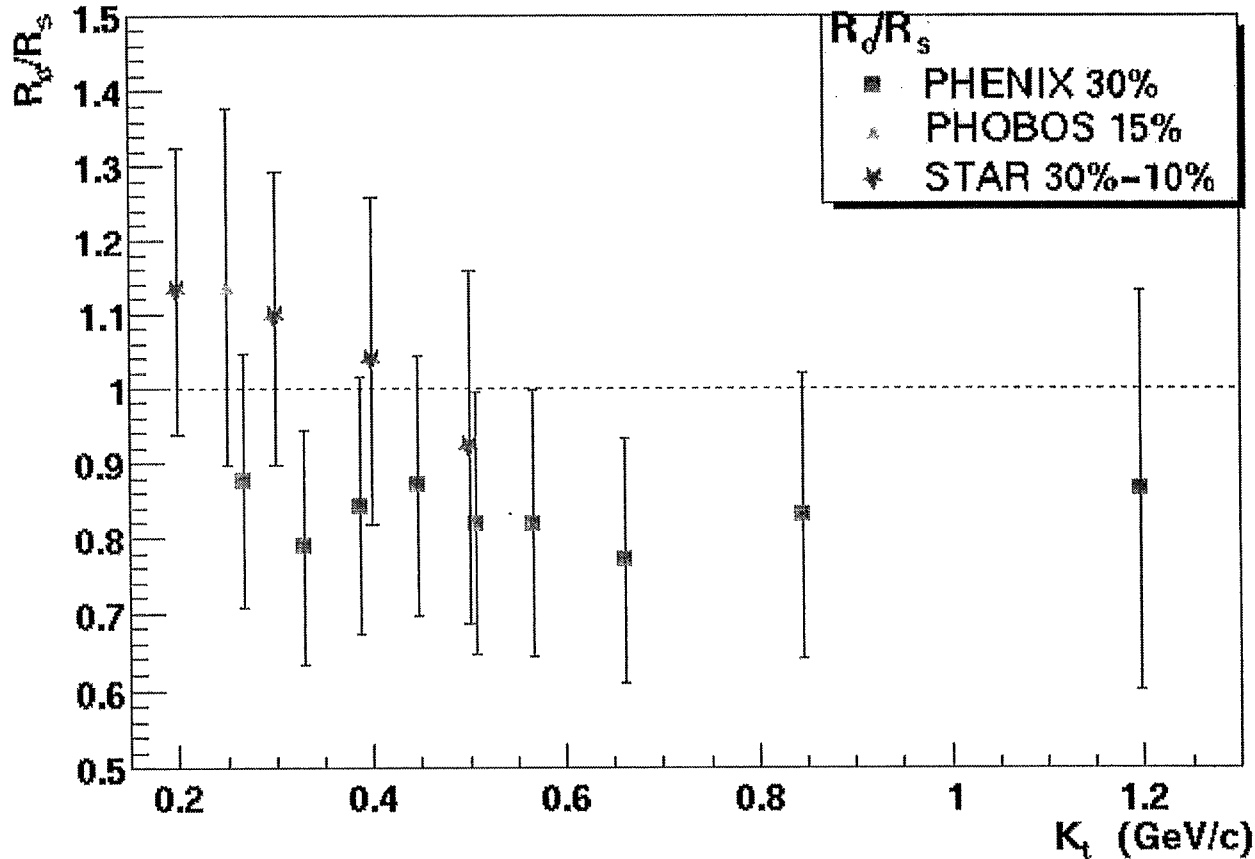
HBT radii decrease with m_T (flow)

Roughly parallel m_T dependence for different centralities

$R_O/R_S \sim 1$
(short emission time)

R_{out}/R_{side} Ratios at 200 GeV

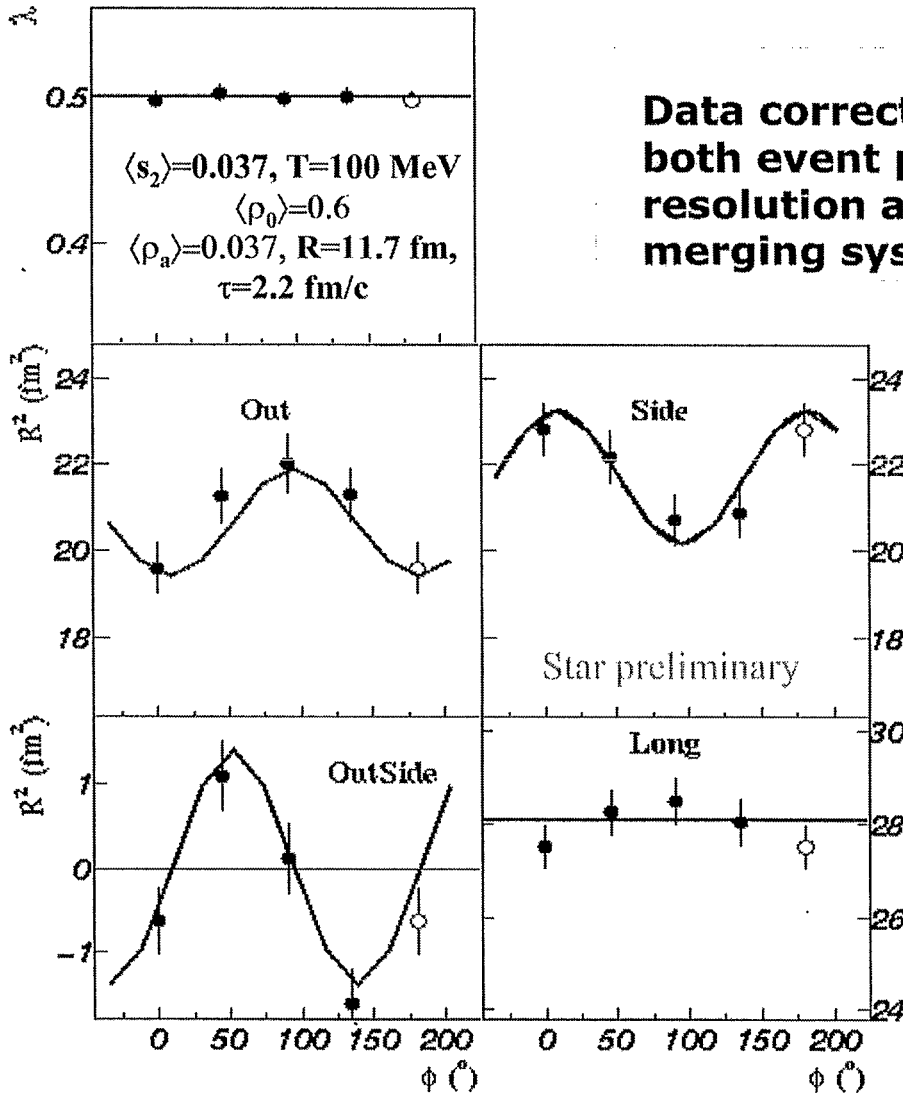
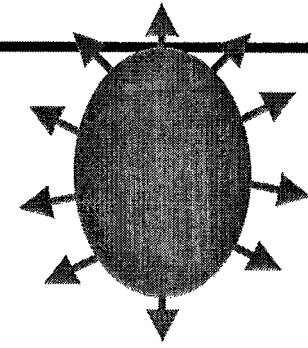
R_0/R_{side} , AuAu 200 GeV, Central



Ratio is <1 at high Pt (but note different centralities!)

Errors are statistical + systematic

HBT(ϕ) Results – 130 GeV



Minbias events @ 130 GeV

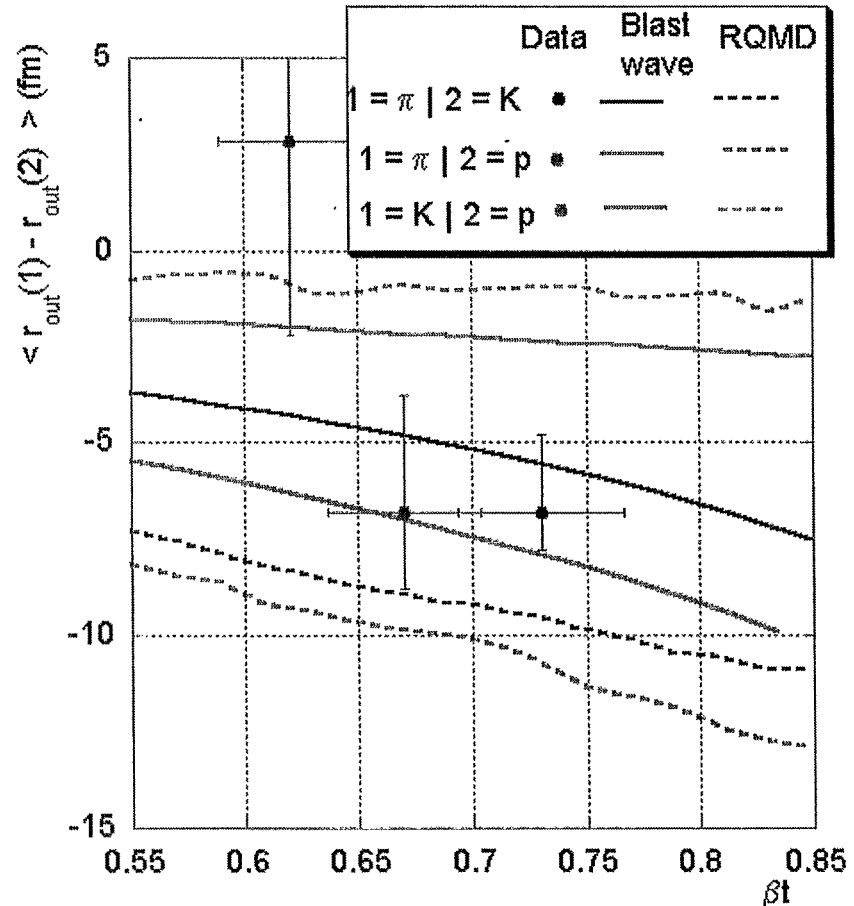
Bolstered statistics by summing results of π^- and π^+ analyses

Blast wave calculation (lines) indicates out-of-plane extended source

97

π -K, π -p and K-p combined

- ★ Blast wave consistent with data
- ★ RQMD overestimate shift between pions and kaons and pions and protons
- ★ Large systematic errors however



I discuss here only those strangeness measurements made by STAR in Au-Au collisions at $\sqrt{s_{NN}}=130$ and 200 GeV, those measurements made by the other RHIC experiments have been presented elsewhere at this workshop.

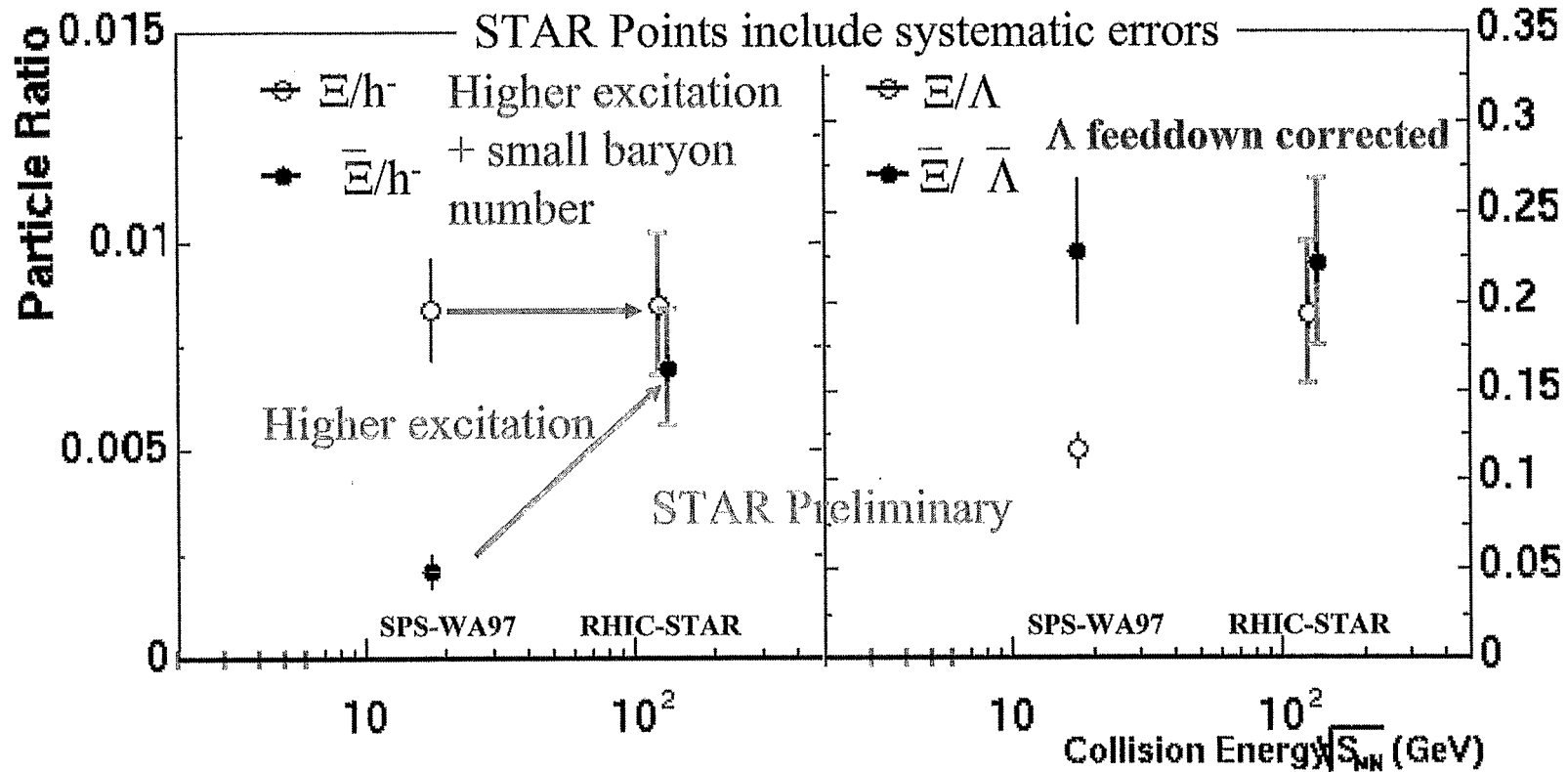
The anti-baryon to baryon ratios, p , Λ , Ξ and Ω , are all substantially higher than those at the SPS, but are still not unity indicating a finite net baryon number in the collisions. These ratios are flat as a function of p_t , rapidity and centrality. The anti- Ξ/h^- ratio increases from SPS to RHIC due to the increased excitation energy from the collision. However the enhancement caused by this increase in energy is, coincidentally, almost exactly canceled by the drop in net-baryon number in the case of the Ξ resulting in the Ξ/h^- ratio staying constant. The K/π is constant as a function of centrality and equal to that at the top SPS energy and centrality indicating that strangeness production per particle has reached saturation, a concept also suggested by the constancy in the ϕ/K^- as a function of centrality at RHIC and that the anti- Ξ /anti- Λ ratio at RHIC equals that of the SPS $\sqrt{s_{NN}}=20$ GeV collisions.

All ratios are well described by thermal models and suggest a chemical freeze-out temperature of ~ 175 MeV, $\mu_q \sim 10$ MeV, $\mu_s = 0$ MeV and $\gamma_s = 1$ at 130 GeV. Surprisingly the K^*/h^- ratio is also described by statistical models. As the K^* lifetime is close to that of the fireball it commonly decays inside the volume and hence does not get reconstructed due to the re-scattering of its daughters. A closer look at the K^* shows that the K^*/K ratio drops by only a factor of 2 from the ratio in pp collisions at the same energy. This can be taken as an indication that the rescattering phase of the collision is short.

Although the hadronic re-scattering phase appears short the m_T spectra indicate the fireball lives long enough to thermalise. The m_T spectra show an increase in inverse slope as a function of both particle mass and centrality suggesting transverse flow develops in the collisions. However many different models currently appear to be able to describe the particle spectra. Among the possible models are 1) Multi-strange (and heavier) particles freeze-out completely at T_{ch} while the lighter particles rescatter and freeze-out thermally only at a later time and with a significantly lower temperature (T_{th}). 2) All particles freeze-out at T_{ch} . 3) All particles freeze-out with a common T_{th} but $T_{th} < T_{ch}$. 4) There is no fixed T_{th} all particles freeze-out with different T_{th} but $T_{th} < T_{ch}$. While the 130 GeV Ω spectra cannot distinguish between the above scenarios they do rule out some possibilities. Fits show that if the Ω s freeze-out at $T_{th}=T_{ch}$ there is already significant flow in the system. This would indicate that a significant fraction of the transverse flow develops in the partonic phase of the collision. However the current spectra are equally well described by a smaller temperature and a higher flow velocity, which could be due solely to rescattering in the hadronic phase. A more detailed study is needed including all the measured particles.

In conclusion, the STAR detector has already provided a wealth of information on strange particle production in Au-Au collisions. The data seem to indicate a saturation of strangeness production per particle and this production is well described by thermal models. The resonance data indicate that the rescattering phase of the collision is short but that the fireball lives long enough to thermalise the system. The current data is unable to distinguish between several different kinematic scenarios and we are eagerly awaiting further running to aid our understanding of the collision dynamics.

Non-identical particle ratios

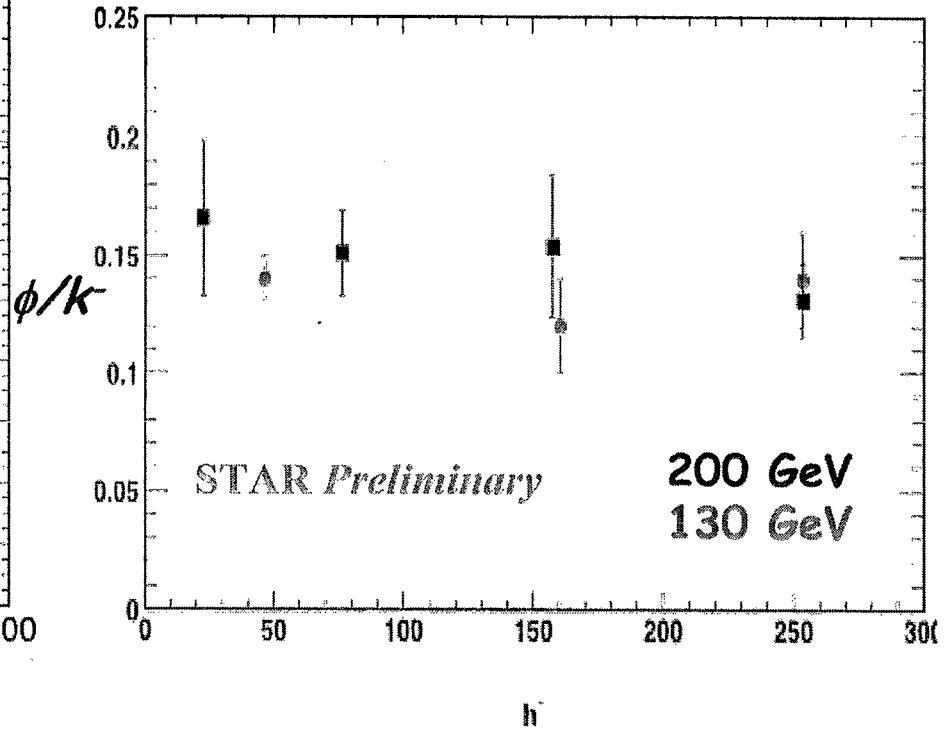
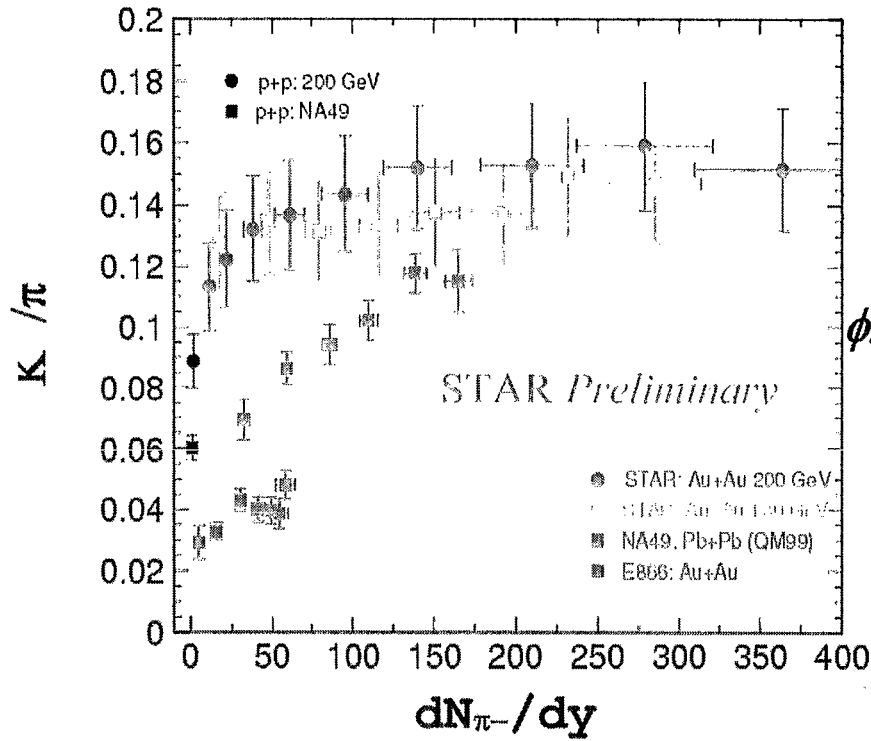


Combined effect of:

- Higher excitation
- Pair production becomes dominant, small net baryon number



Strange Particle Ratios



Appear to reach a saturation of strangeness production



Ratios, experiment vs. a model

Central
130 GeV Au+Au
Preliminary Data

Agreement between
model and data is
very good!

Thermal fits to mid-rapidity
spectra have caveats regarding
non- 4π measurements (local
vs. global equilibrium, boost-
invariance).

M. Kaneta and N. Xu,
J. Phys. G27 (2001) 589

$$\langle N_{\text{part}} \rangle = 345 \pm 7$$

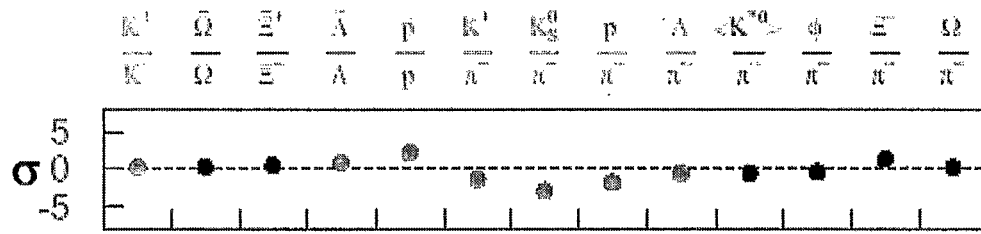
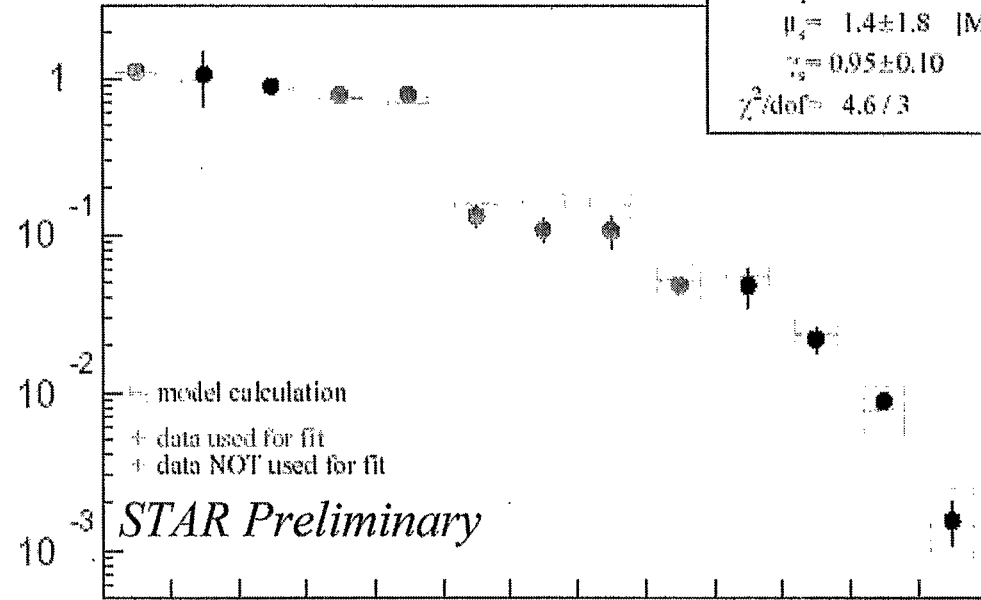
$$T_{\text{ch}} = 176 \pm 9 \text{ [MeV]}$$

$$\mu_q = 12.0 \pm 1.2 \text{ [MeV]}$$

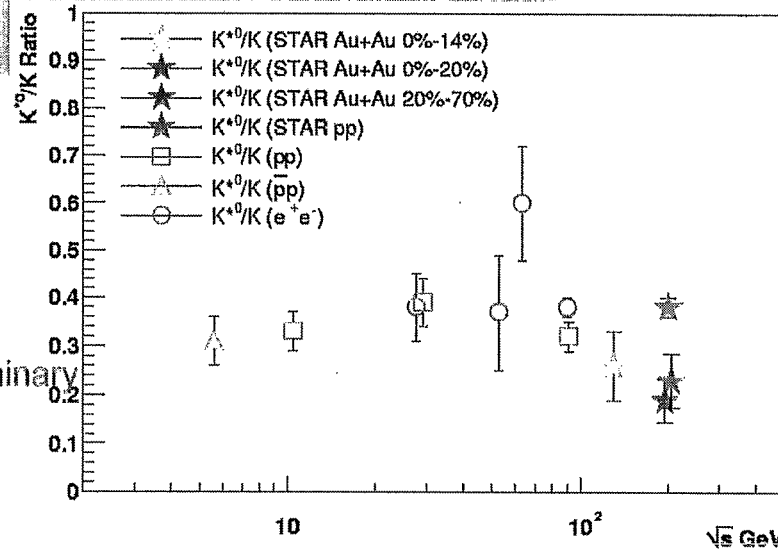
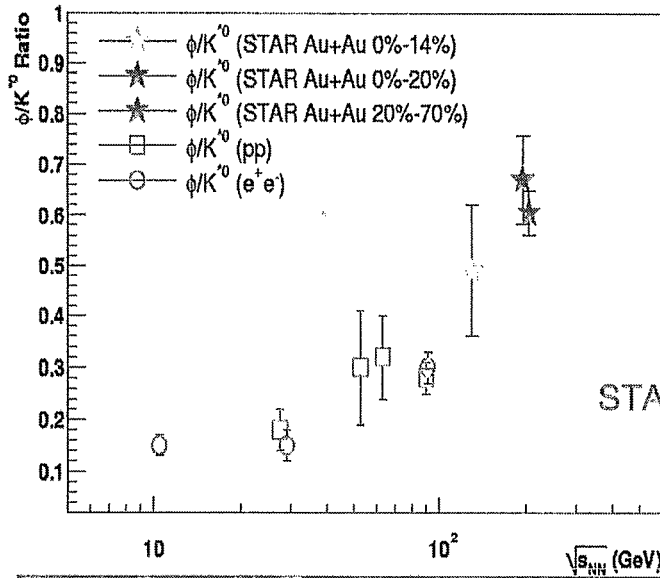
$$\mu_s = 1.4 \pm 1.8 \text{ [MeV]}$$

$$\chi_s = 0.95 \pm 0.10$$

$$\chi^2/\text{dof} = 4.6/3$$



K* ratios



- $\phi/K^{*0} \Rightarrow$ measures strangeness suppression in elementary collisions \Rightarrow small mass difference and $\Delta S = 1$
- ϕ/K^{*0} Au+Au at RHIC \Rightarrow increase compared to pp and e^+e^-
- Strangeness Enhancement? \Rightarrow not that simple due to additional effects on short-lived resonances in heavy ion collisions

$K^{*0} \Rightarrow JP = 1^-$
 $K \Rightarrow JP = 0^-$
 K^{*0} and $K \Rightarrow$ similar quark content and different spin
 $\sqrt{s_{NN}} = 200$ GeV at RHIC \Rightarrow Au+Au K^{*0}/K lower than pp K^{*0}/K by a factor of 2!

- $\sqrt{s_{NN}} = 130$ GeV \Rightarrow statistical and systematic errors added quadratic
- $\sqrt{s_{NN}} = 200$ GeV \Rightarrow statistical error only

Transverse Mass Spectra

130 GeV

Try fitting Ω 's to several Blast wave scenarios

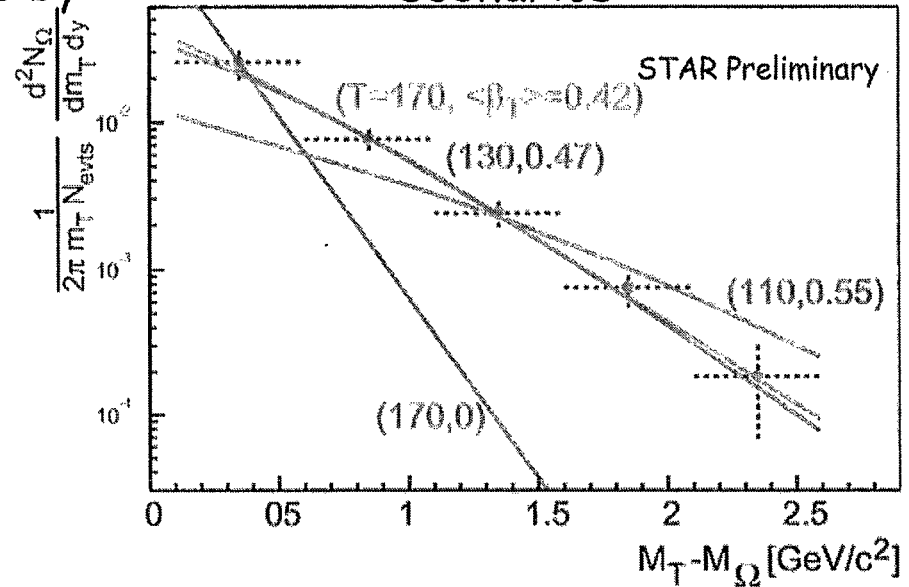
Can currently get equally good fits by using any of these 4 models

Multi-Strange + heavier particles freeze-out at T_{ch}

All particles freeze-out and T_{ch}

All particles freeze-out at common T_{th}

No fixed freeze-out



Clearly the Ω needs some flow.

Not possible to distinguish between high T low flow or low T high flow

104



Jets and Dijets in p+p and Au+Au collisions at RHIC

David Hardtke for the STAR collaboration
Lawrence Berkeley National Laboratory
Berkeley, CA 94720

The origin of high p_T of particles in heavy-ion collisions at RHIC is of considerable interest due to the observation of a suppression of single inclusive high p_T hadron yields relative the binary scaling expectation. In addition, the proton-to-pion ratio has been observed to be rather large (≈ 1) above $p_T = 2$ GeV/c. The suppression of the inclusive yields is what would be expected in the case of parton energy loss, while the p/π ratio would suggest that some other mechanism besides hard scattering and fragmentation contributes to the particle production at moderate to large p_T .

To verify the existence of a hard scattering and fragmentation component at high p_T , STAR uses two-particle azimuthal correlations among high p_T hadrons. At small relative azimuth, an enhancement is seen in both the central Au+Au and minimum bias p+p data. This enhancement has been measured independently for same sign and opposite sign hadron pairs, and the enhancement ≈ 2.5 times larger for the opposite sign hadron pairs. This is consistent with known properties of jet fragmentation.

To compare the azimuthal correlations in p+p and Au+Au, STAR assumes that the only correlations between independent hard scatterings are due to elliptic flow. Making this assumption, and using independently measured v_2 values, STAR shows that the small relative azimuth correlations are similar in p+p and all centralities of Au+Au collisions. In striking contrast, back-to-back azimuthal correlations disappear with increasing collision centrality, and there is a near complete suppression of back-to-back azimuthal correlations in the most central Au+Au collisions.

A simple picture that can explain the suppression of the inclusive hadron yields, the large and saturated v_2 at high p_T and the disappearance of back-to-back azimuthal correlations is a system that is opaque to the propagation of partons. In this picture, only partons produced near the surface of the system are observed.

Two-particle azimuthal correlations

- Identify jets on a *statistical* basis
- Given a trigger particle with $p_T > p_T(\text{trigger})$, associate particles with $p_T > p_T(\text{associated})$,

$$C_2(\Delta\phi, \Delta\eta) = \frac{1}{N_{TRIGGER}} \frac{1}{\text{Efficiency}} N(\Delta\phi, \Delta\eta)$$

- Efficiency for finding trigger particle cancels
- C_2 is probability to find another particle at $(\Delta\phi, \Delta\eta)$
- $p_T(\text{associated}) > 2 \text{ GeV}/c$
- $p_T(\text{trigger})$: 4-6 GeV/c, 3-4 GeV/c, 6-8 GeV/c
- $|\eta| < 0.7 \Rightarrow |\Delta\eta| < 1.4$

- STAR analysis for 200 GeV data:

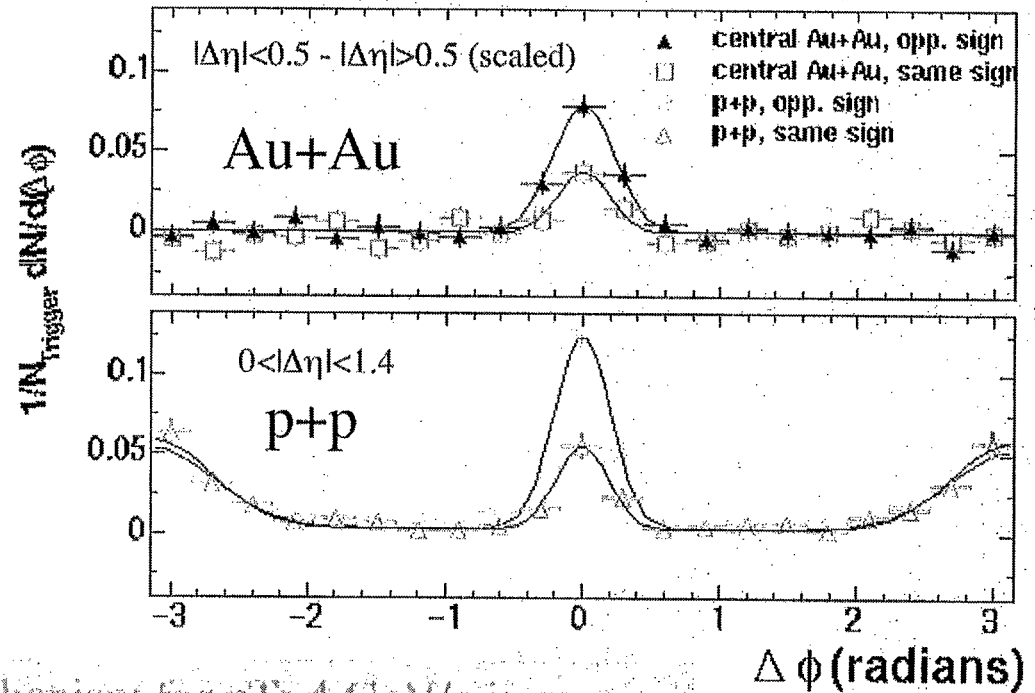
- p+p Minbias: $\approx 10 \text{ M}$ events
- Au+Au Minbias: 1.7 M events, Au+Au central: 1.5 M events

Relative Charge Dependence

Strong dynamical
charge correlations in
jet fragmentation \rightarrow

Compare ++ and --
charged azimuthal
correlations to +-
azimuthal correlations

STAR Preliminary @ 200 GeV/c
0-10% most central Au+Au
p+p minimum bias
 $4 < p_T(\text{trig}) < 6$ GeV/c
 $2 < p_T(\text{assoc.}) < p_T(\text{trig})$



System	(+-)/(++ & --)
p+p	2.7 ± 0.6
0-10% Au+Au	2.4 ± 0.6
Jetset	2.6 ± 0.7

Same particle production mechanism for $p_T > 4$ GeV/c in pp
and central Au+Au

August 8, 2002

David Hardtke - LBNL



Comparing Au+Au and p+p

- Ansatz: high p_T triggered Au+Au event is superposition of high p_T triggered p+p event and elliptic flow:

$$C_2(Au + Au) = C_2(p + p) + A^* (1 + 2v_2^2 \cos(2\Delta\phi))$$

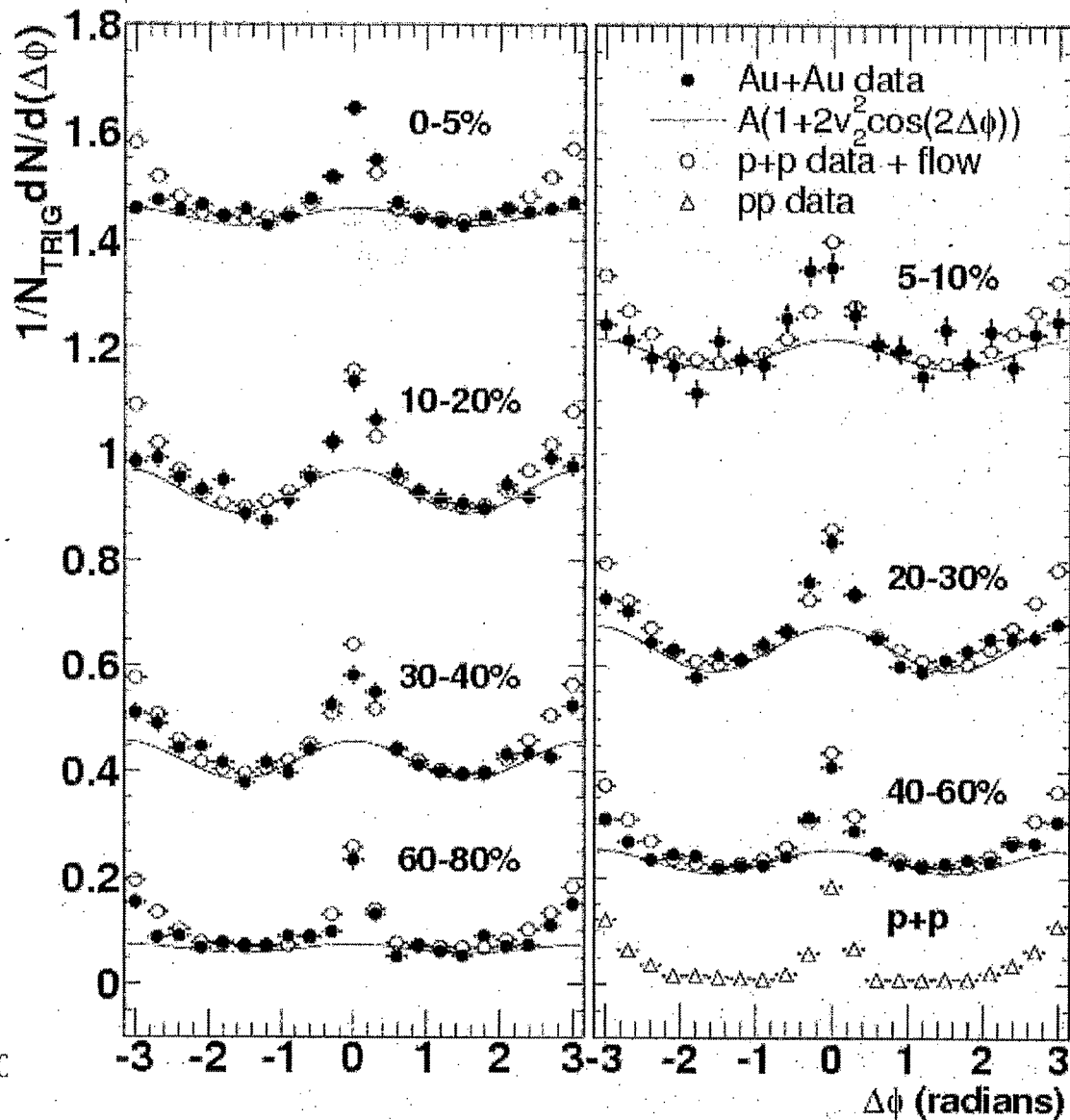
– v_2 from reaction plane analysis

– A fit in non-jet region ($0.75 < |\Delta\phi| < 2.24$)

- Quantify deviations for jet cone region ($|\Delta\phi| < 0.75$) and back-to-back region ($2.24 < |\Delta\phi| < 3.14$):

$$ratio = \frac{\int d(\Delta\phi) [C_2(Au + Au) - A^* (1 + 2v_2^2 \cos(2\Delta\phi))]}{\int d(\Delta\phi) [C_2(p + p)]}$$

$4 < p_t(\text{trig}) < 6 \text{ GeV}/c$ data

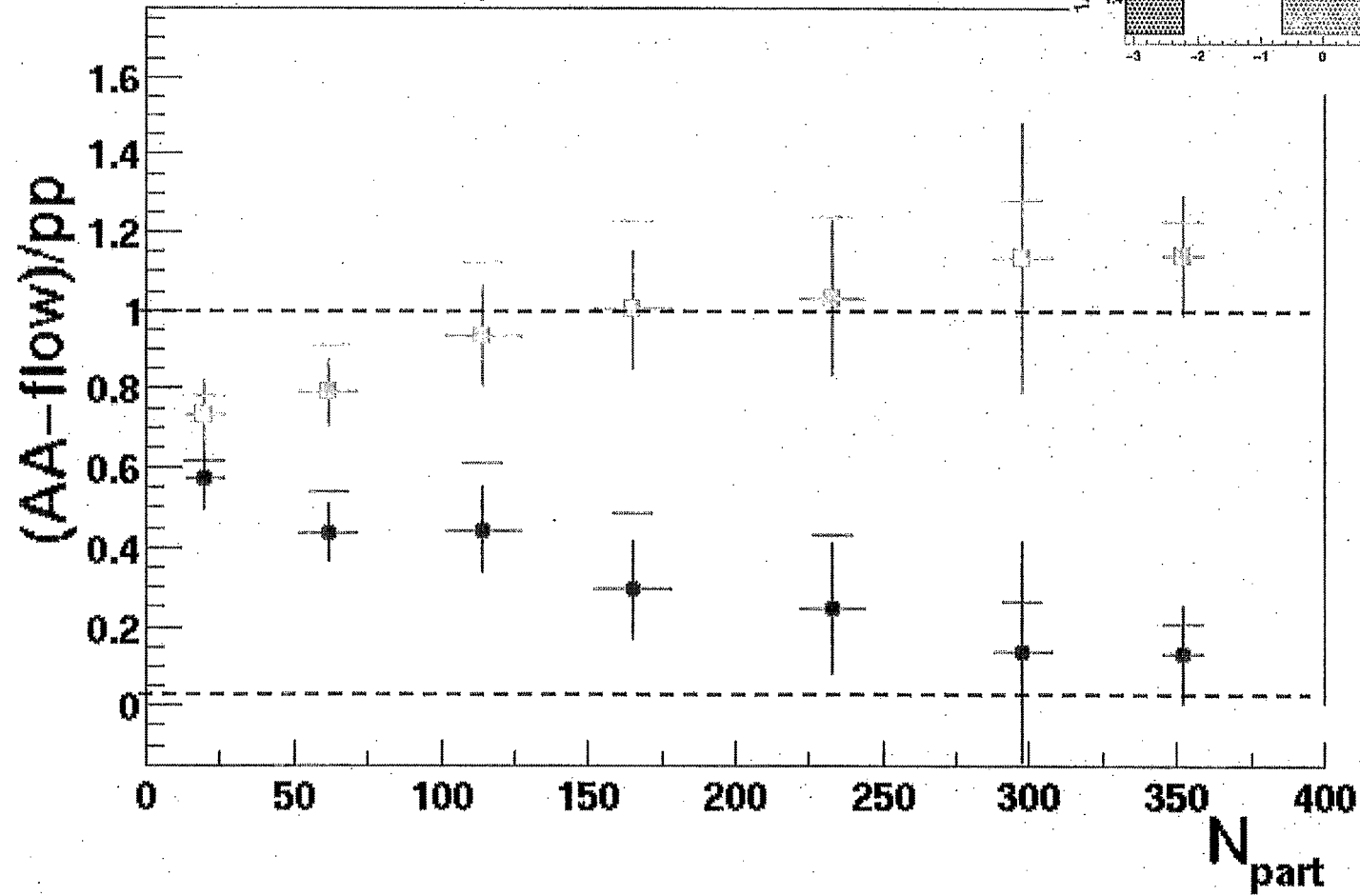
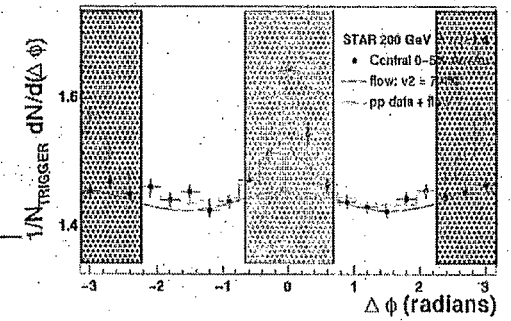


August 8, 200



Ratio vs. # participants

- $|\Delta\phi| < 0.75, 4 < p_T(\text{trig}) < 6 \text{ GeV}/c$
- $|\Delta\phi| > 2.25, 4 < p_T(\text{trig}) < 6 \text{ GeV}/c$



110

August 8, 2002

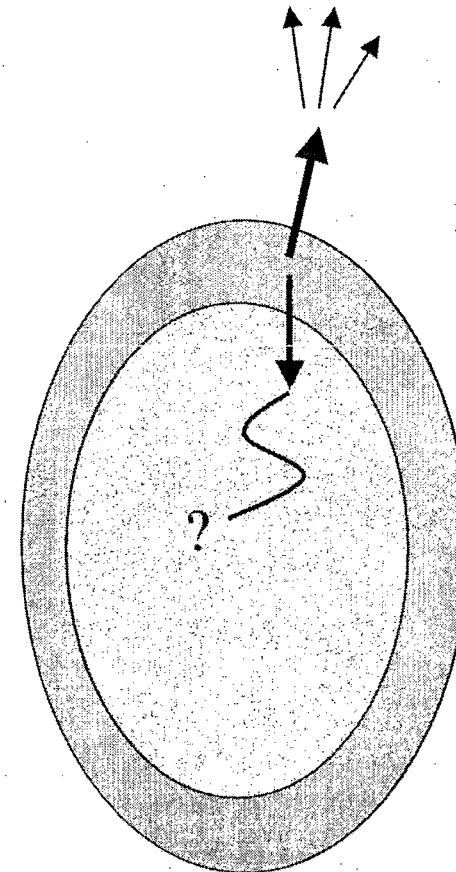
David Hardtke - LBNL



High p_T particle production @ RHIC

- Known previously
 - Suppression of inclusives compared to binary collision scaling
 - Saturation of v_2
- This talk
 - High p_T charged hadrons dominated by jet fragments
 - Relative charge
 - Azimuthal correlation width
 - Evolution of jet cone azimuthal correlation strength with centrality
 - Suppression of back-to-back correlations in most central Au+Au collisions

Surface emission!



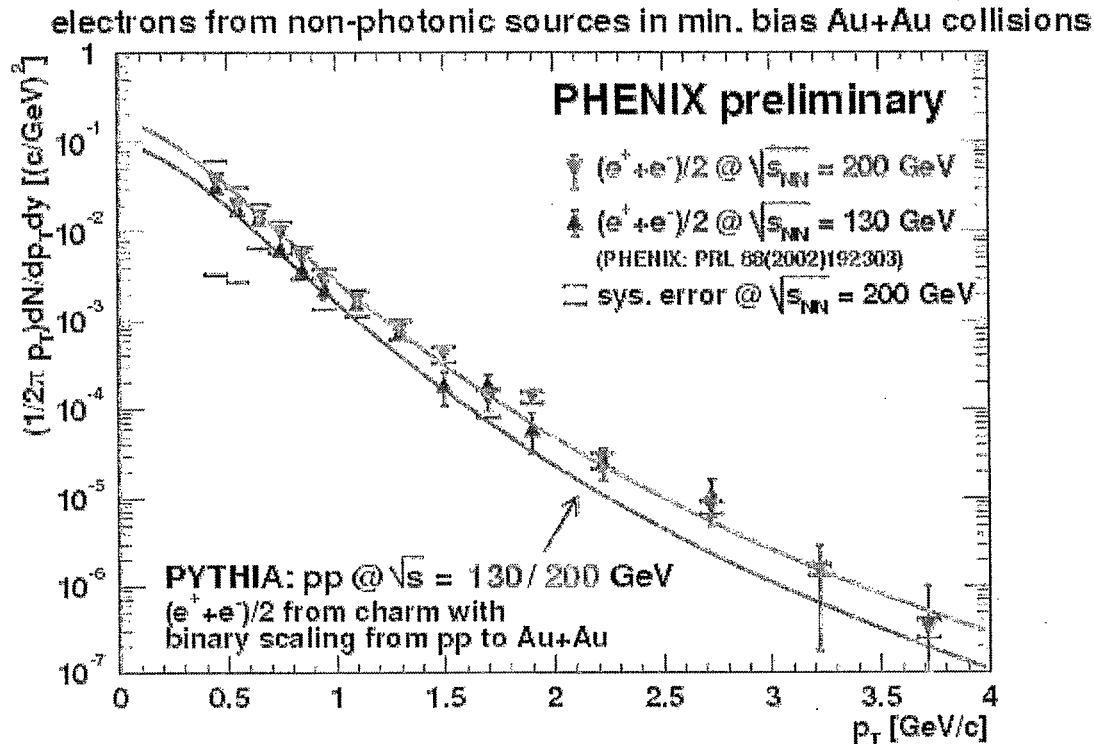
Bjorken '82

Charm and J/PSI measurement at RHIC

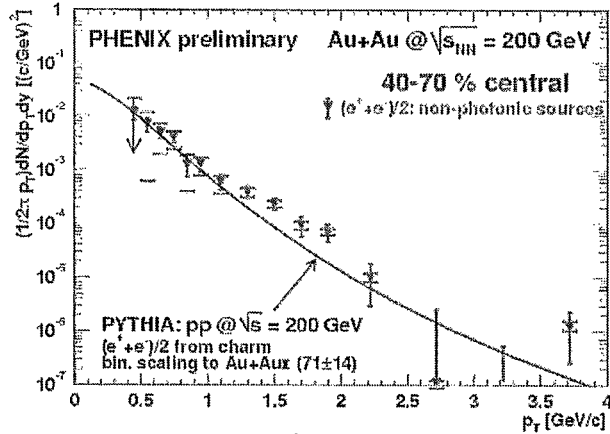
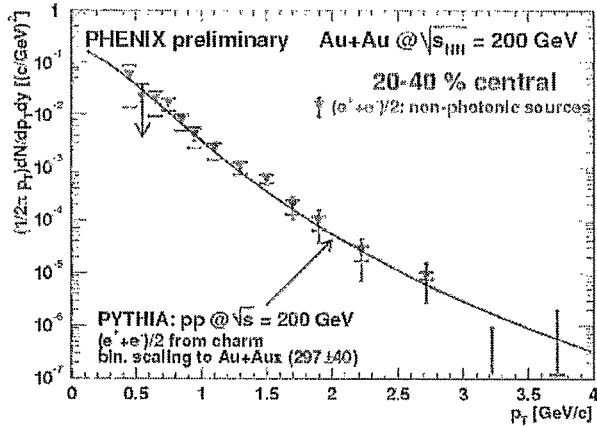
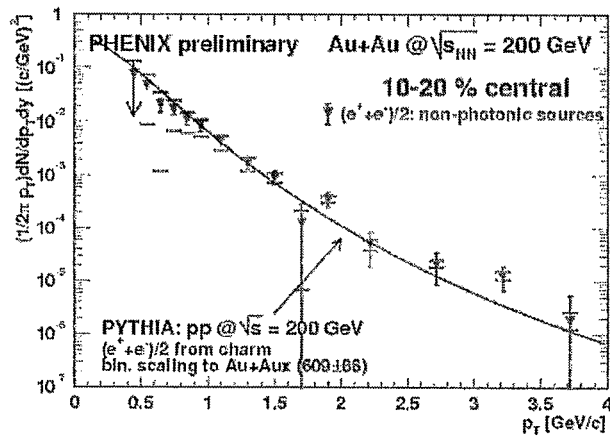
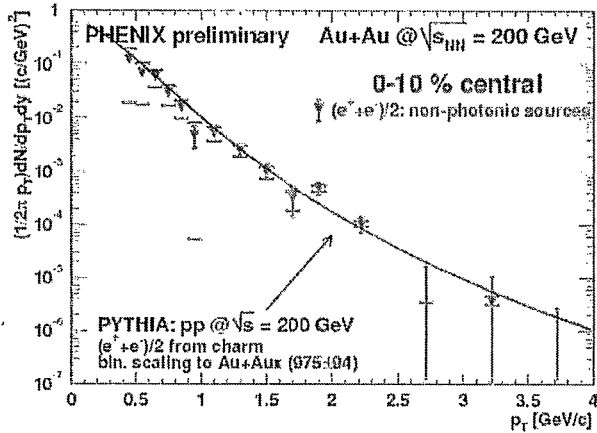
Y. Akiba (KEK)

August 9, 2002

Riken Summer study 2002



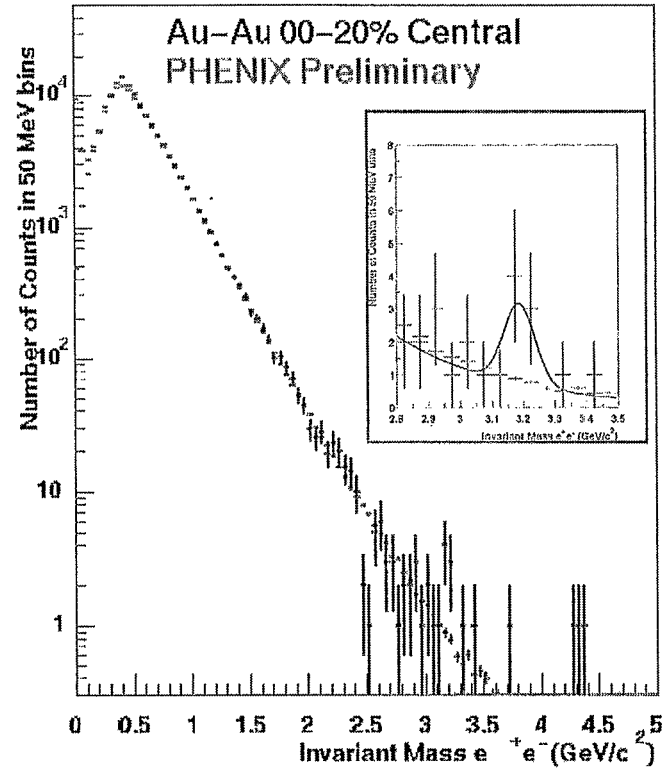
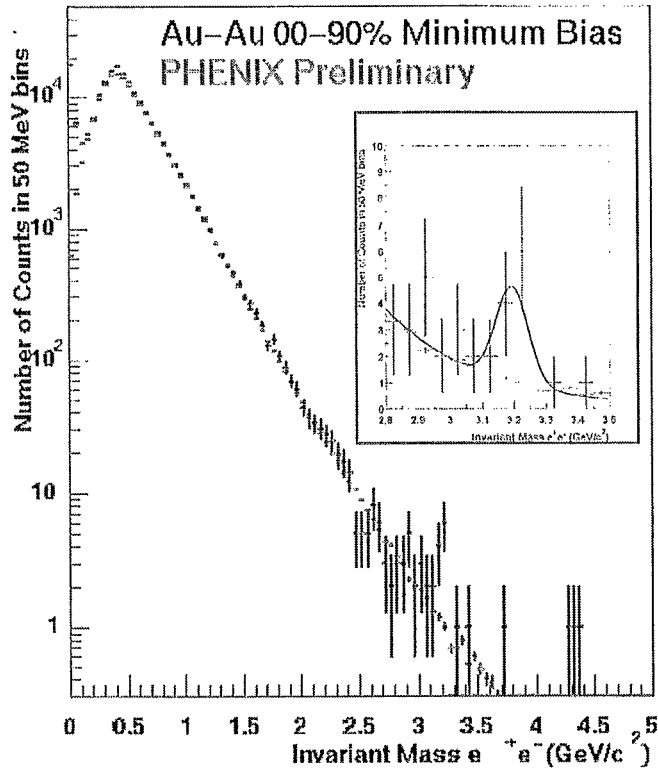
- The yield of non-photonic electron at 200 GeV is higher than 130 GeV
- The increase is consistent with PYTHIA charm calculation
 $(\sigma_{cc}(130\text{GeV})=330 \mu\text{b} \rightarrow \sigma_{cc}(200\text{GeV})=650 \mu\text{b})$
- Large systematic uncertainty due to material thickness without converter. The error will be reduced in the final result.



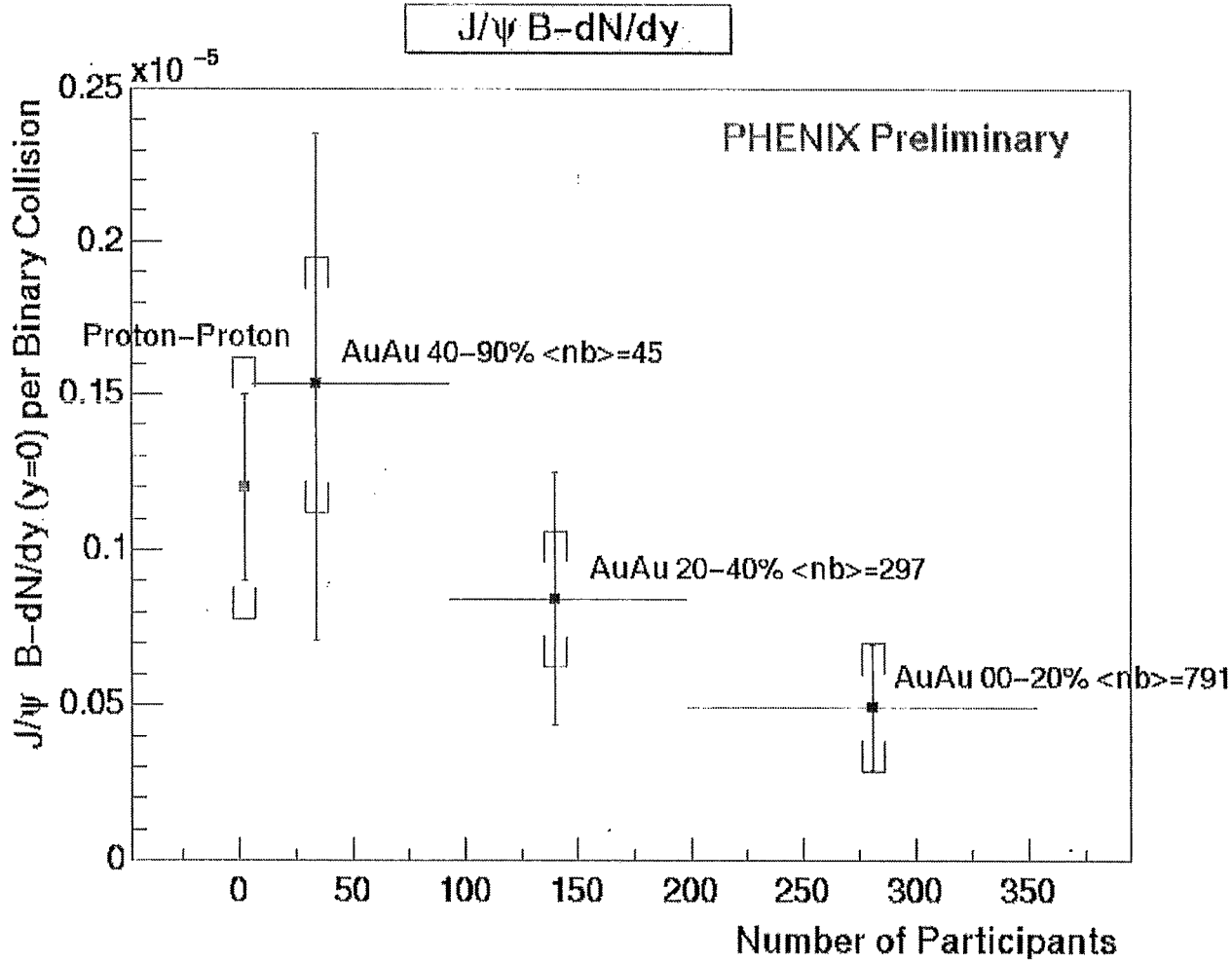
$J/\psi \rightarrow e^+e^-$ in Gold-Gold !

$N = 10.8 \pm 3.2$ (stat) ± 3.8 (sys)

$N = 5.9 \pm 2.4$ (stat) ± 0.7 (sys)



J/ψ B-dN/dy per binary collision



- PHENIX has measured single electrons from charm decay in Au+Au collision at RHIC
- Single electron data is consistent with the binary scaling
 - No or little nuclear shadowing effect in charm production?
 - No or little energy loss for charm quark?
 - Important input to understand high pt suppression
 - We are working to reduce systematic errors of the measurement
- PHENIX made the first measurement of J/Ψ in p+p and Au+Au at RHIC
 - Present statistics is too limited to draw any conclusion on J/Ψ suppression, but some J/Ψ formation models can be excluded from the data
 - We have about factor 2 more statistics in RUN-2
 - Future high statistics Au+Au run is needed to make a decisive measurement of J/Ψ suppression at RHIC

PHENIX AA Related Upgrades

Craig Woody
Brookhaven National Lab

August 9, 2002

The PHENIX experiment at RHIC is a large multipurpose detector designed to discover and explore new states of matter produced in relativistic heavy ion collisions in a new energy regime, and to study the spin structure of the nucleon in polarized proton interactions. It has a wide range of capabilities that allows it to make detailed measurements of the production of leptons, photons, jets, high p_T particles, transverse energy, flow, and numerous other quantities of physics interest in these types of collisions. The RHIC collider has now had two successful physics runs, including the most recent run in which the design luminosity was reached for Au+Au collisions, along with the first polarized proton run. During these first two runs, the PHENIX detector was only partially complete. However, many new and interesting results have already been produced with the data obtained thus far. The final major components of the detector will be installed during the 2002 RHIC shutdown period, which will complete the baseline configuration of the detector in time for the third physics run at RHIC starting in the fall of 2002.

With the successful startup of RHIC and its four experiments, there are now plans to increase the luminosity of the machine, possibly by a factor of 40 above the design value through its proposed upgrade to RHIC II. This will open up many new possibilities for exploring new physics, particularly those involving rare processes in both heavy ion and polarized proton collisions. The PHENIX experiment has also begun to make plans to enhance the physics capabilities and extend the physics reach of its present baseline detector to meet these new challenges as the experimental program moves from the initial "discovery" phase to one of a detailed study of matter at extreme temperatures and densities, and of the spin structure of the nucleon. This talk discusses the present status of these plans along with some of the new physics topics that could be studied with an upgraded detector.

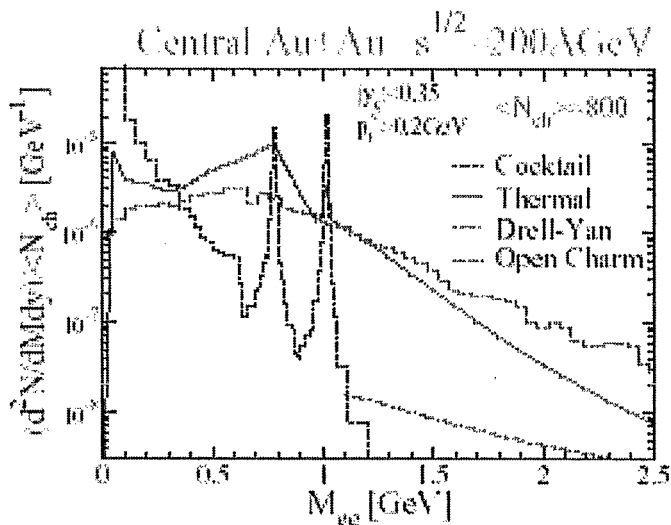
New Physics to be Addressed with an Upgraded PHENIX Detector

- Low mass dilepton pairs
- Improved measurements of heavy flavor (c,b) production
- Jet studies and γ -jet correlations
- High p_T identified particles
- Rare processes
 - Inclusive particle spectra and direct γ s out to high p_T
 - Drell-Yan continuum above the J/ψ
 - Upsilon spectroscopy - $\Upsilon(1S), \Upsilon(2S), \Upsilon(3S)$
 - W-production
 - ...

Low Mass Electron Pairs in PHENIX

Total Combinatorial Background

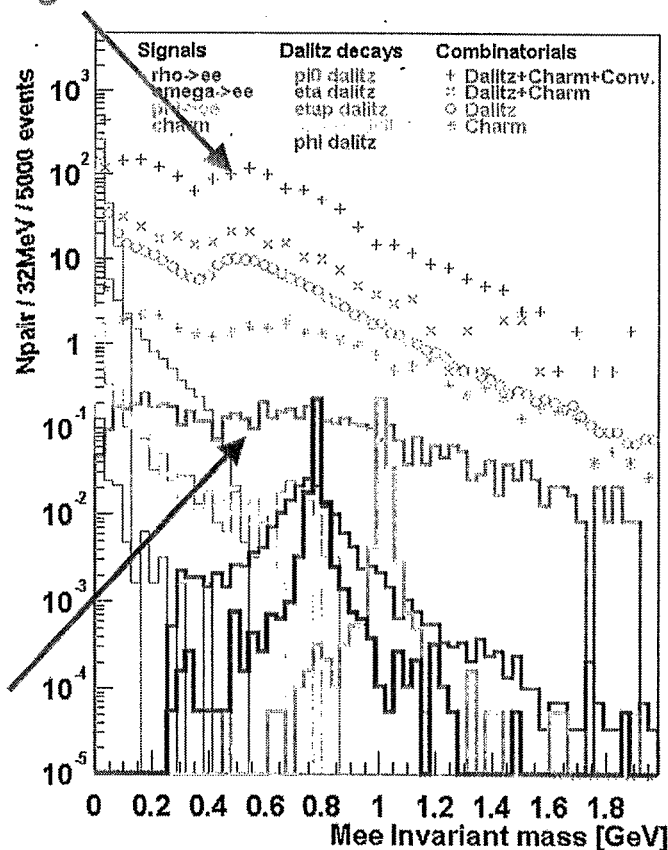
Poster at QM2002
K. Ozawa and C. Aidala

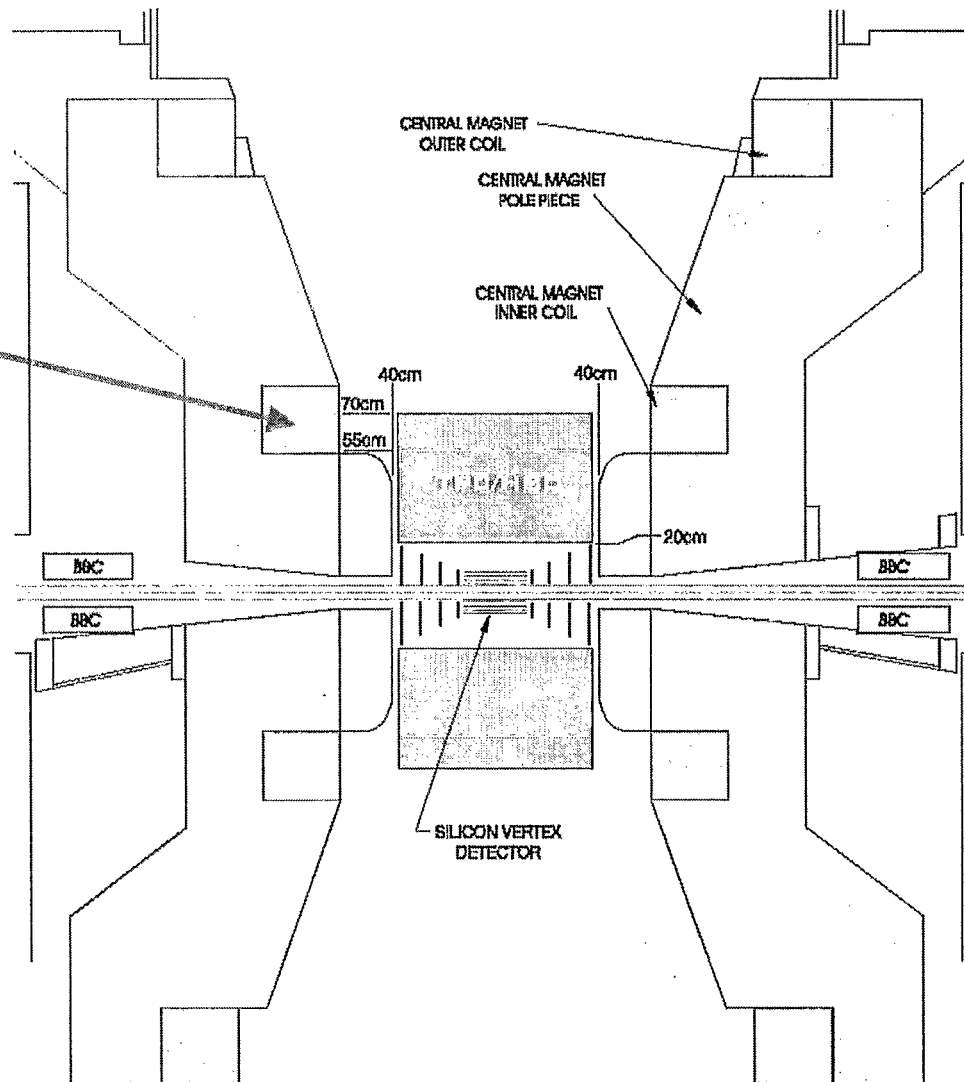


Dilepton spectra from central Au-Au collisions at full RHIC energy

R.Rapp

Charm signal





Inner Coil creates a "field free" ($|B_{\parallel}|=0$) region inside the Central Magnet

TPC tracking coverage

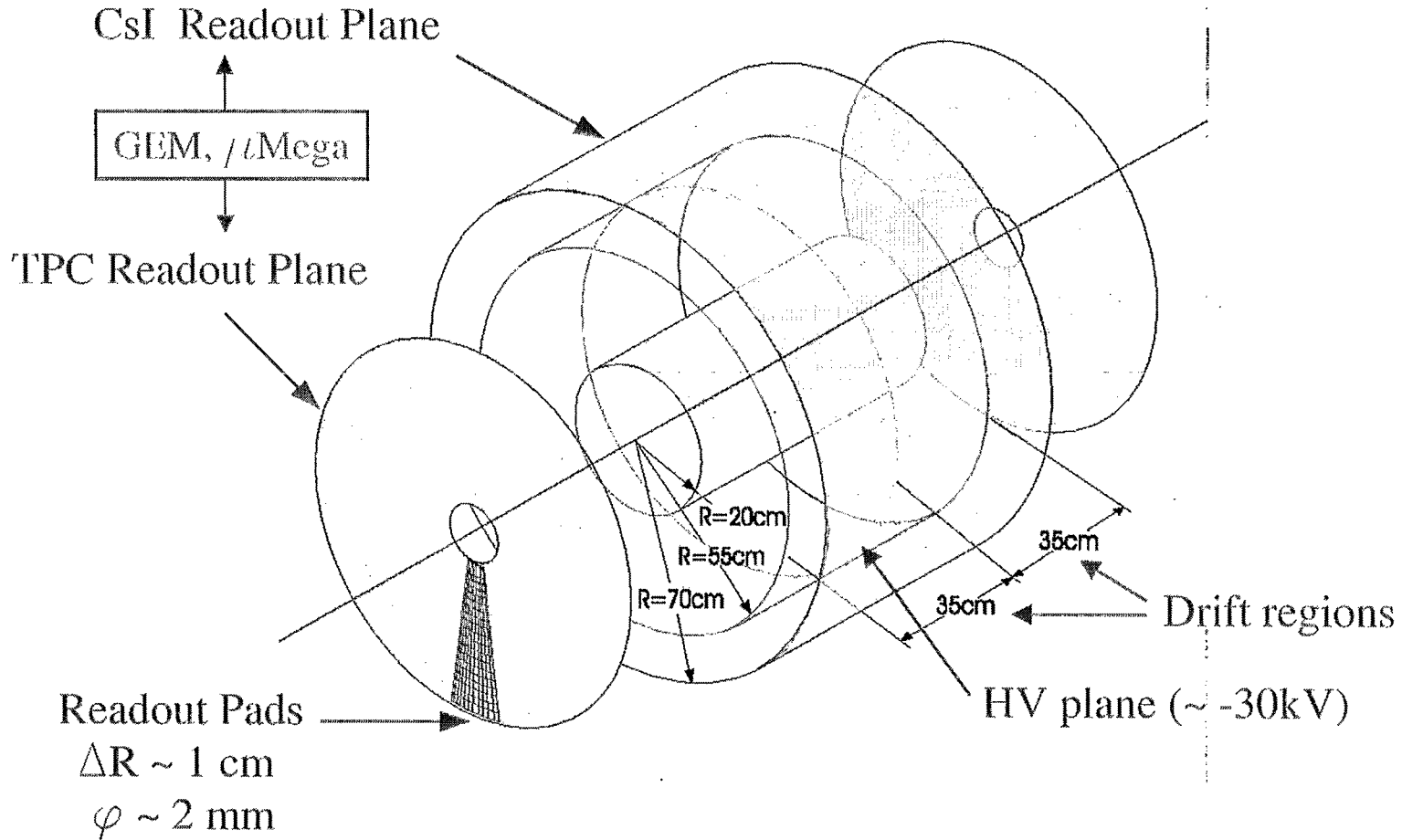
$$\Delta\varphi = 2\pi$$

$$|\eta| < 1.0$$

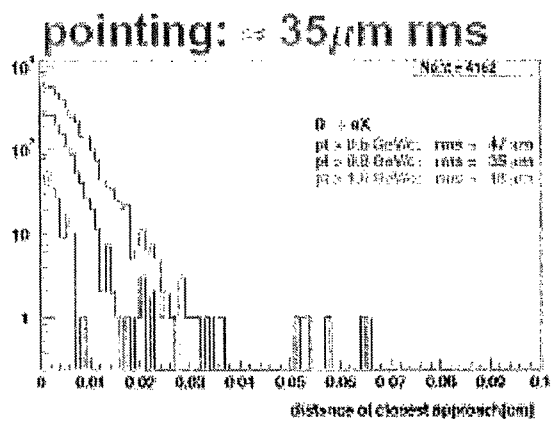
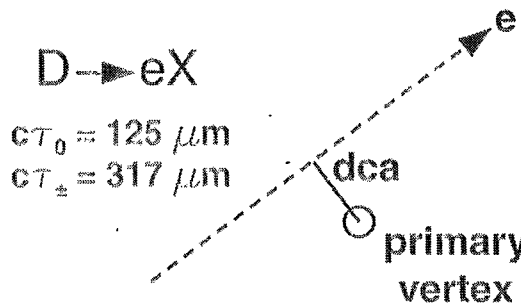
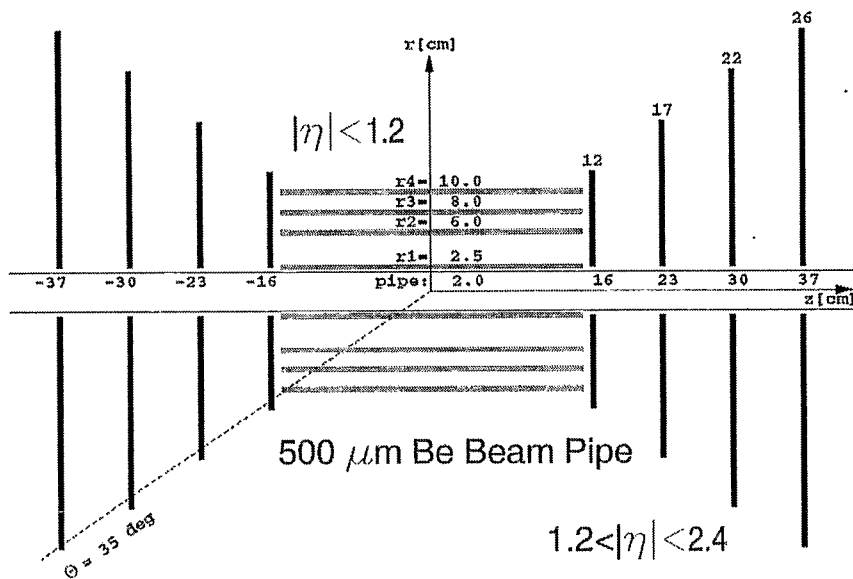
$$\delta p_T/p_T \sim .02p$$

Assembly being installed during 2002 shutdown

TPC/HBD Conceptual Design (PHENIX + STAR)



123

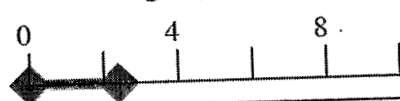
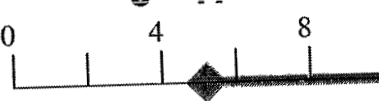
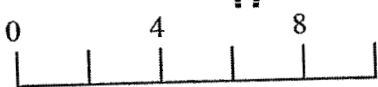
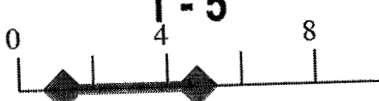


- Pixel barrels ($50 \mu\text{m} \times 425 \mu\text{m}$)
- Strip barrels ($80 \mu\text{m} \times 3 \text{ cm}$)
- Pixel disks ($50 \mu\text{m} \times 4 \text{ mm}$)

1.0% X_0 per layer

Simulation by J. Heuser

Extended PID with Aerogel

		Pion-Kaon separation	Kaon-Proton separation
TOF	$\sigma \sim 100$ ps	0 - 2.5 	0 - 5 
RICH	$n=1.00044$ $\gamma_{th} \sim 34$	5 - 17 	17 - 
Aerogel	$n=1.007$ $\gamma_{th} \sim 8.5$	1 - 5 	5 - 9 

Y. Miake

Aerogel together with TOF can extend the PID capability up to ~ 10 GeV/c

Current and Future Physics at RHIC

Dmitri Kharzeev

*Physics Department,
Brookhaven National Laboratory
Upton, NY 11973, USA*

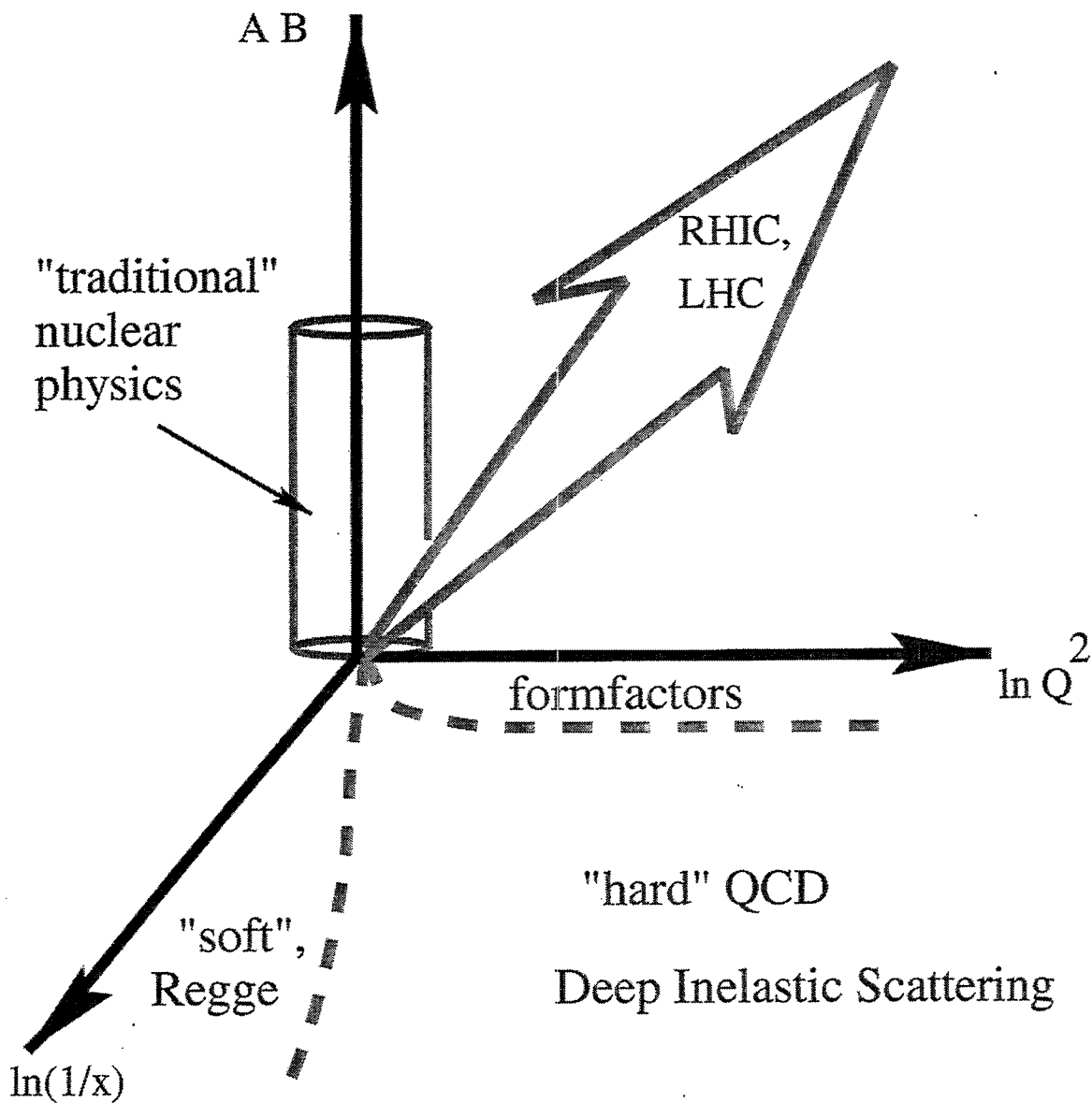
In this talk, I review the physics goals of the RHIC program and the results obtained so far. The highlights include the data on hadron multiplicity and its centrality, energy, and rapidity dependences; particle composition; the azimuthal anisotropy of particle production; suppression of high p_t particles; unusually large baryon component at high transverse momentum; and charm production inferred from the single electron spectrum. I discuss the significance of these results and their theoretical interpretations. The future directions for the RHIC program are discussed as well.

Current and Future Physics at RHIC

D. Kharzeev

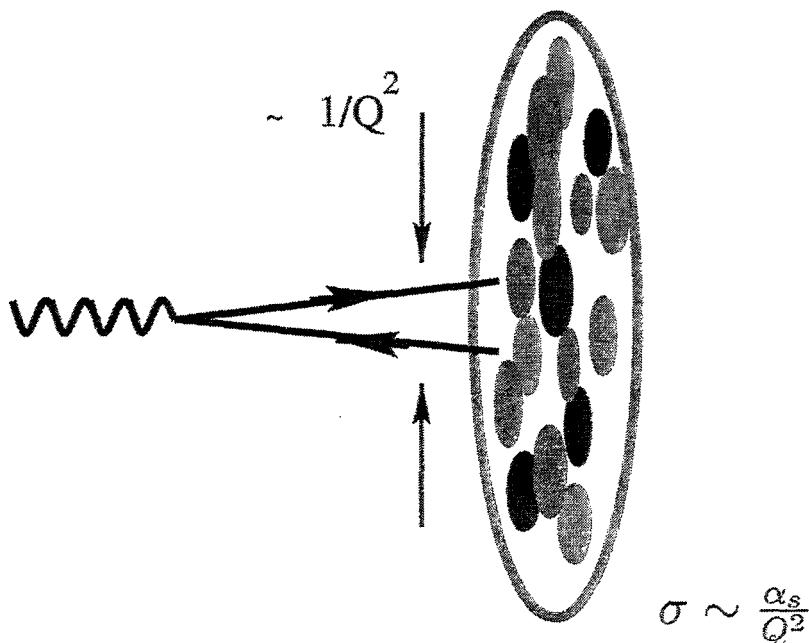
1. Why study QCD at RHIC?
2. What do we expect to find?
3. Looking at the first RHIC data
4. What do we learn?
5. The future

QCD and Heavy Ions



High parton density regime of QCD

$$\rho_A = \frac{\text{Number of partons}}{\text{area}} \simeq \frac{xG_A(x, Q^2)}{\pi R_A^2} \simeq A^{1/3}$$



- $\sigma \rho_A \ll 1$ – dilute regime, incoherent interactions
- $\sigma \rho_A \gg 1$ – dense parton system

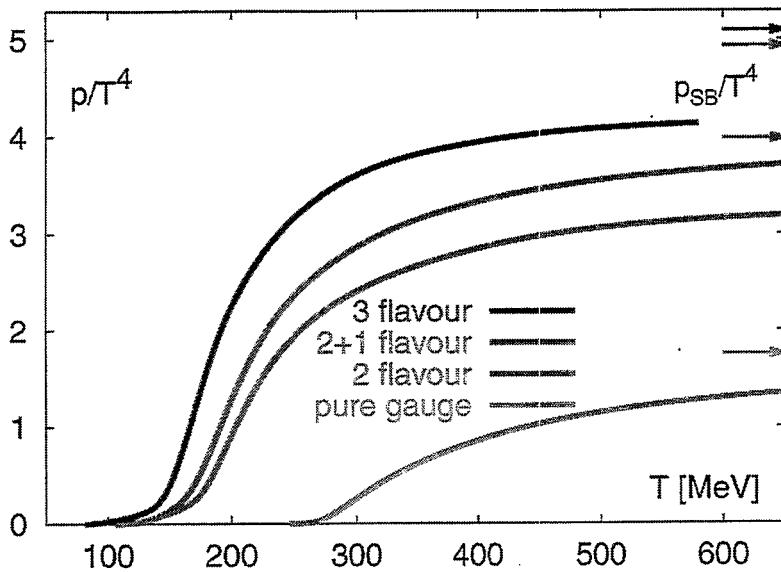
Qualitatively new regime in QCD

“saturation”; “colored glass”; classical theory?

Phase transitions

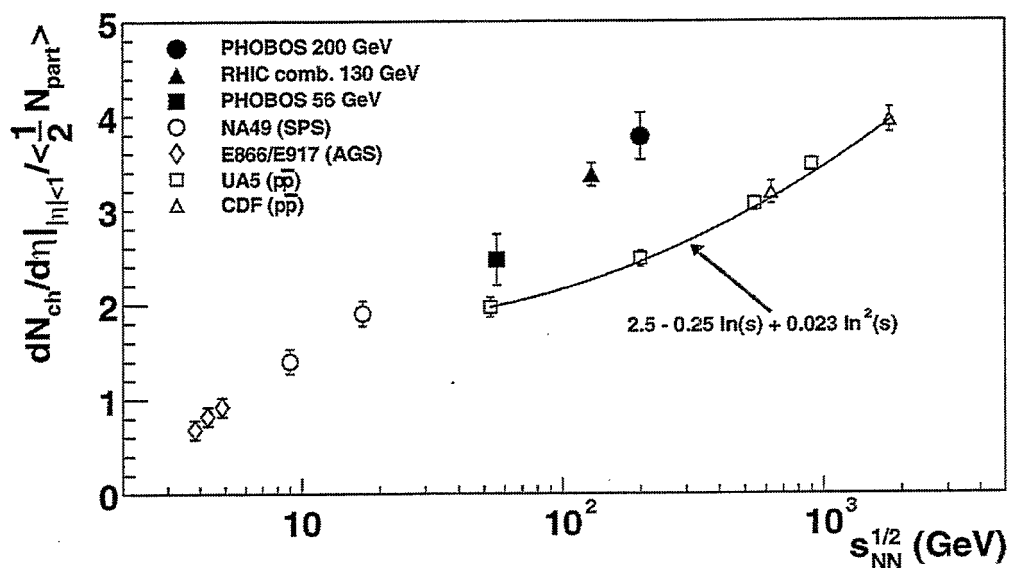
High initial parton density \Rightarrow statistical description,
approach to thermalization

Quark-gluon plasma



F. Karsch, hep-lat/0106019

Energy dependence of multiplicity in Au-Au



B.B. Back et al (PHOBOS Coll.), Phys.Rev.Lett.88:022302,2002

Is this multiplicity “large” or “small”?

Independent NN collisions would yield $N \sim N_{coll} \sim N_{part}^{4/3}$

This is not observed; instead, interactions are coherent

The Future

1. $p(d)A$ program will be crucial in separating initial-state nuclear effects from the signals of thermalized quark-gluon matter
2. Extending the current results in $A - A$:
 - high p_t : better statistics, broader coverage
 - heavy flavors: charm and beauty (luminosity/energy ?)
 - heavy quarkonia: better statistics in J/Ψ , Ψ' , Υ (luminosity/energy ?)
 - continuum dileptons and photons
 - correlations and fluctuations
 - ultra-peripheral and diffractive physics

Heavy Quark Production at RHIC

Jörg Raufeisen

Los Alamos National Laboratory, MS H846, Los Alamos, NM 87545, USA

Talk presented at the RIKEN-BNL Research Center Workshop "Current and Future Directions at RHIC", August 5-23, 2002

At high center of mass energies, heavy quark production can be expressed in terms of the same color dipole cross section as low Bjorken- x DIS. This dipole formulation has first been introduced in 1995 by Nikolaev, Piller and Zakharov with the intention of developing a theoretical framework for the description of nuclear effects. In fact, nuclear shadowing and saturation effects, which will be important at RHIC (and at LHC) are very naturally described in the dipole approach.

Before calculating nuclear effects, one should however first establish the validity of the dipole approach in proton-proton (pp) collisions. The basic formula is given on transparency one: the cross section for heavy quark pair production can be written as convolution of a light-cone wavefunction $\Psi_{G \rightarrow Q\bar{Q}}$ describing the transition $G \rightarrow Q\bar{Q}$ and the cross section $\sigma_{q\bar{q}G}$ for scattering a color neutral quark-antiquark-gluon system on a nucleon. The latter can be expressed in terms of the same dipole cross section as low x DIS, for which we employ the phenomenological parameterization of Golec-Biernat and Wüsthoff. The light-cone wavefunction is calculable in perturbative QCD.

Since the heavy quark cross section varies $\propto 1/m_Q^2$ (modulo logs), most of the theoretical uncertainties arise from the choice of the heavy quark mass m_Q . This is shown for the case of open charm pair production on the second transparency. Of course, the same uncertainty is also present in the NLO parton model. Once free parameters are fixed to describe existing total cross section data, dipole approach and NLO parton model calculations agree numerically well for all energies of practical importance, even though the saturation scale is of order of the charm quark mass, see slide three.

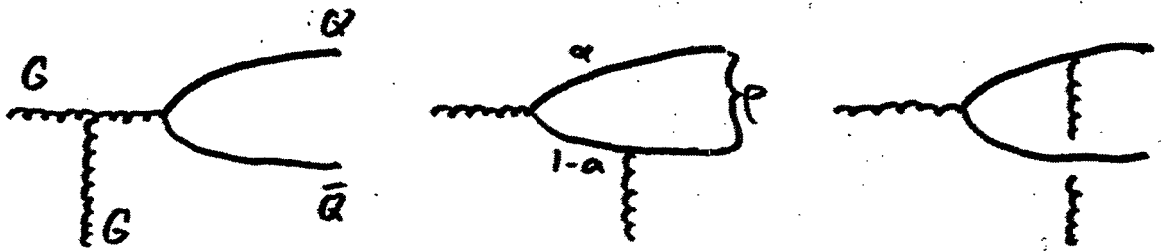
Higher twist effects arising from saturation will only be important for nuclear targets. Since the heavy quark pair is small, $\rho \sim 1/m_Q$, a double scattering like the one shown in the upper figure on the fourth transparency gives a higher twist contribution to shadowing. However, in the case of charm, this higher twist is not small, because it will be enhanced by a power of the saturation scale Q_s^2 . For a nucleus A , $Q_s^2(A) \propto A^{1/3}$. The leading twist contribution to shadowing for heavy quarks originates from rescattering of higher Fock states, containing gluons.

Numerical results for shadowing of open charm, obtained by Kopeliovich and Tarasov, are shown on the fifth slide. The dashed curves single out the contribution of leading twist gluon shadowing. The solid curves include higher twists as well. For comparison, we also show a parton model calculation using EKS98 parameterization. It will be interesting to see, if such higher twists can be identified in experiment. In any case, one should be cautious to identify shadowing for open charm production at RHIC with gluon shadowing.

Dipole Approach to Heavy Quark Production

Nikolaev, Piller, Zakharov, JETP 81 (95) 851

Kopeliovich, Tarasov, hep-ph/0205151



$$\frac{d\sigma_{Q\bar{Q}}}{dy} = \kappa \int_0^1 dx_1 \mu \int_0^1 d\alpha \int d^2\rho |\Psi_{G \rightarrow Q\bar{Q}}(\alpha, \rho)|^2 G_{q\bar{q}G}^N(x_2, \alpha, \rho)$$

$$\mu \sim m_Q$$

General rule:

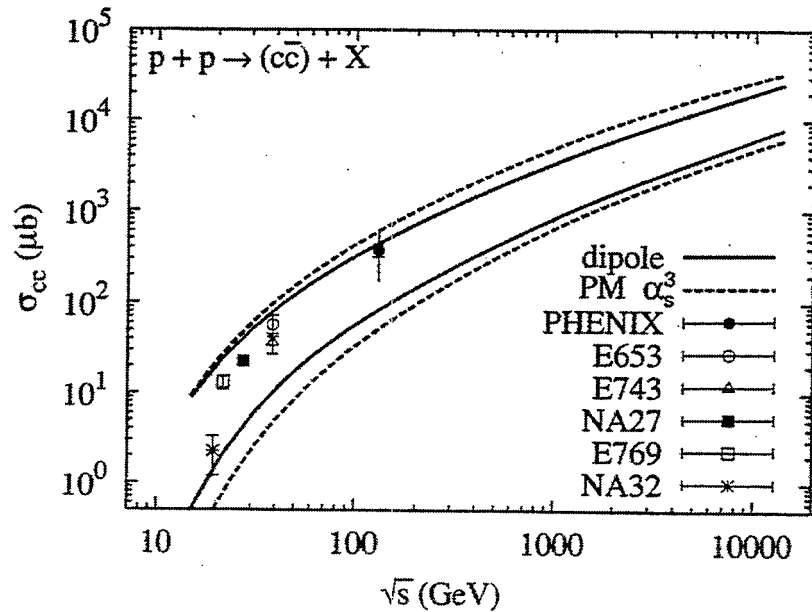
$$\sigma(aN \rightarrow bcX) = \int d\Gamma |\Psi_{a \rightarrow bc}(\Gamma)|^2 G_{bc\bar{a}}^N(\Gamma)$$

Γ : set of all internal variables
of the (bc) -system

$\Psi_{a \rightarrow bc}$: LC wavefunctions for
the transition $a \rightarrow bc$

$G_{bc\bar{a}}^N$: cross section for scattering
the $(bc\bar{a})$ -system on a nucleon

Theoretical uncertainties



Uncertainties arise from the choice of

- i) charm quark mass m_c
- ii) renormalization scale μ_R (enters α_s)
- iii) factorization scale μ_F (enters PDFs)

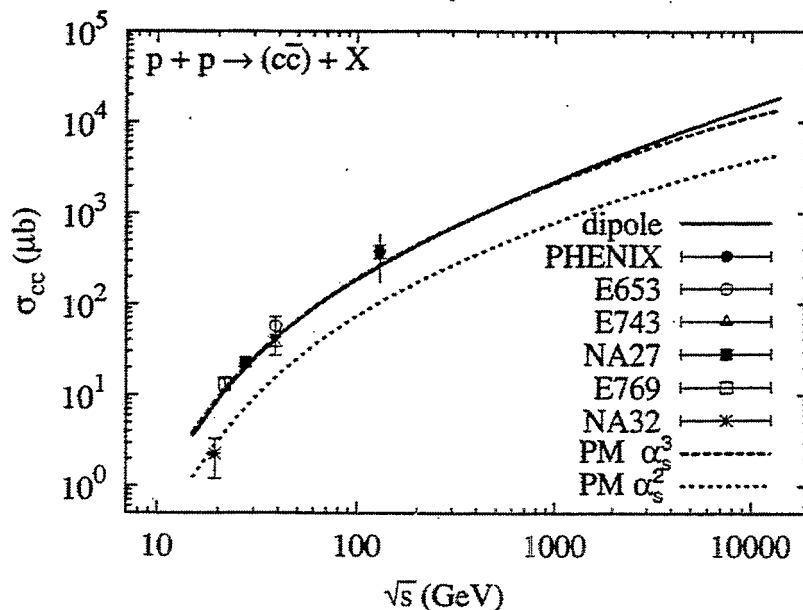
$$1.2 \text{ GeV} \leq m_c \leq 1.8 \text{ GeV}, \quad m_c \leq \mu_R \leq 2m_c$$

$$\mu_F = 2m_c \text{ fixed}$$

fix parameters to describe data

The total $c\bar{c}$ -pair cross section

Before application to nuclei, establish validity of dipole approach to pp -collisions



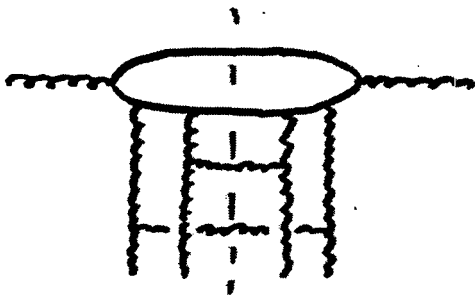
α_s^3 parton model calculation from
Nason, Dawson, Ellis, NPB 303 (88) 607
NPB 327 (89) 49
Mangano, Nason, Ridolfi, NPB 373 (92) 295

- Dipole approach describes all data, even at low energies.
- No significant difference between dipole approach and parton model despite $\alpha_s \sim m_c$.

Nuclear Shadowing in Open Charm Production

Two contributions to shadowing:

1) rescattering of $c\bar{c}$ -Fock state



$c\bar{c}$ -separation $\rho \sim \frac{1}{m_c}$

→ higher twist shadowing

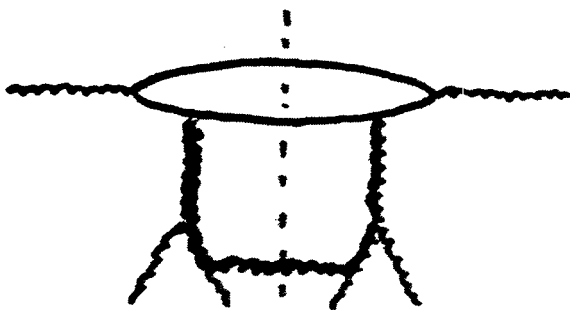
$$\text{but } \frac{\Delta G}{G} \sim \frac{A^{1/3} Q_s^2(x)}{m_c^2}$$

not negligible

(Kopeliovich, Tarasov, hep-ph/0205151)

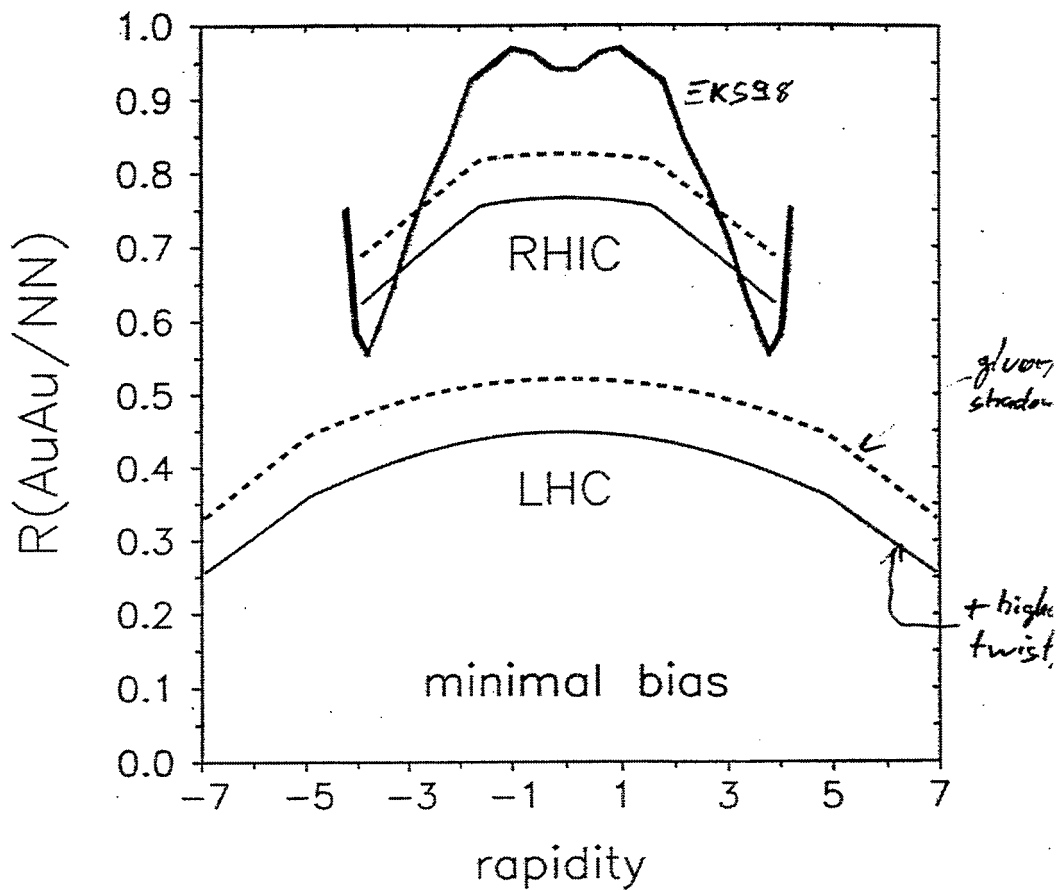
2) rescattering of higher Fock states

(Gluon Shadowing)



single scattering $c\bar{c}$
sees reduced gluon
density

double scattering of $c\bar{c}G$ Fock state
leads to the leading twist gluon shadowing



Kopeliovich, Tarasov, hep-ph/0205151

Violations of Parton-Hadron Duality in DIS Scattering

S. Liuti

University of Virginia

Charlottesville, VA 22904, USA

E-mail: sl4y@virginia.edu

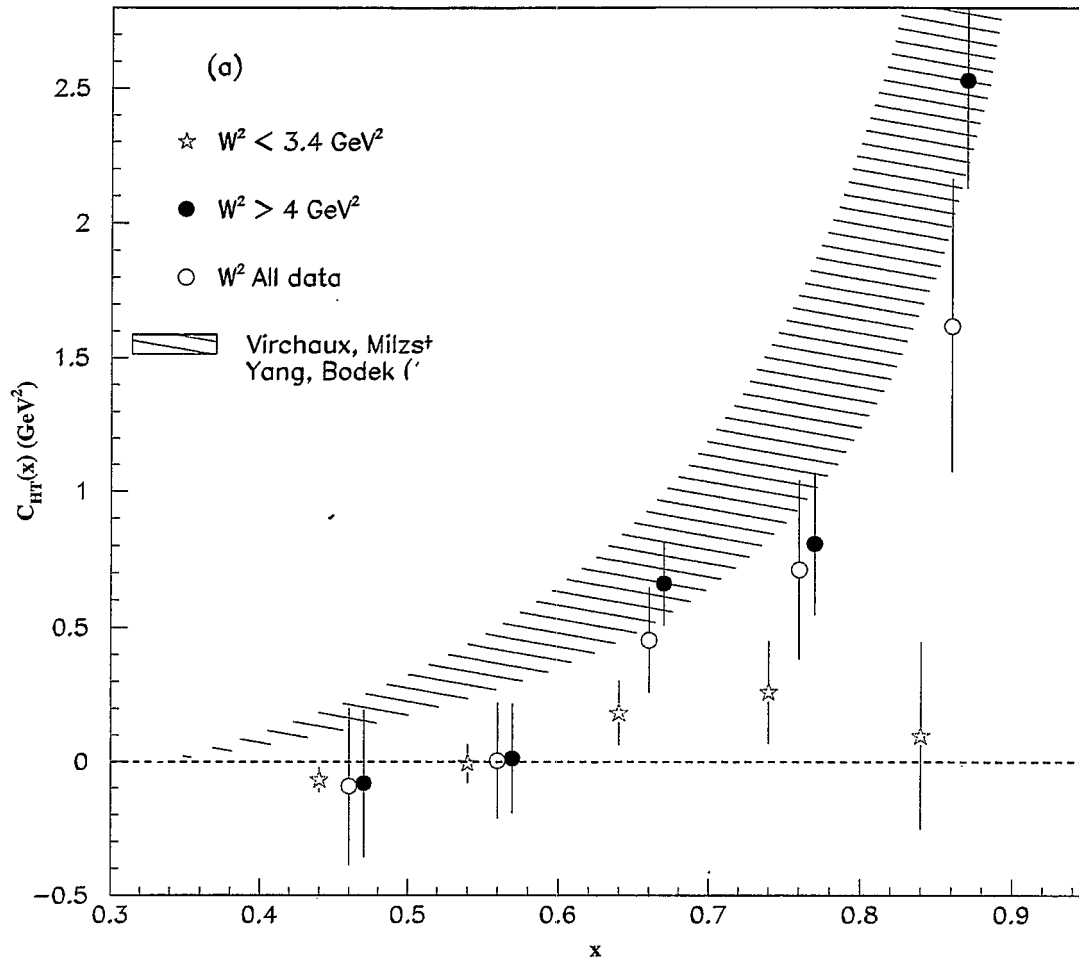
We discuss the limits of validity of parton-hadron duality in ep scattering, in the large x region. The uncovered pattern of violations of duality can be explained by introducing a distribution of color neutral clusters in the initial stage of evolution, whose mass spectrum is predicted within the preconfinement property of QCD.

1.3 Why is it interesting?

General aim: to study the interface between perturbative (quarks and gluons d.o.f.) and non-perturbative (hadronic d.o.f.).

- ★ pQCD phase – parton showers from primary quarks – is well separated from production of secondary gluons and $q\bar{q}$ pairs – soft radiation – eventually responsible for hadron formation.
- ★ Study mechanism by which this radiation is responsible for hadron jets formation, while not affecting the total cross section.
- ★ How far down in Q^2 does pQCD work? What is the meaning of the initial scale?
- ★ What are the consequences of putting all this in a nucleus (e-RHIC)?

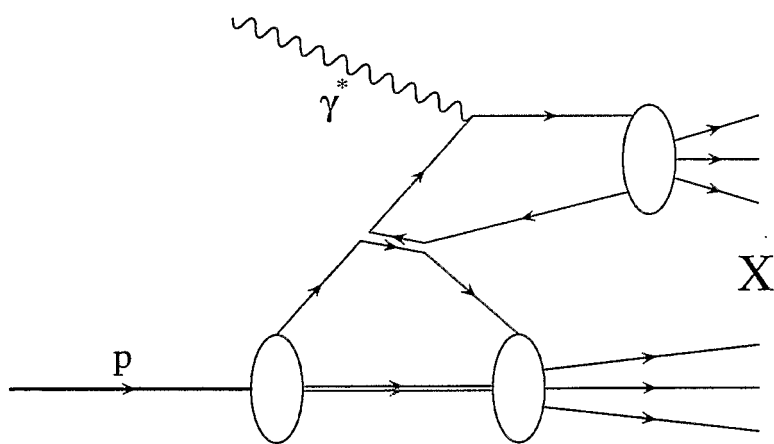
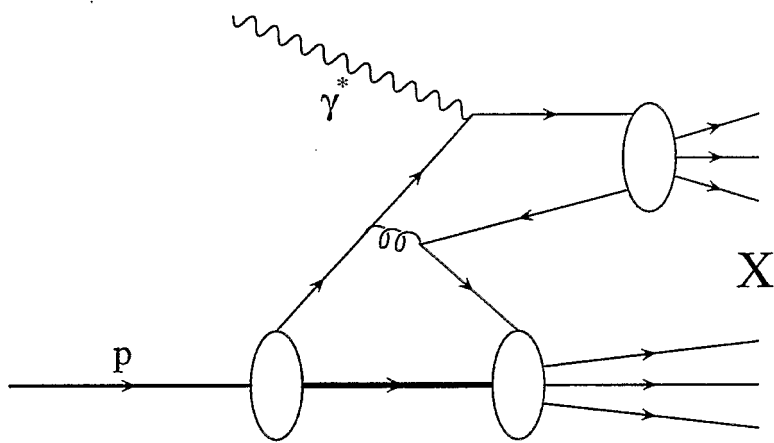
S.L., R.Ent, C. Keppel and I. Niculescu, hep-ph/0111063.



$$F_2(x, Q^2) = F_2^{pQCD+TMC}(x, Q^2) + \frac{H(x, Q^2)}{Q^2} + \mathcal{O}\left(\frac{1}{Q^4}\right)$$

$$H(x, Q^2) = F_2^{pQCD+TMC}(x, Q^2) C_{HT}(x)$$

Large N_c



Working Formula

$$F(x, Q^2) = \sum_i e_i^2 \int_{\mu^2}^{Q^2} \frac{dk^2}{k^2} \frac{\alpha_s(k^2)}{2\pi} \times \\ \times \int_x^1 dy f_i(y, Q^2, k^2) P(y, k^2, \mu^2) \times \mathcal{R}$$

Initial Cluster Mass Dist. \Rightarrow semi-hard evolution

$$P(y, k^2, \mu^2) = \sum_{j, j_1, j_2} \int_{x_1}^{y-x_2} \frac{dz}{y} \int_{x_1}^{x-x_2} \frac{dz}{z} P_{j \rightarrow j_1 j_2}(z/y) \\ \times \frac{x_1}{z} \Gamma_{j_1} \left(\frac{x_1}{z}, k^2, \mu^2 \right) \frac{x_2}{y-z} \Gamma_{j_2} \left(\frac{x_2}{y-z}, k^2, \mu^2 \right)$$

Γ evolves as a color connected distribution \Rightarrow Sudakov type dampening at large k^2 .

Amati & Veneziano, Bassetto, Ciafaloni & Marchesini

$f_j \Rightarrow$ DGLAP Evolution

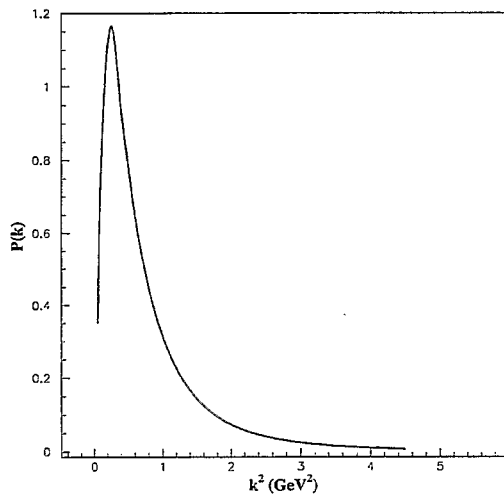
Initial condition: $f_j(y, Q_o^2, Q_o^2) = \delta(1 - y)$

\Rightarrow all structure in P .

Limiting cases

★ Low W^2 (resonances): $P \approx \bar{P}(k^2, \mu^2)$

$$\Rightarrow F_2 \propto \bar{P}(k^2, \mu^2)$$

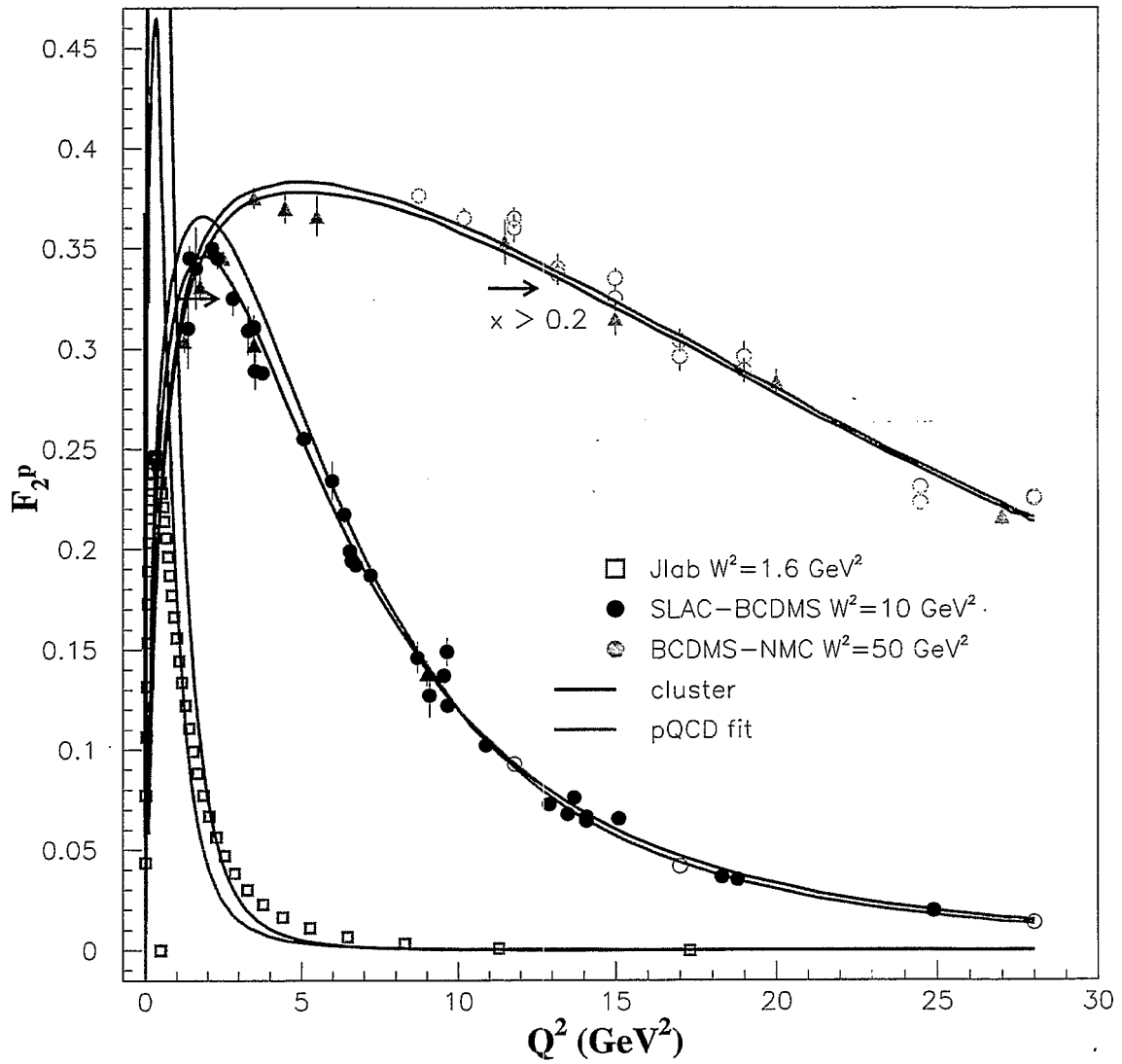


★ Large W^2 : $P \approx \delta(k^2 - \langle k^2 \rangle)$

$$\Rightarrow F_2 \approx f_i(x, Q^2, \langle k^2 \rangle)$$

better definition of initial evolution parameter.

★ “In between” – convolution – expand P in powers of $k^{-2} \Rightarrow$ effective way of obtaining HT contributions.



Leading and Higher Twist in $e + A$ and $p + A$

Rainer Fries

*Department of Physics, Duke University, P.O.Box 90305,
Durham, NC 27708*

In the era of RHIC and LHC hard processes attract more and more attention in heavy ion physics. The application of perturbative quantum chromodynamics (pQCD) in heavy nuclei must therefore be on firm ground to meet the challenge.

pQCD is very successful in explaining scattering reactions involving hadrons at large momentum transfer. pQCD calculations are based on factorization theorems that allow a rigorous separation of short range (perturbative) and long range (non-perturbative) properties. The well known leading twist factorization theorem tells us that the cross section, e.g. for deep inelastic lepton nucleon scattering or Drell Yan production can be written as a convolution of a parton cross section and parton distributions that encode the non-perturbative part of the cross section. This factorization formula is valid at leading twist accuracy, i.e. modulo corrections of order λ^2/Q^2 where Q is the perturbative scale and λ a non-perturbative hadronic scale.

For scattering off large nuclei certain new problems arise in perturbative QCD since the non-perturbative part of the cross section is sensitive to the size of the nucleus. This can invalidate the argument about the suppression of higher twist corrections. In fact there are higher twist contributions that scale like $A^{1/3}\lambda^2/Q^2$, where A is the mass number of the nucleus. The interpretation of these contributions is in terms of multiple scattering on the parton level [2].

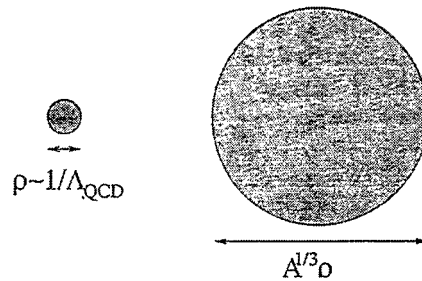
Higher twist corrections of this kind can give sizable contributions to cross sections in $p+A$ or $d+A$ at RHIC and LHC [3]. Furthermore they enter the evolution equations for parton distributions or fragmentation functions. For the parton distributions this could be the key to an understanding of shadowing in a strict pQCD setting. For fragmentation functions these considerations were already used in the literature to derive the energy loss in nuclear matter [4].

References

- [1] M. Luo, J. Qiu and G. Sterman, Phys. Lett. B **279**, 377 (1992); Phys. Rev. D **49**, 4493 (1994); Phys. Rev. D **50**, 1951 (1994).
- [2] X. Guo, Phys. Rev. D **58**, 036001 (1998). R. J. Fries, B. Müller, A. Schäfer and E. Stein, Phys. Rev. Lett. **83** (1999) 4261; Nucl. Phys. **B582** (2000) 537.
- [3] X. Guo and X. Wang, Phys. Rev. Lett. **85**, 3591 (2000); Nucl. Phys. A **696**, 788 (2001). E. Wang and X. N. Wang, arXiv:hep-ph/0202105.

pQCD and Nuclear Collisions

- So do we know everything about perturbative QCD in heavy nuclei?
We should be fine in the asymptotic limit.
- What about the non-perturbative scales?



- The non-perturbative part of the cross section will know about the long-range structure of the nucleus.
Geometric enhancement: $\Lambda_{\text{QCD}} \rightarrow A^\alpha \Lambda_{\text{QCD}}$
- We have to expect a modification of the higher twist suppression:
 $\lambda^2/Q^2 \rightarrow A^{1/3} \lambda^2/Q^2$.
Nuclear Enhancement of Higher Twist.
- Interpretation: Higher Twist = contributions from new matrix elements, beyond simple parton distributions.
Which of them are sensitive to the nuclear size? \Rightarrow Multiple scattering.
 $\langle (FF) \rangle, \langle (FF)(FF) \rangle, \langle (FF)(FF)(FF) \rangle, \dots$
- Rearrange the twist expansion with nuclear enhancement:

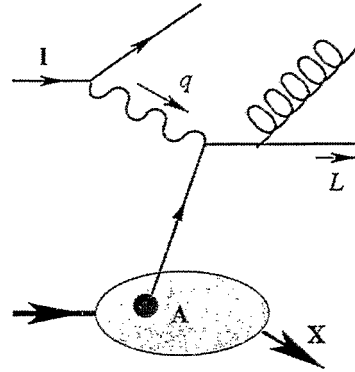
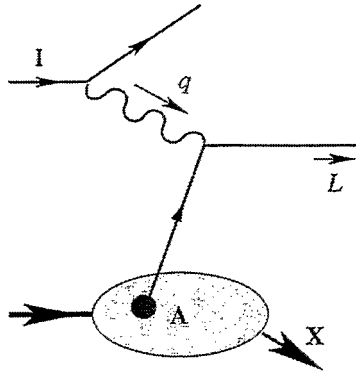
Nuclear enhanced expansion parameter

$$A^{1/3} \lambda^2 / Q^2$$

Luo, Qiu and Sterman

Twist corrections & α_s corrections

Single scat.
(Twist-2)

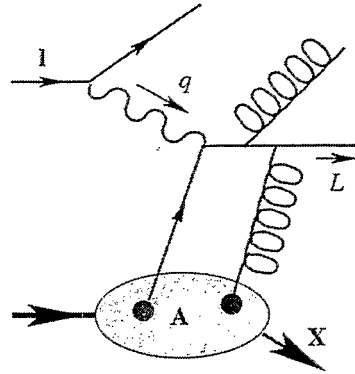
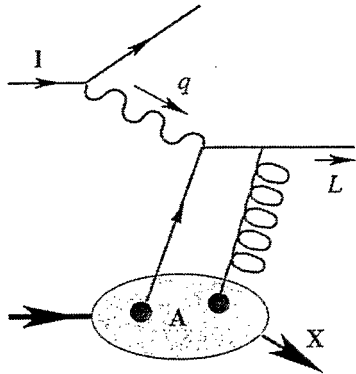


$\mathcal{O}(\dots)$

1

α_s

Double scat.
(Twist-4)



$\mathcal{O}(\dots)$

$$\frac{\alpha_s \lambda^2 A^{1/3}}{Q^2}$$

$$\alpha_s \left(\frac{\alpha_s \lambda^2 A^{1/3}}{Q^2} \right)$$

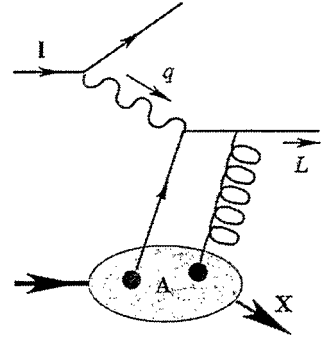
...

...

...

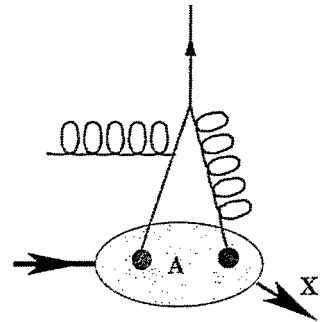
Different Types of Corrections

- Corrections to the hard scattering cross section.

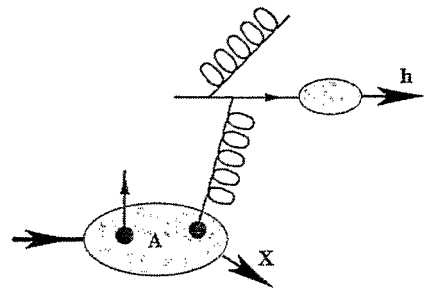


- Modifications internal to the nucleus due to interactions between partons from different nuclei.

GLR type modification to the evolution equations \Rightarrow nuclear modified PDFs.



- Corrections to the evolution of fragmentation functions. These in-medium modifications are not process independent.
(X. Guo, X. Wang, E. Wang)



Probing Twist-4 Correlators in Nuclei

- Lepton pair production at high transverse momentum.

Generic feature: interplay between hard and soft poles (double hard and soft hard scattering).

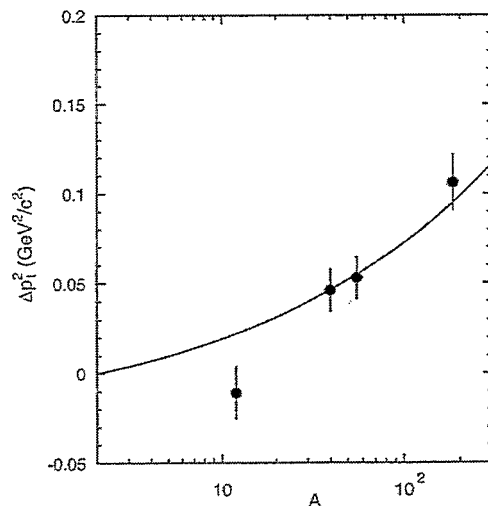
Nuclear enhancement provides a natural explanation for the Cronin effect. Why is it absent at small transverse momentum? \implies Interference effect

- Transverse momentum broadening. (X. Guo)

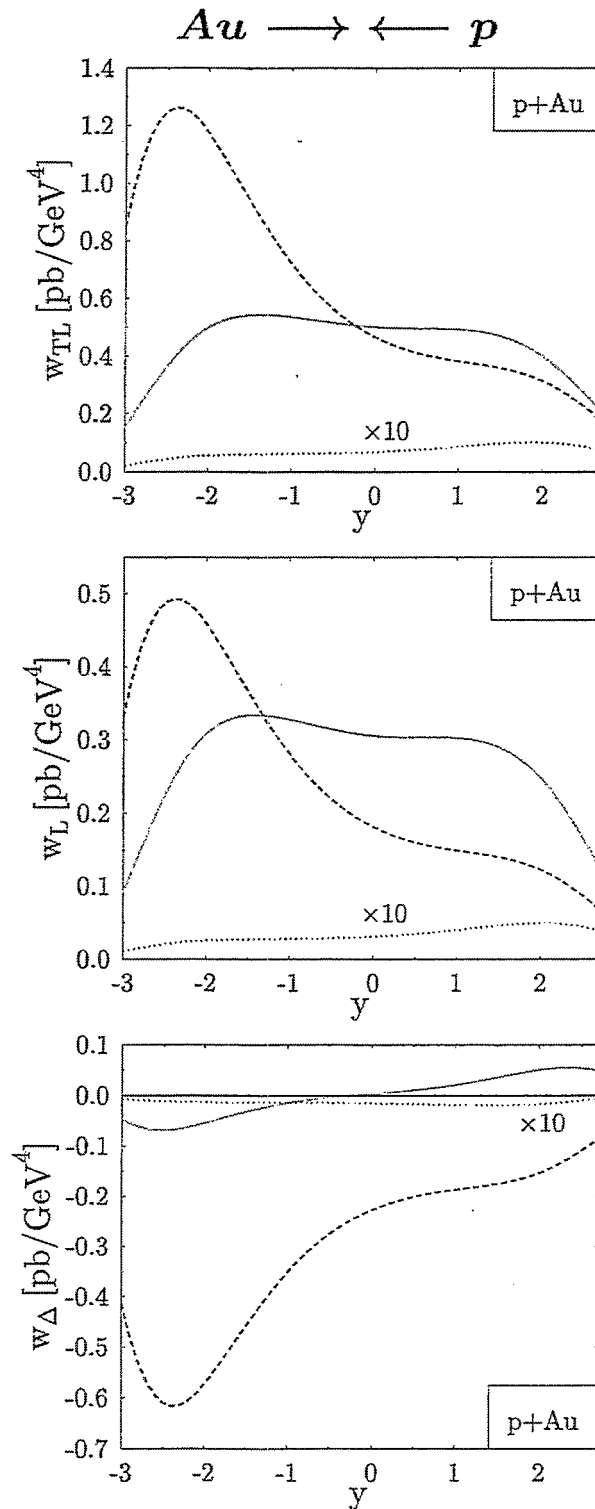
$$\langle q_{\perp} \rangle = \frac{\int dq_{\perp}^2 q_{\perp}^2 d\sigma/dQ^2 dq_{\perp}^2}{d\sigma/dQ^2}$$

$$\begin{aligned} \Delta \langle q_{\perp}^2 \rangle &= \langle q_{\perp}^2 \rangle_{p+A} - \langle q_{\perp}^2 \rangle_{p+p} \\ &= \frac{4\pi^2 \alpha_s \sum_q c_q^2 f_{\bar{q}} \otimes T_{qg}}{N_c \sum_q c_q^2 f_{\bar{q}} \otimes f_q} \sim \frac{4\pi^2 \alpha_s}{N_c} \lambda^2 A^{1/3} \end{aligned}$$

Comparison with Drell Yan data from Fermilab E772 [McGaughey, Moss, Peng]



- RHIC



Rapidity dependence of w_{TL} , w_L and w_{Δ} in the CS frame for 250 GeV protons colliding with 100 GeV/nucleon Au nuclei at $Q = 5$ GeV and $q_{\perp} = 4$ GeV. Single scattering (solid), double-hard (dashed), soft hard (dotted). $w_i = N_{\sigma} W_i$ where W_i are the helicity amplitudes and $N_{\sigma} = \alpha^2 / (64\pi^3 S Q^2)$

RIKEN-BNL Workshop and Summer Program

Current and Future Directions at RHIC

Brookhaven National Laboratory, August 2002

F. Hautmann (Universität Regensburg)

Diffractive deep-inelastic scattering

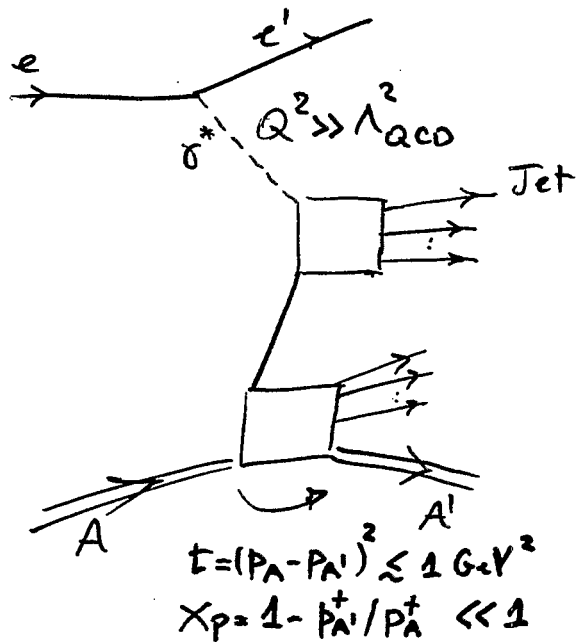
The proposed Electron-Ion Collider (EIC) will explore hadron structure by measuring the hard scattering of virtual photons from the quarks and gluons in the nucleon and nuclear beams with unprecedented precision in the region $10^{-4} < x < 1$, $1 < Q^2/GeV^2 < 10^4$. It will continue and deepen the physics program that has been pursued in electron-proton collisions at HERA, starting in 1992.

Perhaps the most striking experimental results on deep inelastic lepton scattering in the last decade have come from observations of diffraction hard scattering. Experiments at HERA have measured for the first time the diffractive structure functions of the nucleon, and performed the first determinations of diffractive parton distributions. The EIC will be able to measure diffractive parton distributions in nuclei for the first time, and thus provide us with important tests of the QCD conceptual framework for diffractive DIS. Since, as discussed in this contribution, diffractive final states are highly sensitive probes of the gluon distribution, the study of hard diffraction on nuclei at the EIC will provide a remarkable window into the physics of high gluon densities.

In my contribution at this workshop I briefly reviewed the theory of diffractive DIS in QCD and presented new results on calculations for diffractive final states. The theoretical framework I described is based on two main ingredients: i) the factorization of the hard interaction, which leads us to introduce a partonic description in terms of diffractive parton distributions; ii) the application of light-cone hamiltonian methods to these distributions. These methods enable us to exploit systematically the simplicity of the spacetime structure of the scattering in a particular reference frame, the rest frame of the target. In particular they lead us to the observation that if nonperturbative dynamics generates a semihard momentum scale in diffractive DIS, the dependence of the diffractive parton distributions on the longitudinal momentum fraction β becomes calculable by perturbation methods, and gives testable predictions. In my talk I focused on the diffractive production of jets, and presented next-to-leading-order QCD predictions for the diffractive jet cross section.

Diffractive final states in DIS

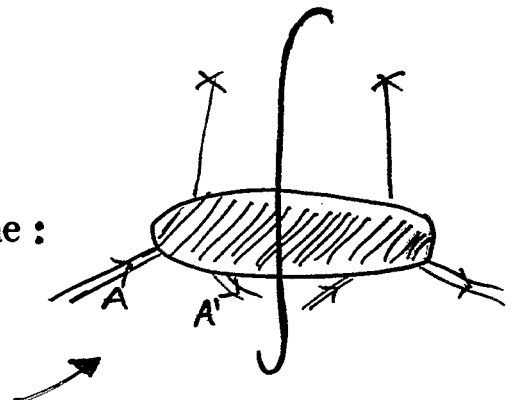
- large- Q^2 interaction occurs
- but hadron is not broken up



- diffractive dissociation preserves quantum numbers of initial particle

⇒ Problem of describing parton dynamics *and* dynamics of vacuum quantum-number exchange

- Useful concept: hadronic matrix elements on the lightcone :



diffractive parton distributions

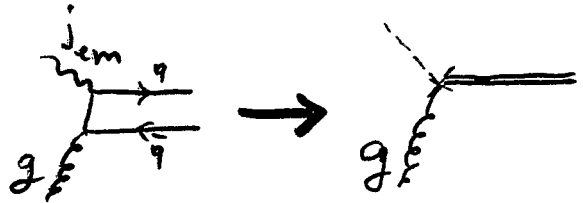
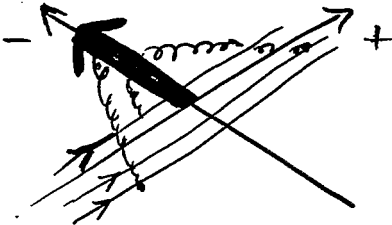
Diffractive gluon distribution:

$$\frac{d\phi_g^{(D)}(\beta, x_P, t, \mu)}{dx_P dt} = \frac{1}{(4\pi)^3 \beta x_{PP_A}^+} \sum_X \int dy^- e^{i\beta x_{PP_A}^+ y^-} \times \langle A | \tilde{G}_a(0)^{+j} | A', X \rangle \langle A', X | \tilde{G}_a(0, y^-, 0)^{+j} | A \rangle,$$

where $\tilde{G}_a(y)^{+j} = E(y)_{ab} G_b(y)^{+j}$, $E(y) = \mathcal{P} \exp\left(-ig \int_{y^-}^{\infty} dx^- A_c^+(y^+, x^-, y) t_c\right)$

Note:

- diffractive requirement on the final state
- UV divergences from operator products renormalized at scale μ
- operator $E \rightarrow$ makes the definition gauge invariant
- physical interpretation in terms of the recoil color flow in a deep inelastic experiment:



- replace $q\bar{q}$ by color-octet eikonal line
- account for this idealization through perturbative corrections to hard scattering

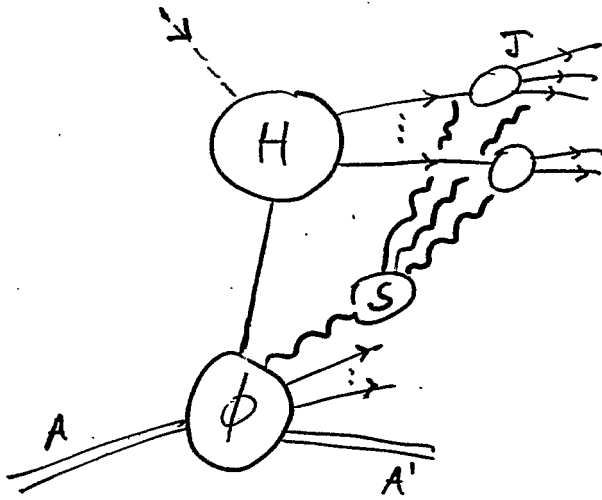
Recall, by comparison, the inclusive distribution:

$$f_g(\xi, \mu) = \frac{1}{2\pi\xi p_A^+} \int dy^- e^{i\xi p_A^+ y^-} \langle A | \tilde{G}_a(0)^{+j} \tilde{G}_a(0, y^-, 0)^{+j} | A \rangle$$

(and its non-diagonal generalization $A' \neq A$)

- utility of diffractive parton distributions comes from factorization formula

Structure of leading-power regions:



soft subgraphs S
"cancel"

physical picture: soft gluons do not see the details of final state jets

\Rightarrow attachments to jets replaced by attachments to eikonal line

note: cancellation holds even though

the beam jet has both initial-state and final-state couplings

- Diffractive jet observable σ :

$$\sigma[W] = \int \phi^{(D)} \otimes H \otimes W + \mathcal{O}(1/\text{hard scattering scale})$$

diffractive
parton distrib.

hard
scattering
function

measurement
function

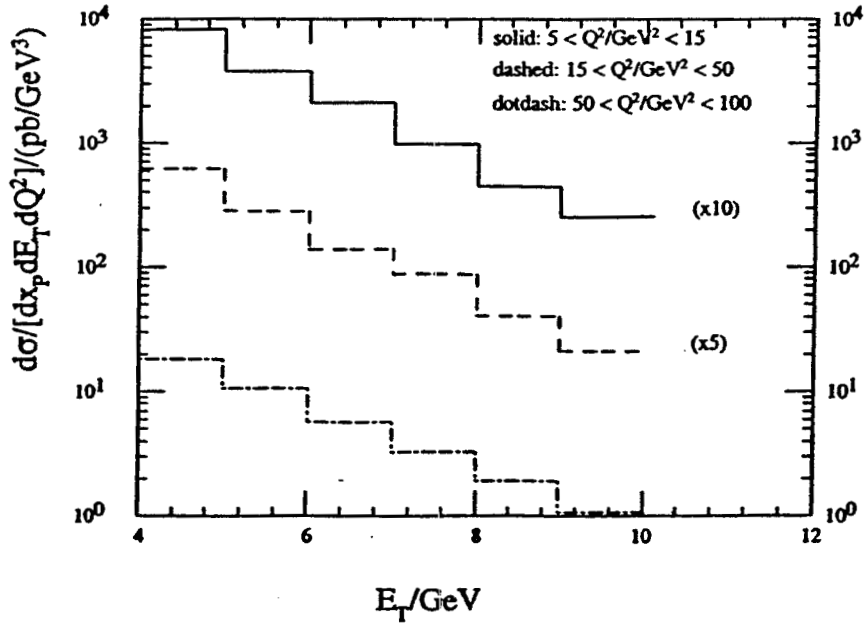
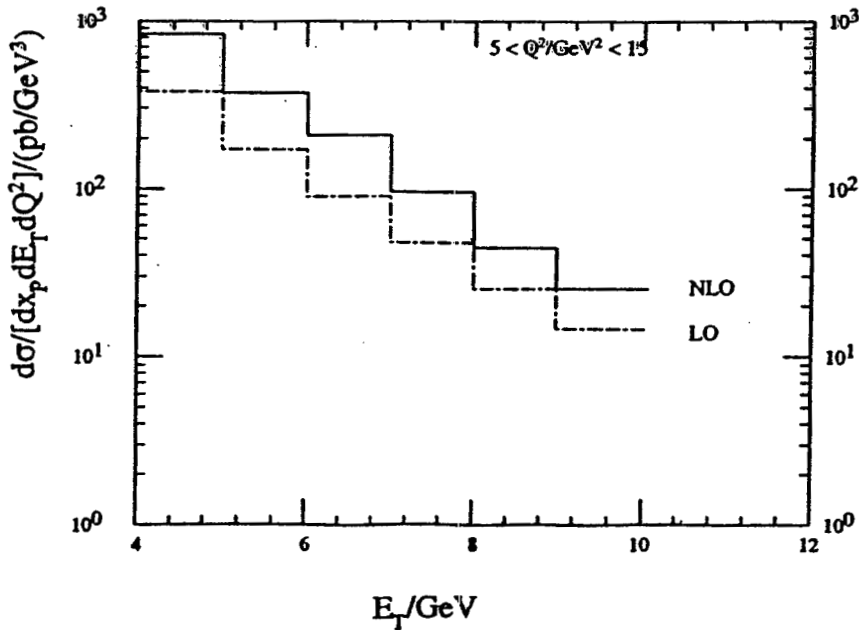
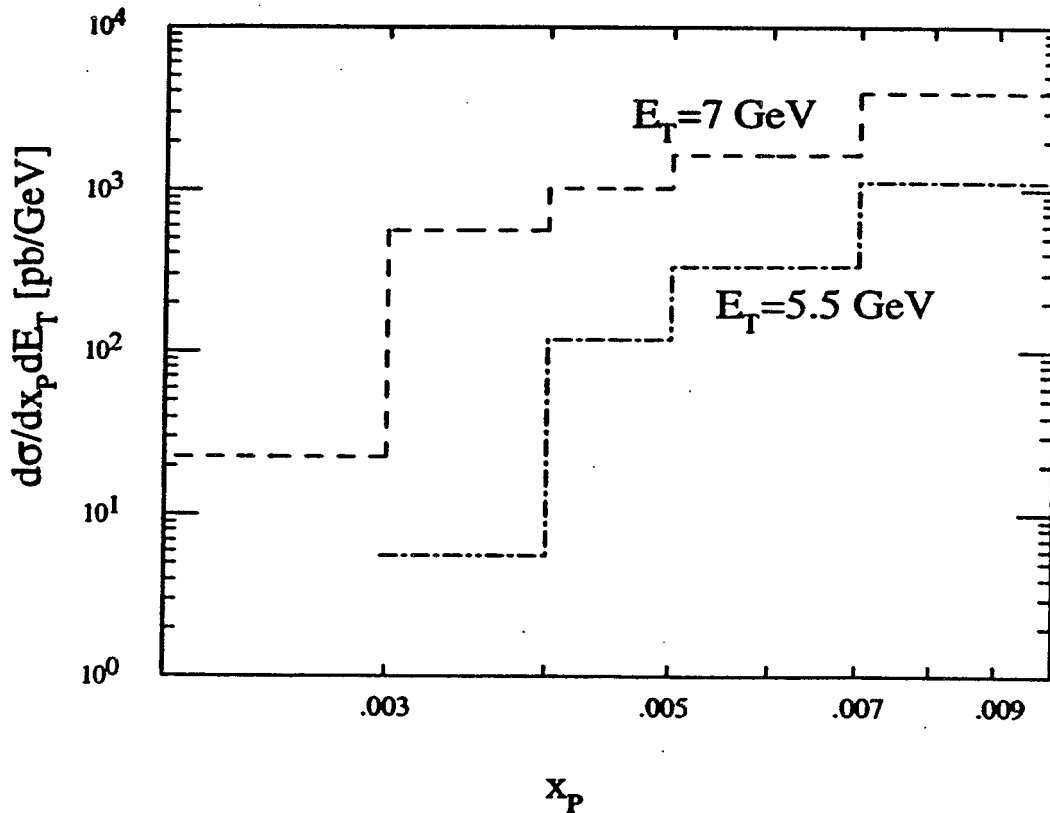


Figure 1: The diffractive one-jet cross section at NLO as a function of the jet transverse energy E_T for different Q^2 bins and $x_P = 0.05$ ($\sqrt{S} = 300$ GeV).

$\mu^2 = \mu_R^2 = Q^2$. Jets are defined by k_T -clustering, with jet resolution parameter $R = 1$.





The diffractive one-jet cross section at NLO as a function of the hadron's momentum loss x_p for different jet transverse energies E_T

ALTHOUGH THE ϕ 'S INCREASE WITH DECREASING x_p ,
 $\sigma^{(jet)}$ DECREASES BECAUSE $\sigma^{(jet)} \sim \int_B^1 \phi \otimes \hat{\sigma}$, $\beta \propto 1/x_p$
 ↑
 non-pointlike coupling
 (unlike F_2)

Small x phenomena with nuclei

M. Strikman

Department of Physics, PSU, USA

It was demonstrated in Ref. [3] how to use the Collins factorization theorem for hard diffraction in DIS [1] to generalize the Gribov theory of nuclear shadowing [2] to calculate the leading twist component of nuclear shadowing for each nuclear parton distribution *separately*. As a result the double scattering term for the shadowing correction to the nuclear parton distributions, $\delta f_{j/A}^{(2)}(x, Q^2)$, is expressed as a convolution of the corresponding diffractive parton distribution function (DPDF) and the appropriate nuclear factor. Since $f_{j/N}^D$ obeys the leading twist DGLAP evolution equation, the Q^2 -evolution of $\delta f_{j/A}^{(2)}$ is also governed by DGLAP, i.e., it is *by definition* a leading twist contribution. This explains why the approach of [3] can legitimately be called the leading twist approach. However one can take into account in this approach also higher twist effects in the diffraction.

The HERA diffractive data are consistent with dominance of the leading twist diffraction in the process $\gamma^* + p \rightarrow M_X + p$ for $Q^2 \geq 4 \text{ GeV}^2$. These studies have determined quark DPDF in a direct way and the gluon diffractive DPDF indirectly through the scaling violation. More recent studies of the charm production and production of diffractive production of two jets in the direct photon kinematics measured directly the gluon DPDF and found them to be consistent (within 30% which is mainly determined by the uncertainties of treating the NLO effects in the two jet production) with the inclusive diffraction in DIS. As a result we were able to determine the strength of interaction in the quark channel and gluon channels. It turns out to be large at the $Q_0^2 \sim 4 \text{ GeV}^2$ where one can set up the boundary condition ¹ It is typically of the order of 20 mb for the quark channel and 30÷40 mb for the gluon channel for $Q^2 \sim 4 \text{ GeV}^2, x \leq 10^{-3}$. Consequently one needs to include the interactions with $N \geq 3$ nucleons in the calculations. These were modeled using quasieikonal approximation. Corrections due to the cross section fluctuations were also analyzed and found to be rather small for reasonable models of fluctuation effects [4]. We have performed recently a detailed analysis of the nuclear shadowing in the leading twist using the current HERA diffractive data [5]. We have analyzed the uncertainties originating from the uncertainties in the input diffractive parton distribution functions related to the uncertainties in the data and find that these uncertainties $\leq 20 \div 30\%$ for $x \leq 10^{-3}$. The biggest uncertainty in the gluon channel originates from the t -dependence of the gluon diffractive pdf which is not measured directly. The results of the calculations for the A -dependence of the light and heavy quarks, and gluon shadowing in the NLO as well for $\sigma_{L,T}$ are presented in [5]. We also performed a comparison with the higher twist shadowing which we estimated in the eikonal approximation and demonstrated that the leading twist contribution dominates down to very small x at large enough Q^2 .

It is worth emphasizing here that the diagrams corresponding to the leading twist shadowing are usually neglected in the BFKL type approaches to the scattering off nuclei. For example, these diagrams are neglected in the model of Balitsky and Kovchegov. Note also that the higher twist effects become important at sufficiently small x and $Q \leq Q_{min}(x)$. Rough estimates indicate that $Q_{min}(10^{-3})$ for the gluon sector and $A \sim 200$ are $\sim 2 \div 5 \text{ GeV}$ depending on the way how one treats the next to leading order effects. Also, $Q_{min}(x)$ should increase with decrease of x .

In conclusion, the leading twist shadowing effects are expected to lead to significant modifications of the cross sections of hard processes at LHC in pA and AA collisions and at RHIC in pA collisions in the proton fragmentation region. Further progress in the studies of the diffraction at HERA will allow to reduce significantly the uncertainties in the predictions.

[1] J. C. Collins. Phys. Rev. D **57**, 3051 (1998) [Erratum-ibid. D **61**, 019902 (2000)] [arXiv:hep-ph/9709499].

[2] V.N.Gribov. Sov.J.Nucl.Phys. **9** 1969) 369; Sov.Phys.JETP **29** 1969, 483; ibid **30** (1970) 709.

[3] L. Frankfurt and M. Strikman, Eur. Phys. J. A **5**, 293 (1999) [arXiv:hep-ph/9812322].

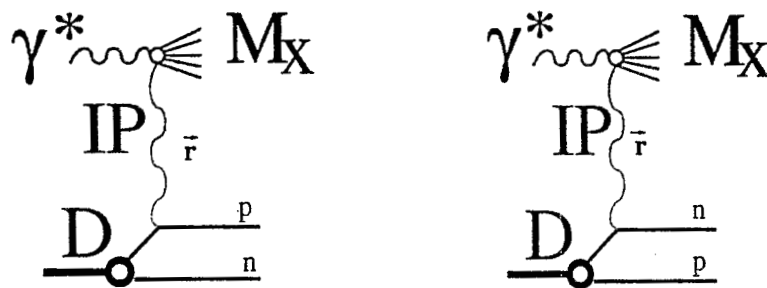
[4] L. Alvero, L. L. Frankfurt and M. I. Strikman, Eur. Phys. J. A **5**, 97 (1999) [arXiv:hep-ph/9810331].

[5] L. Frankfurt, V. Guzey, M. McDermott and M. Strikman, JHEP **0202**, 027 (2002).

¹For $Q^2 \leq 4 \text{ GeV}^2$ higher twist effects in ep diffraction maybe significant leading to higher twist contributions to the nuclear shadowing. In particular, higher twist shadowing may contribute significantly in the shadowing kinematics of the NMC experiment.

Deep connection between high-energy diffraction and phenomenon of nuclear shadowing. Gribov 68

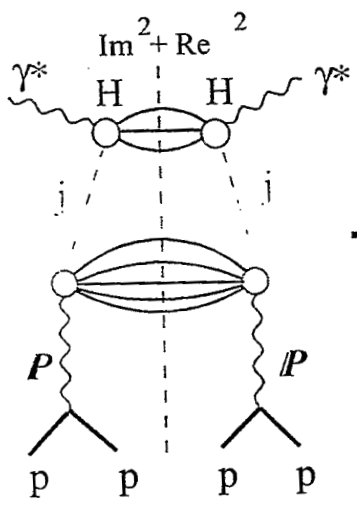
Qualitatively the connection is due to a possibility of small momentum transfer, \vec{r} , in diffractive processes $\gamma^* + N \rightarrow M_{dif} + N$: $\vec{r} = x m_n \sqrt{x(1 + M_{dif}^2/Q^2)}$ comparable to the average average nucleon momentum in a nucleus. In this case amplitudes of diffractive scattering off different nucleons interfere.



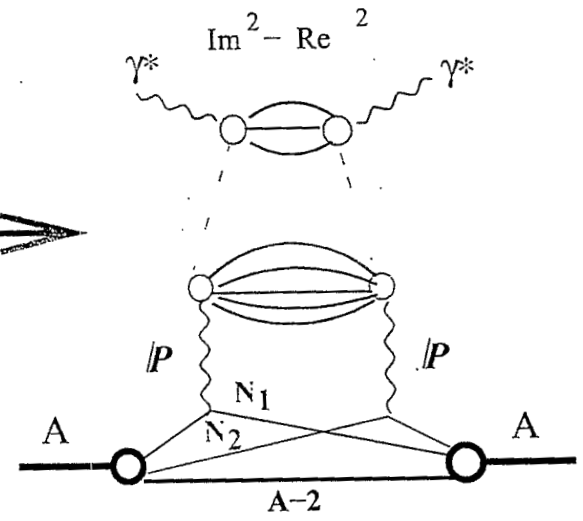
The Gribov theory for $\sigma_{tot}(\gamma^* A)$ agrees well with the $F_2 A / F_2 N$ shadowing data. In early days calculations involved modeling diffraction FS88-89, Kwiecinski89, Brodsky & Liu 90, Nikolaev & Zakharov 91. Use of the HERA diffractive data (this involves a certain extrapolation of the HERA data to smaller W) allows to explain the high precision NMC data.

Theoretical expectations for shadowing - leading twist limit

Theorem: In the low thickness limit the leading twist nuclear shadowing is unambiguously expressed through the diffractive parton densities $f_j^D(\frac{x}{x_P}, Q^2, x_P, t)$ of ep scattering. FS 98



Hard diffraction
off parton "j"



Leading twist contribution
to the nuclear shadowing for
structure function $f_j(x, Q^2)$

Summary of new HERA data
on hard inclusive diffraction.

- $\sigma \approx f_{IP}(x_{IP}) f(\beta, Q^2)$
- scaling violation pattern different from inclusive DIS at large β .
can be fitted using NLO QCD

- Energy dependence

$$d_{IP}^{eff}(Q^2 \gtrsim 10) \sim 1.15 - 1.2$$

- gluon diffractive pdf's \gg quark diffractive pdf's

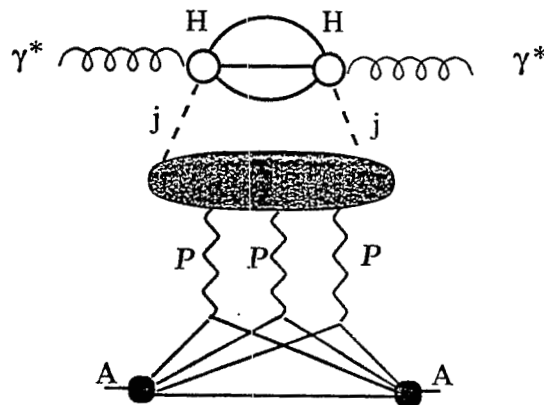
Critical tests of factorization and dominance of gluons in diffractive pdf's
2 jet production [$\gamma + p \rightarrow 2j + X + p$].
charm diffraction.

Warning LT analyses of 2jet & charm.

Leading twist quasieikonal model of shadowing:

(a) Include double scattering exactly using connection to the diffractive pdf's

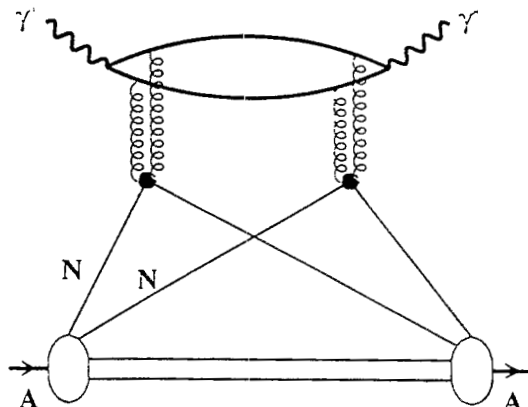
b) Model $N \geq 3$ rescatterings:



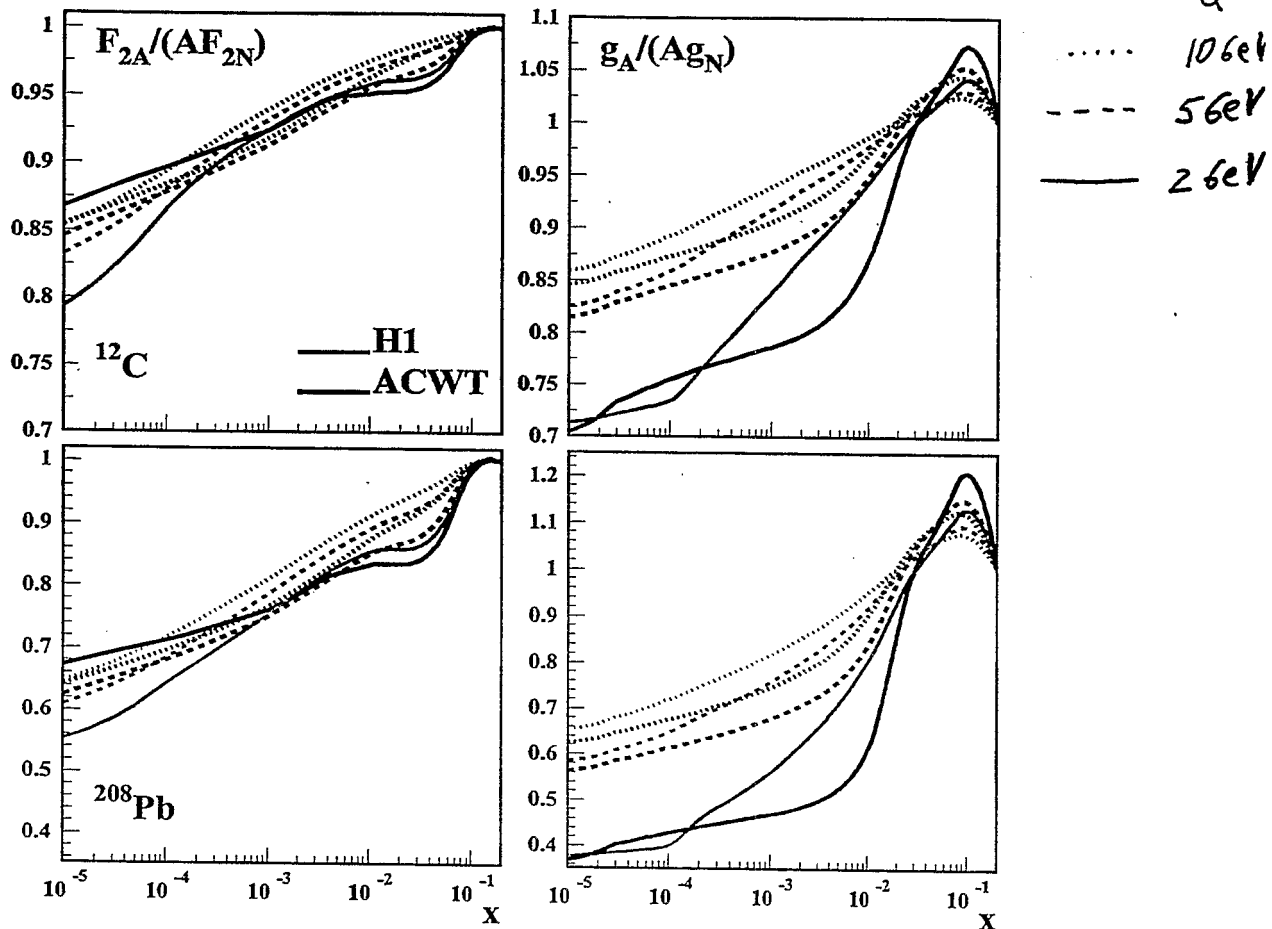
Leading twist triple rescattering.

using quasieikonal approximation (σ_{eff}^j). *Effects of dispersion of σ_{eff} are rather small FS98*

c) Neglect higher twist diagrams with multigluon attachments to the hard block like:



Predictions for F_2^A and g_A



- NLO calculation (with CTEQ5M for $f_{j/N}$)
- Valence quarks are shadowed as the sea quarks; charm quarks are **not** modified at the input scale $Q_0 = 2 \text{ GeV}$
- Predictions with H1 and ACWT are virtually the same for $10^{-4} < x < 10^{-2}$: F_2^D is measured in this range and fitted well by both parameterizations

M.Strikman

Global analysis of nuclear DIS and Drell-Yan data

S. Kumano *

Department of Physics
Saga University
Saga 840-8502
Japan

ABSTRACT

We made a global analysis of deep inelastic scattering and Drell-Yan data for obtaining optimum parton distributions in nuclei [1,2]. The parton distribution functions are provided at $Q^2=1 \text{ GeV}^2$ with a number of parameters, which are determined by a χ^2 analysis of the data. From the analysis, we propose the parton distribution functions at $Q^2=1 \text{ GeV}^2$ for nuclei from deuteron to heavy ones. They are provided by either analytical expressions or computer subroutines for practical usage [3]. Our studies should be important for understanding physics mechanisms of the nuclear modification and also for applications to heavy-ion reactions.

References

- [1] M. Hirai, S. Kumano, and M. Miyama, Phys. Rev. D64 (2001) 034003.
- [2] M. Hirai and S. Kumano, research in progress.
- [3] Nuclear parton-distribution subroutines could be obtained from the web site:
<http://hs.phys.saga-u.ac.jp/nuclp.html>.

* kumanos@cc.saga-u.ac.jp, <http://hs.phys.saga-u.ac.jp>.

- Nuclear parton distributions (per nucleon)
if there *were* no modification

$$A u^A = Z u^p + N u^n, \quad A d^A = Z d^p + N d^n$$

Isospin symmetry: $u^n = d^p \equiv d$, $d^n = u^p \equiv u$

$$\rightarrow u^A = \frac{Z u + N d}{A}, \quad d^A = \frac{Z d + N u}{A}$$

- Take into account the nuclear modification
by the factors $w_i(x, A)$

$$u_v^A(x) = w_{u_v}(x, A) \frac{Z u_v(x) + N d_v(x)}{A}$$

$$d_v^A(x) = w_{d_v}(x, A) \frac{Z d_v(x) + N u_v(x)}{A}$$

$$\bar{q}^A(x) = w_{\bar{q}}(x, A) \bar{q}(x)$$

$$g^A(x) = w_g(x, A) g(x)$$

Functional form of $w_i(x, A)$

$$f_i^A(x) = w_i(x, A) f_i(x), \quad i = u_v, d_v, \bar{q}, g$$

first, assume the A dependence as $1/A^{1/3}$

then, use

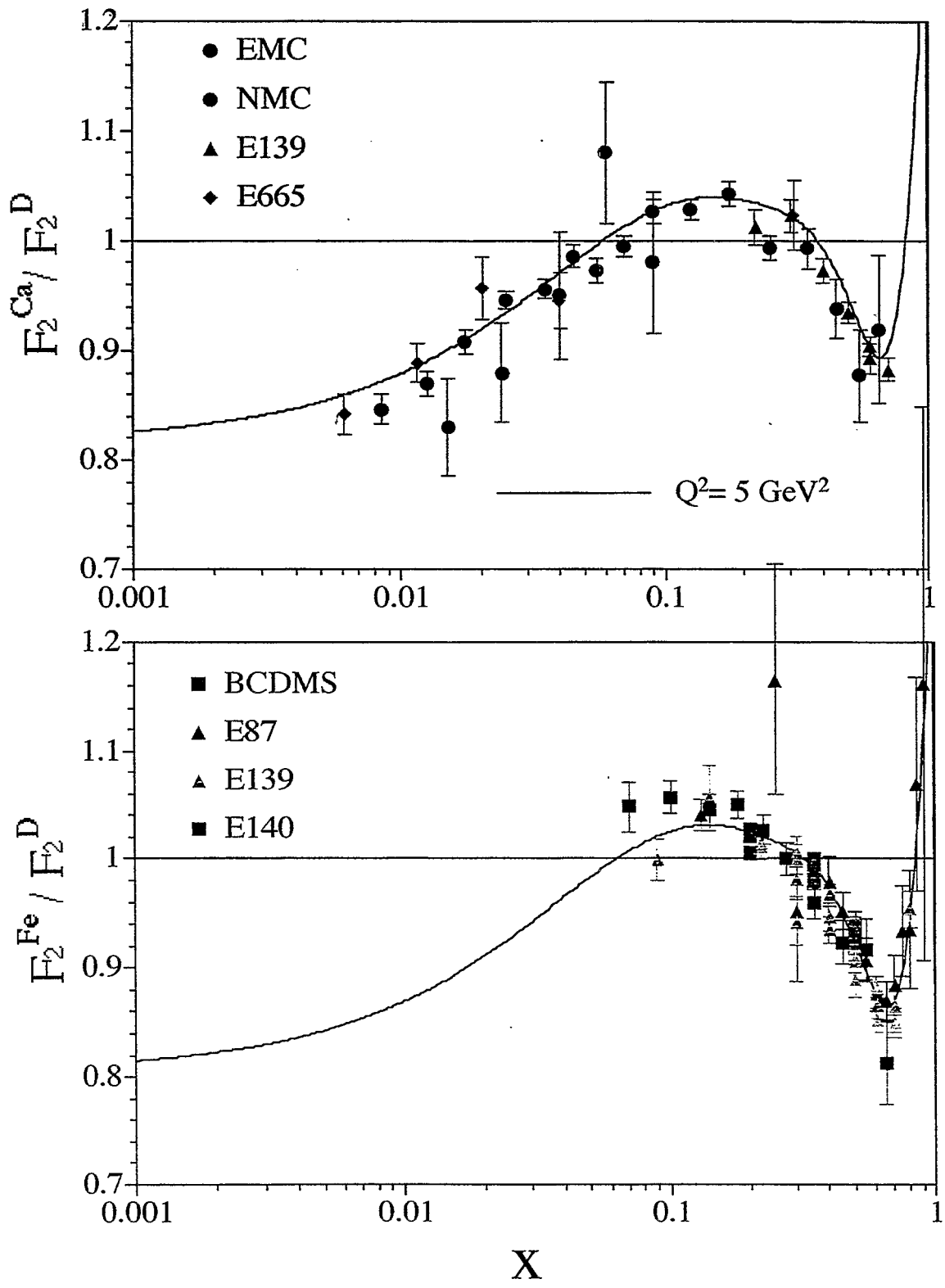
$$w_i(x, A) = 1 + (1 - 1/A^{1/3}) \frac{a_i + b_i x + c_i x^2 + d_i x^3}{(1 - x)^{\beta_i}}$$

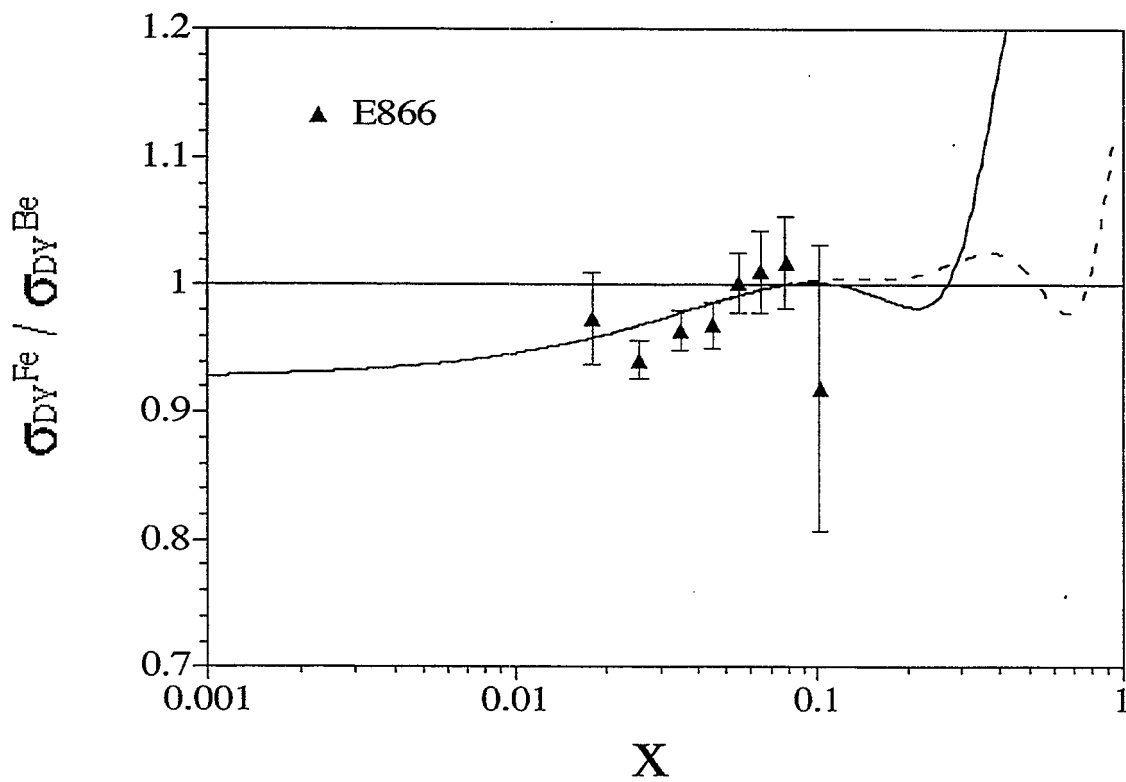
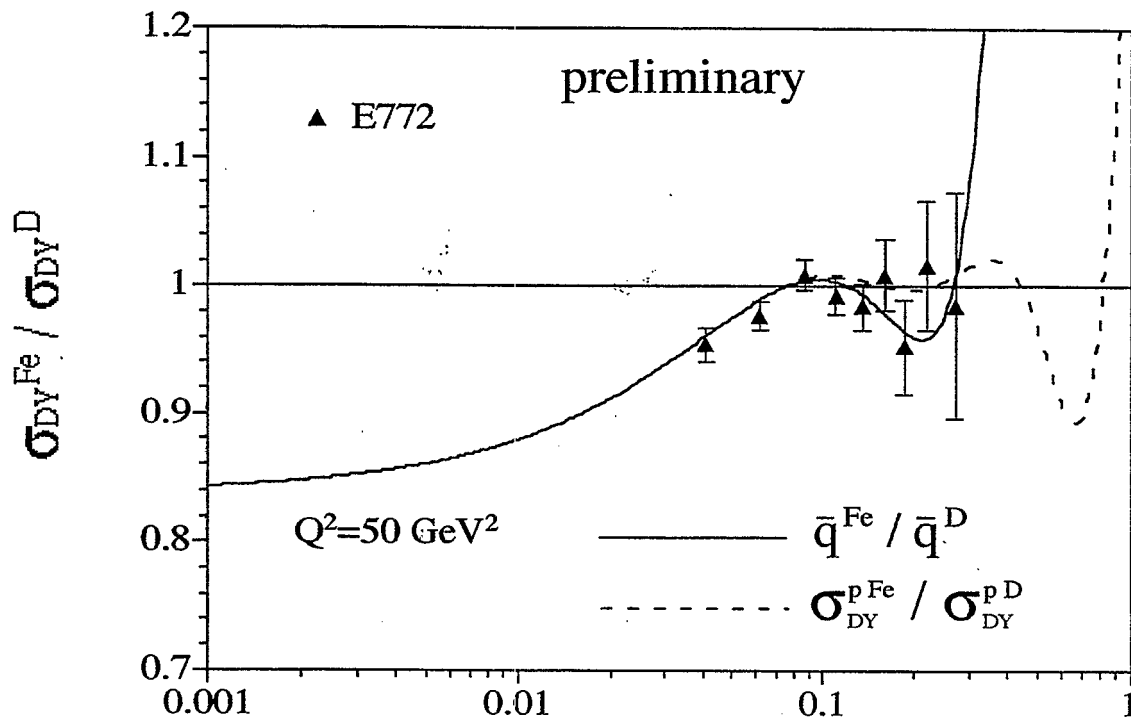
$a_i, b_i, c_i, d_i, \beta_i$: parameters to be determined
by χ^2 analysis

Fermi motion: $\frac{1}{(1 - x)^{\beta_i}} \rightarrow \infty$ as $x \rightarrow 1$ if $\beta_i > 0$

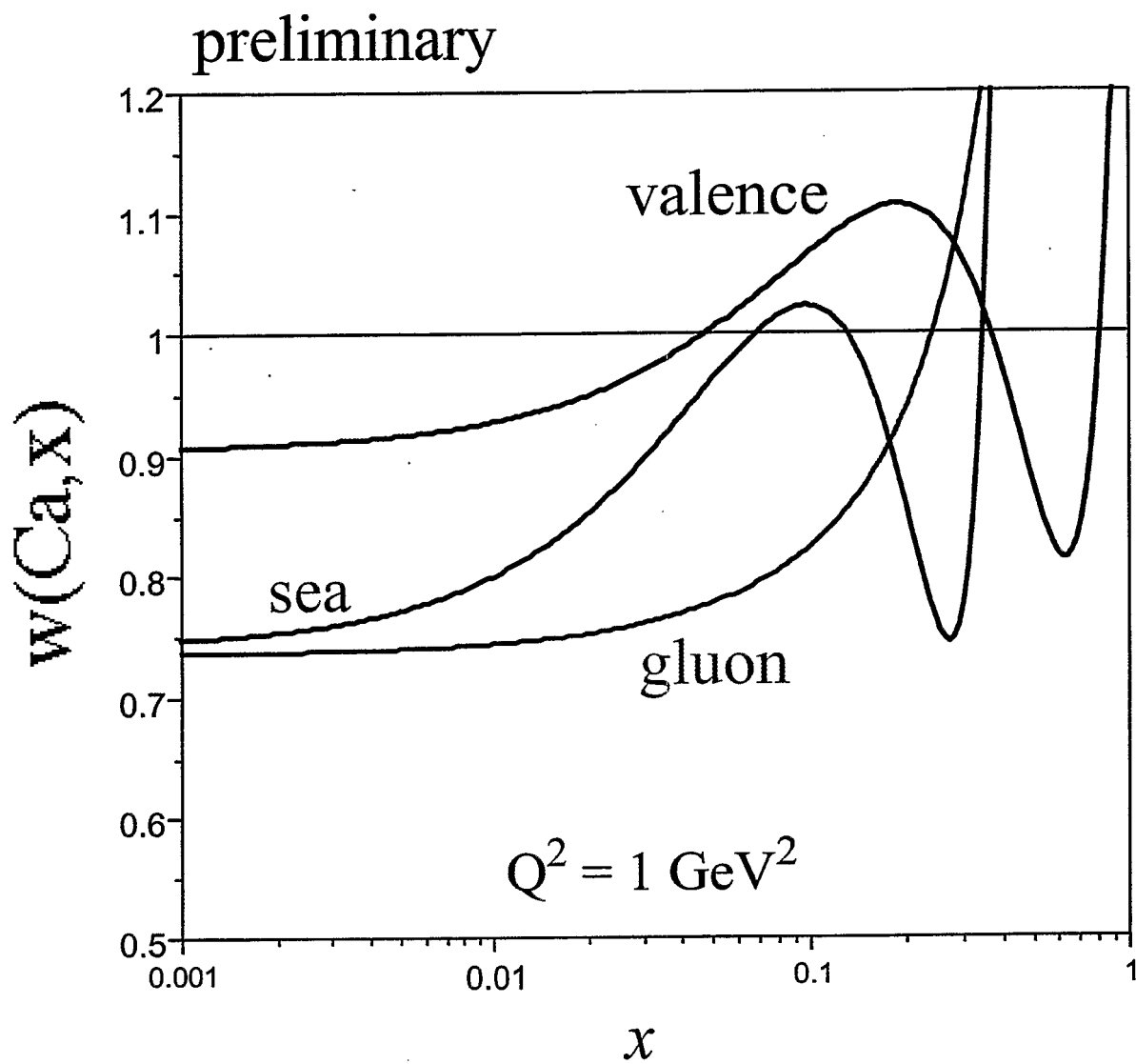
Shadowing: $w_i(x \rightarrow 0, A) = 1 + (1 - 1/A^{1/3}) a_i < 1$

Fine tuning: b_i, c_i, d_i





Nuclear corrections for Ca



Towards a New Global QCD Analysis: P.d.f. for low x

E. Levin

Tel Aviv University / DESY

e-mail: leving@post.tau.ac.il; levin@mail.desy.de

In this talk it will be reported on new global QCD analysis which we started at Tel Aviv university. The main ingredients are two QCD evolution equations. The first one is non-linear evolution equation which has been written in the final form by Balitsky and Kovchegov. this equation sums all high twist contributions while preserving unitarity. It could be a reasonable theoretical basis for matching “hard” and “soft” processes or, in other words, the theoretical method for calculation of DIS in the whole region of photon virtuality Q^2 from very low to high one. The second equation is linear and it is reasonable for short distances since it includes the DGLAP kernel. We present here only our first try in which we achieved a good description all DIS data starting with very low values of Q^2 .

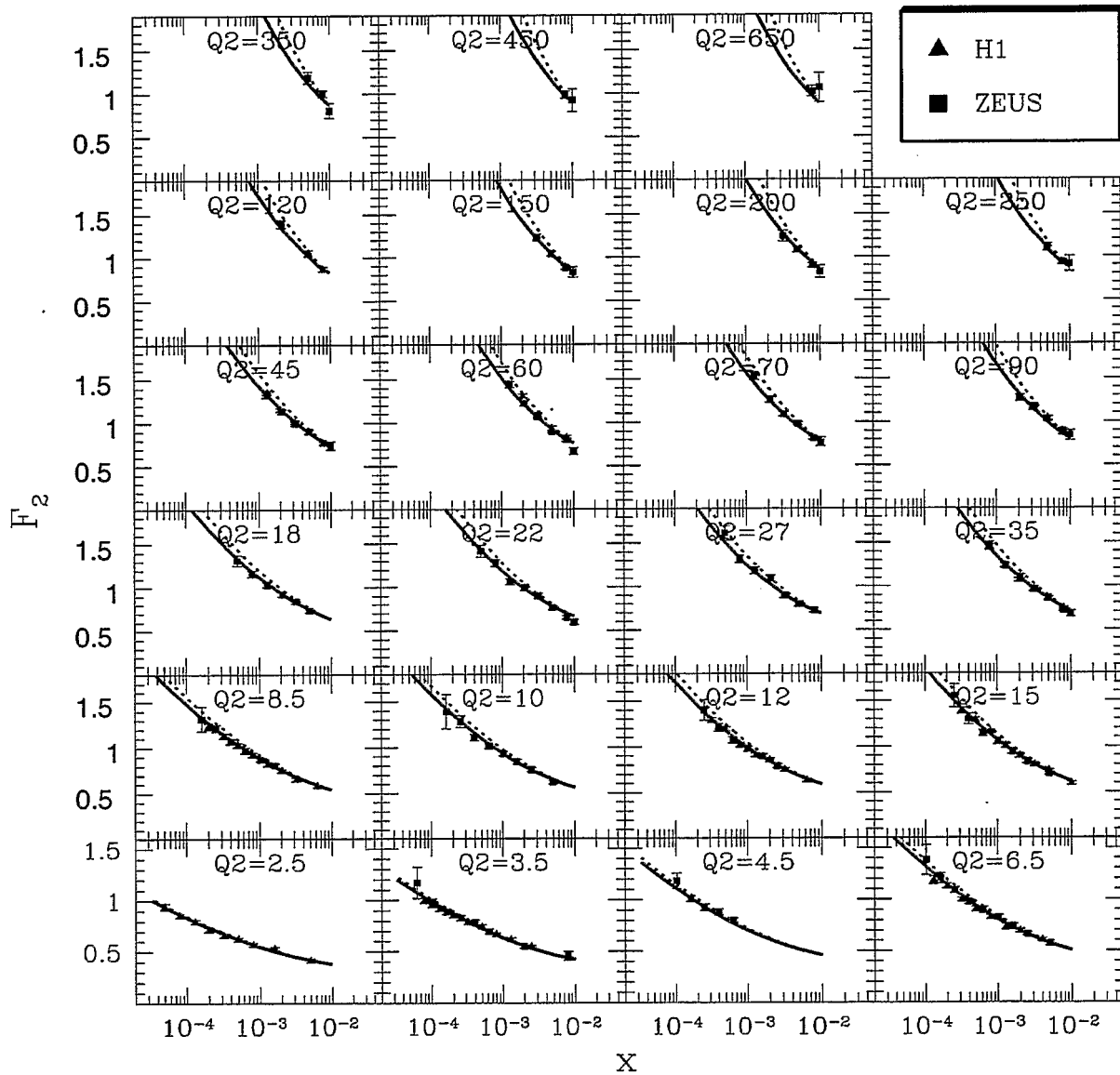
All 354 point F_2 at low x measured by H1,ZEUS and E665 collaborations were included in the fit and we obtain $\chi^2/n.d.f = 1$. We believe that it is an encouraging start.

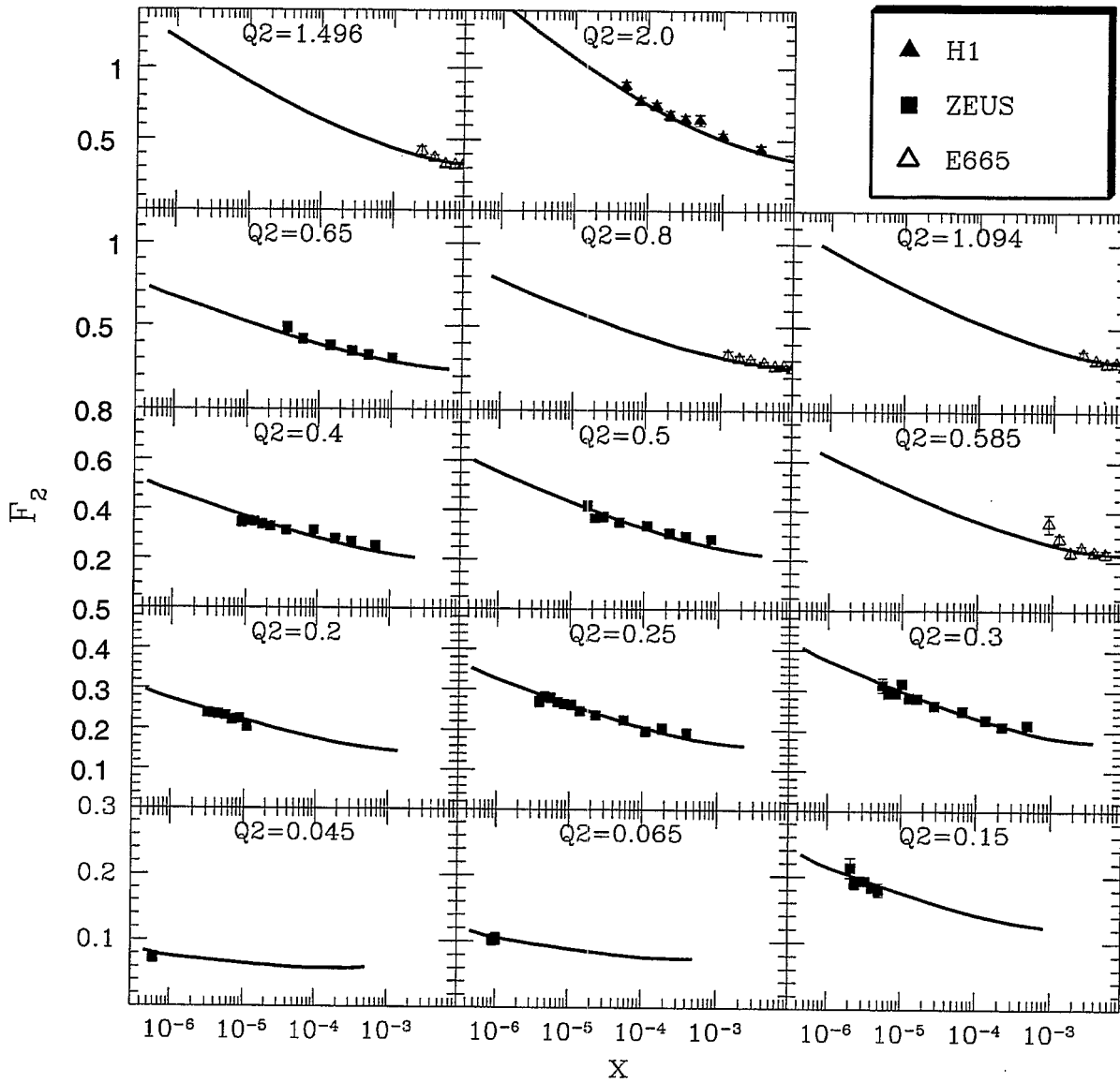
We calculated the Q^2 and x slopes of F_2 : $\frac{dF_2}{d \ln Q^2}$ and $\lambda = \frac{d \ln F_2}{d \ln Q^2}$, at very low x and Q^2 . The calculated slopes give a good description of the experimental data. It is interesting to note that we found $\lambda = 0.08 \div 0.1$ for $Q^2 < 1 \text{ GeV}^2$. This result imitates the “Soft” Pomeron (Donnachie - Landshoff) Pomeron intercept without soft physics involved.

- The first transparency shows the F_2 fit at high values of Q^2 . One can see that we achieved a good description of the data, using actually the only one fitting parameter $R^2 = 3.1 \text{ GeV}^{-2}$. This parameter enters only the initial condition for our evolution which was taken in the form of Glauber-Mueller formula . The small value of the radius is not surprising since this value takes into account a sufficiently strong diffractive production. It is well known that diffractive production stems from rather small distances. In terms of the constituent quark model our R^2 is an average between the size of a hadron and the proper size of the constituent quark;
- Second transparency shows F_2 at low Q^2 . One can see that we describe the transition between long and short distances quite well. We need to note, that we use the normalization factors in our fit: 1.03 (for H1), 0.97 (for E665), 0.98 (ZEUS low Q^2) and 1 (ZEUS high Q^2);
- The calculated $\frac{dF_2}{d \ln Q^2}$ and experimental data is shown in third and fourth transparencies. One can see the experimental data confirm our calculations;
- The slope λ one can see in the fifth and sixth transparencies as well as the fact the we are able to describe what is usually called as “soft” Pomeron.

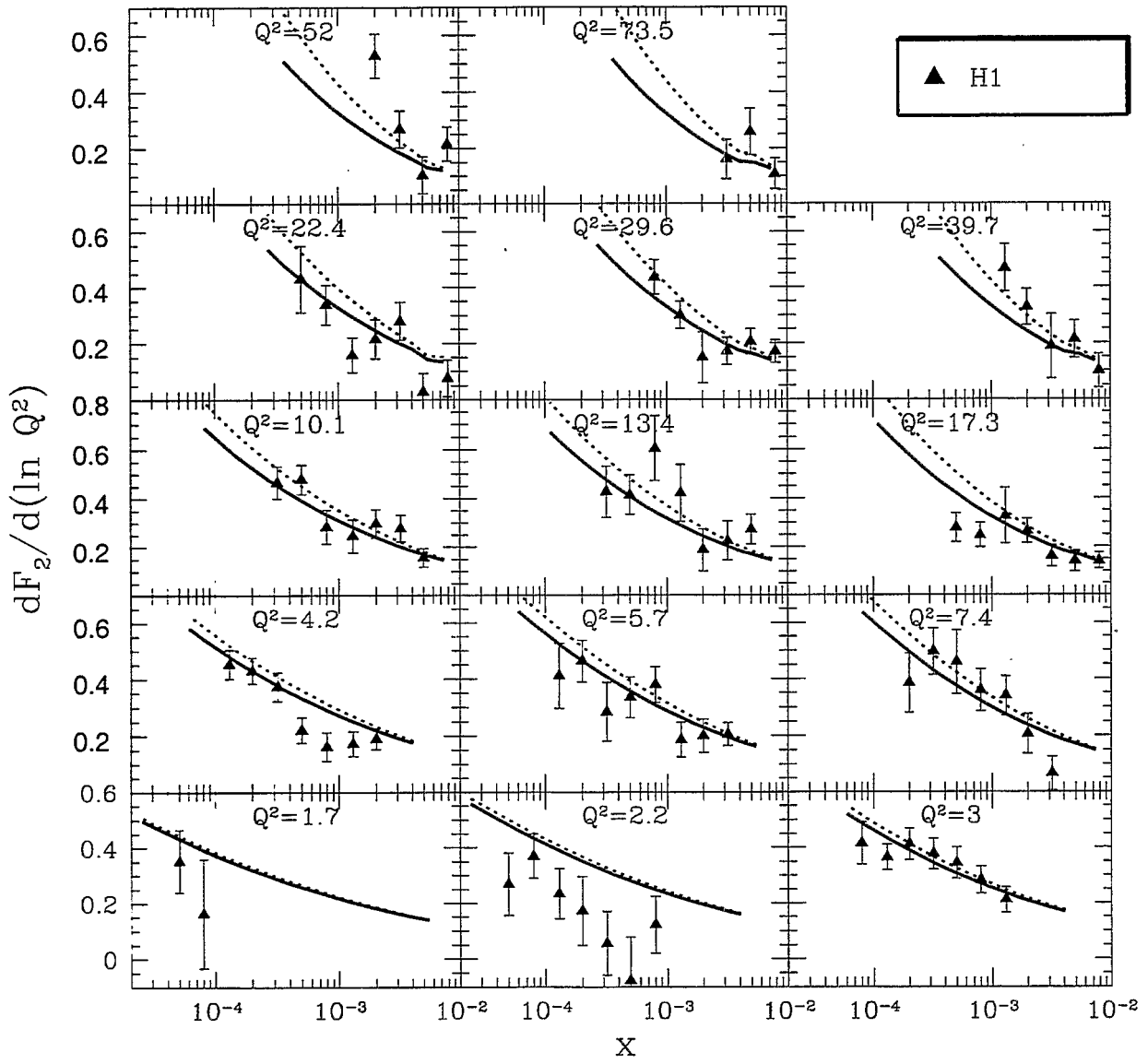
We believe that this work is a good step toward a new global fit of accessible experimental data which will provide a reliable extrapolation for higher energies (LHC, THERA ...) as well as for the DIS with a nuclear target.

$F_2(x, Q^2)$ for nucleon:

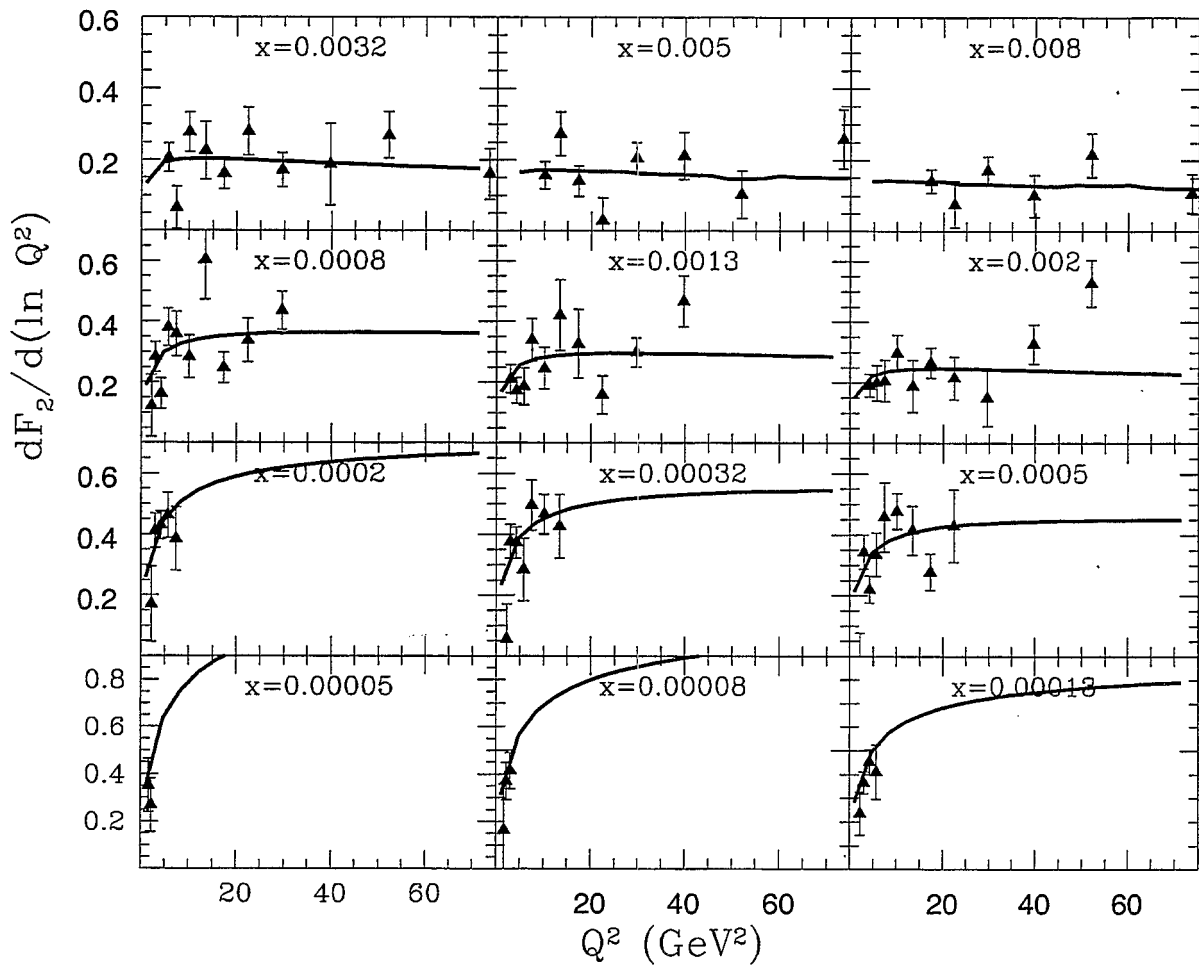




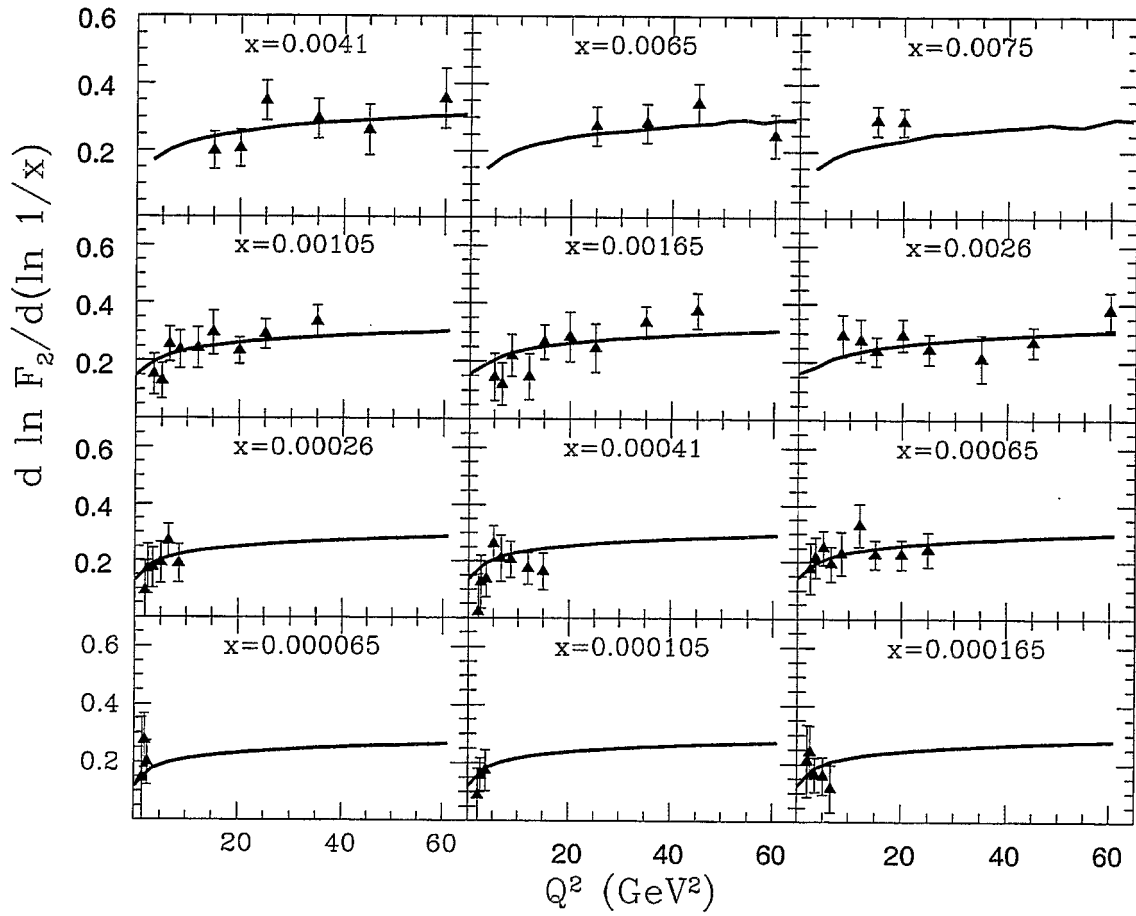
$$\frac{dF_2(x, Q^2)}{d \ln Q^2}$$

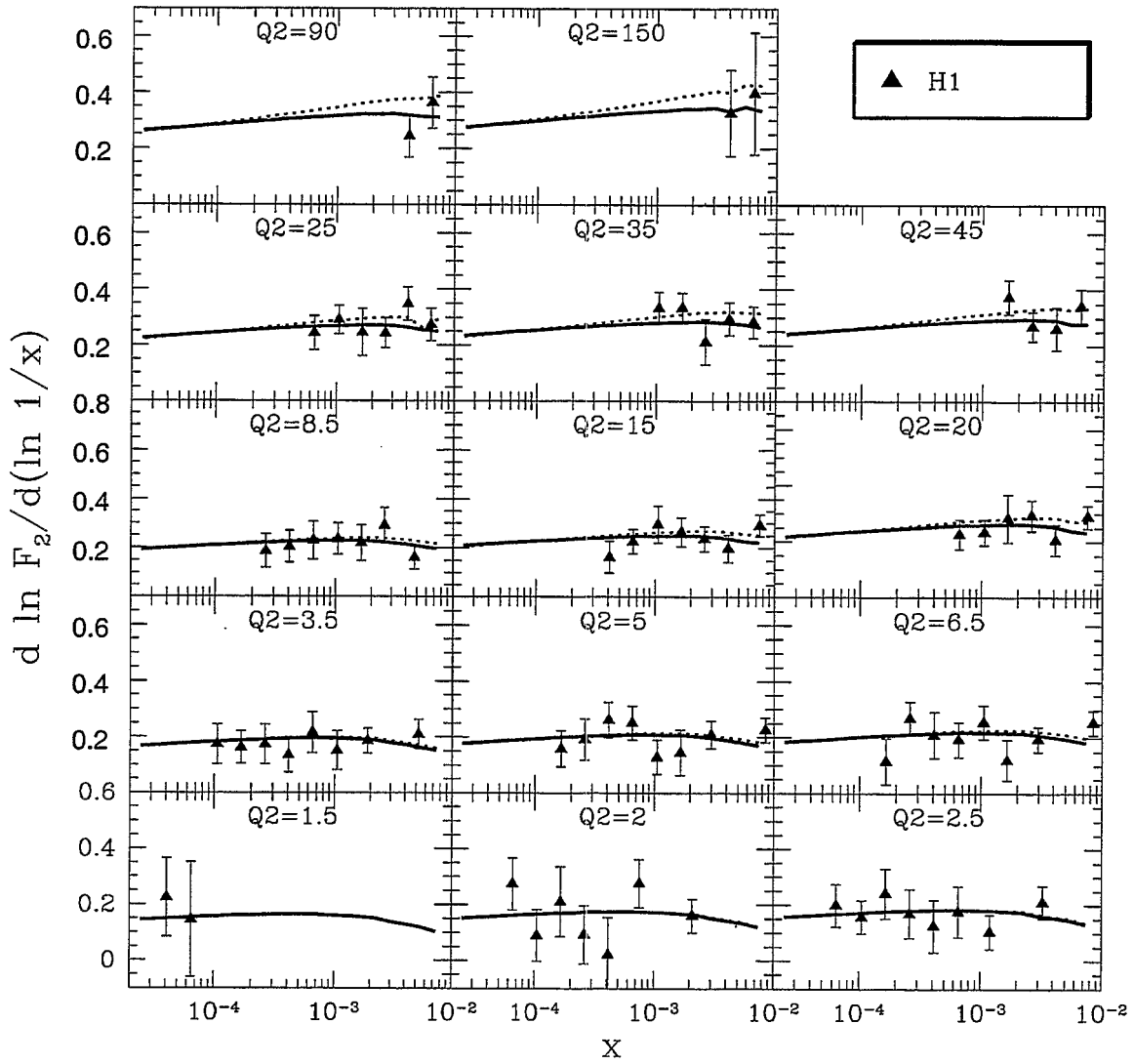


▲ H1



▲ H1





Harry C.S. Lam
McGill University

Gluon Saturation and Wilson Line Distribution

The number of gluons per rapidity interval grows at small x_F like a power of $1/x_F$, according to the DGLAP and the BFKL equations. Present day deeply inelastic data also seem to support this trend. However, such a rapid increase cannot continue forever, because unitarity forbids a growth faster than $\ln^2(1/x_F) \equiv \tau^2$, so saturation must set in at some point. Such a saturation is believed to be provided by the Color Glass Condensate Model, via the JIMWLK renormalization group equation for $W_\tau(\alpha)$, where α is the classical Yang-Mills potential for the dense soft gluons, and $W_\tau(\alpha)$ is its distribution in a nucleus. When probed by a fast parton, the response of the probe to the soft gluons is given by their Wilson line factors v . There are several advantages in dealing with the distribution of the responses of the probe, $\overline{W}_\tau(v)$, rather than the original distribution of $W_\tau(\alpha)$. The former satisfies the JIMWLK equation like the latter, but it is more directly physical, because v is the response of a physical probe, whereas α is gauge dependent. There are far fewer variables v than α , and more importantly, v lives on the compact manifold of the color group. This latter property allows us to construct an orthonormal complete set of polynomials in v and v^\dagger , and the integral of any polynomial to be computed. These properties of $\overline{W}_\tau(v)$ are exploited to obtain the transverse-momentum distribution of the gluon at $x_F = 0$ to be $d(x_F G)/dk^2 = R_A^2(N_c^2 - 1)/8\pi^2\alpha_s N_c$. They are also used to complete Mueller's proof of the JIMWLK equation, though for $\overline{W}_\tau(v)$ and not $W_\tau(\alpha)$. We also use them to derive a set of equations for multipole moments, generalizing the Balitsky-Kovchegov (BK) equation for dipole moments. The non-linearity of the original BK equation leads to saturation. The generalized BK equations for multipole moments are linear but inhomogeneous, driven by the moments of lower multipoles, thus saturation of higher multipoles are driven by the saturation of dipoles. As far as we can see, the multipole moments are the only $\overline{W}_\tau(v)$ that have infrared-finite solutions, so in practice the generalized BK equations may be used to replace the equations for $\overline{W}_\tau(v)$.

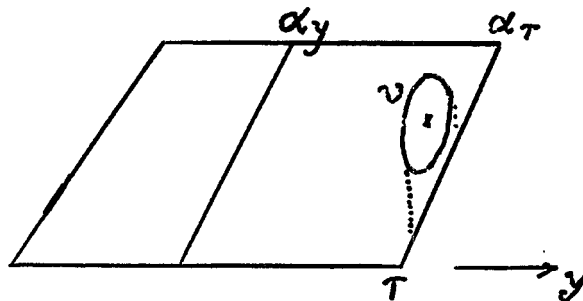
Gluon Saturation and Wilson Line Distribution

C.S. Lam, McGill University

hep-ph 0207058/PRD (CSL, Greg Mahlon, Wei Zhu)

CONTENTS

1. Saturation & Color Glass Condensate Model.
2. Wilson Line Distribution. $W_\tau(\alpha) \rightarrow \overline{W}_\tau(v)$
3. Saturated Gluon Distribution at $x_F = 0$.
$$\frac{d(x_F G)}{dk^2} = \frac{R_A^2 (N_c^2 - 1)}{8\pi^2 \alpha_s N_c}$$
4. Generalized Balitsky-Kovchegov Equation for multipole amplitude
5. Conclusion



Wilson Line Distribution (probe response)

from $W_\tau(\alpha)$ to $\bar{W}_\tau(v)$

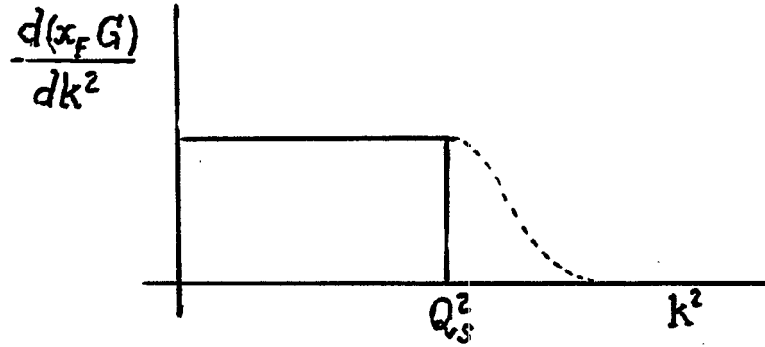
$$v(x) = \bar{P} \exp \left[-ig \int_{-\infty}^{\tau} dy \alpha_y^a(x) t_a \right]$$

- $\bar{W}_\tau(v') = \int W_\tau(\alpha) \delta(v' - v) \mathcal{D}[\alpha] / \mathcal{J}(v)$
(also Blaizot/Iancu/Weigert, hep-ph/0206279)

- Observable:

$$\begin{aligned} \langle O \rangle_\tau &= \int D[\alpha] O(v, v^\dagger, \phi) W_\tau(\alpha) \\ &= \int D_H[v] O(v, v^\dagger) \bar{W}_\tau(v) \end{aligned}$$

- v -space is compact



$$\begin{aligned}
 \frac{d(x_F G)}{dk^2} &= \frac{1}{4\pi^2 N_c} \langle \text{Tr} [F^{+i}(\vec{k}) F^{+i}(-\vec{k})] \rangle \\
 &= \frac{1}{4\pi^2 g^2 N_c} \int d^2 \mathbf{x} d^2 \mathbf{y} \exp [i \mathbf{k} \cdot (\mathbf{x} - \mathbf{y})] \\
 &\quad \cdot \langle \text{Tr} [V(\mathbf{x}) \partial_i V^\dagger(\mathbf{x}) V(\mathbf{y}) \partial_i V^\dagger(\mathbf{y})] \rangle \\
 &= \frac{R_A^2 (N_c^2 - 1)}{8\pi^2 \alpha_s N_c}
 \end{aligned}$$

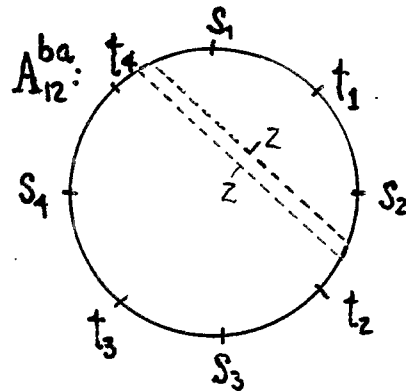
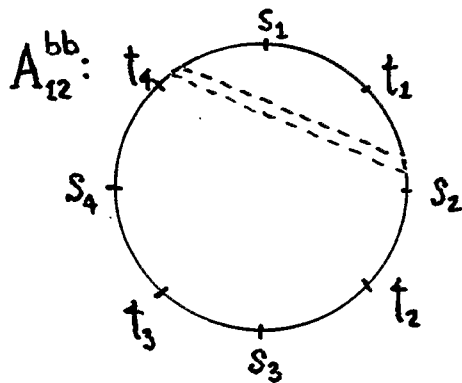
- BK equation: $[A(st) = S_\tau(st)]$

$$\frac{\partial S_\tau(st)}{\partial \tau} = -2\pi\alpha_s N_c \int d^2z I_{st}(z) [S_\tau(st) - S_\tau(sz)S_\tau(zt)]$$

- Generalized BK equation:

$$\frac{\partial A}{\partial \tau} = -2\pi\alpha_s N_c \sum_{i,j=1}^k \int d^2z I_{ij}(z) [A_{ij}^{aa} + A_{ij}^{bb} - A_{ij}^{ba} - A_{ij}^{ab}]$$

$$A_{12}^{bb} = A(|s_1 t_1 | s_2 t_2 \cdots t_k) = A(s_1 t_1) A(s_2 \cdots t_k)$$



- **linear** and inhomogeneous for all $k > 1$
- $I_{ij}(xy|z) = O(1/z^4)$
- replaces IR finite solⁿ of JIMWLK eq?

Conclusion

- Advantages of $\overline{W}_\tau(v)$:
 - more physical; distribution of probe response.
 - $v v^\dagger$ lives on a compact manifold
 - irreducible rep of $U(n)$ forms an orthonormal complete set of polynomials
- Applications:
 - completes Mueller's proof of the JIMWLK eq for $\overline{W}_\tau(v)$
 - derives a generalized BK equation. Replaces Infrared-free JIMWLK eq?
 - saturation: obtains unintegrated gluon distribution at $x_F = 0$

Hard Coherent Phenomena in eA and in pA collisions

L. Frankfurt

Nuclear Physics Dept., Tel Aviv University, Israel

We deduce formulae for a hadron(photon) fragmentation into jets off Coulomb field of nucleus in terms of minimal Fock component of light cone wave function of this hadron. The derivation is based on the theorem which is valid in QCD for a field of equivalent photons produced in the process of fragmentation of a fast hadron(photon) into high k_t jets . We proved that as the consequence of the conservation of e.m. current that field is dominated in the leading order over α_s by the photon radiation from jets.

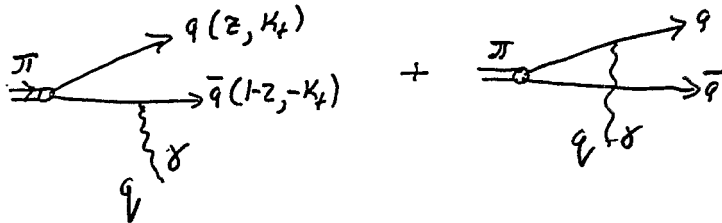
Prediction [3] and observation of squeezing of vector mesons in the electroproduction of vector mesons at HERA . Generalized Color Transparency phenomenon in diffractive electroproduction of vector mesons is explained as one of consequences of proper QCD factorization theorem. [1,3]. Prediction of QCD for the nuclear dependence of the cross section of the process: $\pi + A \rightarrow 2jet + X$ for $X=A$ or nuclear excitations [1] as well as recent discovery of color transparency phenomenon at FNAL are explained. Postselection requirements. High momentum tail of z, k_t dependence of minimal Fock component of pion wf is calculated. Cancellation of infrared divergencies in the renormalization procedure cf. [6]. QCD factorization and the choice of special light cone gauge. [1]. Various color transparency and color opacity phenomena in eA scattering are discussed. [4]

Diffractive proton fragmentation into 3 jets in pA collisions. x, k_t dependencies of cross section. Various color transparency and color opacity phenomena in the process: $p + A \rightarrow 3jets + A$. [7]

-
- [1] L.L. Frankfurt, G.A. Miller and M. Strikman, Phys. Lett. **B304**, 1 (1993);
Found. Phys. **30**, 533 (2000),
Phys.Rev. D65:094015,2002.
 - [2] E. M. Aitala *et al.* [Fermilab E791 Collaboration], Phys. Rev. Lett. **86**, 4773 (2001);
E. M. Aitala *et al.* [Fermilab E791 Collaboration], Phys. Rev. Lett. **86**, 4768 (2001).
 - [3] S. J. Brodsky, L. Frankfurt, J. F. Gunion, A. H. Mueller and M. Strikman, Phys. Rev. **D50**, 3134 (1994).
 - [4] See the review:
L.L. Frankfurt, G.A. Miller and M. Strikman, Ann. Rev. Nucl. Part. Sci. **44**, 501 (1994)
hep-ph/9407274.
 - [5] L.Frankfurt, V. Guzey, M. McDermott and M.Strikman, Phys.Rev.Lett.87:192301,2001
 - [6] S.J. Brodsky G.P. Lepage, Phys. Rev. **D22**, 2157 (1982)
 - [7] E. Lippmaa *et al.* [FELIX Collaboration], CERN-LHCC-97-45, LHCC-I10, J. Phys. G **28**, R117 (2002).

$$\langle \pi | d_{r,t} \cdot q_{r,t} | q\bar{q} \rangle \Rightarrow$$

for small q_t is dominated by photon radiation from quark (jet) lines:



$$\langle \pi | d_{r,t} q_{r,t} | q\bar{q} \rangle = e \chi_{\pi}(z, k_t) \times \sum_i \frac{2(\chi_{E_i}(q_t) e_i)}{z_i}$$

$\frac{e_i (-e_i)}{e}$ is the charge of quark (antiquark)

This formulae is the generalization of V. Eruber formulae for the photon bremsstrahlung which is the basic element of derivation of QCD evolution equation in the momentum space.

$$\chi_{\pi}(z, k_t^2) = \frac{4\pi C_F \alpha_s(k_t^2)}{k_t^2} \sqrt{3} \int_{\pi} z(1-z) \left(\ln \frac{k_t^2}{\lambda_{QCD}^2} \right)^{CF/\beta}$$

$$\varphi_{\pi}(z, Q^2) = \frac{1}{d(Q^2)} \int_0^{Q^2} \chi(k_t^2, z) \frac{dk_t^2}{16\pi^3}$$

$$d_{\frac{q}{g}} = \left(\ln \frac{k_t^2}{\lambda_{QCD}^2} \right) \frac{CF}{\beta}$$

\rightarrow renormalization of quark Green function

Summary

$$h + A \rightarrow \text{jets} + A$$

$$h = \pi, p, \delta, \dots$$

$$A = \frac{-e^2 \cdot S}{(q_{\perp}^2 - t_{\min})} \frac{\mathcal{V}_h(z_i, K_{\perp i})}{M_{\perp}^2(\text{jet})} \sum_i \frac{\mathcal{G}(q_{\perp}, K_{\perp i}) \rho_i}{z_i} \frac{z \cdot F_A(H)}{\prod_i \sqrt{d_i(K_{\perp i}^2)}}$$

$$M_{\perp}^2 = \sum_i \frac{K_{\perp i}^2}{z_i}$$

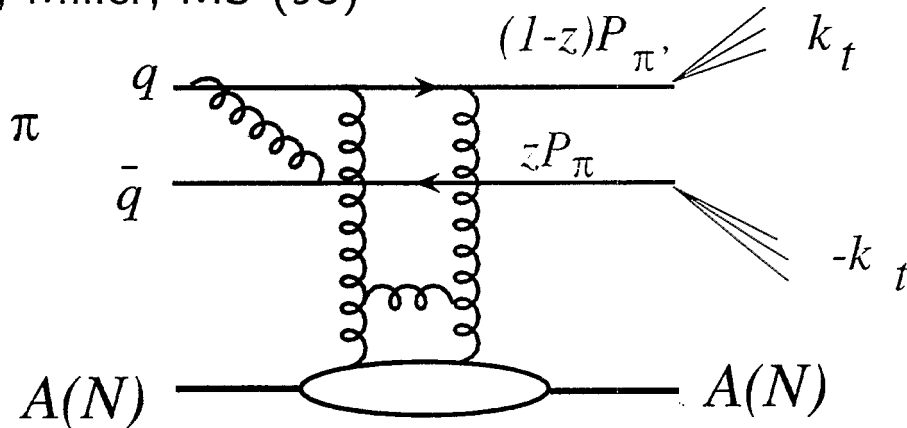
- i). At large energies formulae unambiguously follows from renormalizability of QCD and conservation of e.m. current. Accuracy - $\alpha_s(K_{\perp}^2)$.
- ii). renormalization of amplitude A leads to the cancellation of infrared divergencies (BL82) and to additional factor $\prod_i \sqrt{d_i}$ in the amplitude. (ms)
- iii). High K_{\perp} tail of l.c. w.f. of a fast hadron is observable in the leading order over α_s and all orders over $(\alpha_s \ln \frac{K_{\perp}^2}{\Lambda_{\text{QCD}}^2})$

$$\pi + N(A) \rightarrow \text{"2high } p_t \text{ jets"} + N(A)$$

Mechanism:

Pion approaches the target in a frozen small size $q\bar{q}$ configuration and scatters elastically via interaction with $G_{target}(x, Q^2)$.

the first analysis for πp scattering Randa(80), nuclear effects - Bertsch, Brodsky, Goldhaber, Gunion (81), pQCD treatment: Frankfurt, Miller, MS (93)



$$A(\pi + N \rightarrow 2 \text{ jets} + N)(z, p_t, t=0) \propto$$

$$\int d^2b \psi_\pi^{q\bar{q}}(z, b) \sigma_{q\bar{q}-N(A)}(b, s) \exp(ik_t b)$$

$$b = r_t^q - r_t^{\bar{q}}$$

Calculation resembles jet production off
Coulomb field. (fms 02)

- i). Derivation of Weizsacker, Williams approximation is the same in QED and in QCD because Ward identity is the same in color singlet channel.
- ii). Use of generalization of V. Gribov theorem to prove that gluon radiation from external quark, gluon lines (jets) dominates.
Precision of prove is $d_s(k_+^2)$
- iii). Generalized Color Transparency Phenomenon unambiguously follows from QCD

$$\frac{d}{dt} \sigma(h+A \rightarrow \text{high } p_T \text{ jets} + A) \Big|_{t=0} = \left[\frac{C_A(x_1, x_2, p_T^2)}{C_H(x_1, x_2, p_T^2)} \right]^2 \frac{d\sigma(h+A \rightarrow \text{jets} + A)}{dt}$$

within the region of applicability of QCD evolution equation.

CT should disappear in the proximity to black body regimes: color glasses

Effective probe of onset new QCD regime

\implies A-dependence: $A^{4/3} \left[\frac{G_A(x, k_t^2)}{AG_N(x, k_t^2)} \right]^2$, where $x = M_{dijet}^2/s$.

$\implies \frac{d\sigma(z)}{dz} \propto \phi_\pi^2(z) \approx z^2(1-z)^2$ where $z = E_{jet1}/E_\pi$.

$\implies k_t$ dependence: $\frac{d\sigma}{d^2k_t} \propto \frac{1}{k_t^n}$, $n \approx 8$ for $x \sim 0.02$

\implies Absolute cross section is also predicted

Andrzej M. Sandacz

Sołtan Institute for Nuclear Studies, ul. Hoża 69, Warsaw
PL 00681, Poland

E-mail: sandacz@fuw.edu.pl

Search for Color Transparency

A. Sandacz

Softan Institute for Nuclear Studies, ul. Hoża 69, Warsaw, PL 00681, Poland

E-mail: sandacz@fuw.edu.pl

Color transparency (CT) is a phenomenon of perturbative QCD, whose characteristic feature is that small color-singlet objects interact with hadrons with small cross sections (for references see e.g. [1]). QCD calculations confirmed the hypothesis of F. Low on smallness of the cross section for the interaction of SSC with a hadron, if the gluon density in the hadron is not very high (at moderately small x). They also predict a related phenomenon of *color opacity* when the gluon density becomes very large (at very small x) and SSC interacts with the hadron with large cross section.

Experimental searches for CT started more than a decade ago and encompass various processes (for references see [1]): large- t quasielastic ($p, 2p$) scattering, large- Q^2 quasielastic ($e, e'p$) scattering, J/ψ photoproduction and J/ψ muoproduction, exclusive ρ^0 leptonproduction and coherent diffractive dissociation of the pion into two high- p_t jets.

Among these experiments only few have reported an evidence for CT. For the others an obstacle to clearly demonstrate CT was a relatively low energy of the projectile, and thus low coherence length and formation length. A recent evidence for CT comes from Fermilab E791 experiment on the A -dependence of coherent diffractive dissociation of the pion into two high- p_t jets. Also the E691 results on A -dependence of coherent J/ψ photoproduction and the NMC measurements of A -dependence of coherent and quasielastic J/ψ muoproduction are consistent with CT. Measurements of the nuclear transparency for incoherent exclusive ρ^0 production by Fermilab experiment E665 give a hint for CT. However, due to the low statistics of that data at high Q^2 , it was not possible to disentangle effects of decreasing coherence length at high Q^2 and to demonstrate CT unambiguously.

Unambiguous demonstration of CT and color opacity is still needed and should be a subject of dedicated comprehensive studies. The program of such studies is sketched in Transparency 1.

The potential of the COMPASS experiment at CERN to study color transparency via exclusive ρ^0 production in hard muon-nucleus scattering was examined in [1]. It was proposed to use thin nuclear targets of carbon and lead, with only one nuclear target being exposed to the muon beam at a time and frequent exchanges (every few hours) of different targets. For muon beam energy of 190 GeV and a trigger for medium and large Q^2 ; the covered kinematic range is $2 < Q^2 < 20 \text{ GeV}^2$ and $35 < \nu < 170 \text{ GeV}$. An efficient selection of coherent or incoherent events is possible by applying cuts on p_t^2 . In order to obtain the samples of events initiated with a probability of about 80% by either γ_L^* or γ_T^* , the cuts on the ρ^0 decay angular distribution of $\cos \theta^*$ will be used. The search for CT could be facilitated by using the events with l_c values exceeding the sizes of the target nuclei. The fraction of such events is substantial and the covered Q^2 range seems sufficient to observe CT. The estimates of the yields of accepted events were obtained assuming integrated luminosity $\int \mathcal{L} = 230 \text{ pb}^{-1}$ which corresponds to 37 effective days of muon beam.

The high sensitivity of the measured ratio R_T of nuclear transparencies for lead and carbon for different models of nuclear absorption is shown in Transp. 2. These measurements, taken at different Q^2 intervals, may allow to discriminate between different mechanisms of the interaction of the hadronic components of the virtual photon with the nucleus.

At EIC, taking advantage of its high energy, large luminosity and wide range of nuclear beams, a more precise systematic study could be realised. Results of simulations of hard exclusive J/ψ production, hard exclusive ρ^0 production and of J/ψ quasi-real photoproduction at EIC were presented in [2]. With the assumed Extended Central Tracking Detector covering the range $-3.1 < \eta < 3.1$ the hard vector meson production could be measured with good acceptance in the kinematical range $1 < Q^2 < 50 \text{ GeV}^2$, $10 < W < 55 \text{ GeV}$ and $0.0003 < x < 0.16$ both for ρ^0 and J/ψ . Therefore, the transition from color transparency to color opacity may be observed.

The estimates of accepted numbers of events were obtained assuming integrated luminosity $\int \mathcal{L} = 330 \text{ pb}^{-1}$ for ep collisions and 10 pb^{-1} for $e\text{Au}$ collisions. The total numbers of accepted events for hard exclusive ρ^0 production are 1.1 mln for the proton beam and 4.2 mln for the gold beam. For hard exclusive J/ψ production with J/ψ decaying into either e^+e^- or $\mu^+\mu^-$ the corresponding numbers are 7000 and 210000 events. The event sample for J/ψ photoproduction will be about ten times larger than for hard J/ψ production; 80000 events for the proton beam and 2.2 mln for the gold beam.

The expected statistical accuracy of parameter α , which quantifies A -dependence of cross sections, $\sigma_A = \sigma_0 A^\alpha$, is shown in Transp. 3 for hard exclusive ρ^0 production. Note, that at EIC in general the statistical error $\Delta\alpha$ will be within the range 0.0005 - 0.01, except for the region of the lowest x at high Q^2 values. For the sample of coherent events, with the cut $|t| < 0.02 \text{ GeV}^2$ applied to the events from gold, the values of $\Delta\alpha$ will be practically about the same as those shown for the global sample. For the incoherent events, selected with the cut $|t| > 0.05 \text{ GeV}^2$ for gold, the errors will be about 1.5 to 2 times larger (Transp. 4). Also for J/ψ production the statistical precision will be high. In particular, for the photoproduction data divided between 6 bins in W , $\Delta\alpha$ will be about 0.002 in each W bin (Transp. 5).

At EIC the precision of α will be significantly higher than in previous experiments. For example, the statistical errors $\Delta\alpha$ for the coherent dissociation of pions into high p_t jets from E791 are about 0.1, for the coherent J/ψ photoproduction measured by E691 $\Delta\alpha = 0.06$ and for the NMC results on coherent J/ψ muoproduction it is about 0.02.

In conclusion, the proposed comprehensive studies of exclusive production of vector mesons in eA and ep collisions at EIC will be a decisive step towards experimental verification of the predictions of perturbative QCD on color transparency and color opacity.

References

- [1] A. Sandacz, O.A. Grajek, M. Moinester, E. Piasezky,
Color Transparency at COMPASS, TAUP-2671-2001, hep-ex/0106076.
- [2] A. Sandacz, **Exclusive Processes at EIC - Feasibility Study**,
presented at EIC Workshop, BNL, March 1, 2002, to appear in the proceedings.

Program to unambiguously demonstrate
color transparency and color opacity

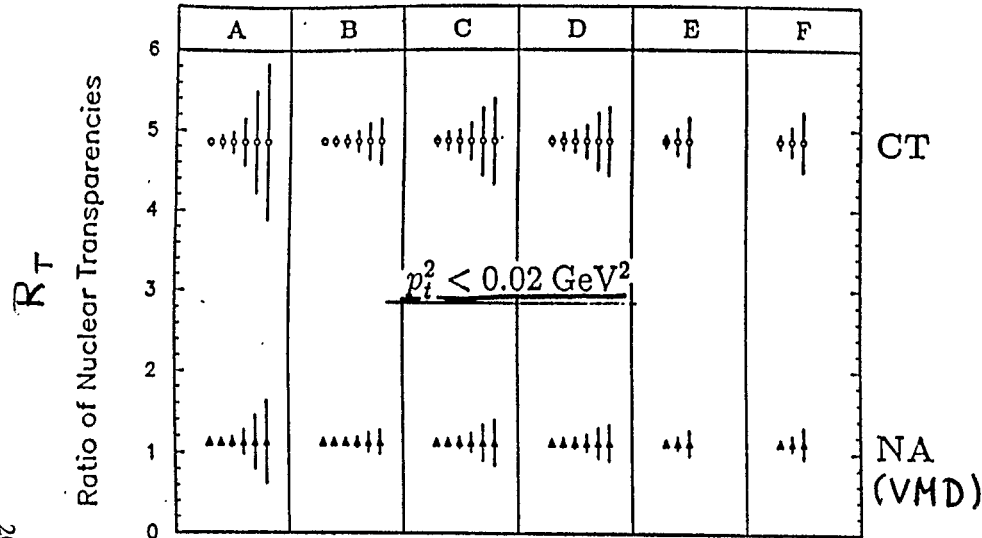
via exclusive vector meson production

- measure $A - Q^2$ and x -dependence of cross sections for exclusive production of various mesons ($\rho^0, \phi, J/\psi, \rho', \psi', \dots$)
- measure both coherent and incoherent cross sections
- sample different polarisation of vector mesons
- control coherence length (and formation length)

prerequisites:

- high energy
- high luminosity

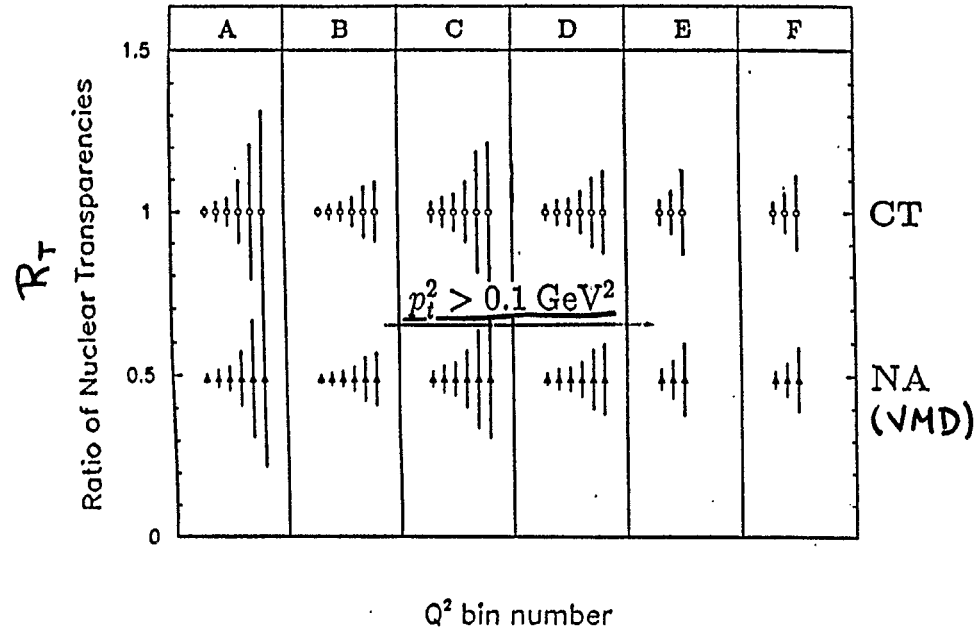
coherent



COMPASS, MC

Bin number	Q^2 bin [GeV ²]	$\langle Q^2 \rangle$ [GeV ²]	$\langle x \rangle$
1	2-3	2.4	0.016
2	3-4	3.4	0.022
3	4-6	4.8	0.031
4	6-9	7.2	0.048
5	9-12	10.2	0.072
6	12-20	14.8	0.11

incoherent



$$R_T = T_{PB} / T_C = (\sigma_{PB} / A_{PB}) / (\sigma_C / A_C)$$

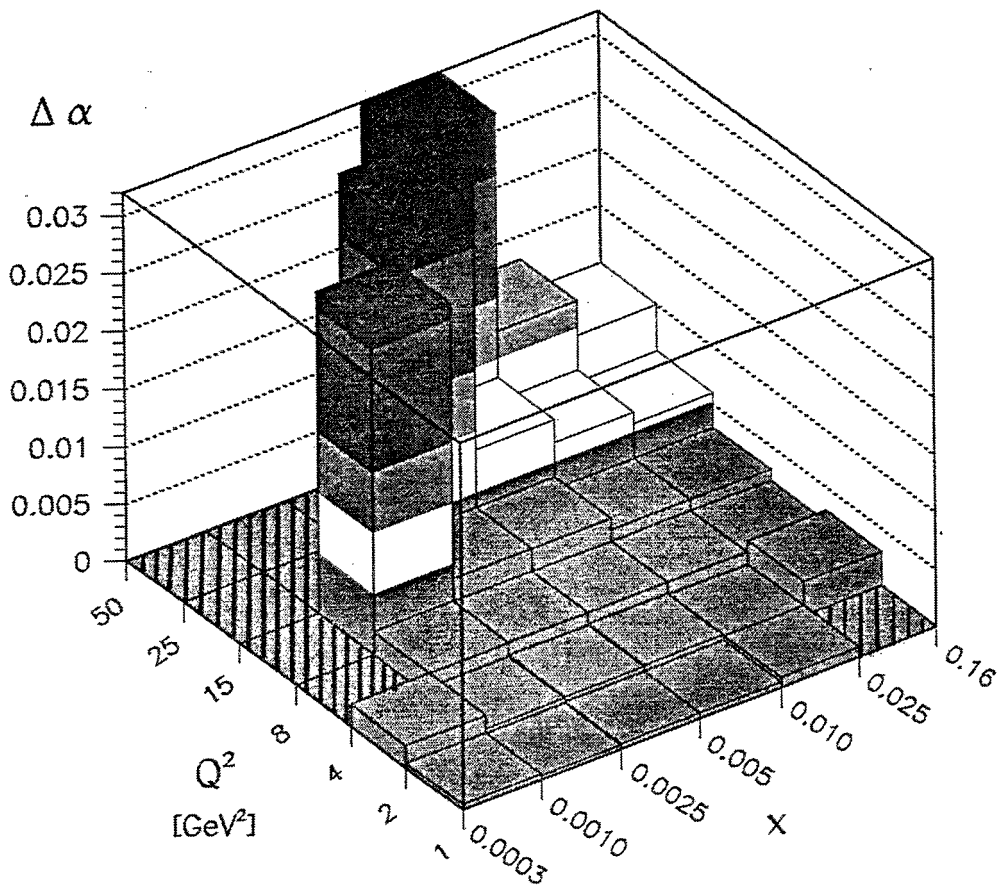
$$(T_A = \frac{\sigma_A}{A \sigma_N})$$

set	conditions
A	MT
B	FT
C	FT + $ \cos \theta < 0.4$
D	FT + $ \cos \theta > 0.7$
E	FT + $ \cos \theta < 0.4$ + $l_c > 11 \text{ fm}$
F	FT + $ \cos \theta > 0.7$ + $l_c > 11 \text{ fm}$

(EIC)

Nuclear dependence of cross sections
for exclusive ρ^0 production at $Q^2 > 1 \text{ GeV}^2$

$$\sigma_A = \sigma_0 A^\alpha$$



\mathcal{L}_{int} : 330 pb $^{-4}$ for ep 10 pb $^{-4}$ for eAu

total numbers of accepted events:
1.1 M for ep 4.2 M for eAu

EIC

Statistical precision of α for various subsamples of exclusive g^0 production at $Q^2 > 1 \text{ GeV}^2$

- coherent selection - $|t| < 0.02 \text{ GeV}^2$
 - incoherent selection - $|t| > 0.05 \text{ GeV}^2$
 - alternative θ^* cuts $\left\{ \begin{array}{l} \text{or } |\cos \theta^*| > 0.7 \text{ to suppress } g_T^0 \\ \text{or } |\cos \theta^*| < 0.4 \text{ to suppress } g_L^0 \end{array} \right.$ } for eAu
- (θ^* cuts applied both for ep and eAu)

(x, Q^2) bin	$\Delta\alpha$				
	all	coherent	incoherent	coherent and θ^* cut	incoherent and θ^* cut
$0.001 \div 0.0025$ $2 \div 4$	0.0008	0.0008	0.0012	0.0014	0.0021
$0.001 \div 0.0025$ $8 \div 15$	0.028	0.028	0.043	0.049	0.075
$0.01 \div 0.025$ $2 \div 4$	0.0009	0.001	0.002	0.002	0.003
$0.01 \div 0.025$ $8 \div 15$	0.003	0.004	0.006	0.006	0.010
$0.01 \div 0.025$ $25 \div 50$	0.013	0.013	0.021	0.023	0.036

Nuclear dependence of J/ψ photoproduction at EIC

Extended CTD

only J/ψ reconstructed

$$W^2 \approx 2(E_{J/\psi} - p_{zJ/\psi}) \cdot E = 4 E_p E_e y$$

$$t = (q - V)^2 \approx -P_{TJ/\psi}^2$$

10 GeV + 100 GeV

$Q_{\min}^2 < Q^2 < 1 \text{ GeV}^2$
$10 < W < 60 \text{ GeV}$

$$|t| < 0.6 \text{ GeV}^2$$

$$Q_{\min}^2 = M_e^2 y^2 / (1-y)$$

(down to 10^{-10} GeV^2)

$$\langle Q^2 \rangle \approx 0.05 \text{ GeV}^2$$

$$10^{-10} \lesssim x \lesssim 10^{-3}$$

\mathcal{L}_{int} : 330 pb^{-1} for ep 10 pb^{-1} for eAu

total numbers of accepted events :

80 k for ep 2.2 M for eAu

dividing W range into 6 bins

\Rightarrow

$\Delta x \approx 0.002$

in each of W bins

eRHIC. Accelerator Issues.

V.Ptitsyn,
Collider-Accelerator Department, BNL

The electron-ion (proton) collider on the basis of the existing RHIC collider is attractive and feasible option. The accelerator objective is to provide e-Au and e-p collisions with luminosities up to 10^{31} and $3 \cdot 10^{32} (s \cdot cm^2)^{-1}$ respectively, for 5-10 GeV electron beam and for proton (or Au) beam at the present RHIC energy range. The electron and proton beams should be polarized with up to 70% polarization degree. Moreover, at a collision point the longitudinal direction of polarization is wanted.

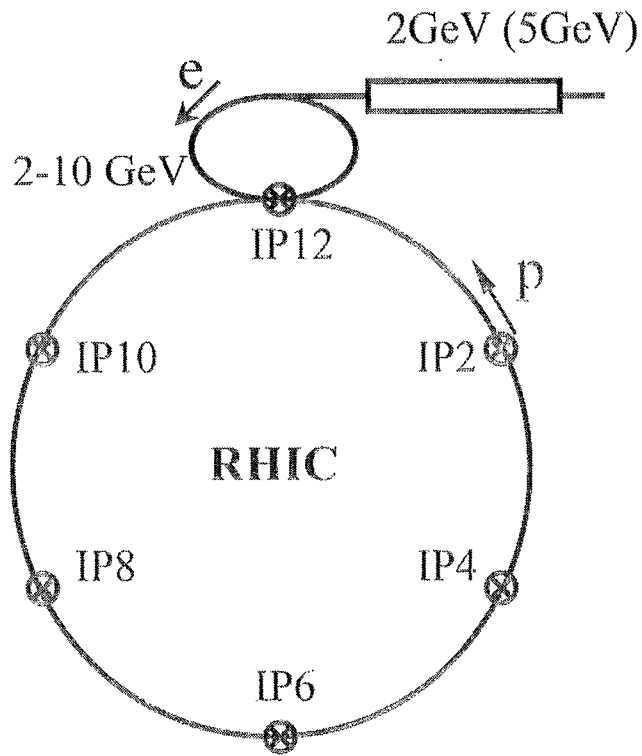
The present collider scheme is based on the layout suggested by Novosibirsk Budker Institute. It assumes the storage electron ring out of the RHIC tunnel which intersects the RHIC ring at one collision point (currently at 12 o'clock). The electron beam acquires its polarization due to synchrotron radiation while circulating in the ring. To provide the sufficiently small polarization time the e-ring lattice uses the special dipole magnets called superbends. The middle high-field region of the superbend magnets has the constant field of 2T while the remaining low-field part of the magnet changes with electron energy to provide the same total bending angle in all electron beam energy range (5-10 GeV). The main issue related with the application of the superbend magnets is the accommodation of high amount of synchrotron radiation power, radiated from high field regions of the magnets.

The realization of cooling of RHIC ion (or proton beam) is necessary condition in order to reach the required luminosities. Also the possible limitations on the RHIC ion current, like intensity driven instabilities (particularly the effect of electron cloud) should be evaluated. The eRHIC design requires using 360 RHIC ion bunches instead of 60 used in RHIC operation runs so far.

There are two basic interaction region design schemes: one involving the beam separation in horizontal plane, another with the separation in the vertical plane. The interaction region designs involve the issues related with detector background and minimizing the beam depolarization. For both interaction region schemes the longitudinal polarization at the collision point can be achieved by using the spin rotators based on the solenoidal field magnets.

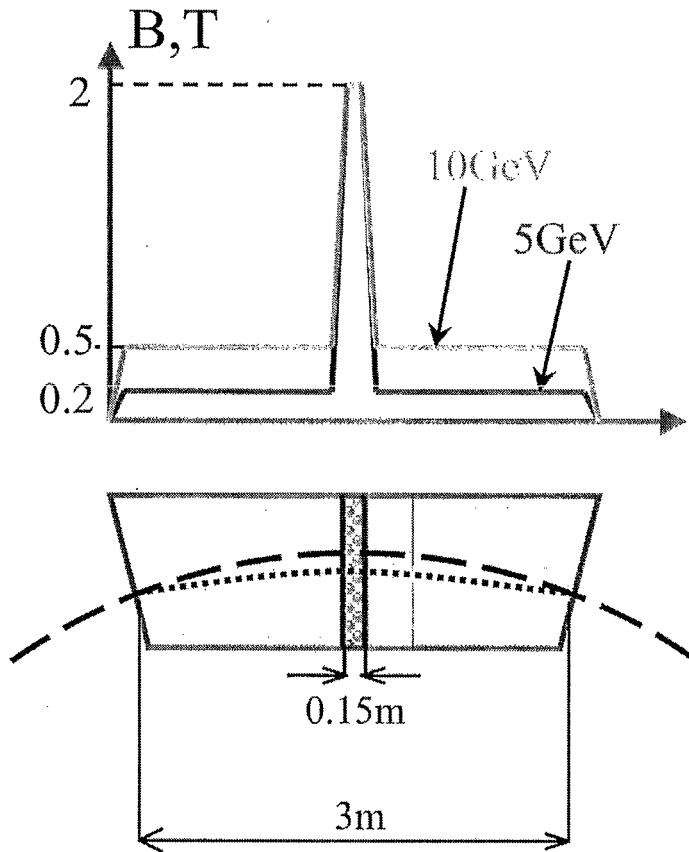
Another possible eRHIC option, with recirculator ring instead of the storage electron ring, have been considered. Such a scheme allows to have lower emittance electron beam from linac and to be less restricted by beam-beam effects, but it requires the high-current polarized source development to be done.

Present collider layout



- Proposed by BINP(Novosibirsk)
- e-ring is $\frac{1}{4}$ of RHIC ring length
- Collisions in one interaction point
- Collision e energies: 5-10 GeV
- Injection linac: 2-5 GeV
- Lattice based on "superbend" magnets
- Polarization time: 4-16 minutes
- RHIC IR12, IR2, IR4 are possible candidates for collision point

Superbend magnet

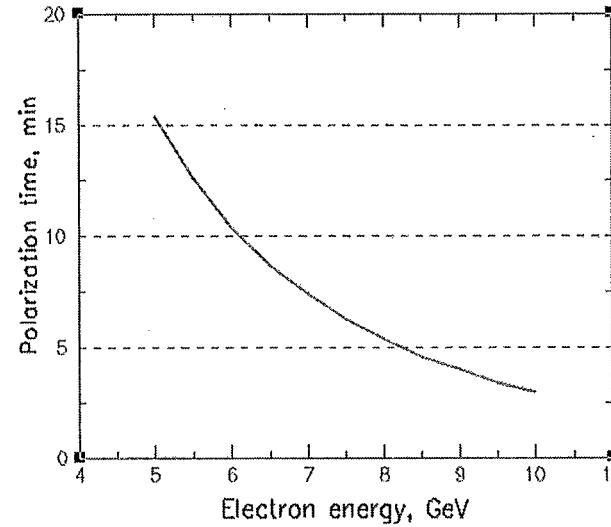
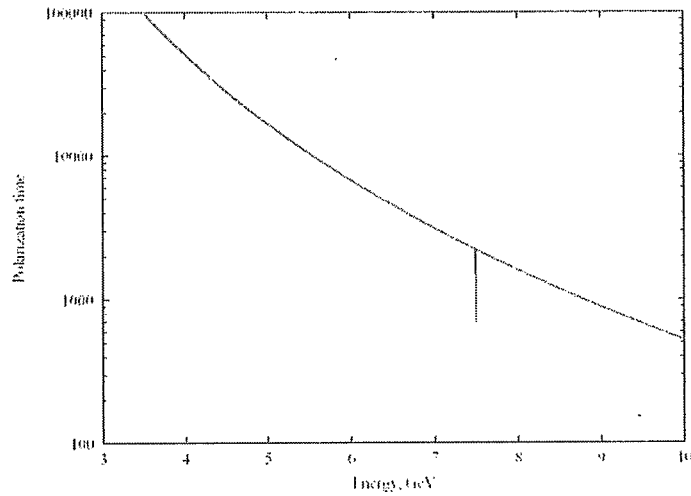


Issues:

- Accomodation of radiated power (9MW radiated at 10 GeV)
- Orbit change versus beam energy
- Orbit lengthening control

$$\tau_{pol}^{-1} \propto \gamma^2 H^3$$

Polarization time with superbend



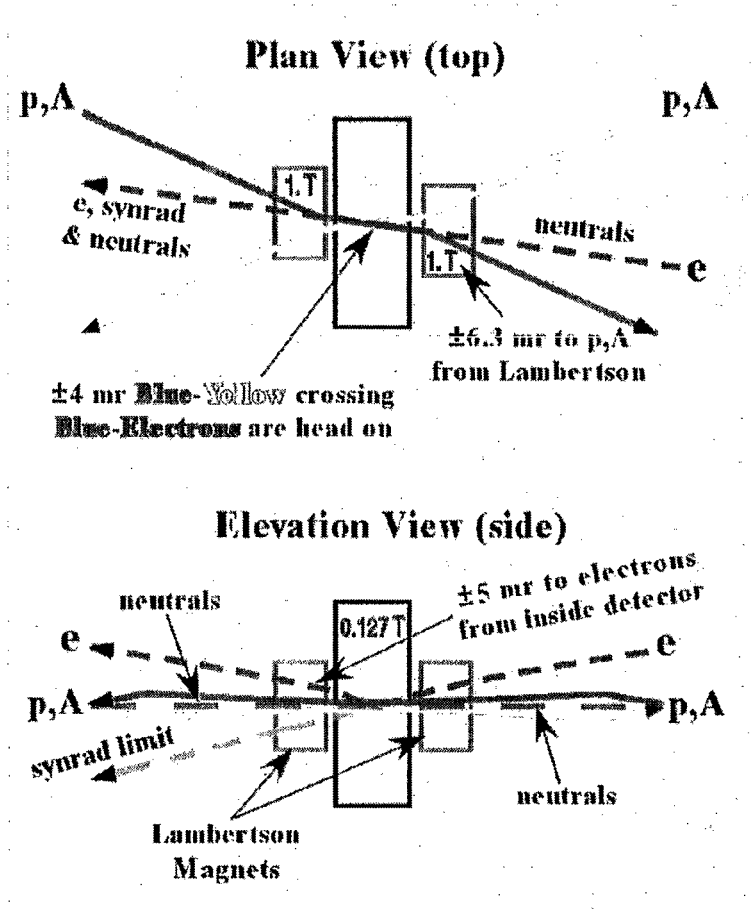
- All magnetic bending field scaled proportionally with energy

$$\tau_{pol}^{-1} \propto \frac{\gamma^5}{\rho^3}$$

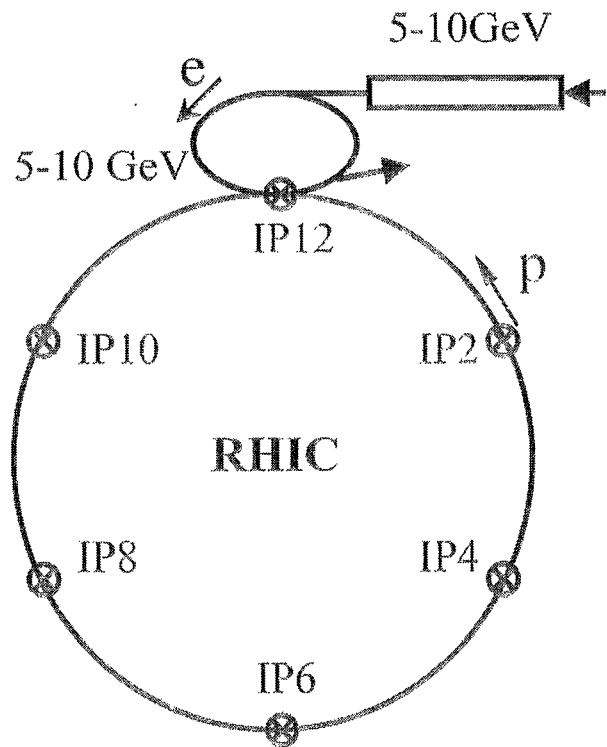
- The central part of the superbend kept at constant field at any energy

$$\tau_{pol}^{-1} \propto \gamma^2 H^3$$

Vertical separation scheme (B.Parker)



Recirculating ring



- ❖ Injected beam circulates in the e-ring for few hundred turns only
- ❖ Allows to keep advantages of linac-ring option:
 - Simpler electron polarization control
 - Smaller electron beam emmitances
 - Electron beam degradation from collisions is not critical factor
- ❖ The more of polarized source studies needed to understand perspectives of the option

HERA III & THERA Plans

15th International Spin Physics Symposium
Henri Kowalski Columbia/BNL/DESY

Most important observations of HERA in the low- x DIS region:

Strong rise of F_2 with diminishing x or equivalently quickly rising total γ^*p cross sections as a function of W

Observation of a leading twist inclusive diffraction

Observation of diffractive VM- production

determination of the proton shape from the diffractive t distributions (in progress)

best described by dipole models with saturation



existence of high density gluonic matter
in a low entropy, coherent state in the protons core



nuclear enhancement $\frac{dxg(..)}{d^2b} = \frac{3}{2 \cdot \pi^2 \alpha_s(Q_s^2)} \cdot Q_s^2 \quad Q_s^2 \sim A^{1/3}$



possible clear spin effects

HERA III Machine and Detector Tasks

improve substantially HERA measurements in areas sensitive to high density gluonic effects



Tune the HERA machine and redesign detectors (see below)

low divergence HERA beams to optimise the performance of forward detectors

rebuild the detectors to close the Q^2 gap in the present measurements

improve electron measurement resolution

build high efficiency forward detectors and/or improve forward detector coverage

Adapt HERA to acceleration of ions see Durham Workshop Dec 2001

Light ions ~ d, C, O

Heavy ions ~ possible but more difficult

HERA III Measurement Program

DIS on protons

measurement of F_2 in the whole Q^2 range of $\sim O(0.1 - 1000)$ GeV² (without gaps)

measurement of inclusive and VM diffractive processes to improve considerably the quality of t dependence

measurement of F_L (*not measured until now*)

Estimated time – two years of measurements

DIS on nuclei

Spin Physics

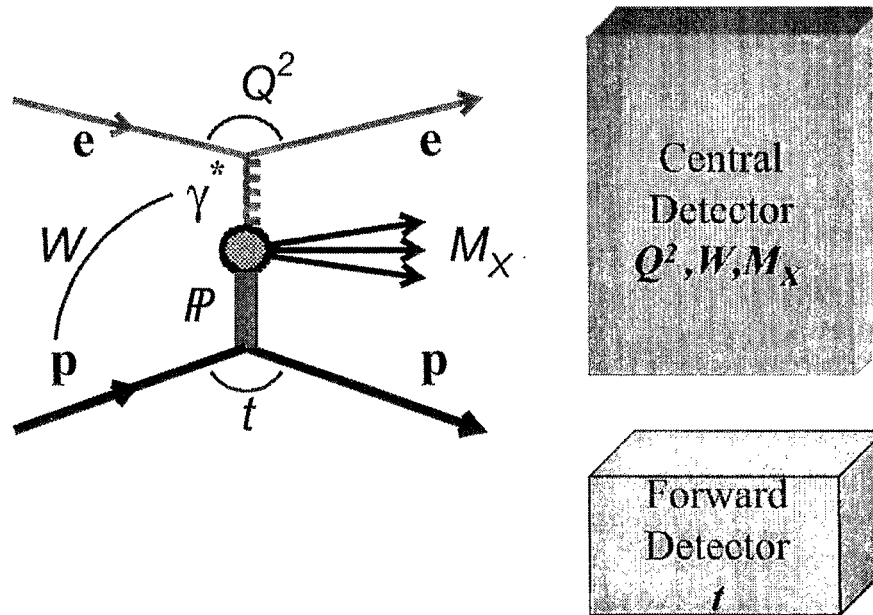
TESLA & HERA = THERA

Extension of W^2 range over an order of magnitude



order of magnitude deeper into the dense matter

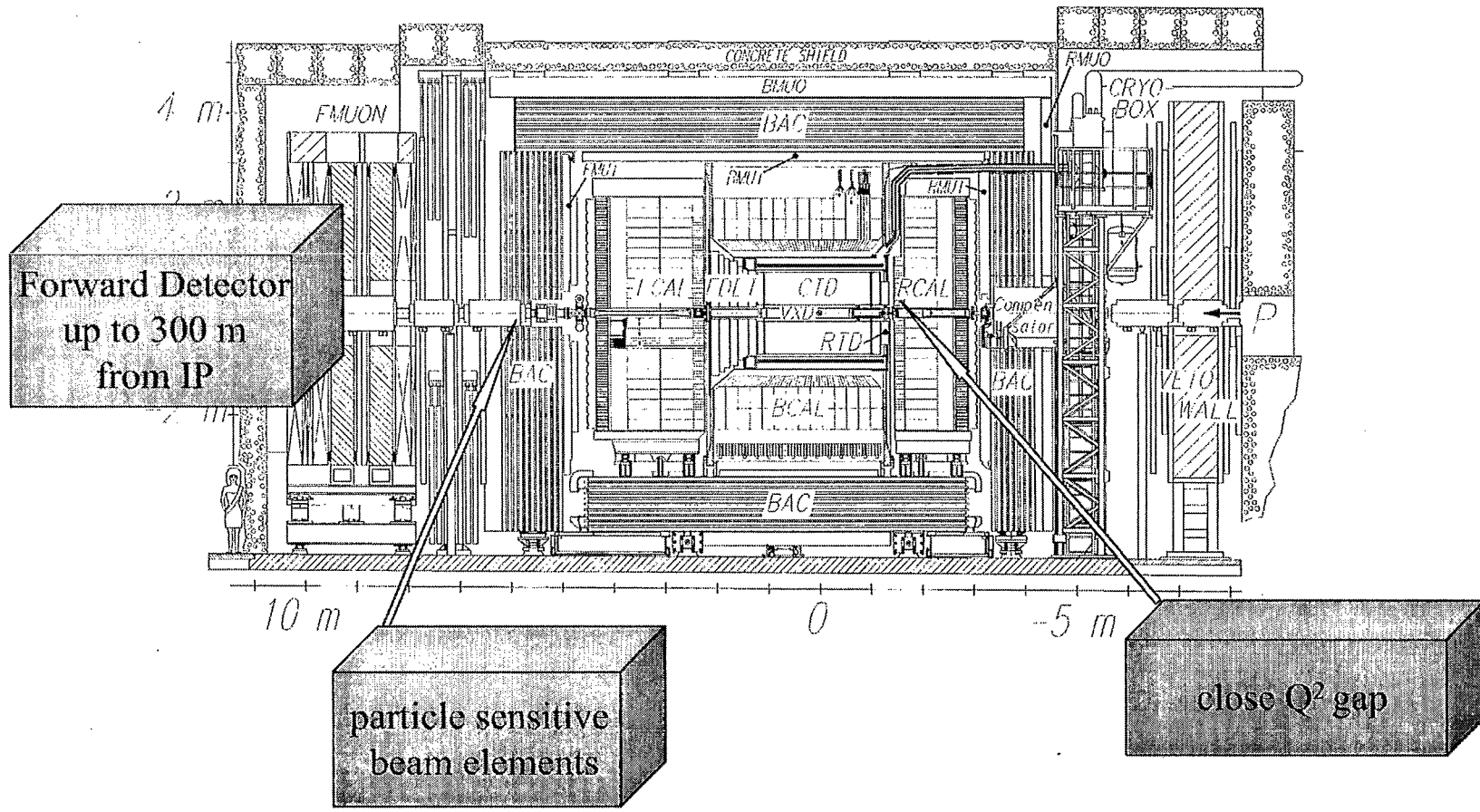
HERA Measurements



- Q^2 - virtuality of the incoming photon
- W - CMS energy of the incoming photon-proton system
- M_X - invariant mass of all particles seen in the central detector
- t - momentum transfer to the diffractively scattered proton
- t - conjugate variable to the impact parameter

Detector improvements

215



QCD Results from CDF

Fumihiko Ukegawa
(CDF Collaboration)

Institute of Physics
University of Tsukuba, Japan

Current and Future Directions at RHIC
Week II : eA and pp Physics

August 12 – 15, 2002

Brookhaven National Laboratory

QCD Results from CDF

Fumihiko Ukegawa¹
(CDF Collaboration)²

*Institute of Physics, University of Tsukuba
Tsukuba, Ibaraki, 305-8571 Japan*

The Collider Detector at Fermilab (CDF) collaboration conducts an experiment at the Tevatron proton-antiproton collider at Fermilab in Batavia, Illinois, USA, and studies proton-antiproton collisions at a center-of-mass energy of $\sqrt{s} = 1.8 - 2.0$ TeV. Since its inception in 1985, CDF has made measurements concerning various aspects of elementary particle physics, such as quantum chromodynamics (QCD), electroweak physics, heavy quarks, and searches for new phenomena beyond the standard model of elementary particles.

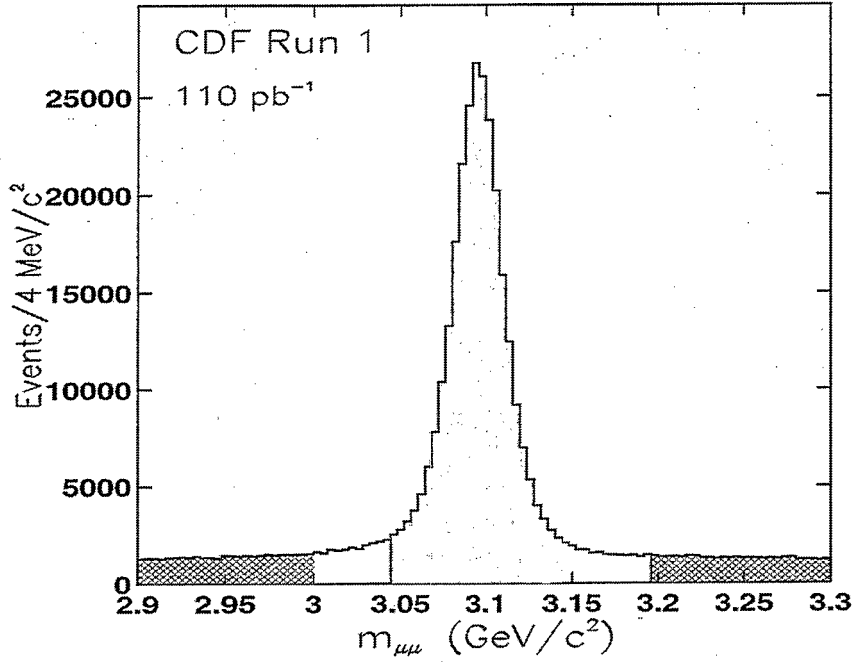
In its previous physics run, Run I (from 1992 to 1996), CDF collected a data sample corresponding to an integrated luminosity of 110 pb^{-1} . We observed production of top quark pairs in this data sample. CDF has also studied various hard QCD processes such as production of (a) high transverse momentum jets, (b) W^\pm bosons, (c) lepton pairs through the Drell-Yan mechanism and Z^0 boson decay, (d) prompt photons, and (e) heavy quarks in their open and hidden (quarkonium) forms. After a brief introduction to the experiment and the particle detection with the CDF detector, we discuss some of these QCD processes and relevant CDF measurements. In general, perturbative QCD calculations give quite satisfactory descriptions of data in many quantities. Here we mention a couple of measurements that are still a bit puzzling: open b -quark production and charmonium production. For the former, data values lie about a factor of two above the next-to-leading order calculations, while for the latter, the nominal theory underestimates direct production of J/ψ and $\psi(2S)$ by a factor of 50.

CDF is now in the new data taking period, Run II, which started in 2001 and is scheduled to continue through 2004 where we expect to accumulate about 2 fb^{-1} of data. The Tevatron accelerator now operates with 36 bunches of protons and antiprotons with increased luminosity provided by the newly constructed Main Injector. The center-of-mass energy has increased from 1.8 TeV to nearly 2 TeV. The detector has also undergone a vast upgrade, and its capabilities have been enhanced greatly while keeping the strengths of the previous detector, namely excellent momentum resolution and lepton identification capabilities. We show that the new CDF detector works very well. We also mention some of preliminary results from the new data, including those which were made available by a new trigger system that makes use of silicon detector information on-line.

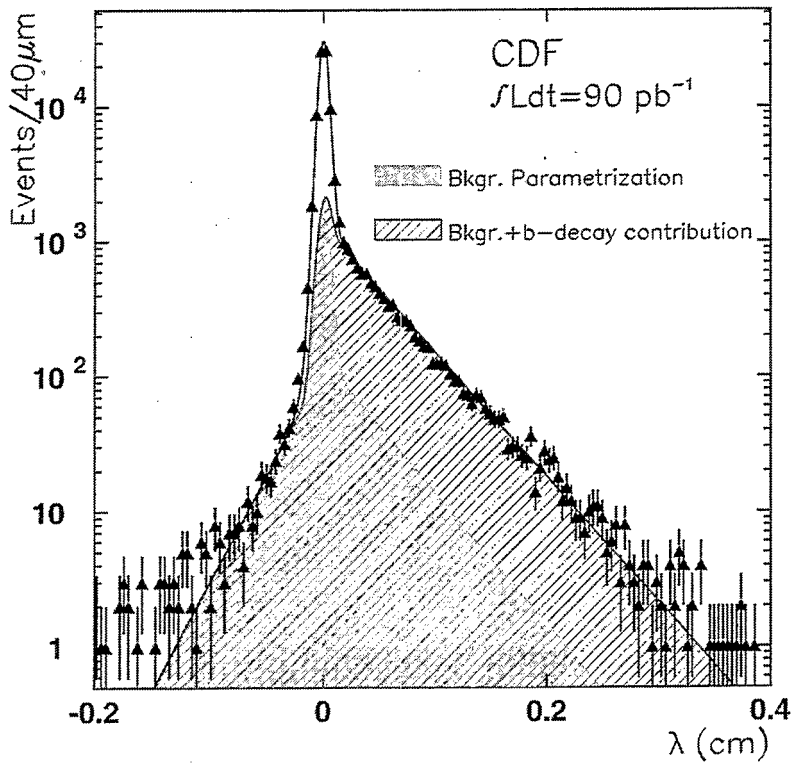
¹ E-mail: ukegawa@hep.px.tsukuba.ac.jp

² <http://www-cdf.fnal.gov/>

$J/\psi \rightarrow \mu^+ \mu^-$ and B decays

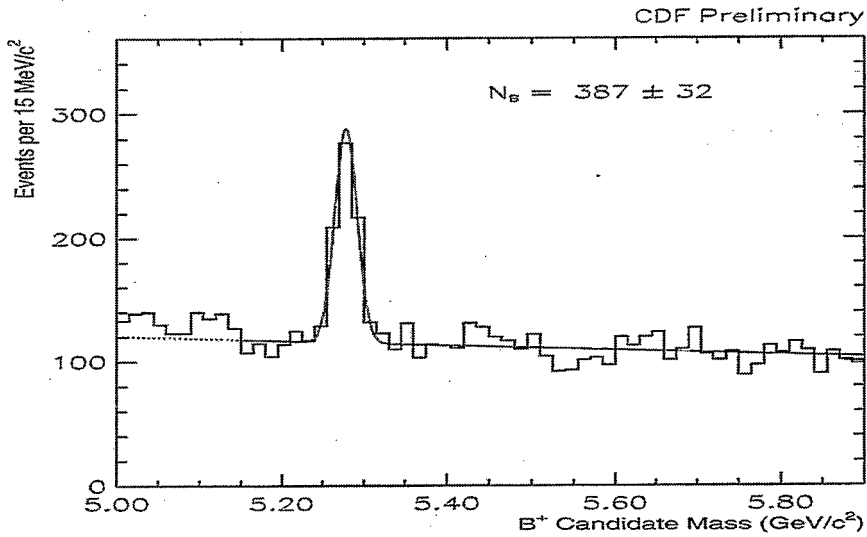


Decay length distribution

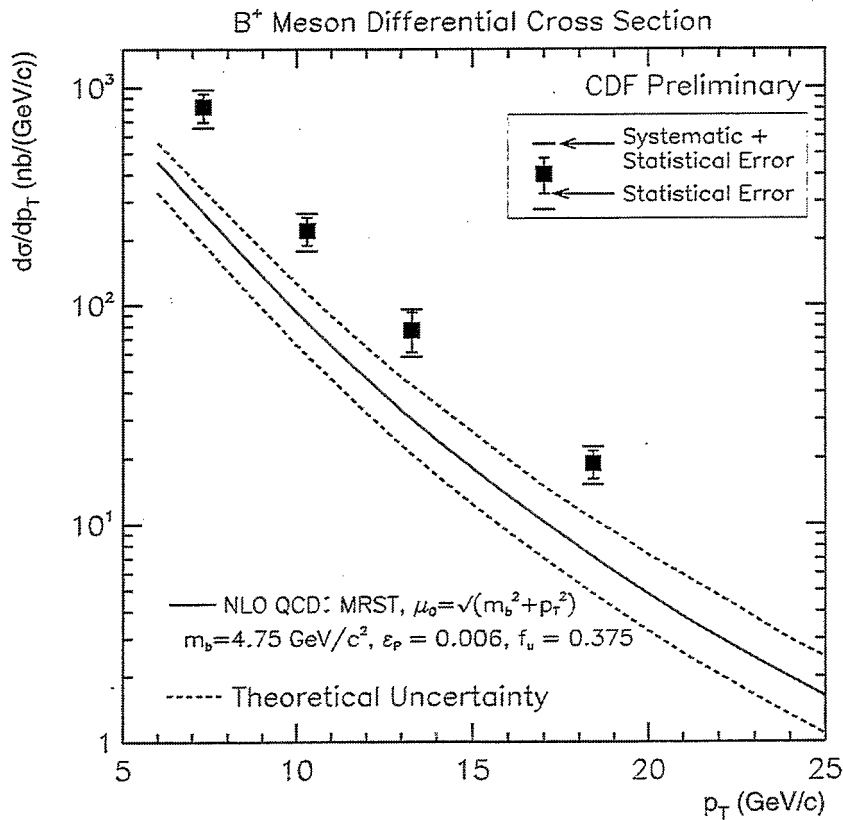


$\sim 20\%$ of J/ψ 's from B decays.

Fully reconstructed $B^+ \rightarrow J/\psi K^+$ decays

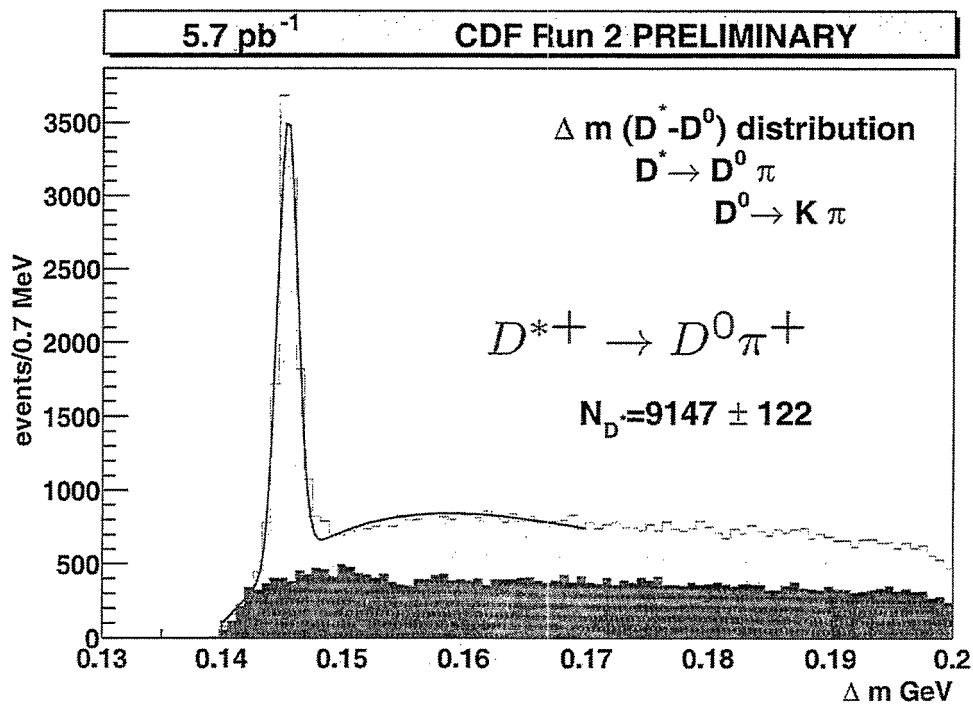
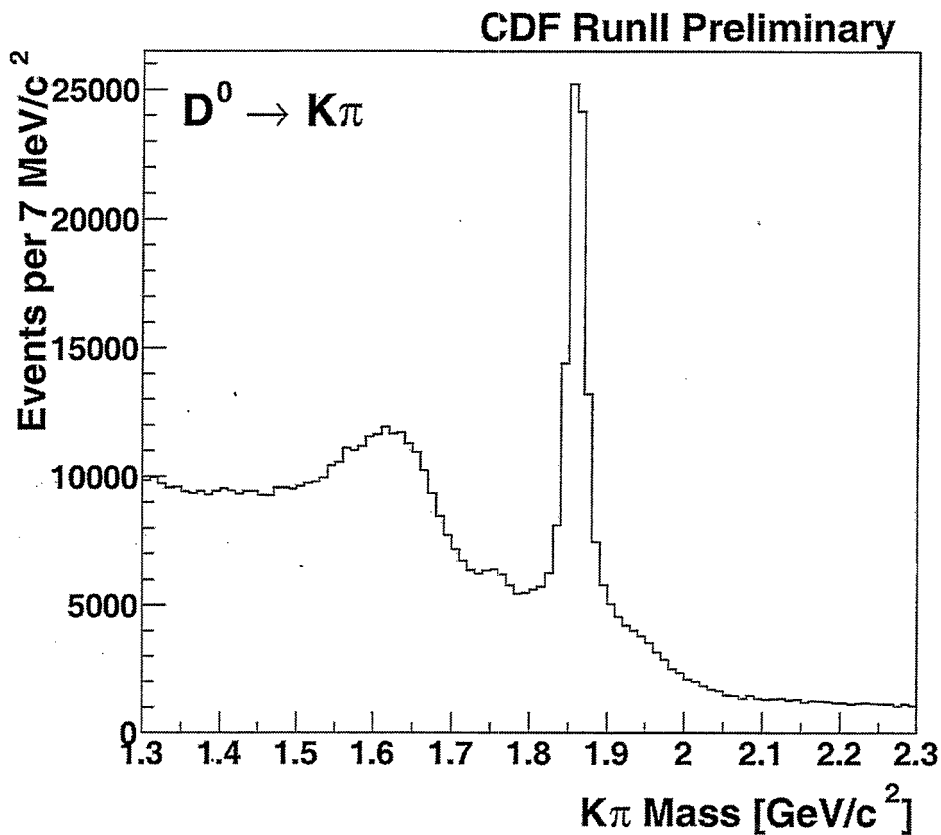


B^+ meson production cross section



$\sigma(\bar{p}p \rightarrow B^+ X) = 3.51 \pm 0.42 \pm 0.53 \mu\text{b}$
 for $p_T > 6 \text{ GeV}/c$ and $|y| < 1.0$.
 PRD 65, 052005 (2002).

Run-II $D^0 \rightarrow K^- \pi^+$ from SVT trigger

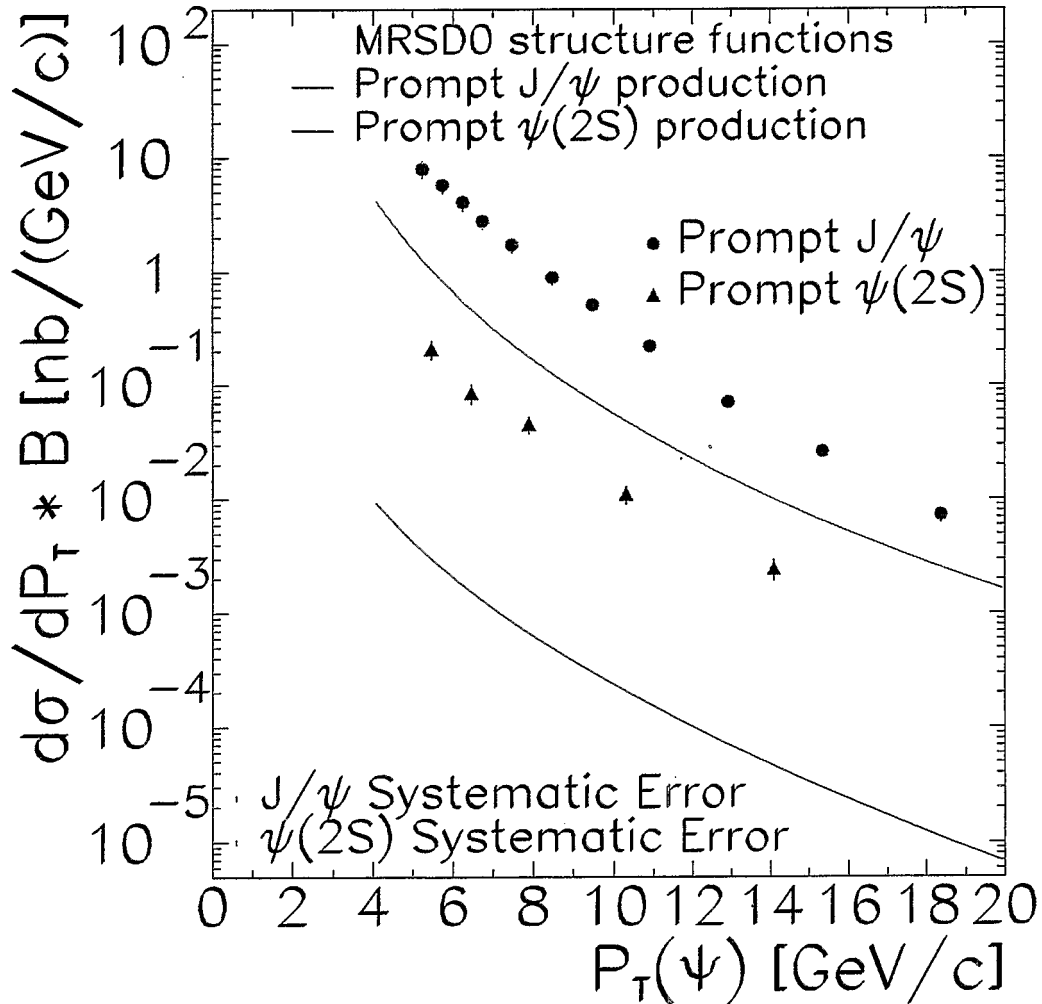


J/ψ and ψ(2S) Production

Sources:

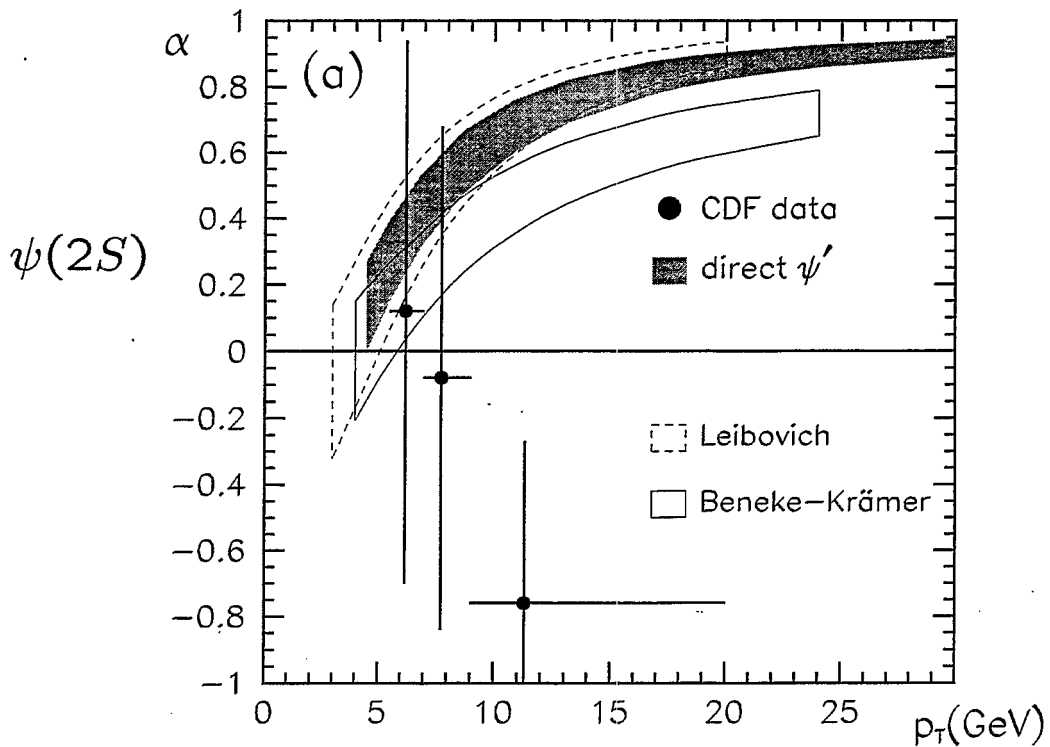
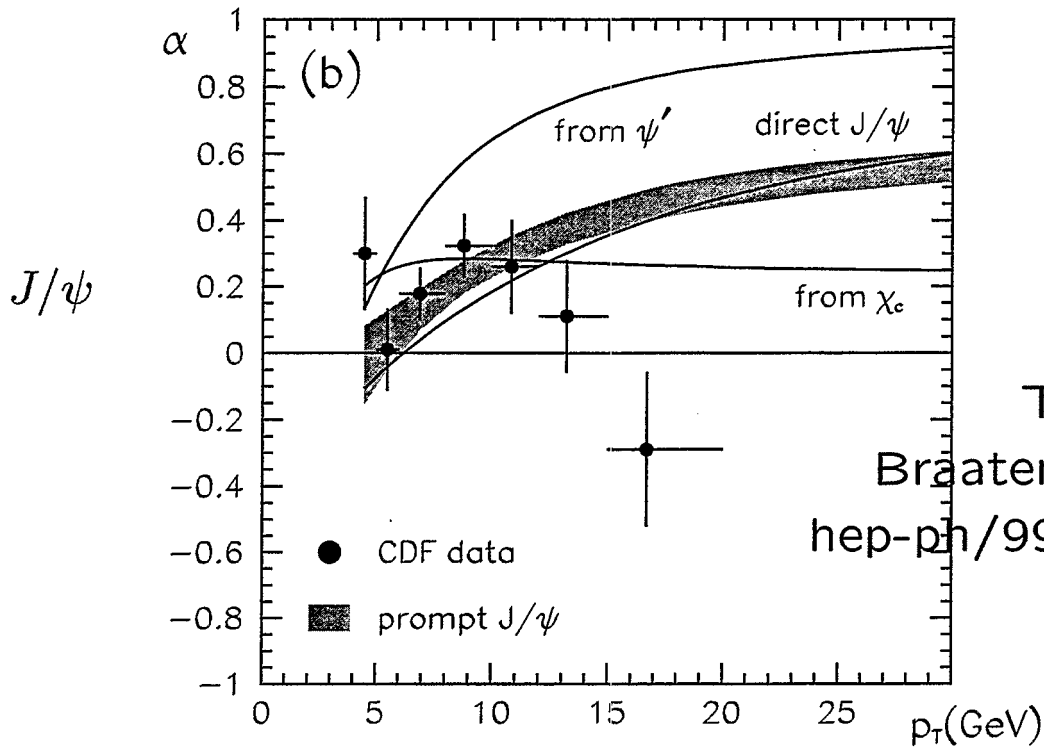
- $B \rightarrow J/\psi, \psi(2S) X$ (lifetime, $\sim 20\%$ of all)
- Direct $J/\psi, \psi(2S)$
- Direct $\chi_c \rightarrow J/\psi \gamma$ (not for $\psi(2S)$)

The latter two have zero lifetime : “prompt”



PRL 79, 572 (1997).

J/ψ and $\psi(2S)$ Polarization



Phys. Rev. Lett. 85, 2886 (2000).

EVIDENCE FOR HADRONIC DECONFINEMENT

In \bar{p} -p Collisions at 1.8 TeV *

R. P. Scharenberg

(E-735 Collaboration Purdue University)

We have measured deconfined hadronic volumes, $4.4 < V < 13.0 \text{ fm}^3$, produced by a one-dimensional (1D) expansion. These volumes are directly proportional to the charged particle pseudorapidity densities $6.75 < dN_C / d\eta < 20.2$. The hadronization temperature is $T = 179.5 \pm 5 \text{ (syst) MeV}$. Using Bjorken's 1D model, the hadronization energy density is $\epsilon_F = 1.10 \pm 0.26 \text{ (stat) GeV/fm}^3$ corresponding to an excitation of $24.8 \pm 6.2 \text{ (stat) quark-gluon degrees of freedom}$.

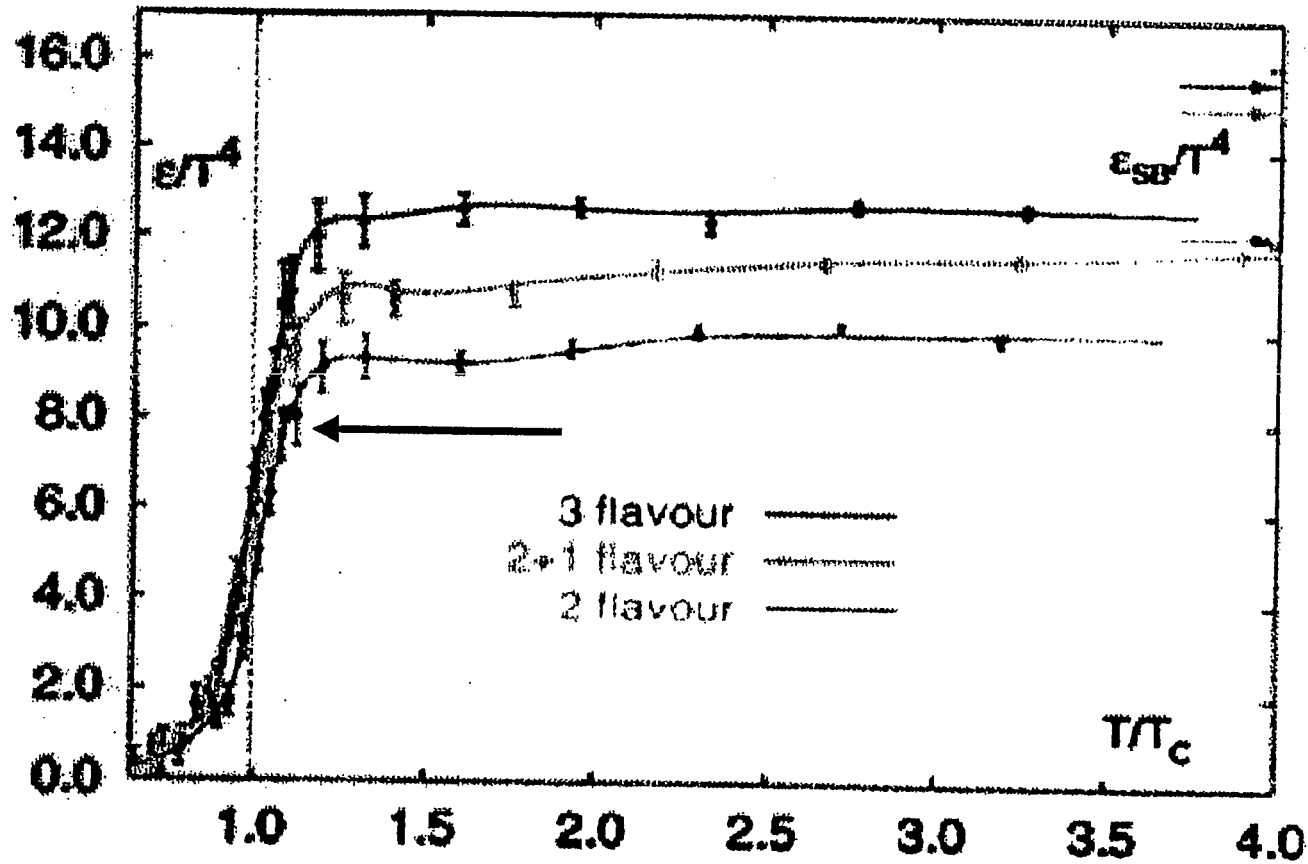
* Phys. Lett. B528(2002)43-48

CONCLUSIONS

- * We have measured the deconfined hadronic volumes produced by a one dimensional isentropic expansion.
 - * The freeze out no. of pions / fm³ $n_{\pi} = 1.64 \pm 0.33$.
 - * The hadronization temperature is $T_{\text{slope}} = 179 \pm 5$ MeV.
 - * The freeze out energy density is $\mathcal{E}_f = 1.10 \pm 0.26$ GeV/ fm³.
 - * The number of DOF in the source is 23.5 ± 6 , 24.8 ± 6.2
In general agreement with those expected for QGP.
- * The measured constant n_{π} , \mathcal{E}_f , T_{slope} values characterize the quark–gluon to hadron thermal phase transition.

Comparison with Lattice Gauge Theory

$$\varepsilon / T_{\text{slope}}^4 = \pi^2 / 30 G(T_{\text{slope}}) = 8.15 \pm 2.0 \text{ (stat)}$$



In Fig.5 the Temperature $T = T_{\text{slope}}$, T_c is the critical temperature

Charged Particle Multiplicity Correlations in $p \bar{p}$ Collisions at $\sqrt{s} = 0.3-1.8$ TeV

R. P. Scharenberg
(E-735 Collaboration, Purdue University)

The Correlations between charged particle multiplicities produced in forward and backward pseudorapidity regions in $p \bar{p}$ interactions have been measured with a 240 element scintillator hodoscope. The correlation coefficient and the variance of the difference of multiplicities in two pseudorapidity regions were determined for $\sqrt{s} = 0.3-1.8$ TeV. These results have been interpreted in terms of a cluster model of particle production.

Phys. Lett. B353(1995)155-160

It is customarily assumed that particles from $p\bar{p}$ collisions are produced in clusters. Clusters are thought of as bodies which provide the common ancestry of the produced particles. The cluster size is the average number of charged particles originating in a cluster and can be obtained by an approach proposed by Chou and Yang. Let $z = n_f - n_b$. For any given total multiplicity $n = n_f + n_b$ there is a distribution in z .

We assume that the net charge in both forward and backward hemispheres is zero. It can be shown that variance of the symmetry distribution, $\langle z^2 \rangle$, is equal to $2n$ provided $\langle z \rangle = 0$. In generalization of this approach, each cluster is assumed to fragment on average into r charged particles plus neutrals. The relation between $\langle z^2 \rangle$ and n then becomes $\langle z^2 \rangle = r n$. The Figure shows a plot of $\langle z^2 \rangle$ vs n for the entire available pseudorapidity range, $|\eta| < 3.5$ at 1.8 TeV.

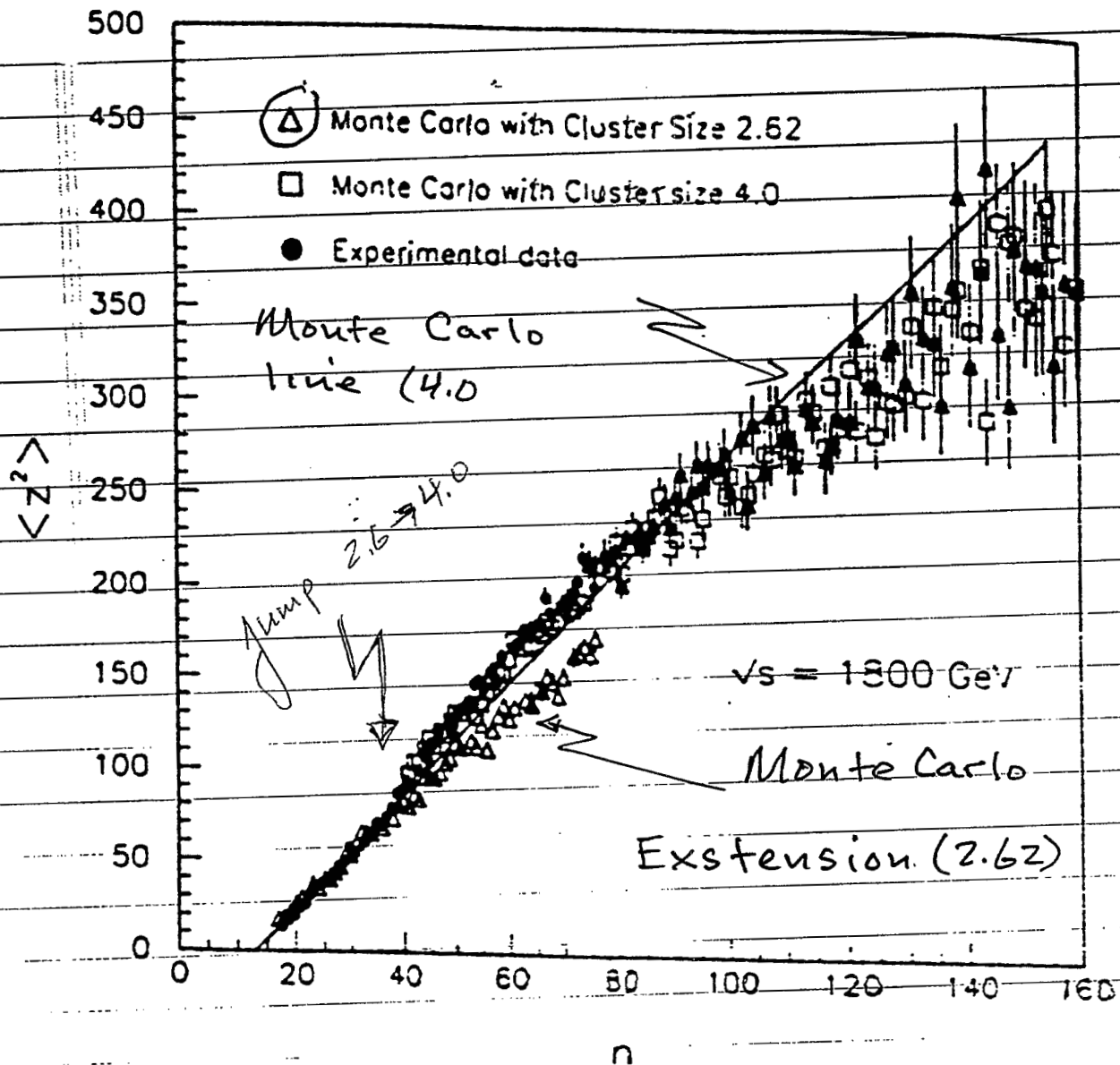


Fig. 4. Variance of the asymmetry distribution for $|\eta| < 3.25$ at 1.8 TeV. \bullet - experimental data; \circ - simulated data assuming cluster size 2.62; \square - simulated data based on the assumption that cluster size increases at $n \approx 40$ to 4.0. The solid line is a linear fit to the data up to $n \approx 40$.

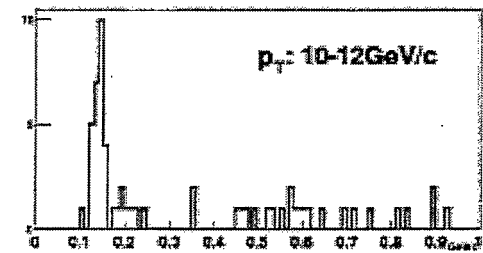
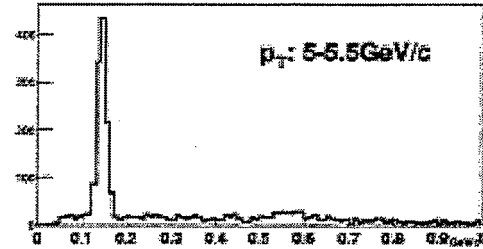
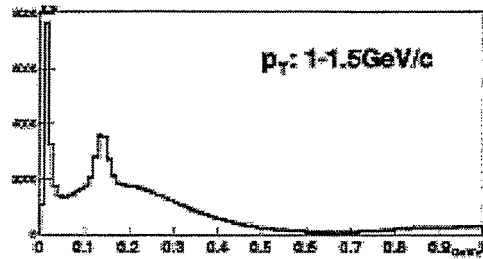
$$\frac{dN_c/d\eta}{d\eta} = n^{1/6.5}$$

pp Neutral pion results from PHENIX Run-2

H. Torii
Kyoto University

π^0 Measurement

- Invariant mass spectrum
- The background is smaller than that of heavy ion collisions
 - 1-1.5GeV/c N/S = 200%
 - $p_T > 5$ GeV/c N/S = 10%
- 2x2 trigger worked very well
 - Rejection Factor = 90
 - Measured 1-15GeV/c π^0
 - 30 π^0 at 10-12GeV/c
 - 10 π^0 at 12-15GeV/c



3

Analysis Procedure

PHENIX

$\mathcal{E}^{(MB)}$ 51%

Minimum Bias (MB) Trigger efficiency

Luminosity normalization

$$\mathcal{E}_{\pi^0}^{(MB)}(p_T) = \frac{N_{\pi^0}^{(MB \& 4 \times 4)}}{N_{\pi^0}^{(4 \times 4)}}$$

π^0 efficiency in Min. Bias trigger 75% flat

Slope correction for Min. Bias trigger

$$\mathcal{E}_{\pi^0}^{(High)}(p_T) = \frac{N_{\pi^0}^{(2 \times 2 \& MB)}}{N_{\pi^0}^{(MB)}}$$

π^0 efficiency in 2x2 trigger 80% flat for $p_T > 3$ GeV

$N_{\pi^0}^{(High)} C_{\pi^0}^{reco}(p_T)$

4

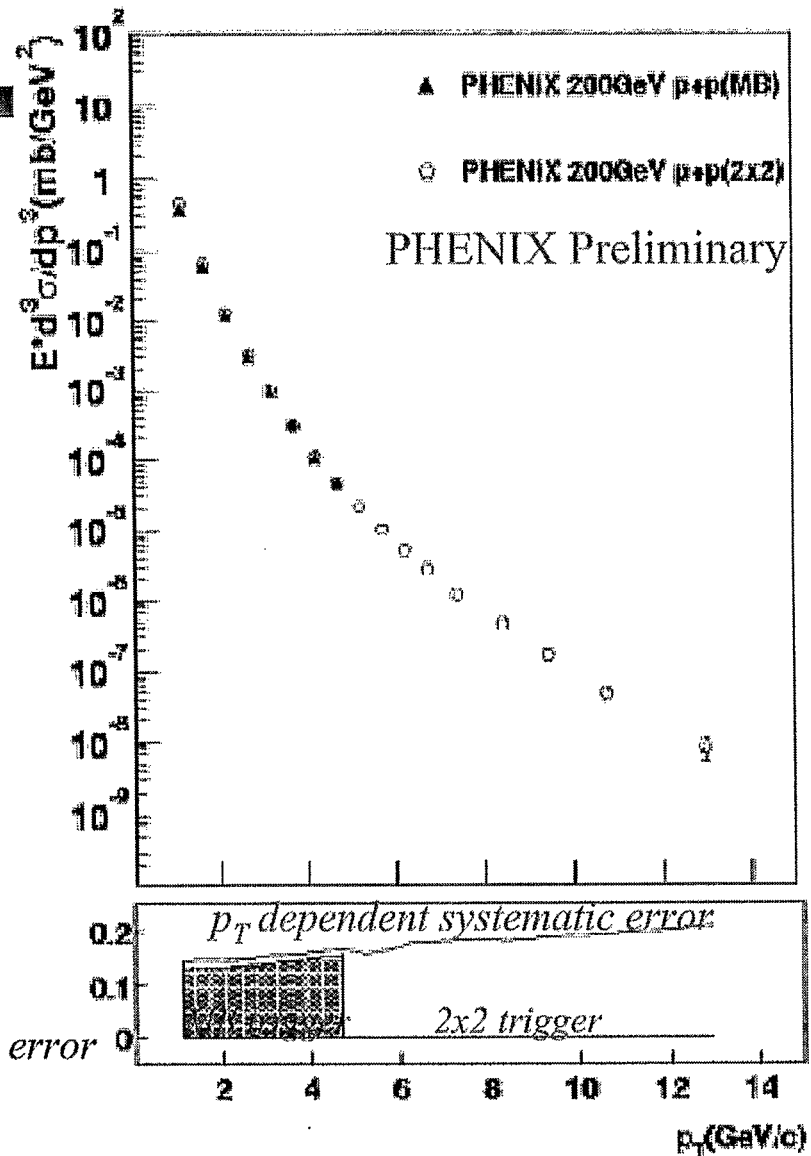
“turn-on” curve for trigger

π^0 Inclusive Cross Section

Cross section measured over 8 orders of magnitude.

- 1-13 GeV/c
- Two triggers
 - Minimum Bias (MB) trigger
 - 2x2 trigger
- They are consistent within systematic error.
- To minimize the systematic error
 - Min. Bias data for 1-3 GeV/c
 - 2x2 trigger for 3-15 GeV/c

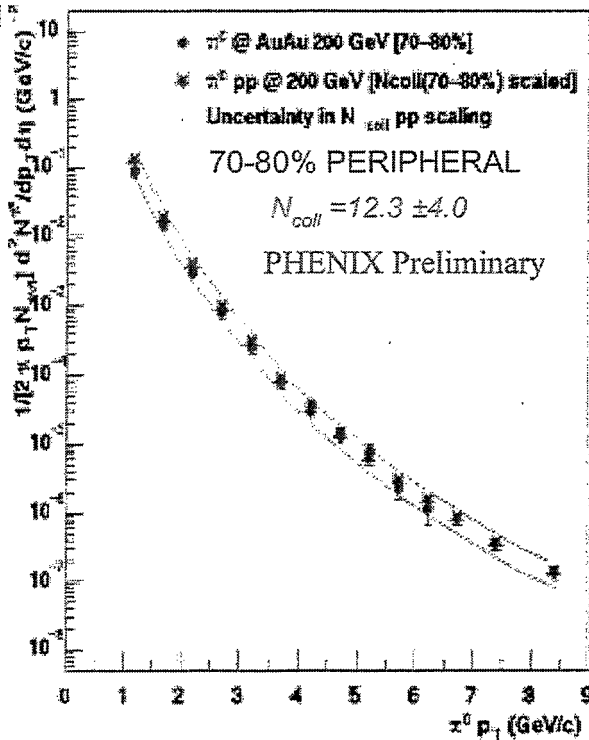
*Normalization systematic error
30% is not included here.*



Comparison with AuAu Peripheral

PHENIX

- AuAu 200GeV peripheral data is up to 6GeV/c
 - The pp data is scaled up by the number of collision.
- They are consistent within Ncoll scaling

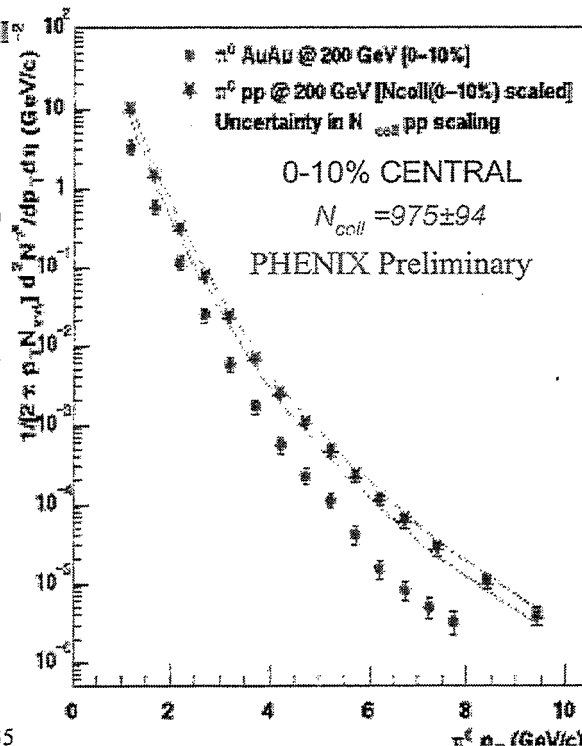


6

Comparison with AuAu Central

PHENIX

- AuAu 200GeV central data is up to 8GeV/c
 - The pp data is scaled up by the number of collision.
- AuAu data shows large suppression.
 - The suppression is dependent of pT
 - This might be understood by the jet quenching effect.



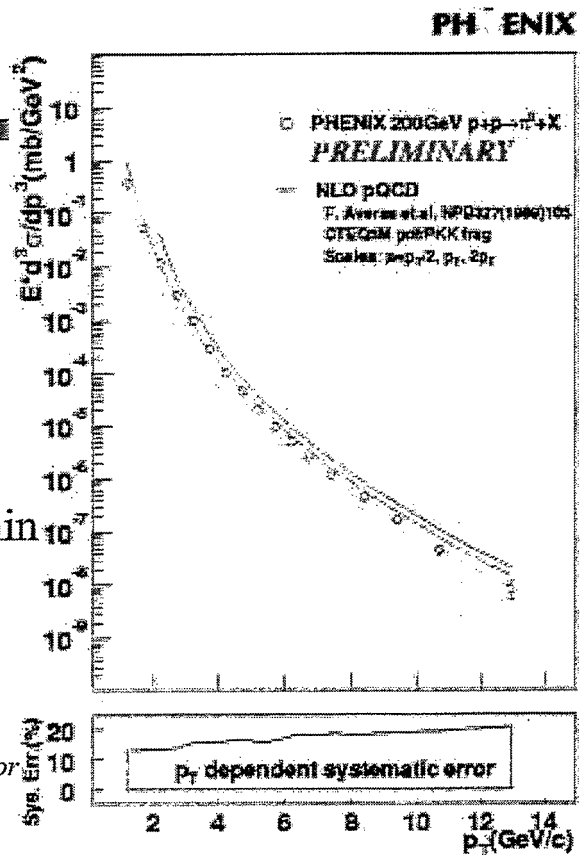
7

Comparison with OCD Calculation

- NLO pQCD calculation
 - CTEQ5M pdf
 - Potter-Kniehl-Kramer fragmentation function
 - $\mu = p_T/2, p_T, 2p_T$
- Consistent with data within the scale dependence.

Thanks to W. Vogelsang

Normalization systematic error
30% is not included here.



Comparison with OCD Calculation

- The deviation of the pQCD calculation is depicted
 - The pQCD calculation with one a set of PDF/FF is consistent within the systematic error of the data and the scale selection

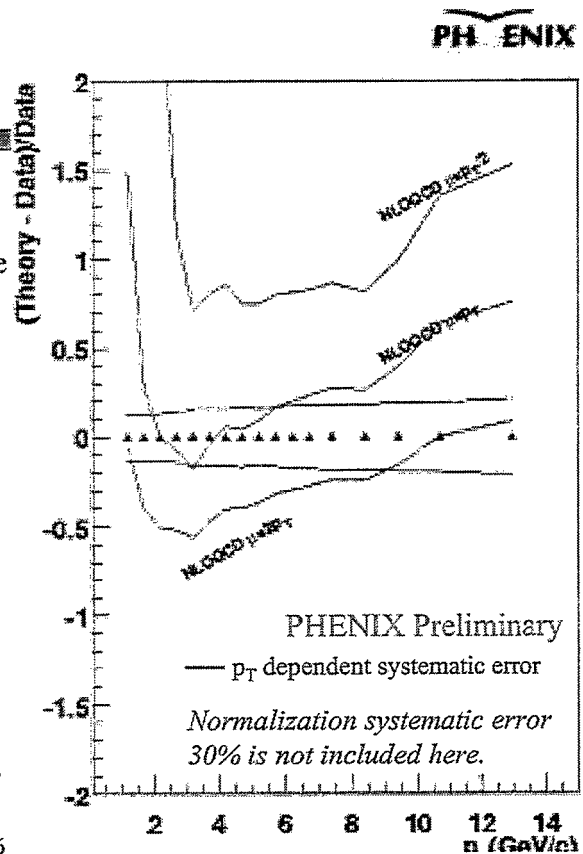
***O.K. So everybody is happy!!!
Let's go to drink beer!!!***

Wait!!!!

What I want to say in this workshop is

“Our data might be one more reference point for study of PDF and FF.”

- Dear all, please don't stop your head and hand !!!



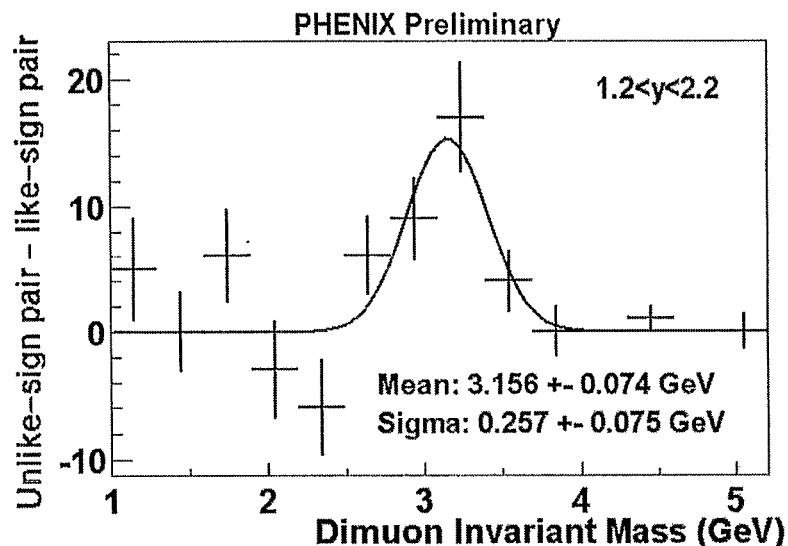
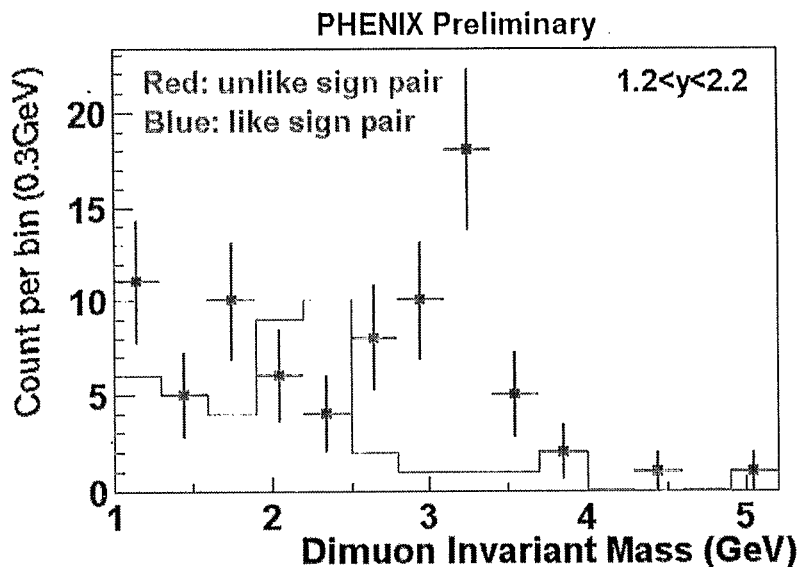
Conclusion

- Measured π^0 cross section.
 - Photon trigger worked well
 - 8 orders of magnitude, 1-13 GeV/c
 - Rejection factor = 90
 - Results from two triggers (Min. Bias and 2x2) are consistent within systematic error
- Comparison with UA1 extrapolation
 - Extrapolation underestimates data at high p_T
 - The data will be an important reference for A+A
- Comparison with AuAu
 - Consistent with AuAu peripheral
 - AuAu central shows large suppression
- Comparison with pQCD with NLO calculation
 - pQCD calculation agree with data

pp J/Psi Results from PHENIX Run-2

Hiroki Sato
RBRC

$J/\psi \rightarrow \mu^+\mu^-$ signal



- Significant enhancement of unlike-sign pair in the J/ψ mass region
 - Peak (3156 ± 74 MeV/ c^2) is consistent with J/ψ mass
 - Mass width (257 ± 75 MeV/ c^2) is consistent with expectation \rightarrow further improvement is expected
- 36 counts in $2.5 < \text{mass} < 3.7$ GeV/ c assuming same count of unlike and like-sign pairs from background (confirmed with simulation)
- Systematic error on the count $\sim 10\%$ by changing mass cut

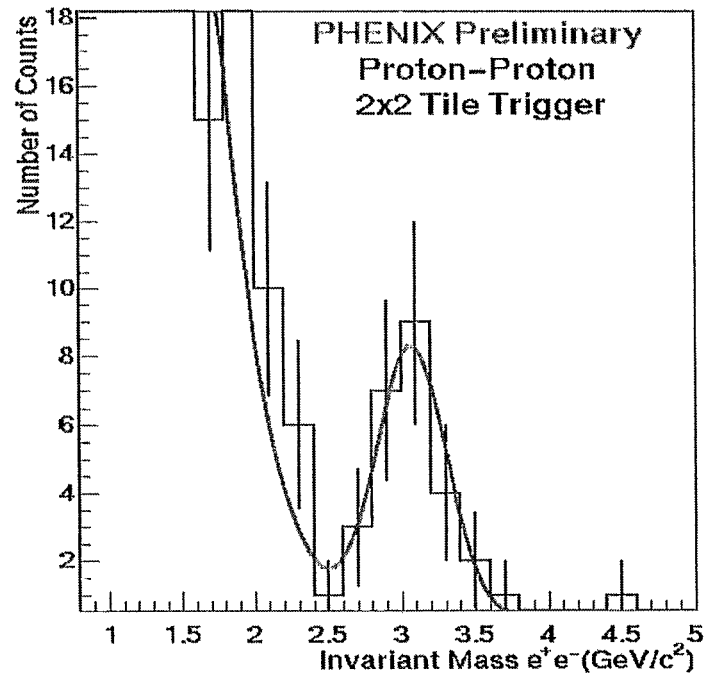
Br dσ/dy|_{y=1.7} result and its uncertainties

	Center value	Uncertainty
$N_{J/\psi}$	36 (2.5 < mass < 3.7 GeV/c ²)	19% (statistical) 10% (cut dependence)
$A_{cc} \epsilon_{MuID} \epsilon_{MuTr}$	0.0163 (1.2 < y < 2.2)	10% (J/ψ pol. dep., α < 0.3) 11% (MuID efficiency) 10% (MuTr efficiency)
$\epsilon_{BBC}^{J/\psi L}$	60 nb ⁻¹	20% (consistency with machine value) <5% (Trigger counter efficiency)

$$\text{Br}(J/\psi \rightarrow \mu^+ \mu^-) d\sigma_{J/\psi}/dy|_{y=1.7} = 37 \pm 7(\text{stat.}) \pm 11(\text{syst.}) \text{ nb}$$

PHENIX Preliminary

J/ψ → e⁺e⁻ Signal



$$N_{J/\psi} = 24 \pm 6 \text{ (stat.)} \pm 4 \text{ (syst.)}$$

Br dσ/dy|_{y=0} result

$$\text{Br} \frac{d\sigma}{dy} \Big|_{y=0} = \frac{N_{J/\psi}}{\epsilon_{acc} \epsilon_{eff} \epsilon_{run-run} \epsilon_{trig} \epsilon_{BBC}^{J/\psi} L \Delta y}$$

$$N_{J/\psi} = 24 \pm 6(\text{stat.}) \pm 4(\text{syst.})$$

$$\epsilon_{acc} \epsilon_{eff} = 0.0163 \pm 0.0020$$

$$\epsilon_{run-run} = 0.87 \pm 0.09 \rightarrow \text{additional Run-by-Run correction factor}$$

$$\epsilon_{trig} = 0.90 + 0.06 - 0.07$$

$$\epsilon_{BBC}^{J/\psi} = 0.75 \pm 0.11$$

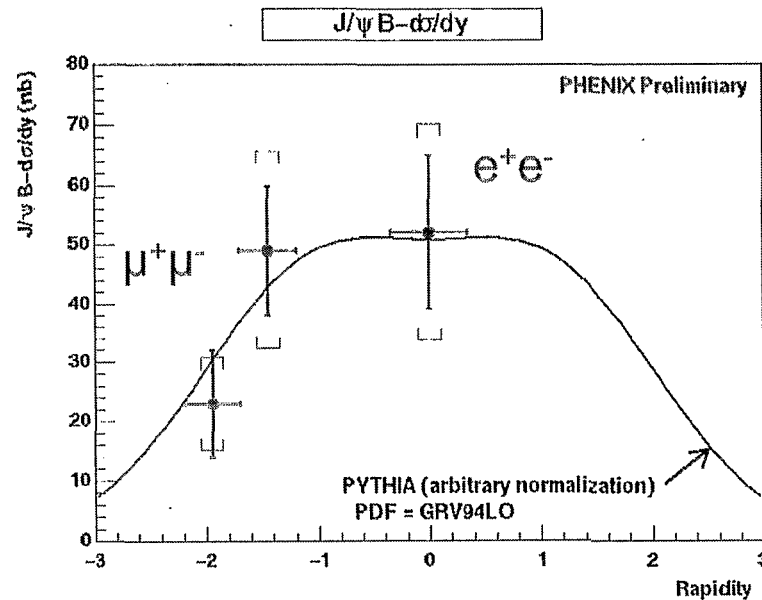
$$L = 48 \pm 10 \text{ nb}^{-1}$$

$$\Delta y = 1.0$$

$$\rightarrow \text{Br}(J/\psi \rightarrow e^+e^-) d\sigma/dy|_{y=0} = 52 \pm 13 (\text{stat.}) \pm 18 (\text{syst.}) \text{ nb}$$

PHENIX Preliminary

J/ψ Rapidity distribution and Total cross section



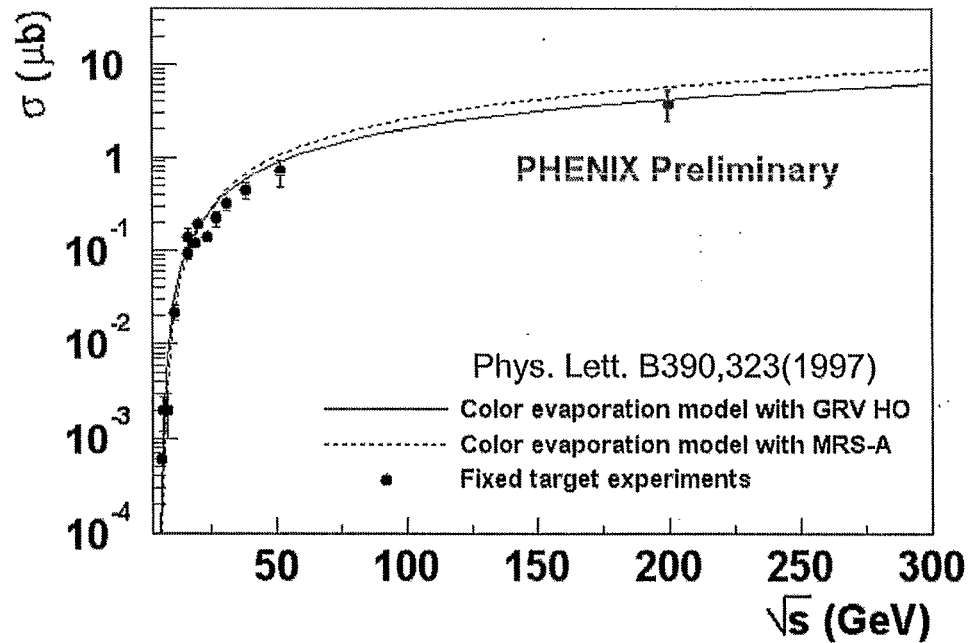
- Rapidity distribution is consistent with PYTHIA
- A global fit gives

PHENIX Preliminary

$$\text{Br}(J/\psi \rightarrow l^+l^-) \sigma(\text{total}) = 226 \pm 36 \text{ (stat.)} \pm 79 \text{ (syst.) nb}$$

$$\sigma(\text{total}) = 3.8 \pm 0.6 \text{ (stat.)} \pm 1.3 \text{ (syst.) } \mu\text{b}$$

Total Cross section compared with the Color-Evaporation Model prediction



- CEM Parameters are fixed by fitting low energy data
- Our result agrees with the CEM prediction at $\sqrt{s}=200\text{GeV}$

Summary

- Cross section of inclusive J/ψ production was measured with PHENIX using both e^+e^- decay channel ($|y| < 0.35$) and $\mu^+\mu^-$ decay channel ($1.2 < y < 2.2$) in Run-2 p+p collisions at $\sqrt{s} = 200\text{GeV}$
- $\text{Br}(J/\psi \rightarrow \mu^+\mu^-) \frac{d\sigma_{J/\psi}}{dy}|_{y=1.7} = 37 \pm 7(\text{stat.}) \pm 11(\text{syst.}) \text{ nb}$
- $\text{Br}(J/\psi \rightarrow e^+e^-) \frac{d\sigma_{J/\psi}}{dy}|_{y=0} = 52 \pm 13(\text{stat.}) \pm 18(\text{syst.}) \text{ nb}$
- Rapidity fit including both results gives
 $\sigma_{J/\psi}(\text{total}) = 3.8 \pm 0.6(\text{stat.}) \pm 1.3(\text{syst.}) \mu\text{b}$
- The result agrees with the Color-Evaporation model prediction and disagrees with the Color-Singlet Model prediction
- In Run-3, measurement of the J/ψ polarization and A_{LL} is expected

Fragmentation Functions in Hard Hadron Production

Xiaofei Zhang and George Fai

Center for Nuclear Research, Department of Physics, Kent State University
Kent, Ohio 44242, USA

Péter Lévai

KFKI Research Institute for Particle and Nuclear Physics, P.O. Box 49, Budapest 1525, Hungary

Hadron spectra at large transverse momentum (p_T), where perturbative Quantum Chromodynamics (pQCD) has good predictive power, are very important for the understanding of the physics at the Relativistic Heavy Ion Collider (RHIC) and at the planned Large Hadron Collider (LHC).

To predict the p_T spectra of final state hadrons in the framework of pQCD, perturbative partonic cross sections need to be convoluted with parton distribution functions (PDF-s) and fragmentation functions (FF-s) according to the factorization theorem. PDF-s and FF-s are assumed to be *universal*, meaning that once extracted from a limited set of data via a fitting procedure, they can then be used with predictive power in other reactions [1–4].

In order to study the role of different regions of z in the FF-s, we define the ratio R_z as [5]

$$R_z(p_T) = \int_0^z dz' \frac{d\sigma}{p_T dp_T dz'} \bigg/ \int_0^1 dz' \frac{d\sigma}{p_T dp_T dz'} \quad (1)$$

where the cross section $d\sigma/p_T dp_T dz$ is differential in p_T and in z , and the ratio depends on the upper limit of the integration in the numerator. We found that the large- z part of the fragmentation function dominates the hard hadron production cross section $d\sigma/p_T dp_T$ in hadronic collisions at RHIC energies. When p_T increases, the effect becomes even more pronounced. Due to phase space effects, the dominant region of the FF-s is very different for fixed target energies, RHIC, and LHC energies. For higher energy, there is more phase space to produce higher p_T partons, which can lose a large fraction of their momentum before becoming a hard hadron. The results also depend on the shape of the FF-s and the dominant regions are different for different species of hadrons.

Most of the FF-s available are extracted from e^+e^- data. The large- z region of the FF-s is constrained by the data from the edge of the phase space of e^+e^- experiments, where the data points are limited and the error bars are large. Therefore, the e^+e^- data do not strongly constrain the FF-s in the large- z region. We illustrate that there is significant freedom in the choice of the large- z behavior of FF-s based on e^+e^- experiments. Since the contribution of gluon fragmentation to the e^+e^- hadron production cross section appears only as a NLO correction, the situation concerning gluon FF-s at large z is even less certain than it is for quarks.

RHIC reported anomalous enhancement of the p/π^+ ratio in central $Au - Au$ collisions. In fact, pQCD already underestimates the p/π^+ ratio by a factor of 3 – 10 in pp collisions. To illustrate the role of FF-s in hard hadron production, we compare the results for the p/π^+ ratio calculated using the KKP form of the proton FF-s, but varying the value of the FF-s in the large- z region. Using the freedom of the proton FF-s in the large- z region, the p/π^+ ratio for $p_T > 6$ GeV in pp collisions at fixed target energies can be reasonably described. After combining the above effects with the idea of different parton intrinsic transverse momenta ($\langle k_T^2 \rangle$) for protons and pions ($\langle k_T^2 \rangle_p \sim 3\text{GeV}^2$, $\langle k_T^2 \rangle_\pi \sim 1\text{GeV}^2$), the p/π^+ ratio for $p_T > 3$ GeV can be satisfactorily described by the theory.

In conclusion, since the large- z details of the fragmentation functions are very important for pQCD predictions of high- p_T hadron production in both pp and AA collisions at RHIC and LHC, a comprehensive study of these fragmentation functions with particular attention to the large- z region is strongly warranted. It appears that available p/π ratios from pp collisions at high p_T can be reproduced by adjusting the large- z behavior of the fragmentation functions and the widths of transverse momentum distributions.

This work was supported in part by the U.S. DOE under DE-FG02-86ER-40251, by the NSF under INT-0000211, and by Hungarian OTKA under T025579 and T032796.

- [1] J. Binnewies, B.A. Kniehl, and G. Kramer, Z. Phys. C **65**, 471 (1995).
- [2] B.A. Kniehl, G. Kramer, and B. Pötter, Nucl. Phys. B **597**, 337 (2001).
- [3] S. Kretzer, E. Leader, and E. Christova, Eur. Phys. J. C **22**, 269. (2001).
- [4] L. Bourhis, M. Fontannaz, J.P. Guillet, and M. Werlen Eur.Phys.J.C **19**, 89 (2001).
- [5] X. F. Zhang, G. Fai and P. Levai, hep-ph/0205008.

FRAGMENTATION FUNCTIONS IN HARD HADRON PRODUCTION

Xiaofei Zhang*
Kent State University

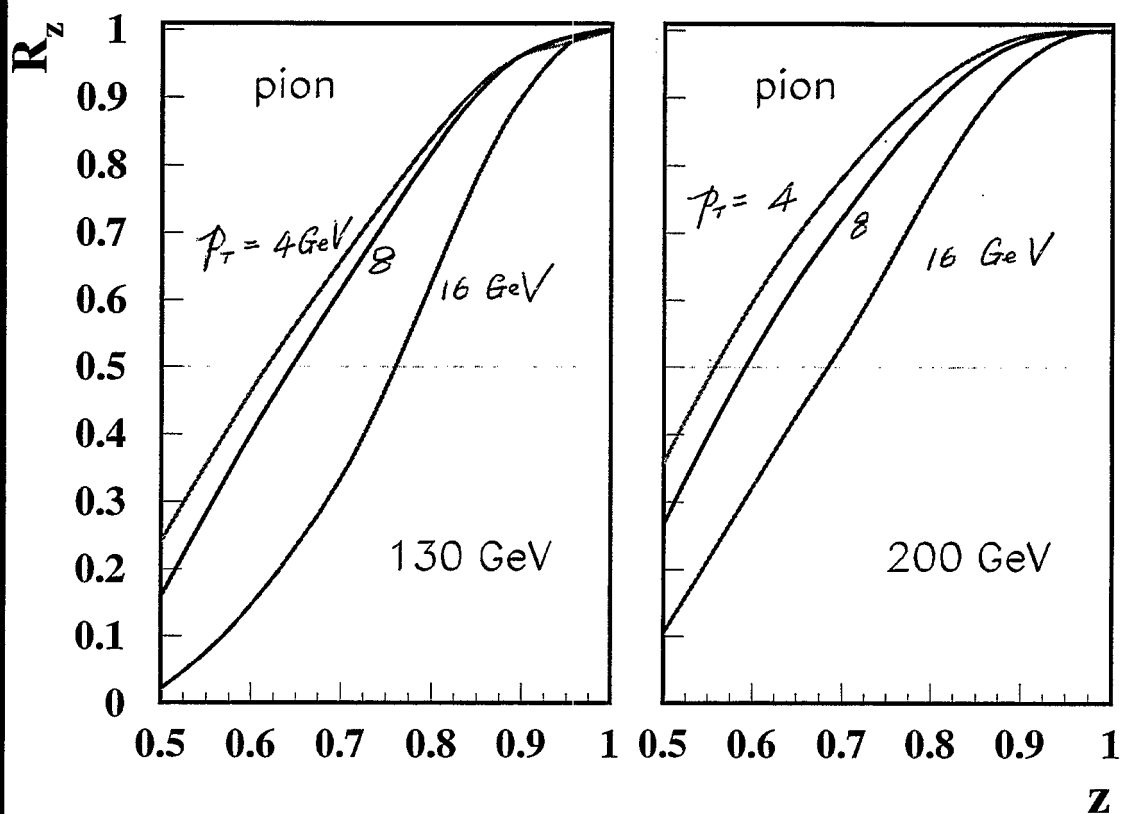
Contents:

1. Introduction
2. Role of Fragmentation Function in Hadronic Collisions
3. Fragmentation Function from e^+e^-
4. p/π Ratio in pp Collisions

*Work done with George Fai and Peter Levai, hep-ph/0205008

FRAGMENTATION FUNCTION IN PP COLLISIONS (PION)

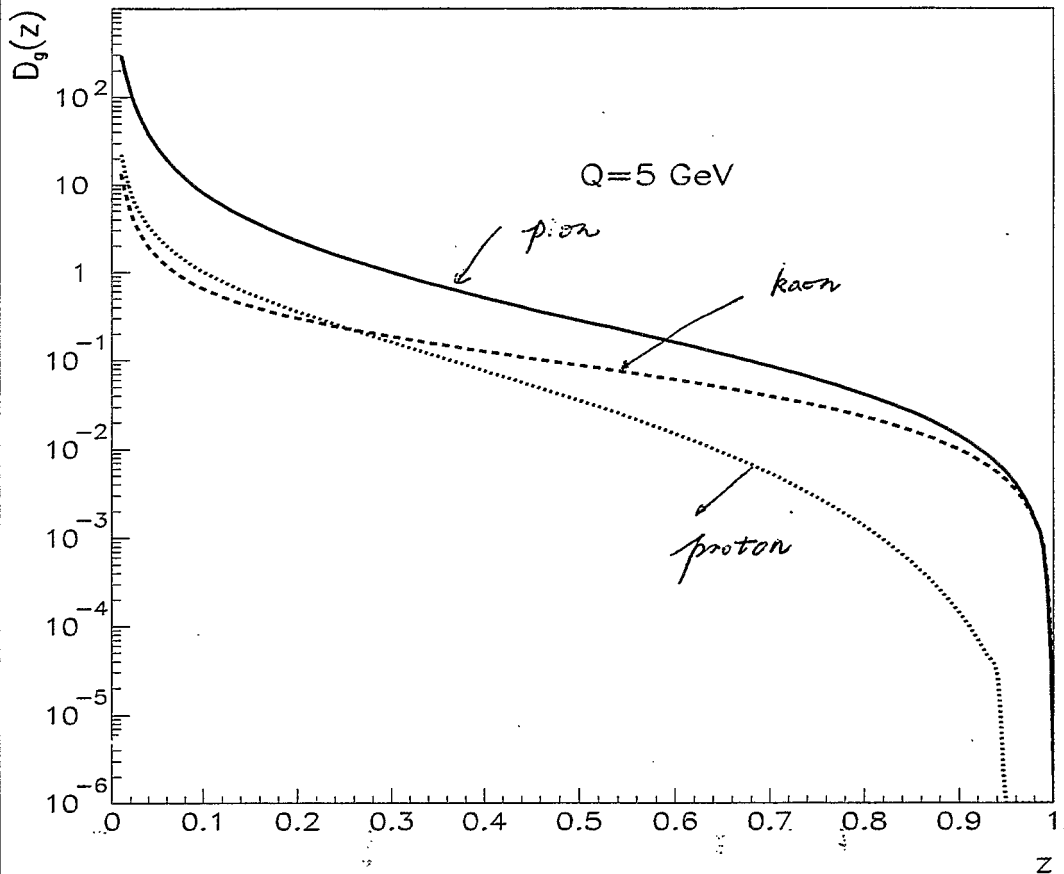
- $$R_z(p_T) = \int_0^z dz' \frac{d\sigma}{p_T dp_T dz'} \bigg/ \int_0^1 dz' \frac{d\sigma}{p_T dp_T dz'}$$



- use KKP FF-s
- Large z part of the FF-s dominates the π production at RHIC
 $p_T \sim xz\sqrt{s}$, two PDF, one FF \rightarrow favor small x , large z
- when p_T increases, the large z region of FF-s becomes even more important (phase space effect)

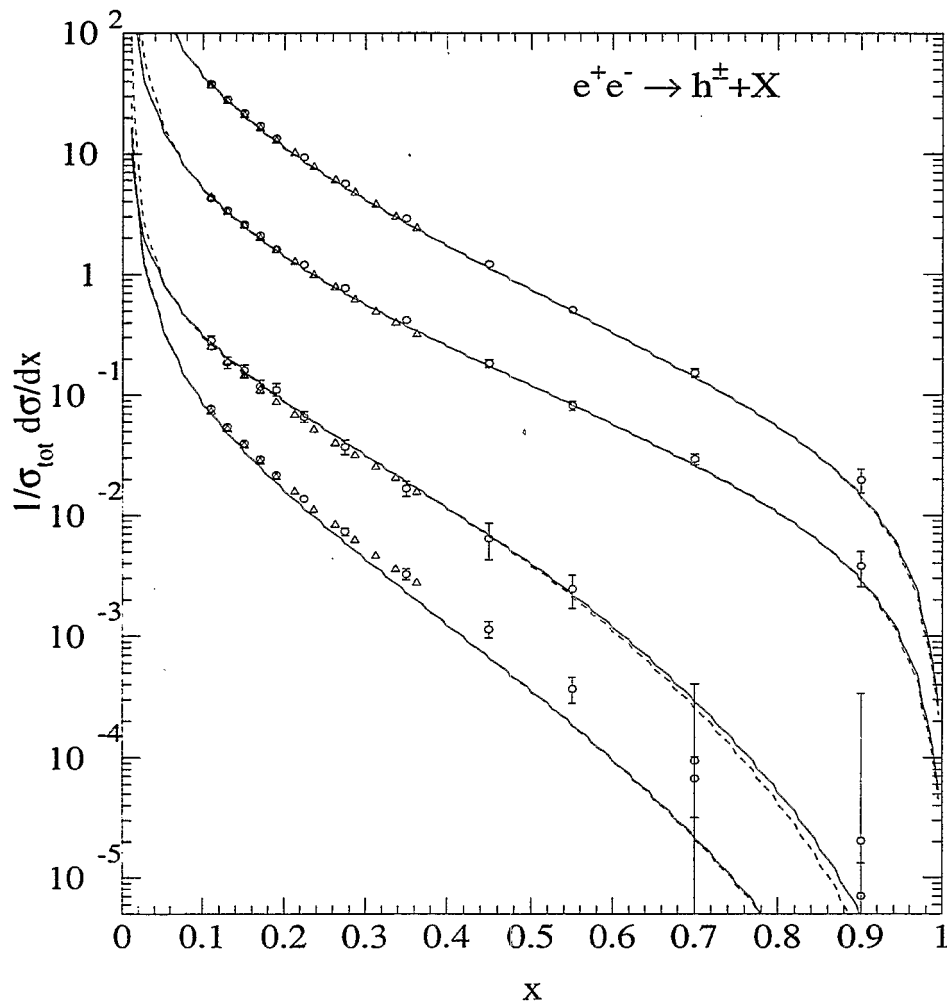
RESULTS DEPEND ON THE SHAPE OF FF-S

- Results depend on the shape of fragmentation function
If FF-s fall less steeply, the dominance of the large z region is even more significant
- Due to the different shape of FF-s for different particles, the dominant region of FF is not the same



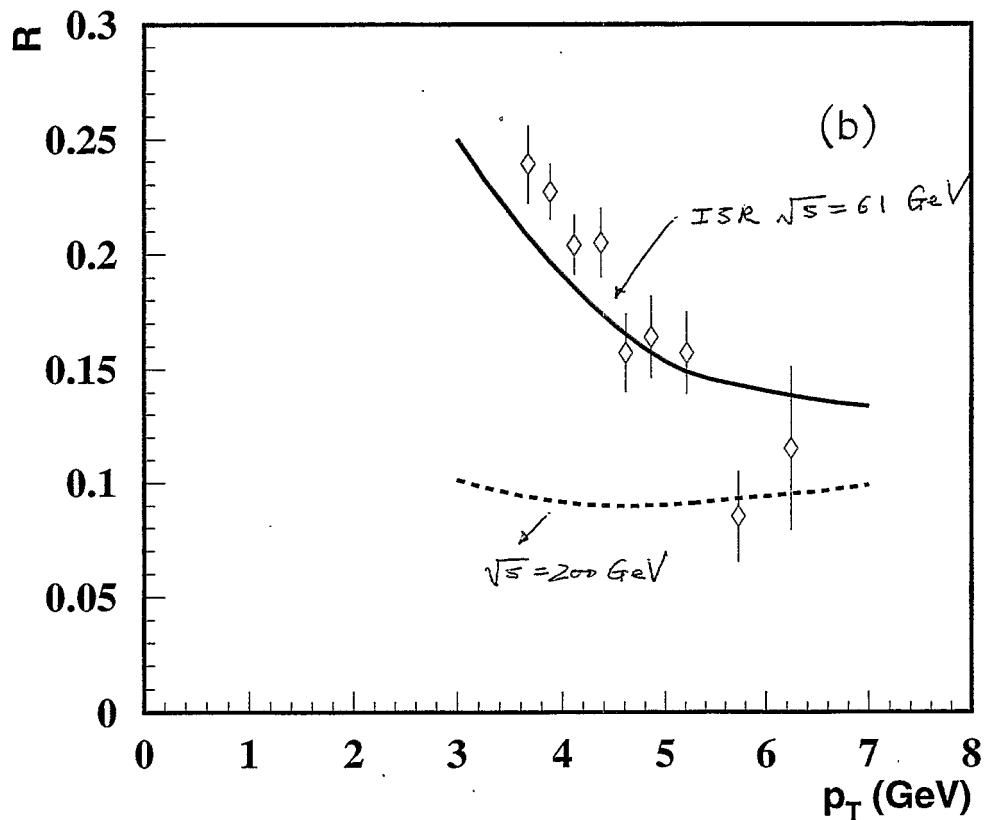
FRAGMENTATION FUNCTION FROM e^+e^- DATA ($h^+ + h^-$)

- $\frac{d\sigma^h}{dx} = \sum_a \int_x^1 \frac{dz}{z} \frac{d\hat{\sigma}_a}{dy}(y, \mu_F, \mu_R) D_a^h(z, \mu_F)$
- $y = x/z$, scale $\sim \sqrt{s}$
- $x = 2E_h/\sqrt{s} \sim z$, $x = z$ in the leading order



- large- z region of FF-s is not strongly constrained by e^+e^- data

P/ π RATIO IN PP COLLISIONS ^a



- $\langle k_T^2 \rangle_\pi = 1 \text{ GeV}^2$, $\langle k_T \rangle_\pi \sim 0.8 \text{ GeV}$

- $\langle k_T^2 \rangle_p = 3.0 \text{ GeV}^2$, $\langle k_T \rangle_p \sim 1.5 \text{ GeV}$

^a data are from A. Breakstone *et. al.*, Z. Phys. C **36**, 567 (1987).

Resummed cross-section for Higgs production at hadron colliders

D. DE FLORIAN
Universidad de Buenos Aires
Argentina

The dominant mechanism for SM Higgs boson production at hadron colliders is gluon–gluon fusion through a heavy (top) quark loop. NLO QCD corrections to this process are known to be large [1, 2]: their effect increases the cross section of about 90–100 % with respect to the LO result. Recently, the calculation of the NNLO corrections has been completed [3, 4, 5, 6]. Their effect is also large: at the LHC, for a light Higgs, the K-factor is about 2.3–2.4, corresponding to an increase of about 25% with respect to NLO. At the Tevatron $K \sim 3$, the increase being of about 50% with respect to NLO. As expected [3, 7], the bulk of the effect is due to soft and collinear radiation, the hard contributions giving only a small effect. The effects of multiple soft gluon emission beyond NNLO can thus be important, especially at the Tevatron.

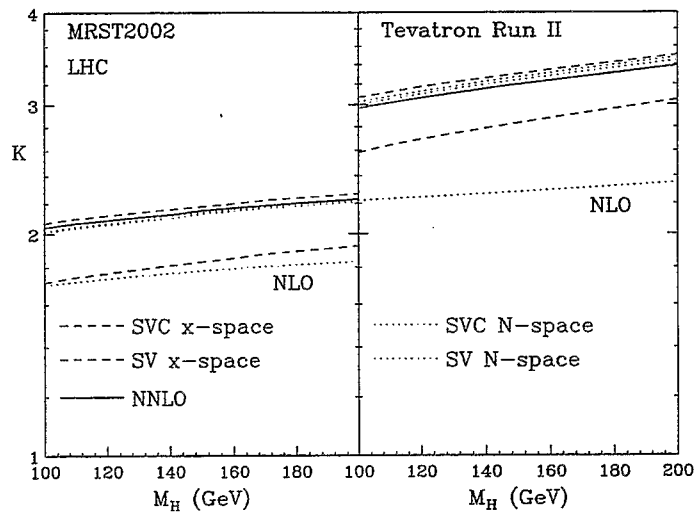
Here we investigate the effects of resummation of soft (Sudakov) emissions to all orders up to NNLL accuracy[8]. In the case of LHC we find that the corrections are moderate, with an increase in the cross section of about 6 % with respect to the NNLO result. In the case of Tevatron the resummation effect is larger. Going from NLO to NLL the increase in the cross section is from 25 to 30%. At NNLL the cross section increases (with respect to the NNLO result) between about 12 and 16 % when M_H goes from 100 to 200 GeV. This result is not unexpected, since at Tevatron the process is certainly closer to threshold and the effect of multiple soft gluon emission is more important.

References

- [1] S. Dawson, Nucl. Phys. B **359** (1991) 283.
- [2] A. Djouadi, M. Spira and P. M. Zerwas, Phys. Lett. **B264** (1991) 440.
- [3] S. Catani, D. de Florian and M. Grazzini, JHEP **0105** (2001) 025.
- [4] R. V. Harlander and W. B. Kilgore, Phys. Rev. D **64** (2001) 013015.
- [5] R. V. Harlander and W. B. Kilgore, Phys. Rev. Lett **88** (2002) 201801.
- [6] C. Anastasiou and K. Melnikov, hep-ph/0207004 (2002).
- [7] S. Catani, D. de Florian and M. Grazzini, JHEP **0201** (2002) 015.
- [8] S. Catani, D. de Florian, M. Grazzini and P. Nason, in preparation.

NNLO

- Compare to full calculation ($\mu_R = \mu_F = M_H$)
 LO : LO pdf and 1 loop α_s (MRST2001/2)
 NNLO : 'NNLO' pdf and 3 loop α_s ($K = NNLO/LO$)
- 'NNLO' with approximated kernels (van Neerven, Vogt)



- wrt NLO: +15% at the LHC +35% at Tevatron
- SVC excellent: 2% at LHC and 4% at Tevatron
- Tevatron closer to threshold \Rightarrow larger corrections
- As expected, SV underestimates the full result
- Much better stability in N-space: both SV and SVC very close to SVC-X
- Differences in X-space due to $\mathcal{O}(1/N)$ contributions
- Corrections clearly dominated by soft emission

Threshold resummation

- Considering the large effect of soft emission close to threshold (contribution of $\ln^i N$ terms) it is worth to perform the resummation of those terms to all orders in $\alpha_s \Rightarrow$ Multiple soft emission beyond NNLO can be important

$$G_{gg,N} = \alpha_s^2 \left\{ 1 + \sum_{n=1}^{+\infty} \alpha_s^n \sum_{m=0}^{2n} G_H^{(n,m)} \ln^m N \right\} + \mathcal{O}(1/N) = G_{gg,N}^{(\text{res})} + \mathcal{O}(1/N)$$

- Particularly relevant for Tevatron RunII, where convergence of the perturbative expansion is 'slower'
- Soft-gluon resummation carried out in N-space (Sterman (1987); Catani, Trentadue (1989))
- The resummed partonic coefficient is organized as

$$G_{gg,N}^{(\text{res})} = \alpha_s^2(\mu_R^2) C_{gg}(\alpha_s(\mu_R^2), M_H^2/\mu_R^2; M_H^2/\mu_F^2) \Delta_N^H(\alpha_s(\mu_R^2), M_H^2/\mu_R^2; M_H^2/\mu_F^2)$$

- The resummation is achieved by exponentiation in the radiative factor Δ_N^H containing the large $\ln N$ -contributions due to soft radiation

$$\Delta_N^H(\alpha_s(\mu_R^2), M_H^2/\mu_R^2; M_H^2/\mu_F^2) = \left[\Delta_N^g(\alpha_s(\mu_R^2), M_H^2/\mu_R^2; M_H^2/\mu_F^2) \right]^2 \times \Delta_N^{(\text{int})H}(\alpha_s(\mu_R^2), M_H^2/\mu_R^2)$$

where

$$\Delta_N^g(\alpha_s(\mu_R^2), M_H^2/\mu_R^2; M_H^2/\mu_F^2) = \exp \left\{ \int_0^1 dz \frac{z^{N-1} - 1}{1-z} \int_{\mu_F^2}^{(1-z)^2 M_H^2} \frac{dq^2}{q^2} A_g(\alpha_s(q^2)) \right\}$$

embodies the effect of soft-collinear radiation, and

$$\Delta_N^{(\text{int})H}(\alpha_s(\mu_R^2), M_H^2/\mu_R^2) = \exp \left\{ \int_0^1 dz \frac{z^{N-1} - 1}{1-z} D_H(\alpha_s((1-z)^2 M_H^2)) \right\}$$

takes into account the effect of soft-gluon emission at large angles

- $C_{gg}(\alpha_s)$: virtual and non-log. soft contributions

LHC

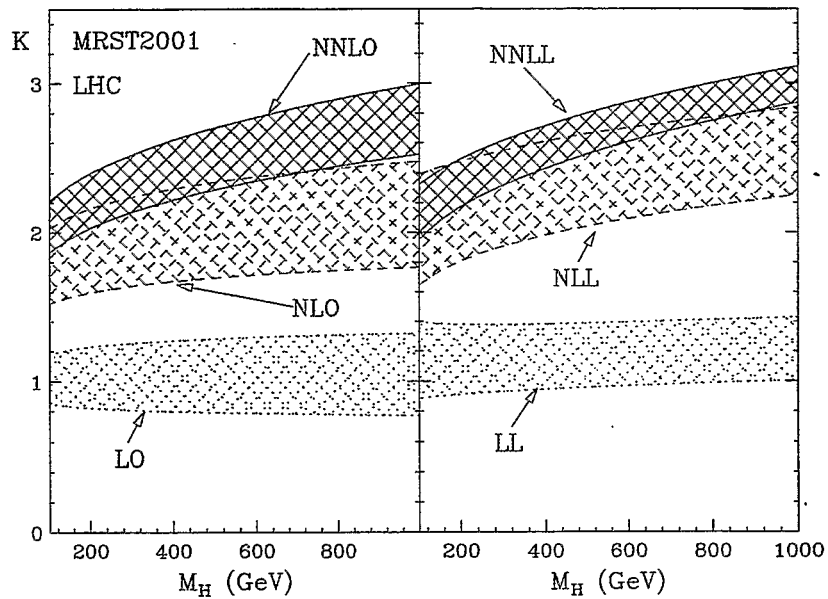
- K factors

$$K = \frac{\sigma^{NL/NNL}(\mu_{F,R})}{\sigma^{LO}(\mu_{F,R} = M_H)}$$

- Uncertainty band:

– Fixed order $\mu_F = \mu_R = \chi M_H$ $1/2 < \chi < 2$

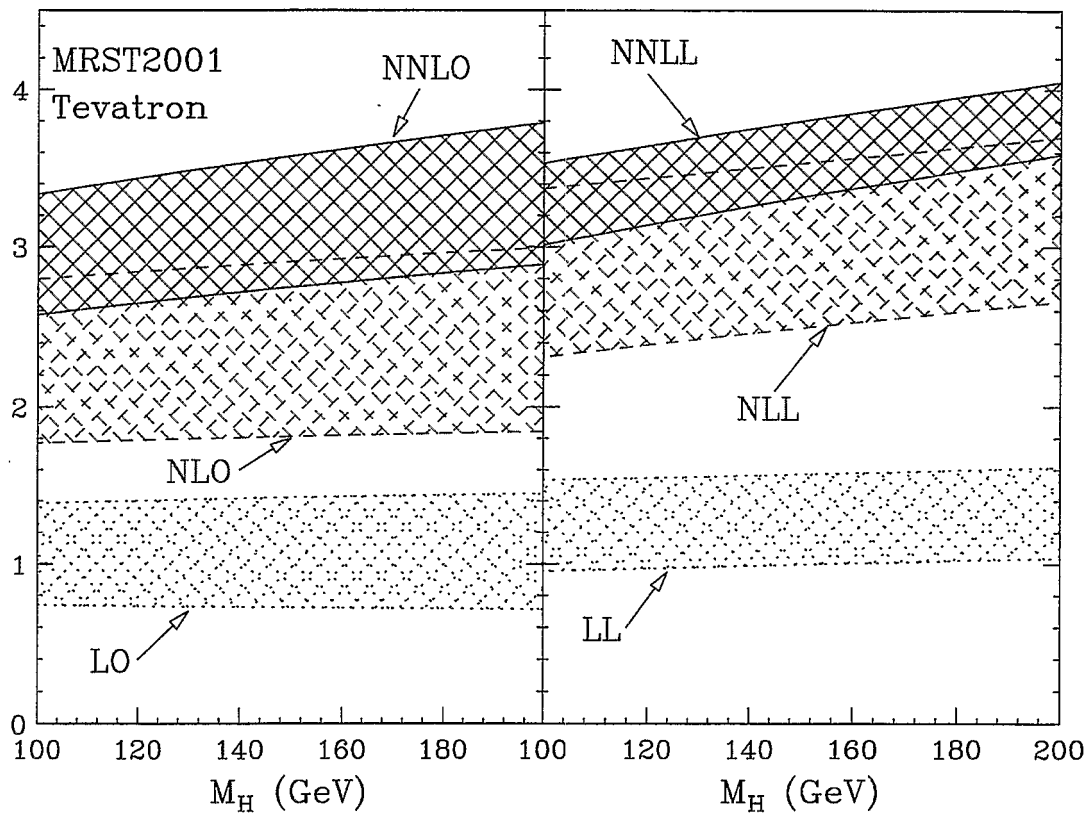
– Resummed $\mu_F = M_H$ $\mu_R = \chi M_H$



- Residual theoretical uncertainty at NNLL of about $\pm 10\%$ ($M_H < 200$ GeV).

Tevatron

- Bands defined as for LHC



- Residual theoretical uncertainty at NNLL of about $\pm 10\%$

Summary

- NNLO calculation for direct Higgs production completed
 - Increase in the cross section of $\sim 15\%$ at the LHC and of $\sim 35\%$ at Tevatron (wrt NLO)
 - 35% of NLO ($K_{NLO} = 2.2$) $\Rightarrow \sim 75\%$ of LO
 - Corrections dominated by soft emission \Rightarrow SVC approximation works very well
- We have evaluated the contributions of multiple soft emission to all orders \Rightarrow Resummation
 - Effect moderate for LHC $\sim +6\%$ for light Higgs
 - More relevant for Tevatron $\Rightarrow \sim +12 - 15\%$
- Perturbative result under better control after threshold resummation

Transverse momentum resummation in DIS production of light and heavy flavors

P. Nadolsky

in collaboration with N. Kidonakis, F. Olness, D. Stump, C.-P. Yuan

August 16, 2002

We present a formalism that improves the applicability of perturbative QCD in the current region of semi-inclusive deep inelastic scattering. The formalism is based on all-order resummation of large logarithms arising in the perturbative treatment of hadron multiplicities and energy flows in this region. It is shown that the current region of semi-inclusive DIS is similar to the region of small transverse momenta in vector boson production at hadron colliders. We use this resummation formalism to describe transverse energy flows and charged particle multiplicity measured at the electron-proton collider HERA. We find good agreement between our theoretical results and experimental data for the transverse energy flows. We also find it necessary to introduce a strong x -dependence in the nonperturbative Sudakov factor to describe broadening of q_T -distributions at $x \lesssim 10^{-2}$. This broadening is a new feature that is not present in Sudakov factors at larger values of x . It will be interesting to further investigate the x and z dependence of Sudakov factors in the upcoming studies at HERA and Electron-Ion Collider.

We next consider the resummation of soft and collinear logarithms in the heavy quark production. The calculation of differential distributions for heavy quark production introduces new kinematic energy scales (in addition to the heavy quark mass), which can yield additional large logarithms that will inhibit accurate predictions. Logarithms involving the heavy quark mass can be summed in the ACOT scheme via the heavy quark parton distribution functions. A second class of logarithms involving the heavy quark transverse momentum can be summed using the CSS (Collins-Soper-Sterman) formalism. We perform a systematic summation of these logarithms, thereby obtaining an accurate description of heavy-quark differential distributions at all energies; our method essentially combines ACOT and CSS approaches. As an example, we present the angular distributions of heavy quarks produced in neutral current events at large momentum transfers at the ep collider HERA.

Soft and collinear radiation in SIDIS

CSS refactorization formalism can be applied to resum large logarithmic terms in the hadronic energy flow (J. Collins, 1993; R. Meng, F. Olness, D. Soper, 1996) and particle cross sections (P. N., D. Stump, C.-P. Yuan, 1999-2000)

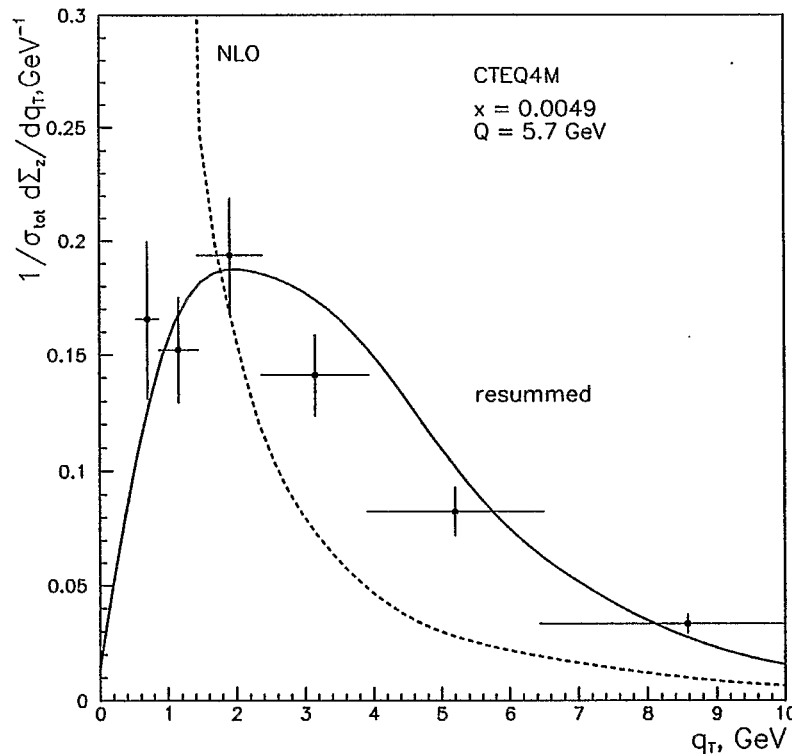
$$q_T = W e^{-\eta_{c.m.}},$$

where

$$W^2 = Q^2 \left(\frac{1}{x} - 1 \right)$$

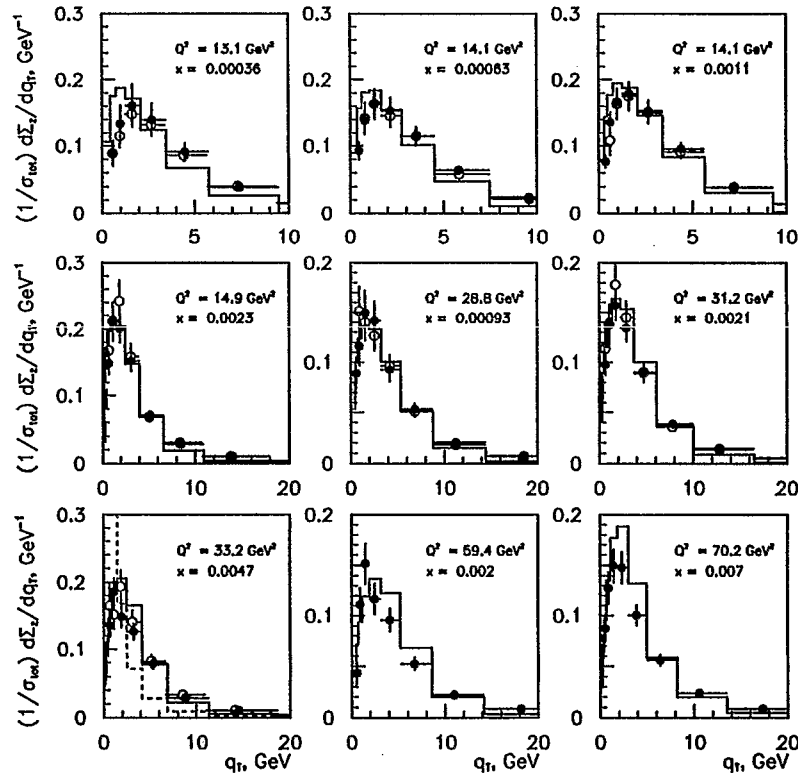
$$\lim_{\theta \rightarrow 0} q_T = \frac{W}{2} \left(\theta + \frac{\theta^3}{12} + \dots \right)$$

Σ_z is a rescaled transverse energy flow in the γ^*p c.m. frame



q_T dependence of E_T flow at small x

Data from H1 Collaboration
(DESY-99-091)



$$13.1 < \langle Q^2 \rangle < 70.2 \text{ GeV}^2, \\ 8 \times 10^{-5} < \langle x \rangle < 7 \times 10^{-3}$$

BFKL cross sections do not factorize

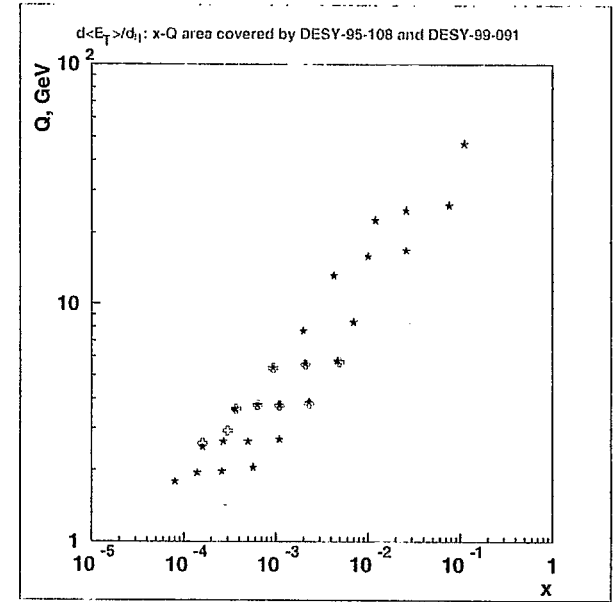
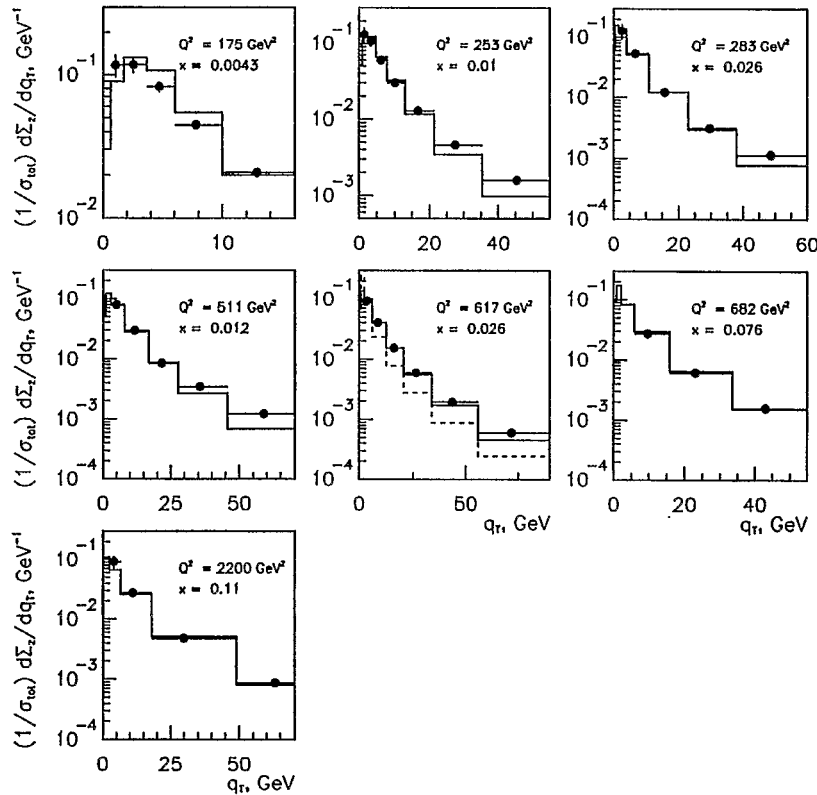
Resummed z -flow: CTEQ5M1 PDFs,

$$S_z^{NP} = b^2 \left\{ 0.013 \frac{(1-x)^3}{x} + 0.19 \ln \left(\frac{Q}{2 \text{ GeV}} \right) \right\}$$

Possible interpretation:
rapid increase of "intrinsic" k_T
when x decreases (first BFKL
signs???)

No mechanism for such
increase in the $\mathcal{O}(\alpha_s)$ part of
the CSS formula

E_T flow at HERA at large x

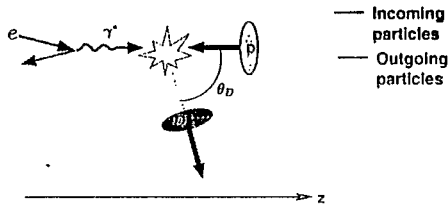


Resolution of the H1 detector not sufficient for studying the q_T distribution at large x

$$175 < \langle Q^2 \rangle < 2200 \text{ GeV}^2, \\ 0.0043 < \langle x \rangle < 0.11$$

⇒ Because of lower energy, resolution at EIC may be better than at HERA

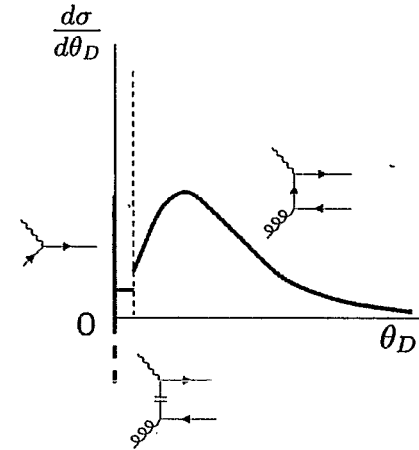
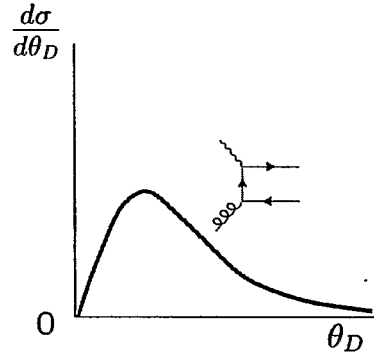
Polar angle distributions of heavy quarks in γ^*p c.m. frame



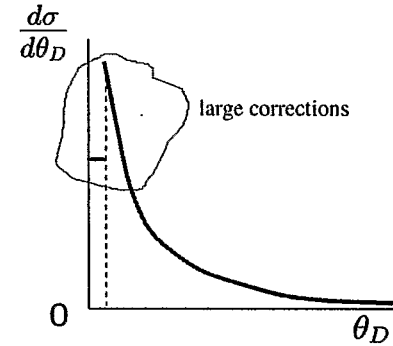
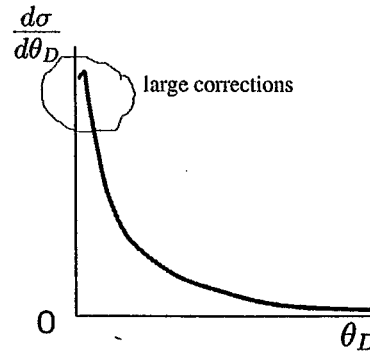
Fixed-flavor number scheme

ACOT

$Q \sim M$



$Q \gg M$



Fixed-order calculations in any scheme have trouble with the region $\theta_D \rightarrow 0$

Conclusions for the heavy flavor part

- ✓ ACOT factorization scheme + CSS = consistent description of distributions in heavy quark production at $\Lambda_{QCD}^2 \ll M^2 \leq Q^2 < \infty$
- ✓ The cross section reproduces fixed-order cross sections at $Q \approx M$, and resummed cross sections at $Q \gg M$
- ✓ An interesting exercise
 - ◆ Resummation that does not use the dimensional regularization for collinear singularities
 - ◆ transition between 2-particle inclusive and 1-particle inclusive kinematics
 - ◆ Large- b physics suppressed by $M^2 \gg \Lambda_{QCD}^2$

Physics Beyond RHIC Spin

Kaoru Hagiwara
KEK Theory Division

I reviewed prospects of spin physics at hadron colliders beyond the RHIC Spin project, including the possibility of physics at Tevatron and LHC with polarized beams.

I examined physics with following types of beam polarizations:

- (1) one proton beam is longitudinally polarized
- (2) both proton beams are longitudinally polarized
- (3) one proton beam is transversely polarized
- (4) one proton beam is longitudinally polarized

(1) Physics with Single Longitudinal Polarization

Parity-violating asymmetry can be used to probe physics with $W/Z/W'/Z'$.

Single top production cross section in the SM can be enhanced at Tevatron, and the polarization asymmetry probes new physics.

WW fusion production cross-section of Higgs at LHC can be enhanced and the background level can be lowered.

CP violation in gluon-fusion production of Higgs boson can be detected by using the asymmetry.

(2) Physics with Double Longitudinal Polarization

Single top production cross-section in the SM, and the WW fusion production of the Higgs boson can be further enhanced.

Gluon-fusion production of the Higgs boson plus b-quark pair may be a promising channel for studying the Higgs boson CP property because the Higgs boson four-momentum can be reconstructed in its tau-pair decay mode. When the colliding protons have the same helicities, the cross section should be largest.

(3) Physics with Single Transverse Polarization

Transverse polarization asymmetries at high transverse momentum can be expected only when there is new physics that violates light-quark chiral symmetry. Such new physics would have difficulty to explain naturally the smallness of up and down quark masses.

I learned during the workshop that there have been studies on chirality flip observables that arise from chiral symmetry breaking in QCD. Such asymmetries are generally expected to arise at relatively small transverse momentum on the order 1GeV or less.

(4) Physics with Double Transverse Polarization

Asymmetry is expected when an initial state quark and an anti-quark annihilate to produce a vector boson, such as virtual photon, Z and Z'. No additional information on the electroweak couplings may be obtained from such asymmetries. New insight on the spin structure of the nucleus may be obtained from the study of those asymmetries.

In summary, proton beam polarization will be a powerful tool to study new physics at hadron colliders, but the expected enhancement in the production cross section is generally a fraction of unity. The physics situation for polarized beams will become clear once a new particle is found and if its property can be probed by using polarization asymmetries.

Physics beyond RHIC Spin

by K. Hagiwara (KEK)

2002. 8. 16

@Riken BNL RCWS

$\vec{P}\vec{P}$: Single Longitudinal Polarization

$\not\propto$ asymmetries ($W, Z, \text{contact}, W', Z'$)

single-top production

WW fusion \rightarrow H @ LHC

~~CP~~ in $gg \rightarrow H$

$\vec{P}\vec{P}$: Double Longitudinal Polarization

Improve S/N further.

$A_{\pm\pm/\pm\mp}$ useful for Higgs production

$gg \rightarrow bbH \rightarrow Z^+Z^-$ @RHIC 650?

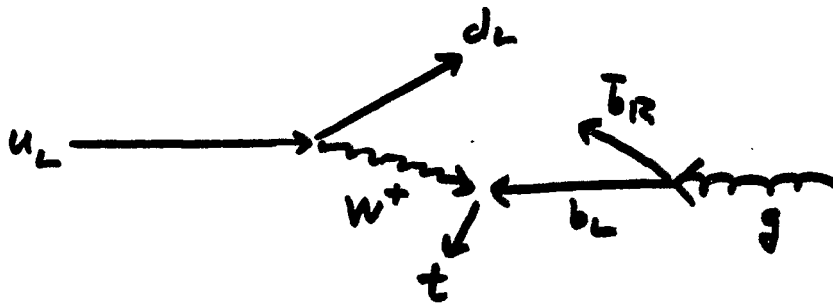
$P_T P_T$: Single Transverse Polarization

Chirality violation $\propto m_u, m_d$: Theorists say!

$P_T P_T$: Double Transverse Polarization

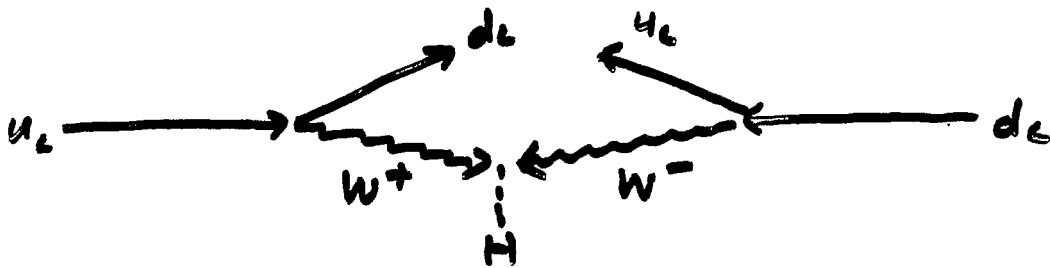
Only the s-channel $\gamma/Z/g$ exchange \Rightarrow no new information?

Single-top production



How about RHIC 650 ?

W-fusion @ LHC



Promising even without polarization

$$H \rightarrow \gamma\gamma, \tau^+\tau^-, WW^*, ZZ^*$$

With the help of \vec{P} QCD background can be better controlled. (Hadronic decay modes of $\tau^+\tau^-$)

\Rightarrow How about $WW \rightarrow t\bar{t}$?

gluon polarization : \vec{s}

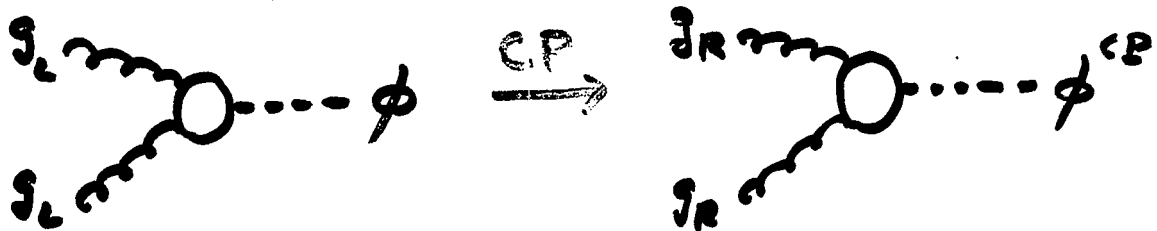
$g_L \bar{q} q$ vs $g_R \bar{q} q$

does not give difference

unless q -line is attached to W/Z .

\Downarrow
just higher-order
QCD correction to
the previous processes.

$g_L \bar{q} q$ vs $g_R \bar{q} q$ probes Higgs



$$\hat{\sigma}(g_L \bar{q} q \rightarrow \phi) \neq \hat{\sigma}(g_R \bar{q} q \rightarrow \phi) \Rightarrow \cancel{CP}$$

Gunion-Yuan-Grazdowski, PRL 71:488:1993

E 71:2681:1993

MSSM : $(h, H) \leftrightarrow A$ mixing at 1-loop
CP-even CP-odd



$g_L \bar{q} q$ vs $g_R \bar{q} q$ probes \vec{s} in tensor boson

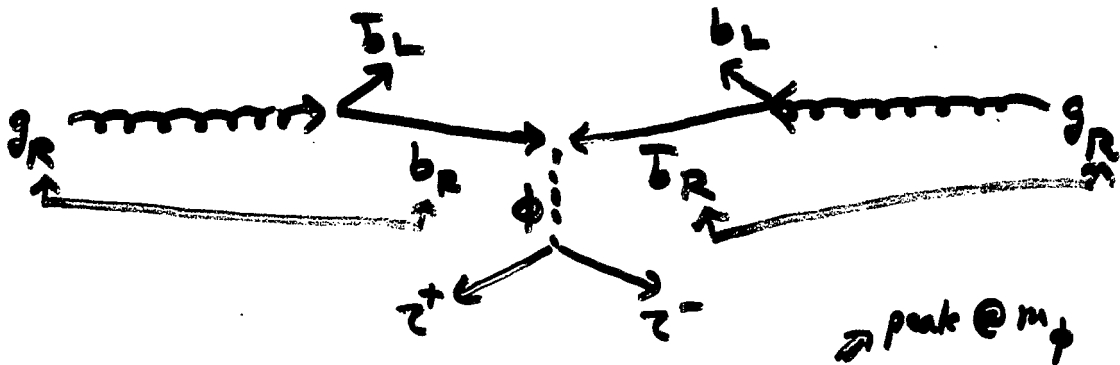
(3) $A_{\pm\pm/\pm\mp}$ Improves S/N for Higgs

ex) Higgs @ RHIC 650

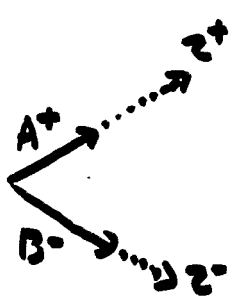
$$QED \cdot QCD \Rightarrow \begin{cases} \sigma(\gamma_{\pm} \gamma_{\pm} \rightarrow f\bar{f}) \ll \sigma(\bar{\nu}_{\pm} \nu_{\pm} \rightarrow f\bar{f}) \\ \sigma(g_{\pm} g_{\pm} \rightarrow g\bar{g}) \ll \sigma(g_{\pm} g_{\mp} \rightarrow g\bar{g}) \end{cases}$$

\downarrow Higgs channel! \uparrow $(\frac{m_{\pm}}{E})^2$

$g g \rightarrow b\bar{b} \phi$
 $\hookrightarrow \tau^+ \tau^-$ @ large $\tan\beta$



ϕ has $\vec{p}_T \Rightarrow m(\tau^+ \tau^-)$ can be reconstructed!



cf. Rainwater-Zappenzfeld-KH, PRD59:014037:1999

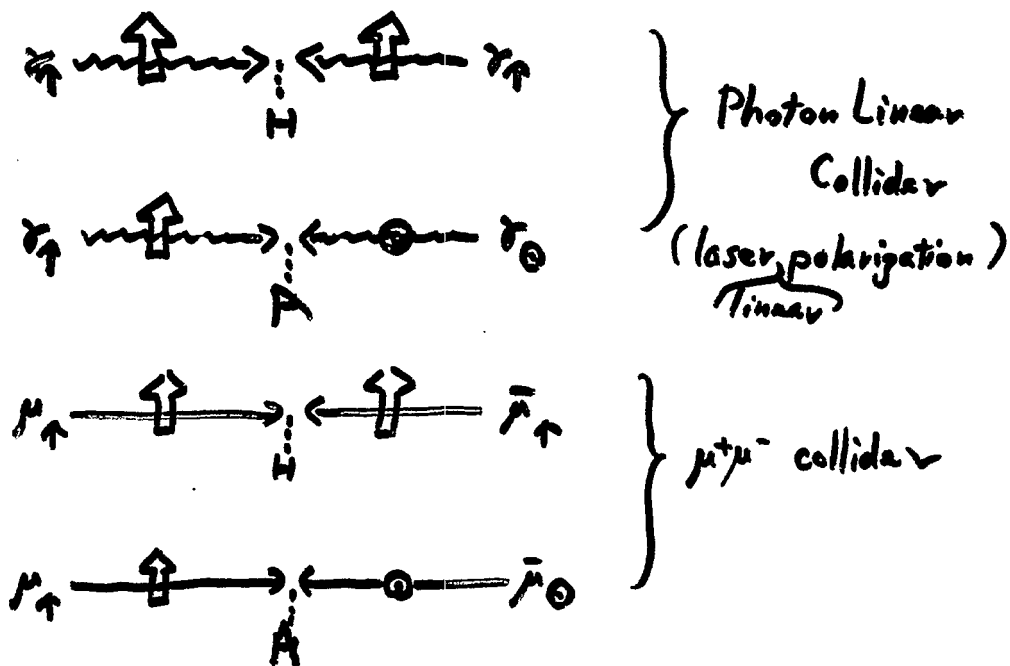
$$\vec{p}_{\tau^+} = \frac{\vec{p}_{A^+}}{x_1} \quad \vec{p}_{\tau^-} = \frac{\vec{p}_{B^-}}{x_2}$$

x_1 & x_2 can be solved from \vec{p}_T conservation if $p_T^{\phi} \neq 0$.

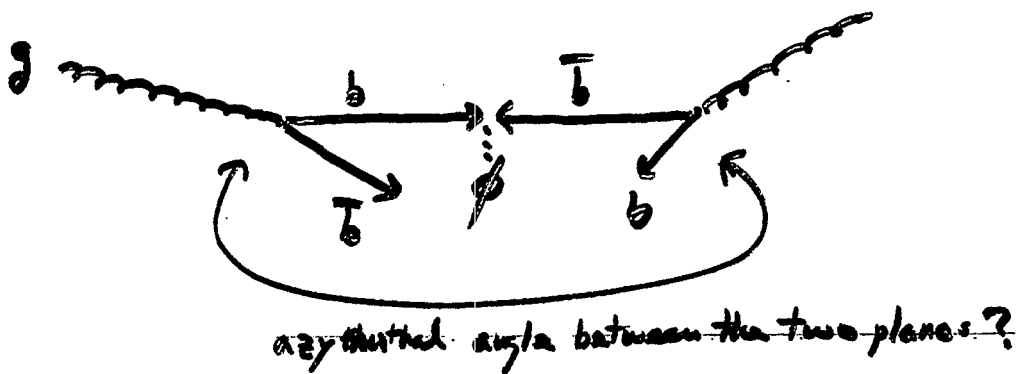
CP parity of ϕ (H vs A)?

Note that $\sigma(\gamma_R \gamma_R \rightarrow \phi) \neq \sigma(\gamma_L \gamma_L \rightarrow \phi)$ tells us ~~CP~~
 but when CP is conserved, no information on the
 CP-parity ($\phi = H$ or A) is obtained.

Transverse polarization



How about



NLO QCD Corrections to A_{LL}^π

Barbara Jäger, Marco Stratmann

*Institute for Theoretical Physics, University of Regensburg,
93040 Regensburg, Germany*

Werner Vogelsang

Brookhaven National Laboratory, Upton, NY 11973-5000

Measurements of the double spin asymmetry A_{LL}^π for inclusive high- p_T pion production are expected to provide first direct information about Δg at RHIC. Based on the factorization theorem in perturbative QCD, the longitudinally polarized cross section is given by

$$d\Delta\sigma^{pp\rightarrow\pi X} = \sum_{abc} \int dx_a dx_b dz_c \Delta f_a(x_a, \mu_f) \Delta f_b(x_b, \mu_f) D_c^\pi(z_c, \mu_{f'}) \\ \times d\Delta\hat{\sigma}^{ab\rightarrow cX'}(x_a P_a, x_b P_b, P^\pi/z_c, \mu_f, \mu_{f'}, \mu_r) ,$$

where the $\Delta f_{a,b}$ are the spin-dependent parton densities and the D_c^π are the fragmentation functions for $c \rightarrow \pi$. LO estimates of the perturbatively calculable partonic cross sections $d\Delta\hat{\sigma}^{ab\rightarrow cX'}$ suffer from a strong dependence on the unphysical renormalization and factorization scales μ_r and $\mu_{f,f'}$, respectively.

This talk reports on the progress of a computation of $d\Delta\hat{\sigma}^{ab\rightarrow cX'}$ in the NLO of QCD which is expected to reduce the theoretical errors considerably and to provide a much more reliable environment for an extraction of Δg . The calculation will provide analytical results for single-inclusive hadron production along similar lines as in the corresponding unpolarized case [1,2]. Our results can be compared to a NLO calculation of A_{LL}^π based on Monte-Carlo methods which was also presented during the workshop [3].

It should be noted that the current knowledge of D_c^π is not fully satisfactory, and one has to carefully estimate its impact on an extraction of Δg . However, future QCD analyses of fragmentation functions will try to quantify these uncertainties [4].

- [1] R.K. Ellis and J.C. Sexton, Nucl. Phys. **B269** (1986) 445.
- [2] F. Aversa et al., Nucl. Phys. **B327** (1989) 105.
- [3] D. de Florian, this workshop.
- [4] S. Kretzer, this workshop.

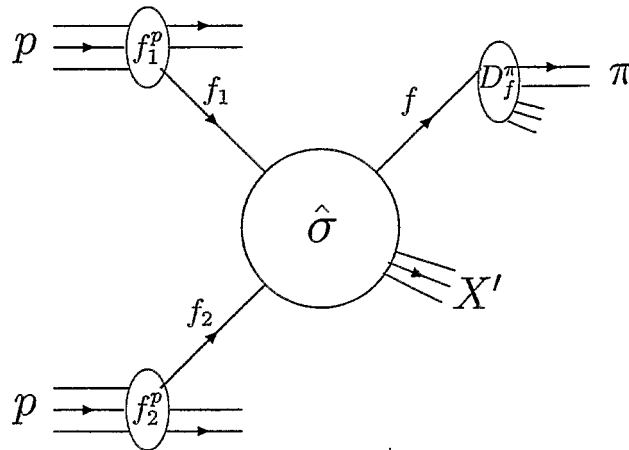
talk presented by Marco Stratmann

general framework for inclusive-pion production:

starting point: factorization theorem

Libby, Sterman; Ellis et al.; Collins et al.; ...

requirement: a hard scale, e.g., pions with high- p_T



cross sections are convolutions:

$$\frac{d\sigma^{pp \rightarrow \pi X}}{d\mathcal{P}} = \sum_{f_1 f_2 f} \int dx_1 dx_2 dz f_1(x_1, \mu_f) f_2(x_2, \mu_f) D_f^\pi(z, \mu_{f'})$$

$$\times \frac{d\hat{\sigma}^{f_1 f_2 \rightarrow f X'}}{d\mathcal{P}}(x_1 P_1, x_2 P_2, P^\pi/z, \mu_f, \mu_{f'}, \mu_r)$$

long-distance
 from exp.; μ -dep.: $d\sigma/d\mu = 0$ (pQCD)
 ↓ ↓ ↓
 ↑
 short-distance
 pQCD: power series in α_s

- \mathcal{P} : appropriate set of kin. variables (p_T, y, \dots)
- arbitrary scales $\mu_{f, f', r}$: separate long- and short-dist. physics

NLO QCD corrections to A_{LL}^π - outline:

at $\mathcal{O}(\alpha_s^2)$ one has:

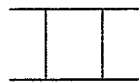
all LO $2 \rightarrow 2$  parton-parton scattering processes

unpol.: 4 processes $qq' \rightarrow qq'$, $qq \rightarrow qq$, $q\bar{q} \rightarrow gg$, $gg \rightarrow gg$
all other processes related by crossing

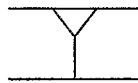
polarized: cannot use crossing, e.g., $q\bar{q} \rightarrow gg \neq qq \rightarrow qq$

at $\mathcal{O}(\alpha_s^3)$ one has:

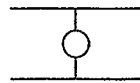
(1) 1-loop (virtual) corrections to all LO processes



'box'



'vertex'



'selfenergy'

(2) all $2 \rightarrow 3$  parton-parton scattering processes

$qq' \rightarrow qq'g$, $q\bar{q} \rightarrow ggg$, $gg \rightarrow ggg$, etc.

important check: unpol. matrix elements in Ellis, Sexton

two different strategies for NLO calculations



'Monte-Carlo approach'

- ✓ different observables
- ✓ exp. cuts easy
- × delicate numerics
- × too slow for fits
- Daniel's talk



'analytical results'

- × 'only' single-incl. x-secs
- × exp. cuts difficult
- ✓ numerically stable
- ✓ fast → useful for global fits
- our approach

final results (I) - $\mathcal{O}(\alpha_s^3)$ parton-parton processes:

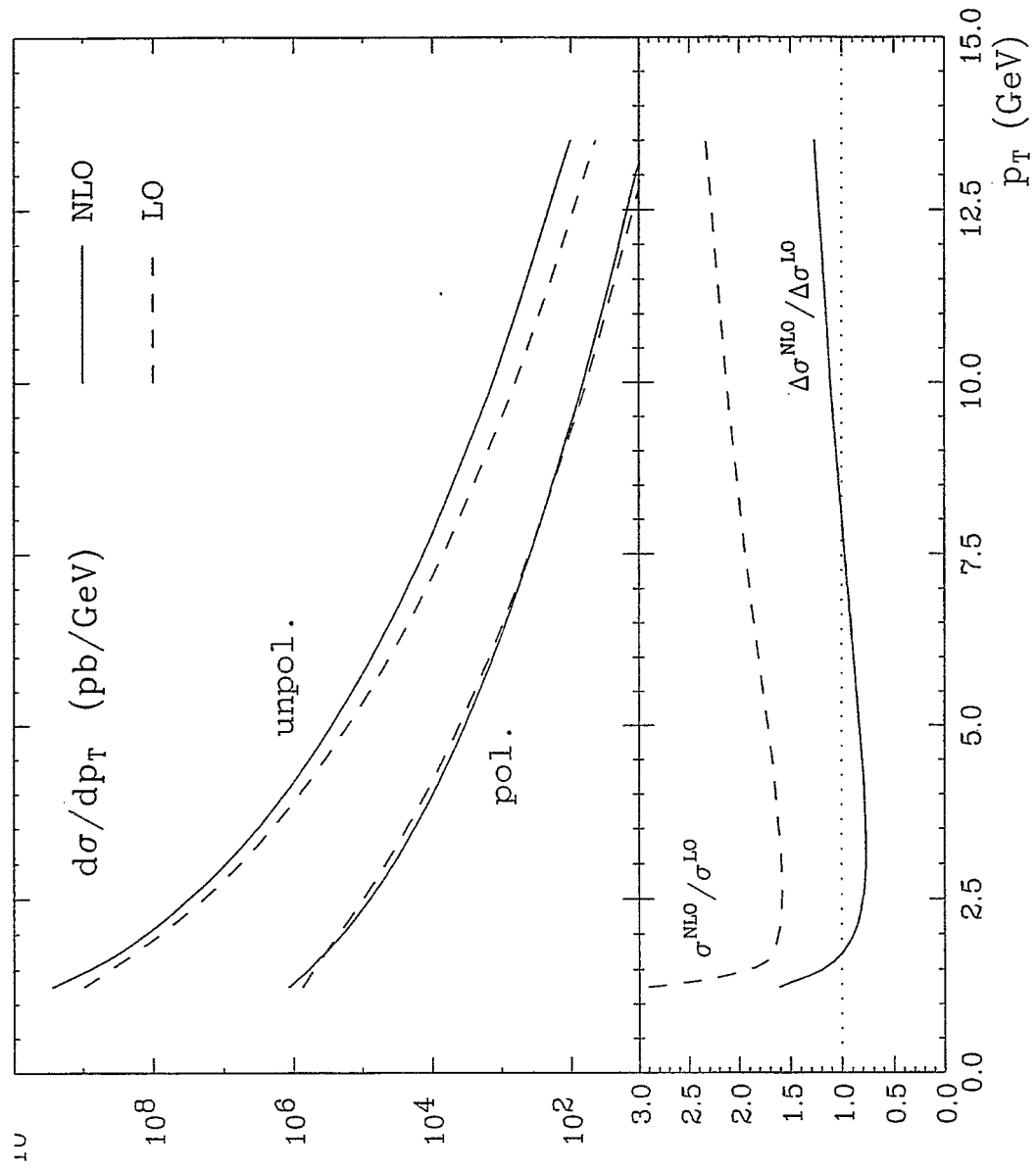
16 different inclusive cross sections contribute:

fragmenting parton	
↓	
qq'	$\rightarrow q + X \quad \checkmark$
	$\rightarrow g + X \quad \checkmark$
$q\bar{q}'$	$\rightarrow q + X \quad \checkmark$
	$\rightarrow g + X \quad \checkmark$
$q\bar{q}$	$\rightarrow q' + X \quad \checkmark$
	$\rightarrow q + X \quad \checkmark$
	$\rightarrow g + X \quad \bullet$
qq	$\rightarrow q + X \quad \checkmark$
	$\rightarrow g + X \quad \checkmark$
qg	$\rightarrow q' + X \quad \checkmark$
	$\rightarrow \bar{q}' + X \quad \checkmark$
	$\rightarrow \bar{q} + X \quad \checkmark$
	$\rightarrow q + X \quad \bullet$
	$\rightarrow g + X \quad \bullet$
gg	$\rightarrow g + X \quad \checkmark$
	$\rightarrow q + X \quad \checkmark$

\checkmark : done & unpolarized results agree with Aversa et al.

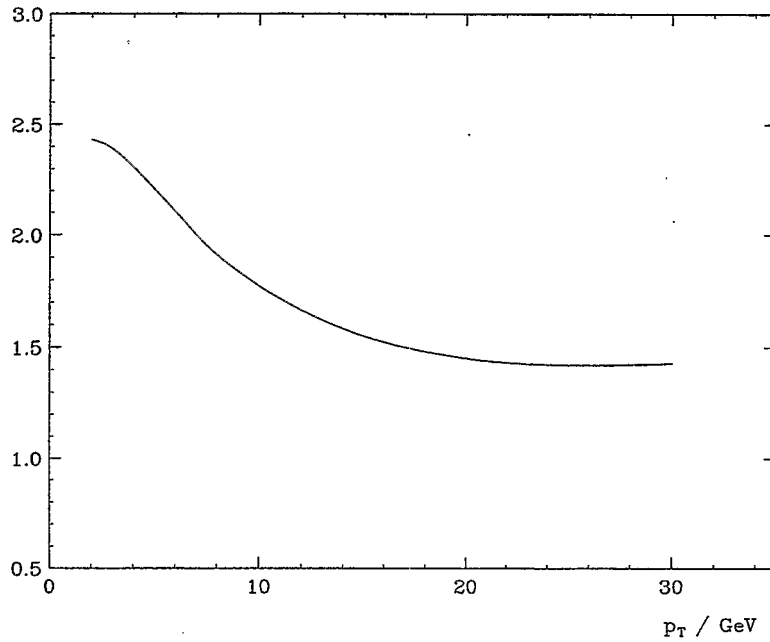
\Rightarrow almost done ... expect to have full NLO results soon

1st preliminary results: gg -induced processes only:

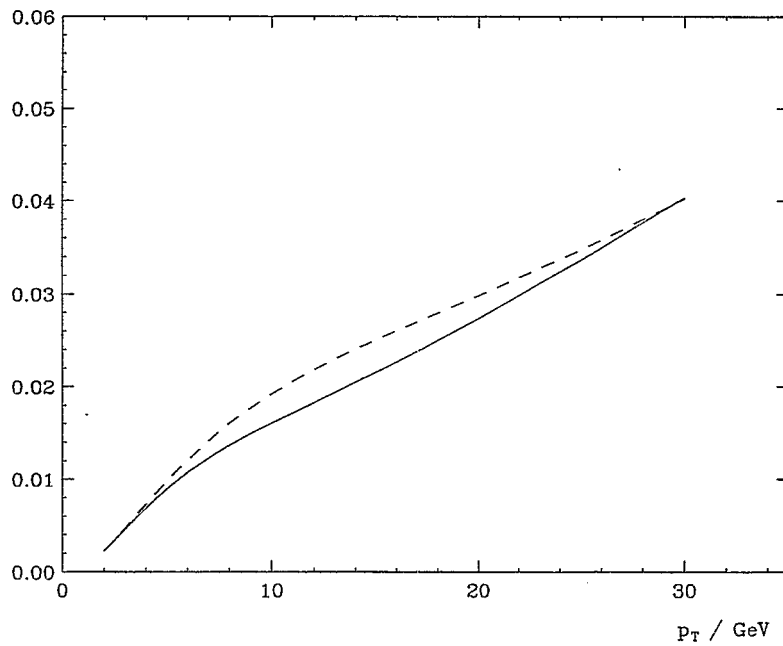


dependence of $\frac{d\sigma}{dp_T}$ and A_{LL}^π on fragmentation functions:

$$d\sigma^{KKP} / d\sigma^{Kretzer}$$



$A_{LL}^\pi(p_T)$ (dashed: KKP; solid: Kretzer)



Hadron production in polarized pp collisions at NLO

D. DE FLORIAN
Universidad de Buenos Aires
Argentina

The measurement of the longitudinally polarized double-spin asymmetry in high- p_T hadron production at RHIC offers a very powerful way to determine the polarized gluon density Δg [1, 2]. In the case of PHENIX, where the limited coverage in rapidity does not allow to observe jets, pions can be used as jet surrogates.

As it is well known, leading-order calculations in hadron-hadron collisions usually provide only qualitative information about the process. When higher order corrections are included, as at next-to-leading-order (NLO), the theoretical uncertainties (due to the dependence on the unphysical renormalization and factorization scales) are considerably reduced and the result follows in a closer way the experimental data.

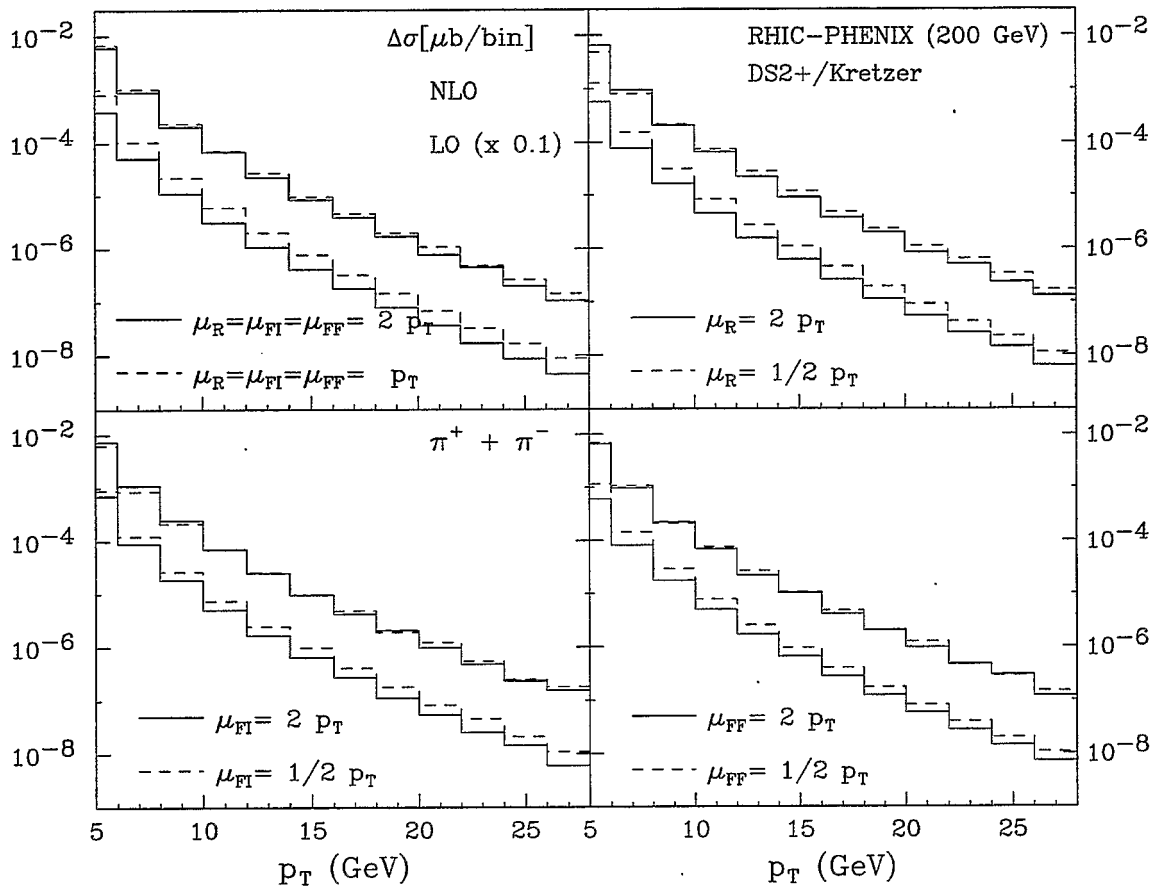
In this talk I present the NLO results for pion production in polarized pp collisions. The calculation [3] is done in the framework of the subtraction method and implemented in a Monte-Carlo code that allows to compute any infrared-safe observable and to implement realistic experimental cuts. As a check of the calculation, we observe agreement with the unpolarized result presented in [4]. Further checks in the polarized sector will be performed with the analytical calculation presented in [5]

It is shown that the perturbative stability of the cross section certainly improves after including the NLO corrections. Also the corrections are found to be non-trivial: K factors are larger for the unpolarized cross section than for the polarized one, resulting in a reduction of the asymmetry at NLO. The possibility of looking at charged pions in the final state is also studied, finding that π^+ and π^0 are the most convenient channels for the determination of the polarized gluon density at values of x between 0.05 and 0.3.

References

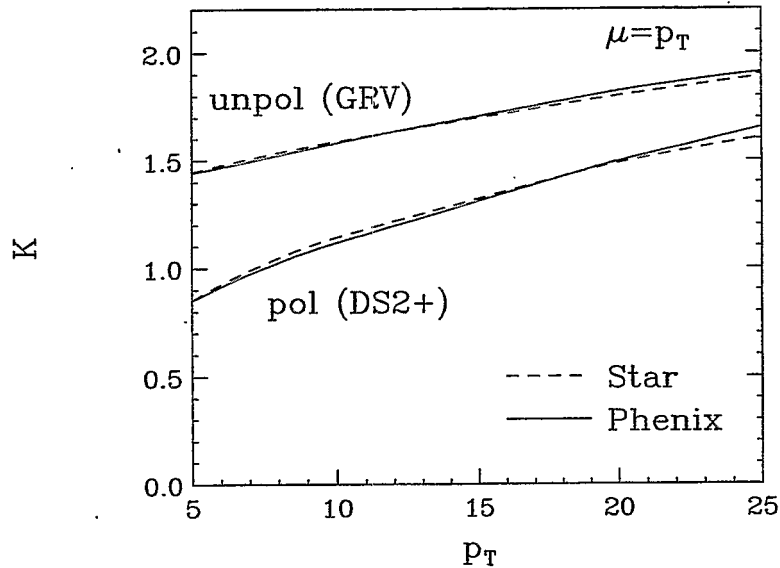
- [1] Y. Goto, Proceedings of Spin Physics at RHIC in Year-1 and Beyond, RIKEN BNL (2001).
- [2] W. Vogelsang, Proceedings of Spin Physics at RHIC in Year-1 and Beyond, RIKEN BNL (2001).
- [3] D. de Florian, in preparation (2002).
- [4] F.Aversa, P.Chiappeta, M.Greco and J.-Ph.Guillet, Nucl. Phys. B **327** (1989) 105.
- [5] M. Stratmann, this workshop.

- Scale dependence in the polarized case: use DS2+

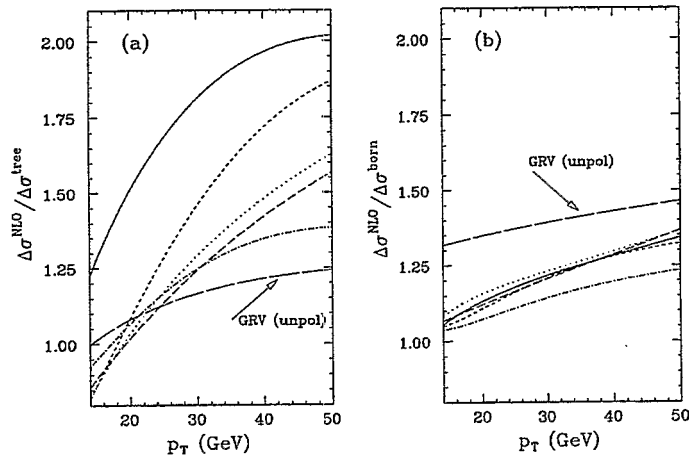


- Again better perturbative stability
- Similar results for other sets/final states hadrons

- K -factors $\frac{(\Delta)\sigma^{NLO}}{(\Delta)\sigma^{Born}}$

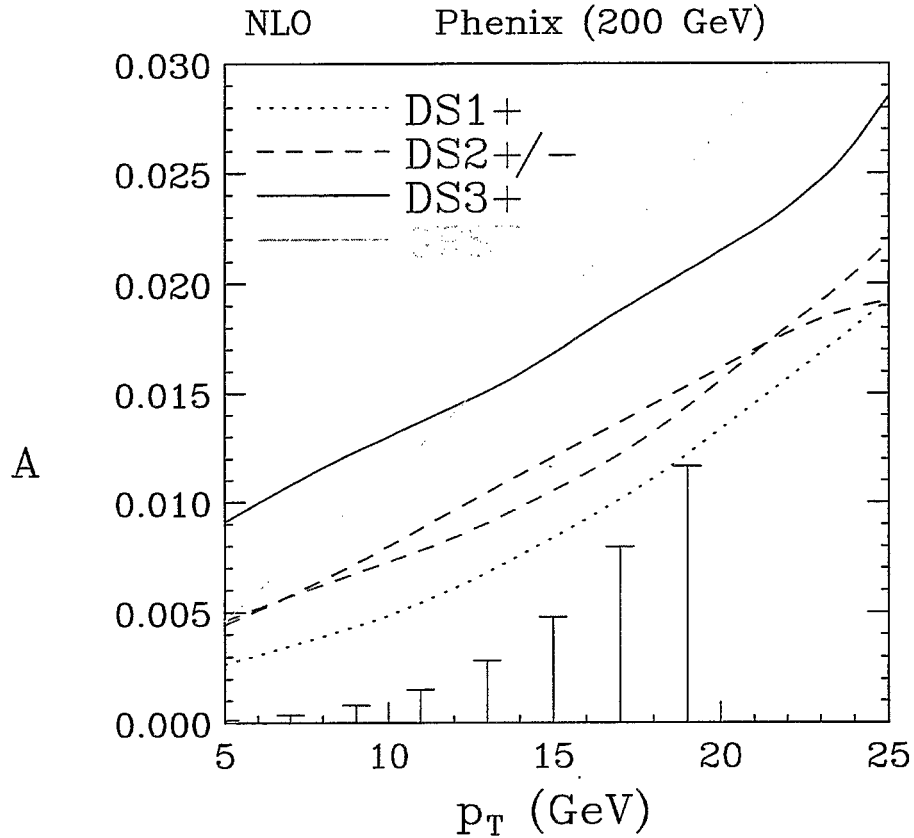


- Notice that the asymmetry is changed: similar to jet production D.de F., S.Frixione, A.Signer, W.Vogelsang



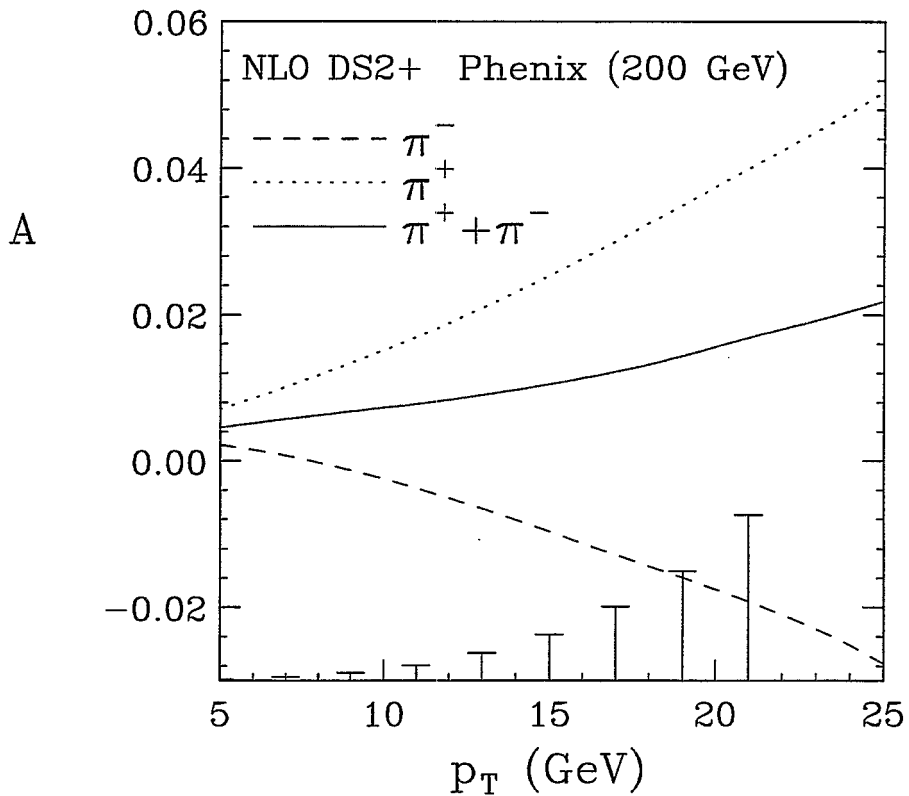
- Remember that K -factor is scale-dependent and has no physical relevance \Rightarrow just an easy number to have an idea of the 'size' of the correction

- Expected asymmetries at NLO $\epsilon_{stat} = 1/P^2 \sqrt{2\epsilon_\pi \sigma \mathcal{L}}$
 $\mathcal{L} = 100\text{pb}^{-1}$ $P = 0.7$ $\epsilon_\pi = 1$ bin size: 2 GeV



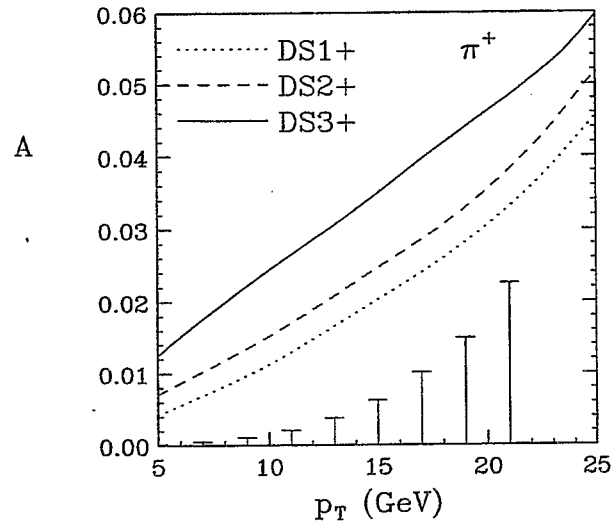
- DS2+ vs DS2-: small difference \Rightarrow gives an idea on the weight of $\Delta\bar{q}$
- Good perspectives to pin down Δg for $p_T < 12$ GeV
 \rightarrow compare to Δg plot

- Possibility to look at different hadrons in the final state: π^+ / π^-

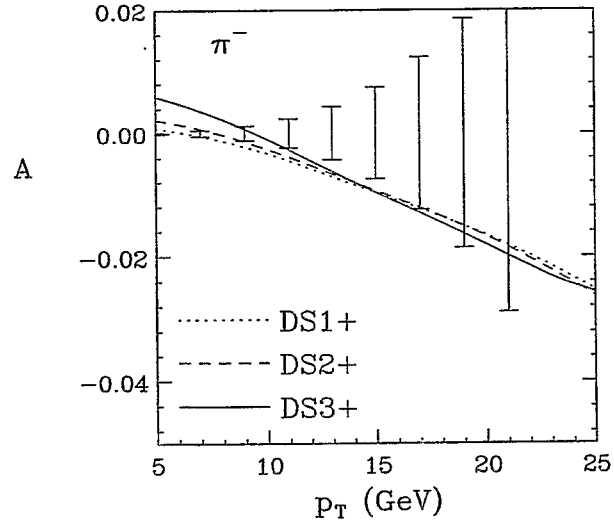


- π^+ provides larger asymmetries
 $\Rightarrow A_{\pi^+} \sim 2A_{\pi^+ + \pi^-}$ with $\epsilon_{\pi^+} \sim \sqrt{2}\epsilon_{\pi^+ + \pi^-}$
- π^- Asymmetry changes sign: might be an indication of smaller sensitivity

- π^+ production (Phenix $\sqrt{s} = 200$ GeV)



- Larger asymmetries and (not much) 'resolution'



- π^- production: only useful at small p_T
- ug and dg dominate $\Rightarrow \Delta g (\Delta u D_u^\pi + \Delta d D_d^\pi)$
 $\Delta u > 0 \quad \Delta d < 0 \quad D_u^{\pi^+} > D_d^{\pi^+}$

Polarization Effects in Drell-Yan

HIROSHI YOKOYA AND JIRO KODAIRA

Dept. of Physics, Hiroshima University

Higashi-Hiroshima 739-8526, JAPAN

Abstract

The lepton helicity distributions in the polarized Drell-Yan process at RHIC energy are investigated. In the absence of the weak interaction, only the measurement of lepton helicity can prove the antisymmetric part of the hadronic tensor. Furthermore, due to the chiral structure of QCD, the symmetric part coming from the $q\bar{q}$ initial state is essentially the same both for the unpolarized and polarized Drell-Yan at least in the leading order of QCD. Therefore it might be interesting to consider the helicity distributions of leptons to obtain more information on the structure of proton from the polarized Drell-Yan process. We estimate the QCD corrections at $\mathcal{O}(\alpha_s)$ to the antisymmetric part of the hadronic tensor including both γ and Z bosons. We report the numerical analyses on the Z pole and show that the $u(\bar{u})$ and $d(\bar{d})$ quarks give different and characteristic contributions to the lepton helicity distributions. We also estimate the lepton helicity asymmetry A which is defined by,

$$A \equiv \frac{d\sigma(\lambda_l = -1) - d\sigma(\lambda_l = +1)}{d\sigma(\lambda_l = -1) + d\sigma(\lambda_l = +1)}$$

This asymmetry amounts to around 50%. Although the helicity measurements might be difficult experimentally, our analyses may have some theoretical interests.

Polarization Effects in Drell-Yan

Jiro Kodaira, Hiroshi Yokoya (Hiroshima University)

2002.8.5-23 RIKEN BNL Research Center Workshop
Brookhaven National Laboratory

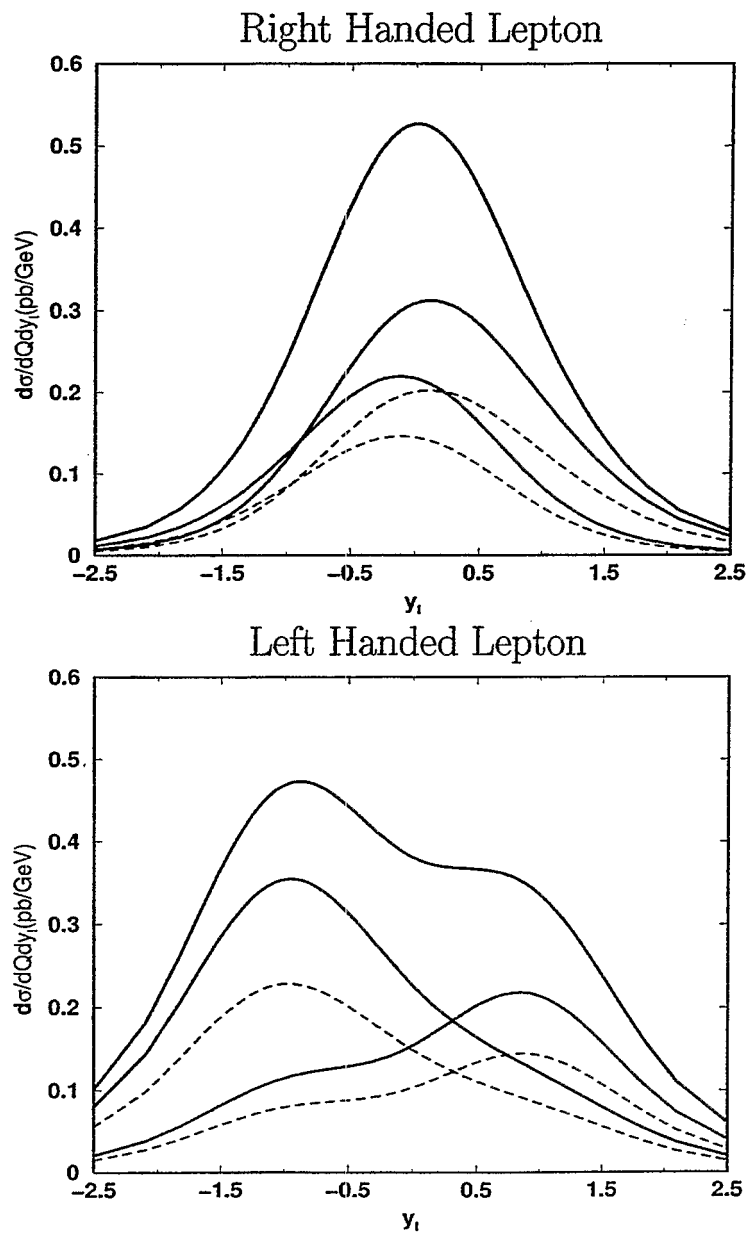
Contents

1. Polarized Drell-Yan Process
2. Spin Dependence of Hard Part
3. QCD Correction
4. Numerical Application : in Z-pole Region
5. Summary

◇ Double Differential Cross Section

Proton Polarizations is " + - " case

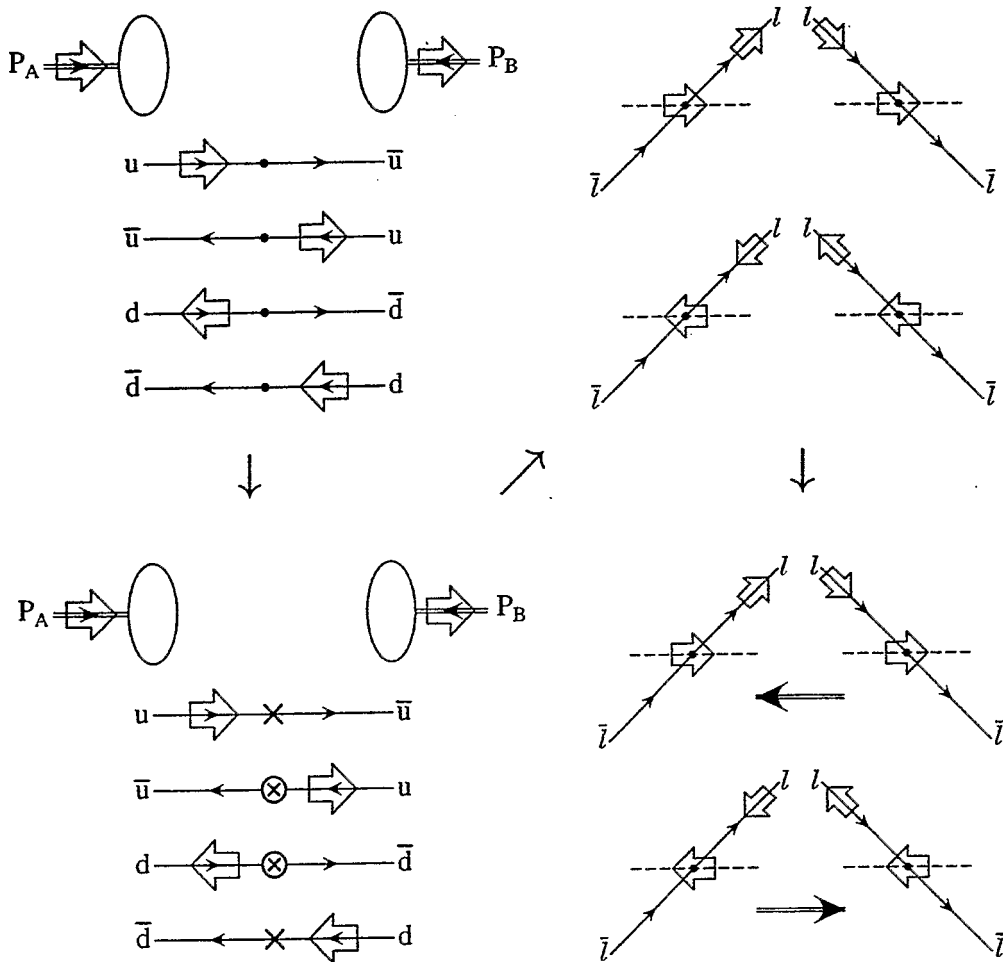
(Blue line → Up Quark, Red line → Down Quark)



◇ Flavor Contributions and Chiral Structure

- (1) Sign of Polarized PDFs : $\Delta u(x) > 0, \Delta d(x) < 0$
- (2) V-A Coupling is larger than V+A Coupling
- (3) Angular Momentum Conservation
- (4) Lorentz Boost

'+-' Polarization case

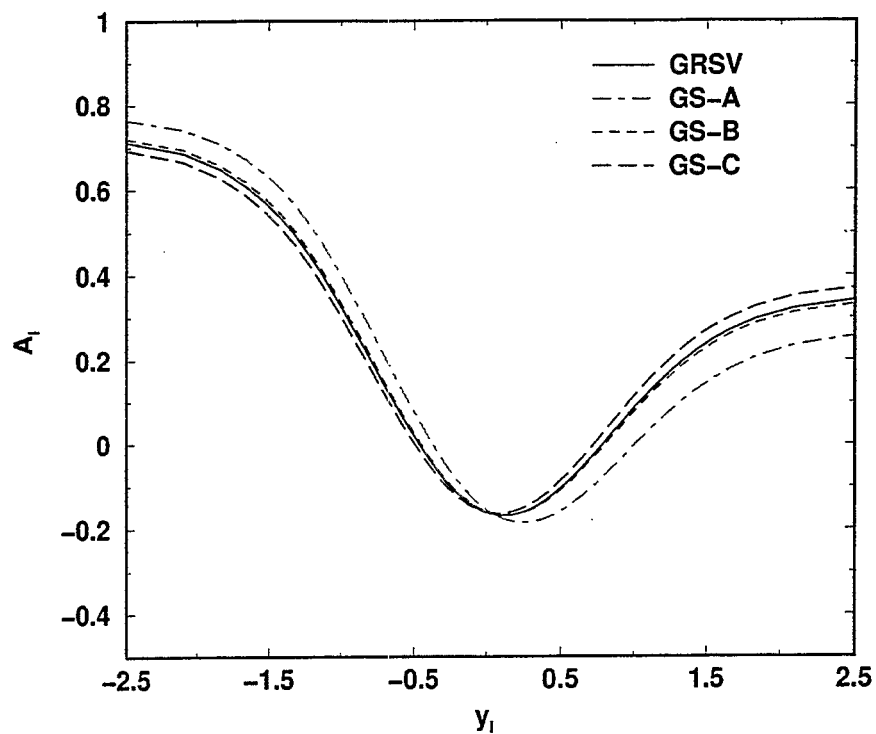


◇ Lepton Helicity Asymmetry

$$A = \frac{d\sigma(\lambda_l = -1) - d\sigma(\lambda_l = +1)}{d\sigma(\lambda_l = -1) + d\sigma(\lambda_l = +1)}$$

Using MRST and GRSV or GS(A,B,C) Data

Proton Polarizations set to '+-'



6. Summary

- We considered Lepton Helicity and Angular Distributions in Polarized Drell-Yan Process up to $O(\alpha_s)$ and studied Numerically in Z-pole Region.
- In Z-pole Region, Down Quark contribution is relatively larger than in photon case.
- Flavor Contributions and Angular Distribution variously changed in different Polarization of Protons and Helicity of Lepton.
- We got Large Asymmetry of Lepton Helicity.
 - ★ Pol. PDFs dependence is small.
- Measuring the Polarized Drell-Yan Process in RHIC Experiments is meaningful to investigate both Soft Part(PDFs) and Hard Part objects.

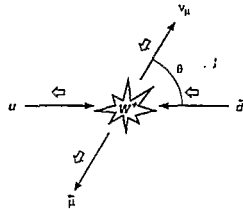
W-boson Physics at the Polarized RHIC

C.-P. Yuan

In collaboration with Pavel Nadolsky

Michigan State University

Current and Future Directions
at RHIC
A RIKEN BNL Workshop
Aug 19, 2002



Massive vector boson production at RHIC

$$pp \rightarrow (W^\pm, Z^0 \rightarrow l_1 \bar{l}_2) X$$

Total cross sections/number of events

	$\sqrt{s} = 200 \text{ GeV}$ $L = 320 \text{ pb}^{-1}$	$\sqrt{s} = 500 \text{ GeV}$ $L = 800 \text{ pb}^{-1}$	$\sqrt{s} = 650 \text{ GeV}$ $L = 10 \text{ fb}^{-1}$
W^+	$10 \pm 5 \text{ pb}$ 3000	$1.20 \pm 0.14 \text{ nb}$ 10^6	$2.3 \pm 0.2 \text{ nb}$ $2 \cdot 10^7$
W^-	$3.0 \pm 1.8 \text{ pb}$ 1000	$0.38 \pm 0.06 \text{ nb}$ $3 \cdot 10^5$	$0.82 \pm 0.11 \text{ nb}$ $8 \cdot 10^6$
Z^0	$3.4 \pm 1.4 \text{ pb}$ 1100	$0.44 \pm 0.05 \text{ nb}$ $3.5 \cdot 10^5$	$0.91 \pm 0.09 \text{ nb}$ $9 \cdot 10^6$

The uncertainties of the cross sections are due to the parton luminosities (the error matrix analysis of CTEQ5 PDFs)

Both proton beams can be polarized ($P = 70\%$)

Highlights

1. The production of W^\pm -bosons at RHIC is a sensitive test of polarized quark densities
2. The correct interpretation of the RHIC data is impossible without a full analysis at the lepton level
3. Lepton-level asymmetry $A(y^{lepton})$ presents an attractive alternative to the W-boson level asymmetry $A(y_W)$: it is directly measurable and sensitive
4. A complete lepton-level study for the polarized beams is now available; the $\mathcal{O}(\alpha_s)$ contributions are combined with an all-order sum of large logarithmic corrections from multiple soft gluon radiations

Unpolarized W-boson Physics

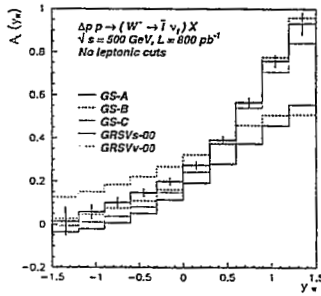
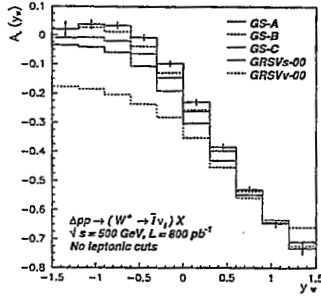
can refine our knowledge on the unpolarized parton distribution functions (PDF) from measuring

- (1) the total production rate of W-boson,
- (2) the rapidity distributions of the charged leptons from the decay of the W^+ and W^- bosons.

⇒ Refine the \bar{u} and \bar{d} PDFs

(This is complementary to the W-boson physics at the Tevatron, which is a $p\bar{p}$ collider, in contrast to a pp collider.)

Some predictions (from a NLO QCD calculation)



Neither PHENIX nor STAR detector is hermetic

PHENIX

Muon detector: $1.2 < |\eta_\mu| < 2.4$, $0 < \varphi < 2\pi$
EM calorimeter; $|\eta_e| < 0.35$, $\Delta\varphi = \pi$

STAR

EM calorimeter: $|\eta_e| < 1.0$, $\Delta\varphi = 2\pi$

⇒ Missing E_T cannot be measured

Irrelevant for γ^* , Z^0

Important for W^\pm :

⇒ the 4-momentum of W^\pm cannot be reconstructed

Reconstruction of $y(W)$ from the charged lepton's momentum (possible at the Born level)

Let $y(l)$ and $p_T(l)$ correspond to the rapidity and transverse momentum of the lepton in the lab frame; $y'(l)$ and $p'_T(l)$ are defined in the rest frame of the W -boson. At the Born level,

$$\begin{aligned} y(l) &= y'(l) + y(W) \\ p_T(l) &= p'_T(l) \end{aligned}$$

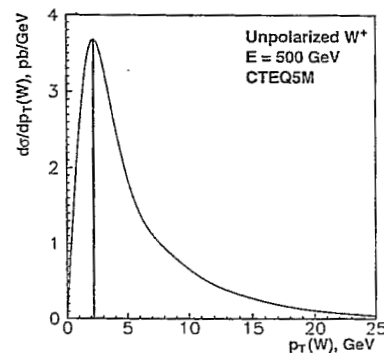
with $p_T(W) = 0$, and in the rest frame of W ,

$$\begin{aligned} y'(l) &= \frac{1}{2} \ln \frac{1 + \cos \theta}{1 - \cos \theta} \\ p'_T(l) &= \frac{M_W}{2} \sin \theta \end{aligned}$$

The above equations have two solutions for $y(W)$ in terms of $y(l)$ and $p_T(l)$.

⇒ One of them can be correctly chosen in some kinematic region ($y(l)$ and $p_T(l)$ dependent).

In reality, $p_T(W)$ does not vanish.

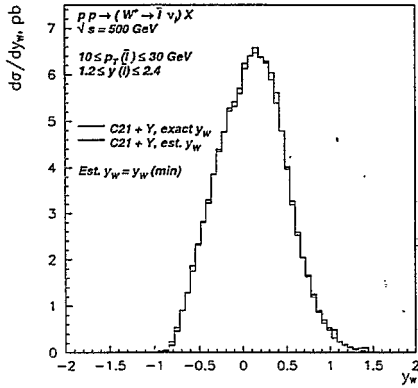


When $p_T(W) \ll M_W$, $p'_T(l)$ is about equal to $p_T(l)$, then the above method can be applied.

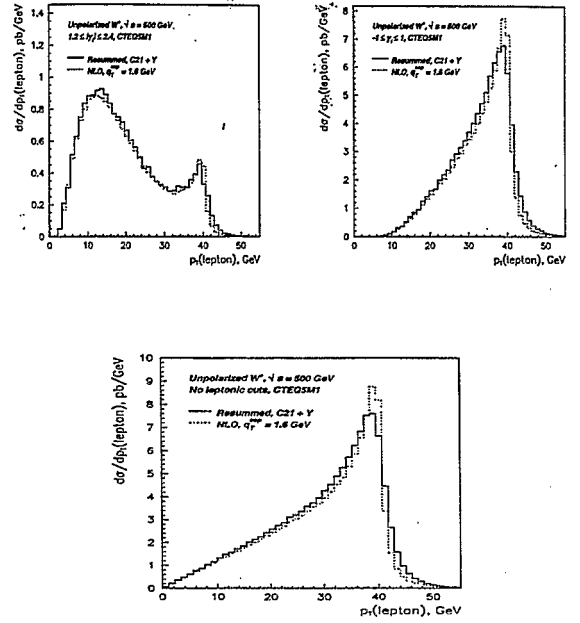
⇒ This approximation can be applied to a higher-order calculation.

Reconstruction of $d\sigma/dy_W$

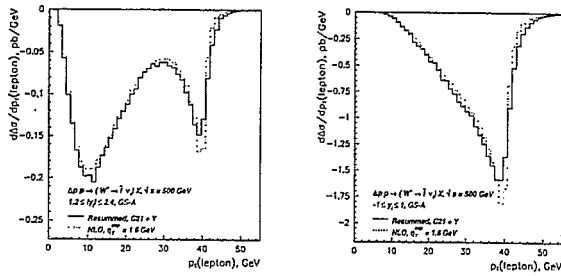
for a special phase space region (where the event rate is small), from a resummation calculation



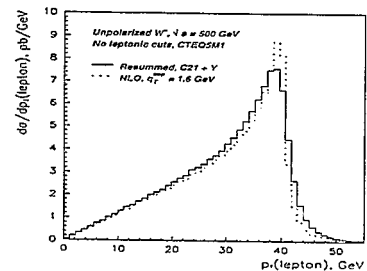
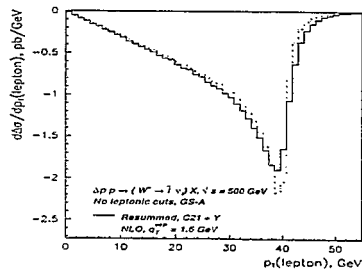
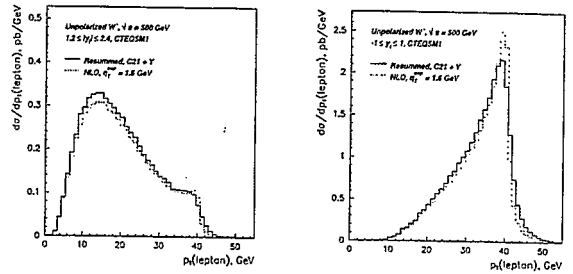
$\frac{d\sigma}{dp_T^l}$ for unpolarized NLO and resummed W^+ rates with $1.2 < |\eta_\mu| < 2.4$ and $|\eta_e| < 1.0$



$\frac{d\Delta\sigma}{dp_T^l}$ for polarized NLO and resummed W^+ rates with $1.2 < |\eta_\mu| < 2.4$ and $|\eta_e| < 1.0$

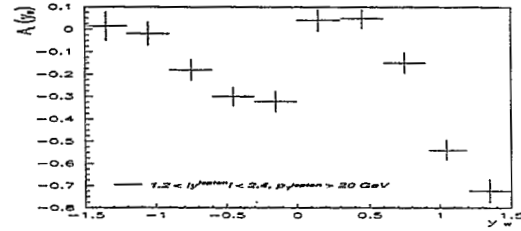
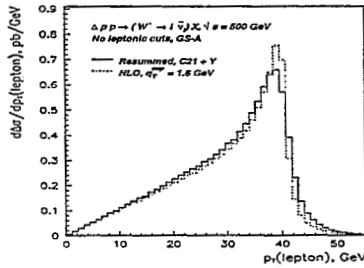
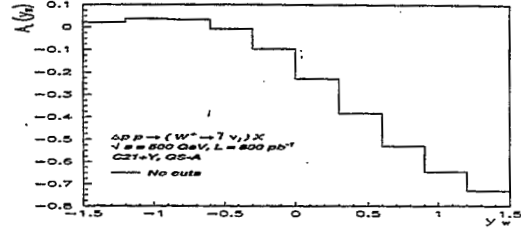
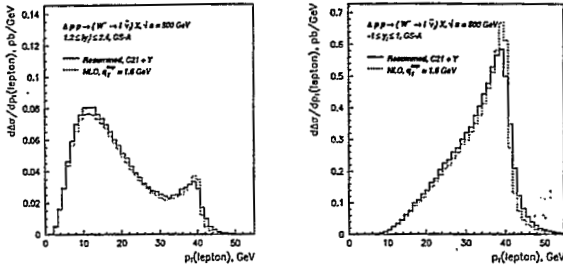


$\frac{d\sigma}{dp_T^l}$ for unpolarized NLO and resummed W^- rates with $1.2 < |\eta_\mu| < 2.4$ and $|\eta_e| < 1.0$

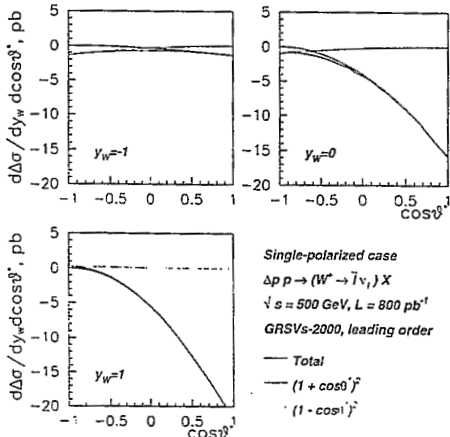
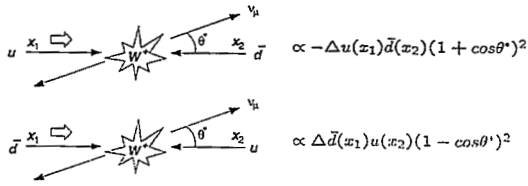


$\frac{d\Delta\sigma}{dp_T^l}$ for polarized NLO and resummed W^- rates
with $1.2 < |\eta_\mu| < 2.4$ and $|\eta_e| < 1.0$

Leptonic Cuts distort $d\sigma/dy_W$



Angular distributions in the W rest frame:
LO single-spin cross sections



To summarize:

- ❖ Reconstruction of y_W significantly reduces the event sample
- ❖ The shape of $A(y_W)$ is significantly distorted by the experimental cuts \Rightarrow direct comparison with the LO formula is not possible
- ❖ The LO analysis of $A(y_W)$ is not accurate itself

Solutions:

- ❖ Direct measurement of the lepton-level asymmetries $A(y^{lepton})$ and $A(p_T^{lepton})$
- ❖ Careful modeling of the kinematics of leptons from the W-boson decay with the effect of multiple gluon radiation included

A better theory calculation

- ❖ $\mathcal{O}(\alpha_S)$ fully differential cross section

$$\frac{d\sigma}{d^3\vec{p}_l d^3\vec{p}_{\nu_l}} [pp \rightarrow (\gamma^*, W^\pm, Z^0)X]$$

for arbitrary longitudinal polarizations of the beams $\Rightarrow A_L, A_{LL}$ at the lepton level

- ❖ In the region $p_T^W \rightarrow 0, \frac{d\sigma}{d^3\vec{p}_l d^3\vec{p}_{\nu_l}}$ is dominated by large terms

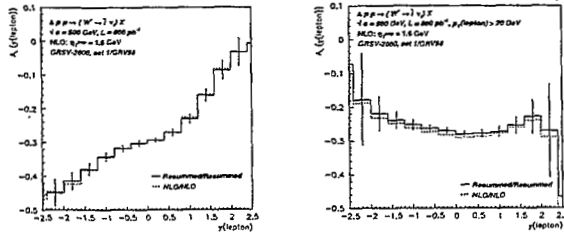
$$\alpha_S^n \left(\frac{1}{p_T^2} \ln^m \frac{Q^2}{p_T^2} \text{ or } \delta(p_T) \right),$$

$$n = 0, \dots, \infty; m = 0, \dots, 2n - 1$$

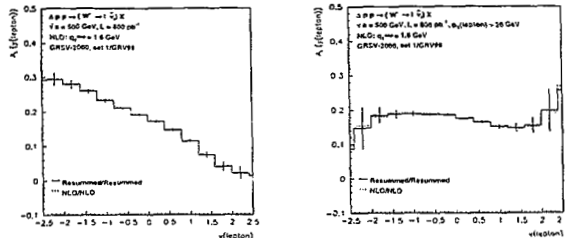
We found the sum of these terms with the help of the impact parameter space resummation formalism (Collins, Soper, Sterman, 1985)

$$\frac{d\sigma_{h_A h_B}}{dQ^2 dy dp_T^2 d\Omega_l} \approx \int \frac{d^2b}{(2\pi)^2} e^{i\vec{p}_T \cdot \vec{b}} \tilde{W}_{h_A h_B}(b, \dots)$$

$A_L(y^{lepton})$ in W^+ events, with $p_T(l) > 0$ GeV and $p_T(l) > 20$ GeV, respectively



$A_L(y^{lepton})$ in W^- events, with $p_T(l) > 0$ GeV and $p_T(l) > 20$ GeV, respectively



Resummed cross section at lepton level

- ❖ The resummation calculation for the polarized hadron beams that also describes spin correlations in the final state is done for the first time
- ❖ The perturbative part of the resummed cross section is now completely known at $\mathcal{O}(\alpha_S)$, with the soft factor known at $\mathcal{O}(\alpha_S^2)$.
- ❖ We combine this sum and the $\mathcal{O}(\alpha_S)$ cross section at large p_T^W to predict the rate in all available phase space
- ❖ The results are implemented in the numerical simulation package (Legacy++ & ResBos)

Summary

1. Neither PHENIX nor STAR detector is hermetic \Rightarrow Missing E_T cannot be measured \Rightarrow W -boson 4-momentum cannot be reconstructed \Rightarrow need predictions at the lepton level
2. We study the production and the decay (at the lepton level) of the W -boson with hadron beams of arbitrary longitudinal polarization up to the NLO QCD. A resummation calculation is also presented.
3. The lepton-level spin asymmetries $A(y^{lepton})$ are sensitive and easily measurable observables that are good alternatives to $A(y_W)$
4. The arbitrariness in the shape of p_T -distribution in the fixed-order QCD analysis is cured by summation of large logarithmic terms arising when p_T of the W -boson is small
5. RHIC can easily test the spin dependence of the perturbative soft, collinear and nonperturbative contributions to $d\sigma/dp_T^{lepton}$

QCD analysis of spin structure function data from present and prospective future measurements

Jechiel LICHTENSTADT

School of Physics and Astronomy
The Raymond and Beverly Sackler Faculty of Exact Sciences
Tel Aviv University, 69978 Tel Aviv, ISRAEL *

1. INTRODUCTION

The measurement of the spin structure function of the proton g_1^p by the EMC [1] concluding that only a small fraction of the nucleon spin is carried by the valence quarks has triggered a new series of experiments. They aimed to reduce the statistical and systematic uncertainties on the measurements, to extend the kinematic range of the data and obtain data on both, the neutron and the proton and thereby test experimentally the Bjorken sum rule. Measurements were performed by the SMC at CERN [2], the E142, E143, E154 and E155 collaborations at SLAC [3-6] and the HERMES [7] collaboration at DESY. The data cover now the entire kinematic range accessible by present day accelerators which are capable of providing polarized beams. Extending further the kinematic range will require new machines, possibly colliders of polarized beams.

The new data have induced much theoretical activity. In QCD the treatment of g_1 follows closely that of the unpolarized structure functions and parton distributions. The evolution of the parton distributions is given by the DGLAP equations [8], for which the coefficient functions and the splitting functions have been computed to next-to-leading-order [NLO] in α_s [9,10], thus allowing for a consistent QCD analysis in NLO of scaling violations in $g_1(x, Q^2)$ [11-14]. The analysis provides the first information on the polarized gluon distribution in the nucleon. Such analyses were carried out by several theoretical groups [11-14] as well as by the SMC [15].

We repeat the QCD analysis performed on the g_1 data and include all the new (recent) data which were not available in the SMC analysis. The results of the analysis were used to project

future measurements in new machines.

2. QCD ANALYSIS OF g_1 DATA

The QCD analysis has been done following Ball Forte and Ridolfi [11] including all available g_1^p , g_1^d and g_1^n data [1-7]. Using the DGLAP equations parton distributions, parameterized at an initial scale Q_0^2 are evolved to the Q^2 value of the experimental data at the measured x , thereby fitting the initial parameterization to the data. The form for each parton distribution at the initial scale ($Q_0^2=1 \text{ GeV}^2$) was taken as:

$$\Delta f = N(\alpha_f, \beta_f, a_f, \rho_f) \eta_f x^{\alpha_f} (1-x)^{\beta_f} (1+a_f x + \rho_f \sqrt{x})$$

where N is a normalization factor ($\int_0^1 N x^\alpha (1-x)^\beta (1+ax + \beta\sqrt{x}) dx = 1$) and η_f is the first moment of the Δf . The analysis has been carried out in the AB scheme [11]. Our results [17] for the first moments of the singlet parton distribution and the polarized gluon distribution are:

$$\eta_q = 0.40 \pm 0.02 \quad (\Delta\Sigma \pm \delta(\Delta\Sigma))$$

$$\eta_g = 0.63_{-0.19}^{+0.20} \quad (\Delta g \pm \delta(\Delta g))$$

Errors are statistical only. The systematic error is essentially the same as that determined in the QCD analysis performed by the SMC [15]. The best fit parton distributions at the initial scale are shown in the attached figures.

3. PROSPECTIVE MEASUREMENTS AT e-RHIC AND HERA

The results of the QCD analysis were used to project values of measurements in the extended kinematic region which may become possible in the future and examine their impact on the determination of Δg . Two future machines were considered:

- A new electron-proton collider at RHIC (e-RHIC) [18] with beam energies of $E_p=250$

*This work is supported by The Israel Science Foundation founded by The Israel Academy of Sciences and Humanities.

GeV and $E_e=10$ GeV.

- Polarized HERA [19], with polarized electron (available) and proton beams of 27 and 820 GeV respectively.

The estimates were done assuming beam polarizations of 0.7 for both beams, and detector parameters similar to those of H1 at HERA. A total integrated luminosity of $\mathcal{L} = 12.6 \text{ fb}^{-1}$ was assumed for the expected e-RHIC data and $\mathcal{L} = 500 \text{ pb}^{-1}$ for HERA. Such luminosities should be obtainable in three years according to the proposed design parameters.

The parton distributions from the QCD analysis were used to project the g_1 values at the extended kinematic region, and the statistical errors were estimated according to the detector and machine parameters. The projected 'data' were then added to the real data and the QCD analysis was repeated to assess the uncertainty on the polarized gluon distribution.

The new g_1 data will reduce significantly the uncertainty on the first moment of the polarized gluon distribution in the nucleon, Δg :

- Inclusion of projected HERA data ($\mathcal{L} = 500 \text{ pb}^{-1}$) will result with:
 $\Delta g = 0.6 \pm 0.14$ and $\Delta \Sigma = 0.40 \pm 0.02$
- Inclusion of projected e-RHIC data ($\mathcal{L} = 12.6 \text{ fb}^{-1}$) will result with:
 $\Delta g = 0.7 \pm 0.08$ and $\Delta \Sigma = 0.41 \pm 0.015$

The estimated errors are statistical only.

4. COMBINED ANALYSIS OF g_1 AND DI-JET ASYMMETRIES DATA

New experiments which measure processes in which Δg contributes in leading order, such as COMPASS at CERN or RHIC-Spin are underway. These data will provide a direct measurement of $\Delta g(x)$. Future facilities will enable measurements of two-jet asymmetries where Δg contributes in leading order as well. These data which will determine the shape of the gluon distribution, can also be included in the QCD analysis in a self-consistent way [16]. They will constrain the (presently) assumed shape of the polarized gluon distribution as well as reduce the uncertainty on its first moment. The expected uncertainties on the di-jet asymmetries were evaluated by Rädcl and DeRoeck [20]. They are shown in the attached figures. Including such di-jet asymmetries in the QCD analysis, will further reduce the uncertainty on the first

moment of the the polarized gluon distribution:
 $\Delta g = 0.6 \pm 0.04$

The expected uncertainties on the polarized gluon distribution which will be obtained from QCD analysis of present and future data are summarized in the attached table.

REFERENCES

1. EMC, J. Ashman *et al*; Nucl. Phys. B **328** (1989) 1.
2. SMC, B. Adeva *et al*; Phys. Rev. **D58** (1998) 112001.
3. E-142 P. L. Anthony *et al*; Phys. Rev. **D 54** (1996) 6620.
4. E-143, K. Abe *et al*; Phys. Rev. **D 58** (1998) 112003.
5. E-154 K. Abe *et al*; Phys. Rev. Lett. **79** (1997) 26.
6. E-155, P. L. Anthony *et al*; Phys. Lett **B 493** (2000) 19. Phys. Lett **B 463** (1999) 339.
7. HERMES Coll. K. Ackestaff *et al*; Phys. Lett **B 404** (1997) 383. A. Airapetian *et al*; Phys. Lett **B 442** (1998) 484.
8. V. N. Gribov and L. N. Lipatov, Sov. J. Nucl. Phys. **15** (1972) 438; **15** (1972) 675; G. Altarelli and G. Parisi Nucl. Phys. **B 126** (1977) 298; Yu. L. Dokshitzer, Sov. Phys. JETP **46** (1977) 641.
9. J. Kodaira, Nucl. Phys. **B 165** (1980) 129.
10. R. Mertig and W. L. van Neerven Z. Phys. **C 70** (1996) 637; W. Vogelsang, Nucl. Phys. **B 475** (1996) 47.
11. R. D. Ball, S. Forte and G. Ridolfi Phys. Lett. **B378** (1996) 255
12. M. Glück *et al*., Phys. Rev. **D53** (1996) 4775.
13. T. Gehrmann and W. J. Stirling Z. Phys. **C65** (1995) 461; Phys. Rev **D53** (1996) 6100.
14. G. Altarelli *et al*; Nucl. Phys. **B 496** (1997) 337
15. SMC, B. Adeva *et al*; Phys. Rev. **D58** (1998) 112002.
16. A. De Roeck, *et al*; Eur. Phys. **J C 6** (1999) 121.
17. J. Lichtenstadt, Nucl. Phys. **B (Proc. Suppl.) 105** (2002) 86.
18. The 2nd eRHIC Workshop, L. McLerran *et al*; Yale University April 2000. BNL-52592 Formal Report.
19. Workshop on Future Physics at HERA, G. Ingelman, A. DeRoeck and R. Klanner Ed. HERA, Hamburg Germany 1995-1996.
20. G. Rädcl and A. De Roeck, Nucl. Phys. **B (Proc. Suppl.) 105** (2002) 90.

New QCD analysis in NLO

J. Lichtenstadt, Preliminary

- Include new and revised data (E143, E155, HERMES).
- Fit 12 parameters.
- Parton Distributions at $Q_0^2 = 1 \text{ GeV}^2$:

$$\Delta f = N(\alpha_f, \beta_f, a_f, \rho_f) \eta_f x^{\alpha_f} (1-x)^{\beta_f} (1+a_f x + \rho_f \sqrt{x})$$

- Evaluate only statistical errors.
- Significant improvement in χ^2 : 194.5/174
(Compared to 239.3/177 with 9 parameters).
- Systematic and theoretical are still significant (same).
- Analysis in AB scheme.

NEW QCD fit in NLO of world data

- Use only data with $Q^2 > 1 \text{ GeV}^2$
- Fit results at $Q^2 = 1 \text{ GeV}^2$ (preliminary):

$$\eta_q = 0.40 \pm 0.02 \quad (\Delta\Sigma \pm \delta(\Delta\Sigma))$$

$$\alpha_q = 1.6 \pm 0.2$$

$$\beta_q = 4.4 \pm 0.4$$

$$a_q = 0.0 \text{ (Fixed)}$$

$$\rho_q = 0.0 \text{ (Fixed)}$$

$$\eta_g = \mathbf{0.63}_{-0.19}^{+0.20} \quad (\Delta g \pm \delta(\Delta g))$$

$$\alpha_g = -0.15 \pm 0.21$$

$$\beta_g = 4.0 \text{ (Fixed)}$$

$$a_g = 7.4 \pm 0.7$$

$$\rho_g = -5.6 \pm 0.3$$

$$\eta_{NS}^{p(n)} = (-)0.75g_A + 0.25a_8$$

$$\alpha_{NS}^p = -0.75 \pm 0.07$$

$$\beta_{NS}^p = 2.4 \pm 0.1$$

$$a_{NS}^p = 27.5 \pm 14.8$$

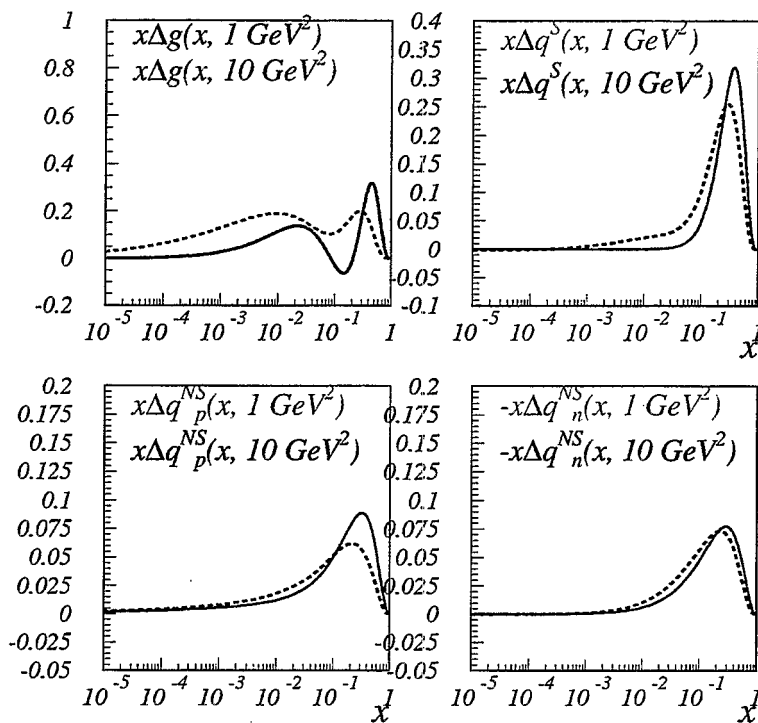
$$\alpha_{NS}^n = 0.01 \pm 0.1$$

$$\beta_{NS}^n = 2.5 \pm 0.4$$

$$\chi^2 = 194.5 \text{ for } 174 \text{ deg. of freedom}$$

Parton Distributions

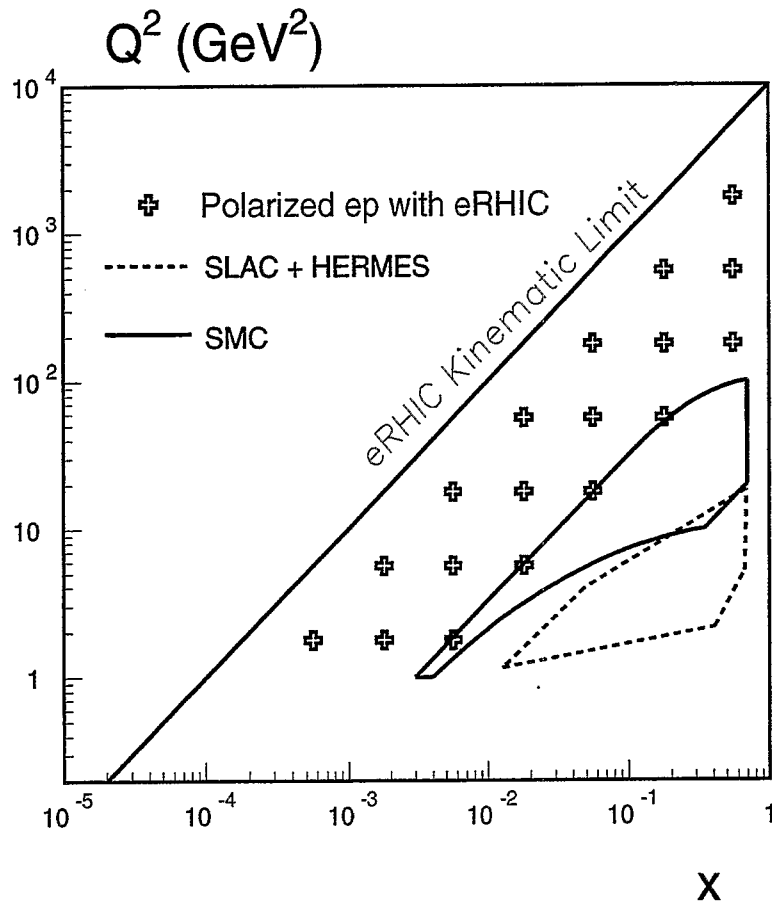
AB scheme



(PRELIMINARY)

Measurement of $g_1(x, Q^2)$ at e-RHIC

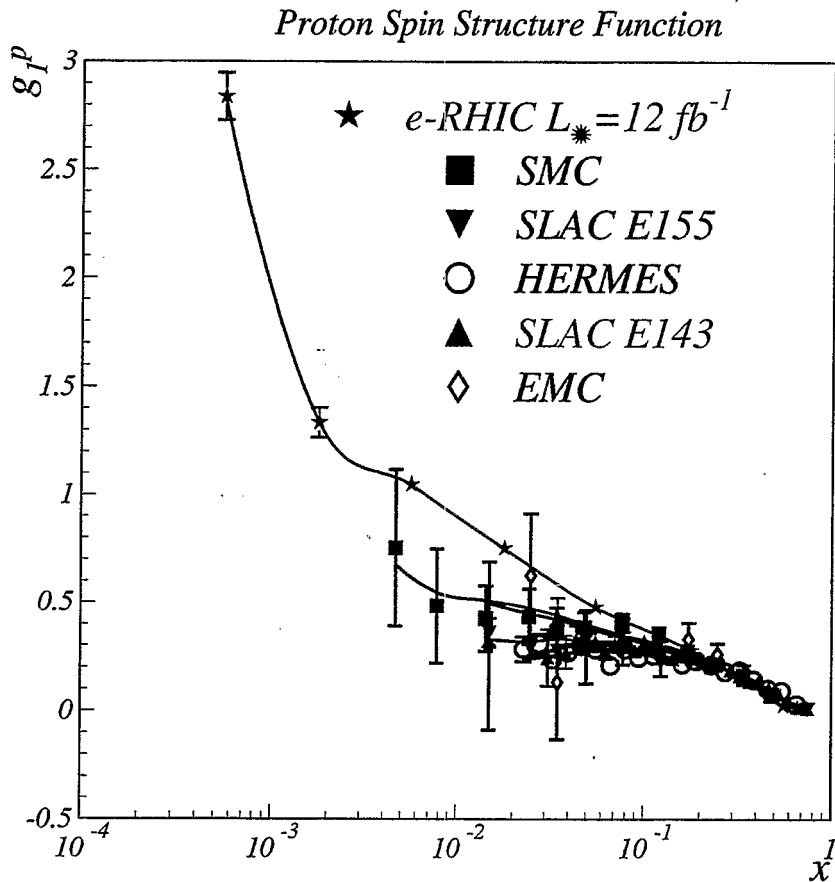
Kinematic range:



- Beam energies $E_p = 250$ GeV: $E_e = 10$ GeV provide $\sqrt{s} \sim 100$ GeV
A significant improvement compared to **fixed target** experiments.

Fit to world data and e-RHIC projections

Three years - 12.6 fb^{-1}



From QCD analysis (in NLO) at 1 GeV^2 :

$$\eta_g = \int_0^1 \Delta g(x) dx = 0.7^{+0.08}_{-0.08} \text{ (statistical)}$$

$$\eta_q = \Delta\Sigma = 0.41 \pm 0.015 \text{ (statistical)}$$

Combined analysis of g_1 and 2-jet data

A. Polarized gluon distribution Δg

From QCD analysis (in NLO) at 1 GeV²:

$$\mathcal{L} = 12.6 \text{ fb}^{-1}$$

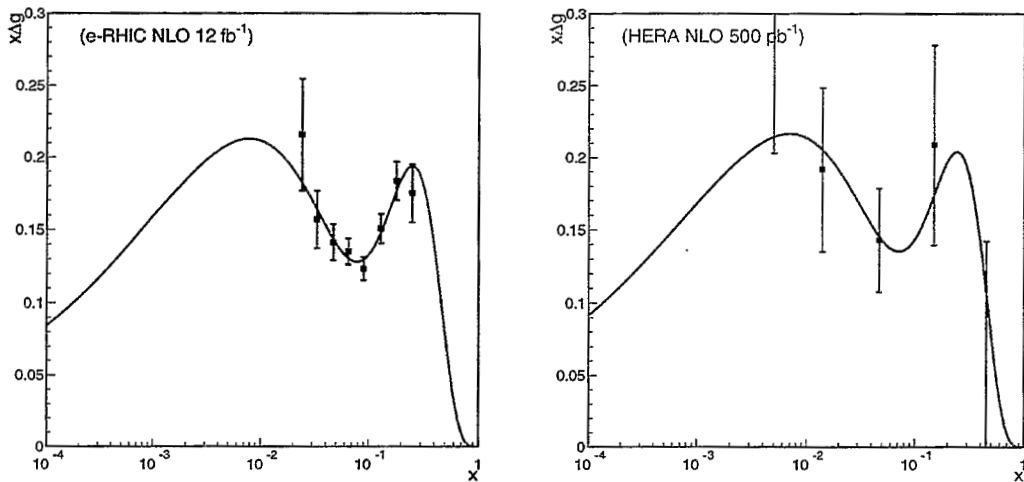
$$\eta_g = \int_0^1 \Delta g(x) dx = 0.64 \pm 0.04 \text{ (statistical)}$$

$$\eta_q = \Delta\Sigma = 0.40 \pm 0.02 \text{ (statistical)}$$

B. Sensitivity to the shape of Δg

Polarized gluon distributions

Fits compared to $\Delta g(x)$ from 2-jet asymmetries



- **Experiments in a polarized collider (e-RHIC or pol-HERA) which will include also measurements of di-jet asymmetries are expected to determine the polarized gluon distribution with about 7% accuracy as well as constrain its shape.**

Data used	$\delta(f \Delta g)$	$\delta(f \Delta q_S)$
QCD Anal. g_1 data ("D")	± 0.20	± 0.02
"D" + e-RHIC g_1^P ($420 pb^{-1}$)	± 0.15	± 0.02
"D" + e-RHIC g_1^P ($4.2 fb^{-1}$)	± 0.10	± 0.02
"D" + e-RHIC g_1^P ($12.6 fb^{-1}$)	± 0.08	± 0.016
"D" + HERA g_1^P ($500 pb^{-1}$)	± 0.15	± 0.02
"D" + HERA g_1^P + Δg -jets	± 0.10	± 0.02
"D" + e-RHIC g_1^P + Δg -jets ($12.6 fb^{-1}$)	± 0.04	± 0.014

Polarized light-antiquark flavor asymmetry

S. Kumano *

Department of Physics
Saga University
Saga 840-8502
Japan

ABSTRACT

Flavor asymmetry of polarized antiquark distributions is investigated. Because of extensive studies of \bar{u}/\bar{d} asymmetry in the last ten years, the unpolarized flavor asymmetry is now well established [1]. However, little is known for the polarized flavor asymmetry. First, it is investigated in a meson-cloud model [2]. In this model, a polarized proton splits into a meson and a baryon, then the meson interacts with the virtual photon. For polarized antiquark distributions, a contribution comes from the spin-one ρ meson. The $\Delta\bar{u} - \Delta\bar{d}$ distribution is expressed in terms of ρ momentum distributions in the proton and the polarized valence-quark distribution in ρ . We include ρNN and $\rho N\Delta$ splitting processes in the calculation by keeping $1/Q^2$ terms. As a result, we find that $\rho N\Delta$ process terms are small in comparison with the ρNN terms. The g_2^p -type contributions become significant in the medium- x region. Numerical estimates indicate that the ρ meson contributes $\Delta\bar{d}$ excess over $\Delta\bar{u}$. Second, a polarized proton-deuteron (pd) Drell-Yan process is investigated for finding the polarized flavor asymmetry [3] because the transversity flavor asymmetry cannot be found in the W production unlike the longitudinally-polarized one. Numerical estimates indicate that the pd reaction could be used for measuring the asymmetry particularly in the large x_F region.

References

- [1] S. Kumano, Phys. Rep. 303 (1998) 183.
- [2] S. Kumano and M. Miyama, Phys. Rev. D65 (2002) 034012.
- [3] S. Kumano and M. Miyama, Phys. Lett. B497 (2000) 149.

* kumanos@cc.saga-u.ac.jp, <http://hs.phys.saga-u.ac.jp>.

$\Delta\bar{u} - \Delta\bar{d}$ distribution

naive quark model

$$\rho^+(\bar{u}\bar{d}), \quad \rho^0((\bar{u}\bar{u} - \bar{d}\bar{d}) / \sqrt{2}), \quad \rho^-(\bar{u}\bar{d})$$

$$\begin{aligned} [\Delta\bar{u} - \Delta\bar{d}]_{\rho\text{NB}} &= \Delta f_{\rho^+\text{pn}} \otimes [\Delta\bar{u} - \Delta\bar{d}]_{\rho^+} \\ &+ \Delta f_{\rho^0\text{pp}} \otimes [\Delta\bar{u} - \Delta\bar{d}]_{\rho^0} \\ &+ \Delta f_{\rho^+\text{p}\Delta^0} \otimes [\Delta\bar{u} - \Delta\bar{d}]_{\rho^+} \\ &+ \Delta f_{\rho^0\text{p}\Delta^+} \otimes [\Delta\bar{u} - \Delta\bar{d}]_{\rho^0} \\ &+ \Delta f_{\rho^-\text{p}\Delta^{++}} \otimes [\Delta\bar{u} - \Delta\bar{d}]_{\rho^-} \end{aligned}$$

Charge symmetry in ρ

$$\Delta\bar{u}_{\rho^-}^{\text{val}} = \Delta\bar{d}_{\rho^+}^{\text{val}} = 2\Delta\bar{u}_{\rho^0}^{\text{val}} = 2\Delta\bar{d}_{\rho^0}^{\text{val}} = \Delta v_{\rho}$$

$$[\Delta\bar{u} - \Delta\bar{d}]_{\rho\text{NB}} = \left(-2 \Delta f_{\rho\text{NN}} + \frac{2}{3} \Delta f_{\rho\text{N}\Delta} \right) \otimes \Delta v_{\rho}$$

ρ -meson contribution to g_1

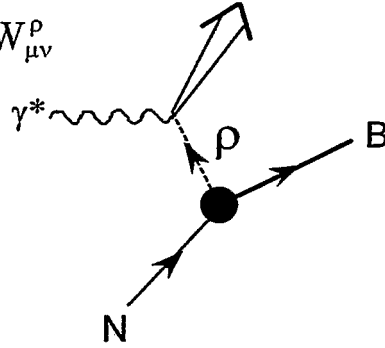
$$W_{\mu\nu} = \int \frac{d^3 p_B}{(2\pi)^3} \frac{2 m_\rho m_B}{E_B} |\Gamma_{\rho NB}|^2 W_{\mu\nu}^\rho$$

calculate $P^{\mu\nu} W_{\mu\nu}$

Longitudinal polarization

$$\left[g_1(x) - \gamma^2 g_2(x) \right]_{\rho NB}$$

$$= \int_x^1 \frac{dy}{y} \left[\Delta f_{\rho NB}^{1L}(y) g_1^\rho\left(\frac{x}{y}\right) - \Delta f_{\rho NB}^{2L}(y) g_2^\rho\left(\frac{x}{y}\right) \right]$$



Transverse polarization

$$\gamma^2 \left[g_1(x) + g_2(x) \right]_{\rho NB}$$

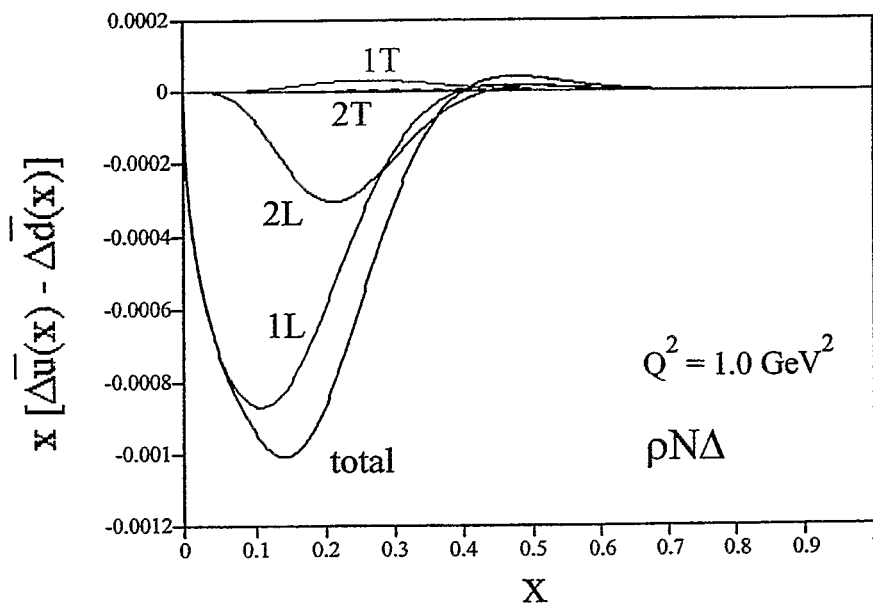
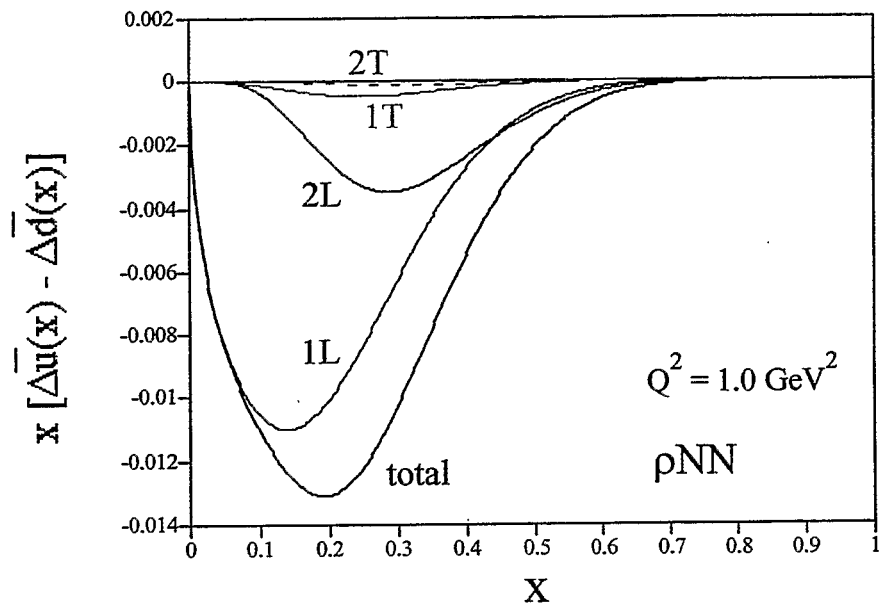
$$= \int_x^1 \frac{dy}{y} \left[\Delta f_{\rho NB}^{1T}(y) g_1^\rho\left(\frac{x}{y}\right) - \Delta f_{\rho NB}^{2T}(y) g_2^\rho\left(\frac{x}{y}\right) \right]$$

$$\left[g_1(x) \right]_{\rho NB}$$



$$= \frac{1}{1 + \gamma^2} \int_x^1 \frac{dy}{y} \left[\Delta f_{\rho NB}^{1L}(y) g_1^\rho\left(\frac{x}{y}\right) - \Delta f_{\rho NB}^{2L}(y) g_2^\rho\left(\frac{x}{y}\right) \right. \\ \left. + \Delta f_{\rho NB}^{1T}(y) g_1^\rho\left(\frac{x}{y}\right) - \Delta f_{\rho NB}^{2T}(y) g_2^\rho\left(\frac{x}{y}\right) \right]$$

$\Delta\bar{u} - \Delta\bar{d}$ distributions



Comments on previous works

(1) Fries - Schäfer (FS, 1998)

(2) Cao - Signal (CS, 2001)

The situation was confusing in the sense that CS pointed out two major mistakes in the FS calculations.

- $f_{\rho NN} g_{\rho NN}$ should be replaced by $-f_{\rho NN} g_{\rho NN}$ in $\Delta f(y)$
- $\rho N\Delta$ results are wrong

As far as we checked, the FS results are right.

(except for a minor misprint)

→ consistency with the unpolarized distributions

by Melnitchouk and Thomas (1993)

→ consistency with Machleidt (1986)

→ detailed studies of helicity amplitudes

Numerical analysis

$$r_{\bar{q}} \equiv \frac{\Delta_{(T)}\bar{u}}{\Delta_{(T)}\bar{d}} = 0.7, 1.0, \text{ or } 1.3 \quad \text{at } Q^2 = 1 \text{ GeV}^2$$

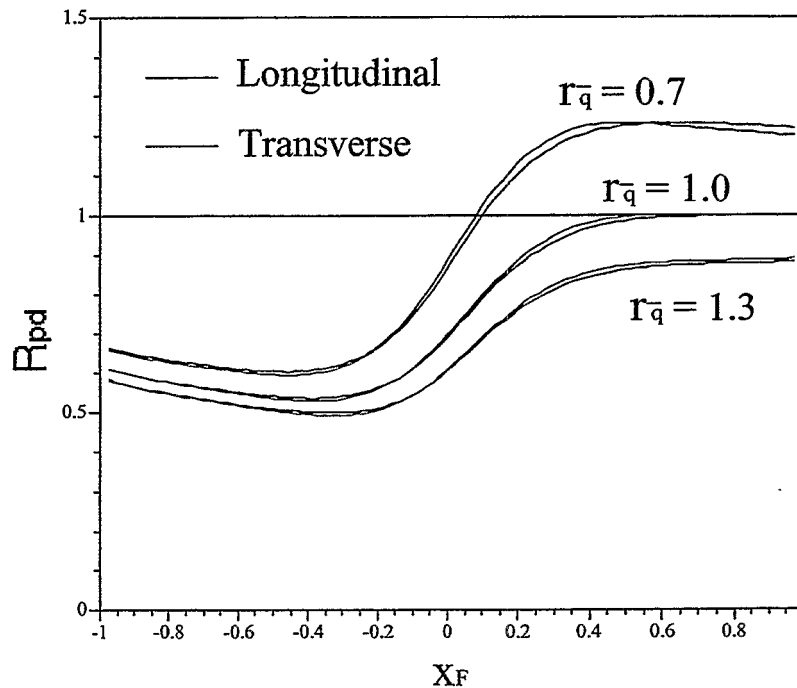
$$M_{\mu\mu} = 5 \text{ GeV}, \quad \sqrt{s} = 50 \text{ GeV}$$

parton distributions: LSS-99 at $Q^2 = 1 \text{ GeV}^2$

$$Q^2 = 1 \text{ GeV}^2 \quad \text{evolution} \Rightarrow \quad Q^2 = M_{\mu\mu}^2$$

$$\Rightarrow \quad R_{pd} \equiv \frac{\Delta_{(T)}\sigma^{pd}}{2 \Delta_{(T)}\sigma^{pd}}$$

assume $\Delta_{Tq}(x) = \Delta q(x)$ at $Q^2 = 1 \text{ GeV}^2$



Nucleon matrix elements with domain wall fermions

Konstantinos Orginos
RBC collaboration*
RIKEN-BNL Research Center

September 10, 2002

The structure of the nucleon is one of the fundamental problems that lattice QCD can address. In the last few years, substantial efforts have been made by several groups [1, 2, 3] in calculating the non-perturbative matrix elements relevant to nucleon structure. Up to now only Wilson fermions, improved and unimproved, have been used in both the quenched approximation and in full QCD. In this report we examine the feasibility of studying nucleon matrix elements with domain wall fermions in the quenched approximation. Domain wall fermions have only $\mathcal{O}(a^2)$ lattice artifacts, non-perturbative renormalization works very well, and have no problem with exceptional configurations [4, 5]. Furthermore, the chiral symmetry they preserve on the lattice eliminates mixings with lower dimensional operators, rendering the renormalization of certain matrix elements significantly simpler. For the above reasons, a study of the nucleon structure with domain wall fermions is definitely important.

We study the nucleon matrix elements relevant to the leading twist contributions to the moments of the nucleon structure functions. The leading twist matrix elements are:

$$\begin{aligned} \frac{1}{2} \sum_s \langle p, s | \mathcal{O}_{\{\mu_1 \mu_2 \dots \mu_n\}}^q | p, s \rangle &= 2 \langle x^{n-1} \rangle_q(\mu) \times [p_{\mu_1} p_{\mu_2} \dots p_{\mu_n} + \dots - tr] \\ - \langle p, s | \mathcal{O}_{\{\sigma \mu_1 \mu_2 \dots \mu_n\}}^{5q} | p, s \rangle &= \frac{2}{n+1} \langle x^n \rangle_{\Delta q}(\mu) \times [s_\sigma p_{\mu_1} p_{\mu_2} \dots p_{\mu_n} + \dots - tr] \\ \langle p, s | \mathcal{O}_{\{\sigma \{\mu_1\} \mu_2 \dots \mu_n\}}^{[5]q} | p, s \rangle &= \frac{1}{n+1} d_n^q(\mu) \times [(s_\sigma p_{\mu_1} - s_{\mu_1} p_\sigma) p_{\mu_2} \dots p_{\mu_n} + \dots - tr] \\ \langle p, s | \mathcal{O}_{\rho\nu \{\mu_1 \mu_2 \dots \mu_n\}}^{\sigma q} | p, s \rangle &= \frac{2}{m_N} \langle x^n \rangle_{\delta q}(\mu) \times [(s_\rho p_\nu - s_\nu p_\rho) p_{\mu_1} p_{\mu_2} \dots p_{\mu_n} + \dots - tr] \end{aligned}$$

where p_μ and s_μ are the nucleon momentum and spin vectors, m_N the nucleon mass, and

$$\begin{aligned} \mathcal{O}_{\mu_1 \mu_2 \dots \mu_n}^q &= \left(\frac{i}{2}\right)^{n-1} \bar{q} \gamma_{\mu_1} \overleftrightarrow{D}_{\mu_2} \dots \overleftrightarrow{D}_{\mu_n} q - trace \\ \mathcal{O}_{\sigma \mu_1 \mu_2 \dots \mu_n}^{5q} &= \left(\frac{i}{2}\right)^n \bar{q} \gamma_\sigma \gamma_5 \overleftrightarrow{D}_{\mu_2} \dots \overleftrightarrow{D}_{\mu_n} q - trace \\ \mathcal{O}_{\rho\nu \mu_1 \mu_2 \dots \mu_n}^{\sigma q} &= \left(\frac{i}{2}\right)^n \bar{q} \gamma_5 \sigma_{\rho\nu} \overleftrightarrow{D}_{\mu_1} \dots \overleftrightarrow{D}_{\mu_n} q - trace \end{aligned}$$

{ } implies symmetrization and [] implies anti-symmetrization. For the conventions used see [3].

In conclusion, we have started the computation of moments of nucleon structure functions with domain wall fermions. Our current results are unrenormalized and restricted to those matrix elements that can be computed with zero momentum nucleon states. Yet we already have hints of a couple of potentially interesting results. First we have an indication of the possible onset of chiral log behavior for $\langle x \rangle_{u-d}$. Also it is very encouraging, although expected, to see the lack of power divergent contributions for d_1 . Our project is ongoing. We hope to have more statistics and non-perturbative renormalization of the presented matrix elements in the near future.

References

- [1] M. Gockeler *et al.*, Phys. Rev. **D63**, 074506 (2001).
- [2] M. Gockeler *et al.*, Phys. Rev. **D53**, 2317 (1996).
- [3] D. Dolgov *et al.*, (2002).
- [4] T. Blum *et al.*, hep-lat/0007038 (2000).
- [5] T. Blum *et al.*, Phys. Rev. **D66**, 014504 (2002).

*The current members of the RBC collaboration are: Y. Aoki, T. Blum, N. Christ, C. Dawson, T. Izubuchi, L. Levkova, X. Liao, G. Liu, R. Mawhinney, Y. Nemoto, J. Noaki, S. Ohta, K. Orginos, S. Prelovsek, S. Sasaki and A. Soni. We thank RIKEN, BNL and the U.S. DOE for providing the facilities essential for the completion of this work.

RBC Simulation

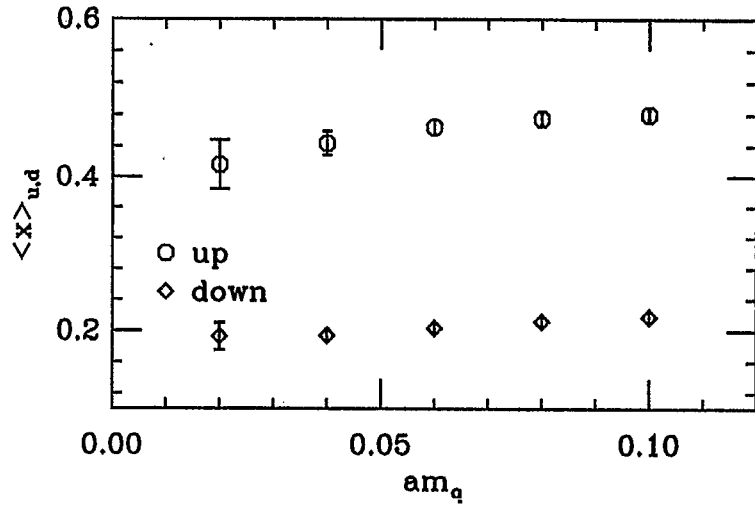
- Gauge Action: DBW2

$$S_g = \frac{\beta}{3} \text{Re Tr} \left[(1 - 8c_1) \langle 1 - \text{[square]} \rangle + 2c_1 \langle 1 - \text{[rectangle]} \rangle \right]$$

With $c_1 = -1.4067$ computed by non-perturbative RG blocking.

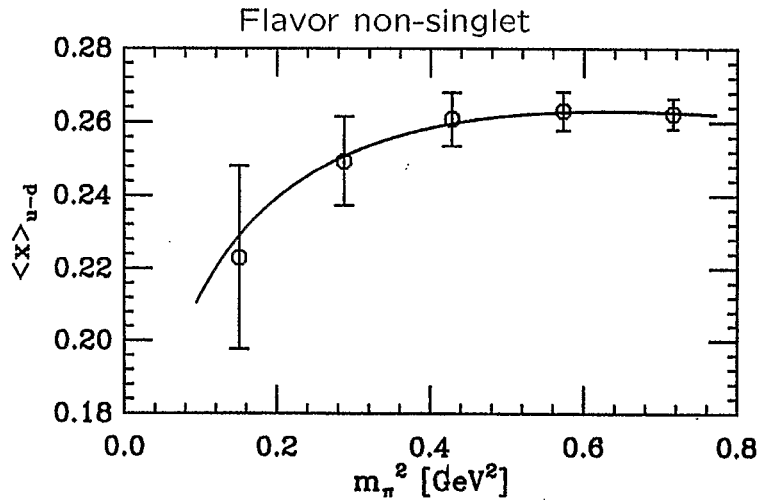
[Takaishi Phys.Rev. D54 (1996)]

- $\beta = 0.870$ or $a^{-1} = 1.3\text{GeV}$, Volume: $16^3 \times 32 \sim 2.4^3 fm^3$ box.
- Fermion Action: Domain wall fermions $L_s = 16 \rightarrow m_{res} \sim .7\text{MeV}$
- Statistics: 100 Lattices QCDSP 300Gflops for 3 weeks
- Status: PRELIMINARY!



Note:

- Unrenormalized
- Curvature in the chiral limit



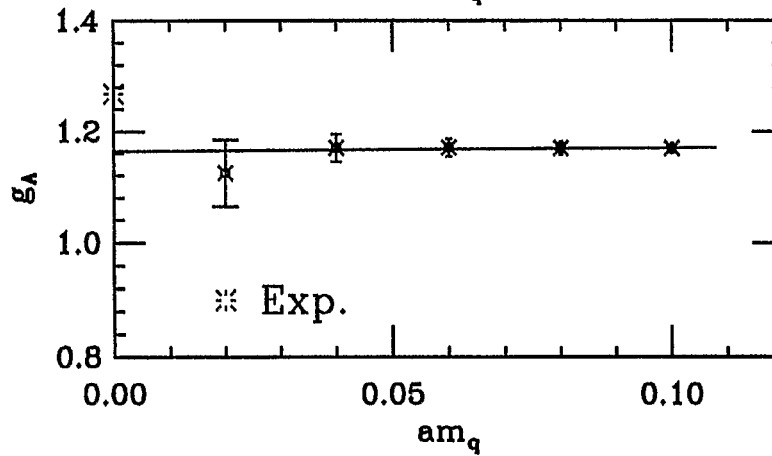
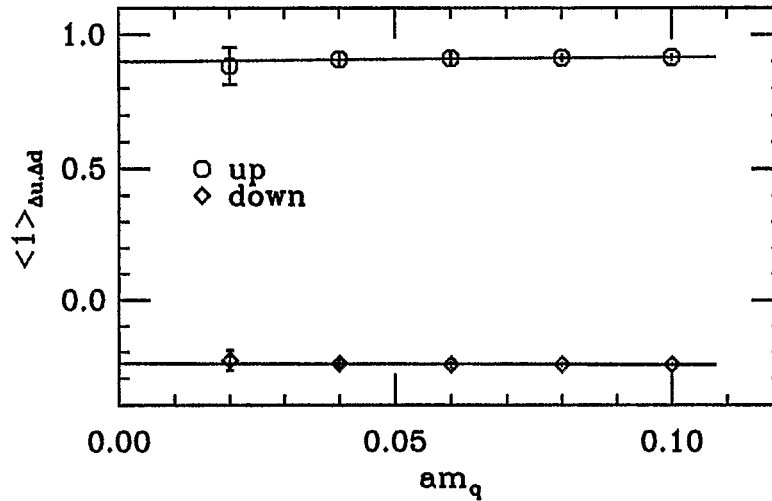
$$\langle x \rangle_{u-d} \sim a_1 \left[1 - \frac{(3g_A^2 + 1)m_\pi^2}{(4\pi f_\pi)^2} \ln\left(\frac{m_\pi^2}{m_\pi^2 + \mu^2}\right) \right] + b_1 m_\pi^2.$$

Where $g_A = 1.14$, $f_\pi a = .1$, $\mu = 550 MeV$

Valid for full QCD

[Detmold et.al. Phys.Rev.D87 2001]

plateaus



Axial Charge

- Renormalization:

$$\langle A^{cons} \bar{q} \gamma_5 q \rangle = Z_A \langle A^{loc} \bar{q} \gamma_5 q \rangle$$

[Y. Aoki LAT01]

$$Z_A = 0.77759(45)$$

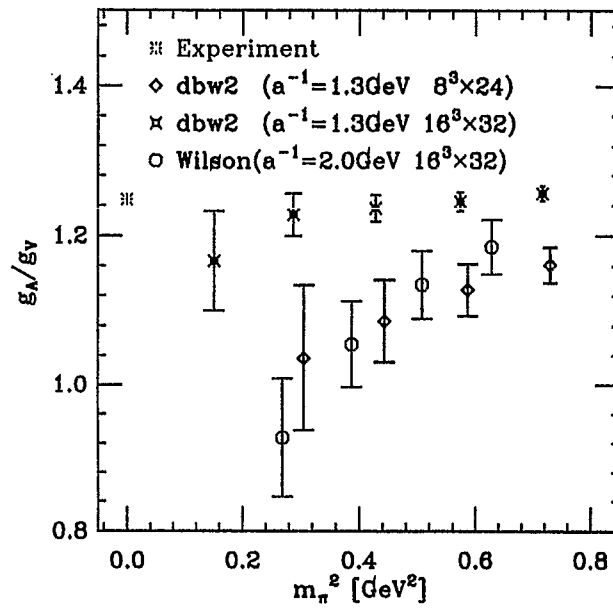
- Chiral limit (Linear fit):

$$g_A = 1.16(3)$$

See S. Ohta's LAT02 poster.

plateaus

Finite volume effect for g_A



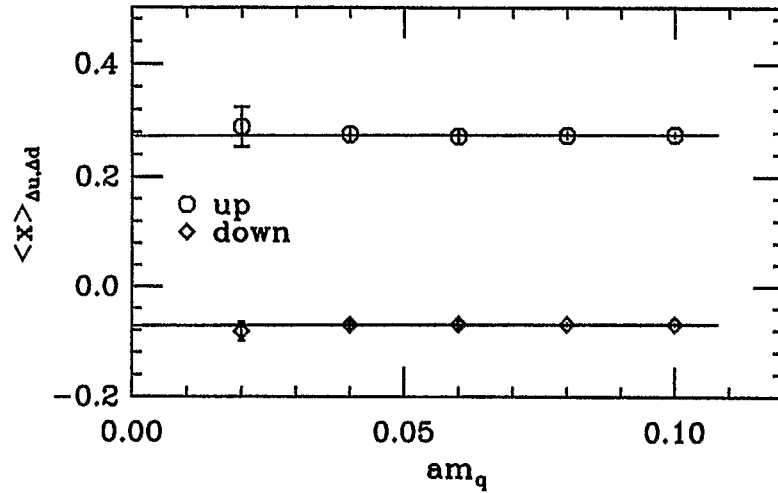
Previous RBC study:

[Blum, Ohta, Sasaki] 1.6fm box

New RBC study:

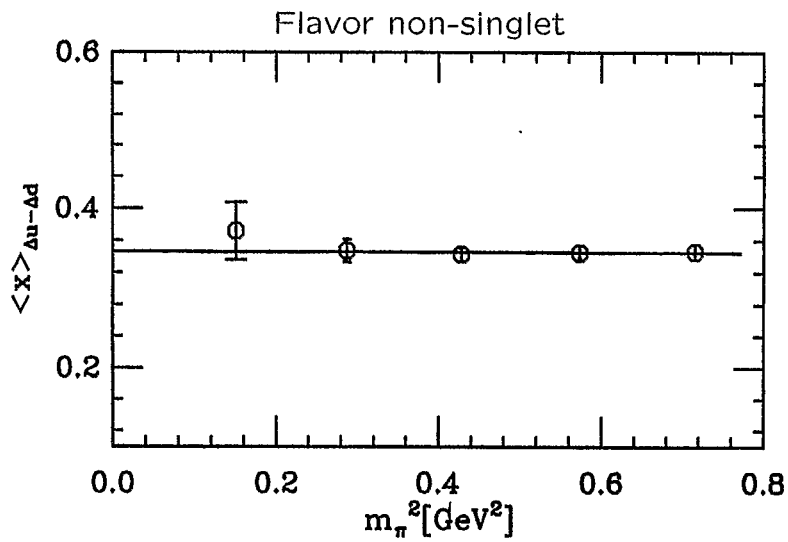
2.4fm and 1.2fm box

Clear finite volume effect

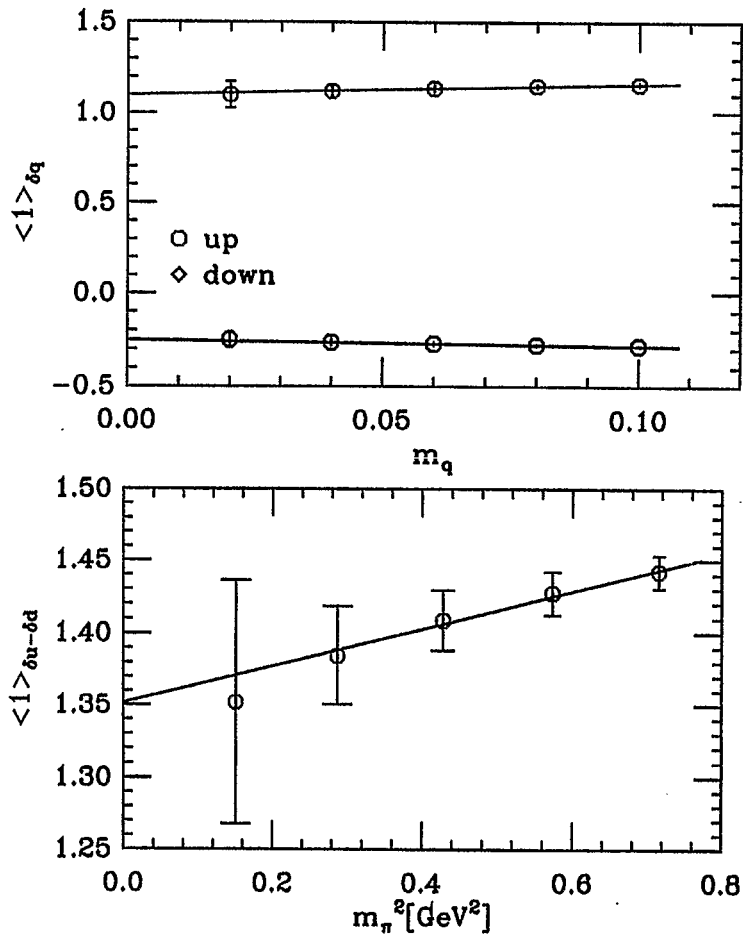


Note:

- Unrenormalized
- No curvature in the chiral limit
- Light mass needs more statistics



plateaus



Note:

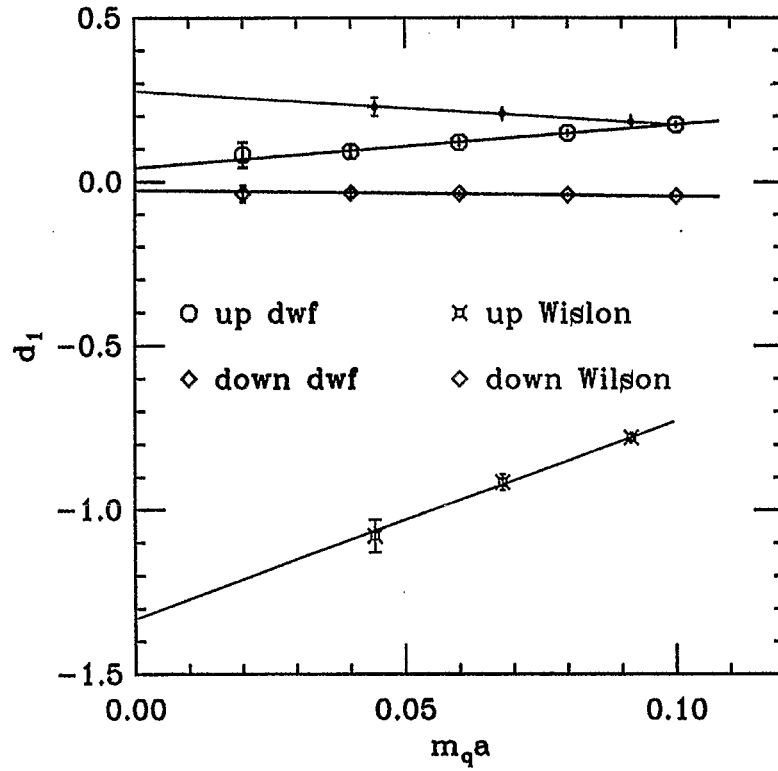
- Unrenormalized

NPR has been done

Result coming soon

[C. Dawson LAT02]

plateaus



Note:

- Unrenormalized
- Disagreement with the Wilson results
- Power divergent mixing
- [LHPC-SESAM: hep-lat/0201021]
- Small at chiral limit

plateaus

Single spin asymmetries in pp and ep collisions

Yuji Koike

Department of Physics, Niigata University, Ikarashi, Niigata 950-2181, Japan

In this talk, I will discuss the single transverse-spin asymmetry in the pion production, $\{e, p\} + p^\uparrow \rightarrow \pi(\ell) + X$, and the Λ hyperon polarization, $\{e, p\} + p \rightarrow \Lambda^\uparrow(\ell) + X$, in the framework of the collinear factorization. These asymmetries occur as the twist-3 effect which represent particular quark-gluon correlations in the hadrons.

We first classify the complete set of the twist-3 distribution and fragmentation functions. Then we summarize how they appear in the analysis, and present cross section formula. By introducing a model for the twist-3 functions, we discuss qualitative features of the asymmetries. The model is constructed in order to reproduce approximately the existing data of the asymmetries in pp collisions and then applied to ep collisions. Finally a comparison with another approach based on T -odd, k_\perp distribution and fragmentation functions is briefly discussed.

At large x_F .

★ PP collisions: valence-quark soft-gluon approx.

$p \uparrow p \rightarrow \pi X$ keep only $\frac{d}{dx} G_F(x)$ etc.

$$\Rightarrow \text{(i)} \quad \frac{d}{dx} G_F(x) \otimes \left\{ \begin{array}{l} f_1(x') \\ G(x') \end{array} \right\} \otimes \hat{f}_1(z) \otimes \hat{\sigma}_1 \quad (\text{Qiu \& Stermann '99})$$

$$\text{(ii)} \quad h_1(x) \otimes \frac{d}{dx'} E_F(x', x') \otimes \hat{f}_1(z) \otimes \hat{\sigma}_2 \quad (\text{Kanazawa \& Y.K. P.L. B490})$$

\uparrow chiral-odd $\quad \quad \quad \uparrow$ This is negligible!

$$\Rightarrow \text{(iii)} \quad h_1(x) \otimes \left\{ \begin{array}{l} f_1(x') \\ G(x') \end{array} \right\} \otimes \frac{d}{dz} \hat{E}_F(z, z) \otimes \hat{\sigma}_3 \quad (\text{This work})$$

$PP \rightarrow \Lambda^+ X$ $p \quad p \quad \Lambda^+$

$$\text{(i)} \quad \frac{d}{dx} E_F(x, x) \otimes \left\{ \begin{array}{l} f_1(x') \\ G(x') \end{array} \right\} \otimes \hat{h}_1(z) \otimes \hat{\sigma}_1' \quad (\text{Kanazawa \& Y.K. P.R. D64 (2001)})$$

$$\text{(ii)} \quad f_1(x) \otimes \left\{ \begin{array}{l} f_1(x') \\ G(x') \end{array} \right\} \otimes \frac{d}{dz} \hat{G}_F(z, z) \otimes \hat{\sigma}_2' \quad (\text{This work})$$

Parametrization of twist-3 functions (soft-gluon component)

$$N \left\{ \begin{array}{l} \cdot G_F^a(x, x) \equiv K_a f_1^a(x) \quad (\text{Qiu \& Stermann}) \\ \quad K_u = 0.07, K_d = -0.07 \quad \cdot f_1: \text{GRV, LC} \\ \cdot E_F^a(x, x) \equiv K'_a h_1^a(x) \quad \cdot h_1 \equiv g_1: \text{GRSV} \\ \quad K'_u = 0.07, K'_d = -0.07 \end{array} \right.$$

↙ same Dirac structure

$$\Lambda : \hat{G}_F^a(z, z) \equiv \hat{K}_a \hat{f}_1^a(z) \quad \hat{f}_1 \text{ for } \Lambda : \text{de Florian et al. ('98)}$$

$$\hat{K}_u = 0.07, \hat{K}_d = -0.07$$

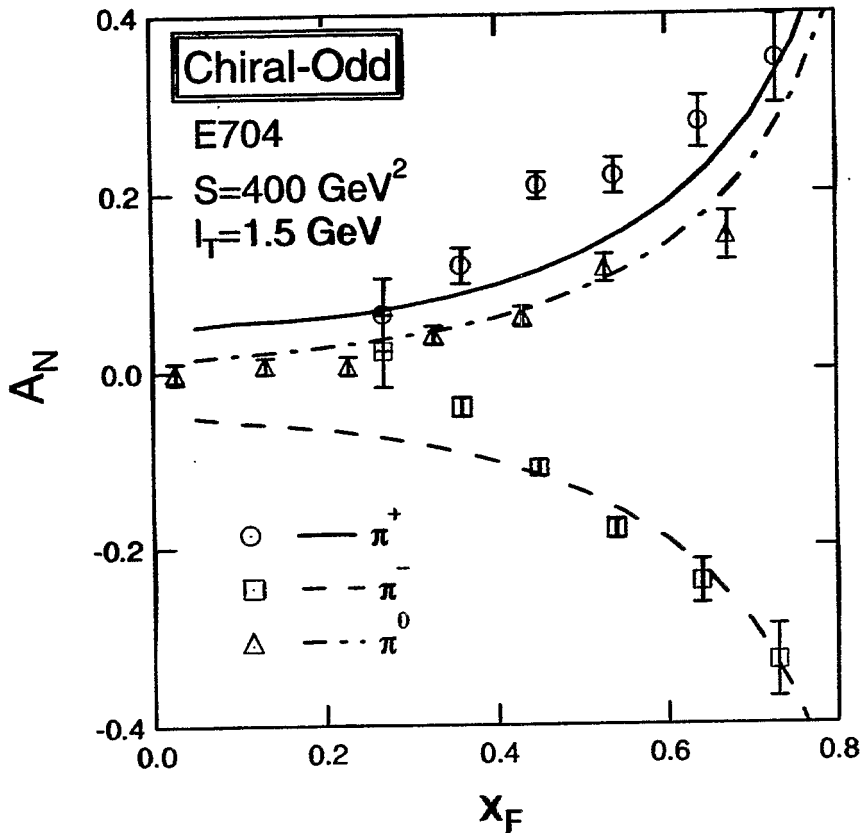
$$\pi : \hat{E}_F^a(z, z) \equiv \hat{K}'_a \hat{f}_1^a(z) \quad \hat{f}_1 \text{ for } \pi : \text{BKK/95}$$

$$\hat{K}'_u = -0.11 \quad \hat{K}'_d = -0.19 \quad \text{to fit } A_N$$

(π has no \hat{h}_1 !)

$$h_1(x) \otimes \begin{Bmatrix} f_1(x') \\ G(x') \end{Bmatrix} \otimes \frac{d}{dz} \hat{E}_F(z, z) \otimes \hat{\sigma}$$

↑
transversity
($\equiv g_1(x)$)

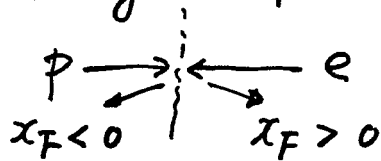


Qualitatively the same behavior as

$$\frac{d}{dx} G_F(x) \otimes \begin{Bmatrix} f_1(x) \\ G(x) \end{Bmatrix} \otimes \hat{f}_1(z) \otimes \hat{\sigma}$$

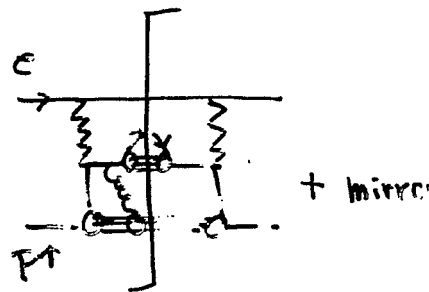
★ ep collisions

Keep all soft-gluon-poles. Valid at $-1 < x_F < 1$

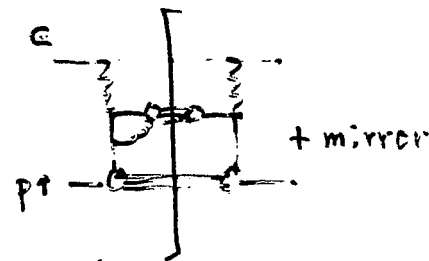


ep⁺ → πX

$$(i) \left\{ \begin{array}{l} G_F(x, x) \\ \frac{d}{dx} G_F(x, x) \end{array} \right\} \otimes \hat{f}_1(z) \otimes \hat{\sigma}_1$$



$$(ii) h_1(x) \otimes \left\{ \begin{array}{l} \hat{E}_F(z, z) \\ \frac{d}{dz} \hat{E}_F(z, z) \end{array} \right\} \otimes \hat{\sigma}_2$$



$$\text{large } x_F \sim \frac{K\pi M x_T}{(-T)} \frac{1}{1-x_F} \sin \varphi \sim \frac{K\pi M}{x_T} \frac{1}{1-x_F} \sin \varphi$$

ep → Λ⁺X

$$(i) \left\{ \begin{array}{l} E_F(x, x) \\ \frac{d}{dx} E_F(x, x) \end{array} \right\} \otimes \hat{h}_1(z) \otimes \hat{\sigma}_1'$$

$$(ii) f_1(x) \otimes \left\{ \begin{array}{l} \hat{G}_F(z, z) \\ \frac{d}{dz} \hat{G}_F(z, z) \end{array} \right\} \otimes \hat{\sigma}_2'$$

Summary

(1) Single spin asymmetries

$$p^\uparrow p \rightarrow \pi(P_T)X, \quad ep^\uparrow \rightarrow \pi(P_T)X$$

$$pp \rightarrow \Lambda^\uparrow(P_T)X, \quad ep \rightarrow \Lambda^\uparrow(P_T)X$$

are studied within QCD factorization theorem.

All twist-3 contributions are identified and the formulas are given.

(2) PP case: Valence-quark soft-gluon approx. keeping only derivatives of twist-3 functions is adopted.

$$\text{A model } \Gamma(x) \sim (\text{twist-2}) \sim (1-x)^\beta$$

$\hat{F}(z) \sim (\quad) \sim (1-z)^{\beta'}$ is used to see qualitative behavior of asymmetries.

2-1) $p^\uparrow p \rightarrow \pi X$: $h_1(x) \otimes \frac{d}{dz} \hat{E}_F(z)$ can be an equally good source as $\frac{d}{dz} G_T(x)$ studied by Qiu & Sterman.

2-2) $pp \rightarrow \Lambda^\uparrow X$: two contributions give rising P_Λ at large x_F .

(3) ep case: The formula include all the soft-gluon pole contributions. A model for $\Gamma(x)$ and $\hat{F}(z)$ determined in PP case is tested.

3-1) A_N^{ep} and $P_\Lambda^{ep} \approx 0$ at $x_F < 0$, and steep rise at $x_F \geq 0.3$.

3-2) Signs of A_N^{ep} and P_Λ^{ep} are opposite to PP case, and their magnitudes are larger due to color

Extraction Of Polarized Parton Distributions From Semi-inclusive HERMES Data

Patricia Liebing, DESY-Zeuthen *On behalf of the HERMES Collaboration*

August 20, 2002

HERMES collected large statistics of inclusive and semi-inclusive DIS on polarized hydrogen and deuterium targets. From the inclusive data the polarized structure functions g_1^p and g_1^d were extracted with high precision. The measurements were extended down to $x_{Bj} \simeq 0.004$. Good consistency between the preliminary HERMES data on g_1/F_1 with an earlier measurement of SMC [1] is observed despite the fact that the average Q^2 of SMC is about a factor of ten larger than that of HERMES.

The semi-inclusive asymmetries are based on 1.8(6.5) million DIS events taken on hydrogen (deuterium) in the region of $Q^2 > 1 \text{ GeV}^2$ and $W^2 > 10 \text{ GeV}^2$. For the hydrogen data, pions could be identified using the information from a threshold Cherenkov counter. For the deuterium data the RICH detector provided the possibility to identify pions and kaons. The semi-inclusive and the inclusive asymmetries from both targets in the same kinematic region were used for the flavor decomposition of the individual quark polarizations. The purity formalism was applied, in which in LO QCD the semi-inclusive asymmetry can be written as

$$A_1^h(x, Q^2) \simeq \frac{1 + R(x, Q^2)}{1 + \gamma^2} \sum_q P_q^h(x, Q^2) \frac{\Delta q(x, Q^2)}{q(x, Q^2)}, \quad (1)$$

where $R = \frac{\sigma_L}{\sigma_T}$, $\gamma = \sqrt{Q^2/\nu^2}$ and

$$P_q^h(x, Q^2) = \frac{e_q^2 q(x_i, Q_i^2) \int_{z_{min}}^{z_{max}} dz D_q^h(z, Q_i^2)}{\sum_q e_q^2 q(x_i, Q_i^2) \int_{z_{min}}^{z_{max}} dz D_q^h(z, Q_i^2)} \quad (2)$$

is the purity for a quark of type q and a hadron h . $q(x, Q^2)$ is the unpolarized PDF. JETSET with the LUND string model was used to obtain the fragmentation functions $D_q^h(z, Q_i^2)$ which were integrated over z from $z_{min} = 0.2$ to $z_{max} = 0.8$ in the HERMES acceptance. The LUND fragmentation parameters were tuned to fit hadron multiplicities measured at HERMES. They were varied for an estimation of the associated systematic uncertainties. Integrating over the Q^2 -range in each x_{Bj} -bin one can obtain the quark polarizations by solving

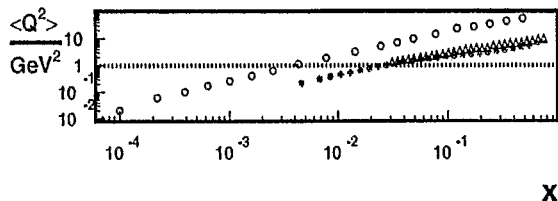
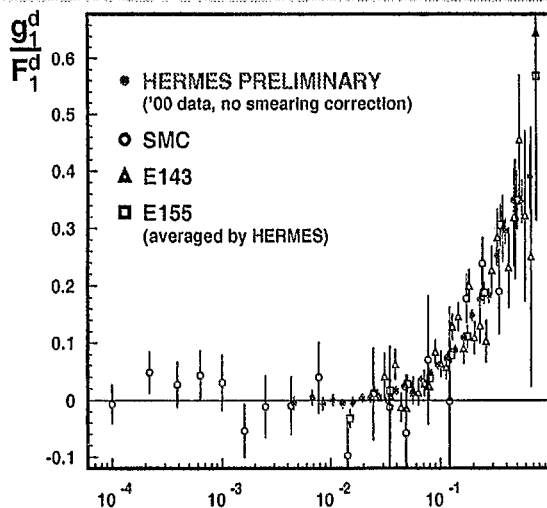
$$\vec{A}(x) = P(x)\vec{Q}(x) \quad (3)$$

where $\vec{A}(x)$ is the vector of input asymmetries, $P(x)$ is the purity matrix and $\vec{Q}(x) = \left(\frac{\Delta u}{u}, \frac{\Delta d}{d}, \frac{\Delta \bar{u}}{\bar{u}}, \frac{\Delta \bar{d}}{\bar{d}}, \frac{\Delta s}{s} = \frac{\Delta \bar{s}}{\bar{s}} \right)$ is the solution vector. Except for $\Delta s/s = \Delta \bar{s}/\bar{s}$ there is no symmetry assumption on the sea flavors. The results on $\frac{\Delta u}{u}$ and $\frac{\Delta d}{d}$ are in good agreement with [2]. The strange sea polarization is slightly positive. The HERMES data on $\Delta \bar{u} - \Delta \bar{d}$ are consistent with zero favoring an unbroken $SU(2)_f$ symmetry.

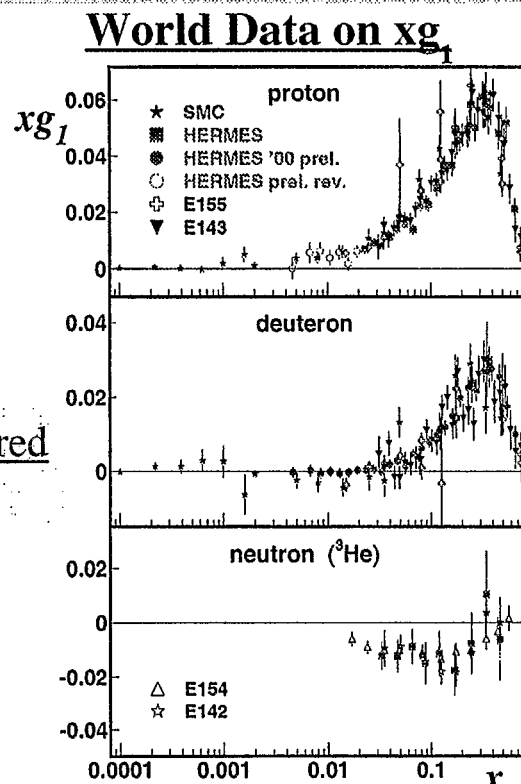
[1] D. Adeva et al., Phys. Rev. D 58, 112001 (1998)

[2] K. Ackerstaff et al., Phys. Lett. B 464, 123 (1999)

INCLUSIVE ASYMMETRIES AND G_1



All Data at measured Q^2



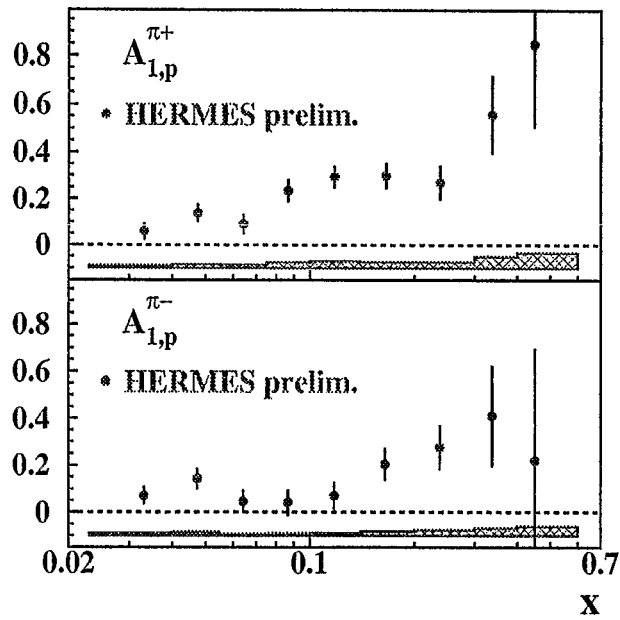
No significant Q^2 -dependence of g_1/F_1 observed ...

P. Liang
HERMES DESY

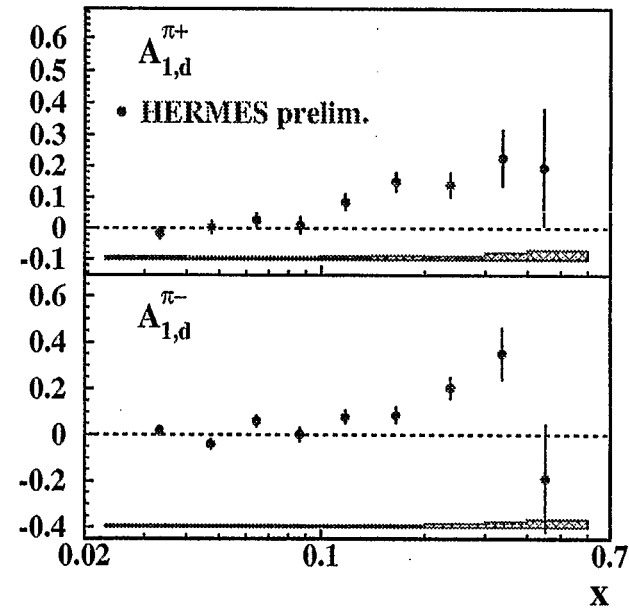
... but small Q^2 -dependence of g_1 visible

THE SEMI-INCLUSIVE ASYMMETRIES

Pions (Proton)



Pions (Deuteron)



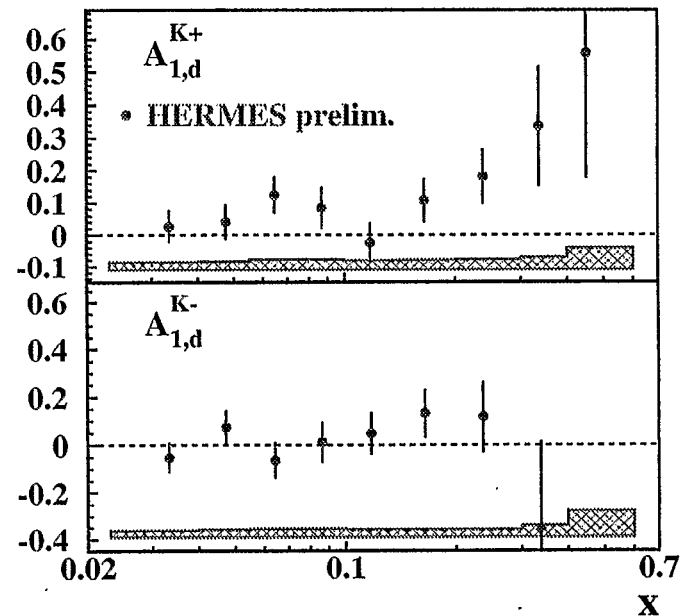
$4 < p_{\pi} < 13.8 \text{ GeV}$

THE SEMI-INCLUSIVE ASYMMETRIES

Kaons(Deuteron)

First measurement of semiinclusive Kaon Asymmetries !

- K^+ -Asymmetry positive
→ dominated by u-quark?
- K^- -Asymmetry ≈ 0
→ K^- = sea-object!



$4 < p_K < 13.8 \text{ GeV}$

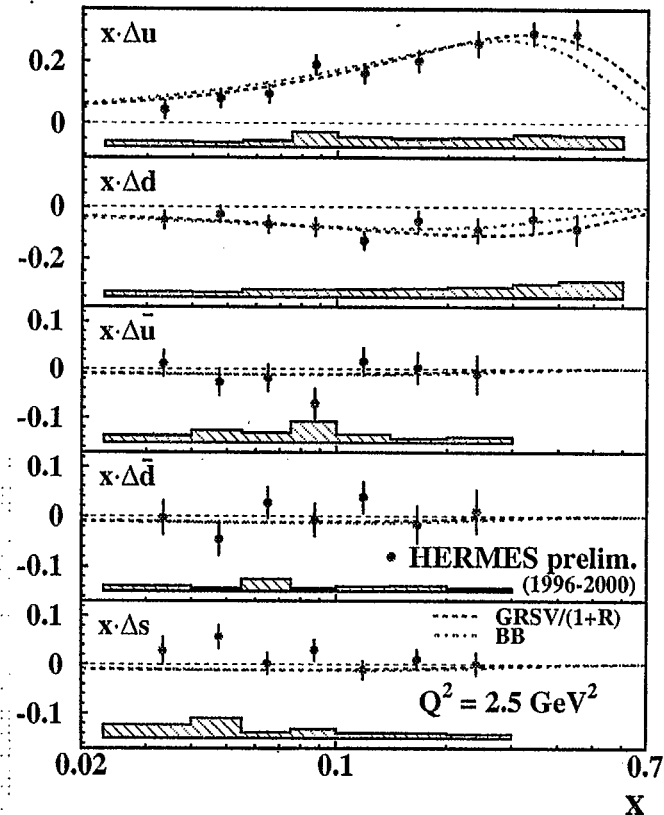
POLARIZED QUARK DISTRIBUTIONS

x-weighted polarized Quark Densities

P. Liebing
HERMES DESY

$$\Delta q(x_i, Q^2 = 2.5 \text{ GeV}^2) = \underbrace{\frac{\Delta q(x_i, Q_i^2)}{q(x_i, Q_i^2)}}_{\text{HERMES data}} \cdot \underbrace{q(x_i, Q^2 = 2.5 \text{ GeV}^2)}_{\text{CTEQ5LO}}$$

- Theoretical curves from
 - GRSV (Phys. Rev. D53 (1996) 4775, 'standard' scenario, leading order)
 - Blümlein-Böttcher (hep-ph/0203155, leading order – Scenario 1)
- No negative strange sea!!



A?-SYMMETRY OF THE LIGHT POLARIZED SEA

$$\Delta\bar{u} - \Delta\bar{d}$$

P. Liebing


- A variety of models for SU(3)-breaking

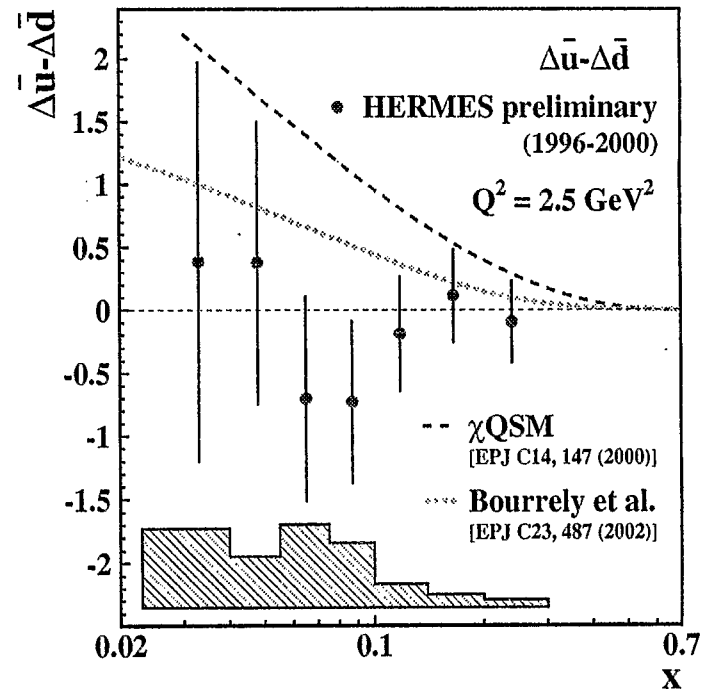
$$\Delta\bar{u} \neq \Delta\bar{d} \neq \Delta s$$

exists, e.g.:

- Chiral Quark Soliton model
 (Dressler et. al., EPJC14(2000) 147)
- Statistical model
 (Bourrely et al., EPJC23(2002)479)

- Data show no significant breaking of the light sea symmetry

→ χ QSM model not favoured



Thoughts on Measuring Δs in Semi-Inclusive DIS

E.R. Kinney

University of Colorado, Boulder, CO 80309-0390, USA

August 23, 2002

Precise determination of the quark spin and flavor structure of the nucleon has been one of the central goals in the study of quark-gluon dynamics. In particular, the contribution of the strange quarks to the nucleon spin has been sought in order to test the hypothesis that the small total contribution of quark spins to the total spin of the nucleon implies a relatively large and negative strange sea contribution.

While the spin structure is becoming better determined in the range of intermediate Bjorken x where valence quarks predominate, there is still large uncertainty in the structure of the virtual sea at low x as well as in the valence region at high x . Within the widely used common assumption of $\Delta s = \Delta \bar{s}$, only a very small strange sea polarization is found. Considerable effort will be required to determine this quantity with precision over a broad range in Bjorken x . Recent projections for the statistical accuracies of experimental results from HERMES[1], COMPASS[2] and the 5 GeV on 50 GeV EIC design[3] were presented, all of which use the technique of flavor tagging in semi-inclusive deep inelastic scattering. Already, the HERMES measurements have statistical uncertainties comparable to the systematic uncertainties which result from the uncertainties in the unpolarized strange quark distribution, the fragmentation process, and the effects of higher order QCD in the analysis of the semi-inclusive asymmetries.

Programs of measurements using parity-violating electron scattering and elastic neutrino scattering are also underway; first results from the former also are consistent with a very small strange contribution to the nucleon spin. Plans are also underway at RHIC to determine the spin components. In the far future, a neutrino factory could provide an ideal tool for these studies.

It seems possible that within 5 to 10 years, before the EIC program will start, we will know this particular quantity as a function of x to about 20-30%, although it should be kept in mind that we may get a big surprise and

find the assumption of equal strange and anti-strange distributions is false. In that case, we will still have a lot to do to get to the 20-30% level. To progress further using semi-inclusive DIS it will be necessary to find ways to decrease the systematic uncertainties of the technique; this implies more precise determination of the strange quark content and better understanding of the fragmentation to allow more complicated but more efficient hadron tagging. The theoretical community has already been at work to understand the extension of the technique to higher orders.

I think it is appropriate at this time to step back and ask ourselves what goals we have in making these precise measurements before undertaking the very large effort to make them. In the spirit of this workshop, I then ask the question of whether we can expect in 10 years to have calculations of the nucleon structure at a level where we not only test our understanding of the nucleon but also, perhaps, test our understanding of QCD. While not a true “heavy” quark, the strange quark appears to offer some handle to the nucleon structure because their mass is significantly different than up and down quarks. Whether models or lattice calculations can make precise and testable predictions remains an open question. Understanding the nucleon structure also means understanding confinement; it is important to determine whether a precise flavor decomposition will also offer new insight to the confinement problem.

In conclusion, while the EIC offers exciting possibilities of studying the nucleon, it is clear that there is much work to be done both on the theoretical and experimental fronts to make a new level of precision measurements of basic importance to advancing our understanding.

This work was supported in part by the U.S. Department of Energy, grant DE-FG03-95ER-40913.

References

- [1] The HERMES Collaboration, “The HERMES Physics Program and Plans for 2001–2006,” HERMES Report No. 03-003 (2000).
- [2] The COMPASS Collaboration, CERN/SPSLC 96-14 (1996) (available at www.compass.cern.ch).
- [3] The EIC Collaboration, “The EIC Collider,” BNL-68933, p. 61 (2002).

Outline

- Introduction
 - Why measure Δ_s ?
 - Semi-Inclusive Deep Inelastic Scattering
- Semi-Inclusive Results and Projections
 - Hermes Flavor Decomposition Results
 - Compass Projections
 - EIC Projections
- Open Questions and Opinions

Nucleon Spin Structure

Whence spin?

$$J_q + J_g = \frac{1}{2}\Delta\Sigma + L_q + \Delta G + L_g = \frac{1}{2}$$

$\Delta\Sigma$ is small!

- 1980: First measurements at SLAC (E80,E130)
- 1988: $\Delta\Sigma = 0.012 \pm 0.17$ at EMC \ll Ellis-Jaffe Sum
- 2000: SLAC,CERN, DESY give $\Delta\Sigma \approx 0.2 \leftrightarrow 0.4$

Explanations?

- Strange sea polarization Δ_s large and negative?
- Larger than expected gluon polarization ΔG ?
- Large orbital angular momentum contributions L_q, L_g ?

Goals for a Δ_S Measurement

- Separate Δ_S and $\Delta_{\bar{S}}$
- Precise Δ_S over broad x range
- Why?
 - Data for the world, e.g., LHC, Ultrahigh Cosmic rays
 - Test models of nucleon structure
 - Test Lattice calculations of nucleon structure
 - Test QCD(!)
- This requires a belief in future theoretical success!

Concerns

- Present measurements nearly dominated by limited knowledge of fragmentation functions and unpolarized q_f 's.
 - Where will better knowledge of D and q_f 's come from?
- Δ_s appears small (but not if $\Delta_s = -\Delta_{\bar{s}}$)
 - How well can we separate and determine these distributions?
- How will measurements of ΔG , " L_q " affect the motivation?
- Can we count on "1%" calculations?

Conclusions

- New studies for EIC should probably focus equally on systematics as well statistics: the experiment will run in the era of precision QCD
- Theorists should explore the ramifications of precise flavor-spin determinations, especially beyond models



S. Kretzer
(Michigan State University)

presentation @ RIKEN BNL on 21/08/2002:

Fragmentation Functions from e^+e^- Annihilations and Semi-Inclusive DIS

- Fragmentation Functions from e^+e^- Collisions:
Phys. Rev. D62, 054001 (2000), other Fits
- FFs from SIDIS; *Purities* for polarized SIDIS
Collab. with E. Christova. E. Leader:
Eur. Phys. J. C (2001)
- From “PDFs with errors” to “FFs with errors”: $D(z) \pm \delta D(z)$
 $\rightarrow \sigma \pm \delta\sigma$ for any $\sigma = f \otimes \hat{\sigma} \otimes D$
Collab. with E. Christova, E. Leader, W.-K. Tung.
- Last minute inclusions here at the workshop ...

- What is determined by the e^+e^- data ?

$$D_{\text{meas}}^{\pi^+\pi^-} = \sum_{q=u,d,s} \left(D_q^{\pi^+\pi^-} + D_{\bar{q}}^{\pi^+\pi^-} \right) \hat{e}_q^2(s)$$

$$\hat{e}_q^2(s) : \text{SU}(2) \times \text{U}(1)$$

$$\hat{e}_u^2(s) = \hat{e}_d^2(s) \quad @ \sqrt{s} = 78, 113 \text{ GeV}$$

$$\hat{e}_u^2(s)/\hat{e}_d^2(s) \Big|_{s=M_Z^2} \simeq 3/4$$

The singlet combination

$$\begin{aligned} D_{\Sigma}^{\pi^+} &\equiv \left(D_u^{\pi^+} + D_{\bar{u}}^{\pi^+} + D_d^{\pi^+} + D_{\bar{d}}^{\pi^+} + D_s^{\pi^+} + D_{\bar{s}}^{\pi^+} \right) \\ &= 2 \left(D_u^{\pi^+} + D_d^{\pi^+} + D_s^{\pi^+} \right) \end{aligned}$$

within extreme flavour assumptions

$$0 < (D_s^{\pi^+} + D_{\bar{s}}^{\pi^+}) < (D_u^{\pi^+} + D_{\bar{u}}^{\pi^+})$$

is fixed by e^+e^- data to $\sim 5\%$:

$$\begin{aligned} \bar{D}_{\text{meas}}^{\pi^+\pi^-} &= D_{\text{meas}}^{\pi^+\pi^-} / \hat{e}_d^2(s) \\ D_{\Sigma}^{\pi^+} &= \frac{4}{7} \bar{D}_{\text{meas}}^{\pi^+\pi^-} - \frac{1}{7} \left(D_s^{\pi^+} + D_{\bar{s}}^{\pi^+} \right) \end{aligned}$$

$$\rightarrow \frac{4}{7} \bar{D}_{\text{meas}}^{\pi^+\pi^-} < D_{\Sigma}^{\pi^+} < \frac{6}{11} \bar{D}_{\text{meas}}^{\pi^+\pi^-}$$

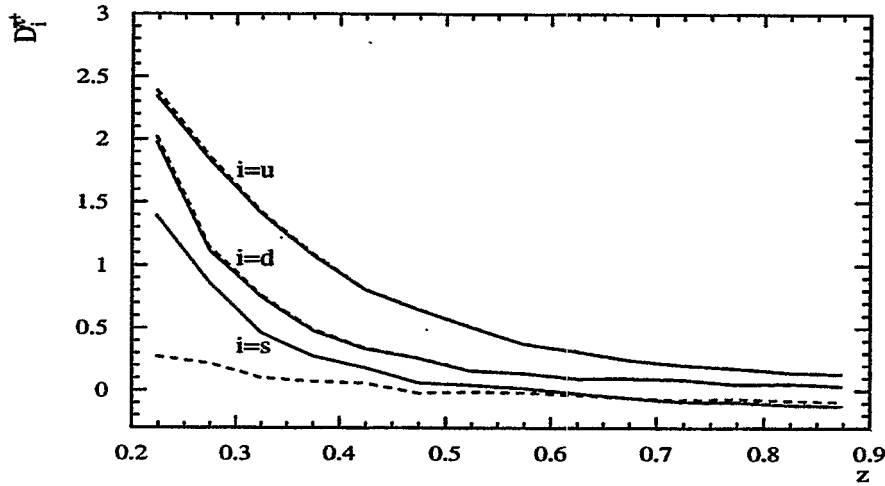
And similar estimates hold for $D_{\Sigma}^{\Lambda, K}$.

- Light-Flavour FFs from HERMES data:

$$D_u^{\pi^+} - D_d^{\pi^+} = \frac{9(R_p^{\pi^+} - R_p^{\pi^-})\tilde{\sigma}_p^{DIS}}{4u_V - d_V}$$

$$D_u^{\pi^+} + D_d^{\pi^-} = \frac{9(R_p^{\pi^+} + R_p^{\pi^-})\tilde{\sigma}_p^{DIS} - 2sD_\Sigma^{\pi^+}}{4(u + \bar{u} - s) + d + \bar{d}}$$

$$D_s^{\pi^+} = \frac{-18(R_p^{\pi^+} + R_p^{\pi^-})\tilde{\sigma}_p^{DIS} + [4(u + \bar{u}) + d + \bar{d}]D_\Sigma^{\pi^+}}{2[4(u + \bar{u} - s) + d + \bar{d}]}$$



HERMES data $\oplus D_\Sigma$ [K(solid), KKP(dashed)]

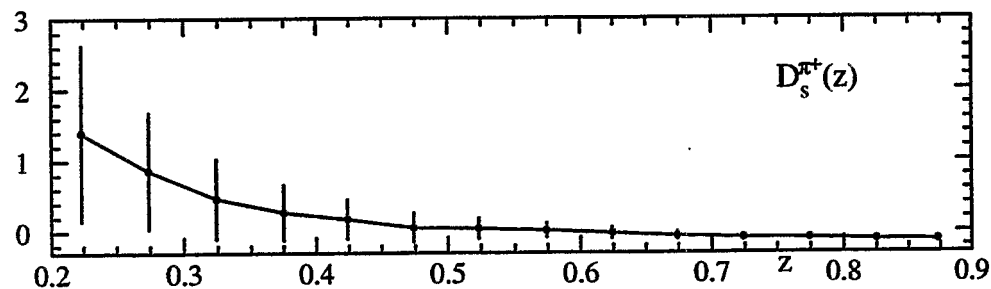
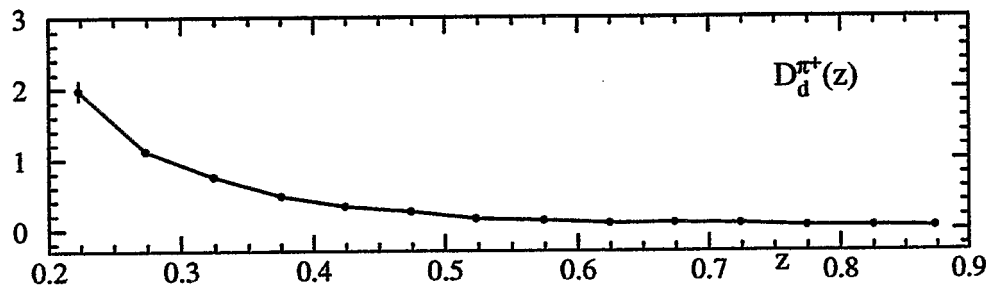
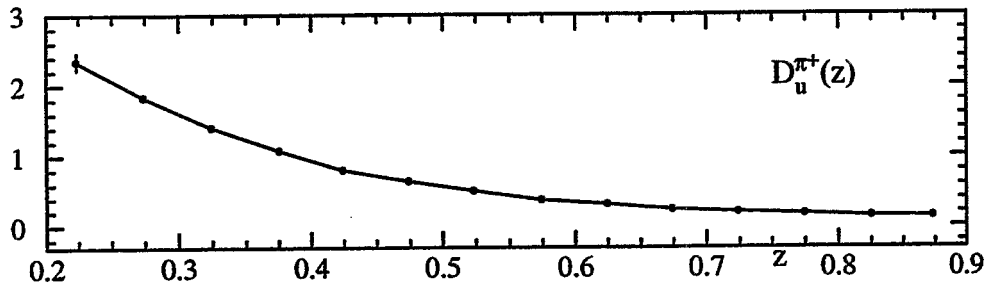
- Isospin:

$$D_d^{\pi^+} = D_{\bar{d}}^{\pi^-} = D_u^{\pi^-} = D_{\bar{u}}^{\pi^+}$$

$$D_{\bar{d}}^{\pi^+} = D_d^{\pi^-} = D_{\bar{u}}^{\pi^-} = D_u^{\pi^+}$$

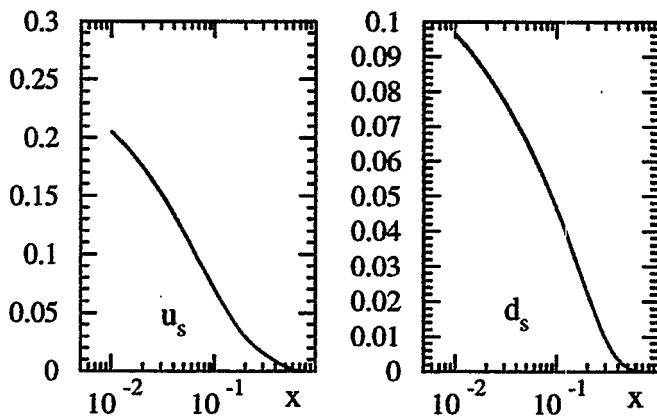
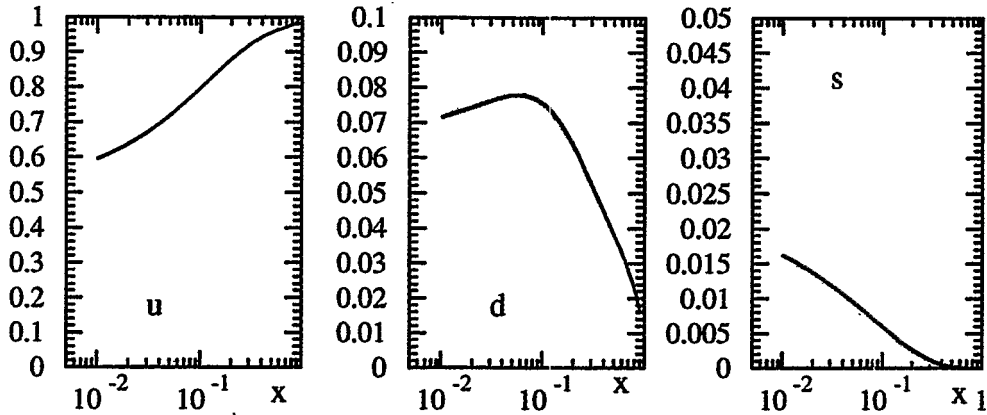
$$D_{\bar{s}}^{\pi^+} = D_s^{\pi^-} = D_{\bar{s}}^{\pi^-} = D_s^{\pi^+}$$

• Light-Flavour FFs within Errors (from LO extraction)



- SU(2) sector ($D_u^{\pi^+}, D_d^{\pi^+}$) well determined
- $D_s^{\pi^+}$ anything within $[0, D_d^{\pi^+}]$
- Knowledge of $D_{\Sigma}^{\pi^+}$ ($\mu = \text{DIS}$) within $\sim 5\%$ would fix $D_s^{\pi^+}$ within $\sim 20 - 30\%$

• Purities $P_q^{\pi^+}$ within uncertainties



$$P_f^h(x) = \frac{e_f^2 q_f(x) \int_{0.2}^1 D_f^h(z) dz}{\sum_{f'} e_{f'}^2 q_{f'}(x) \int_{0.2}^1 D_{f'}^h(z') dz'}$$

effective coupling for SIDIS

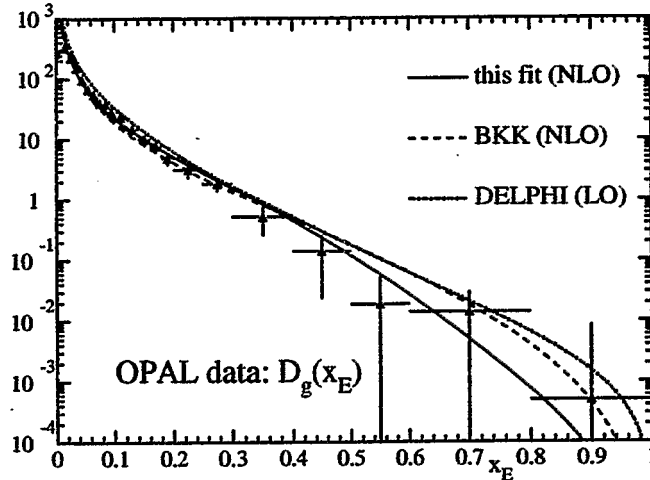
$$A^h(x) = \sum_f P_f^h(x) \frac{\Delta q_f(x)}{q_f(x)}$$

• Gluon Fragmentation in $b\bar{b}g$ 3-jet topologies

only h^\pm ; no π, \dots

Curves:

$$D_g(z = x_E, \mu = E_g^{\text{jet}})$$



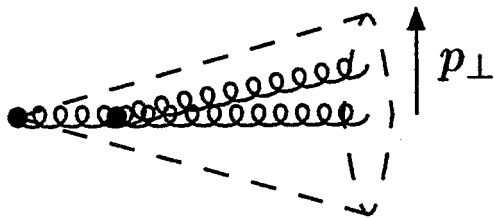
experimental Fragmentation Function

$$D_g^h(x_E, \mu^2) \equiv \frac{1}{N_{\text{tot}}} \frac{\Delta N_g^h}{\Delta x_E}; \quad x_E \equiv \frac{E_h}{E_g^{\text{jet}}}$$

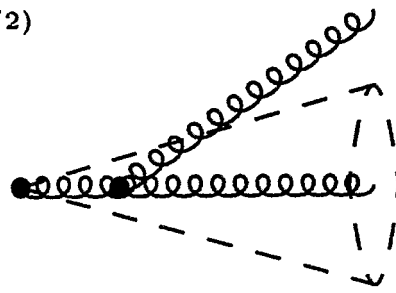
LO QCD scaling violations

$$\int_{\mu^2}^{(p_\perp^{\text{max}})^2} \frac{dp_\perp^2}{p_\perp^2} [P_{ji}^{(0)}(z)]_{p_\perp=0} = P_{ji}^{(0)}(z) \ln \left(\frac{p_\perp^{\text{max}}}{\mu} \right)^2$$

$$\rightarrow \left. \frac{dD_g^h(x_E, \mu^2)}{d \ln \mu^2} \right|_{\mu = E^{\text{jet}} \sin(\theta/2)} : \text{LO - DGLAP}$$



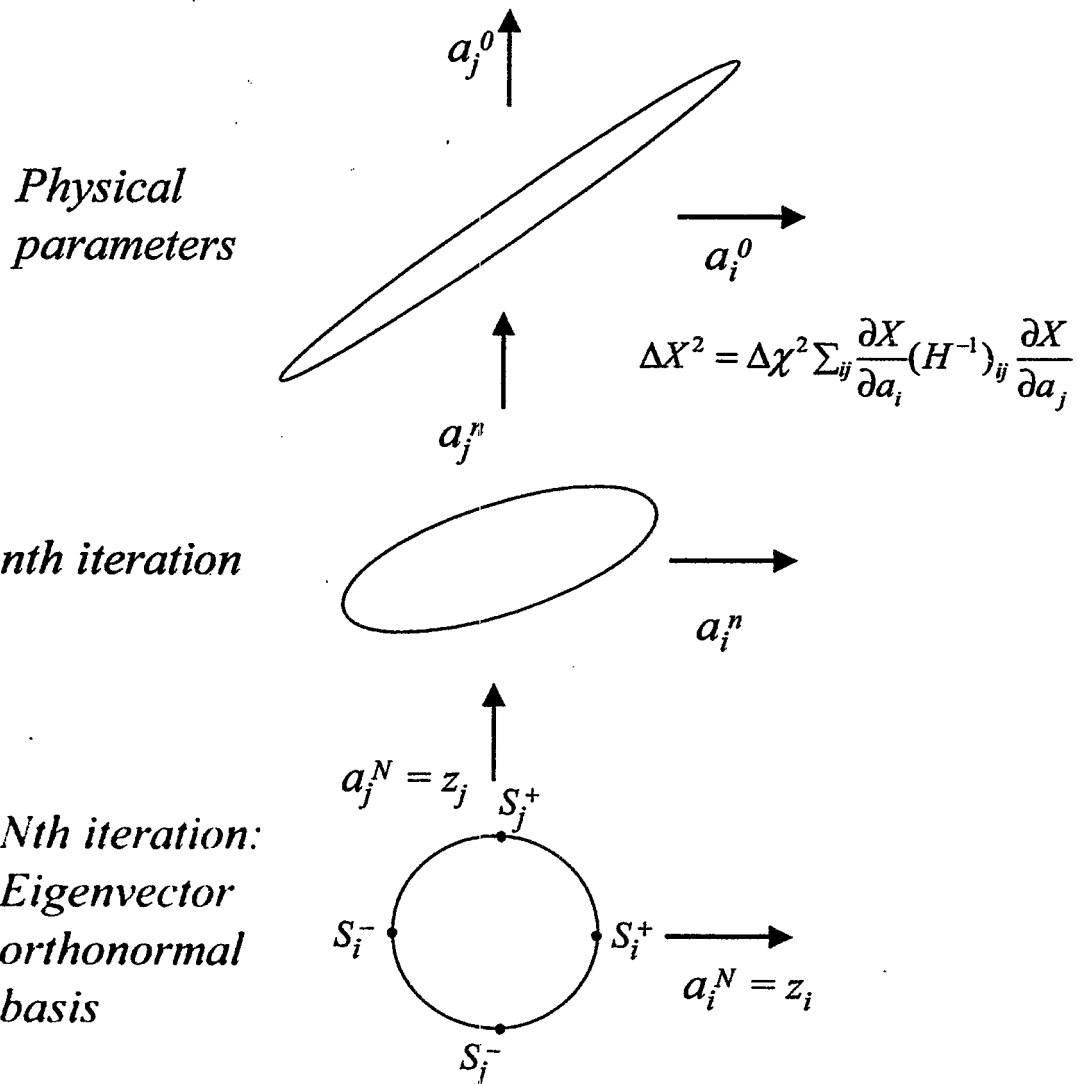
LO!



NLO?

Iterative Method to generate Eigenvectors: (and dramatically improve numerical reliability)

the $\chi^2 = \text{const.}$ ellipsoid



$$\Delta X^2 = \Delta \chi^2 \sum_i \left(\frac{\partial X}{\partial z_i} \right)^2 = \sum_i [X(S_i^+) - X(S_i^-)]^2$$

νp elastic scattering: a direct measure of Δs

Steven D. Bass

HEP Group, Institute for Experimental Physics and Institute for Theoretical Physics, Universität Innsbruck, Technikerstrasse 25, A-6020 Innsbruck, Austria

Parity violating νp elastic scattering offers an exciting new opportunity to probe the strange quark contribution to the spin structure of the proton. This process involves elastic Z^0 exchange and measures the axial charge $g_A^{(Z)}$ for protons to couple to the weak neutral current

$$J_{\mu 5}^Z = \frac{1}{2} \left\{ \sum_{q=u,c,t} - \sum_{q=d,s,b} \right\} \bar{q} \gamma_\mu \gamma_5 q, \quad (1)$$

viz: $2g_A^{(Z)} = (\Delta u - \Delta d - \Delta s) + (\Delta c - \Delta b + \Delta t)$ where Δq refers to the expectation value $\langle p, s | \bar{q} \gamma_\mu \gamma_5 q | p, s \rangle = 2m_p s_\mu \Delta q$ for a proton of spin s_μ and mass m_p . The heavy-quark contributions to $g_A^{(Z)}$ have recently been evaluated to next-to-leading order (S.D. Bass, R.J. Crewther, F.M. Steffens and A.W. Thomas (hep-ph/0207071)). They are small, both at LO and at NLO. One finds that, when first t , then b , and finally c are decoupled using heavy-quark renormalization group techniques, the full NLO result is:

$$2g_A^{(Z)} = (\Delta u - \Delta d - \Delta s)_{\text{inv}} + \mathcal{P}(\Delta u + \Delta d + \Delta s)_{\text{inv}} + O(m_{t,b,c}^{-1}) \quad (2)$$

Here \mathcal{P} is a polynomial in the running couplings $\tilde{\alpha}_h$,

$$\begin{aligned} \mathcal{P} &= \frac{6}{23\pi} (\tilde{\alpha}_b - \tilde{\alpha}_t) \left\{ 1 + \frac{125663}{82800\pi} \tilde{\alpha}_b + \frac{6167}{3312\pi} \tilde{\alpha}_t - \frac{22}{75\pi} \tilde{\alpha}_c \right\} \\ &\quad - \frac{6}{27\pi} \tilde{\alpha}_c - \frac{181}{648\pi^2} \tilde{\alpha}_c^2 + O(\tilde{\alpha}_{t,b,c}^3), \\ &= -0.02 \end{aligned} \quad (3)$$

Δq_{inv} denotes the scale-invariant version of Δq and $\tilde{\alpha}_h$ denotes Witten's renormalization group invariant coupling for a heavy quark h . Given the small value of the heavy-quark contributions, $g_A^{(Z)}$ provides a direct measure of Δs_{inv} independent of assumptions about the small Bjorken x behaviour of g_1 . In particular, the value of Δs_{inv} extractable from νp elastic scattering includes any contribution to the spin associated with Bjorken $x = 0$, including the possibility of a contribution associated with non-perturbative gluon topology (S.D. Bass, Mod. Phys. Lett. A13 (1998) 791), which, if present, would be missed by deep inelastic scattering ($x > 0$).

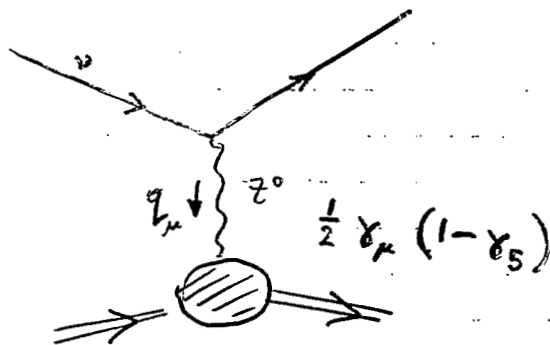
A definitive measurement of νp elastic scattering may be possible using the miniBooNE set-up at FNAL (R. Tayloe, Nucl. Phys. B (Proc. Suppl.) 105 (2002) 62). The projected error on Δs_{inv} from this experiment is 0.03, comparable with the error from the present polarized deep inelastic measurements.

Spin Structure of the Nucleon

THREE EXPERIMENTS

Hard processes $\rightarrow \Delta q, \Delta g$

1. Polarized Deep Inelastic Scattering
(incl. semi-inclusive)
2. Polarized pp, RHIC Spin
3. np elastic



Measure axial form-factor as $q^2 \rightarrow 0$

$$g_A^z = \Delta u - \Delta d - \Delta s + (\Delta c - \Delta b + \Delta t)$$

Independent measure of " Δs "

Process	Axial Charge	#
n β -decay	Non Singlet $g_A^3 = \Delta u - \Delta d$	1.26
hyperon β -decays	Non Singlet $g_A^8 = \Delta u + \Delta d - 2\Delta s$	0.58 \pm 0.03
elastic νp	Non Singlet $g_A^z = \frac{1}{2} \left[(\Delta u - \Delta d - \Delta s) + (\Delta c - \Delta b + \Delta t) \right]$	$\Delta s = -0.15 \pm 0.08$ E-734 @BNL

$$-5 < a^2 < 1$$

Polarized DIS $\left(\frac{1}{12} g_A^3 C_{NS}^3 + \frac{1}{36} g_A^8 C_{NS}^8 + \frac{1}{9} g_A^0 C^0 \right) \sim \int_0^1 dx g_1^P$

Singlet $g_A^0 \Big|_{inv} = (\Delta u + \Delta d + \Delta s)_{inv} = E(\alpha_s) (\Delta u + \Delta d + \Delta s)$

$$g_A^0 = 0.2 - 0.35$$

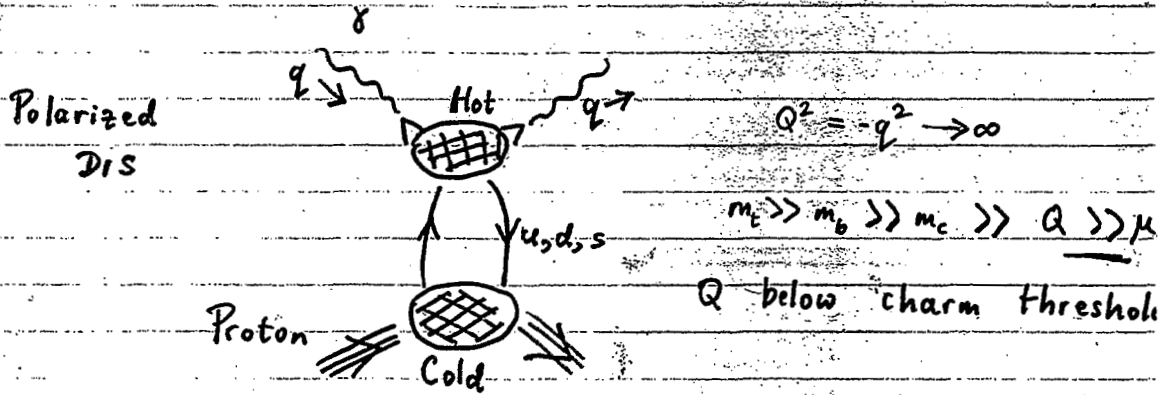
Ellis-Jaffe

1 g_A^3, g_A^8 , Assume $\Delta s = 0$

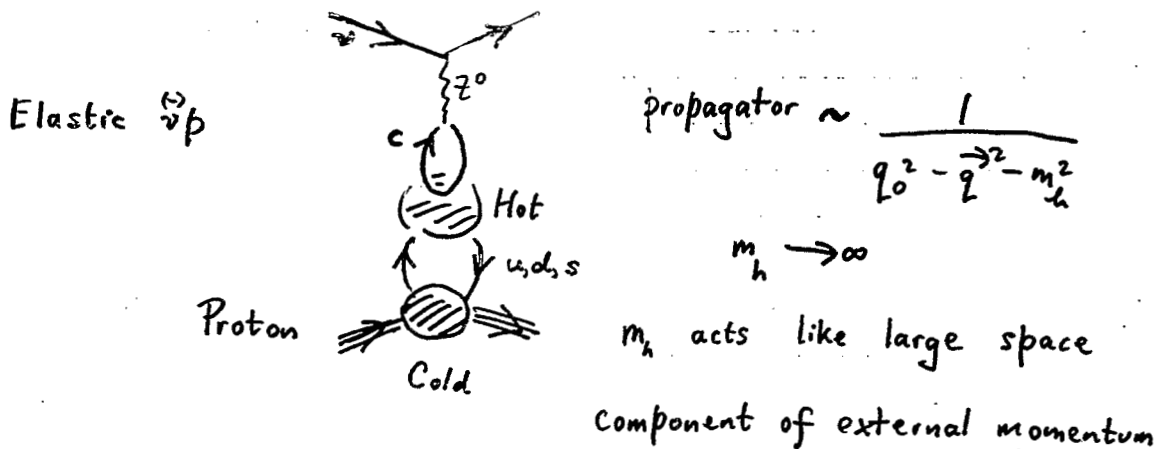
2 g_A^3, g_A^8, g_A^z with $\Delta c, \Delta b, \Delta t = 0$

3 Eqⁿs, 3 Unknowns $\rightarrow g_A^0$

Operator Product Expansions



$$\int_0^1 dx g_1^P = \frac{1}{2} \sum_q e_q^2 \Delta q_{\text{lin}} \left\{ 1 + \sum_e c_e \alpha_s(Q) \right\}$$

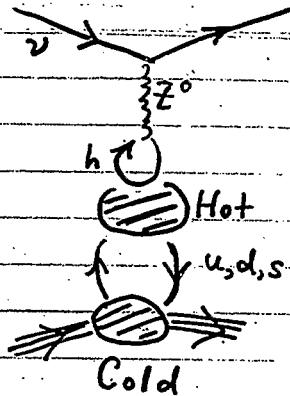


$$g_A^z = \frac{1}{2} \left\{ \Delta u - \Delta d - \Delta s + \Delta c - \Delta b + \Delta t \right\}$$

Calculate using heavy quark theory

Heavy Quark Contributions

- Want answer in terms of Renormalization group invariants
(Δ_{linv} , RG invariant couplings)



$$g_A^Z = \text{Scale Indep.}$$

Use Witten's RG

$$\begin{aligned} 2g_A^Z &= \Delta u - \Delta d - \Delta s + \Delta c - \Delta b + \Delta t \\ &= (\Delta u - \Delta d - \Delta s)_{\text{inv}} + C (\Delta u + \Delta d + \Delta s)_{\text{inv}} + O(1/m) \end{aligned}$$

$$\begin{aligned} C &= \frac{6}{23\pi} (\tilde{\alpha}_b - \tilde{\alpha}_t) \left\{ 1 + \frac{125663}{82800\pi} \tilde{\alpha}_b + \frac{6167}{3312\pi} \tilde{\alpha}_t - \frac{22}{75\pi} \tilde{\alpha}_c \right\} \\ &\quad - \frac{6}{27\pi} \tilde{\alpha}_c - \frac{181}{648\pi^2} \tilde{\alpha}_c^2 + O(\tilde{\alpha}_h^3) \end{aligned}$$

$$= -0.02$$

SDB, Crewther, Steffens, Thomas, hep-ph/020707

$$\tilde{\alpha}_h = \text{Witten coupling}, \quad \ln m_h = \int \tilde{\alpha}_h d - 1 - \delta_F(x)$$

? If $\Delta S_{\text{DIS}}^{\text{RHIC}} \neq \Delta S_{\text{ep elastic}}^{\text{ep elastic}}$?

(Violation of E7 #2)

- νp elastic measures matrix element

$$\langle \bar{s} \gamma_\mu \gamma_5 s \rangle = 2 m_s \Delta s$$

→ Does not rely on small x extrapolation

Indep. of $\left\{ \begin{array}{l} \text{Anomalous behaviour at } x \sim 0 \text{ (?) } \\ \text{SU(3)}_F \text{ violation (?) } \end{array} \right.$

Can help pin down "missing spin"

Possible $\delta(x)$ term in $g_1 \dots$

Andrzej M. Sandacz

Soltan Institute for Nuclear Studies, ul. Hoża 69, Warsaw
PL 00681, Poland

E-mail: sandacz@fuw.edu.pl

Studies of Exclusive Processes in ep Scattering at EIC

A. Sandacz

Soltan Institute for Nuclear Studies, ul. Hoża 69, Warsaw, PL 00681, Poland

E-mail: sandacz@fuw.edu.pl

In recent years significant progress has been made in the theory of *generalized parton distributions* (GPD). Unifying the concepts of parton distributions and of hadronic form factors, they contain a wealth of information about how quarks and gluons make up hadrons. The reactions where GPDs can be accessed are deeply virtual Compton scattering (DVCS) and exclusive meson electroproduction, $ep \rightarrow epM$, where M is either vector or pseudoscalar meson. DVCS is special, because it interferes with Bethe-Heitler process when the real photon is radiated from the lepton. This offers the unique possibility to study DVCS at the amplitude level, including its phase.

To fully explore the physics of GPDs one will want to disentangle contributions from various spin and flavor combinations. This requires measurements of various reactions in unpolarised collisions as well as with polarised lepton and proton [1].

In the following we present results of studies of several exclusive processes in ep scattering at EIC, with $E_e = 10$ GeV and $E_p = 250$ GeV. The considered processes are: DVCS, hard ρ^0 production, J/ψ photoproduction and J/ψ hard production. The effects of the detector acceptance on the data were included in the simulation. The main features of the assumed detector are listed in Transparency 1. In Transp. 2 details are given for the considered Roman Pot Spectrometer to be used for the tracking of the final state proton. For the considered setup the acceptance is good (0.3 - 0.6) for $|t| > 0.04 \text{ GeV}^2$. For estimates of the statistical accuracies of the data the moderate luminosity of 330 pb^{-1} was assumed for all analysed channels, except for the estimates of precision for double spin asymmetry.

The kinematics of the real photon from DVCS is shown in Transp. 3. It clearly demonstrates a need to extend calorimetric measurements of energy of electromagnetic showers down to about 1 GeV, and to extend measurements to the region close to the beam. The correlation of E_γ with the accessible kinematic range of W and x can be seen in Transp. 4. With $E_\gamma > 1$ GeV, the resulting kinematical range is $Q^2 > 1 \text{ GeV}^2$, $20 < W < 95 \text{ GeV}$, $|t| > 0.01 \text{ GeV}^2$ and the total number of accepted DVCS events will be about 60000 (6000 for $Q^2 > 4 \text{ GeV}^2$). This will allow to determine $d\sigma/dW$ with statistical accuracy of about 1% at several (6) W values.

The estimated precision of the measured azimuthal asymmetry, which results from the interference between DVCS and Bethe-Heitler amplitudes, is shown in Transp. 5. The statistical precision is good, $\delta A/A < 0.1$ in most of the region. However, at the lowest and highest W values systematic errors, which are due to the acceptance corrections, are expected to be large.

For the hard production of ρ^0 and J/ψ the kinematics of the vector mesons and decay particles is shown in Transp. 6. It illustrates the importance of tracking of decay particles in a wide angular range, $5 < \theta < 175^\circ$. The effect of the acceptance of the central tracking detector on the accessible kinematical range is shown in Transp. 7. With the proposed detector the kinematical range for hard ρ^0 and J/ψ production is $1 < Q^2 < 50 \text{ GeV}^2$, $15 < W < 95 \text{ GeV}$.

For the ρ channel the total number of accepted events will be about 650000 (52000 for $Q^2 > 4 \text{ GeV}^2$) and the double-differential cross section $d^2\sigma/dxdQ^2$ will be measured with accuracy better than 2% in the most of the region of $Q^2 < 15 \text{ GeV}^2$, cf. Transp. 8.

The accuracy of measuring the longitudinal double spin asymmetry $A_{\gamma^*p \rightarrow \rho^0 p}$ is shown in Transp. 9. To obtain the shown accuracy the high luminosity of the order of several fb^{-1} will be needed.

For hard J/ψ production the total number of accepted events in the decay channels $J/\psi \rightarrow \mu^+\mu^-$ and $J/\psi \rightarrow e^+e^-$ will be about 5000. This will allow to determine $d\sigma/dx$ with accuracy of about 3% at several x values.

Finally, we studied J/ψ photoproduction, where the exchanged virtual photon is quasi-real. In most of these events scattered electron escapes into the beam pipe, and the energy W has to be estimated using the reconstructed J/ψ . The kinematics of J/ψ and distributions of Q^2 and W are shown in Transp. 10. For the accessible kinematic range $Q_{min} < Q^2 < 1 \text{ GeV}^2$, $15 < W < 95 \text{ GeV}$ the accepted number of events will be about 70000. This will allow to measure cross section $d\sigma/dW$ with an accuracy of about 1% at several W values.

In summary, unpolarised cross sections for the studied channels could be measured at EIC already at a moderate luminosity of about 300 pb^{-1} . Measurements of azimuthal asymmetries for DVCS are possible, but systematic errors due to acceptance corrections may be large in certain kinematical regions. Studies of double spin asymmetries will require luminosities which are at least an order of magnitude higher. Studies of exclusive processes will present several challenges for the future detector at EIC. In particular, wide angular coverage of the central tracking detector, measurements and isolation of electromagnetic showers with low energy, and large acceptance Roman Pot Spectrometer will be needed.

References

- [1] M.Diehl, **Exploring skewed parton distributions with polarised targets**, Proceedings of the Nuclear Theory Summer Meeting on eRHIC, July 26 - July 14, 2000, BNL-52606, p.123.

Proposed Detector

- Extended Central Tracking Detector (ECTD) and Vertex Detector

$$5 < \Theta < 175^\circ \quad (|\eta| < 3.1) \quad !$$

Resolution for charged particles

$$\frac{\sigma_{PT}}{P_T} = 0.0058 p_T \oplus 0.0065 \oplus 0.0044/p_T$$

$$\sigma_{\eta} = 0.0045 \oplus 0.0047/p_T \quad \text{like ZEUS}$$

$$\sigma_{\varphi} = 0.0006 \oplus 0.002/p_T$$

- Scattered Electron Detector (precise angular measurements for e')

$$\sigma_{\theta} = \sigma_{\varphi} = 0.0003$$

for those e' not covered by ECTD, E'_e from CM:

$$E'_e = \frac{2E_e - \xi(E_i - p_{zi})}{1 - \cos\Theta_{e'}}$$

- Electromagnetic Calorimeter

Shower energy down to 1 GeV !

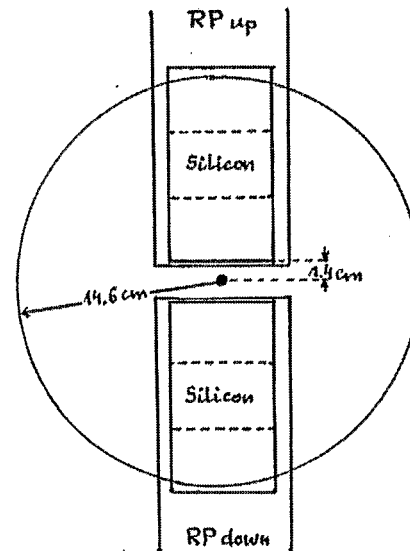
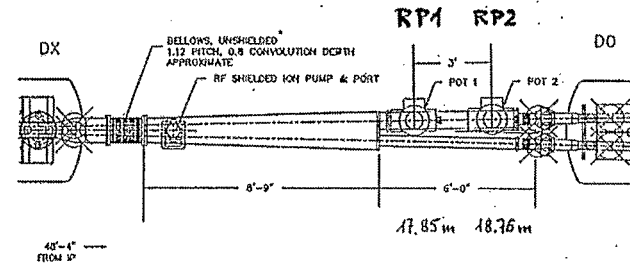
$$\frac{\Delta E}{E} = \frac{0.075}{\sqrt{E}} \oplus 0.025 \quad \text{like SPACAL of H1}$$

- Muon Identifier

- Roman Pot Spectrometer

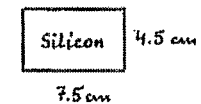
Roman Pot Spectrometer

OVERLAY OF H1 ROMAN POTS ON DX-DO TRANSITION REGION
6 FEET BETWEEN BEAMLINE MERGE PLATE AND ISOLATION VALVES APARTING DO.



cross section of the ring at RP1 or RP2

size of a single pp2pp detector



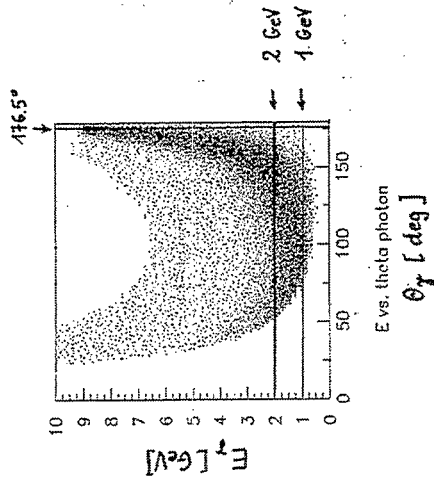
Photon kinematics in DVCS

$ep \rightarrow ep\gamma$ at 250 GeV

$$Q^2 > 1 \text{ GeV}^2$$

$$20 < W < 95 \text{ GeV}$$

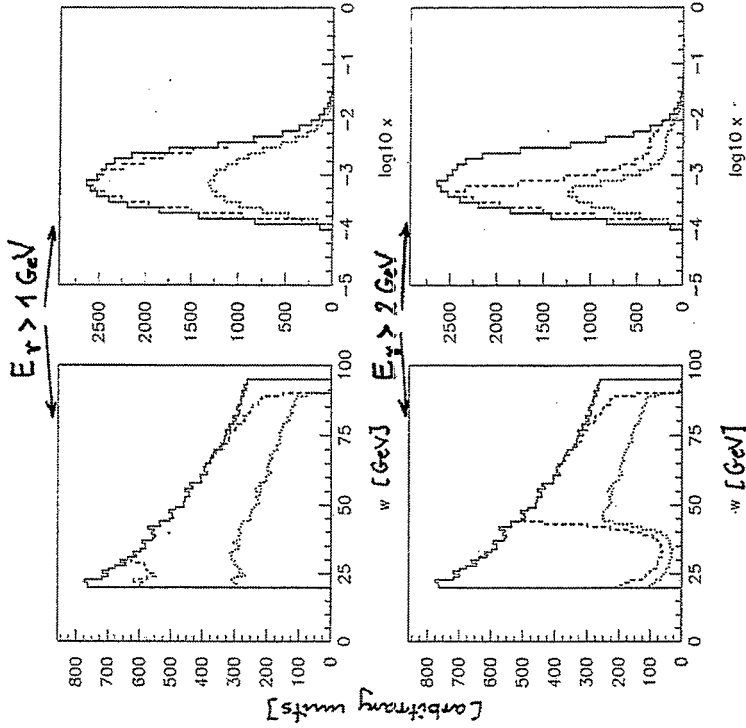
$$0.01 < |t| < 1.0 \text{ GeV}^2$$



Effect of acceptance in E_γ on kinematical range

DVCS

Event distributions



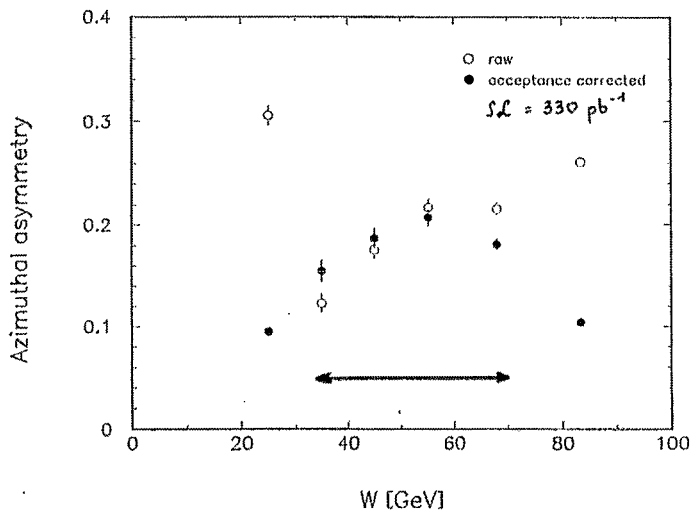
— generated - - - - - accepted by CD accepted by all

Measurements of E_γ must extend to low energies $\approx 1 \text{ GeV}$

Azimuthal asymmetry

DVCS + BH

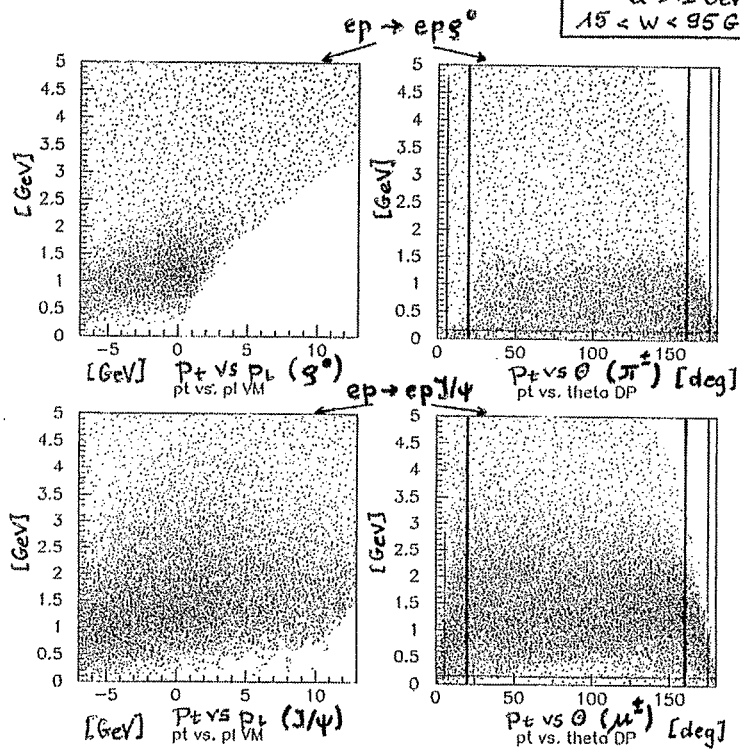
$$A = \frac{\int_{-\pi/2}^{\pi/2} d\phi_T d\sigma_{\text{DVCS} + \text{BH}} - \int_{\pi/2}^{3\pi/2} d\phi_T d\sigma_{\text{DVCS} + \text{BH}}}{\int_0^{2\pi} d\phi_T d\sigma_{\text{DVCS} + \text{BH}}}$$



Kinematics of VM exclusive production

$ep \rightarrow ep\gamma^0$ $ep \rightarrow epJ/\psi$ at 250 GeV

$Q^2 > 1 \text{ GeV}^2$
 $15 < W < 95 \text{ GeV}$



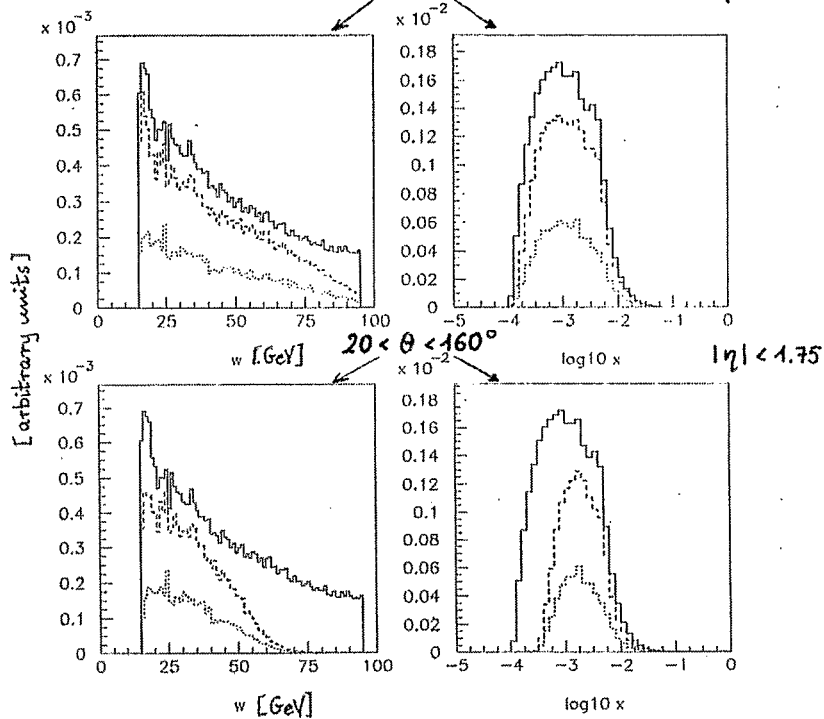
Effect of acceptance for decay particles on kinematical range

$ep \rightarrow ep\gamma^0$
 $Q^2 > 1 \text{ GeV}^2$

Event distributions

$5 < \theta < 175^\circ$

$|\eta| < 3.1$



— generated - - - - - accepted by CD accepted by all

⇒ Tracking of decay particles must extend to mid-forward and mid-rear region

363

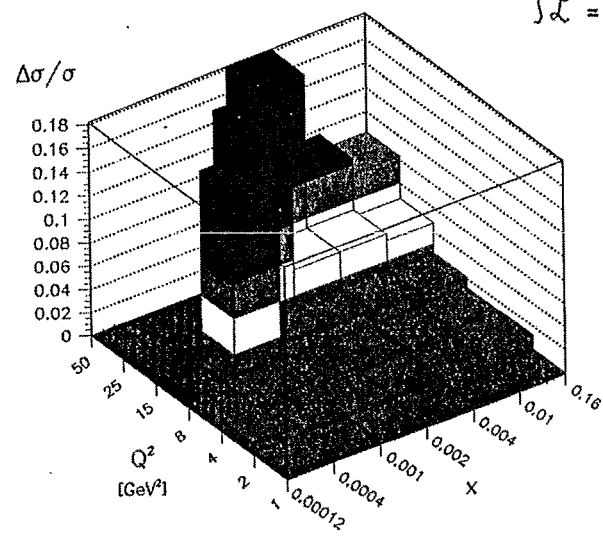
Statistical precision of $d^2\sigma/dx dQ^2$

$ep \rightarrow ep\gamma^0$

$1 < Q^2 < 50 \text{ GeV}^2$
 $15 < W < 95 \text{ GeV}$

$\sigma_{ep \rightarrow ep\gamma^0} = 7.3 \text{ nb}$

$\int \mathcal{L} = 330 \text{ pb}^{-1}$

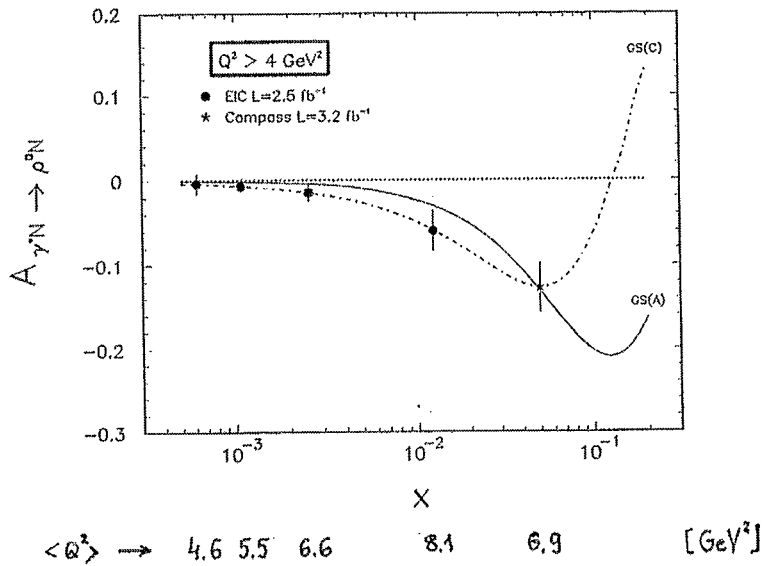


Total number of accepted events

$Q^2 > 1 \text{ GeV}^2$	656 000
$Q^2 > 4 \text{ GeV}^2$	52 500

$$\delta A_{\gamma^* p \rightarrow S^* p}$$

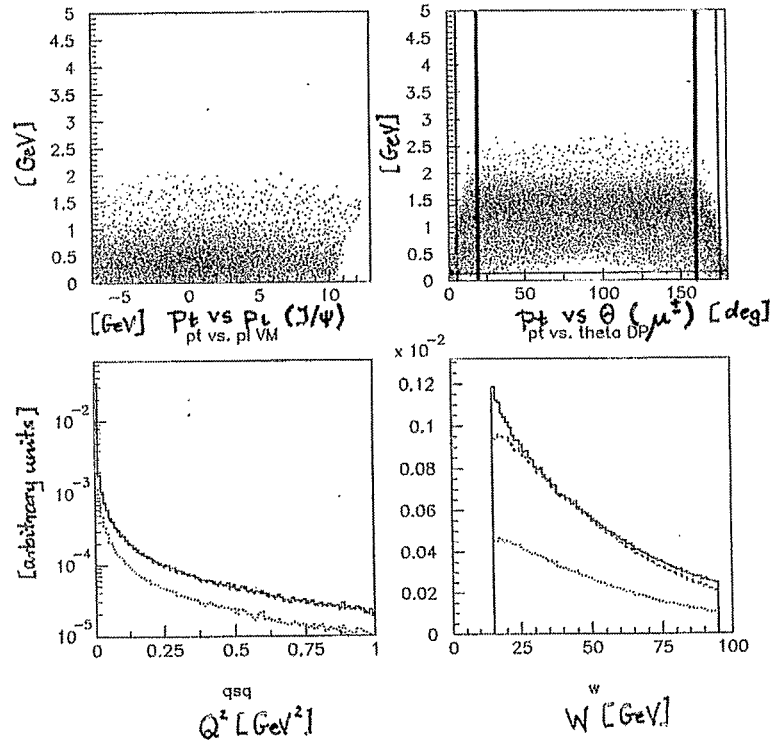
curves: predictions from model of Ryskin (97)
 using
 different sets of polarised PDF's of GS(L0)'96
 and
unpolarised gluon distributions of GRV(L0)'92 } evaluated
 at $\bar{K}^2 = 1.3$
 GeV^2
 for details see A.S., COMPASS Note 1998-5
<http://www.compass.cern.ch/compass/notes>



Note: requirement of recoil detection relaxed
 in this analysis

Photoproduction of J/ψ

electron escapes into the beam pipe
 $\Rightarrow W^2 \approx 2(E_{J/\psi} - P_{zJ/\psi})E_p = 4E_p E_e y$



— generated - - - - - accepted by CD accepted by all

$\langle Q^2 \rangle = 0.05 \text{ GeV}^2$ $\langle x \rangle = 5 \cdot 10^{-5}$

IMPACT PARAMETER SPACE INTERPRETATION FOR THE
GENERALIZED PARTON DISTRIBUTIONS $H(X, 0, T)$ AND
 $E(X, 0, T)$.

M.BURKARDT

*Department of Physics, New Mexico State University
Las Cruces, New Mexico 88011, U.S.A.*

The Fourier transform of generalized parton distribution functions at $\xi = 0$ describes the distribution of partons in the transverse plane. The physical significance of these impact parameter dependent parton distribution functions is discussed. In particular, it is shown that they satisfy positivity constraints which justify their physical interpretation as a probability density. The generalized parton distribution H is related to impact parameter distribution of unpolarized quarks for an unpolarized nucleon, \tilde{H} is related to the distribution of longitudinally polarized quarks in a longitudinally polarized nucleon, and E is related to the distortion of the unpolarized quark distribution in the transverse plane when the nucleon has transverse polarization. The magnitude of the resulting transverse flavor dipole moment can be related to the anomalous magnetic moment for that flavor in a model independent way.

References

1. M. Burkardt, hep-ph/0207047.



366

Physical Interpretation for the Generalized Parton Distributions $H(x, 0, -\Delta_{\perp}^2)$ and $E(x, 0, -\Delta_{\perp}^2)$ *or: What DVCS has to do with the distribution of partons in the transverse plane*

Matthias Burkardt

burkardt@nmsu.edu

New Mexico State University
Las Cruces, NM, 88003, U.S.A.



Form Factors vs. GPDs

operator	forward matrix elem.	off-forward matrix elem.	position
$\bar{q}\gamma^+q$	Q	$F(t)$	ρ
$\int \frac{dx^- e^{ixp^+x^-}}{4\pi} \bar{q}\left(\frac{-x^-}{2}\right) \gamma^+ q\left(\frac{x^-}{2}\right)$	$q(x)$	$H(x, 0, t)$	$q(x,$

$q(x, \mathbf{b}_\perp) =$ impact parameter dependent PDF

Physical Interpretation for the Generalized Parton Distributions $H(x, 0, -\Delta_\perp^2)$ and $E(x, 0, -\Delta_\perp^2) - p.$



Summary

- DVCS allows probing GPDS

$$\int \frac{dx^-}{2\pi} e^{ixp^+x^-} \left\langle p' \left| \bar{\psi} \left(-\frac{x^-}{2} \right) \gamma^+ \psi \left(\frac{x^-}{2} \right) \right| p \right\rangle$$

- GPDs resemble both PDFs and form factors: defined through matrix elements of light-cone correlation, but $\Delta \equiv p' - p \neq 0$.
 - t -dependence of GPDs at $\xi = 0$ (only \perp momentum transfer) \Rightarrow Fourier transform of impact parameter dependent parton distributions $q(x, \mathbf{b}_\perp)$
- \hookrightarrow knowledge of GPDs for $\xi = 0$ allows determining distribution of partons in the \perp plane

Physical Interpretation for the Generalized Parton Distributions $H(x, 0, -\Delta_\perp^2)$ and $E(x, 0, -\Delta_\perp^2) - p$:



$$q(x, \mathbf{b}_\perp) = \int \frac{d^2 \mathbf{b}_\perp}{(2\pi)^2} H(x, 0, -\Delta_\perp^2) e^{-i\mathbf{b}_\perp \cdot \Delta_\perp}$$
$$\Delta q(x, \mathbf{b}_\perp) = \int \frac{d^2 \mathbf{b}_\perp}{(2\pi)^2} \tilde{H}(x, 0, -\Delta_\perp^2) e^{-i\mathbf{b}_\perp \cdot \Delta_\perp}$$

↪ GPDs provide novel information about nonperturbative parton structure of nucleons: distribution of partons in \perp plane
 $L_x \sim \langle yp_z - zp_y \rangle$ only lowest \mathbf{b}_\perp moment of the information

- $q(x, \mathbf{b}_\perp), \Delta q(x, \mathbf{b}_\perp)$ have probabilistic interpretation, e.g. $q(x, \mathbf{b}_\perp) > 0$ for $x > 0$
- universal prediction: large x partons more localized in \mathbf{b}_\perp than small x partons



- $\frac{\Delta_{\perp}}{2M} E(x, -\Delta_{\perp}^2)$ describes how the momentum distribution of unpolarized partons in the \perp plane gets transversely shifted (distorted) if is nucleon polarized in \perp direction..
- published in: M.B., PRD **62**, 71503 (2000), hep-ph/0105324, and hep-ph/0207047; see also ($\xi \neq 0$) M.Diehl, hep-ph/0205208.

Azimuthal asymmetries in semi-inclusive DIS

Pavel Nadolsky

in collaboration with

D. Stump, C.-P. Yuan (Phys. Lett., B515, 175 (2001))

Contents

- ✓ Perturbative aspects ($q_T^2 \gg \Lambda_{QCD}^2$)
 - ◆ Unpolarized azimuthal asymmetry as a probe of the vector nature of QCD; recent ZEUS data

- ✓ Nonperturbative aspects ($q_T^2 \sim \Lambda_{QCD}^2$)
 - ◆ Small- q_T factorization
 - ◆ Sudakov factors & Collins fragmentation function; strong Sudakov suppression of Collins asymmetry?

- ✓ Merging perturbative and nonperturbative regions

Fixed-order SIDIS cross section $d\sigma/(dx dQ^2 d\theta)$ is unreliable in the limit $\theta \rightarrow 0$

$$\left(\frac{d\sigma}{dx dQ^2 d\theta}\right)_{\theta \rightarrow 0} \propto \frac{1}{\theta^2} \sum_{n=1}^{\infty} \left(\frac{\alpha_S}{\pi}\right)^n \sum_{m=0}^{2n-1} \ln^m\left(\frac{\theta^2}{4}\right)$$

There is a powerful machinery for summation of such logarithms originally introduced in e^+e^- hadroproduction and Drell-Yan processes (*Dokshitzer, Dyakonov, Troyan, 1978; Parisi, Petronzio, 1979; Collins, Soper, Serman, 1981-1985; Altarelli, Ellis, Greco, Martinelli, 1984;...*)

Hard cross sections in SIDIS, e^+e^- hadroproduction and Drell-Yan processes are "kinematically isomorphic" (described by same Feynman diagrams in different crossing channels)

When formulated in Lorentz-invariant terms, the most part of the resummation formalism is identical in three processes

ZEUS (*Phys. Lett., B481, 199 (2000)*) measured p_T -dependence of $\langle \cos \varphi \rangle$ and $\langle \cos 2\varphi \rangle$ in the charged hadron production

Extra complications in the ZEUS analysis

1. p_T distributions mix fixed-order perturbative and nonperturbative contributions in both $\langle \cos \varphi \rangle$ and $\langle \cos 2\varphi \rangle$. The nonperturbative contributions are not just "intrinsic k_T " contributions, but also include PQCD Sudakov factors at $\Lambda_{QCD}^2 \ll q_T^2 \ll Q^2$
2. They contribute both to the numerator and denominator
3. Fragmentation functions $D(z)$ in $\langle \cos n\varphi \rangle$ do not cancel
4. $\mathcal{O}(\alpha_S^2)$ corrections to SIDIS are expected to be large

A simple alternative:

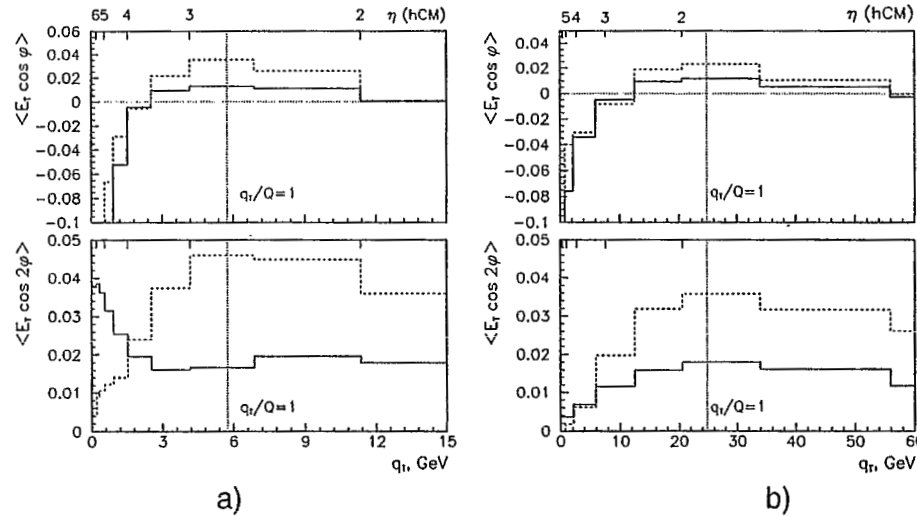
azimuthal asymmetries of the transverse energy flow $\langle E_T \rangle$ in the γ^*p c.m. frame as a function of q_T

$$\frac{d\langle E_T \rangle}{dx dQ^2 dq_T} = \frac{1}{d\sigma/(dx dQ^2)} \sum_B \int dz E_T \frac{d\sigma(e + A \rightarrow e + B + X)}{dx dQ^2 dz dq_T}$$

$$\langle E_T \cos n\phi \rangle(q_T) = \frac{\int d\Phi \int_0^{2\pi} d\phi \cos n\phi \frac{d\langle E_T \rangle}{dx dQ^2 dq_T^2 d\phi}}{\int d\Phi \int_0^{2\pi} d\phi \frac{d\langle E_T \rangle}{dx dQ^2 dq_T^2 d\phi}}$$

- ✓ The perturbative ($q_T^2/Q^2 \sim 1$) and nonperturbative ($q_T^2/Q^2 \ll 1$) contributions are well separated
- ✓ $D(z)$ are integrated out
- ✓ Nonperturbative terms in the denominator are well understood in the framework of small- q_T factorization
- ✓ $q_T = W e^{-\eta_{c.m.}}$ can be easily measured

Estimates of $\langle E_T \cos n\varphi \rangle(q_T)$ in data bins from H1 E_T -flow analysis (DESY-99-091)



(a) $\langle x \rangle = 0.0047$,
 $Q^2 = 33.2 \text{ GeV}^2$;

(b) $\langle x \rangle = 0.026$,
 $Q^2 = 617 \text{ GeV}^2$

$\int_0^{2\pi} d\varphi \cos n\varphi \frac{d\langle E_T \rangle}{dx dQ^2 dq_T^2 d\varphi}$ is calculated at $\mathcal{O}(\alpha_S)$; $\int_0^{2\pi} d\varphi \frac{d\langle E_T \rangle}{dx dQ^2 dq_T^2 d\varphi}$ is calculated in the resummation formalism (solid) and at $\mathcal{O}(\alpha_S)$ (dashed)
 PQCD is trustworthy at $q_T/Q \sim 1$ and fails as $q_T/Q \rightarrow 0$, where $\langle E_T \cos \varphi \rangle$ is large and negative (even diverges for the resummed denominator)

Conclusions

1. Azimuthal asymmetries in unpolarized SIDIS provide sensitive tests of PQCD
2. In particular, the measurement of $\langle \cos \varphi \rangle$ and $\langle \cos 2\varphi \rangle$ in the E_T -flow as a function of η in the γ^*p c.m. frame is simple and cleanly separates perturbative and nonperturbative contributions
3. We need to understand better how azim. asymmetries are affected by multiple parton radiation at $\Lambda_{QCD}^2 \ll q_T^2 \ll Q^2$
4. In the presence of perturbative radiation, Collins transverse spin asymmetries do not have to vanish as $1/Q^{0.64}$ due to Sudakov factors; additional studies are needed that consider effects from the region $\Lambda_{QCD}^2 \ll q_T^2 \ll Q^2$

Measurements of the structure of proton and virtual photon at HERA

Stefan Schlenstedt (DESY Zeuthen)

Abstract

This talk deals mainly with the progress of the measurements of deep inelastic scattering in neutral current interactions performed by the collider experiments at HERA. The impressive improvement of the precision of the proton structure function F_2 in the last ten years is described. New measurements of F_2 extending the phase space towards small momentum transfers Q^2 are introduced. The analysis of the gluon density, and the precise extraction of α_s is discussed. Important cross-checks as the extrapolation of the charm structure function F_2^c , and different ways to determine the longitudinal structure function F_L are depicted. This is followed by a discussion of the F_2 measurements at very small momentum transfers. The analysis of the derivatives of F_2 is described. The high Q^2 cross sections and the structure function xF_3 are presented with regard to the potential to extract the valence quark distributions.

The second part of the talk is devoted to measurements of cross sections of event classes where a second scale besides Q^2 becomes important. An interpretation in terms of the resolved photon in deep inelastic scattering is discussed.

The third part of the talk is dedicated to an outlook of in the HERA II running phase, prediction for measurements and improvements in precision are presented.

Measurements of the structure of proton and virtual photon at HERA

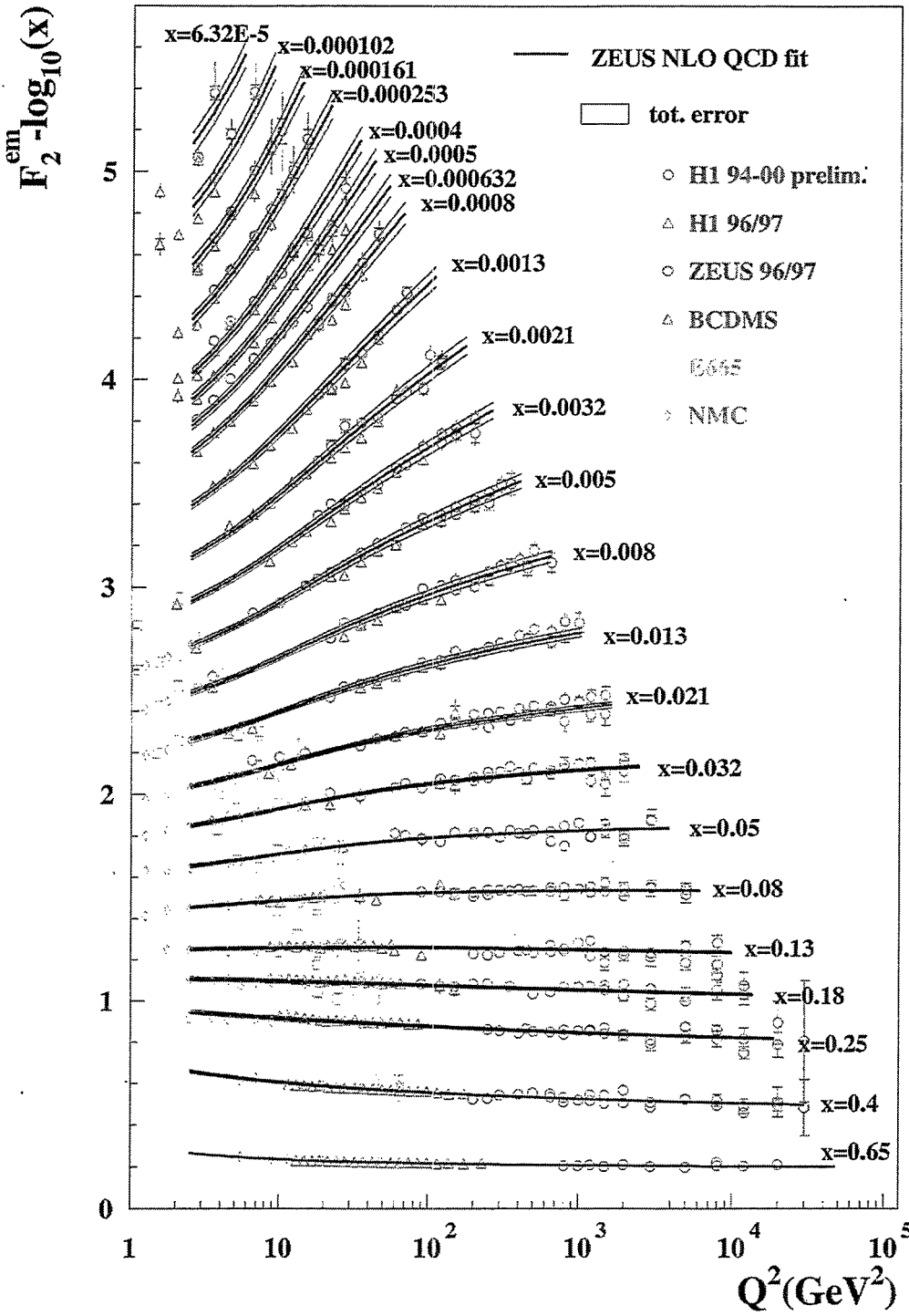
Stefan Schlenstedt (DESY Zeuthen)

Outline

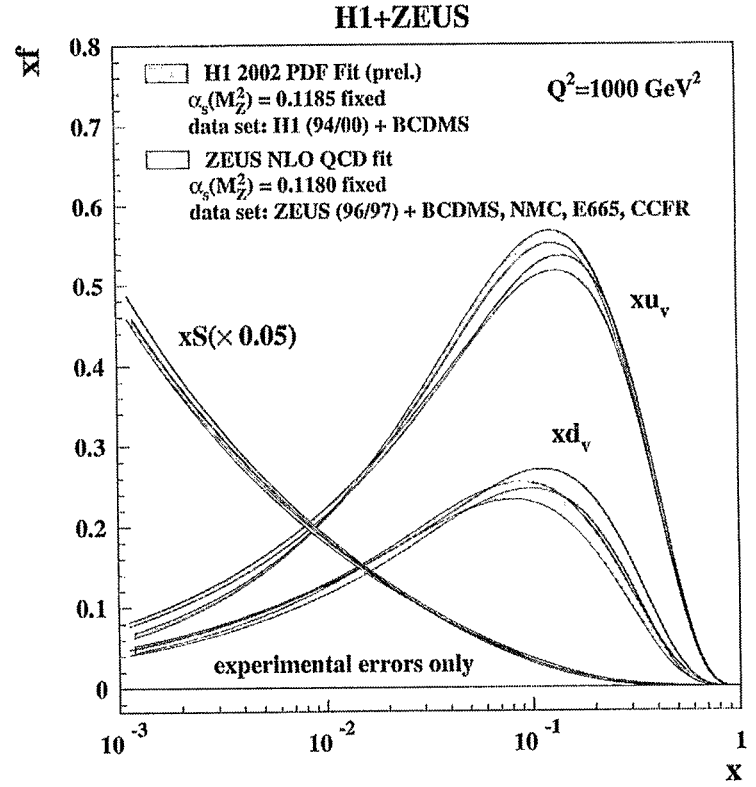
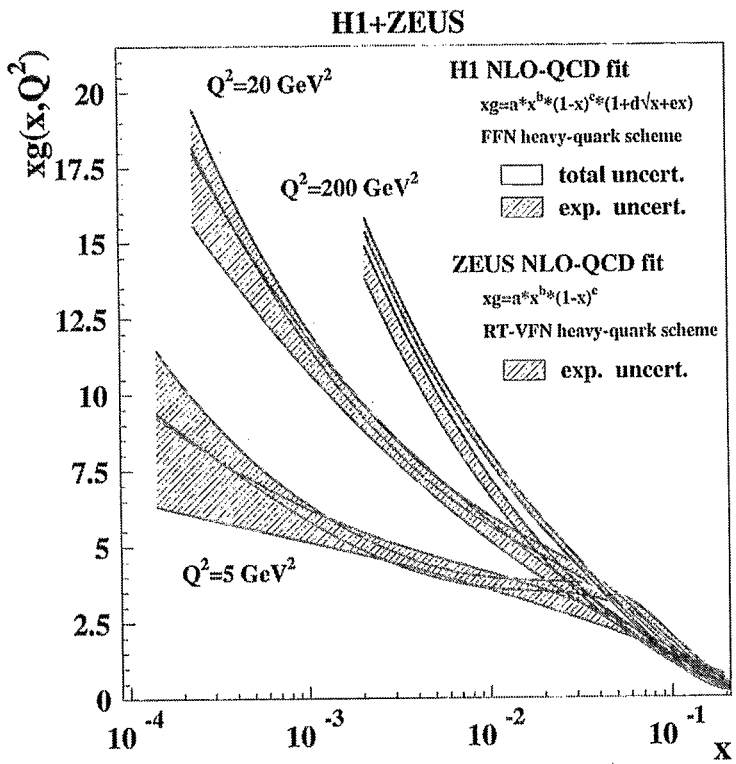
- ▷ Introduction
- ▷ The proton structure
 - The structure function F_2 at medium Q^2
 - Gluon density and charm in the proton
 - The longitudinal structure function F_L
 - Extraction of α_s
 - xF_3 from high Q^2 neutral current events
 - Charged current interactions
 - Lowest Q^2 's
- ▷ The virtual photon
 - Forward particles and jets
 - Photon structure and remnant
 - Virtual photons
- ▷ Summary and outlook

F₂ scaling violation

HERA F₂



Comparison and PDF fits



Summary and Outlook

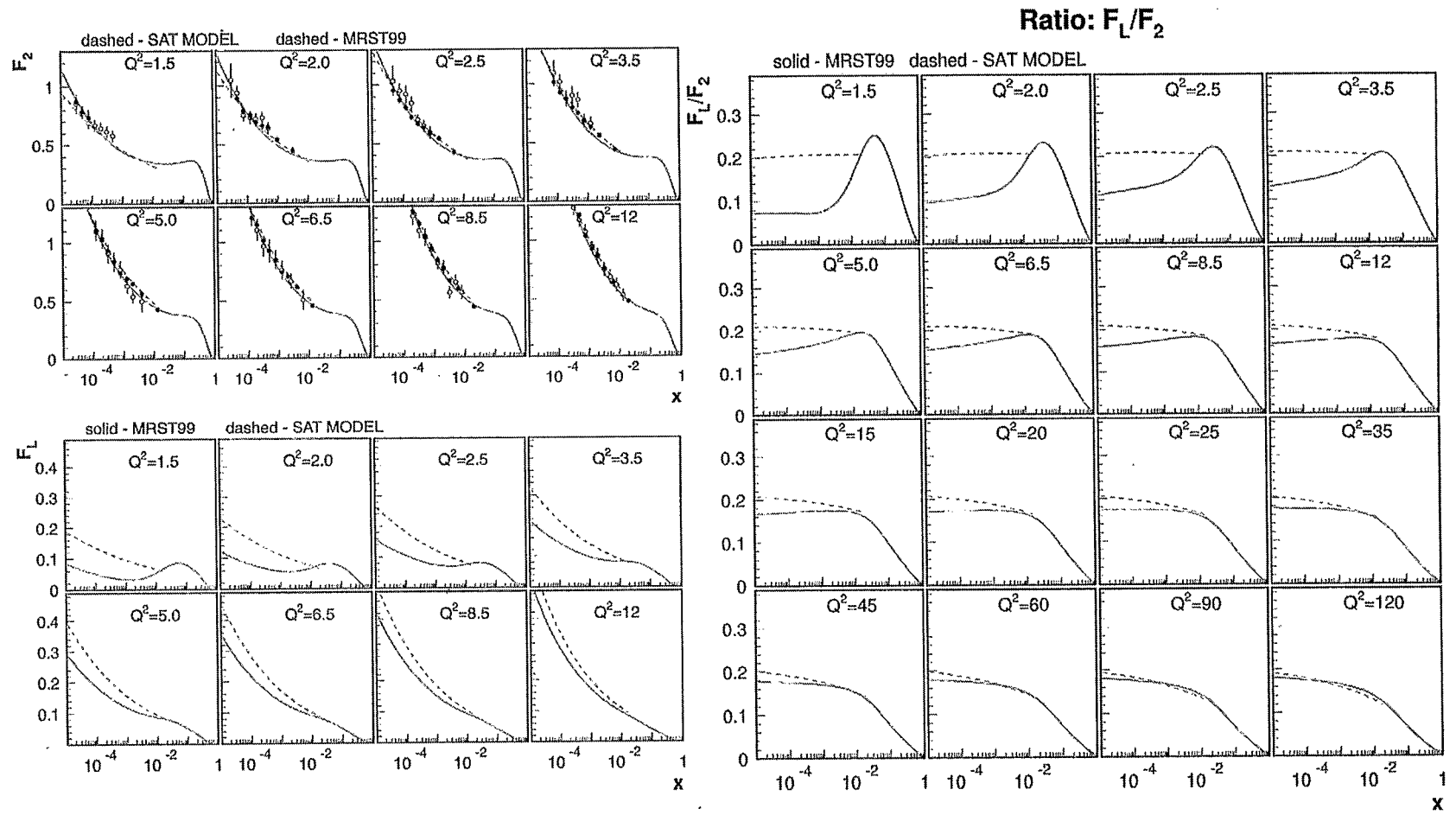
- The HERA collider experiments H1 and ZEUS are working since 1992 and exploit and extend their detector(s) with better and better understanding
- HERA physics reveals unique knowledge of the proton structure and the QCD at high parton densities
- The structure of the virtual photon is investigated
- The HERA program is rich: there are many other unique and competitive results of QCD, diffraction, heavy flavour physics, real photon structure and beyond the Standard Model
- HERA's goal is to deliver 1 fb^{-1} with polarized electrons (positrons) between 2002-06 mainly for high Q^2 physics

HERA Parameters			
	1997	Design	Upgrade
p beam energy (GeV)	820	820	820*
e beam energy (GeV)	27.5	30	30†
Number of bunches	180/189	210	180/189
Number of protons/bunch	7.7×10^{10}	10×10^{10}	10×10^{10}
Number of electrons/bunch	2.9×10^{10}	3.6×10^{10}	4.2×10^{10}
Proton current (mA)	105	160	140
Electron current (mA)	43	58	58
Hor. proton emittance (nm rad)	5.5	5.7	5.7
Hor. electron emittance (nm rad)	40	39	22
Proton beta function x/y (m)	7/0.5	10/1	2.45/0.18
Electron beta function x/y (m)	1/0.7	2/0.7	0.63/0.26
beam size $\sigma_x \times \sigma_y$ (μm)	200×54	247×78	118×32
Synchrotron Rad. at IP (kW)	6.9	9.7	25
Specific luminosity ($\text{cm}^{-2} \text{s}^{-1} \text{mA}^{-2}$)	7.6×10^{29}	3.4×10^{29}	1.64×10^{30}
Luminosity ($\text{cm}^{-2} \text{s}^{-1}$)	1.4×10^{31}	1.5×10^{31}	7.36×10^{31}

* Possible increase to 920 GeV, tests in 1997 and 1998

† 30 GeV maximum energy assumed for background calculation

Different F_L predictions



F_2 is described by both calculation/ fits
 F_L seems to be much more sensitive

Calculation by K Golec-Biernat

Helicity Selection and Semi-Exclusive Meson Production

J. Lenaghan
The Niels Bohr Institute

The Size of $\gamma u \rightarrow \pi^+ d$

The semiexclusive cross section is

$$(1) \frac{d\sigma}{dt} (\gamma p \rightarrow \pi^+ Y) = \sum_{q=u,d} f_{q/p}(x) \frac{d\hat{\sigma}}{dt} (\gamma q \rightarrow \pi^+ q')$$

$$(2) \frac{d\hat{\sigma}}{dt} = \frac{256\pi^2 \alpha \alpha_s^2 (e_u - e_d)^2}{27\hat{s}^2 |t|} \left\{ \int_0^1 \frac{dz}{z^2} \phi_\pi(z) \right\}^2$$

There is presently ~~no~~ data for $\gamma p \rightarrow \pi^+ Y$ in the semi-exclusive kinematic limit.

↪ Assumes a compact valence Fock state $\sim \mathcal{O}(1/\sqrt{E})$

However, the measured $\gamma p \rightarrow \pi n$ cross section is so large that Bloom-Gilman duality would have to fail by 2 orders of magnitude!

Eden, Hoyer, Khodjamirian

⇒ (1) seriously underestimates the cross section due to lack of color transparency.

- Use the γ virtuality as a probe of the subprocess size

- The cross section should be independent of Q^2 when the scattering region is small compared to $1/Q$.

$\frac{d\hat{\sigma}}{dt}(\gamma u \rightarrow \pi^+ d)$ is finite for $Q^2 \rightarrow 0$;
 however, its slope is logarithmically infinite.

$$M_{u, \pi^+}^{AB}(\gamma^* u \rightarrow u \bar{d} \pi^+) = S_{AB} \int_0^1 dz \left[H_{u, \pi^+}^{+-}(z) - H_{u, \pi^+}^{-+}(z) \right] \phi_{\pi}(z)$$

$$H_{u, \pi^+}^{+-} = -\frac{2T_2 e(4\pi\alpha_s) C_F}{1-t} \left\{ \frac{e u}{z - \bar{z} Q^2/t} - \frac{e \bar{z}}{z(\bar{z} - z Q^2/t)} \right\}$$

→ Since $\phi_{\pi} \approx z(1-z)$, the integral is not enhanced near $z=0, 1$.

- BL factorization fails in this endpoint region.

The subprocess is not transversally compact:

$$\frac{1}{|\vec{l}_u|} = \frac{1}{|z\vec{k} + \vec{F}|} \sim \mathcal{O}(1/\Lambda_{QCD})$$

- Large only when γ couples to slow quark since

$$z \approx 1 - \frac{\Lambda_{QCD}}{\sqrt{s}} \implies l_u^2 \approx \frac{s}{4} \\ l_q^2 \approx \frac{s}{4} \frac{1-z}{1+z}$$

The V.M. should be longitudinally polarized since quark helicity is conserved at all vertices.

!!! The data show over the full t -range that the p has a transverse polarization!!!

BL factorization then implies a quark helicity flip with a $\frac{m_q^2}{|t|}$ suppression factor,
i.e. $n=4$.

Puzzle: a) Data consistent w/ $n=3$
b) ϕ/p flavor symmetry indicates an insensitivity to m_q^2 .
c) p carries the δ -helicity

Consider the form of the factorized amplitude:

$$M_{\mu, \lambda \lambda'}^{vv'}(Ng \rightarrow pg) = \int_0^1 dz G_{\mu, \lambda \lambda'}^{vv'}(z) \Phi_{\rho}^{\delta}(z)$$

$$\delta \equiv \frac{v v'}{z}$$

No quark helicity flip:

$$G_{\mu, \lambda \lambda'}^{+-} = \frac{\sqrt{2} e e_q}{\sqrt{3} \sqrt{-t}} \frac{Q^2 / (-t)}{z \bar{z}} \frac{4\pi \kappa_s}{(z - \bar{z} Q^2 / t - m_q^2 / t)(\bar{z} - z Q^2 / t - m_q^2 / t)}$$

Vanishes in photoproduction ($Q^2 = 0$)

Helicity flip amplitude:

$$G_{\mu, \lambda \lambda'}^{++} = \frac{-\sqrt{2} e e_q 4\pi \kappa_s}{\sqrt{3} \sqrt{-t}} \frac{\sqrt{m_q^2 / (-t)}}{z \bar{z} (z - m_q^2 / t)(\bar{z} - m_q^2 / t)}$$

$$= \frac{-\sqrt{2} e e_q 4\pi \kappa_s}{\sqrt{3} \sqrt{-t}} \frac{\sqrt{m_q^2 / (-t)}}{(z \bar{z})^2} \left\{ 1 + \mathcal{O}\left(\frac{m_q^2}{t}\right) \right\}$$

→ Enhances endpoints for D.A. which vanishes linearly at endpoints!

The Drell-Hearn-Gerasimov sum-rule at EIC

Steven D. Bass

HEP Group, Institute for Experimental Physics and Institute for Theoretical Physics, Universität Innsbruck, Technikerstrasse 25, A-6020 Innsbruck, Austria

Future measurements of the spin dependent part of the total γp cross-section at large values of the real-photon proton centre of mass energy $s_{\gamma p}$ will help to constrain the high-energy part of the fundamental Drell-Hearn-Gerasimov sum-rule. Exploring the “transition region” in g_1 – varying Q^2 between 0.01 and 1 GeV² – would yield valuable new constraints on the transition between the realms of Regge predictions and hard-scale perturbative QCD dynamics.

The DHG sum-rule is derived from fundamental principles plus the single assumption that the spin-dependent part of the forward Compton amplitude satisfies an unsubtracted dispersion relation. Failure of the sum-rule would imply a subtraction constant (“subtraction at infinity”), challenging our understanding of spin dependent phenomena in QCD. Given the fundamental nature of the DHG sum-rule, it is very important to measure the high-energy Regge contribution. The EIC could measure $(\sigma_A - \sigma_P)$ between $20 < s_{\gamma p}^{1/2} < 90$ GeV – considerably extending the first measurements planned at SLAC (up to 9 GeV centre of mass energy).

The transition region for g_1 is particularly interesting because much larger changes are expected in the effective intercept λ which describes the shape of the structure functions at small Bjorken x , ($f(x, Q^2) \sim x^{-\lambda}$), in g_1 than in the unpolarized structure function F_2 which has been extensively studied at HERA. The effective intercept changes between 0.1 and 0.35 for unpolarized data as we increase Q^2 from zero to about 100 GeV². For g_1 , the corresponding change $\delta\lambda$ may be as much as five times larger, yielding new opportunities to study the transition region and new challenges for models which aim to describe the Regge to hard Q^2 transition. Open questions which may be addressed with the EIC are: At which Q^2 does the effective intercept for g_1 start to grow? What is the rate of growth with increasing Q^2 ? Where in Q^2 will perturbative QCD start to describe future g_1 data at small x ?

With appropriate small angle tagging detectors in both the electron and proton direction at the EIC very precise data on low Q^2 asymmetries can be collected. The high luminosity of the EIC makes it the optimal proposed polarized ep collider to perform these measurements. The use of deuteron beams with spectator tagging could help to disentangle different exchange contributions in the Regge regime.

For a detailed study, see: S.D. Bass and A. De Roeck, Eur. Phys. J C18 (2001) 538.

SDB, A De Roeck
EPJ C18 (2001)

The DHEG sum-rule at EIC

g_1 @ low x and low Q^2 with EIC

Steven Bass

Physics issues

• DHEG sum-rule at $Q^2 = 0$

$$\int_{\nu_{th}}^{\infty} \frac{d\nu}{\nu} \Delta\sigma(\nu) = -\frac{2\pi^2 dK^2}{m^2}$$

Assuming no "subtraction @ ∞ " ($J=1$ Regge fixed)

Constrain high-energy part of sum-rule

• Regge \rightarrow perturbative QCD transition @ low Q^2

$$g_1 \sim x^{\alpha_{eff}}$$

$$\Delta \alpha_{eff}^{spin} \sim 5 \Delta \alpha_{eff}^{(F_2)}$$

how fast? what Q^2 ?

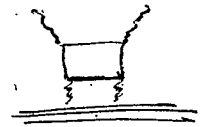
Low x , low Q^2

Unpolarized

$$\sigma_{tot}^{\gamma^* P}(s, Q^2) = \frac{M_0^2}{M_0^2 + Q^2} \left(A_R s^{\alpha_R - 1} + A_P s^{\alpha_P - 1} \right)$$

$M_0^2 \rightarrow 52 \pm 0.4 \text{ GeV}^2$
 $\alpha_R \rightarrow +0.5$
 $A_R \rightarrow 147.8 \pm 4.6 \mu\text{b}$
 $\alpha_P \rightarrow 1.102 \pm 0.007$
 $A_P \rightarrow 62.0 \pm 2.3 \mu\text{b}$

Polarized Regge



$$\sigma_A - \sigma_P \sim N_3 s^{\alpha_{a_1} - 1} + N_0 s^{\alpha_{f_1} - 1} + N_g \frac{\ln s/\mu^2}{s} + \dots$$

$$\Delta\sigma \approx \frac{4\pi^2\alpha}{r} g_1$$

$$f_1 \sim \alpha^{-1}$$

$$g_1 \sim N_3 \alpha^{-1} + N_g \dots$$

$\alpha^2 = ?$

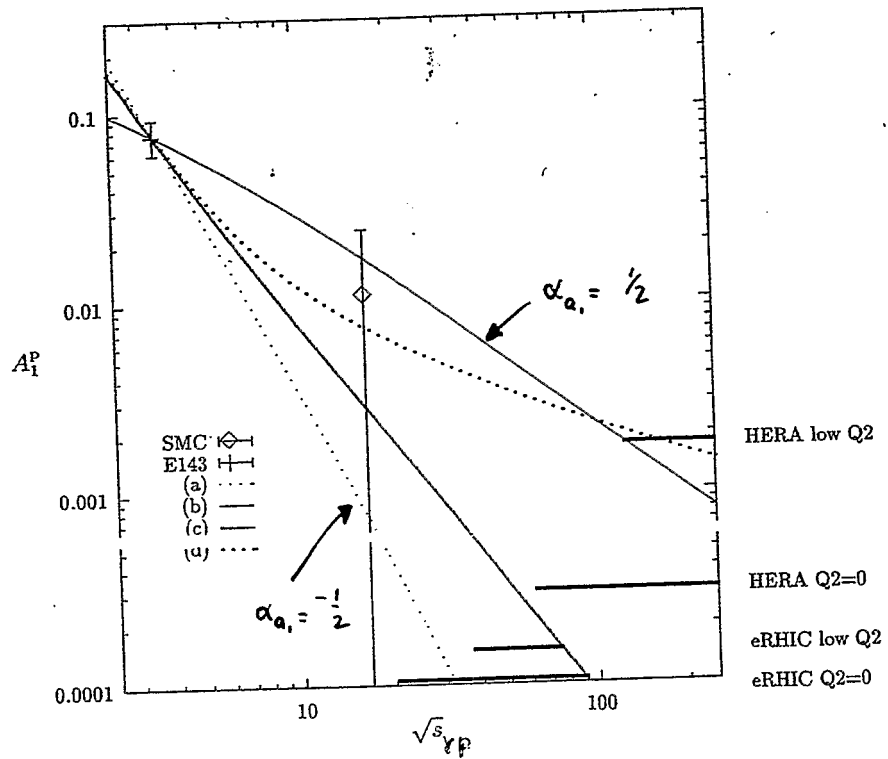
Straight, parallel Regge trajectories

$$\Rightarrow \alpha_{a_1} \approx \alpha_{f_1} \approx -0.4$$

$$\sigma_A - \sigma_P \approx \frac{4\pi^2\alpha}{r} g_1$$

α^2

Estimating asymmetries



Reggè

$$\Delta\sigma = N_3 s^{\alpha_{a_1}-1} + N_0 s^{\alpha_{f_1}-1} + N_g \frac{\ln s/\mu^2}{s} + N_p \frac{1}{\ln^2 s/\mu^2}$$

Isotriplet

$$N_3^p = -N_3^n$$

Isosinglet

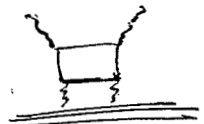
Low x , low Q^2

Unpolarized

$$\sigma_{tot}^{\gamma^*P}(s, Q^2) = \frac{M_0^2}{M_0^2 + Q^2} \left(A_R s^{\alpha_R - 1} + A_P s^{\alpha_P - 1} \right)$$

$M_0^2 = 52 \pm 0.4 \text{ GeV}^2$
 $\alpha_R = +0.5$
 $A_R = 147.8 \pm 4.6 \mu\text{b}$
 $\alpha_P = 1.102 \pm 0.007$
 $A_P = 62.0 \pm 2.3 \mu\text{b}$

Polarized Regge



$$\sigma_A - \sigma_P \sim N_3 s^{d_{a_1} - 1} + N_0 s^{d_{f_1} - 1} + N_g \frac{\ln s/\mu^2}{s} + \dots$$

$$\Delta\sigma \pm \frac{4\pi^2\alpha}{v} g_i$$

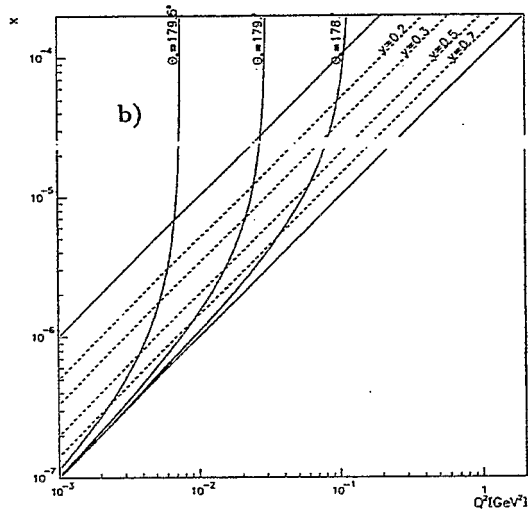
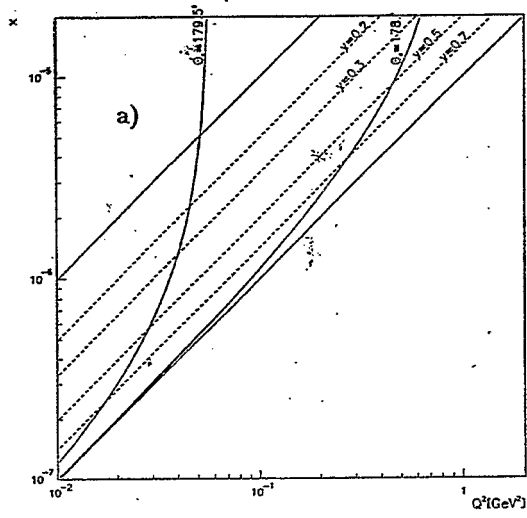
$$g_i \sim N_i x^{-d_i}$$

$\left. \begin{matrix} \text{Regge} \\ \text{} \end{matrix} \right\} \alpha^2 = ?$

Straight, parallel Regge trajectories

$$\sigma_A - \sigma_P \pm \frac{4\pi^2\alpha}{v} s$$

Kinematics



Conclusions and Opportunities

- EIC optimal polarized ep collider to explore transition region @ low x , low Q^2

Regge \rightarrow hard Q^2 physics

Large effects expected

$$\Delta\alpha_{\text{eff}}^{\text{spin}} \sim 5 \Delta\alpha_{\text{eff}}^{(F_2)}$$

E.g. $g_1^{p,n} \sim x^{0.4} \xrightarrow{\text{Regge}} x^{-1/2}$
SLAC "low x "

EP strategy: measure with decreasing Q^2 until A_1 "disappears"

New constraints for models

- Drell-Hearn-Gerasimov Sum-rule

Important to measure high-energy part

? Does sum-rule work?

If not, new non-perturbative phenomenon

ΔG at RHIC-SPIN via Double J/ψ Production

JIRO KODAIRA

*Dept. of Physics, Hiroshima University
Higashi-Hiroshima 739-8526, JAPAN*

Abstract

The major emphasis and strength of RHIC-Spin is to measure the gluon polarization, so it is important and interesting to investigate various processes which are attainable experimentally to this aim. In this talk, I want to show that the double heavy quarkonium production in the polarized proton-proton collision would provide an ideal means of detecting the polarized gluon distributions, and which may at least play a supplemental role to the presently proposed program at RHIC to this end. It should be stressed that the double quarkonium production has several advantage over the single quarkonium production in reducing the theoretical uncertainties. (1) By considering double production, the relativistic corrections and color-octet uncertainties are reasonable highly suppressed. (2) The total contribution from the higher excited states are also doubly suppressed. (3) The higher order QCD correction can be well controlled by applying a suitable p_T cut for the Charmonium system. (4) Since the prevailing partonic process is the gluon-gluon fusion into double quarkoniums, it stands as very sensitive method in measuring the gluon polarization. In the RHIC energy region, and for the $p-p$ collision, the $q\bar{q}$ initiated process might be negligible.

After giving an analytical expression for the polarized process (new result), we show the numerical result for the asymmetry,

$$\begin{aligned} A &\equiv \frac{d\sigma(p_+p_+ \rightarrow J/\psi J/\psi) - d\sigma(p_+p_- \rightarrow J/\psi J/\psi)}{d\sigma(p_+p_+ \rightarrow J/\psi J/\psi) + d\sigma(p_+p_- \rightarrow J/\psi J/\psi)} \\ &= \frac{\int dx_1 dx_2 d\Delta\hat{\sigma}\Delta G(x_1, Q^2)\Delta G(x_2, Q^2)}{\int dx_1 dx_2 d\hat{\sigma}G(x_1, Q^2)G(x_2, Q^2)} \end{aligned}$$

Our study shows that the asymmetry measurement at RHIC-SPIN experiments is pretty realistic to extract the polarized gluon distribution function $\Delta G(x)$.

ΔG at RHIC-SPIN via Double J/ψ Production

J.Kodaira (Hiroshima)

hep-ph/0207318
at RBRC Workshop
August 2002

Double spin asymmetry for J/ψ pair productions at
RHIC-SPIN is investigated.
Asymmetry measurement is pretty realistic to extract
 $\Delta G(x)$.

1. Major Emphasis and Strength of RHIC-Spin

Polarized Gluon Distribution

2. Double Heavy Quarkonium Production

Some Advantage

3. Numerical Studies

Feasibility

in collaboration with

C.- F. Qiao (Hiroshima)

♣ Double Heavy Quarkonium Production

Some advantages
in reducing the theoretical uncertainties

1. Relativistic corrections and color-octet uncertainties
→ highly suppressed
2. Total contribution from the higher excited states
→ doubly suppressed
3. Higher order QCD correction
→ well controlled
with suitable p_T cut for
Charmonium system
4. Prevailing partonic process is gluon-gluon fusion
in RHIC energy region, and for $p - p$ collision
 $q\bar{q}$ initiated process is negligible

Similar analyses so far

- S.P. Baranov and H. Jung, Z. Phys. C**66**, 467 (1995)
- T. Gehrmann, Phys. Rev. D**53**, 5310 (1996)

Main emphasis were not on RHIC physics
Analytical expressions were not given

The polarized partonic differential cross section

$$\begin{aligned}
\frac{d\Delta\hat{\sigma}}{dt} = & \frac{-16\alpha_s^4\pi|R(0)|^4}{81s^8(m^2-t)^4(m^2-u)^4} \times [2744m^{24} - 15240m^{22}(t+u) \\
& + m^{20}(32110t^2 + 90076tu + 32110u^2) \\
& - 16m^{18}(2025t^3 + 12673t^2u + 12673tu^2 + 2025u^3) \\
& + 2t^4u^4(349t^4 - 908t^3u + 1374t^2u^2 - 908tu^3 + 349u^4) \\
& + 4m^{16}(3903t^4 + 57292t^3u + 117766t^2u^2 + 57292tu^3 + 3903u^4) \\
& - 4m^{14}(510t^5 + 36713t^4u + 135685t^3u^2 + 135685t^2u^3 + \\
& \quad + 36713tu^4 + 510u^5) \\
& + m^{12}(-1461t^6 + 58600t^5u + 364313t^4u^2 \\
& \quad + 594840t^3u^3 + 364313t^2u^4 + 58600tu^5 - 1461u^6) \\
& + 4m^2t^2u^2(9t^7 - 505t^6u + 44t^5u^2 - 556t^4u^3 \\
& \quad - 556t^3u^4 + 44t^2u^5 - 505tu^6 + 9u^7) \\
& + 2m^{10}(381t^7 - 7111t^6u - 83783t^5u^2 - 180639t^4u^3 \\
& \quad - 180639t^3u^4 - 83783t^2u^5 - 7111tu^6 + 381u^7) \\
& + m^8(-79t^8 + 1272t^7u + 54526t^6u^2 + 156224t^5u^3 \\
& \quad + 163850t^4u^4 + 156224t^3u^5 + 54526t^2u^6 + 1272tu^7 - 79u^8) \\
& + m^4tu(-36t^8 + 1471t^7u + 9764t^6u^2 + 12863t^5u^3 \\
& \quad + 7196t^4u^4 + 12863t^3u^5 + 9764t^2u^6 + 1471tu^7 - 36u^8) \\
& - 2m^6(2t^9 + 17t^8u + 5151t^7u^2 + 25947t^6u^3 + 24439t^5u^4 \\
& \quad + 24439t^4u^5 + 25947t^3u^6 + 5151t^2u^7 + 17tu^8 + 2u^9)].
\end{aligned}$$

♣ Numerical Studies

Parameters

- $\sqrt{s} = 500 \text{ GeV}$
- Scale Q^2
 $Q^2 = p_T^2$ for p_T distributions.
 $Q^2 = m^2$ for angular dist. and total
- $m = 2 m_c$ with $m_c = 1.5 \text{ GeV}$
- $|R(0)|^2 = 0.8 \text{ GeV}^3$

Total cross section

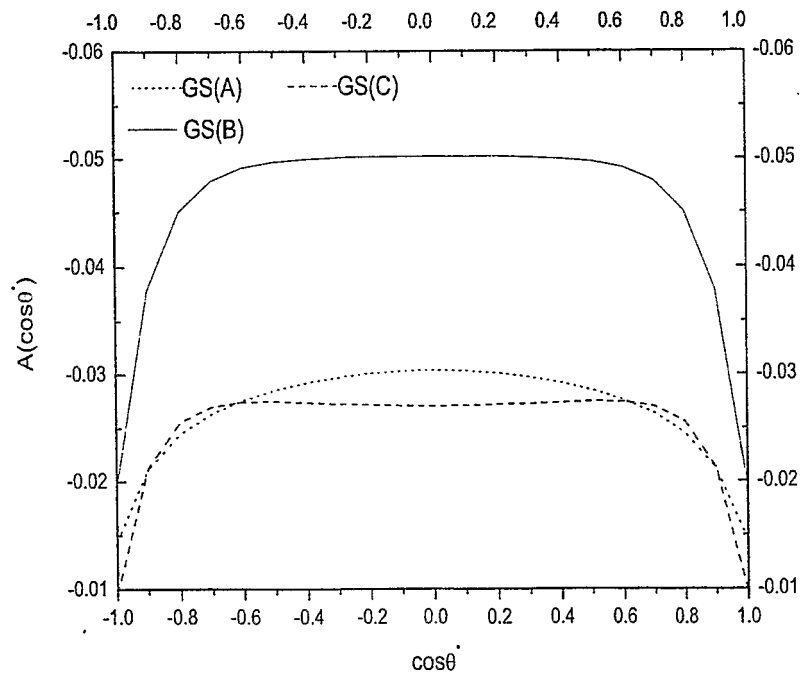
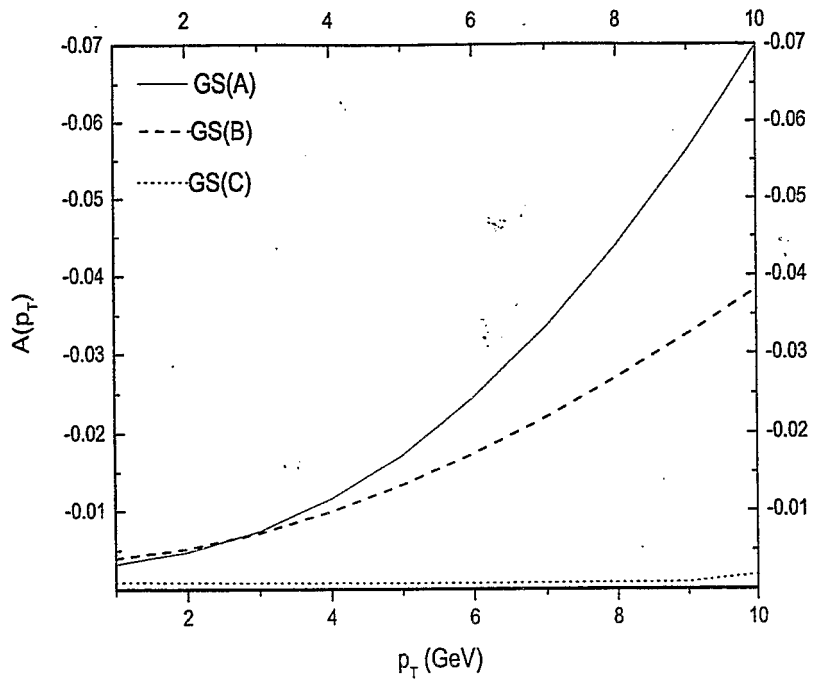
	$\sigma_{\mu^+\mu^-}^{tot}$	$\sigma_{\mu^+\mu^-}(p_T > 1 \text{ GeV})$
CTEQ5L	11.8 pb	7.3 pb
MRST	6.5 pb	4.3 pb
GRV	7.4 pb	4.7 pb

NOTE

$$B(\psi \rightarrow \mu^+\mu^-) = 0.0588$$

is included

- For the time being $\sigma_{\mu^+\mu^-} \approx 10 \text{ pb}$
- Accumulated luminosity $800 \text{ pb}^{-1} \rightarrow \text{ENOUGH!!}$
 In the next run?



Perturbative Aspects of Azimuthal Asymmetries in Polarized ep

K.A. Oganessyan ^{1,2}

¹ *LNF-INFN, I-00040, Enrico Fermi 40, Frascati, Italy*

² *DESY, Notkestrasse 85, 22603 Hamburg, Germany*

E-mail: kogan@mail.desy.de

Abstract

It is widely recognized that the study of azimuthal asymmetries in hard scattering processes provide interesting variables to study of both the non-perturbative and perturbative effects. In particular, for testing pQCD through azimuthal asymmetries in polarized ep at high Q^2 the following asymmetries are of interest:

- unpolarized azimuthal asymmetries, $\cos\phi$, $\cos 2\phi$ – a good test of pQCD at $\mathcal{O}(\alpha_S^{(1)})$.
- Single spin (beam/target) azimuthal asymmetries: may appear only at $\mathcal{O}(\alpha_S^{(2)})$ - clear evidence for the existence of the three-gluon coupling.
- Double-spin azimuthal asymmetries, $\cos\phi$, $\cos 2\phi$ ($\mathcal{O}(\alpha_S^{(1)})$) - another way for testing pQCD.

These asymmetries, from the point of view of future collider and fixed target facilities, are discussed in detail.

Perturbative Aspects of Azimuthal Asymmetries in Polarized ep

K.A. Oganessyan

INFN – Laboratori Nazionali di Frascati

DESY – Deutscher Electronen Synchrotron

Current and future directions at RHIC

August 5-23, 2002

A RIKEN BNL Research Center

- Azimuthal Asymmetries
 - ⇒ Kinematics
 - ⇒ Parity Invariance
- Testing pQCD Through Azimuthal Asymmetries
 - ⇒ Non-perturbative (brief) & pQCD Aspects
 - ⇒ Spin-independent asymmetries
 - ⇒ Double-spin asymmetries
 - ⇒ Single (beam/target) spin asymmetries



Azimuthal asymmetries in Hard Scattering Processes

Parity Invariance

Single-spin azimuthal asymmetries

$$A_S(\phi) = N^+(\phi) - N^-(\phi)$$

$$\Downarrow$$
$$ODD \equiv \sum_{m=1} \delta N^{(m)} \sin m\phi$$

Double-spin azimuthal asymmetries

$$A_{\lambda S}(\phi) = N^{++}(\phi) + N^{--}(\phi) - N^{+-}(\phi) - N^{-+}(\phi)$$

$$\Downarrow$$
$$EVEN \equiv \sum_{m=0} \Delta N^{(m)} \cos m\phi$$

$$A_{\lambda S}(\phi) = N^{++}(\phi) + N^{--}(\phi) + N^{+-}(\phi) + N^{-+}(\phi)$$

$$\Downarrow$$
$$EVEN \equiv \sum_{m=0} N^{(m)} \cos m\phi$$

Spin-independent $\cos 2\phi \Rightarrow F_L(x, Q^2)$

T. Gehrmann, PLB 480 (2000) 77.

The coefficient of $\cos 2\phi$ is proportional to $F_L(x, Q^2)$ and the second moment (with respect to \hat{z}) of $\cos 2\phi$ asymmetry will look like

$$A_{(2)}^{\cos 2\phi} \equiv \frac{\sum_h \int_0^1 dz \int_0^{2\pi} d\phi \cos 2\phi d\sigma}{\sum_h \int_0^1 dz \int_0^{2\pi} d\phi d\sigma}$$
$$= \frac{1}{2} \frac{(1-y)F_L(x, Q^2)}{(1+(1-y)^2)F_2(x, Q^2) - y^2F_L(x, Q^2)}$$

↓

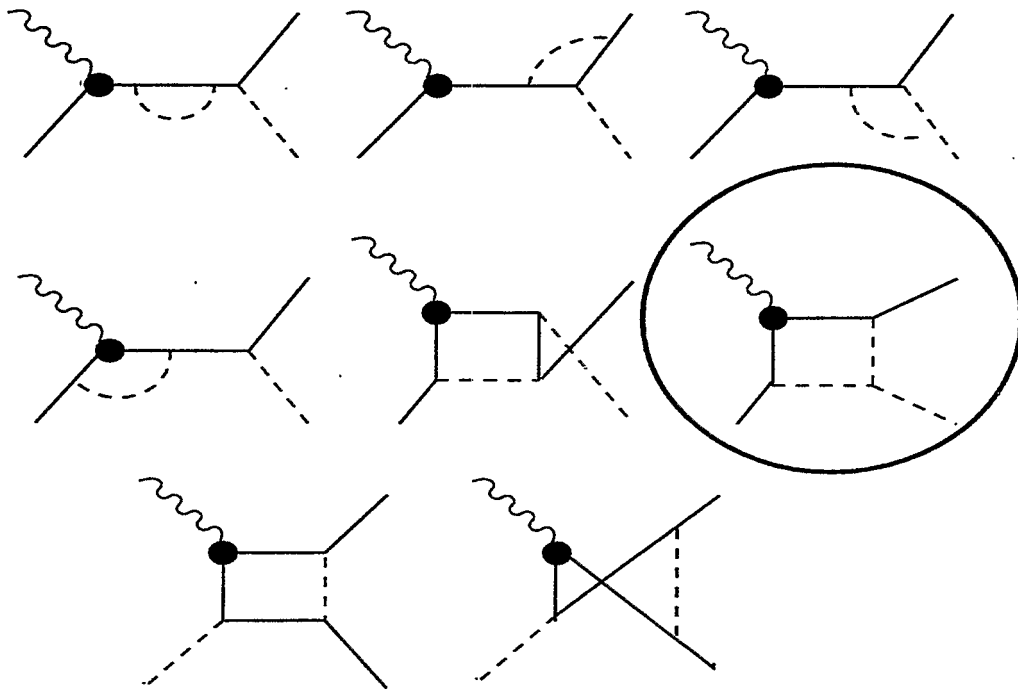
$$\frac{F_L(x, Q^2)}{F_2(x, Q^2)}$$

Single-Spin Azimuthal Asymmetries

- Longitudinally polarized beam; UNpolarized target

pQCD aspect

K.Hagiwara, K. Hikasa, N. Kai, PRD 27 (1983) 84.



Highly sensitive to the gluon self-coupling

⇒ observation of the asymmetry with the expected sign should provide clear evidence for the existence of the three-gluon coupling

Azimuthal asymmetries \Leftarrow EIC

- Wide range of collision energies:
 \Rightarrow NP + pQCD effects

$$\langle W \rangle = \frac{\int d\phi W \cdot [d\sigma^{np} + d\sigma^{\alpha^m S}]}{\int d\phi \cdot [d\sigma^{np} + d\sigma^{\alpha^m S}]}$$

$$W = \cos \phi, \cos 2\phi, \sin \phi, \sin 2\phi$$

- Polarization of electron and proton spins:

\Rightarrow measurement of different asymmetries simultaneously:

$$A_{\cos m\phi} \equiv \frac{[d\sigma^{\rightarrow\leftarrow} + d\sigma^{\leftarrow\Rightarrow}] - [d\sigma^{\rightarrow\Rightarrow} + d\sigma^{\leftarrow\leftarrow}]}{d\sigma^{\rightarrow\leftarrow} + d\sigma^{\leftarrow\Rightarrow} + d\sigma^{\rightarrow\Rightarrow} + d\sigma^{\leftarrow\leftarrow}}$$

$$A(\sin m\phi) = \frac{[d\sigma^{\rightarrow\leftarrow} - d\sigma^{\leftarrow\leftarrow}] - [d\sigma^{\leftarrow\Rightarrow} - d\sigma^{\rightarrow\Rightarrow}]}{[d\sigma^{\rightarrow\leftarrow} - d\sigma^{\rightarrow\Rightarrow}] - [d\sigma^{\leftarrow\Rightarrow} - d\sigma^{\leftarrow\leftarrow}]}$$

- Luminosity:
 \Rightarrow High precision

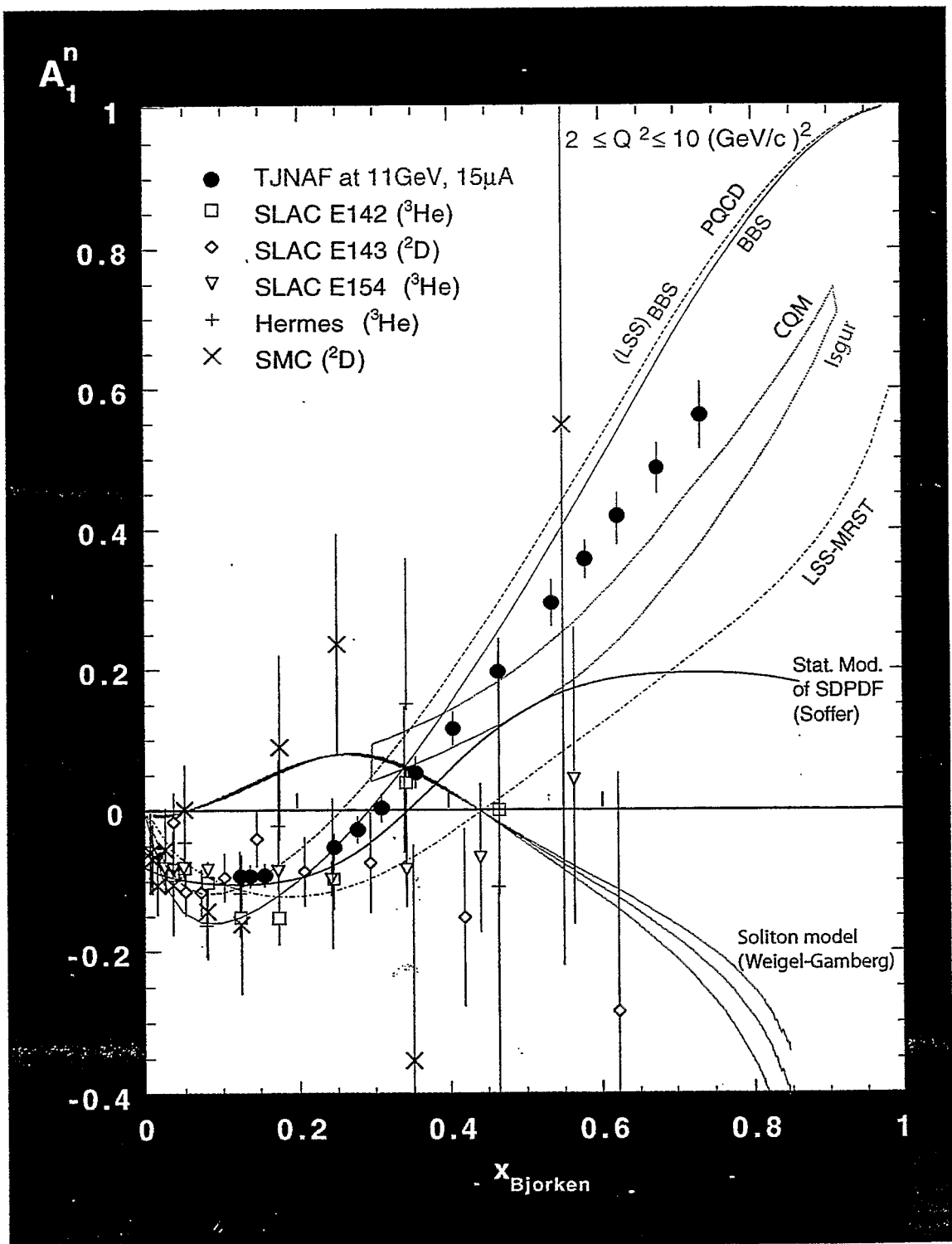
Nucleon spin physics at Jefferson Lab using the 12 GeV upgrade

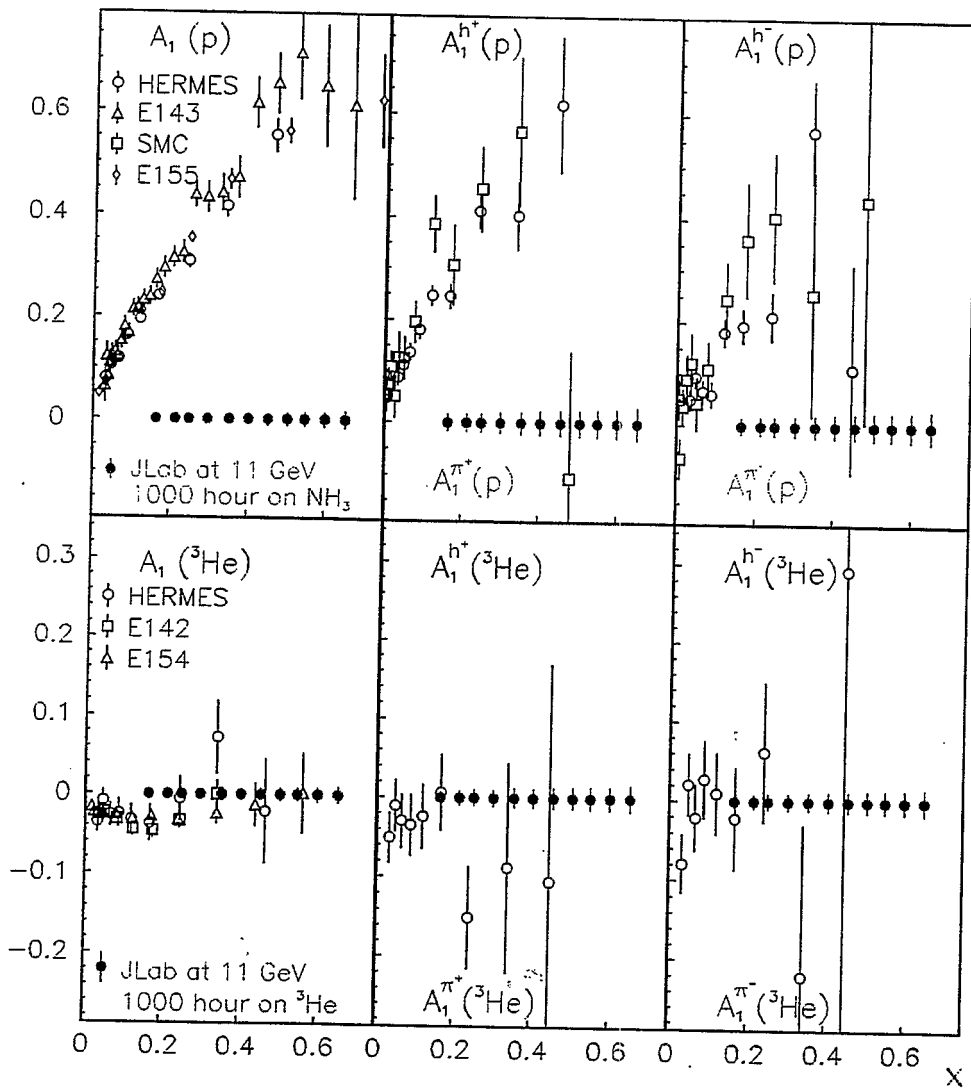
Z.E. Meziani
Temple University

- Nucleon spin and flavor structure in the valence quark region.
- Twist-three matrix element d_2 : electric and magnetic polarizabilities of the color field.
- Single spin asymmetries in semi-inclusive; A quest for transversity.
- Precision measurement of the Q^2 evolution of the extended GDH, the BC and the Bjorken sum rules.

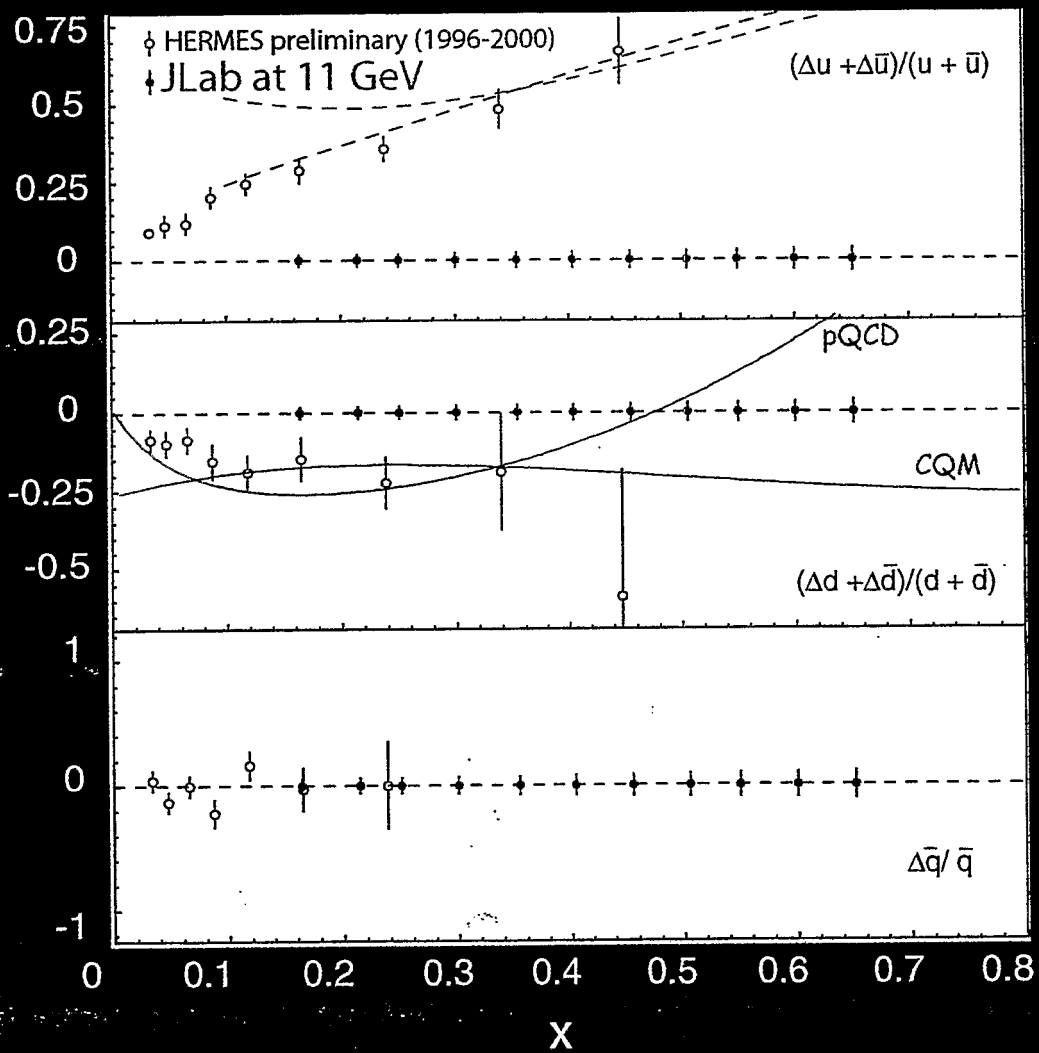
August 23, 2002

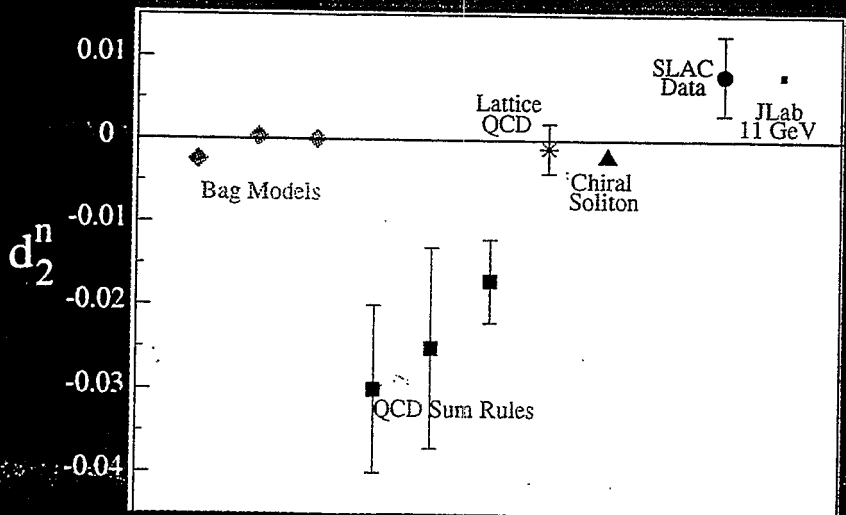
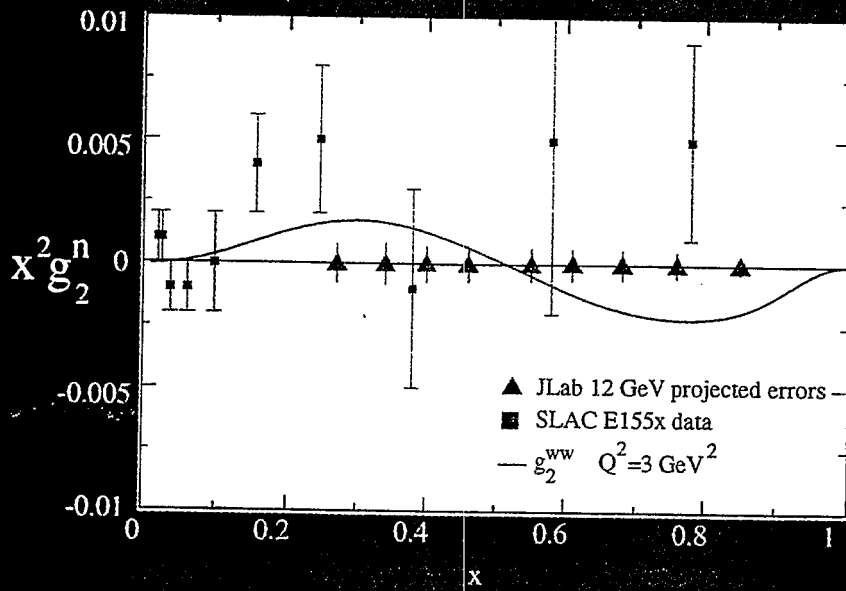
Current and Future Directions at RHIC





VALENCE SPIN STRUCTURE USING SEMI-INCLUSIVE DEEP INELASTIC SCATTERING





Current and Future Directions at RHIC

August 5-23, 2002

REGISTERED PARTICIPANTS

Christine Aidala	Physics – 510A Brookhaven National Laboratory Upton, NY 11973-5000	caidala@bnl.gov
Sam Aronson	Physics – 510A Brookhaven National Laboratory Upton, NY 11973-5000	aronsons@bnl.gov
Elke-Caroline Aschenauer	DESY - Hermes Building 1e/407 Notkestrasse 85 D - 22603 Hamburg Germany	Elke.Aschenauer@desy.de
Mark Baker	Chemistry – 555A Brookhaven National Laboratory Upton, NY 11973-5000	Mark.Baker@bnl.gov
Anthony Baltz	Physics – 510A Brookhaven National Laboratory Upton, NY 11973-5000	baltz@bnl.gov
Kenneth Neil Barish	Physics Department University of California 900 University Avenue Riverside, CA 92521	Kenneth.Barish@ucr.edu
Steven Bass	Institute for Theoretical Physics University of Innsbruck Technikerstrasse 25 A-6020 Innsbruck Austria	Steven.Bass@cern.ch
Frank Bauer	Physics – 510C Brookhaven National Laboratory Upton, NY 11973-5000	fbauer@rcf.rhic.bnl.gov
Carola Berger	C.N. Yang Inst. of Theoretical Physics SUNY Stony Brook Stony Brook, NY 11794	carola.berger@sunysb.edu
Les Bland	Physics – 510A Brookhaven National Laboratory Upton, NY 11973-5000	bland@bnl.gov
Antje Bruell	Massachusetts Institute of Technology Building 26-551 77 Massachusetts Avenue Cambridge, MA 02139	abr@mitlns.mit.edu

Current and Future Directions at RHIC

August 5-23, 2002

REGISTERED PARTICIPANTS

Stephen Bueltmann	Physics – 510D Brookhaven National Laboratory Upton, NY 11973-5000	buelmann@bnl.gov
Gerry Bunce	Physics – 510A Brookhaven National Laboratory Upton, NY 11973-5000	bunce@bnl.gov
Matthias Burkardt	Department of Physics New Mexico State University Las Cruces, NM 88003	burkardt@nmsu.edu
Helen Caines	Wright Lab 272 Whitney Avenue Yale University New Haven, CT 06520	caines@star.physics.yale.edu
Daniel de Florian	Departamento de Fisica Facultad de Ciencias Exactas y Naturales Univ de Buenos Aires Pabellón I Ciudad Univ. (1428) Capital Federal Argentina	deflo@df.uba.ar
Abhay Deshpande	Physics – 510A Brookhaven National Laboratory Upton, NY 11973-5000	abhay@bnl.gov
Adrian Dumitru	Physics – 510A Brookhaven National Laboratory Upton, NY 11973-5000	dumitru@quark.phy.bnl.gov
George Fai	Department of Physics Kent State University Kent, OH 44242	fai@cnrred.kent.edu
Kirill Filimonov	LBNL, MS70-319 1 Cyclotron Road Berkeley, CA 94720	KVFilimonov@lbl.gov
Leonid Frankfurt	Tel Aviv University Ramat-Aviv 61390 Tel Aviv, P.O.B. 39040 Israel	frankfur@lev.tau.ac.il
Rainer Fries	Physics Department Duke University P.O. Box 90305 Durham, NC 27708	rjfries@phy.duke.edu

Current and Future Directions at RHIC

August 5-23, 2002

REGISTERED PARTICIPANTS

Todd Fugleberg	Physics – 510A Brookhaven National Laboratory Upton, NY 11973-5000	Fugle@quark.phy.bnl.gov
Yoshinori Fukao	Physics Department Kyoto University Kitashirakawa Oiwake-cho Sakyo-ku, Kyoto 606-8502 Japan	fukao@nh.scphys.kyoto-u.ac.jp
Dominik Gabbert	Hessstr. 64 80798 Muenchen Germany	allegro_con_fuoco@hotmail.com
Francois Gelis	Lab de Physique Theorique Universite Paris XI, Etat 210 91405 Orsay Cedex France	gelis@th.u-psud.fr
Lars Gerland	Institute for Nuclear Physics Ramat Aviv, 69978 Tel-Aviv Israel	gerland@lev.tau.ac.il
Yuji Goto	RBRC / RIKEN Physics – 510A Brookhaven National Laboratory Upton, NY 11973-5000	goto@bnl.gov
Matthias Grosse Perdekamp	Physics – 510A Brookhaven National Laboratory Upton, NY 11973-5000	Matthias@bnl.gov
Wlodek Gryn	Physics – 510D Brookhaven National Laboratory Upton, NY 11973-5000	gryn@bnl.gov
Kaoru Hagiwara	Theory Group KEK Tsukuba 305-0801 Japan	kaoru.hagiwara@kek.jp
David Hardtke	LBNL MS 70-319 Berkeley, CA 94720	DHHardtke@lbl.gov
Francesco Hautmann	Institute for Theoretical Physics University of Regensburg D-93053 Regensburg Germany	francesco.hautmann@physik.uni-regensburg.de

Current and Future Directions at RHIC

August 5-23, 2002

REGISTERED PARTICIPANTS

L. Donald Isenhower	Abilene Christian Univ. Box 27963 Abilene, TX 79699-796	isenhowe@acu.edu
Barbara Jacak	Physics Department SUNY at Stony Brook Stony Brook, NY 11794	jacak@skipper.physics.sunysb.edu
Barbara Jaeger	Institute for Theoretical Physics University of Regensburg D-93053 Regensburg Germany	barbara.jaeger@physik.uni-regensburg.de
Jamal Jalilian-Marian	Physics – 510A Brookhaven National Laboratory Upton, NY 11973-5000	jamal@bnl.gov
Dmitri Kharzeev	Physics – 510A Brookhaven National Laboratory Upton, NY 11973-5000	kharzeev@bnl.gov
Edward Kinney	390 UCB University of Colorado Boulder, CO 80309-0390	Edward.Kinney@colorado.edu
Jiro Kodaira	Department of Physics Hiroshima University Higashi-Hiroshima 739-8526 Japan	jkodaira@hiroshima-u.ac.jp
Yuji Koike	Physics Department Niigata University Ikarashi, Niigata 950-2181 Japan	koike@nt.sc.niigata-u.ac.jp
Yuri Kovchegov	Dept. of Physics, Box 351560 University of Washington Seattle, WA 98195	yuri@phys.washington.edu
Henri Kowalski	Columbia University Nevis Lab PO Box 137 Irvington, NY 10533	Kowalski@nevis.columbia.edu
Alexander Krasnitz	FCT, Univ. do Algarve Campus de Gambelas P-8000-117 Faro Portugal	krasnitz@ualg.pt

Current and Future Directions at RHIC

August 5-23, 2002

REGISTERED PARTICIPANTS

Stefan Kretzer	Department of Physics and Astronomy Michigan State University 3231 Biomed Phys Sciences East Lansing, MI 48824	kretzer@pa.msu.edu
Shunzo Kumano	Department of Physics Saga University Saga 840-8502 Japan	kumano@cc.saga-u.ac.jp
Krishna Kumar	Department of Physics University of Massachusetts Amherst, MA 01003	kkumar@physics.umass.edu
Gerd Kunde	Physics Department Yale University New Haven, CT 06520 USA	g.j.kunde@yale.edu
Harry Lam	Department of Physics McGill University 3600 University Street Montreal, Quebec Canada H3A 2T8	Lam@physics.mcgill.ca
J.-H. Lee	Physics – 510D Brookhaven National Laboratory Upton, NY 11973-5000	jhlee@bnl.gov
Jonathan Lenaghan	The Niels Bohr Institute 17 Blegdamsvej 2100 - Copenhagen Denmark	lenaghan@alf.nbi.dk
Evgeny Levin	HEP Department School of Physics Tel Aviv University Tel Aviv, 69978 Israel	leving@post.tau.ac.il
Jechiel Lichtenstadt	School of Physics and Astronomy Tel Aviv University 69978 Tel Aviv Israel	jech@lepton.tau.ac.il
Patricia Liebing	DESY Notkestrasse 85 22607 Hamburg Germany	patricia.liebing@desy.de

Current and Future Directions at RHIC

August 5-23, 2002

REGISTERED PARTICIPANTS

Simonetta Liuti	Department of Physics University of Virginia 382 McCormick Road PO Box 400714 Charlottesville, VA 22904	sl4y@virginia.edu
Dan Magestro	Ohio State University C/O Brookhaven National Laboratory Building 510A Upton, NY 11973	magestro@bnl.gov
Naomi Makins	University of Illinois Loomis Lab of Physics 1110 W Green Street Urbana, IL 61801-3080	makins@uiuc.edu
Robert McCarthy	Dept. of Physics and Astronomy State University of New York Stony Brook, NY 11794	mccarthy@sbhep.physics.sunysb.edu
Melvin Mckenzie, Jr.	US Army, Retired Middle Island, NY 11953	melnsel@msn.com
Zein-Eddine Meziani	Temple University Physics - Barton Hall (009) A323 1900 N. 13th Street Philadelphia, PA 19122	meziani@unix.temple.edu
Denes Molnar	Columbia University 538 West 120th Street New York, NY 10027	molnard@phys.columbia.edu
Pavel Nadolsky	Department of Physics Fondren Science Building Southern Methodist University Dallas, TX 75275-0175	nadolsky@mail.physics.smu.edu
Yasushi Nara	Physics – 510A Brookhaven National Laboratory Upton, NY 11973-5000	ynara@quark.phy.bnl.gov
Gouranga Nayak	Theoretical Division T-8, MSB285 Los Alamos National Laboratory Los Alamos, NM 87545	nayak@shakti.lanl.gov
Karo Oganessyan	INFN-LNF Via E. Fermi 40 C.P. 13, I-00044 Frascati, Italy	kogan@lnf.infn.it

Current and Future Directions at RHIC

August 5-23, 2002

REGISTERED PARTICIPANTS

Sergey Panitkin	Physics – 510A Brookhaven National Laboratory Upton, NY 11973-5000	panitkin@bnl.gov
Joerg Raufeisen	Los Alamos National Laboratory MS H846 Los Alamos, NM 87545	jorgr@lanl.gov
Gunther Roland	Massachusetts Institute of Technology 77 Massachusetts Avenue Room 24-504 Cambridge MA 02139	Gunther.Roland@cern.ch
Marzia Rosati	Iowa State University Department of Physics and Astronomy 12 Physics Hall Ames, IA 50011	mrosati@iastate.edu
Naohito Saito	Physics Department Kyoto University Kitashirakawa Oiwake-cho Sakyo-ku, Kyoto 606-8502 Japan	saito@nh.scphys.kyoto-u.ac.jp
Andrzej Sandacz	Soltan Inst for Nucl Studies ul Hoza 69 PL 00-681 Warsaw Poland	sandacz@fuw.edu.pl
Jurgen Schaffner-Bielich	Columbia University 538 West 120th Street New York, NY 10027	schaffne@nt3.phys.columbia.edu
Rolf Scharenberg	Purdue University West Lafayette, IN 47907	schrnrg@purdue.edu
Stefan Schlenstedt	DESY Zeuthen Platanenallee 6 15735 Zeuthen Germany	stefan.schlenstedt@ifh.de
Viktor Siegle	Physics – 510A Brookhaven National Laboratory Upton, NY 11973-5000	victor@bnl.gov
Misha Stephanov	Physics Department 2256 SES MC 273 University of Illinois Chicago, IL 60612	stephanov@bnl.gov

Current and Future Directions at RHIC

August 5-23, 2002

REGISTERED PARTICIPANTS

George Sterman	C.N. Yang Inst. of Theoretical Physics SUNY Stony Brook Stony Brook, NY 11794	sterman@insti.physics.sunysb.edu
Marco Stratmann	Institute for Theoretical Physics University of Regensburg D-93053 Regensburg Germany	marco.stratmann@physik.uni-regensburg.de
Mark Strikman	104 Davey Lab Pennsylvania State University University Park, PA 16802	strikm@phys.psu.edu
Bernd Surrow	Physics – 510A Brookhaven National Laboratory Upton, NY 11973-5000	surrow@bnl.gov
Hiroshi Takahashi	Building 475B Brookhaven National Laboratory Upton, NY 11973-5000	takahash@bnl.gov
Kiyoshi Tanida	Radiation Laboratory RIKEN 2-1 Hirosawa, Wako-shi, Saitama 351-0198 Japan	tanida@rarfaxp.riken.go.jp
Michael Tannenbaum	Physics – 510C Brookhaven National Laboratory Upton, NY 11973-5000	mjt@bnl.gov
Derek Teaney	Physics – 510A Brookhaven National Laboratory Upton, NY 11973-5000	dteaney@quark.phy.bnl.gov
Manabu Togawa	Physics Department Kyoto University Kitashirakawa Oiwake-cho Sakyo-ku, Kyoto 606-8502 Japan	togawa@nh.scphys.kyoto-u.ac.jp
Hisayuki Torii	Physics – 510A Brookhaven National Lab Upton, NY 11973	htorii@bnl.gov
Kirill Tuchin	Institute for Nuclear Theory Physics/Astronomy Building University of Washington Box 351550 Seattle, WA 98195-1550	tuchin@phys.washington.edu

Current and Future Directions at RHIC

August 5-23, 2002

REGISTERED PARTICIPANTS

Fumi Ukegawa	Institute of Physics University of Tsukuba Ten'noudai 1-1-1 Tsukuba-shi, Ibaraki-ken 305-8571 Japan	ukegawa@hep.px.tsukuba.ac.jp
Raju Venugopalan	Physics – 510A Brookhaven National Laboratory Upton, NY 11973-5000	raju@bnl.gov
Ivan Vitev	Physics, 704 Pupin Hall Columbia University 538 West 120th Street New York, NY 10027	ivitev@nt4.phys.columbia.edu
Werner Vogelsang	Physics – 510A Brookhaven National Laboratory Upton, NY 11973-5000	wvogelsang@bnl.gov
Hiroshi Yokoya	Department of Physics Hiroshima University Higashi-Hiroshima 739-8526 Japan	yokoya@theo.phys.sci.hiroshima-u.ac.jp
C.-P. Yuan	Department of Physics and Astronomy Biomedical Physical Science Building Michigan State University East Lansing, MI 48824	yuan@pa.msu.edu
Xiaofei Zhang	Department of Physics Kent State University Kent, OH 44242	Xzhang3@kent.edu

2002 SUMMER PROGRAM : "CURRENT AND FUTURE DIRECTIONS AT RHIC"

A RIKEN BNL Research Center Workshop

~~~~~  
August 5-23, 2002  
Physics Dept., Bldg. 510, Large Seminar Room  
~~~~~

Organizers: A. Deshpande, A. Dumitru, J. Jalilian-Marian,
N. Saito, D. Teaney, R. Venugopalan, W. Vogelsang

Note: Daily *Discussion* sessions are for specific discussions on the day's topics; however, may also be used for brief additional presentations.

Week I (Aug. 5 - 9): AA and pA physics

Monday, Aug. 5: pA physics

10:30 - 11:15	R. McCarthy	<i>Nuclear Effects Observed at High PT at Fermilab</i>
11:15 - 12:00	I. Vitev	<i>pA at RHIC</i>
14:00 - 14:45	D. Isenhower	<i>pA at Fermilab</i>
14:45 - 15:30	F. Gelis	<i>pA in the Color Glass Condensate Model</i>
15:30 -		<i>Round table discussion on dA at RHIC</i>

Tuesday, Aug. 6: New RHIC results (I)

10:00 - 10:45	M. Baker	<i>New Experimental Results from RHIC</i>
10:45 - 11:30	B. Jacak	<i>What's happening at high pt? New Results from Phenix</i>
11:30 - 12:00	Y. Nara	<i>v2 from Classical Yang-Mills</i>
13:30 - 14:00	K. Tuchin	<i>Azimuthal Correlations from Minijets</i>
14:00 - 14:30	K. Filimonov	<i>Elliptic Flow at High pt</i>
14:30 - 15:15		<i>Discussion</i>

Wednesday, Aug. 7: New RHIC results (II), saturation physics

10:30 - 11:15	G. Roland	<i>News from PHOBOS</i>
11:15 - 12:00	E. Levin	<i>Saturation and RHIC data</i>

14:00 - 14:45	J.H. Lee	<i>News from Brahm</i> s
14:45 - 15:30	Y. Kovchegov	<i>Particle production in AA collisions at RHIC from saturation physics</i>
15:30 -		<i>Discussion</i>
18:30 -		WORKSHOP DINNER (Patio of BNL Center)

Thursday, Aug. 8:

10:30 - 11:15	M. Tannenbaum	<i>ET distributions and other event-by-event fluctuations</i>
11:15 - 12:00	S. Panitkin	<i>Two-particle interferometry at RHIC</i>
14:00 - 14:45	H. Caines	<i>Strangeness</i>
14:45 - 15:30	D. Hardtke	<i>Jets and Dijets in AA at RHIC</i>
15:30 -		<i>Discussion</i>

Friday, Aug. 9:

10:00 - 11:15	G. Kunde	<i>High PT particles in STAR</i>
11:15 - 12:00	Y. Akiba	<i>Continuum leptons</i>
13:30 - 14:15	C. Woody	<i>AA upgrade PHENIX</i>
14:15 - 15:00	T. Roser	<i>RHIC machine upgrades</i>
15:00 - 15:45	D. Kharzeev	<i>Current and Future Physics at RHIC</i>
15:45 -		<i>Discussion on RHIC upgrades</i>

Week II (Aug. 12 - 16): eA and pp physics

Monday, Aug. 12:

10:30 - 11:15	J. Raufeisen	<i>Heavy quark production at RHIC</i>
11:15 - 12:00	S. Liuti	<i>Violations of Duality in Deep Inelastic Scattering</i>
14:00 - 14:45	R. Fries	<i>Leading twist and higher twist in eA and pA collisions</i>
14:45 - 15:30	F. Hautmann	<i>Diffraction DIS</i>
15:30 -		<i>Discussion</i>

Tuesday, Aug. 13:

10:45 - 11:30	M. Strikman	<i>Small-x phenomena with nuclei</i>
11:30 - 12:15	S. Kumano	<i>Parton distribution functions in nuclei</i>
14:00 - 14:45	E. Levin	<i>Low-x pdfs and Diffraction</i>
14:45 - 15:15		<i>Discussion</i>

Wednesday, Aug. 14:

10:30 - 11:15	H. Lam	<i>Gluon saturation and Wilson line distribution</i>
11:15 - 12:00	L. Frankfurt	<i>Hard coherent phenomena in eA and pA collisions</i>
14:00 - 14:45	A. Sandacz	<i>Search for color transparency</i>
14:45 - 15:30	V. Ptitsyn	<i>eRHIC. Accelerator issues</i>
15:30 - 16:15	H. Kowalski	<i>Proton shape in the saturation picture from VM-DIS data</i>
16:15 -		<i>Discussion</i>
18:30 -		WORKSHOP DINNER (Patio of BNL Center)

Thursday, Aug. 15: Experimental results in ppbar and pp

10:30 - 11:15	F. Ukegawa	<i>QCD results from CDF</i>
11:15 - 12:00	R. Scharenberg	<i>Evidence for hadronic deconfinement and for a significant change in the hadronization conditions in pbar-p collisions @ 1.8 TeV</i>
14:00 - 14:30	H. Torii	<i>pp Neutral pion results from PHENIX Run-2</i>
14:30 - 15:00	H. Sato	<i>pp J/Psi results from PHENIX Run-2</i>
15:00 - 15:30	X.-F. Zhang	<i>Decisive Role of Fragmentation Functions in Hadron Production</i>
15:30 -		<i>Discussion</i>

Friday, Aug. 16: QCD studies (I)

10:30 - 11:15	D. de Florian	<i>Resumed cross-section for Higgs production at hadron colliders</i>
11:15 - 12:00	P. Nadolsky	<i>Resumation in SIDIS and for heavy flavors</i>
14:00 - 14:45	A. Bruell	<i>Shadowing in Nuclei</i>
		BEYOND THE STANDARD MODEL
14:45 - 15:30	K. Hagiwara	<i>Physics beyond RHIC Spin</i>
15:30 -		<i>Discussion</i>

Week III (Aug. 19 - 23): polarized pp and ep physics

Monday, Aug. 19: QCD studies (II) – polarized scattering

10:00 - 10:45	M. Stratmann	<i>A_{LL} for pion production at NLO</i>
10:45 - 11:30	D. de Florian	<i>Hadron production in polarized pp collisions at NLO</i>
14:00 - 14:45	H. Yokoya	<i>Polarization effects in Drell-Yan</i>
14:45 - 15:30	C.-P. Yuan	<i>W-boson physics at the polarized RHIC</i>
15:30 -		<i>Discussion</i>

Tuesday, Aug. 20: Spin structure of the nucleon from lp and pp

10:00 - 10:45	J. Lichtenstadt	<i>Polarized PDFs, recent data, uncertainty estimates</i>
10:45 - 11:30	S. Kumano	<i>Polarized antiquark distributions</i>
11:30 - 12:15	K. Orginos	<i>Spin structure on the lattice</i>
13:45 - 14:30	Y. Koike	<i>Single spin asymmetries in pp and ep collisions</i>
14:30 - 15:15	L. Bland	<i>STAR plans for polarized proton collision physics</i>
15:45 - 16:30	B. Fox	<i>PHENIX plans for polarized proton collision physics</i>
16:30 -		<i>Discussion</i>

Wednesday, Aug. 21: Polarized Nucleon Structure from semi-inclusive measurements

10:00 - 10:45	P. Liebing	<i>Extraction of polarized parton distributions from semi-inclusive HERMES data</i>
10:45 - 11:30	E. Kinney	<i>Delta s in semi-inclusive DIS</i>
11:30 - 12:15	S. Kretzer	<i>Fragmentation functions</i>
12:15 -		<i>Discussion</i>
14:00 - 14:45	S. Bass	<i>Neutrino proton elastic scattering and the spin structure of the proton</i>
14:45 - 15:30	A. Sandacz	<i>Studies of exclusive processes in ep scattering at EIC</i>
15:30 -		<i>Discussion</i>
18:30 -		WORKSHOP DINNER (Patio of BNL Center)

Thursday, Aug. 22: EXCLUSIVE PHYSICS, DVCS, OFPD's (II)

09:30 - 10:15	M. Burkardt	<i>Physical Interpretation for Generalized Parton Distributions</i>
10:15 - 11:00	P. Nadolsky	<i>Azimuthal asymmetries in SIDIS</i>
		MORE QCD IN ep SCATTERING
11:00 - 12:00	S. Schlenstedt	<i>Measurements of the structure of the proton and photon at HERA</i>
14:00 - 14:45	J. Lenaghan	<i>Helicity selection and semi-exclusive meson production</i>
14:45 - 15:15	S. Bass	<i>The DHG sum rule</i>
15:15 - 15:40	K. Kumar	<i>Spin asymmetries at low Q²</i>
15:40 - 16:00	J. Kodaira	<i>Detecting Delta g at RHIC via Double Quarkonium Production</i>
16:00 -		<i>Discussion</i>

Friday, Aug. 23: Future ep facilities

09:30 - 10:15	K. Oganessyan	<i>Perturbative Aspects of Azimuthal Asymmetries in Polarized ep</i>
10:15 - 11:00	E. Aschenauer	<i>The Physics Program for HERMES Run II</i>
11:00 - 11:45	Z. Mezziani	<i>Nucleon Spin Physics at Jefferson Lab using the 12 GeV upgrade</i>
11:45 -		<i>Discussion on future facilities</i>

Additional RIKEN BNL Research Center Proceedings:

- Volume 44 – RHIC Spin Collaboration Meetings VIII, IX, X, XI – BNL-
- Volume 43 – RIKEN Winter School – Quark-Gluon Structure of the Nucleon and QCD – BNL-52672
- Volume 42 – Baryon Dynamics at RHIC – BNL-52669
- Volume 41 – Hadron Structure from Lattice QCD – BNL-52672
- Volume 40 – Theory Studies for RHIC-Spin – BNL-52662
- Volume 39 – RHIC Spin Collaboration Meeting VII – BNL-52659
- Volume 38 – RBRC Scientific Review Committee Meeting – BNL-52649
- Volume 37 – RHIC Spin Collaboration Meeting VI (Part 2) – BNL-52660
- Volume 36 – RHIC Spin Collaboration Meeting VI – BNL-52642
- Volume 35 – RIKEN Winter School – Quarks, Hadrons and Nuclei – QCD Hard Processes and the Nucleon Spin – BNL-52643
- Volume 34 – High Energy QCD: Beyond the Pomeron – BNL-52641
- Volume 33 – Spin Physics at RHIC in Year-1 and Beyond – BNL-52635
- Volume 32 – RHIC Spin Physics V – BNL-52628
- Volume 31 – RHIC Spin Physics III & IV Polarized Partons at High Q^2 Region – BNL-52617
- Volume 30 – RBRC Scientific Review Committee Meeting – BNL-52603
- Volume 29 – Future Transversity Measurements – BNL-52612
- Volume 28 – Equilibrium & Non-Equilibrium Aspects of Hot, Dense QCD – BNL-52613
- Volume 27 – Predictions and Uncertainties for RHIC Spin Physics & Event Generator for RHIC Spin Physics III – Towards Precision Spin Physics at RHIC – BNL-52596
- Volume 26 – Circum-Pan-Pacific RIKEN Symposium on High Energy Spin Physics – BNL-52588
- Volume 25 – RHIC Spin – BNL-52581
- Volume 24 – Physics Society of Japan Biannual Meeting Symposium on QCD Physics at RIKEN BNL Research Center – BNL-52578
- Volume 23 – Coulomb and Pion-Asymmetry Polarimetry and Hadronic Spin Dependence at RHIC Energies – BNL-52589
- Volume 22 – OSCAR II: Predictions for RHIC – BNL-52591
- Volume 21 – RBRC Scientific Review Committee Meeting – BNL-52568
- Volume 20 – Gauge-Invariant Variables in Gauge Theories – BNL-52590
- Volume 19 – Numerical Algorithms at Non-Zero Chemical Potential – BNL-52573
- Volume 18 – Event Generator for RHIC Spin Physics – BNL-52571
- Volume 17 – Hard Parton Physics in High-Energy Nuclear Collisions – BNL-52574
- Volume 16 – RIKEN Winter School - Structure of Hadrons - Introduction to QCD Hard Processes – BNL-52569
- Volume 15 – QCD Phase Transitions – BNL-52561
- Volume 14 – Quantum Fields In and Out of Equilibrium – BNL-52560

Additional RIKEN BNL Research Center Proceedings:

- Volume 13 – Physics of the 1 Teraflop RIKEN-BNL-Columbia QCD Project First Anniversary Celebration – BNL-66299
- Volume 12 – Quarkonium Production in Relativistic Nuclear Collisions – BNL-52559
- Volume 11 – Event Generator for RHIC Spin Physics – BNL-66116
- Volume 10 – Physics of Polarimetry at RHIC – BNL-65926
- Volume 9 – High Density Matter in AGS, SPS and RHIC Collisions – BNL-65762
- Volume 8 – Fermion Frontiers in Vector Lattice Gauge Theories – BNL-65634
- Volume 7 – RHIC Spin Physics – BNL-65615
- Volume 6 – Quarks and Gluons in the Nucleon – BNL-65234
- Volume 5 – Color Superconductivity, Instantons and Parity (Non?)-Conservation at High Baryon Density – BNL-65105
- Volume 4 – Inauguration Ceremony, September 22 and Non -Equilibrium Many Body Dynamics – BNL-64912
- Volume 3 – Hadron Spin-Flip at RHIC Energies – BNL-64724
- Volume 2 – Perturbative QCD as a Probe of Hadron Structure – BNL-64723
- Volume 1 – Open Standards for Cascade Models for RHIC – BNL-64722

For information please contact:

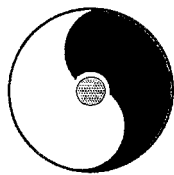
Ms. Pamela Esposito
RIKEN BNL Research Center
Building 510A
Brookhaven National Laboratory
Upton, NY 11973-5000 USA

Phone: (631) 344-3097
Fax: (631) 344-4067
E-Mail: pesposit@bnl.gov

Ms. Tammy Heinz
RIKEN BNL Research Center
Building 510A
Brookhaven National Laboratory
Upton, NY 11973-5000 USA

(631) 344-5864
(631) 344-2562
theinz@bnl.gov

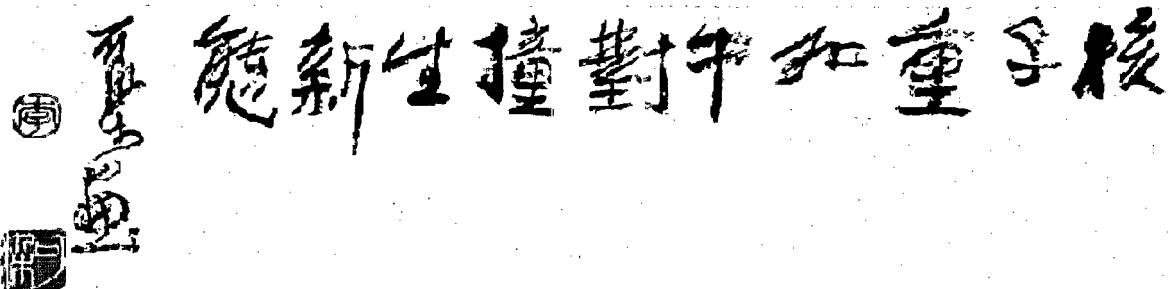
Homepage: <http://quark.phy.bnl.gov/www/riken/index.html>



RIKEN BNL RESEARCH CENTER

2002 Summer Program:
Current and Future Directions at RHIC

August 5-23, 2002



Li Keran

*Nuclei as heavy as bulls
Through collision
Generate new states of matter.
T.D. Lee*

Copyright©CCASTA

Speakers:

- | | | | | | |
|-------------|----------------|----------------|-----------------|---------------|---------------|
| Y. Akiba | E. Aschenauer | M. Baker | S. Bass | L. Bland | A. Bruell |
| M. Burkardt | H. Caines | D. de Florian | K. Filimonov | B. Fox | L. Frankfurt |
| R. Fries | F. Gelis | K. Hagiwara | D. Hardtke | F. Hautmann | D. Isenhower |
| B. Jacak | E. Kinney | D. Kharzeev | J. Kodaira | Y. Koike | Y. Kovchegov |
| H. Kowalski | S. Kretzer | S. Kumano | K. Kumar | G. Kunde | H. Lam |
| J.H. Lee | J. Lenaghan | E. Levin | J. Lichtenstadt | P. Liebing | S. Liuti |
| R. McCarthy | Z. Meziani | P. Nadolsky | Y. Nara | K. Oganessyan | K. Orginos |
| S. Panitkin | V. Ptitsyn | J. Raufeisen | G. Roland | T. Roser | A. Sandacz |
| H. Sato | R. Scharenberg | S. Schlenstedt | M. Stratmann | M. Strikman | M. Tannenbaum |
| H. Torii | K. Tuchin | F. Ukegawa | I. Vitev | C. Woody | H. Yokoya |
| C.-P. Yuan | X.-F. Zhang | | | | |

Organizers: A. Deshpande, A. Dumitru, J. Jalilian-Marian, N. Saito, D. Teaney, R. Venugopalan, W. Vogelsang